PROFILING RETINOID SIGNALING IN TRIPLE-NEGATIVE BREAST CANCER: TOWARDS PRECISION APPLICATIONS

by

Krysta Mila Coyle

Submitted in partial fulfilment of the requirements
for the degree of Doctor of Philosophy

at

Dalhousie University
Halifax, Nova Scotia
March 2018

Nevertheless, she persisted.

TABLE OF CONTENTS

LIST OF TABLES

List of Figures

ABSTRACT

Breast cancer is the most common malignancy diagnosed in women, affecting approximately one in eight Canadian women in their lifetime. Clinical decision-making for breast cancer focuses on targeting growth factor signals through the estrogen receptor (ER) and human epidermal growth factor receptor 2 (HER2). Tumors which lack expression of the progesterone receptor, ER, and HER2 (known as triple-negative breast cancers, TNBCs), cannot be effectively treated with these agents and often face worse prognoses. This illustrates a need for novel therapeutic approaches for the management of TNBC. One potential agent, all-*trans* retinoic acid (atRA) is already used clinically in the treatment of acute promyelocytic leukemia with a limited side-effect profile. I hypothesized that atRA would be an effective treatment for some patients with TNBC following the identification of determinants of sensitivity.

This study characterizes the response of TNBC models to atRA using *in vitro*, *in vivo*, and *in silico* methods. I demonstrate that atRA signaling contributes to expression of a new-age tumor suppressor, RARRES1, and describe the related contributions of DNA methylation and key regulatory factors in establishing its wide range of expression across TNBCs. This formed the basis for large-scale transcriptional profiling of two distinct models of TNBC, in which I identify that the transcriptional response to atRA is largely non-classical and independent of the classical retinoic acid response element; the largely-independent profiles of the two models illustrate the contribution of additional regulatory factors. I further explored the transcriptional response to atRA and the regulatory contributions of DNA methylation across 13 TNBC cell lines and utilized this response to describe a predictive profile which can be used to identify TNBC patients who will benefit from atRA therapy. This was validated against four patient-derived xenografts. Finally, using an *in vivo* genome-wide RNAi screen, I identify SCN1A and GABRA3 as putative mediators of the pro-tumorigenic effects of atRA and suggest that GABAergic signaling may mediate primary or secondary resistance. This research describes non-canonical pathways mediating cellular responses to atRA and provides convincing pre-clinical evidence to support the precision use of atRA for patients with TNBC.

LIST OF ABBREVIATIONS AND SYMBOLS USED

-/-	knockout
µg	micrograms
µm	micrometres
µM	micromoles per litre
°C	degrees Celsius
13cRA	13-*cis* retinoic acid
2D	2-dimensional
3D	3-dimensional
5-mC	5-methylcytosine
7-AAD	7-aminoactinomycin D
9cRA	9-*cis* retinoic acid
A	adenine (nucleotide)
ADP	adenosine diphosphate
AI	aromatase inhibitor
AIC	Akaike Information Criterion
AJCC	American Joint Committee on Cancer
aka	also known as
AKT	RAC-alpha serine/threonine-protein kinase, aka protein kinase B
ALDH	aldehyde dehydrogenase (isoforms 1A1, 1A2, 1A3, 8A1)
AML	acute myeloid leukemia
AMPH	amphiphysin
ANKRD6	ankyrin-repeat domain 6
ANOVA	analysis of variance
AP1	activator protein 1
APL	acute promyelocytic leukemia
AR	androgen receptor
ARF1	ADP-ribosylation factor 1
ARL14EPL	ADP-ribosylation factor like GTPase 14 effector protein-like
As_2O_3	arsenic trioxide
ATCC	American Type Culture Collection
ATRA	all-*trans* retinoic acid
AU	arbitrary units
AXL	tyrosine-protein kinase receptor UFO
B.C.E.	Before Current Era
B2M	β-2 microglobulin
BALB/cfC3H	Bagg-albino inbred mouse model / cfC3H
BCO1	beta-carotene oxygenase 1
bp	base pair
BRCA	breast cancer susceptibility gene (type 1, type 2)
BSA	bovine serum albumin
C	cytosine (nucleotide)
Ca^{2+}	calcium ion
CAF	cancer associated fibroblast

CB17-SCID	CB-17/Icr-*Prkdc*$^{scid/scid}$/Rj
CBP/p300	CREB-binding protein / E1A binding protein p300
CCLE	Cancer Cell Line Encyclopedia
CD	cluster of differentiation (8, 22, 24, 44)
CDH5	cadherin 5
cDNA	complementary deoxyribonucleic acid
ChIP	chromatin immunoprecipitation
Cl^-	chloride ion
CNGA1	cyclic nucleotide gated channel alpha 1
CNS	central nervous system
CO_2	carbon dioxide
COLCA2	colorectal cancer associated 2
CpG	5'—cytosine—phosphate—guanine—3'
CRABP	cellular retinoic acid binding protein
CRBP1	cellular retinol binding protein 1
Cre-*loxP*	Cre recombinase - *loxP* site
CRISP	cysteine-rich secretory protein (2, 3)
CSC	cancer stem cell
CST2	cystatin SA
CTCF	CCCTC-binding factor, aka 11-zinc finger protein
CTSS	cathepsin S
Cy2, 3, 5	cyanine, indocarbocyanine, indodicarbocyanine
CYP	cytochromes P450
DAC	decitabine, 5-aza-2'-deoxycytidine
DAVID	Database for Annotation, Visualization, and Integrated Discovery
DCIS	ductal carcinoma *in situ*
DHRS3	dehydrogenase/reductase 3
DMEM	Dulbecco's Modified Eagle's Medium
DNA	deoxyribonucleic acid
DNase	deoxyribonuclease
DNMT	DNA methyltransferase
DR	direct repeat
DR5	direct repeat, separated by 5 nucleotides
DTT	1,4-dithiothreitol
E10.5	Embryonic day 10.5 (mouse)
EDTA	ethylenediaminetetraacetic acid
EGF	epidermal growth factor
EGFR	epidermal growth factor receptor
ELISA	enzyme-linked immunosorbent assay
EMT	epithelial-to-mesenchymal transition
ER	endoplasmic reticulum
ER	estrogen receptor (α, β)
ERBB2/neu	receptor tyrosine-protein kinase ERBB2, see also HER2
ESM1	endothelial cell specific molecule 1
ESR1	estrogen receptor 1

EYA2	eyes absent homolog 2
F12	Ham's F12 nutrient mixture
FABP	fatty acid binding protein
FACS	fluorescence-activated cell sorting
FBS	fetal bovine serum
FGF	fibroblast growth factor
FGFR1	fibroblast growth factor receptor 1
FOS/JUN	c-FOS, c-JUN heterodimer
FOX	forkhead box (A1, P1)
FSC	forward scatter
G	guanine (nucleotide)
g	gram
GABA	γ-aminobutyric acid
GABRA3	γ-aminobutyric acid receptor subunit alpha-3
GAPDH	glyceraldehyde 3-phosphate dehydrogenase
GBP4	guanylate binding protein 4
GDF15	growth/differentiation factor 15
GEO	Gene Expression Omnibus
GFP	green fluorescent protein
GO BP	gene ontology biological process
GPRC5B	G protein-coupled receptor class C group 5 member B
h	hour
H&E	hematoxylin & eosin
H_0	null hypothesis
H-2Kd	MHC class I alloantigen haplotype d
H#K#	histone #, lysine #
HDAC	histone deacetylase
HEK293T	human embryonic kidney cells 293
HEPES	4-(2-hydroxyethyl)-1-piperazineethanesulfonic acid
HER2	human epidermal growth factor receptor 2, see also ERBB2/neu
HM450	human methylation 450 array (Illlumina)
HOXB2	homeobox B2
HPLC	high-performance liquid chromatography
HRE	hormone response element
HTR4	5-hydroxytryptamine receptor 4
HuGene 2.0ST	GeneChip® Human Gene 2.0 ST Array (Affymetrix)
IC_{50}	inhibitory concentration, 50%
ICD	immunogenic cell death
ICGC	International Cancer Genome Consortium
IDO1	indoleamine 2,3-dioxygenase
IgG	immunoglobulin, G
$IL2Rg^{-/-}$	interleukin 2 receptor gamma chain deficient
EPIC	Infinium MethylationEPIC
IMDM	Iscove's Modified Dulbecco's Medium
IQGAP2	IQ motif containing GTPase activating protein 2

IRF1	interferon regulatory factor 1
IU	International Units
IWK	Izaak Walton Killam
K	keto (nucleotide), guanine or thymine (G or T)
kb	kilobase
kDa	kilodalton
$KHCO_3$	potassium bicarbonate
KRT7	keratin 7
L-15	Leibovitz's L-15 Medium
linc	long intergenic non-coding
LMP	latent membrane protein
loc	gene symbol; published symbol or orthologs are not available
LRAT	lecithin:retinol acyltransferase
LTBP3	latent transforming growth factor beta binding protein 3
MAPK	mitogen-activated protein kinase (p38, p42/44: 38, 42/44 kDa)
MEF2	myocyte enhancer factor 2
MEM	Minimum Essential Media
mg	milligrams
MHC	major histocompatibility complex
min	minutes
mL	millilitre
mm^3	cubic millimetre
MMTV-LTR	mouse mammary tumor virus, long terminal repeat
MOI	multiplicity of infection
mRNA	messenger RNA
MS3	three-stage mass spectrometry
MSK1	ribosomal protein S6 kinase A5 (RPS6KA5)
MYC	myelocytomatosis viral oncogene
N.B.	nota bene
n.d.	not determined or not detected, as specified
n.s.	not significant
Na^+	sodium ion
Na_2EDTA	disodium ethylenediaminetetraacetate dihydrate
NAD	nicotinamide adenine dinucleotide
NADP	nicotinamide adenine dinucleotide phosphate
NCBI	National Center for Biotechnology Information
NCOA	nuclear receptor coactivator (1, 2, 3)
NCOR	nuclear receptor co-repressor
NCSTN	nicastrin
NEAA	non-essential amino acids
NFKBIZ	nuclear factor kappa-beta inhibitor zeta
ng	nanogram
NH_4Cl	ammonium chloride
NHR	nuclear hormone receptor
NK	natural killer cell

nM	nanomole per litre
NOD	non-obese diabetic
NOG/NSG	NOD-*scid* IL2Rg$^{-/-}$
NOTCH4	neurogenic locus notch homolog protein 4
NRIP1	nuclear receptor interacting protein 1
NRP2	neuropilin 2
OCT4	octamer-binding transcription factor 4 (aka POU5F1)
PAM50	Prediction Analysis of Microarray 50
PARP-1	poly [ADP-ribose] polymerase 1
PASTAA	predicting associated transcription factors from annotated affinities
PBS	phosphate buffered saline
PDI	protein disulfide-isomerase
PDK1	phosphoinositide-dependent kinase-1
PDX	patient derived xenograft
PFS	progression-free survival
pGIPZ	GIPZ lentiviral vector plasmid
PIK3CA	phosphatidylinositol-4,5-bisphosphate 3-kinase catalytic subunit α
PML	promyelocytic leukemia (gene)
PPAR	peroxisome-proliferator activated receptor (α, β, δ, γ)
PPRE	peroxisome proliferator response element
PR	progesterone receptor
PRDM1	PR domain zinc finger protein 1
PRKDC	protein kinase, DNA-activated, catalytic polypeptide
PTEN	phosphatase and tensin homolog
PTGES	prostaglandin E synthase
PUM1	pumilio RNA binding family member 1
QEII HSC	Queen Elizabeth II Health Sciences Centre
qPCR	quantitative polymerase chain reaction
R	purine (nucleotide), adenine or guanine (A or G)
RA	retinoic acid
RAG	recombination activating gene (1, 2)
RALDH3	retinaldehyde dehydrogenase 3 *(Mus musculus)*
RANT	retinoic acid naphthalene triazole
RAR	retinoic acid receptor (α, β, γ)
RARE	retinoic acid response element
RARRES	retinoic acid receptor responder protein (1,3)
RAS	rat sarcoma
RBBP4	retinoblastoma binding protein 4
RBP	retinol-binding protein
RMA	robust multi-array average
RMF/EG	reduction mammary fibroblasts, with GFP
RNA	ribonucleic acid
RNAi	RNA interference
ROC	receiver operating characteristic
RPMI	Roswell Park Memorial Institute

RXR	retinoid X receptor (α, β, γ)
S100A7	S100 calcium-binding protein A, psoriasin
SCEL	sciellin
scid	severe combined immunodeficiency
SCN1A	sodium channel protein type 1 subunit α, aka Nav1.1
SERM	selective estrogen receptor modulator
shRNA	short hairpin RNA
SMRT	silencing mediator of retinoic acid and thyroid hormone receptor
SRPX2	sushi repeat-containing protein X-linked 2
SSC	side scatter
SSX	synovial sarcoma, X
STAT1	signal transducer and activator of transcription 1
STR	short tandem repeat
STRA6	stimulated by retinoic acid 6
STRING	Search Tool for the Retrieval of Interacting Genes/Proteins
SUMO2	small ubiquitin-like modifier 2
T	thymine (nucleotide)
TAP	transporter associated with antigen processing (1,2)
TCGA	the cancer genome atlas
TDLU	terminal ductal lobular unit
TET	tetracycline
TGF-β	transforming growth factor-beta
TINAGL1	tubulointerstitial nephritis antigen-like 1
TMPRSS4	transmembrane protease, serine 4
TMT	tandem mass tag
TNBC	triple-negative breast cancer
TNFSF10	tumor necrosis factor superfamily member 10; aka TRAIL
TNM	staging system: tumor size, nodal involvement, metastasis
TP53	tumor protein 53
TR2	testicular receptor 2, aka NR2C1
TRAIL	tumor necrosis factor apoptosis-inducing ligand; aka TNFSF10
Treg	regulatory T cell
TSA	trichostatin A
TSS	transcription start site
TU	transfection units
tubulinEE	detyrosinated tubulin
U	units
V(D)J	variable (diversity) joining
VEGF	vascular endothelial growth factor
V_m	membrane potential
WAP	whey acidic protein
xg	times gravity

N.B. Abbreviations for genes appearing only in high-density figures and tables appear in Appendix 3.

ACKNOWLEDGEMENTS

To my supervisor, Dr. Paola Marcato, who took a chance on a stranger…your confidence in me has never wavered, from the first time you left me alone in the lab to the multitudes of experiments that followed. We have learned so much together and I will continue to learn from your guidance. I am proud of the work I have done with you and I trust you share my pride.

I am blessed to have learned from phenomenal educators in my lifetime: this would not have been possible without your support and belief. And to Dr. Eileen Denovan-Wright, thank you for believing in this day even when I couldn't. You have certainly helped make this possible and I will always carry the life lessons you have shared with me.

I am grateful to have worked with the many members of the Marcato lab, past and present. Many of them have contributed time, energy, and thoughtful feedback to the work in this thesis. To Meg, my partner-in-crime: you have challenged and encouraged me, and shared late-night take-out… this entire experience has been made better by you.

Many thanks to the members of my committee, Drs Graham Dellaire, Karen Bedard, and David Waisman. Your input and encouragement along the way has made me a stronger scientist. To the past and present students, postdocs, and technicians of the Pathology department, thank you for your encouragement, your questions, and your friendship. It would be difficult to overstate the value of the Tupper community: Jordan, Linda, Carolyn, Anna, Eric, Derek, Victoria, Vicky… there are too many to name and too many words to say.

I am so thankful for the love and support of my family, near and far, during this process. To my Nova Scotia family – Mary, Emilie, Lauren, Lindi, Dave, and all your wonderful folks – thank you for welcoming me into your fold with love, laughter, glitter, and occasional tears. My mom has consistently reminded me of the humanity in this work. Much love as always to my sister and to Cadel – who have both reminded me that laughter can really be the greatest medicine! Thanks to Dad for encouraging me to face my fears, and to the rest of my Sahasrabudhe, Coyle, and Dawson families – you have all made even the toughest day a little easier.

This would not be complete without acknowledging the support of my four-legged confidante, Princess Mira the Fluff. She reminds me that we all need to eat, to sleep, to play at 2 in the morning, and to feel loved. Thanks of course to members of my Guiding family who have offered advice, distractions, and more glitter!

I would like to acknowledge financial support from Dalhousie University, the Killam Trusts, Beatrice Hunter Cancer Research Institute, QEII Foundation, Nova Scotia Health Research Foundation, Alberta Advanced Education, and the Canadian Institutes of Health Research.

Finally, this work was made possible by patients who have contributed to research in numerous ways, many with the hope of ensuring future patients will have better experiences. Thank you – especially Mom, Mary, and Jackie – for sharing your hope.

CHAPTER 1: INTRODUCTION

Copyright statement

Portions of this chapter have been previously published in the following manuscripts. The corresponding text has been edited for length, consistency, and to include recent findings.

Coyle KM, Sultan M, Thomas ML, Vaghar-Kashani A, Marcato P. Retinoid signaling in cancer and its promise for therapy. Journal of Carcinogenesis and Mutagenesis 2013; S7:006.

Coyle KM, Boudreau JE, Marcato P. Genetic mutations and epigenetic modifications: Driving cancer and informing precision medicine. BioMed Research International. 2017; 2017: 9620870.

Contribution statement

I prepared the included manuscripts and figures for publication with the guidance of Dr. Paola Marcato. Mohammad Sultan, Margaret Thomas, Ahmad Vaghar-Kashani, and Dr. Jeanette Boudreau supported the writing of the respective manuscripts. All manuscripts were reviewed and edited by all indicated authors.

1.1 CANCER

Cancer refers to a collection of diseases that are characterized by abnormal cellular proliferation, with the potential for local invasion or metastasis to distant tissues. Cancer was described in the Edwin Smith Papyrus, dated as early as 3000 B.C.E., as an incurable disease (discussed in Hajdu, 2004). Today, the lifetime risk for developing cancer is approximately one in two Canadians: 45% for women and 49% for men (Canadian Cancer Society's Advisory Committee on Cancer Statistics, 2017). Despite advances in treatment, cancer remains the leading cause of death for Canadians, accounting for approximately 30% of deaths. Increased cancer occurrence in an aging population, coupled with increasing survivorship, demonstrates a need to improve therapeutic outcomes for patients diagnosed with cancer.

1.1.1 *DEVELOPMENT OF CANCER*

The specific characteristics of individual cancers are derived from, and are as varied as, their tissues, cell types of origin, and the mutations that drive them. Regardless of the tissue of origin, cancers are hypothesized to have eight key biological capabilities, which were termed 'hallmarks' by Hanahan and Weinberg: sustained proliferative signaling, evading growth suppressors, resisting cell death, enabling replicative immortality, inducing angiogenesis, activating invasion and metastasis, metabolic reprogramming, and evading immune destruction (Hanahan and Weinberg, 2000, 2011). The enabling characteristics of genome instability and inflammation support these hallmarks. Collectively, these characteristics position the development and progression of cancer as the result of a complex network of genetic and epigenetic factors, and

interactions between cancer cells and other cells of the body: tissue stromal cells, cells of the immune system, and endothelial cells.

Two key cell-intrinsic factors determining cell behavior are genetics, or heritable nucleotide sequences; and epigenetics, which has traditionally been defined as heritable changes to gene expression that do not involve changes of nucleotide sequences. While genetics plays a key role in cancer, it is not the focus of this thesis and is not discussed in detail.

Canonical epigenetic modifications can alter the transcription and translation of particular genes to increase or decrease their functional levels (Baylin, 2005). Perhaps the most well-studied modification, DNA methylation refers to the addition of methyl groups to CpG dinucleotides in DNA (Irvine et al., 2002; Newell-Price et al., 2000). Although DNA methylation is canonically associated with gene silencing, the implications of DNA methylation vary significantly with genomic context (Jones, 2012). CpG islands, regions of the genome with a high density of CpG dinucleotides, are typically found in gene promoters and rarely methylated (Bird et al., 1985; Cooper et al., 1983). Weak CpG islands, which contain a relatively lower frequency of CpG dinucleotides, may be more susceptible to regulation by DNA methylation (Weber et al., 2007). Genes may have unmethylated promoters and still be transcriptionally inactive, thus the added CpG methylation has been hypothesized to support irrevocable silencing (Bird, 2002).

Other epigenetic modifications that contribute to transcription and translational control of gene expression, while not the primary focus of this work, include the post-translational modification of histone proteins (by acetylation, methylation, phosphorylation, ubiquitylation, or sumoylation) (Jenuwein and Allis, 2001; Peterson and

Laniel, 2004; Strahl and Allis, 2000), and the interactions of non-coding RNAs with proteins or other nucleic acids (Esteller, 2011). These epigenetic processes function normally to provide a framework for development and differentiation, contributing to tissue-specific gene expression, inactivation of the X-chromosome, and genomic imprinting (Ferguson-Smith, 2011; Lau et al., 2004; Mohandas et al., 1981).

While there are many well-described genetic pathways to oncogenesis, the contributions of epigenetics to the development and progression of cancer are more elusive, and both genetic and epigenetic factors collude to provide cancer with the required hallmark capabilities. This thesis focuses on epigenetic factors in cancer.

1.1.2 *Genetic and Epigenetic Factors Driving Cancer*

Key alterations, including mutations, are required for the initiation and development of cancer. Broadly, these genetic aberrations enable growth-promoting signals to cancer genes and/or destabilize the genome to allow continuous malignant transformation by facilitating increased rates of mutation (Cahill et al., 1999; Lengauer et al., 1998; Modrich, 1994; Vogelstein and Kinzler, 2004). These alterations can be found in proto-oncogenes, genes which when activated contribute to cell transformation; and tumor suppressors, genes which normally function to inhibit cellular proliferation. Together, these mutations drive cancer.

Inappropriate activation of oncogenes.

Oncogenes are most often inappropriately activated by mutations, but the removal of epigenetic marks may also be responsible for activating oncogenes (e.g. in rat sarcoma viral oncogene homolog, RAS) and the rate of mutation varies significantly across

cancers of different tissues (Feinberg and Vogelstein, 1983; Fernández-Medarde and Santos, 2011; Kandoth et al., 2013). The emergence of candidate oncogenes from the comprehensive data available through The Cancer Genome Atlas (TCGA) and the International Cancer Genome Consortium (ICGC) databases provides continued insight into the relative frequency of somatic mutations in oncogenes and tumor suppressor genes (Y. Chen et al., 2014; Tamborero et al., 2013).

Several of the most common oncogenes identified as drivers in breast cancer are human epidermal growth factor receptor 2 (HER2, or ERBB2/neu), fibroblast growth factor receptor 1 (FGFR1), MYC proto-oncogene, and phosphatidylinositol-4,5-bisphosphate 3-kinase catalytic subunit α (PIK3CA) (Berns et al., 1992; Pereira et al., 2016). Amplifications or mutations in these genes can potentiate growth factor signaling and support cellular proliferation.

Genetic inactivation or epigenetic silencing of tumor suppressor and genomic stability genes.

The majority of tumor suppressor genes require mutations on both alleles (Stratton et al., 2009), resulting in the inactivation of a gene product that controls excessive cell growth under healthy homeostatic conditions. Typically, loss of cellular integrity followed by persistent and uncontrolled cellular division requires inactivation of protective cellular mechanisms (i.e. tumor suppressor genes) and mutations that facilitate tumor growth, either directly (i.e. by activation of an oncogene) or indirectly (i.e. by enhancing sensitivity to growth factors).

Tumor suppressors which are notable in breast cancer include TP53, breast cancer type 1 and 2 susceptibility proteins (BRCA1, BRCA2), and phosphatase and tensin homolog (PTEN) (Buchholz et al., 1999; Lee and Muller, 2010). TP53 is one of the most common mutations found in cancers, recently estimated to be mutated in over 40% of all human tumors (Kandoth et al., 2013). TP53, BRCA1 and BRCA2 play important roles in DNA repair, and inactivating mutations can promote increased mutagenesis or inhibit apoptosis in the presence of severe DNA damage (Petitjean et al., 2007; Zámborszky et al., 2017); inactivation of PTEN leads to increased AKT signaling and subsequent cellular proliferation (Keniry and Parsons, 2008).

The "two-hit" hypothesis, first described by Knudson in the 1970s (Knudson, 2001, 1971), postulates that at least two mutations of a tumor suppressor gene are required for cancer to develop: first, mutation of one allele; then, loss of heterozygosity, leading to functional loss of the repression of cell division and subsequent development of cancer. Classical tumor suppressor genes, typically defined by inactivation *via* mutation, may also be silenced by epigenetic mechanisms (Birgisdottir et al., 2006; Dobrovic and Simpfendorfer, 1997; Nakamura et al., 2001; Toyota and Issa, 2005). We and others have posited that these "silenced" tumor suppressors may make excellent drug targets as they could potentially be reactivated by reversing these silencing modifications (Balmain, 2002; Coyle et al., 2016), or may indicate pathways and downstream alterations that may be targeted by precise therapeutics.

Normal epigenetic regulation can impact the mutation frequency as highly expressed genes have been demonstrated to have higher mutation rates (C. Park et al., 2012). Epigenetic aberrations can also impact the mutation rate of cancer cells; for

example, spontaneous deamination of methylated cytosines, nucleosome occupancy, and chromatin acetylation can contribute to regional variation in mutation rates. (De and Michor, 2011; Makova and Hardison, 2015; Schuster-Böckler and Lehner, 2012; Timp and Feinberg, 2013; Xia et al., 2012).

Cancer is typically broadly characterized by genome-wide DNA hypomethylation and promoter hypermethylation (Cadieux et al., 2006; de Capoa et al., 2003; Ehrlich, 2009, 2002; Seifert et al., 2007); however, the view and interpretation of epigenetics in the context of precision medicine should be expanded beyond a gene-centric view. The epigenome is not just a surrogate for mutations or variations in gene expression and can have distal effects which range beyond canonical promoter methylation (Aran et al., 2013; Timp and Feinberg, 2013). Evidence suggesting that methylation of distal regulatory elements is related to gene expression poses a complex question that genome-wide studies are now beginning to answer. The hypomethylation observed in cancer often occurs at satellite DNAs, the main component of functional centromeres, and at other repeating sequences that do not function as transcriptional units. Hypomethylation in these DNAs is not likely to have a *cis* effect on gene expression, unless it spreads into neighboring chromatin (Ehrlich, 2002). However, gene expression can be affected by nuclear positioning, and hypomethylation near centromeres could affect gene expression in *trans*. Centromeric heterochromatin has been shown to act as a reservoir for transcriptional control proteins that may be disrupted by hypomethylation (Cobb et al., 2000; Sabbattini, 2001). This hypomethylation may also disrupt interactions between heterochromatin and euchromatin (Brown et al., 1999; Ehrlich et al., 2001; Gasser, 2001). Gene-specific hypermethylation is likely to be a consequence of another cancer-

associated mechanism, such as histone aberrations or variations in transcription rates due to transcription factor control, rather than a direct cause of tumor development or progression (Bestor, 2003; Hosoya et al., 2009; Levanon et al., 2011). This suggests that a gene-centric study of cancer epigenetics may be overly reductive for determining the effects of global epigenetic aberrations.

1.1.3 *Cancer Stem Cells*

A hierarchical model of cancer suggests that a relatively small population of cells, cancer stem cells (CSCs), can repopulate a heterogeneous tumor or leukemia. This contrasts with a stochastic model which implies that all cells of a tumor are equally tumorigenic (reviewed in Coyle and Marcato, 2013). Thus, CSCs represent a stem-like subset of cancer cells which contribute to tumor progression.

CSC biology reflects a number of key stemness features: capacities for self-renewal, proliferation, and multipotency (reviewed in Coyle and Marcato, 2013). Initial research in acute myeloid leukemia (AML), breast cancer, and brain tumors validated the hierarchical model by demonstrating that a population of CSCs could differentiate into a heterogeneous cancer similar to the cancer it originated from (Al-Hajj et al., 2003; Lapidot et al., 1994; Singh et al., 2003). Breast CSCs are typically identified by cell-surface expression of CD44 and CD24 ($CD44^{+}$ $CD24^{-/low}$) or by high aldehyde dehydrogenase ($ALDH^{high}$) enzymatic activity as determined by the commercially-available Aldefluor™ assay (Stem Cell Technologies, Inc.) (Al-Hajj et al., 2003; Ginestier et al., 2007).

The Aldefluor™ assay contains BODIPY-aminoacetaldehyde (BAAA), which is a fluorescent non-toxic substrate for ALDH enzymes. BAAA can freely diffuse into viable

cells, where it is oxidized by ALDH enzymes to BODIPY-aminoacetate (BAA^-). BAA^- is retained in the cell due to its negative charge and fluorescence therefore accumulates due to the activity of ALDH enzymes.

CSCs may be of particular importance for TNBC, as a higher proportion of $CD44^+$ $CD24^{-/low}$ CSCs was identified in clinical TNBC cases. This was associated with worse prognosis when compared with non-TNBC cases (Chang et al., 2016; Idowu et al., 2012). Stem-like cells have also been identified in breast cancer cell lines, with a higher prevalence of $Aldefluor^{high}$ cells in basal-like and claudin-low cell lines (Charafe-Jauffret et al., 2009). High Aldefluor activity has also been associated with CSCs from other tumor types, such as melanoma, lung cancer, and hepatocellular carcinoma (Jiang et al., 2009; Luo et al., 2012; Ma et al., 2008). Recent basic science and clinical research proposes that many of these CSC populations may be resistant to conventional chemotherapy and radiation treatment due to increased drug export or inactivation, quiescence, enhanced DNA repair, or a variety of other mechanisms (D'Andrea et al., 2011; Dobbin et al., 2014; Steg et al., 2012; Yamashina et al., 2014). While presence of high Aldefluor activity or specific cell-surface markers seems to enrich for a population of tumor cells with stem-like characteristics, the presence of CSCs is still contested by the theory of clonal evolution (Adams and Strasser, 2008; Nakshatri et al., 2009; Shipitsin et al., 2007). The relationship between stem-like characteristics, clonal heterogeneity, and tumor progression is an important area of continued investigation.

1.1.4 *Breast Cancer*

Breast cancer is the most common malignancy diagnosed in women, and approximately one in eight Canadian women are expected to develop breast cancer in

their lifetime. The incidence of breast cancer increased with the implementation of mammography screening, but has mostly stabilized since the early 2000s (Canadian Cancer Society's Advisory Committee on Cancer Statistics, 2017). The use of screening mammography and more effective therapies following surgical resection have contributed to the steady decline in mortality from breast cancer since the 1980s (Canadian Cancer Society's Advisory Committee on Cancer Statistics, 2017).

Breast cancer is not a single disease; a variety of factors contribute to a high degree of inter-tumoral heterogeneity. Most breast tumors are classified as adenocarcinomas, arising from the epithelial cells of the breast; although fibroadenomas, inflammatory cancers, or Phyllodes tumors can also occur in the breast. Histologically, breast tumors are classified as ductal or lobular. This was initially thought to be representative of the origin of the tumor, from the ducts or lobules of the breast, respectively. However, both ductal and lobular breast tumors originate from cells of the terminal duct lobular unit (TDLU), and differences may point to distinct cells of origin within the TDLU, or the point in maturation at which cancer was initiated (Zhao et al., 2004). This work focuses on the more common ductal tumors.

Approximately 20% of breast cancers are ductal carcinoma *in situ* (DCIS, Figure 1-1). DCIS is a non-malignant proliferation of breast epithelial cells which is contained by the basement membrane of the duct. Untreated, approximately 40% of patients with DCIS will progress to invasive ductal carcinoma (Figure 1-1), where the cancerous proliferation of cells extends beyond the duct and may invade local blood vessels and lymphatic channels. DCIS is not necessary for the development of invasive breast cancer (Cowell et al., 2013), and molecular studies are underway to identify factors which are

necessary and sufficient for the development of invasive disease from DCIS (Hernandez et al., 2012; Heselmeyer-Haddad et al., 2012). One rare type of invasive ductal carcinoma is inflammatory breast cancer, which can be characterized by skin which is red, warm to the touch, and thickened (Jaiyesimi et al., 1992). These symptoms, which mimic inflammation, are caused by blockage of the lymphatic system due to the highly invasive nature of the tumor (Yamauchi et al., 2012).

A variety of clinical tools have been developed to classify and subtype this highly heterogeneous disease. These approaches can be used clinically to stage tumors, identify and modulate treatment modalities, estimate prognoses, and predict responses to novel therapeutics. In laboratory settings, these molecular features can be used to build response profiles to cancer treatments and identify novel prognostic indicators and stratification approaches to inform patient care.

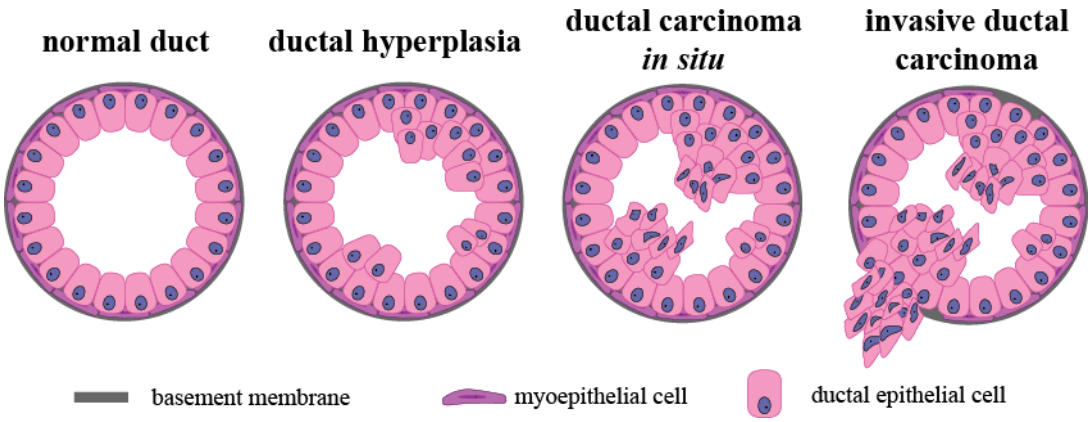

Figure 1-1 Progression of invasive ductal carcinoma.

Normal ductal structure in breast tissue consists of epithelial cells organized inside a structure of myoepithelial cells and contained by a basement membrane. Non-malignant ductal hyperplasia remains contained by both myoepithelial cells and the basement membrane. Subsequent hyperplasia and the appearance of irregular cells and nuclei represent a transition to ductal carcinoma *in situ* (DCIS). Further irregularities and the escape of malignant cells beyond myoepithelial cells with degradation of the basement membrane are characteristic of invasive ductal carcinoma. DCIS is not an obligate precursor to invasive ductal carcinoma.

Clinical classification of breast cancer.

Breast cancer is most often staged by the American Joint Committee on Cancer (AJCC) TNM method which accounts for the size of the primary tumor (T), the number of nearby lymph nodes in which cancer can be detected (N), and the absence or presence of distant metastasis (M). These categories can be collapsed into stages I through IV through a process called 'stage grouping'. Tumors of similar stages are thought to have similar prognoses and are often treated with similar regimens.

Following staging, breast cancer can be classified by expression of the estrogen receptor (ER) and progesterone receptor (PR), and amplification of HER2. The expression of these receptors can be used to select from several targeted therapies, which are discussed in section 1.1.5. Receptor expression is also used to approximate the molecular subtype of breast tumors. Tumors with $ER^{+}/PR^{+/-}HER2^{-}$ are classified as luminal A; $ER^{+}/PR^{+/-}HER2^{+}$ are luminal B; $ER^{-}/PR^{+/-}HER2^{+}$ are classified as HER2-like; and triple-negative breast cancers (TNBCs, $ER^{-}/PR^{-}/HER2^{-}$) are predominantly basal-like (as in Figure 1-2). These approximations are not specific and other tools which incorporate more molecular information can be used to accurately subtype breast tumors.

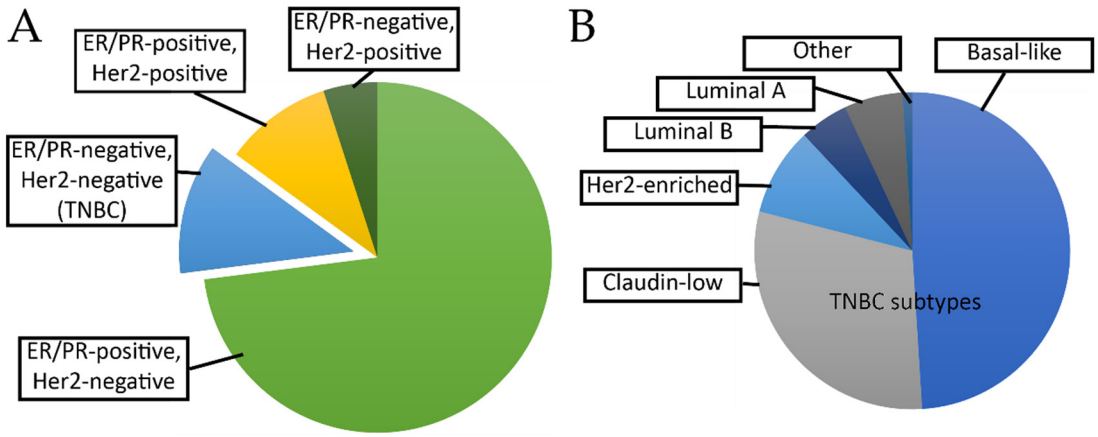

Figure 1-2 Breast cancer is a heterogeneous disease.

A. Approximately 15% of breast cancers are triple-negative (in blue), meaning they do not express ER, PR, or HER2. TNBCs cannot be effectively treated with hormone receptor antagonists. **B.** Within the TNBC classification, there is a high degree of heterogeneity based on gene expression and response to therapy.

Data adapted from (Prat and Perou, 2011).

Molecular classification of breast cancer.

A variety of molecular studies have contributed to our understanding of the wide heterogeneity in breast cancer. The PAM50 tool separates breast tumors into five subtypes: luminal A, luminal B, Her2-like, basal, and normal-like (Parker et al., 2009; Perou et al., 2000). The PAM50 'normal-like' subtype is considered to represent tumors with an overrepresentation of normal epithelial cells, as opposed to a truly distinct subset of tumors (Prat et al., 2010); thus, this classification is not common. A new subtype was later described as claudin-low, which is primarily composed of TNBCs, and has low expression of genes involved in tight junctions and epithelial cell adhesion (e.g. claudins 3, 4 and 7, occludin and E-cadherin) (Prat et al., 2010; Sabatier et al., 2014). This subtype is loosely recapitulated by the alternative identification of mesenchymal and mesenchymal stem-like subtypes of TNBC (Lehmann et al., 2016, 2011) These five subtypes (luminal A, luminal B, HER2-like, basal-like, and claudin-low) are characterized by different survival outcomes and can be treated with different therapeutic agents. Basal-like and claudin-low tumors, as primarily $ER^-/PR^-/HER2^-$, confer poor survival and have limited treatment options available (Dias et al., 2017). These are discussed in further detail in section 1.1.5.

A landmark study of breast cancer in TCGA characterized 10 integrative subgroups of breast cancer with different mutational and gene expression profiles which were associated with distinct patient outcomes (Curtis et al., 2012). Even within clinical or molecular subtypes (such as TNBC), there is a high degree of molecular heterogeneity. TNBC tumors can be classified as luminal, HER2-like, basal-like, and claudin-low

(Figure 1-2B). This intertumoral heterogeneity has important implications for guiding selection of therapies (Abramson and Mayer, 2014; Bianchini et al., 2016).

1.1.5 *Current Therapy for Breast Cancer.*

Therapy for breast cancer is guided by several molecular characteristics and may include a combination of surgical resection, radiation, hormone therapy, and chemotherapy. The use of targeted therapy and immunotherapies in breast cancer is a topic of emerging research.

Hormone therapies.

The use of hormone therapies in breast cancer capitalizes on the characterization of ER and PR expression on breast tumors. A molecular understanding of tissue development, hormones, and required signals for cell proliferation pushed the development of tamoxifen, a selective ER modulator (SERM), originally developed in an attempt to find new contraceptives and cholesterol-lowering drugs (Cole et al., 1971; Harper and Walpole, 1967). Tamoxifen was first licensed for use in the US in 1972 for patients with advanced breast cancer, and its current success in treating patients with ER^+ breast cancers has been called a catalyst for the precision medicine approach to cancer therapy (Jordan, 2008). While values differ between laboratories, breast tumors are most often classified as ER^+ based on a cut-off of 10% of cells expressing ER; however, a response to therapy may be seen in patients in whom as few as 1% of cells express ER (Lin et al., 2013; Yi et al., 2014). The 10% cut-off does not accurately predict response to SERMs (e.g. tamoxifen), thus it is plausible that molecular heterogeneity affects the response of tumors to treatment (Harbeck and Rody, 2012; Lumachi et al., 2013; McDonald et al., 1990). It is clear that the binary distinction between ER^+ and ER^- does

not differentiate between those who will respond to tamoxifen and those who will not, and molecular heterogeneity may help explain this finding. One possibility is the ratio of ERα and ERβ in the targeted tissue (Madeira et al., 2013). Other SERMs such as raloxifene may have similar efficacy in the treatment of ER^+ breast cancer, with variations in side effects including a reduced risk of endometrial cancer or thromboembolic disorders (Swaby et al., 2007).

Aromatase inhibitors (AIs) are also used in the treatment of ER^+ breast cancer. The selective AIs such as anastrozole and letrozole function by reversible competition for the aromatase enzyme, thus inhibiting the synthesis of estrogen (Miller, 2003). A combination of treatment options targeting the estrogen signaling pathway can benefit patients who develop resistance to either treatment (Fan and Jordan, 2014).

Targeting PR has proven more difficult. Early clinical trials suggested that antiprogestins, such as mifepristone (RU486), could be of use in treating breast cancer (Klijn et al., 1989; Romieu et al., 1987). High toxicity and limited efficacy spurred the development of second- and third-generation PR antagonists (Helle et al., 1998; Perrault et al., 1996; Robertson et al., 1999); however, most recent findings with lonaprisan showed limited efficacy and failed to meet clinical targets in phase II study (Jonat et al., 2013). The activity of PR may vary among breast cancers, and the action of progesterone in breast cancer may be context-dependent (Hagan and Lange, 2014). This provides further weight to the pursuit of more targeted applications of therapeutic agents.

Cytotoxic chemotherapies.

Cytotoxic chemotherapies are used to treat advanced breast cancers or those with a moderate-to-high risk of recurrence. A variety of chemotherapeutic agents are used in the treatment of breast cancer. Plant alkaloids, including the taxanes (paclitaxel, docetaxel) and the vinca alkaloids (vinorelbine) are cell-cycle specific and prevent mitosis through interactions with tubulin (Dumontet and Jordan, 2010). Alkylating agents (cyclophosphamide, carboplatin) bind to DNA, resulting in crosslinking of nucleic acids and inhibition of protein synthesis (Hall and Tilby, 1992; Warwick, 1963). Anthracyclines (doxorubicin, epirubicin) intercalate with DNA, inhibiting DNA and RNA synthesis and complexing with topoisomerase II to prevent religation of repaired strands (Zunino and Capranico, 1990). Pyrimidine antagonists (5-fluorouracil, capecitabine, gemcitabine) are pro-drugs which are processed to active metabolites that can be incorporated into DNA and RNA (Maring et al., 2005). Nucleotide imbalances are also introduced by interactions with nucleotide synthesizing enzymes (Longley et al., 2003). Chemotherapies can be given as single agents, in combination, or as successive regimens. The efficacy of chemotherapy (ranging from curative to wholly ineffective) this depend on pharmacological variability between patients (Lin, 2007).

Immunotherapy.

There is consistent evidence for a correlation between survival and immune infiltration in breast cancer (Ali et al., 2016; Mahmoud et al., 2011; Perez et al., 2015), particularly in TNBC and $HER2^{+}$ tumors. This suggests an important role for the immune system in breast cancer, and several clinical trials are investigating the use of checkpoint inhibitors. These agents block inhibitory interactions between tumors and infiltrating

immune cells, enabling anti-tumor immune responses. Preliminary findings show promising responses (Dirix et al., 2016; Nanda et al., 2015; Vonderheide et al., 2010); however, breast cancers do not typically have a highly-mutated phenotype (Kandoth et al., 2013). The limited presence of neoantigens in breast cancer may therefore limit clinical success of immunotherapies.

Targeted therapies.

In breast cancer, the most impressive use of targeted therapy, beyond tamoxifen, is the development and application of the anti-HER2 antibody, trastuzumab, for $HER2^+$ tumors. Trastuzumab significantly improved progression-free and overall survival of women with $HER2^+$ breast tumors (Cobleigh et al., 1999; Slamon et al., 2001). Another promising approach is the use of PARP1 inhibitors in BRCA-mutant tumors to induce synthetic lethality (Balmaña et al., 2014; de Bono et al., 2017). Pre-selection of patients will improve the use of targeted therapies; this demonstrates the need to characterize biomarkers for novel therapies (Figure 1-3).

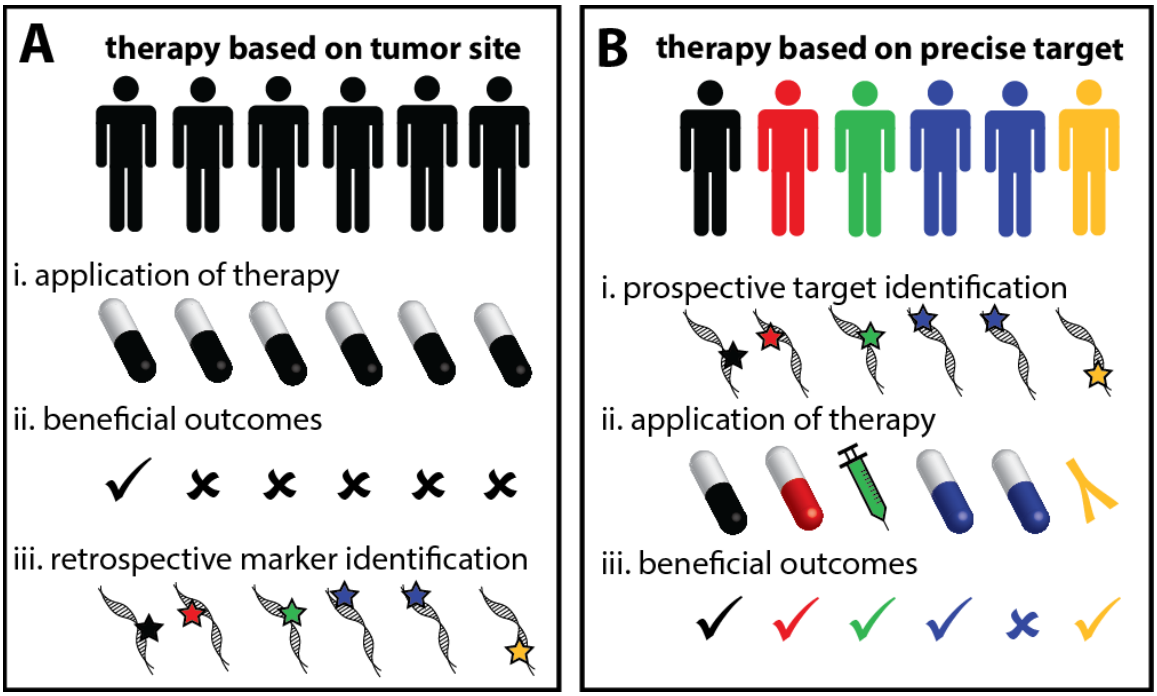

Figure 1-3 Retrospective and prospective identification of biomarkers and actionable targets can improve patient outcomes by allowing more precise therapeutic choices.

A. Traditional treatment of cancers by site of origin. (i) Patients with tumors from the same tissue of origin have typically been treated with the same therapeutic agent. (ii) Treatment outcomes from this type of therapy have been beneficial only in a subset of patients. (iii) With increasing availability of molecular testing, however, we are now retrospectively identifying biomarkers that can predict the outcomes of treatment based on the characteristics of their tumor.
B. Precise patient stratification considers the tumors and the molecular characteristics to determine the best treatment approach. (i) Molecular technologies can identify prospective biomarkers and actionable aberrations. (ii) This allows patients to be given therapies most likely to foster beneficial treatment. (iii) With patient stratification and precise application of therapies, beneficial outcomes are observed in a greater proportion of patients.

1.2 EXPERIMENTAL MODELS OF BREAST CANCER

One of the biggest challenges for breast cancer research is the identification of an ideal preclinical model. For an ideal model system to recapitulate human disease, it must demonstrate several key characteristics: mimic the heterogeneity of human breast tumors; support the study of tumor progression from initiation to metastasis; be cost-effective; and, be on an accessible time scale. The very nature of studying human cancer outside of its natural host is challenging. While there are numerous models of breast cancer, they all have limitations which prevent their use as the perfect model. Many models are missing inter- and intra-tumoral heterogeneity, and where this heterogeneity does exist, it is not always genetically and epigenetically parallel to human tumors. Very few models can mimic the progression of human disease; however, a combination of model systems may be collectively able to appropriately represent human breast cancer.

1.2.1 *MODELING BREAST CANCER* IN VITRO

The use of human cell lines for *in vitro* modeling of breast cancer is widespread. Established cell lines are readily available, can be grown inexpensively, and can be easily used in numerous experimental assays. Cell lines have been derived from various disease states including primary tumors, metastases, and pleural effusions.

Breast cancer cell lines (Table 1-1) can collectively represent most intrinsic subtypes of breast cancer, with one notable exception. Although the PAM50 subtyping tool identifies a subset of breast tumors as ‘normal-like’, this subtype cannot be identified in breast cancer cell lines (Parker et al., 2009; Prat et al., 2010), and perhaps is reflective of the identification of ‘normal-like’ tumors as samples with a high proportion of non-malignant cells (Prat et al., 2010). Additionally, there is some debate about whether cell

lines can represent both the luminal A and luminal B subsets of breast cancer (Jiang et al., 2016; Prat et al., 2013, 2010). While individual cell lines are not entirely relevant models for human disease, the use of cell lines as a system can represent the heterogeneity of breast cancer (Jiang et al., 2016; Kao et al., 2009; Neve et al., 2006; Prat et al., 2013, 2010). A selection of the most common breast cancer cell lines is described in Table 1-1 with reference to their likely subtype and hormone receptor status.

The ease of *in vitro* manipulation and treatment of breast cancer cell lines has allowed comprehensive evaluation of the responses to many drugs (Barretina et al., 2012; Jack et al., 2014; Yang et al., 2013). Additionally, there are several non-malignant immortalized breast cell lines (indicated in Table 1-1) which allow for the study of drug responses and cell signaling in relatively normal cells prior to *in vivo* modeling.

While breast cancer cell lines can collectively model intertumoral heterogeneity, there are several limitations to their exclusive use as model systems. Breast cancer can be described a set of interactions between tumor cells, normal mammary epithelium, endothelial cells, and cells of the immune system. These interactions are conspicuously absent in many *in vitro* experimental assays aside from complex co-culture systems which attempt to replicate one or two of these interactions. There are other propagation methods which attempt to correct some of the flaws in 2D culture, including the use of non-adherent mammosphere models or reconstituted basement membrane cultures. Importantly, the use of 3D models can introduce additional limitations such as a failure to arrest growth and a lack of cell polarity (Bissell et al., 2002; Debnath and Brugge, 2005).

Table 1-1 Selected characteristics of human breast cancer cell lines.

Cell line	ER	PR	HER2	Subtype	Derived
SUM190PT	-	-	+	HER2-like (Prat et al., 2013)	(Forozan et al., 1999)
HCC1954	-	-	+	HER2-like (Jiang et al., 2016)	(Gazdar et al., 1998)
AU565	-	-	+	HER2-like (Jiang et al., 2016)	(Bacus et al., 1990)
HCC202	-	-	+	HER2-like (Jiang et al., 2016)	(Gazdar et al., 1998)
SKBR3	-	-	+	HER2-like (Jiang et al., 2016; Prat et al., 2013)	(Trempe, 1976)
UACC812	+	-	+	HER2-like (Jiang et al., 2016)	(Meltzer et al., 1991)
ZR7530	+	-	+	HER2-like (Jiang et al., 2016)	(Engel et al., 1978)
BT474	+	+	+	HER2-like (Prat et al., 2013)	(Lasfargues et al., 1978)
CAMA1	+	-		HER2-like (Prat et al., 2013)	(Fogh et al., 1977)
BT549	-	-		Claudin-low (Lehmann et al., 2011; Prat et al., 2013, 2010)	*N.B. deposited with ATCC, 1978 (Coutinho & Lasfargues)*
HS578T	-	-		Claudin-low (Lehmann et al., 2011; Prat et al., 2013, 2010)	(Hackett et al., 1977)
MDA-MB-157	-	-		Claudin-low (Prat et al., 2010)	(Cailleau et al., 1978)
MDA-MB-231	-	-		Claudin-low (Lehmann et al., 2011; Prat et al., 2013, 2010)	(Cailleau et al., 1978)
MDA-MB-436	-	-		Claudin-low (Lehmann et al., 2011; Prat et al., 2013, 2010)	(Cailleau et al., 1978)
MDA-MB-435	-	-		*Claudin-low* (Prat et al., 2013, 2010) **see note*	*(Cailleau et al., 1978)*
SUM1315MO2	-	-		Claudin-low (Prat et al., 2013, 2010)	(Forozan et al., 1999)
SUM159PT	-	-		Claudin-low (Prat et al., 2013, 2010)	(Forozan et al., 1999)
HCC1395	-	-		Claudin-low (Prat et al., 2013)	(Gazdar et al., 1998)
HCC38	-	-		Mixed claudin-low / basal (Prat et al., 2013)	(Gazdar et al., 1998)

Cell line	ER	PR	HER2	Subtype	Derived
HCC1143	-	-		Mixed claudin-low / basal (Prat et al., 2013)	(Gazdar et al., 1998)
Du4475	-	-		Basal / immunomodulatory (Lehmann et al., 2011)	(Langlois et al., 1979)
HCC1187	-	-		Basal / immunomodulatory (Lehmann et al., 2011)	(Gazdar et al., 1998)
HCC1599	-	-	+	Basal (Jiang et al., 2016; Lehmann et al., 2011)	(Gazdar et al., 1998)
HCC2157	-	-		Basal (Jiang et al., 2016; Lehmann et al., 2011)	(Gazdar et al., 1998)
HCC70	-	-		Basal (Jiang et al., 2016; Lehmann et al., 2011)	(Gazdar et al., 1998)
MDA-MB-468	-	-		Basal (Jiang et al., 2016; Lehmann et al., 2011)	(Cailleau et al., 1978)
HCC1937	-	-		Basal (Lehmann et al., 2011; Prat et al., 2013)	(Gazdar et al., 1998)
HCC3153	-	-		Basal (Kao et al., 2009; Lehmann et al., 2011)	(Gazdar et al., 1998)
BT20	-	-		Basal (Jiang et al., 2016)	(Lasfargues and Ozzello, 1958)
SUM149PT	-	-		Basal (Lehmann et al., 2011; Prat et al., 2013)	(Forozan et al., 1999)
HCC1806	-	-		Basal (Lehmann et al., 2011)	(Gazdar et al., 1998)
SUM225CWN	-	-	+	Basal / HER2-like (Grigoriadis et al., 2012)	(Forozan et al., 1999)
HCC1500	-	-		Basal (Neve et al., 2006) / luminal (Jiang et al., 2016; Prat et al., 2013)	(Gazdar et al., 1998)
HCC2185	-	-		Luminal (AR) (Lehmann et al., 2011)	(Gazdar et al., 1998)
MDA-MB-453	-	-		Luminal (AR) (Lehmann et al., 2011)	(Cailleau et al., 1978)
SUM185PE	-	-		Luminal (AR) (Lehmann et al., 2011)	(Forozan et al., 1999)
BT483	+	+		Luminal (Jiang et al., 2016)	(Lasfargues et al., 1978)
MCF7	+	+		Luminal (Jiang et al., 2016)	Soule
MDA-MB-134-VI	+	-		Luminal (Jiang et al., 2016)	(Cailleau et al., 1978)
ZR-75-1	+	-		Luminal (Jiang et al., 2016)	(Engel et al., 1978)
MDA-MB-175-VII	+	-		Luminal (Jiang et al., 2016)	(Cailleau et al., 1978)

Cell line	ER	PR	HER2	Subtype	Derived
MDA-MB-361	+	-	+	Luminal (Jiang et al., 2016)	(Cailleau et al., 1978)
MDA-MB-415	+	-		Luminal (Jiang et al., 2016)	(Cailleau et al., 1978)
T-47D	+	+		Luminal (Jiang et al., 2016)	(Keydar et al., 1979)
600MPE	+	-		Luminal (Heiser et al., 2009)	(Smith et al., 1987)
HCC1007	+	-		Luminal (Kao et al., 2009)	(Gazdar et al., 1998)
HCC1428	+	+		Luminal (Prat et al., 2013)	(Gazdar et al., 1998)
LY2	+	-		Luminal (Neve et al., 2006)	(Bronzert et al., 1985)
SUM44PE	+	-		Luminal (Neve et al., 2006)	(Ethier et al., 1993)
SUM52PE	+	-		Luminal (Kao et al., 2009)	(Ethier et al., 1996)
ZR75B	+	-		Luminal (Neve et al., 2006)	(Engel et al., 1978)
HBL100	-	-		Claudin-low (Prat et al., 2010) *N.B. misidentified* (Masters et al., 2001)	(Gaffney, 1982)
RMF/EG	-	-		n/a	(Kuperwasser et al., 2005)
Hs578Bst	-	-		n/a	(Hackett et al., 1977)
MCF10A	-	-		n/a	(Soule et al., 1990)
MCF12A	-	-		n/a	(Paine et al., 1992)

*** MDA-MB-435**: There is substantial evidence which suggests that all existing stocks of MDA-MB-435 cells are derived from the M14 melanoma cell line (Ellison et al., 2002; Korch et al., 2018; Rae et al., 2007; Ross et al., 2000). This evidence includes karyotype analysis, comparative genomic hybridization, microsatellite and single nucleotide polymorphism data, and gene expression. Additional evidence suggests that the identification of MDA-MB-435 as melanoma in origin is due to lineage instability, and that MDA-MB-435 and M14 may both be of mammary origin (Chambers, 2009; Nerlich and Bachmeier, 2013; Sellappan et al., 2004).

Despite these caveats, cell lines have been used to characterize the majority of cancer mechanisms, to identify therapeutic targets, and to test novel agents prior to clinical trials. The use of cancer cell lines as preclinical models for drug discovery and drug response relies on an understanding of the similarities and differences between cell lines and primary tumors. It is possible for the derivation process and continuous growth to introduce profound differences between a cell line and the tumor from which it was initially derived, particularly when considering the most malleable properties of cancer cells (i.e. epigenetic modifications). Interest in characterizing these differences has grown and these studies provide important context for the challenge of translating preclinical successes to clinical success (Burdall et al., 2003; Lacroix and Leclercq, 2004; Thompson et al., 2008; van Staveren et al., 2009; Vincent et al., 2015; Wistuba et al., 1998).

Cancer cell lines have similar patterns of genomic rearrangements as found in primary tumors (Stephens et al., 2009; Wistuba et al., 1998), although continued propagation *in vitro* allows for the accumulation of additional alterations. It is not entirely clear whether the methylation of breast cancer cell lines is similar to that of primary tumors. An early study, which included three breast cancer cell lines (Hs578T, T-47D, and MDA-MB-435), identified hypermethylation of CpG islands in cell lines which was not seen in primary tumors (Smiraglia et al., 2001); however, more recent work concluded that the methylation profiles of 55 cancer cell lines largely mimicked those found in human tumors (Cope et al., 2014). Importantly, Cope et al. identified a subset of cell lines which are ER^- and positive for a CpG-island methylator phenotype with no parallel in primary tumors (Cope et al., 2014). Several of these cell lines are among the most widely used (i.e. MDA-MB-231, MDA-MB-468); therefore, it is especially

important to consider a system of cell lines especially when examining unstable cell characteristics.

The use of a system of human cell lines as an *in vitro* model for breast cancer is relevant and highly feasible for many research questions. Several of the key limitations of *in vitro* assays can be addressed by utilizing *in vivo* modeling; however, the ease and speed of *in vitro* experimentation position cell culture as an essential preclinical model, particularly for high-throughput work.

1.2.2 *Immunocompromised Models of Breast Cancer*

Following *in vitro* culture of human cell lines, the xenografting of cell lines or patient-derived tumors is a common technique to study breast cancers in a model which allows for the interactions of tumor cells with mammary stroma. Most models utilize immunocompromised mice such as the athymic nude mouse or variants of the non-obese diabetic (NOD) severe combined immunodeficiency (*scid*) mouse. Additionally, zebrafish embryos can be used as a model system, particularly of metastasis (Konantz et al., 2012; Ren et al., 2017). There are several key limitations to the use of zebrafish models, including an inability to use orthotopic breast tumor xenografts, and a large mismatch between growth factors (Berman et al., 2014).

Immunocompromised mice lack a fully functional immune system and are required for the study of human cells in mice. The nude mouse, with a mutation in the FOXN1 gene, lacks a thymus, and is thus unable to generate mature subsets of T cells (Nehls et al., 1994; Pelleitier and Montplaisir, 1975). Since T cells are required for graft rejection, nude mice do not reject allografts or xenografts, allowing for the study of human cells. Most strains of nude mice are ‘leaky’ and have a few T cells (Manjili,

2011), so other immunodeficient models, such as the NOD-*scid* mouse, are more commonly used. CB17-*scid* mice are unable to complete V(D)J recombination due to a defect in PRKDC (protein kinase, DNA-activated, catalytic polypeptide) (Bosma et al., 1983). As a result, they lack mature T and B cells and are similarly unable to reject allografts or xenografts. CB17-*scid* mice were crossed with NOD mice (Shultz et al., 1995), which, as a result of inbreeding, have defects in complement activity, T and B lymphocytes, and dendritic cells. The NOD models also display reduced activation of NK cells and defects in macrophage maturation as compared to the *scid* mouse (Bosma et al., 1983; Prochazka et al., 1992). The resultant NOD-*scid* mouse thus supports engraftment of numerous cell types. The NOD-*scid* mouse has been crossed with an IL-2 receptor (IL2R) γ-chain deficient mouse resulting in the NOD-*scid IL2Rg*$^{-/-}$ (colloquially referred to as NOG or NSG) mouse with even more severe impairment of immune function (Ito et al., 2002). Other models of immunodeficiency include recombination activating gene (RAG)1- and RAG2-knockout mice; these may be better models for the study of radiation as they have intact DNA repair mechanisms (Shultz et al., 2007).

There are several factors to consider when choosing a cell line for xenografting. Not all breast cancer cell lines are tumorigenic, even within the immunocompromised NOD-*scid* model (Holliday and Speirs, 2011). Additionally, estrogen-sensitive cell lines require the addition of estrogen in order to engraft (Clarke, 1996). Orthotopic implantation in the mammary fat pad is ideal for breast cancer cell lines and this can increase the take rate over sub-cutaneous implantation (Price et al., 1990). Metastasis of breast cancer cell lines is rare, and occurs most often to the lung (Price, 1996); in contrast, the most common metastatic site in human breast cancer is bone (Manders et al.,

2006). The importance of the immune system in promoting the metastatic cascade is a likely explanation for the rarity of metastases in immunocompromised hosts (Kitamura et al., 2015). More complex experiments have resulted in a series of MDA-MB-231 clones which metastasize to different tissues of the mouse (Kang et al., 2003); additionally, SUM1315MO2 will preferentially metastasize to human bone grafts over mouse bone (Kuperwasser et al., 2005).

An alternative to cell-line xenografts is patient-derived xenografts (PDXs, Figure 1-4). PDXs can be established from implantation of cells or pieces of tissue from human tumors (Tentler et al., 2012). Successive passaging of breast cancer PDXs in mice results in gradual replacement of the human mammary stroma with mouse mammary stroma (Cassidy et al., 2015). Not all tumor types support engraftment as PDXs. Much like TNBC is overrepresented in available cell lines, triple-negative xenografts have a higher take rate than hormone-sensitive tumors (Bruna et al., 2016; Whittle et al., 2015). Additionally, basal-like TNBCs engraft more readily than claudin-low xenografts, making it challenging to fully represent the heterogeneity of human breast cancer with xenografts alone (Zhang et al., 2013). Similar to cell line xenografts, PDXs rarely metastasize (Paez-Ribes et al., 2016); however, PDXs present several advantages over cell line xenografts. PDXs display more fidelity with human tumors in terms of intratumoral heterogeneity and tumor architecture and are passaged less often than in vitro cell culture. This allows the initial characteristics of the clinical sample to be preserved more reliably.

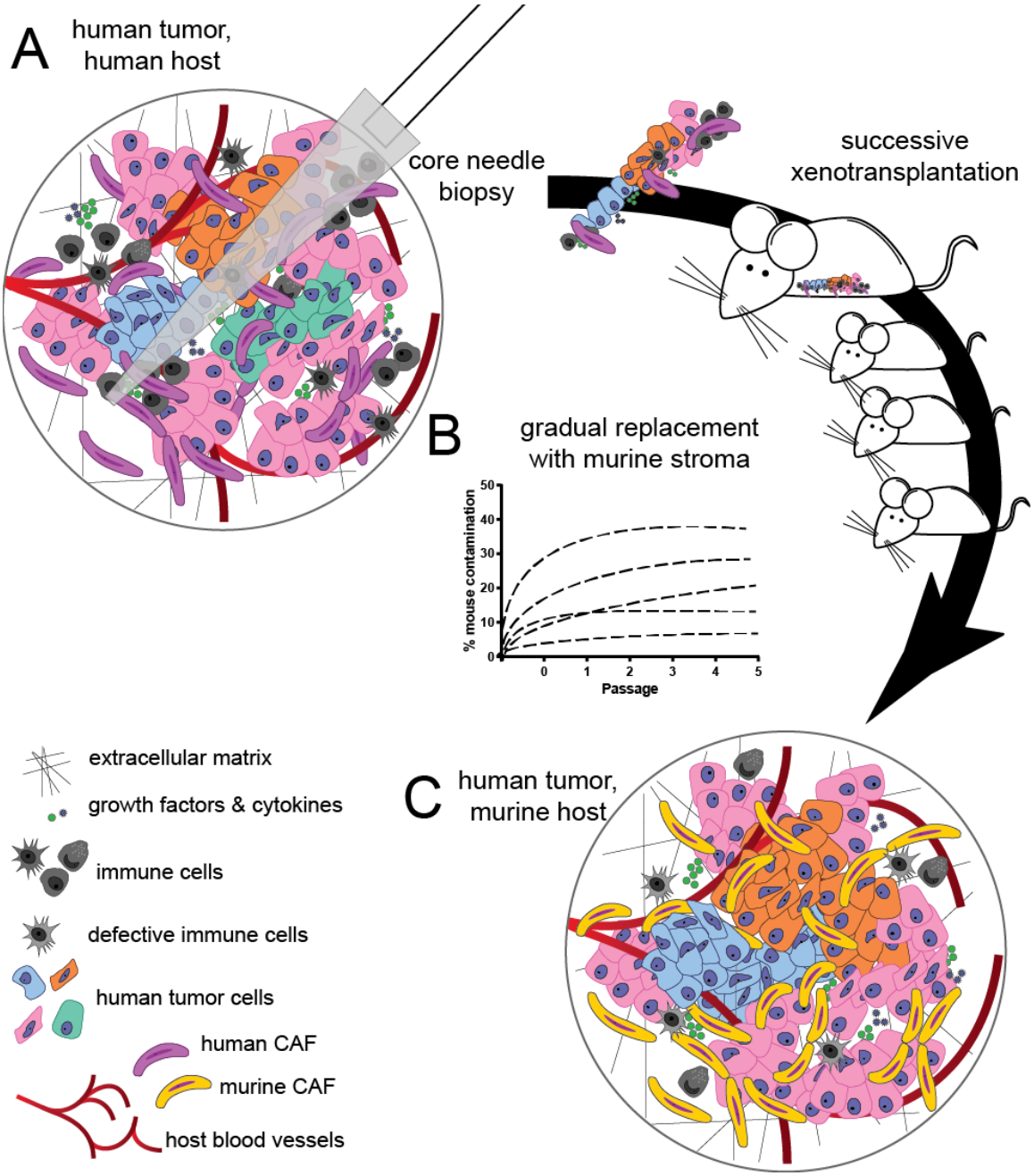

Figure 1-4 Patient derived xenografts result in the replacement of human stroma cells with murine stroma.

A. The first step in establishing a patient-derived xenograft (PDX) is a biopsy of the tumor. This sample will likely contain endothelial cells, cancer-associated fibroblasts (CAFs, stromal cells), tumor cells, immune cells, growth factors, cytokines, and components of the extracellular matrix. **B.** Biopsies are implanted in an immunocompromised murine host and allowed to grow. The human stromal cells are gradually replaced by murine stromal cells throughout successive passaging; the dynamics of this process can differ substantially. **C.** The human stromal component is completely replaced by murine cells.

The use of human cell line and patient-derived xenografts in immunodeficient animal models is common. It is relatively inexpensive, takes little time to develop, and tumors grow relatively synchronously. Experimentally, they are readily available, and many models exist which can recapitulate much of the intertumoral heterogeneity in breast cancer. However, these models are not entirely realistic and there are several pitfalls associated with their exclusive use. First, there is a species mismatch between the stromal cells of the mammary epithelium and the xenografted cancer cells, which may limit cross-talk between the tumor and the supportive stroma. This can be addressed by clearing of the mammary fat pad and humanization with immortalized human fibroblasts (Brill et al., 2008); but this is most typical in studies of normal mammary development, and may inhibit the growth of cancerous xenografts (Zhang et al., 2013). Second, research is unable to investigate the interactions between the human tumor cells and host immune cells. The lack of a chronic inflammatory milieu means that studies of these tumor models are not complete mimics of human cancer. Third, the implantation of large numbers of cells does not imitate the multi-step progression of spontaneous human cancer. There are several approaches in immunocompetent models which can address some of these flaws.

1.2.3 *Immunocompetent Models for Breast Cancer*

There is a wide variety of immunocompetent models for breast cancer which encompass two broad approaches: spontaneous syngeneic models, and genetically engineered transgenic models. The most common host utilized for this work is the laboratory mouse *Mus musculus*, though syngeneic models also exist in the rat (*Rattus norvegicus*). A critical limitation of rat models is that the tumors rarely metastasize.

Genetic manipulation strategies for rats are also not as well-established as those in mice, precluding widespread use of rats as transgenic models.

Syngeneic mouse models of breast cancer are typically derived from spontaneous tumors which arise in murine mammary tissue, and their use combines *in vitro* and *in vivo* methods. The most well-studied is the 4T1 cell-line model, which, along with several sister lines, was derived from a spontaneous tumor in a BALB/cfC3H mouse. The 4T1 variant is a thioguanine-resistant cell line which spontaneously metastasizes *in vivo* to the lung and liver. The sister lines fail at various points in the *in vivo* metastatic cascade; thus, the model has been utilized as a model for metastasis and the epithelial-to-mesenchymal transition (Yang et al., 2004). While syngeneic models are useful to understand essential elements of tumor biology, there are only a few cell lines available (Galli et al., 2000). This makes it difficult to fully represent the wide molecular heterogeneity found in human breast cancer. Additionally, syngeneic cell lines are typically expanded *in vitro* prior to implantation, thus the large number of cells implanted in mice do not represent the early stages of breast cancer progression, and rarely model intratumoral heterogeneity.

Compared to the number of syngeneic models, there is a multitude of transgenic models. These allow the forced expression of a specific oncogene (such as HER2/ERBB2) or can result in the loss of a tumor suppressor (e.g. TP53). Most transgenic models of breast cancer use the murine mammary tumor virus long terminal repeat (MMTV-LTR) or the whey acidic protein (WAP) promoter to drive expression of the transgene. Both MMTV and WAP are hormonally regulated and their expression is not specific to the mammary gland, which suggests that some transgenic models may

have undesirable systemic effects (Wajjwalku et al., 1991; Wen et al., 1995). Thousands of transgenic mice have been generated to study different aspects of breast cancer.

Other models make use of inducible systems such as the tetracycline (tet)-controlled inducible systems (tet-on and tet-off), or the Cre-*loxP* recombination system (Furth et al., 1994; Sauer, 1998). These conditional and inducible models may be more relevant to the study of cancers resulting from spontaneous mutations; whereas germline-altered models are more closely related to tumors arising in individuals with inherited mutations.

It is essential to recognize that no individual model system can recapitulate the vast diversity and heterogeneity of human breast cancer. There are some transgenic models, such as the c-ERBB2-induced model, which are able to more accurately recapitulate human tumors, and several models even demonstrate driver-independent heterogeneity (Ben-David et al., 2016; Hollern and Andrechek, 2014). Although transgenic models allow for the study of cancer initiation and progression, there are significant limitations to direct comparison of transgenic models to human tumors (Cardiff et al., 2000). Most murine mammary tumors are hormone-independent, which is in direct contrast to the over 50% of human breast tumors which are hormone-responsive. Additionally, there is debate about whether similar oncogenic events are responsible for murine and human mammary tumor initiation (Hu et al., 2004; Rangarajan et al., 2004; Rangarajan and Weinberg, 2003). Given the large differences between murine models and human tumors, it is not surprising that transgenic models are not able to represent the detailed molecular stratification of breast cancer.

1.3 VITAMIN A AND ITS DERIVATIVES

In vitro preclinical work and the use of *in vivo* models suggested that vitamin A signaling contributed to breast cancer progression and may be a therapeutic target. For example, retinoic acid receptor β2 expression (RARβ2) is lost in many breast cancer cell lines (Widschwendter et al., 2000), and treatment with 9-*cis* retinoic acid suppresses tumorigenesis in a transgenic model (Wu et al., 2000). This thesis focuses on the role of retinoid signaling in breast cancer, and I first review several important physiological features of this pathway below, before discussing this signaling pathway in the context of cancer.

Vitamin A is an essential physiological molecule which plays a key role in bone metabolism, embryogenesis, vision, skin, and immune function (Clagett-Dame and DeLuca, 2002; Semba, 1998; Tanumihardjo, 2011). Mammals are unable to synthesize vitamin A *de novo*, and it is obtained through diet. It is primarily obtained as β-carotene (Figure 1-5), or pro-vitamin A, from fruits and vegetables; or pre-formed from animal products. Broadly, vitamin A refers to biologically-active molecules in the retinoid class, which consist of a beta-ionone ring with a polyunsaturated carbon chain (Figure 1-5). Synthetic analogues, which may be biologically active, are not designated as vitamin A if they lack this structure.

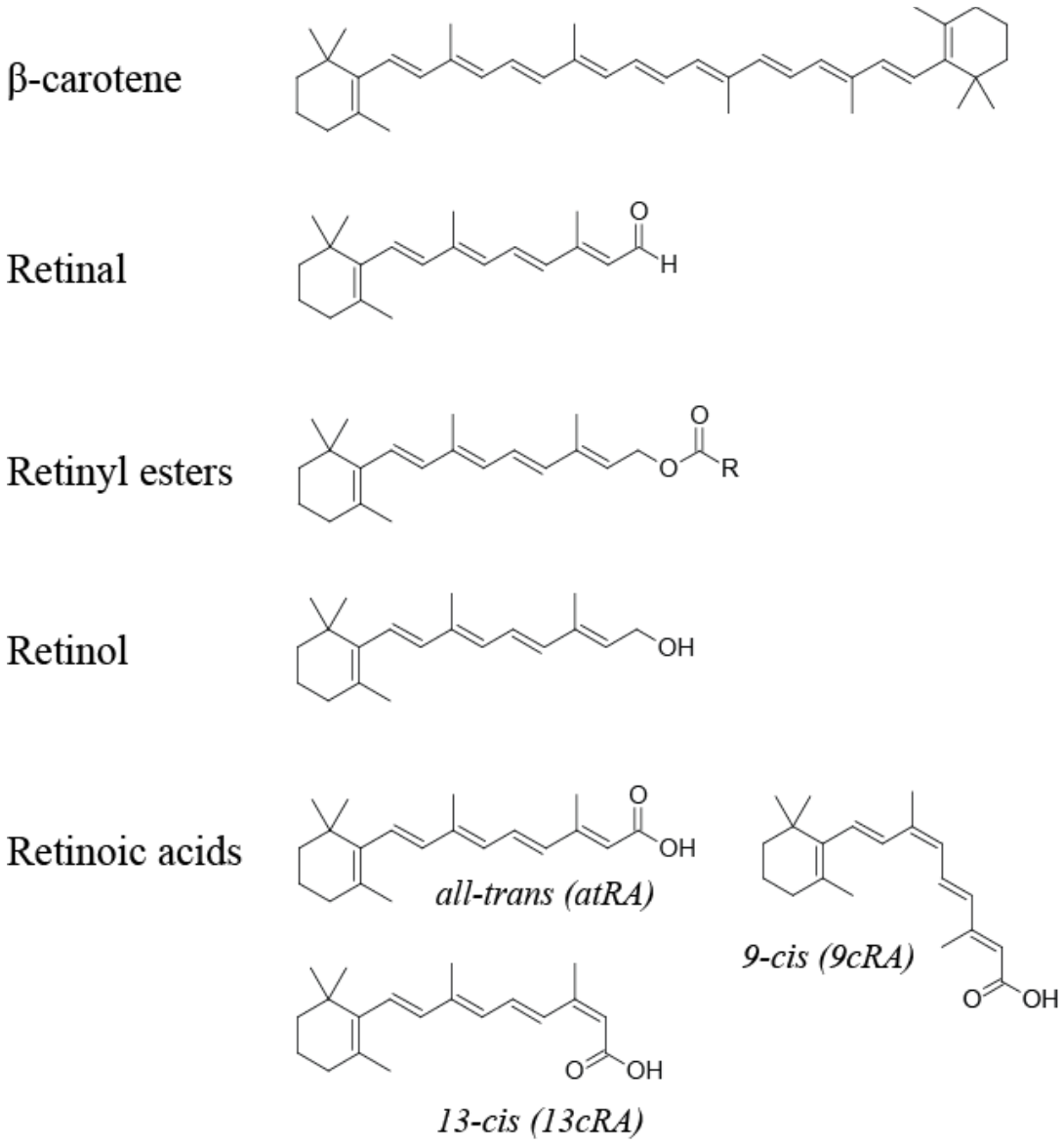

Figure 1-5 Chemical structure of β-carotene and common physiological retinoids.

Retinoids are synthesized from β-carotene in a 1:2 ratio. These physiological retinoids have a cyclic end group, a conjugated side chain, and a polar end group. Most retinoids can exist as several isomers *in vivo* including all-*trans*, 9-*cis*, and 13-*cis*.

Adapted from (Coyle et al., 2013) and used with permission granted under the terms of the Creative Commons Attribution License.

1.3.1 *Retinoid Metabolism and Catabolism*

In the small intestine, β-carotene is cleaved at the 15,15' double-bond by β-carotene oxygenase 1 (BCO1) to form two molecules of retinal (Lintig and Vogt, 2000; Redmond et al., 2001; Wyss et al., 2000). Retinal plays a key role in mammalian vision (Wald, 1968). Retinal can be reduced to retinol by reductase enzymes such as dehydrogenase-reductase 3 (DHRS3).

Retinol is esterified by lecithin:retinol acyltransferase (LRAT) and stored primarily in the liver as retinyl esters (Figure 1-6) (Ong, 1987). Retinyl esters must be hydrolyzed to retinol by one of many retinyl ester hydrolases before it is released into the plasma and circulates bound to retinol-binding protein 4 (RBP4) (Fex and Hansson, 1979; Kopelman et al., 1976). In some cells, the retinol-RBP4 complex binds to a cell-surface receptor, stimulated by retinoic acid 6 (STRA6) which removes retinol from RBP and transports retinol into the cell (Bouillet et al., 1997; Kawaguchi et al., 2007; Sivaprasadarao et al., 1994; Sundaram et al., 1998), where it is transferred to cellular retinoid binding protein 1 (CRBP1). Retinol can also enter the cell via passive diffusion (Hollander and Muralidhara, 1977).

CRBP1 can deliver retinol to retinol dehydrogenases (Boerman and Napoli, 1995) where, in the presence of NAD^+ or $NADP^+$, it is reversibly oxidized to retinal. Retinal can be further oxidized by cytosolic aldehyde dehydrogenases (ALDHs) to retinoic acid (RA) (Zhao et al., 1996). This reaction is irreversible. RA is transferred to the nucleus by cellular RA binding proteins (CRABP1, 2) or fatty-acid binding proteins (e.g. FABP5), and the nuclear effects of RA are discussed in further detail in section 1.3.2. Both CRABP1 and CRABP2 are able to deliver RA to cytochrome P450 (CYP) enzymes

CYP26A1, CYP26B1, and CYP26C1 where RA is hydrolyzed and targeted for excretion (Thatcher and Isoherranen, 2009).

Retinaldehyde dehydrogenases.

The human genome contains 19 distinct ALDH genes which catalyze a wide variety of cellular reactions (Vasiliou and Nebert, 2005). Additionally, ALDH enzymes have non-catalytic properties, binding to numerous molecules (Vasiliou and Nebert, 2005). The activity of several ALDH enzymes can be characterized by an intracellular fluorescent assay such as the commercially-available Aldefluor assay (Stem Cell Technologies, Inc.). This is used to identify and isolate hematopoietic and cancer stem cells.

In humans, four known enzymes are involved in retinoid metabolism: ALDH1A1, ALDH1A2, ALDH1A3, and ALDH8A1 (Hsu et al., 1994; Lin and Napoli, 2000; Rexer et al., 2001; Wang et al., 1996; Yoshida et al., 1992; Zhao et al., 1996). The primary substrate for the ALDH1A isoforms is all-trans retinal; while ALDH8A1 preferentially recognizes 9-*cis* retinal. The ALDH1A isoforms are highly similar, sharing approximately 70% amino acid sequence identity with each other (Moretti et al., 2016). Murine knockout models of ALDH1A enzymes reveal different roles for each isoform in development: *Aldh1a1*$^{-/-}$ mice are viable but demonstrate reduced RA synthesis in the liver (Fan et al., 2003); *Aldh1a2*$^{-/-}$ mice exhibit numerous embryonic defects, resulting in lethality at embryonic day E10.5 (Niederreither et al., 1999; Sandell et al., 2012); and *Aldh1a3*$^{-/-}$ mice die shortly after birth due to nasal malformations (Dupé et al., 2003). The role of ALDH8A1 in physiological retinoid signaling has not yet been determined.

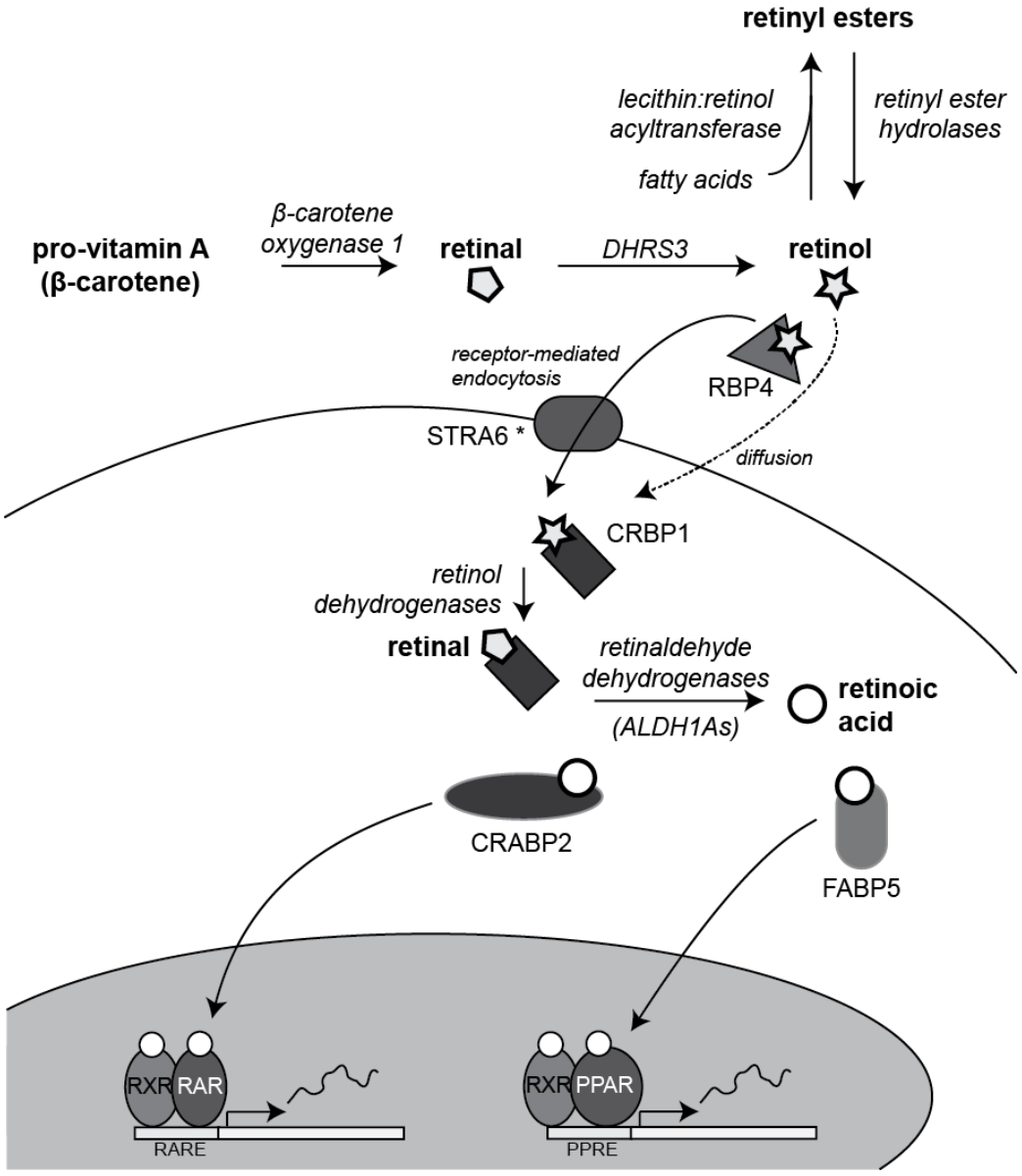

Figure 1-6 Retinoid metabolism and classical signaling.

β-carotene is cleaved by BCO1 to retinal. Retinal can be reduced to retinol and stored bound to fatty acids in the liver; or it can enter cells. Retinol/RBP4 complexes enter cells via STRA6*-mediated endocytosis or via diffusion. Inside the cell, retinol is oxidized to retinal which is subsequently irreversibly oxidized by RALDHs (or ALDH1A isoforms) to retinoic acid. CRABP2 binds retinoic acid and delivers it to RARs within the nucleus. RA-bound RARs and RXRs heterodimerize to activate transcription of genes containing RAREs. Alternative binding to FABP5 can activate transcription of PPREs.

* STRA6 is not present in all cells.

1.3.2 *Genomic Effects of atRA*

The oxidation of retinal by ALDH enzymes generates an important signaling molecule, retinoic acid (RA). The primary effect of RA is to induce transcriptional changes *via* its binding to nuclear hormone receptors (NHRs): retinoic acid receptors (RARs) α, β, and γ; and retinoid X receptors (RXRs) α, β, and γ. RARs can be activated by all-*trans* (atRA), 9-cis (9cRA), and 13-cis RA (13cRA), however; RXRs preferentially bind and are activated by 9cRA (Heyman et al., 1992).

RAR and RXR predominantly exist as a heterodimer, bound to specific DNA sequences termed retinoic acid response elements (RAREs). The consensus RARE sequence is a direct repeat (DR) of the hormone response element (HRE) RGKTCA, separated by five nucleotides (DR5); however, candidate RAREs have been identified with DRs containing zero to ten nucleotides. In the absence of ligand, RAR/RXR heterodimers are bound to RAREs, though evidence suggests that ligand binding increases the occupancy of RAREs by RAR/RXR (Dey et al., 1994; Lefebvre et al., 1998). Over 3000 human genes have been found to be associated with RAREs (Lalevée et al., 2011), leading to a wide variety of possible biological functions from both primary retinoid response genes (those with RAREs) and secondary retinoid response genes.

Unliganded RAR/RXR heterodimers are typically found bound to DNA with corepressors nuclear corepressor (NCOR) and silencing mediator for retinoid and thyroid receptors (SMRT) (Chen and Evans, 1995; Hörlein et al., 1995; Kurokawa et al., 1995). NCOR and SMRT form complexes with histone deacetylases (HDACs) and activate HDAC3 (Guenther et al., 2001; Heinzel et al., 1997; Ishizuka and Lazar, 2003; Li et al., 2000). The HDAC activity associated with these corepressors removes histone

acetylation marks [e.g. H4K5, K8, K13, K16 (Hartman et al., 2005)], maintaining condensed chromatin and repressing transcription of the target gene (Heinzel et al., 1997; Nagy et al., 1997).

Once RA binds RARs in the nucleus, ligand binding induces a conformational change in the RAR/RXR heterodimer which releases the corepressors and recruits coactivators to enhance transcriptional activity. The RAR/RXR-associated coactivators include the p160 subfamily of nuclear receptor coactivators (NCOA) 1, 2, and 3 (Glass and Rosenfeld, 2000), as well as the CBP/p300 coactivator (Dietze et al., 2003, 2002; Yao et al., 1996). The NCOA complex, which contains acetyltransferases and methyltransferases, and the histone acetyltransferase activity of NCOA1 and NCOA3, function to open chromatin and allow transcription to occur (H. Chen et al., 1997; Leo and Chen, 2000; Spencer et al., 1997).

In addition to ligand-binding-directed transcriptional mediation, a new paradigm for phosphorylation of RARs, much like that of other NHRs, has arisen (Keriel et al., 2002; Rochette-Egly, 2003; Taneja et al., 1997). Phosphorylation of RARα recruits RARα to target promoters and enhances recruitment of transcriptional machinery (Bruck et al., 2009). Additional phosphorylation steps may direct ubiquitin- and proteasomal-mediated degradation of RARs (Bour et al., 2007; Perissi et al., 2004).

RAR/RXR binding to regulatory elements is generally thought to activate transcription; however, a number of studies have identified genes which are downregulated in the presence of RA (Madsen et al., 1998; Miller et al., 1990; Roberts et al., 2005; Salbert et al., 1993). Several mechanisms may be possible for this transcriptional repression. Many nuclear receptors share coactivators and corepressors;

sequestration or increased availability of these molecules mediated by RARs may affect the activity of other NHRs (Zhang et al., 1998; Zhao et al., 2001). The interactions of RARs or RXRs with other transcription factors is discussed in section 1.3.3.

RARRES1: a classical retinoid responsive gene.

Many genes were initially characterized based on their responsiveness to retinoids or retinoid receptors. Among these genes is retinoic acid receptor response protein 1 (RARRES1). RARRES1, also known as TIG1 (tazarotene-induced gene 1), was identified in skin raft cultures and is a transmembrane protein of unclear function (Nagpal et al., 1996; Sahab et al., 2011). Investigations in cancer models identified tumor suppressive properties for RARRES1 (Kwok et al., 2009; Oldridge et al., 2013; Sahab et al., 2011). RARRES1 is often silenced by DNA methylation in cancer, adding credence to its role in tumor suppression (Peng et al., 2012). However, this is contested by findings in inflammatory breast cancer which suggest it plays an oncogenic role (Wang et al., 2013). It has been suggested that RARRES1 plays a role in tubulin stability, activation of the AXL receptor tyrosine kinase, or autophagy (Roy et al., 2017; Sahab et al., 2011; Wang et al., 2013). The role of RARRES1 as a classical retinoid response gene in cancer has yet to be precisely characterized.

1.3.3 *Interactions With Other Transcription Factors*

In addition to genes with RAREs, RA can also directly regulate expression of genes without RAREs by interacting with other NHRs and transcription factors. The interactions between RA, peroxisome proliferator-activated receptor (PPAR), as well as with activator protein 1 (AP1) transcriptional activation have been implicated in cancer.

As well, there is evidence to support cross-talk between the estrogen and RA signaling pathways.

Peroxisome proliferator-activated receptor.

In the absence of abundant CRABP2 in the cytoplasm (Figure 1-6), RA can bind other chaperones such as FABP5 with decreased affinity (Dong et al., 1999; Sussman and de Lera, 2005; Tan et al., 2002). Binding to FABP5 delivers RA to PPARβ/δ isoforms instead of to RARs (Schug et al., 2007; Shaw et al., 2003; Tan et al., 2002). PPARβ/δ heterodimerize with RXRs (Figure 1-6) and bind to peroxisome proliferator response elements (PPREs, a DR1 of the classical HRE, AGGTCA), leading to the transcription of genes typically involved in cell growth, such as 3-phosphoinositide-dependent protein kinase 1 (PDK1) (Bardot et al., 1993; Di-Poï et al., 2002; Kliewer et al., 1992; Tugwood et al., 1992). Therefore, predominant RA signaling via FABP5/PPAR can induce cell proliferation as opposed to the more typical cell cycle arrest induced by CRABP2/RAR signaling (Schug et al., 2007).

Activator protein 1.

It is well documented that RARs antagonize the action of AP1 transcription factor (Dedieu and Lefebvre, 2006; Wu et al., 2002). Transrepression of AP1 by RA is possibly coordinated by the interaction of the RARα DNA-binding domain with the c-Jun portion of the AP1 heterodimer (Kliewer et al., 1992), which leads to a decrease in RNA polymerase II recruitment (Benkoussa et al., 2002). AP1-dependent transcription regulates the expression of oncogenic proteins and those involved in proliferation, such

as metalloproteinases, vascular endothelial growth factor (VEGF) and transforming growth factor β (TGF-β) (Liacini et al., 2002; Shih and Claffey, 2001).

Estrogen receptor.

RARα expression is induced by estrogen (Laganière et al., 2005; Roman et al., 1993); as well, there is evidence for extensive cross-talk between RA/estradiol transcriptional activities. SMRT, an RAR/RXR corepressor, is recruited to estrogen receptor α (ERα) in the presence of estradiol and its expression is required for full transcriptional activity of ER responsive genes (Peterson et al., 2007). There is evidence for competitive antagonism between RA- and estrogen-mediated transcription (Hua et al., 2009; Salvatori et al., 2011; Saumet et al., 2012), as well as cooperation between the two pathways (Ross-Innes et al., 2010). It is not clear what factors drive these opposing conclusions.

1.3.4 *Non-Genomic Effects of atRA*

While atRA primarily functions via binding to nuclear receptors, it also has non-genomic, extra-nuclear effects on important cellular functions. One function of retinoids is to influence cell membranes. RA can inhibit keratinization by interfering with calcium ion (Ca^{2+}) entry and the Ca^{2+}-dependent activation of transglutaminase (Yaar et al., 1981; Yuspa et al., 1982). RA may also affect cell-cell signaling by influencing the formation of gap junctions and contact-dependent growth inhibition (Dion et al., 1977; Elias et al., 1980). While molecular networks may reveal that some of these effects are dependent on genomic signaling, one experiment demonstrated that atRA can protect against fibronectin loss even in the absence of nuclei (Bolmer and Wolf, 1982).

Upon binding to RARs, atRA can initiate kinase cascades. Depending on the cell type, ligand-bound RARα can activate p38MAPK or p42/44MAPK, which subsequently activate MSK1. MAPKs and MSK1 can then phosphorylate RARs and other transcription factors (Bruck et al., 2009). Phosphorylation of other factors such as NCOR and NCOA3 affect the transcription of RA-target genes (Giannì et al., 2006). Additionally, non-target genes may be affected as is the case in the phosphorylation of testicular nuclear receptor 2 (TR2) which represses the stemness gene octamer-binding transcription factor 4 (OCT4), supporting RA-mediated differentiation (Gupta et al., 2008). These non-genomic effects of RA are difficult to validate without similar ligands that lack receptor activation (Hammes and Davis, 2015; Persaud et al., 2016). This is an area for further investigation.

1.4 Retinoid Signaling in Cancer

Retinoid signaling plays a controversial role in cancer; evidence suggests it can both suppress and promote tumor development and progression. This has been attributed to the levels of different intracellular proteins such as CRABP2 and FABP5 (as in section 1.3.3), or to the expression of RARβ. The nature of cancer as a complex set of interactions between cancer cells and cells of the tumor microenvironment necessitates consideration of retinoid signaling within tumor cells and within cells of the tumor stroma.

1.4.1 *Intracellular Retinoid Signaling*

At physiological levels of approximately 4-14 nM (Blaner and Olsen, 1994), retinoid signaling is implicated in the development and progression of cancer. With respect to breast cancer, several studies have demonstrated that breast cancer cells exhibit

decreased RA synthesis compared to non-tumorigenic breast epithelial cells (Hayden and Satre, 2002; Mira-Y-Lopez et al., 2000; Rexer et al., 2001); however, the transcriptional consequences of this defect are not well understood.

ALDH enzymes, essential for the generation of retinoic acid (Figure 1-6), also play an important role in cancer. Tumorigenic CSCs can be identified by ALDH enzymatic activity via the Aldefluor assay, and the contribution of different ALDH enzymes to Aldefluor activity depends on the type of cancer under investigation (Marcato et al., 2011a). ALDH1A3 has been identified as the primary contributor to the Aldefluor activity of breast CSCs (Marcato et al., 2011b); and subsequently as playing a role in the progression of TNBC due to the production of RA (Marcato et al., 2015). Expression of ALDH1A3 in tumor cells contributes to the expression of RARE-containing genes including RARβ and tissue transglutaminase, illustrating its importance in regulating retinoid signaling in cancer (Marcato et al., 2015; Sullivan et al., 2017).

Studies of numerous cancer types have identified hypermethylation of RARβ, which has also been associated with prognostic value (Ameri et al., 2011; T. Gao et al., 2013; Tang et al., 2013). In a study of biological effects of atRA on breast cancer, atRA was not able to induce expression of RARβ2 in two-thirds of patients (Toma et al., 2000b); these patients were later shown to have hypermethylation of the promoter (Sirchia et al., 2002). While widespread hypermethylation of RARβ would suggest it has tumor suppressive functions, its expression has also been associated with poor prognosis in patients with non-small cell lung cancer (Khuri et al., 2000); and knockdown of RARβ2 identified both tumor-suppressive and tumor-promoting roles (Pappas et al.,

2011). This contributes to our understanding of a dual role for retinoid signaling in cancer.

Treatment of cancer models with atRA has also demonstrated opposing roles for retinoid signaling. The addition of supraphysiologic levels of atRA (ranging from 100 nM to 1 μM) has been investigated in many cancer models. In breast cancer, it is highly effective in suppressing the growth of many cultured cell lines, although some cell lines (e.g. MDA-MB-231) are highly resistant and proliferation may even be stimulated when cultured with atRA (A. C. Chen et al., 1997; Cho et al., 1997; Fontana, 1987; Hong and Lee-Kim, 2009; Kaleagasioglu et al., 1993; Lotan, 1979; Marth et al., 1984; Mira-Y-Lopez et al., 2000; Somenzi et al., 2007; Van heusden et al., 1998; Wetherall and Taylor, 1986). Using *in vivo* models of TNBC, we have previously shown directly opposing responses: expression of ALDH1A3 or treatment with atRA increased the growth of MDA-MB-231 and MDA-MB-435 xenografts, while similar manipulations decreased the growth of MDA-MB-468 xenografts (Marcato et al., 2015). While a major hypothesis for this finding was differential shuttling of atRA to RAR/RXR heterodimers at RAREs or to RXR/PPAR heterodimers at PPREs, we demonstrated that a substantial portion of the transcriptional response to ALDH1A3 was neither associated with RAREs nor PPREs.

The interactions of RARs and RXRs with other transcription factors, as discussed in section 1.3.3, also play an important role in cancer-associated retinoid signaling. For example, RARα has been clinically associated with tamoxifen resistance in two independent breast cancer patient cohorts, which suggests that RARα may be required to maintain coactivators for ER-mediated transcription (Johansson et al., 2013). This may

have important consequences for hormonal therapy, particularly for patients with primary or acquired resistance to first-line SERMs.

1.4.2 *Retinoid Signaling in the Tumor Microenvironment*

There is increasing evidence of a significant role for the tumor stroma in cancer progression and metastasis (Chang et al., 2004; Hwang et al., 2008; Mazzocca et al., 2010). Activation of stromal fibroblasts occurs early in tumor development (Brentnall et al., 2012; Tuxhorn et al., 2002), and stromal cells cross-talk with the cancer cells of the tumor, resulting in increased tumorigenesis (Dong et al., 2004; Fukumura et al., 1998; Skobe and Fusenig, 1998). There is support for aberrant RA signaling via the tumor stroma as well as from cancerous cells.

Cancer-associated fibroblasts.

Cancer-associated fibroblasts (CAFs) co-evolve with malignant tumor cells and represent an important supportive cell population in the tumor stroma; however, CAFs remain relatively understudied, particularly in characterization of drug responses. There is limited evidence describing the role of retinoid signaling in CAFs; and much of this data is dependent on the tissue and model of choice. ALDH1A1 is often expressed highly in the stromal cells of breast cancer patient tumors and has been correlated with better survival in breast cancer (Resetkova et al., 2010); however, there is conflicting data with respect to the expression of RA-inducible genes such as RARβ in the tumor stroma. Supporting its likely role as a tumor suppressor, RARβ expression is frequently lost in the tissue adjacent to tumors (Widschwendter et al., 2001). Confounding this theory, in ERBB2- and WNT1-induced mammary tumorigenesis model, stromally-expressed RARβ promotes mammary tumorigenesis (X. Liu et al., 2011; Liu and Giguère, 2014). This

finding is validated in a recent study which identified a significant upregulation of RARβ in CAFs compared to normal fibroblasts (Chan et al., 2017). RARβ appears to play a role in the epithelial-to-mesenchymal transition (EMT) which may contribute to its tumor-promoting effects (Liu and Giguère, 2014). Not only do these findings provide evidence of a potential role for RARβ in promoting cancer, they also illustrate that RA signaling in the stroma can be tumorigenic, and may be best targeted with RAR antagonists (Chan et al., 2017).

Cells of the immune system.

For a cancer to develop and progress, it must continually evade immunosurveillance and escape targeting and destruction by the host immune system. Cancers have several immune evasion mechanisms; for instance, tumor cells have decreased antigen presentation by reduced expression of antigen-processing machinery such as transporter associated with antigen processing 1 (TAP1) and TAP2, as well as low molecular mass protein 2 (LMP2) and LMP7 which are associated with the major histocompatibility complexes (MHCs) (Chen et al., 1996; Dissemond et al., 2003; Restifo et al., 1993).

A variety of evidence in different model systems suggests that RA upregulates MHC components and enhances antigen processing and presentation. (Santin et al., 1998; Segars et al., 1993; Vertuani et al., 2007, 2003). Modulation of antigen processing and presentation by RA may contribute to the anti-tumor effects seen in some cancers. Other mechanisms by which RA affects the immune system include contributing to $CD8^+$ T-cell expansion and accumulation (Guo et al., 2012; Tan et al., 2011), and supporting the development of regulatory T (Treg) cells (Benson et al., 2007; Dunham et al., 2013;

Nolting et al., 2009). Understanding the balance between the pro- and anti-inflammatory roles of retinoid signaling in cancer may be an important target for anti-cancer immunotherapy (Galvin et al., 2013).

1.5 Retinoids for Cancer Prevention and Treatment

The general anti-proliferative effects of atRA and the clear role for retinoid signaling in differentiation supported the investigation of retinoids as preventative agents and as anti-cancer therapeutics.

1.5.1 *Retinoids in Cancer Prevention*

Despite evidence in the late 1990s that supplementation of β-carotene with retinyl ester among workers at high risk showed adverse effects on the incidence of lung cancer among patients (Omenn et al., 1996), and a similar study of β-carotene supplementation which revealed no effect on lung cancer incidence (Hennekens et al., 1996), retinoids continue to be studied in prevention and treatment of lung cancer. A 2011 meta-analysis of evidence pertaining to the use of retinoids in lung cancer concluded that there is little support for the use of vitamin A and its natural derivatives in the treatment and prevention of lung cancer; however, the synthetic retinoid bexarotene may hold some promise (Fritz et al., 2011).

Fenretinide, a synthetic retinol analogue, has also been investigated as a preventative agent as it is associated with fewer adverse events than the biological retinoids (Miller, 1998). After five years of oral fenretinide, there was no significant difference in breast cancer recurrence (Veronesi et al., 1999). After fifteen years, recurrence of breast cancer among premenopausal women was decreased by 30%, and significantly fewer women developed ovarian cancer (Veronesi et al., 2006, 1999). The

patients who developed ovarian cancer did so after treatment cessation. (De Palo et al., 2002, 1995; Veronesi et al., 1999). This suggests that fenretinide may exhibit a preventative effect on ovarian tumors, but that this effect does not persist after treatment is discontinued. Despite the ability of both fenretinide and tamoxifen to reduce breast cancer risk, a trial of combination therapy revealed no effect versus placebo (Decensi et al., 2009). The negative-to-modest effects of retinoids on cancer prevention may be attributed to the molecular heterogeneity of retinoid signaling in cancer.

1.5.2 *atRA in Cancer Therapy*

atRA for acute promyelocytic leukemia.

To date, the most successful use of RA in cancer therapy has been in the treatment of acute promyelocytic leukemia (APL). APL represents approximately 5-8% of all acute myeloid leukemia cases and is considered very severe. The vast majority (98%) of APL patients present with the chromosomal rearrangement t(15:17) and resulting fusion of the promyelocytic leukemia (PML) gene with RARα (de Thé et al., 1991; Kakizuka et al., 1991). This fusion protein delays apoptosis (Rogaia et al., 1995); this is likely due to the inability of the PML-RARα fusion protein to appropriately induce physiological RA-mediated differentiation and apoptotic pathways as a result of enhanced recruitment of co-repressor complexes (Altucci et al., 2007; Minucci et al., 2000). These complexes and their accompanying HDAC activity prevent induction of RA-responsive genes at physiological RA concentrations (Minucci et al., 2000). This causes an accumulation of granulocyte precursors, promyelocytes.

Treatment of APL with supraphysiologic concentrations of atRA induces terminal differentiation of these cells and degradation of the oncogenic PML-RARα protein, and significantly improves patient outcomes (Huang et al., 1988). Most recently, the addition of arsenic trioxide (As_2O_3) to atRA has improved efficacy: decreasing time to achieve complete remission, and increasing event-free and overall survival over atRA alone (Aribi et al., 2007; Lo-Coco et al., 2013; Shen et al., 2004). These studies suggest that atRA and As_2O_3 work synergistically to enhance apoptosis and differentiation (Zhou et al., 2007).

As many as one-third of APL patients treated with atRA, As_2O_3, or the combination therapy develop differentiation syndrome (previously known as retinoic acid syndrome) (Frankel et al., 1992; Montesinos and Sanz, 2011). The syndrome is most often characterized by the presence of fever and respiratory distress with no alternative explanations; however, other symptoms may include weight gain, pulmonary infiltrates, pleural or pericardial effusions, hypotension, or renal failure (Botton et al., 1998; Frankel et al., 1992; Tallman et al., 2000). The mechanisms underlying the development of differentiation syndrome are not well understood, but it is hypothesized that atRA-induced changes in adhesive properties and the secretion of various cytokines supports the infiltration of differentiating promyelocytes into various tissues (Dubois et al., 1994; Larson et al., 1997; Marchetti et al., 1996; Seale et al., 1996). Differentiation syndrome only occurs when patients are treated with induction therapy, suggesting that the presence of differentiating APL cells is necessary for these side effects. Co-administration of cytotoxic chemotherapies may reduce the incidence of differentiation syndrome, and the use of corticosteroids when clinical symptoms appear is now standard therapy.

The success of atRA in treating APL has led to earnest attempts to use retinoids in the treatment of other cancers. However; despite the effectiveness displayed in the treatment of APL, retinoids have had limited success in studies of solid tumors.

The use of retinoids for neuroblastoma.

In solid tumors, retinoids have been most successful in the treatment of neuroblastoma. 13cRA is more potent than atRA in models of neuroblastoma (Reynolds et al., 1994). The use of high-dose pulse 13cRA was associated with a number of complete responses in patients with minimal residual disease following myeloablative

therapy (Matthay et al., 1999; Villablanca et al., 1995). This dosing schedule was found to be most effective in obtaining plasma concentrations of 13cRA comparable to those used *in vitro*. Fenretinide may be effective in patients with atRA- and 13cRA-resistant neuroblastoma; however, it has poor bioavailability (Reynolds et al., 2003; Villablanca et al., 2011). Although there is work ongoing to stratify and subtype neuroblastoma based on its molecular features, it is not clear whether this heterogeneity contributes to the modest findings in retinoid-based clinical trials (Van Roy et al., 2009)

Retinoid treatment for glioblastoma.

Early *in vitro* studies in glioblastoma demonstrated anti-proliferative effects of retinoids (Bouterfa et al., 2000). Clinical studies have demonstrated modest effects of 13cRA for some glioblastoma patients, but these responses are not typical and the majority of patients display disease progression (See et al., 2004; Yung et al., 1996). Retinoid derivatives such as RA naphthalene triazole (RANT) may be more effective than 13cRA (Jia et al., 2015). Additionally, combination retinoid therapy may be effective: temozolomide and 13cRA improved progression-free survival (PFS) over temozolomide alone (Jaeckle et al., 2003). Recent evidence suggests that DNA methylation may play an important role in determining the sensitivity of glioblastomas to retinoid therapy (Schmoch et al., 2016). Thus, there is some indication that retinoids could have clinical application in the management of some glioblastomas; however, the factors which dictate response need to be further characterized

Retinoids in breast cancer.

Despite numerous pre-clinical studies, there have been relatively few clinical trials with retinoids in breast cancer. The only clinical trial with atRA as a single agent concluded that atRA did not have significant antitumor capabilities in patients with hormone-refractory, metastatic breast cancer (Sutton et al., 1997). Pharmacokinetic data revealed high variability in the plasma concentration of atRA, ranging from peak concentrations of 17 to 831 ng/mL. This variability suggests that further work is needed to characterize the determinants of retinoid processing and transport.

Other trials testing combinations including retinoids (tamoxifen with atRA, paclitaxel with atRA, tamoxifen with 13cRA) have shown negligible-to-modest responses (Bryan et al., 2011; Budd et al., 1998; Chiesa et al., 2007). We and others have suggested that a failure to account for molecular heterogeneity in breast cancer clinical trials with retinoids is a contributing factor to these disappointing results (Garattini et al., 2014; Marcato et al., 2015). Breast cancer is highly heterogeneous, even when separated by hormone receptor expression; thus, molecular determinants of retinoid sensitivity will play an important role in predicting the response of breast tumors to retinoid-based therapies.

1.5.3 *Determinants of Retinoid Sensitivity*

The relatively few clinical trials of retinoids in breast cancer prohibit the robust identification of clinical biomarkers for retinoid sensitivity; thus, molecular determinants have largely been characterized using *in vitro* and *in vivo* models. One leading hypothesis for retinoid sensitivity is the ratio of CRABP2/FABP5, as discussed in section 1.3.3.

The expression of retinoid receptors is also hypothesized to determine retinoid sensitivity. In ER^+ models, RARα agonists inhibit growth, while silencing of RARα reduces these effects, and overexpression of RARα in MDA-MB-231 cells can confer sensitivity to atRA (Sheikh et al., 1994; Terao et al., 2011). A ratio of RARα/RARγ has been proposed as a predictor for retinoid sensitivity, potentially correlated with ER-positivity and HER2 amplifications (Bosch et al., 2012). Additionally, while RARβ plays a controversial role in cancer models, it is often silenced in breast tumors and its ability to be induced by atRA correlates with inhibition of cell proliferation (Liu et al., 1996).

More recent studies have attempted to use larger data sets to develop a predictive profile for sensitivity to atRA. A tumor-type independent model predicts APL as the most highly sensitive malignancy, whereas breast cancer cell lines display a range of predicted sensitivities (Bolis et al., 2017). Broadly, this sensitivity is described as high for ER^+ tumors and low for TNBC tumors, which is consistent with many *in vitro* studies of retinoid sensitivity in breast cancer (Centritto et al., 2015). Transcriptomic and proteomic characterization of the retinoid-sensitive ER^+ MCF7 and retinoid-resistant $HER2^+$ BT474 cells demonstrate substantial differences between the two cell lines, including in canonical RA target genes (e.g. CYP26A1, STRA6). The authors propose that alterations in canonical RAR signaling as well as in adjacent transcription factors or chromatin modifiers may play an important role in the discrepant phosphoproteome and transcriptome (Carrier et al., 2016).

1.6 Research Rationale and Objectives

While atRA and other retinoids have failed in multiple clinical trials for the treatment of cancer, the accumulating evidence for opposing roles of retinoid signaling in cancer suggests that a more complete understanding of the cellular context in which retinoid signaling operates would allow for a refined use of retinoids in cancer treatment. The overarching goal of this work is to develop an understanding of the possible contexts for atRA signaling in TNBC, in order to develop a predictive signature which can be used to stratify patients who will respond to atRA treatment. This goal is accomplished through the following objectives (Figure 1-7):

- establish a paradigm for epigenetic factors, mainly DNA methylation, as secondary determinants of retinoid signaling (Chapter 2);
- Characterize the transcriptional response of TNBC cells to ALDH1A3 and atRA (Chapter 3);
- Understand the range of responses to atRA in TNBC cell line xenografts and PDXs (Chapter 4);
- Identify and validate a transcriptional and epigenetic signature which predicts the response of TNBCs to atRA *in vivo* (Chapter 4); and
- Identify and confirm functional effectors of the pro-tumor responses of TNBC models to atRA (Chapter 5).

The characterization of atRA sensitivity in TNBC and the cellular contexts governing these responses will support future use of atRA in the clinical management of TNBC.

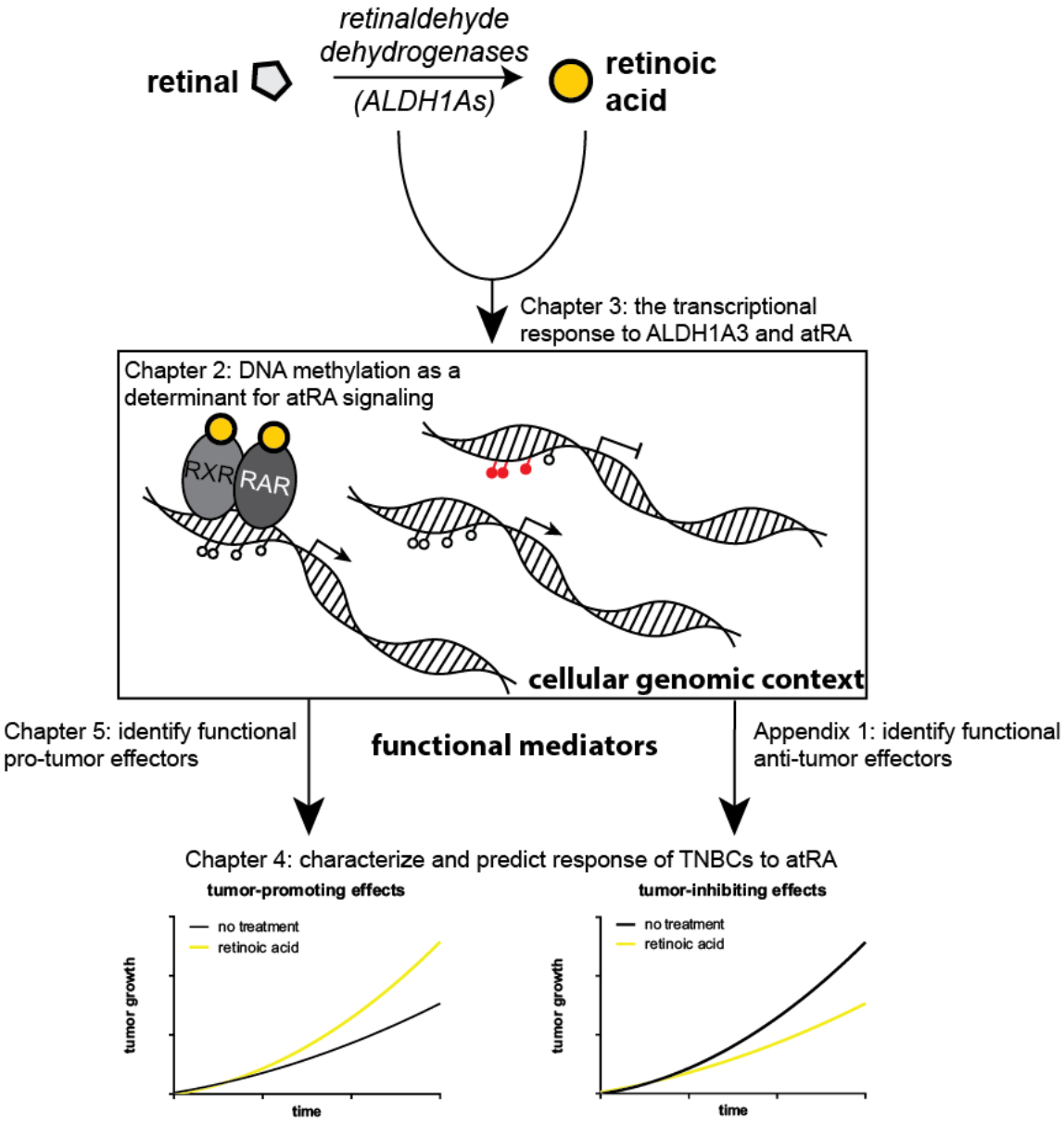

Figure 1-7 Context-dependent atRA signaling: objectives of this thesis.

Chapter 2 will establish DNA methylation as a determinant of atRA signaling; Chapter 3 will further describe the cellular context by comparing the transcriptional response to atRA in two TNBC cell lines with differing responses to atRA. Chapter 4 will demonstrate a range of responses to atRA in TNBC models and establish a predictive profile. Chapter 5 and Appendix 1 identify putative functional effectors of this diversity of responses.

CHAPTER 2: BREAST CANCER SUBTYPE DICTATES DNA METHYLATION AND ALDH1A3-MEDIATED EXPRESSION OF TUMOR SUPPRESSOR RARRES1

Copyright statement

Contribution statement

I wrote the manuscript and designed the experiments with the guidance of Dr. Paola Marcato. The manuscript was reviewed and edited by all authors. I performed experiments and collected data with assistance as follows:

Dr. J Patrick Murphy, mass spectrometry sample preparation, data collection and normalization; Dejan Vidovic, cellular localization; Ahmad Vaghar-Kashani, *in vitro* cell proliferation; Cheryl Dean, histology of clinical samples; Mohammad Sultan, paclitaxel IC_{50} determination; Derek Clements, Western blots (SUMO2, AXL, tubulinEE); Melissa Wallace, qPCR proof-of-principle; Margaret Thomas, Amos Hundert and Dr. Ian Weaver, ChIP data collection and analysis; Dr. Carman Giacomantonio and Dr. Lucy Helyer, collection of clinical samples.

2.1 INTRODUCTION

Although mortality from breast cancer has significantly declined over the past 20 years, breast cancer remains a leading cause of death for women around the world (DeSantis et al., 2016). Novel therapeutic strategies are required to continue making strides against this prevalent disease. Breast cancer has five major molecular subtypes; luminal A/B, HER2 positive, basal-like, and claudin-low. Luminal A/B breast cancers typically express the estrogen receptor (ER) and progesterone receptor (PR), while HER2-like are typically characterized by overexpression of the human epidermal growth factor receptor (HER2, ERBB2/neu) (Van Poznak et al., 2015). Expression of these receptors allows for treatment with hormone receptor antagonist therapies (e.g. tamoxifen), which have vastly improved the survival of breast cancer patients with hormone-receptor-positive tumors (Osborne, 1998). This contrasts with basal-like and claudin-low tumors, which are predominately hormone receptor negative (triple-negative breast cancer; TNBC) and are not treatable by hormone receptor antagonists. Patients with claudin-low or basal-like TNBCs have poorer outcomes with a greater likelihood of metastasis development and more limited treatment options.

Adding to the complexity of patient outcomes, basal-like and claudin-low subtypes differ with respect to prognosis and can be stratified by gene copy-number alterations, genomic instability, gene expression profiles, and distinct drug sensitivities (Sabatier et al., 2014). It is almost certain that differences in the genes expressed in these tumors are responsible for their responses to select agents. Understanding the molecular basis of these breast cancer subtypes will lead to the development of more effective treatment options for TNBC.

Genes can be identified as correlative (e.g. biomarkers) or causative (oncogenes or tumor suppressors) when examining the response of breast cancer subtypes to different therapies. Several approaches exist to identify causative genes. First, mutations and epigenetic modifications can affect the expression of genes such that their role as a tumor suppressor or oncogene is amplified or diminished in different subtypes. DNA methylation is one of the most studied mechanisms affecting gene expression: changes in methylation in many human diseases have been reported, with over 20 000 papers describing these alterations in cancer. Within these studies, several reports have identified promoter-associated hypermethylation in the context of genomic hypomethylation in breast cancer tissue when compared to normal or benign lesions (Bernardino et al., 1997; Soares et al., 1999). Additional studies have observed subtype-specific methylation patterns (Grigoriadis et al., 2012; S. Y. Park et al., 2012; Roll et al., 2013; Sproul et al., 2011; Stefansson et al., 2015); and several tumor-promoting and tumor-suppressing genes have already been identified as differentially methylated in breast cancer subtypes, affecting their expression (Bediaga et al., 2010; Li and Li, 2015). Second, genes and gene products may have different roles and functions depending on their cellular context. For example, the androgen receptor has been suggested as a tumor suppressor in ER-positive tumors, while playing an oncogenic role in ER-negative tumors (Hickey et al., 2012). Our earlier work identified the cancer stem cell marker and retinoic-acid (RA) producing enzyme, aldehyde dehydrogenase 1A3 (ALDH1A3), as promoting or suppressing tumor growth in a context-dependent manner in TNBC (Marcato et al., 2015). The RA receptor responder protein 1 (RARRES1) has also been identified as either suppressing or promoting tumor growth, depending on the study (Peng et al., 2012; Wang et al., 2013).

In this study, we focus on RARRES1 as a paradigm to determine if protein function and gene expression regulation in breast cancer is dictated by subtype. Gene expression studies with a panel of 26 cell lines and analyses of patient data sets reveal that RARRES1 expression is associated with TNBCs, specific to the basal-like subtype. Cell proliferation, tumor growth assays, proteome and cellular localization studies demonstrate it acts as a tumor suppressor in TNBC. HumanMethylation450 arrays and chromatin immunoprecipitation (ChIP) analyses demonstrate that RARRES1 expression is subtype-dependent and regulated dually by DNA methylation and the expression of ALDH1A3, which produces its transcription-inducing factor, all-*trans* (at)RA. These findings provide a precedent for a therapeutically-inducible tumor suppressor and suggest potential avenues of therapeutic intervention for TNBC patients who lack targeted therapies.

2.2 Materials and Methods

2.2.1 *Ethics Statement*

Animal investigations detailed in this manuscript have been conducted in accordance with the ethical standards and according to the Declaration of Helsinki and according to national and international guidelines. All experiments were conducted in accordance with the Canadian Council on Animal Care standards and a protocol approved by Dalhousie University Committee on Laboratory Animals (#13-010). Patient samples were collected and analyzed in accordance with protocol #1007106, approved by the IWK Health Centre Research Ethics Board.

2.2.2 *Cell Lines, Vectors, and Reagents*

Cell lines were obtained from the American Type Culture Collection (ATCC) and cultured as described in Table 2-1. RARRES1 shRNA knockdown clones were generated as previously described (Marcato et al., 2011, 2015), using the pGipZ lentiviral vector (shRNA 1: V3LHS_398249; shRNA 2: V3LHS_398251; Dharmacon). Western blotting was used to verify RARRES1 expression (R&D anti-RARRES1, cat#AF4255, 1/300).

ALDH1A3 knockdown and overexpression cells were generated previously and validated by Western blotting as described previously (Marcato et al., 2011, 2015). Cells were selected with 1.5 μg/mL puromycin (Sigma) and maintained in 0.25 μg/mL puromycin.

For 5-aza-2′-deoxycytidine (DAC) treatment, 1 μM DAC (Sigma) was added for 72 h and replaced every 24 h. When used in combination with all-trans retinoic acid (atRA), 100 nM atRA (Sigma) was added for the last 18 h.

2.2.3 *Quantitative PCR*

qPCR was performed on cDNA generated from extracted RNA as previously described (Marcato et al., 2015)using gene-specific primers (Table 2-2). Standard curves for each primer set were generated, and primer efficiencies were incorporated into the CFX Manager software (Bio-Rad). mRNA expression of all samples was calculated relative to two reference genes [glyceraldehyde 3-phosphate dehydrogenase (GAPDH) and β-2-microglobulin (B2M) for analyses within cell lines; ADP-ribosylation factor 1 (ARF1) and pumilio homolog 1 (PUM1) for analyses between cell lines].

Table 2-1 Cell line subtypes and cell culture conditions.

Cell line	**Hormone Receptor Status**			**Subtype**	**Reference**	**Cell culture specifications**				
	ER	PR	Her2			Basal medium	Additives		Conditions	Passaging
HCC38	-	-	-	claudin-low	(Prat et al., 2013)	RPMI-1640	10% FBS		5% CO_2	0.25% trypsin
BT-549	-	-	-	claudin-low	(Prat et al., 2010)	RPMI-1640	10% FBS	0.023 IU/mL human insulin	5% CO_2	0.25% trypsin
Hs 578T	-	-	-	claudin-low	(Prat et al., 2010)	DMEM	10% FBS	0.01 mg/mL bovine insulin	5% CO_2	0.25% trypsin
MDA-MB-231	-	-	-	claudin-low	(Prat et al., 2010)	L-15	10% FBS		0% CO_2	0.25% trypsin
MDA-MB-436	-	-	-	claudin-low	(Prat et al., 2010)	L-15	10% FBS	10 µg/mL insulin, 16 µg/mL glutathione	0% CO_2	scraped
MDA-MB-157	-	-	-	claudin-low	(Prat et al., 2010)	L-15	10% FBS		0% CO_2	0.25% trypsin
HCC1395	-	-	-	claudin-low	(Prat et al., 2013)	RPMI-1640	10% FBS		5% CO_2	0.25% trypsin
SUM159PT	-	-	-	claudin-low	(Prat et al., 2010)	F12	5% FBS	HEPES, 1 µg/mL hydro-cortisone, 5 µg/mL human insulin	5% CO_2	0.25% trypsin

Cell line	Hormone Receptor Status			Subtype	Reference		Cell culture specifications					
	ER	PR	Her2				Basal medium	Additives			Conditions	Passaging
SUM1315MO2	-	-	-	claudin-low	(Prat et al., 2010)		F12	5% FBS	10 ng/mL EGF, HEPES, 5 µg/mL human insulin		5% CO_2	0.25% trypsin
HCC1937	-	-	-	basal	(Prat et al., 2010)		RPMI-1640	10% FBS			5% CO_2	0.25% trypsin
HCC1143	-	-	-	basal	(Prat et al., 2013)		RPMI-1640	10% FBS			5% CO_2	0.25% trypsin
MDA-MB-468	-	-	-	basal	(Prat et al., 2010)		L-15	10% FBS			0% CO_2	0.25% trypsin
HCC70	-	-	-	basal	(Prat et al., 2010)		RPMI-1640	10% FBS			5% CO_2	0.25% trypsin
HCC1806	-	-	-	basal	(Riaz et al., 2013)		RPMI-1640	10% FBS			5% CO_2	0.25% trypsin
HCC1187	-	-	-	basal	(Prat et al., 2010)		RPMI-1640	10% FBS			5% CO_2	mixed
BT-20	-	-	-	basal	(Prat et al., 2010)		MEM	10% FBS	NEAA, sodium pyruvate		5% CO_2	0.25% trypsin
SUM149PT	-	-	-	basal	(Prat et al., 2010)		F12	5% FBS	HEPES, 1 µg/mL hydrocortisone, 5 µg/mL human insulin		5% CO_2	0.25% trypsin
HCC1599	-	-	-	basal	(Prat et al., 2010)		RPMI-1640	10% FBS			5% CO_2	suspension

Cell line	Hormone Receptor Status			Subtype	Reference		Cell culture specifications					
	ER	PR	Her2				Basal medium	Additives			Conditions	Passaging
Du4475	-	-	-	other	(Riaz et al., 2013)		RPMI-1640	10% FBS			5% CO_2	suspension
MDA-MB-453	-	-	-	Her2	(Riaz et al., 2013)		L-15	10% FBS			0% CO_2	0.25% trypsin
SKBR3	-	-	+	Her2	(Prat et al., 2013)		DMEM	10% FBS			5% CO_2	0.05% trypsin
BT474	+	+	+	Her2 / luminal	(Prat et al., 2013)		IMDM	10% FBS			5% CO_2	0.25% trypsin
MCF-7	+	+	-	luminal	(Prat et al., 2010)		DMEM	10% FBS			5% CO_2	0.05% trypsin
T-47D	+	+	-	luminal	(Prat et al., 2010)		DMEM	10% FBS			5% CO_2	0.05% trypsin
Hs578Bst				normal	(Hackett et al., 1977)		IMDM	10% FBS			5% CO_2	0.25% trypsin
MCF-10A				normal	(Soule et al., 1990)		DMEM/ F12	5% horse serum	20 ng/mL EGF, 0.5 mg/mL hydrocortisone, 10 µg/mL bovine insulin		5% CO_2	0.05% trypsin

Table 2-2 Primers utilized for qPCR and ChIP.

Gene	Primer		Reference
RARRES1	F	ACGGCTCATCGAGAAAAAGA	(Marcato et al., 2015)
	R	GAAAGCCAAATCCCAGATGA	
ALDH1A1	F	TGTTAGCTGATGCCGACTTG	(Marcato et al., 2011b)
	R	TTCTTAGCCCGCTCAACACT	
ALDH1A2	F	CTGGCAATAGTTCGGCTCTC	
	R	TGATCCTGCAAACACTGCTC	
ALDH1A3	F	TCTCGACAAAGCCCTGAAGT	
	R	TATTCGGCCAAAGCGTATTC	
Reference genes			
GAPDH	F	GGAGTCAACGGATTTGGTCGTA	(Marcato et al., 2015)
	R	TTCTCCATGGTGGTGAAGAC	
B2M	F	AGGCTATCCAGCGTACTCCA	
	R	CGGATGGATGAAACCCAGACA	
ARF1	F	GTGTTCGCCAACAAGCAGG	
	R	CAGTTCCTGTGGCGTAGTGA	
PUM1	F	GGCGTTAGCATGGTGGAGTA	
	R	CATCCCTTGGGCCAAATCCT	
ChIP regions			
RARRES1 region A	F	TGCCCGGCTAATTTTTGTAT	(Peng et al., 2012)
	R	GCTCACGAGGTCAGGAGTTT	
Region B	F	CACTGTGCGAGGCAGATTTA	
	R	AACACTTGCTGCCTCCATTC	
Region C	F	CCAAGCATTAGGGCTGTGAT	
	R	GACTTCTCCCACCTCCACAG	
Region D & CTCF response element	F	CACTCCTTTTCCACGTTTCC	
	R	ATGCCGCATCCTAGCACTAA	
RARα response element	F	TTGGTCTGGGTTTCTGATTCTT	
	R	CTCAATCTTGTGTGTGCTTGTG	

2.2.4 *Cell Proliferation Analyses*

Cells were seeded in 6 well plates at 2.5×10^4 cells/well. Cells were counted 24 h after seeding and 144 h after seeding. Data was normalized to the number of cells at 24 h, and proliferation was determined relative to the scramble shRNA.

2.2.5 *Tumor Tissue Histological Analysis by Immunofluorescence Microscopy*

Formalin-fixed and paraffin embedded breast cancer patient tumor core biopsy tissue were taken post-surgery from consenting patients who were diagnosed with breast cancer at the Queen Elizabeth II Health Sciences Centre (QEII HSC) in Halifax, NS, Canada between 2007 and 2014. Standard pathological assessments of patient tumors were performed by staff pathologists at the QEII HSC (Table 2-3). Sequential sections were stained with anti-ALDH1A3 (Abgent) and anti-RARRES1 (Abcam, ab92884) and species-specific secondary antibodies, conjugated to either Cy2 or Cy3 (Jackson Immunoresearch) and nuclear stain ToPro3 (Invitrogen). Images were captured with a Zeiss LSM 510 laser scanning confocal microscope and quantified as previously described (Marcato et al., 2011).

2.2.6 *RARRES1 Immunohistochemical Staining for Localization*

MDA-MB-468 and SUM149 cells were seeded at approximately 35% confluency onto poly-L-lysine coated coverslips, in 12 well plates. After 24 h, the coverslips were fixed in 3% paraformaldehyde, and permeabilized with 0.1% Triton-X-100 in PBS. Following permeabilization the cells were blocked with 1% bovine serum albumin (BSA) and then incubated overnight with 1/500 dilution of primary antibodies: monoclonal mouse anti-RARRES1 (Abcam, ab92884), monoclonal rabbit anti-PDI (Covance, PRB-114P), and polyclonal rabbit anti-giantin (Abcam, ab31811). Coverslips were stained

with species-specific Alexafluor 488nm or Cy3 conjugated secondary antibodies (Jackson Immunoresearch) and ToPro3 (ThermoFisher). Mounted coverslips were imaged with the Zeiss 510 Laser Scanning Confocal Microscope, using the Zen 2012 software. Images of MDA-MB-468 cells were captured under a 40x oil immersion objective lens, with a 10x optical lens, for a total magnification of 400x. Images of SUM149 cells were captured under a 63x oil immersion objective lens, with a 10x optical lens, for a total magnification of 630x. Quantitative image analysis was done using ImageJ (Fiji). The Colocalization Threshold plugin was used to determine the tM1 coefficient (a value from 0 to 1) using the Costes' method (red channel overlapping with green) (Costes et al., 2004). Each image was analysed using the Colocalization Threshold plugin to determine the Costes coefficient. The 5 technical replicates per slide and three experimental replicates were averaged.

2.2.7 *Tumor Xenograft Studies*

Eight-to-ten-week-old NOD-*scid* mice were injected orthotopically in the mammary fat pad with 2×10^6 MDA-MB-231 or MDA-MB-468 cells (vector control and RARRES1 shRNA clones). Injected cells were mixed 1:1 with high-concentration Matrigel (BD Biosciences). Primary tumor growth was quantified (mm^3, length × width × depth × 0.5) and modeled using a quadratic non-linear regression and compared with an extra sum-of-squares F test.

Table 2-3 Patient cohort details.

Sample details		**Sample size (n)**
ER status	Positive	52
	Negative	10
PR status	Positive	47
	Negative	15
HER2 status	Positive	11
	Negative	48
	Not determined	3
Stage	I	12
	IIA	22
	IIB	11
	IIIA	8
	IIIB	4
	IIIC	3
	IV	2
Lymphovascular Invasion	Present	33

2.2.8 *Methylation Profiling*

DNA was collected from untreated and DAC-treated cells using the PureLink DNA kit (Invitrogen). Methylation analyses using the HM450 array (Illumina) was performed by The Centre for Applied Genomics at the Hospital for Sick Children (Toronto, Ontario, Canada) including bisulfite conversion, hybridization, background subtraction, and normalization (Geo Series Accession #GSE78875). β-values for Illumina probes near RARRES1 were extracted from the data, and locations determined relative to the protein-coding regions.

2.2.9 *cBioportal Data Analysis*

Data from TCGA (Ciriello et al., 2015; Network, 2012) were analyzed with cBioportal (Cerami et al., 2012; Gao et al., 2013) or extracted from the TCGA Data Portal as indicated.

2.2.10 *Chromatin Immunoprecipitation*

ChIP assays (Crane-Robinson et al., 1999) were performed following the ChIP assay kit protocol (cat#06-599, Upstate Biotechnology) as previously described (Weaver et al., 2014) using antibodies against 5-mC (cat#BI-MECY-0500, AnaSpec, Inc.), RARα (cat#ab41934, Abcam), CTCF (cat#07-729, Millipore) as well as the control normal rabbit IgG (cat#sc-2027, Santa Cruz Biotechnology). After dissociating the DNA-protein complexes, pulled-down DNA along with the input DNA (devoid of antibody) was subject to qPCR analysis with primers to interrogate the RARRES1 promoter (Table 2-2). Results are expressed as the amount of DNA detected in the immunoprecipitated fraction minus the amount of DNA detected in the nonimmune IgG (negative control) fraction normalized to the input DNA. For sequential ChIP (ChIP–reChIP) experiments, the

protein bound to the beads with the first antibody was incubated (30 min, 37°C) twice with DTT (20 mM) and the combined elutes were suspended in ChIP dilution buffer, which was then immunoprecipitated (14 h, 4°C) with the second antibody.

2.2.11 *Protein Analyses and Mass Spectrometry*

Western blotting was used to detect changes in AXL expression (R&D, cat#AF154, 1/300) and detyrosinated tubulin (tubulinEE, AbD serotec, cat#obt1660, 1/1000; α-tubulin, Sigma-Aldrich, cat#T9026-DM1A, 1/1000).

For mass spectrometry, preparation of lysates, protein digestion, and peptide labelling were performed as previously described (Erickson et al., 2015). Labelled and mixed peptides were fractionated into 12 fractions using basic pH reverse-phase HPLC on a monolithic (100 mm × 4.6 mm) reversed phase column (Phenomenex). Fractions were analyzed using 3 hr gradients from 0-40% acetonitrile (0.1% formic acid) on an Orbitrap Velos Pro mass spectrometer (Thermo-Fisher) using MS3 acquisition as described (Ting et al., 2011). All mass spectrometry data were processed as previously described (Murphy et al., 2014).

2.2.12 *Statistical Analyses*

All statistical analyses were calculated in GraphPad Prism 6 unless indicated otherwise. Paired t-tests were used to compare two treatments, one-way ANOVA was used for multiple treatments. Unpaired t-tests were used to compare groups of cell lines or mice. For all comparisons, * $p < 0.05$, ** $p < 0.01$, *** $p < 0.001$.

2.3 RESULTS

2.3.1 *BASAL-LIKE BREAST CANCER TUMORS EXPRESS HIGHER LEVELS OF RARRES1*

To investigate if RARRES1 represents a gene that is differentially expressed in the molecular subtypes of breast cancer, we obtained data from the 2012 TCGA breast cancer data set (The Cancer Genome Atlas Network, 2012) using the cBioportal interface (Cerami et al., 2012; J. Gao et al., 2013). The arrangement of RARRES1 expression in individual tumors allowed us to identify that ER^-, PR^- and HER2-negative status was associated with higher RARRES1 expression. Additionally, the data set was examined for PAM50 subtype which allowed separation into the luminal A/B, HER2-enriched, and basal-like subtypes based on expression of 50 genes (PAM50 classification does not include the claudin-low subtype). High expression of RARRES1 was associated with the basal-like subtype (Figure 2-1A).

Since TNBCs are primarily basal-like (50% of TNBCs) (Prat and Perou, 2011), we expected that RARRES1 would also be higher in TNBC tumors. We separated the 2015 TCGA data set (Ciriello et al., 2015) using the cBioportal interface for TNBC and non-TNBC tumors. RARRES1 expression was significantly higher in the TNBC tumors (Figure 2-1B). From this data analysis, it is unclear how many of the high RARRES1-expressing TNBC are claudin-low (approximately 30% of TNBC are claudin-low) (Prat and Perou, 2011), and if the association of RARRES1 with TNBCs is specific to either the basal-like or claudin-low subtype.

Figure 2-1 RARRES1 is highly expressed in triple-negative breast cancer.

A. Expression of RARRES1 mRNA was obtained from cBioportal (The Cancer Genome Atlas Network, 2012) and plotted by patient in ascending order with corresponding ER / HER2 / PR status, mutation status, and PAM50 subtype. Samples without mRNA expression data are listed separately. **B.** Expression of RARRES1 mRNA was obtained from cBioportal (Ciriello et al., 2015) and plotted by TNBC / non-TNBC.

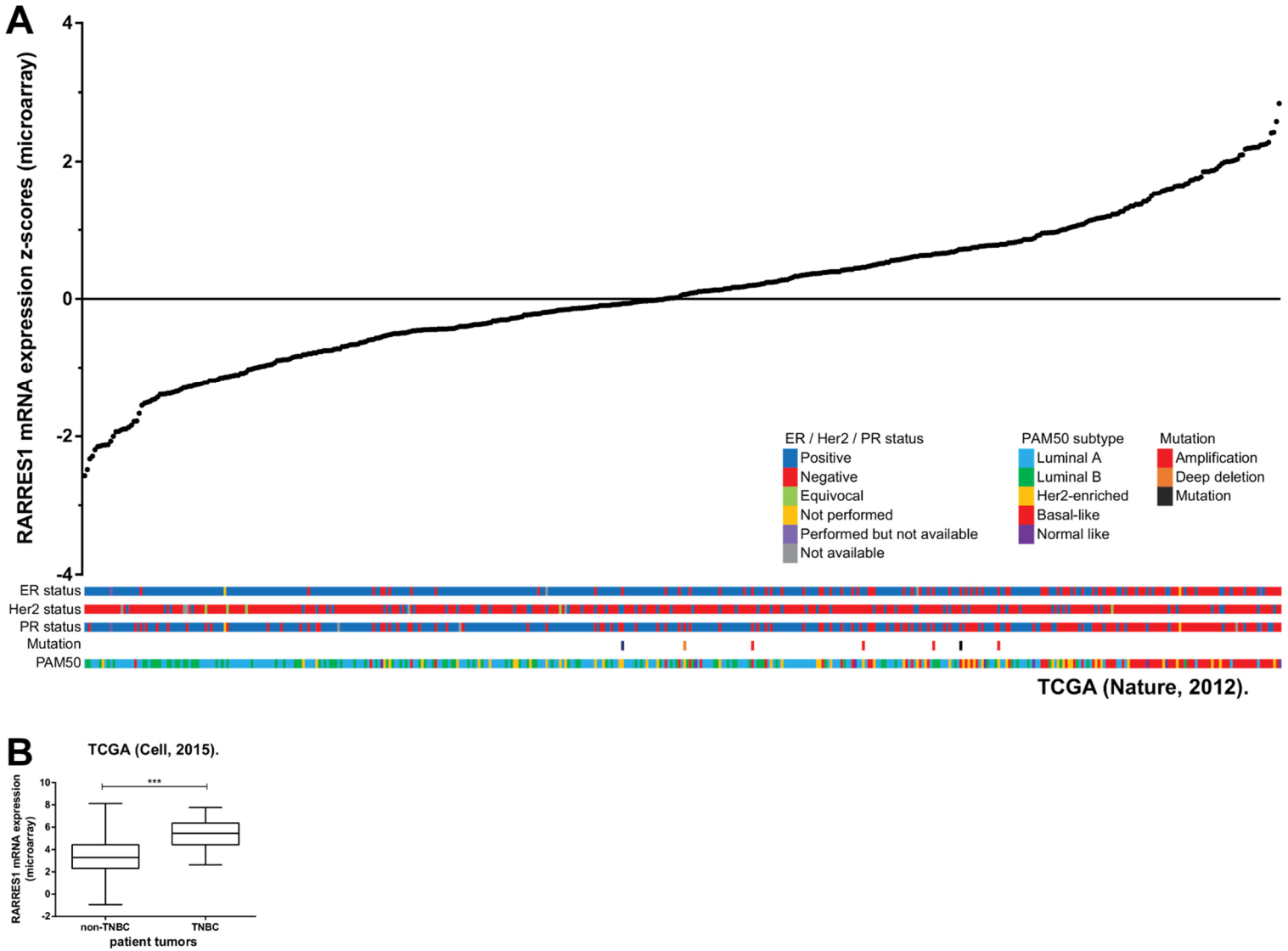

Figure 2-1 RARRES1 is highly expressed in triple-negative breast cancer.

To answer this question and validate these findings, we selected 24 cell lines which have been previously characterized as claudin-low, basal-like, HER2-like, luminal, or other (Table 2-1), as well as two normal immortalized breast cell lines (Hs78Bst and MCF-10A). This series includes 20 TNBC cell lines, with representation of both claudin-low and basal-like TNBCs, and would allow us to confirm that RARRES1 expression is associated with TNBC and if it is specific to the claudin-low or basal-like subtypes. Analysis of existing cell-line databases revealed no known mutations in RARRES1 (Barretina et al., 2012; Forbes et al., 2015), which is consistent with the low frequency of mutations in patient tumors observed in Figure 2-1. We quantified RARRES1 expression in these cell lines by quantitative PCR (qPCR, Figure 2-2A). RARRES1 was detected in all but four cell lines (SUM159, SUM1315, HCC1806, and MCF10A). While the number of HER2-like, luminal, and normal breast cell lines prohibited robust statistical analysis, the cell line data mirrored the patient data and we determined that basal-like cell lines had significantly higher mRNA expression of RARRES1 than the claudin-low cell lines (Figure 2-2B). We also identified significant variability of RARRES1 expression within the basal-like cell lines, which may reflect the heterogeneity known to exist within this breast cancer subtype (Metzger-Filho et al., 2012). Taken together, our data suggest that high expression of RARRES1 in TNBCs is predominantly due to the high expression of RARRES1 in the basal-like subtype. This prompted our focus on TNBCs in the following functional assays.

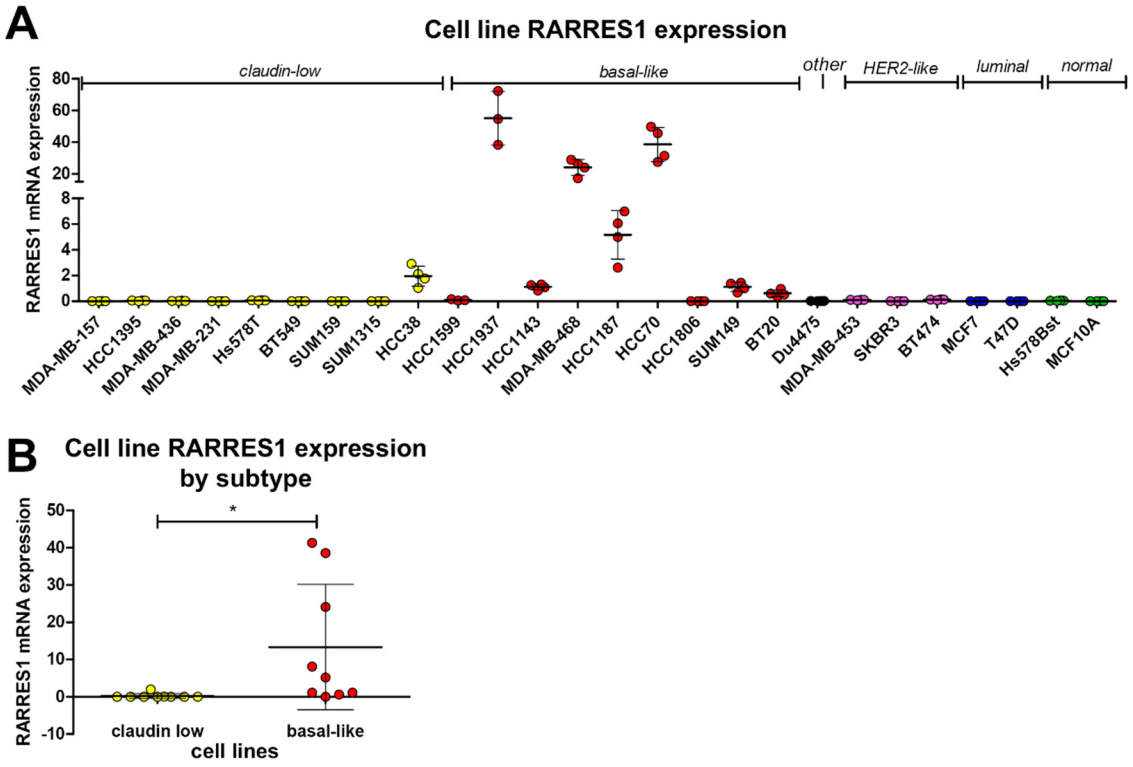

Figure 2-2 RARRES1 is highly expressed in basal-like cell lines.

A. RARRES1 expression in 24 cancerous and 2 normal breast cell lines was determined by qPCR. **B.** the mean value from each claudin low and basal-like cell line were plotted and compared by a student's t-test (* $p < 0.05$). (Subtypes: yellow, claudin-low; red, basal-like; black, other; pink, HER2-like; blue, luminal; green, normal.)

2.3.2 *RARRES1 Exhibits Tumor Suppressive Effects in TNBC*

RARRES1 has been reported to have tumor suppressor function in a number of cancer types (Jing et al., 2002). These are in contrast to a functional study in the rare inflammatory subtype of breast cancer (representing less than 5% of all breast cancers), where RARRES1 was oncogenic (Wang et al., 2013). Furthermore, given these prior reports of both tumor suppressing and oncogenic effects of RARRES1, we considered if RARRES1 expression in a breast cancer subtype influences its function. We generated pooled lentiviral-based shRNA knockdowns of RARRES1 in claudin-low MDA-MB-231 cells, and basal-like MDA-MB-468 and HCC1937 cells. These had reduced mRNA and protein expression of RARRES1 (Figure 2-3). Next, using an *in vitro* proliferation analysis, we determined that knockdown of RARRES1 with shRNA 1 increased *in vitro* proliferation in claudin-low MDA-MB-231 cells, and basal-like MDA-MB-468 and HCC1937 cells (Figure 2-4A). These results were confirmed using shRNA 2 in MDA-MB-231 and MDA-MB-468 cells. Additionally, the cell proliferation experiments agreed with tumor growth studies. Tumor volume (Figure 2-4B) and weight (Figure 2-4C) of mammary fat pad-implanted MDA-MB-231 and MDA-MB-468 cells were significantly increased upon knockdown of RARRES1. The increased tumor burden did not result in increased pulmonary metastasis (MDA-MB-231, Figure 2-4D; MDA-MB-468, non-metastatic and metastasis not measured). Together, these results suggest that RARRES1 has a tumor suppressing role in TNBC regardless of molecular subtype.

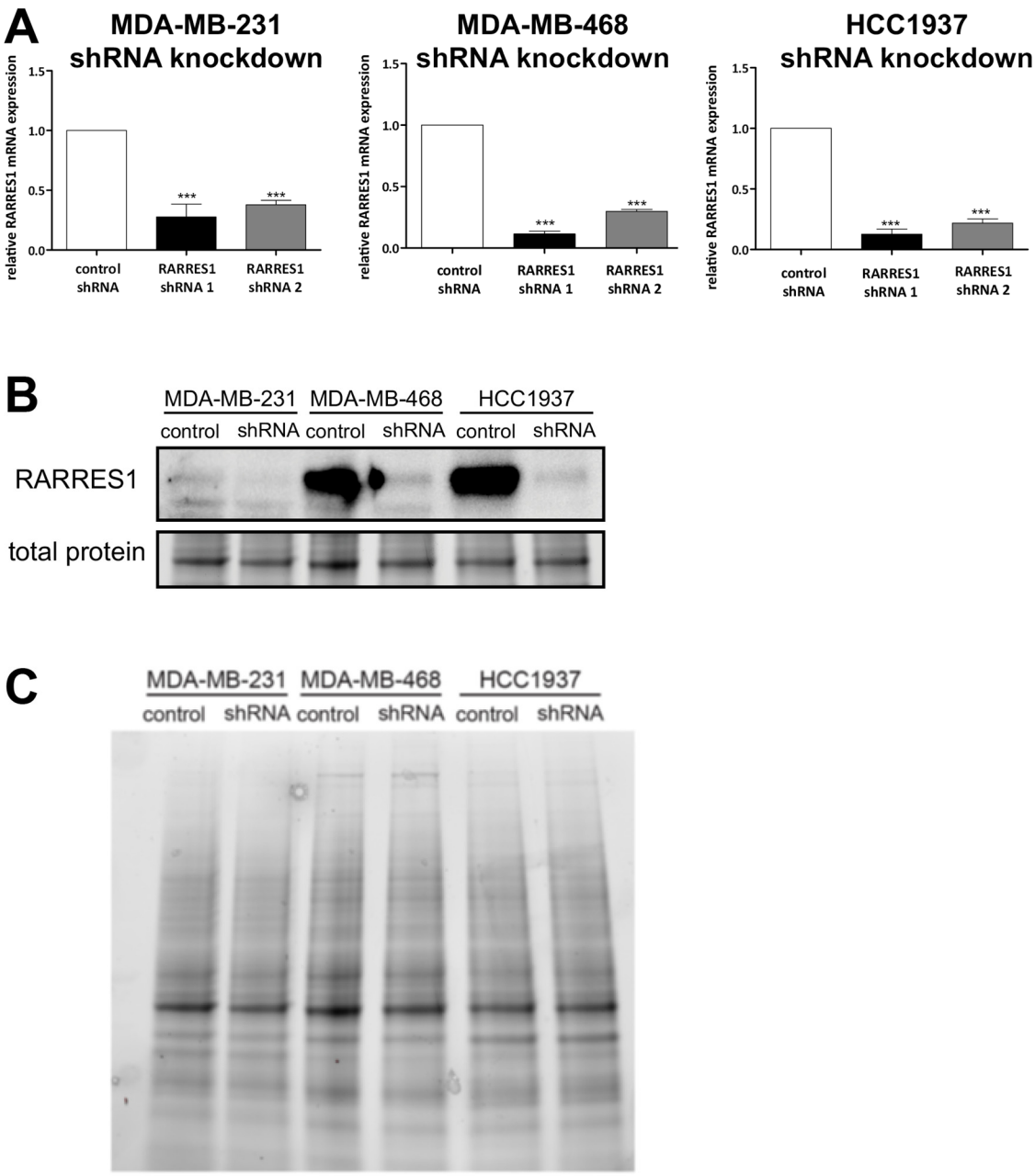

Figure 2-3 shRNA knockdown of RARRES1 decreases mRNA and protein expression.

shRNA knockdowns of MDA-MB-231, MDA-MB-468 and HCC1937 were verified by **A.** qPCR and **B.** Western blot. **C.** Total protein staining demonstrates similar amounts of loaded protein. mRNA expression was compared to scramble shRNA by one-way ANOVA, *** $p < 0.001$.

Figure 2-4 RARRES1 knockdown increases *in vitro* and *in vivo* cell proliferation.

A. The effect of RARRES1 knockdown on *in vitro* cell proliferation as compared to the scramble shRNA (by paired student's t-test). **B.** Effect of RARRES1 knockdown on tumor volume was quantified in MDA-MB-231 and MDA-MB-468 cells implanted into NOD-*scid* female mice. Tumor growth was modeled using a non-linear (exponential) regression and compared by extra-sum-of-squares F test. **C.** Xenografts isolated from MDA-MB-231 and MDA-MB-468 tumor-bearing mice were weighed and compared by a student's T test. **D.** Lungs were harvested from tumor-bearing mice, formalin-fixed and paraffin-embedded and 5 μm thin sections generated for metastasis visualization by haematoxylin and eosin (H&E) staining. Metastasis quantification of each lung were performed blinded using a standardized grid imposed on Axiocam HRC. Color images captured of at least two random H&E-stained thin sections/tissue. Percentage of metastatic lung tissue was calculated by dividing metastatic grid cell counts by the entire tissue grid cell counts. For all statistical comparisons, * $p < 0.05$, ** $p < 0.01$, *** $p < 0.001$.

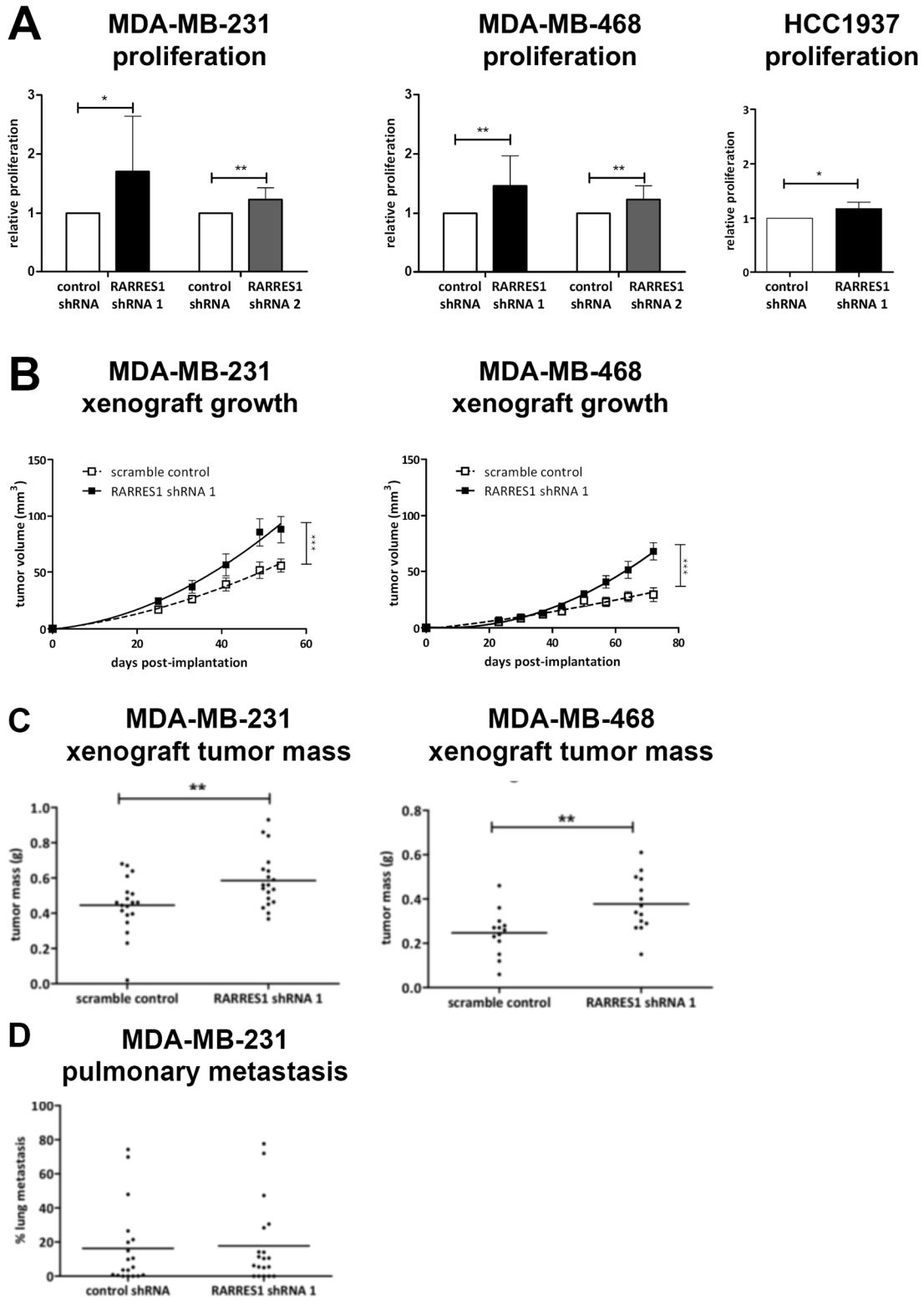

Figure 2-4 RARRES1 knockdown increases *in vitro* and *in vivo* cell proliferation.

2.3.3 *Functional Analysis of RARRES1*

Our finding that RARRES1 has tumor suppressive effects in TNBC regardless of subtype differs from previous findings which suggested that RARRES1 is oncogenic in inflammatory breast cancer (Wang et al., 2013). To attempt to rectify this discrepancy, we first investigated expression of the receptor-tyrosine kinase, AXL, which has been implicated in the oncogenic role of RARRES1. We expected that AXL expression would not be affected in MDA-MB-231 and MDA-MB-468 cells as this mechanism was associated with oncogenic RARRES1. We found no difference in AXL expression following RARRES1 knockdown (Figure 2-5A). This is consistent with previous findings that AXL stabilization is an oncogenic mechanism for RARRES1 (Wang et al., 2013), and with our own findings that RARRES1 is tumor suppressive in TNBC.

Alternatively, in cells of mesenchymal origin, RARRES1 is functionally involved in the tyrosination of α-tubulin (Sahab et al., 2011). We found a modest decrease in the level of detyrosinated α-tubulin when RARRES1 was depleted (Figure 2-5B). To determine if this affected tubulin stability, we investigated if knockdown of RARRES1 affected the sensitivity of MDA-MB-231 and MDA-MB-468 to paclitaxel, which stabilizes microtubules and prevents disassembly. We found no differences in the response of the scramble shRNA-bearing and the RARRES1 shRNA-bearing cells (Figure 2-5C). Therefore, at least in cells of basal-like origin, RARRES1 function appears independent of tubulin stability.

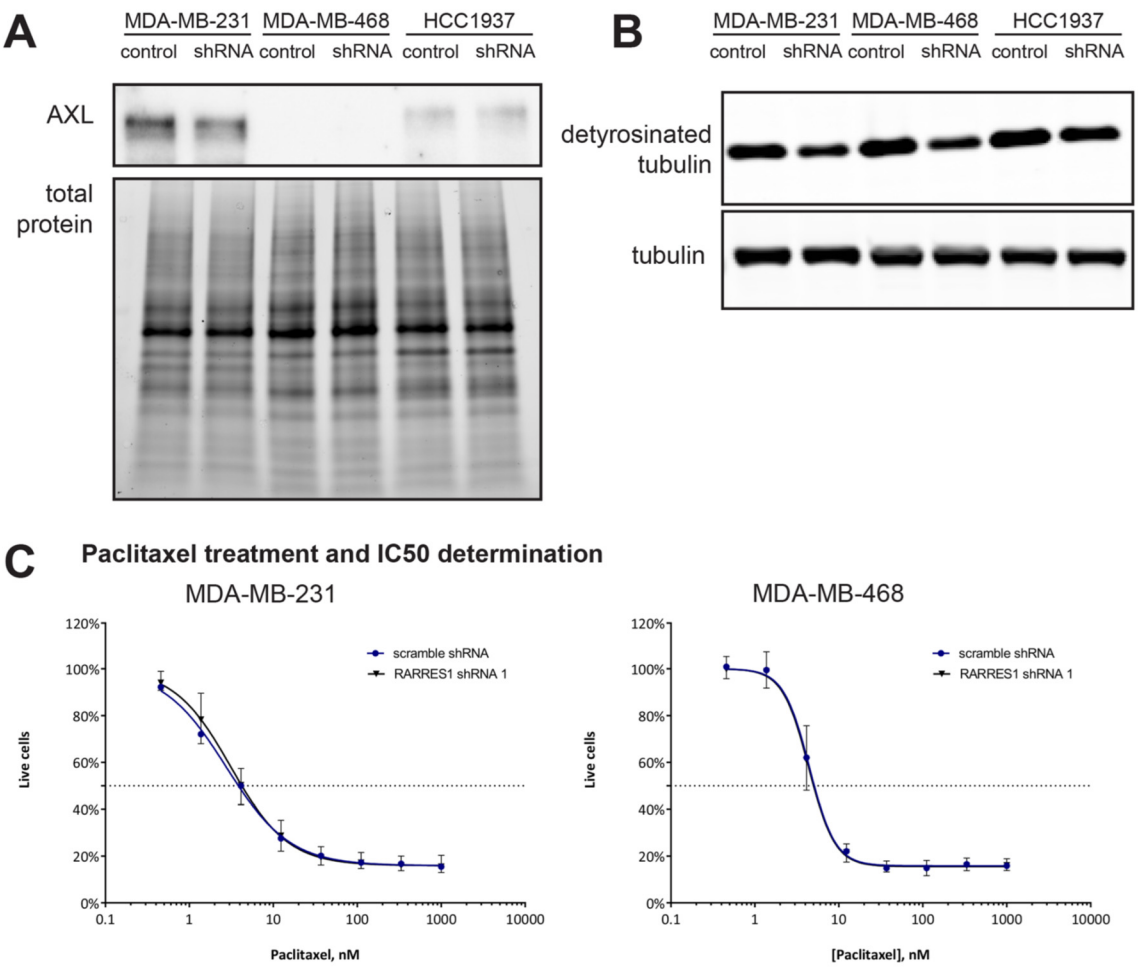

Figure 2-5 The tumor suppressive function of RARRES1 is not related to AXL expression or tubulin tyrosination.

RARRES1 knockdown cells in MDA-MB-231, MDA-MB-468, and HCC1937 cells were examined for **A.** AXL expression; and **B.** detyrosinated tubulin via Western blot. A representative image is presented, n=3. **C.** MDA-MB-231 and MDA-MB-468 scramble control and RARRES1 shRNA-bearing cells were treated with varying amounts of paclitaxel and the IC50 was determined (n=3).

The lack of changes to AXL and tubulin stability suggested the existence of other mechanisms by which RARRES1 acts as a tumor suppressor in TNBC. We performed proteomic analyses with tandem mass tag (TMT) mass spectrometry using the three TNBC cell lines where RARRES1 suppresses cell proliferation and tumor growth (MDA-MB-231, MDA-MB-468, and HCC1937, as in Figure 2-4) to identify functional effects and associations. RARRES1 peptide expression was 3.15-fold higher in HCC1937 cells compared to MDA-MB-468 cells, which is consistent with our qPCR analysis (2.29-fold, Figure 2-2A).We first identified those genes which were consistently regulated between cell lines (Figure 2-6). Fifteen genes are either consistently up- or down-regulated in all three cell lines. We used genes up- or down-regulated in at least two of the three cell lines (as in Figure 2-7) to generate a STRING (Szklarczyk et al., 2015) network (Figure 2-8A). Notably, we identified SUMO2 at the center of the network. SUMO2 is downregulated in both MDA-MB-468 and HCC1937 (see Figure 2-7). SUMO2 is a small ubiquitin-like modifier which is often bound to target proteins to influence a variety of cellular processes. This supports previous findings in which RARRES1 expression was associated with SUMO2 expression in HCT116 colon cancer cells (Wu et al., 2011). In a DAVID analysis (D. W. Huang et al., 2009a, 2009b), we identified those Gene Ontology Biological Processes enriched in at least two of the three cell lines (Figure 2-8B). RARRES1 appears to affect metabolism, nucleic acid processing, and post-translational processes; however, these biological processes were not consistently identified.

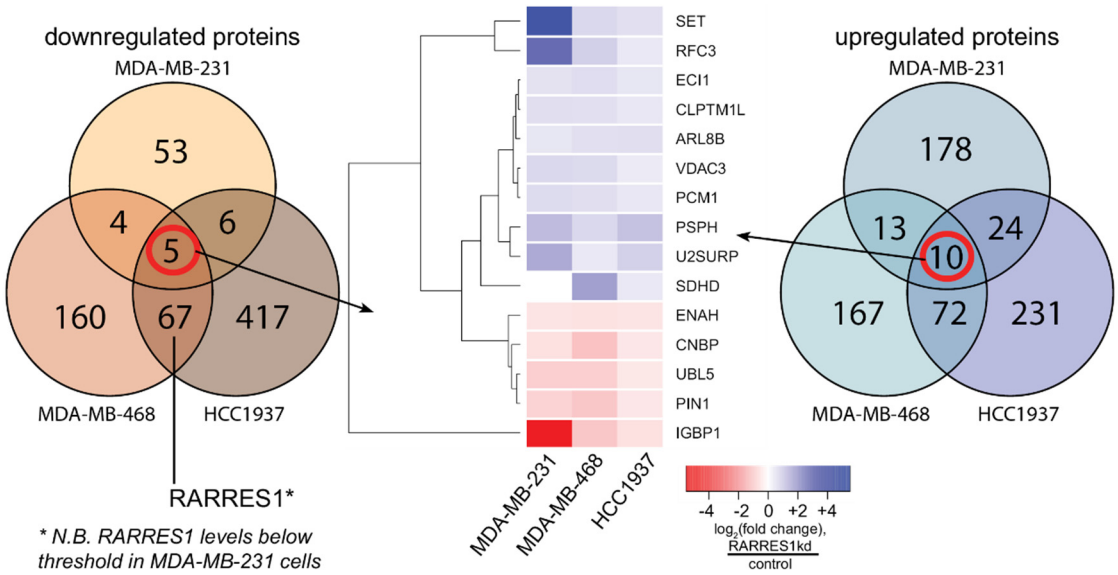

Figure 2-6 RARRES1 regulates hundreds of proteins corresponding to diverse cellular processes.

The effect of RARRES1 knockdown compared to scramble control on the proteome was quantified in MDA-MB-231, MDA-MB-468, and HCC1937 cells by tandem mass tag mass spectrometry of cell lysates, allowing for the detected relative protein changes. We determined a threshold for protein expression and excluded all proteins where all samples fell below the threshold. Proteins with a log2(fold change) > 0.379 were classified as upregulated and < -0.515 were classified as downregulated. Upregulated and downregulated proteins visualized using a Venn diagram; 15 consistently regulated proteins were clustered using heatmap.2 (gplots, R).

Figure 2-7 Knockdown of RARRES1 affecting expression of proteins in two of the three cell lines.

All proteins upregulated or downregulated in at least two cell lines (as described in Figure 4) were clustered using the heatmap.2 function (gplots, R).

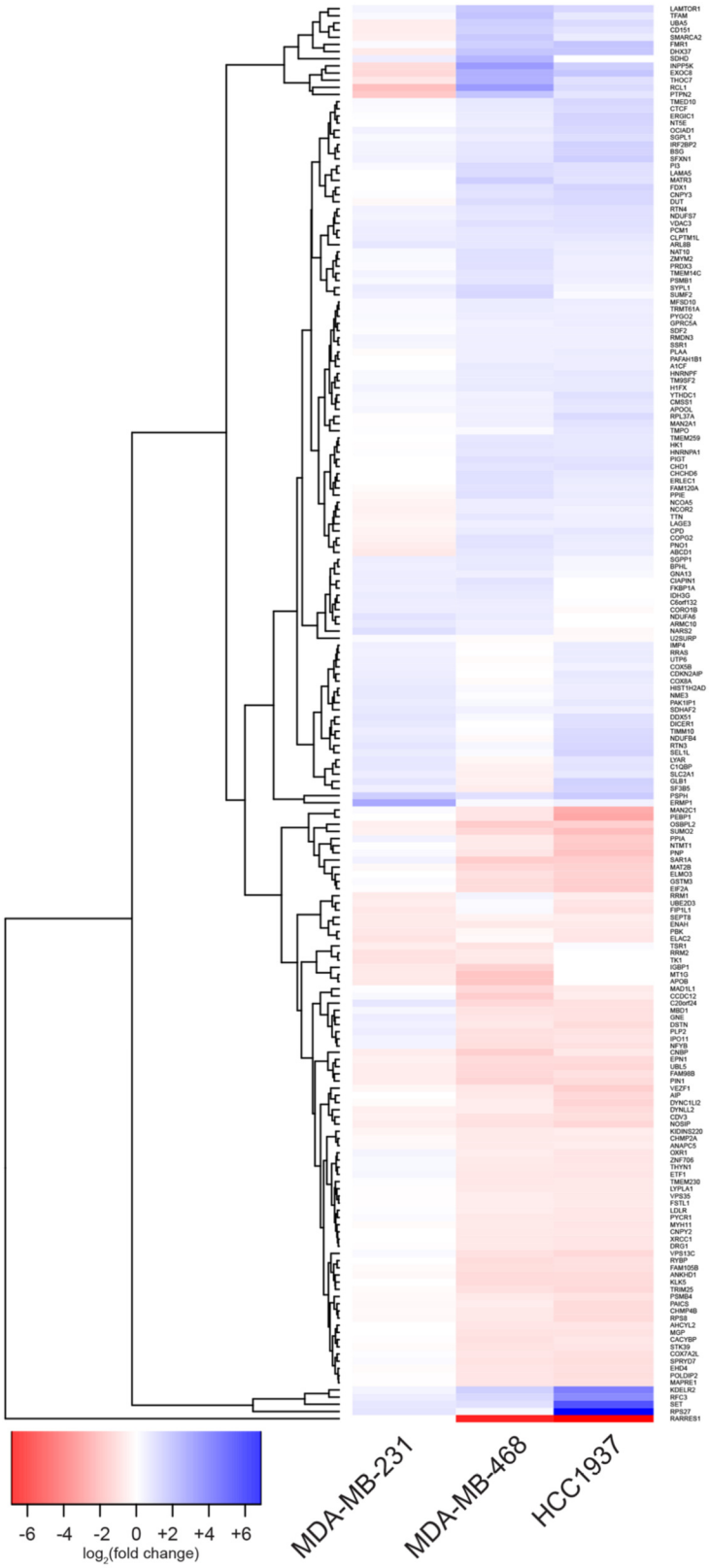

Figure 2-7 Knockdown of RARRES1 affecting expression of proteins in two of the three cell lines.

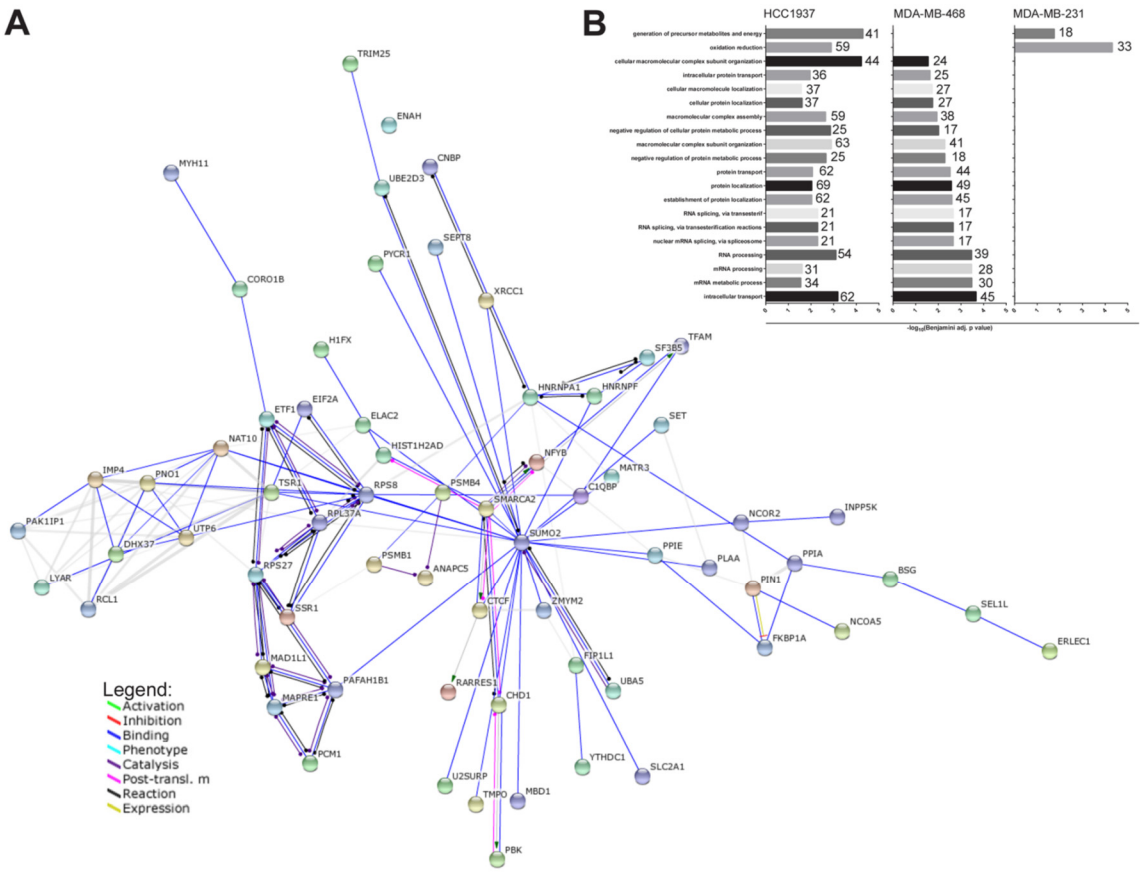

Figure 2-8 Knockdown of RARRES1 affects a complex network of proteins represented in numerous pathways.

A. Proteins upregulated (log2(fold change) > 0.379) or downregulated (log2(fold change) < -0.515), in at least two of three cell lines following RARRES1 knockdown, were input into STRING. Proteins which were not connected to the displayed central network by evidence-based interactions were removed. **B.** All proteins upregulated or downregulated in each cell line were input into DAVID. Any Gene Ontology Biological Processes (GO BP) which were enriched (Benjamini adjusted p-value < 0.05) are displayed with the corresponding number of hits represented.

To determine if the cellular localization of RARRES1 is consistent with its potential roles as suggested by the network analyses of the proteomic data, we performed confocal immunofluorescence. We examined whether RARRES1 colocalized with the endoplasmic reticulum marker, protein disulfide isomerase (PDI, Figure 2-9A), with a Golgi apparatus marker, giantin (Figure 2-9B) or with a nuclear ToPro 3 stain. Notably, RARRES1 was predominately absent from the nucleus (as seen in Figure 2-9A and Figure 2-9B), however; we observed a significant colocalization with PDI when compared to giantin as determined by the Costes coefficient (Figure 2-9C), suggesting that RARRES1 primarily localizes to the endoplasmic reticulum. The predominant localization of RARRES1 in the endoplasmic reticulum is consistent with its function in post-translational processes and metabolism as indicated by the DAVID and STRING analyses of the mass spectrometry-identified proteins.

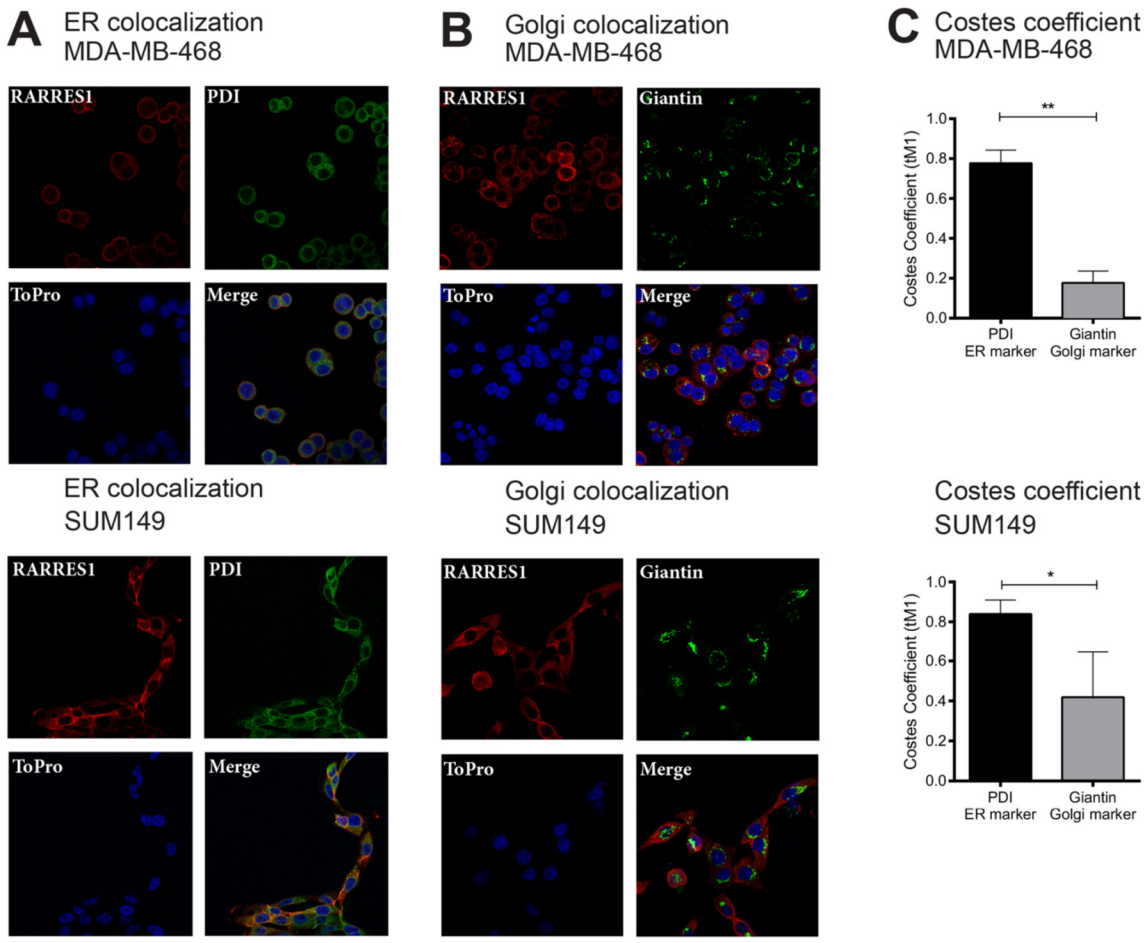

Figure 2-9 RARRES1 is localized to the endoplasmic reticulum in MDA-MB-468 and SUM149.

Representative images from immunofluorescence and confocal microscopy of **A.** RARRES1 and endoplasmic reticulum (ER) colocalization using PDI; and **B.** RARRES1 and Golgi apparatus colocalization using giantin in both MDA-MB-468 and SUM149. **C.** The Costes coefficient (a measure of colocalization) was calculated in both cell lines for RARRES1 with PDI and with giantin. These were compared by paired t-tests (* $p < 0.05$, ** $p < 0.01$).

2.3.4 *RARRES1 is Hypomethylated in Basal-Like Breast Cancers in the Context of Genome-Wide Hypermethylation*

We then investigated the possible mechanisms for the differential expression of RARRES1 across the breast cancer subtypes. Mutations did not appear to contribute significantly to RARRES1 expression (Figure 2-1), suggesting epigenetic (e.g. DNA methylation) and other transcriptional mechanisms as likely contributors.

We performed Illumina HumanMethylation450 bead chip (HM450) arrays for 26 cell lines and submitted this data to NCBI (Geo Series Accession #GSE78875). The β-values of all claudin-low cell lines (n=9) and all basal-like cell lines (n=9) were averaged and the frequency of these values were plotted (Figure 2-10A). The distribution of methylation in these breast cancer subtypes were significantly different, suggesting higher overall methylation in the basal-like cell lines (Figure 2-10B). Consistent with the overall higher methylation of the basal-like cell lines, basal-like tumors (n=81) had significantly higher levels of maintenance methyltransferase DNMT1 and *de novo* DNMT3B than the claudin-low tumors (n=8) (Figure 2-10C). Furthermore, the methylation of RARRES1 at cg08977270 was only weakly negatively correlated with levels of DNMT1 (r=-0.2933), or the *de novo* methyltransferases DNMT3A (r=-0.05230) and DNMT3B (r=-0.3821) (Figure 2-10D, N=220), in the 2015 TCGA data set (Ciriello et al., 2015).Therefore, the increased expression of RARRES1 in basal-like tumors is not due to overall greater hypomethylation of basal-like cancers, and suggests an alternative hypothesis – the specific hypomethylation of RARRES1 in basal-like breast cancer.

Figure 2-10 Basal-like breast cancer is more highly methylated than claudin-low breast cancer.

The HumanMethylation450 β-values were averaged for all claudin-low and all basal-like cell lines and are plotted **A.** as a histogram, and **B.** as a boxplot (compared by a Mann-Whitney test). **C.** Utilizing the 2015 TCGA breast cancer data set accessed via cBioportal (Ciriello et al., 2015), the expression of DNMT1, 3A and 3B was compared between basal-like and claudin-low patient tumors. **D.** RARRES1 methylation is plotted against DNMT 1, 3A, and 3B expression and linear correlation calculated. For all comparisons, * $p < 0.05$, *** $p < 0.001$, *n.s.* not significant.

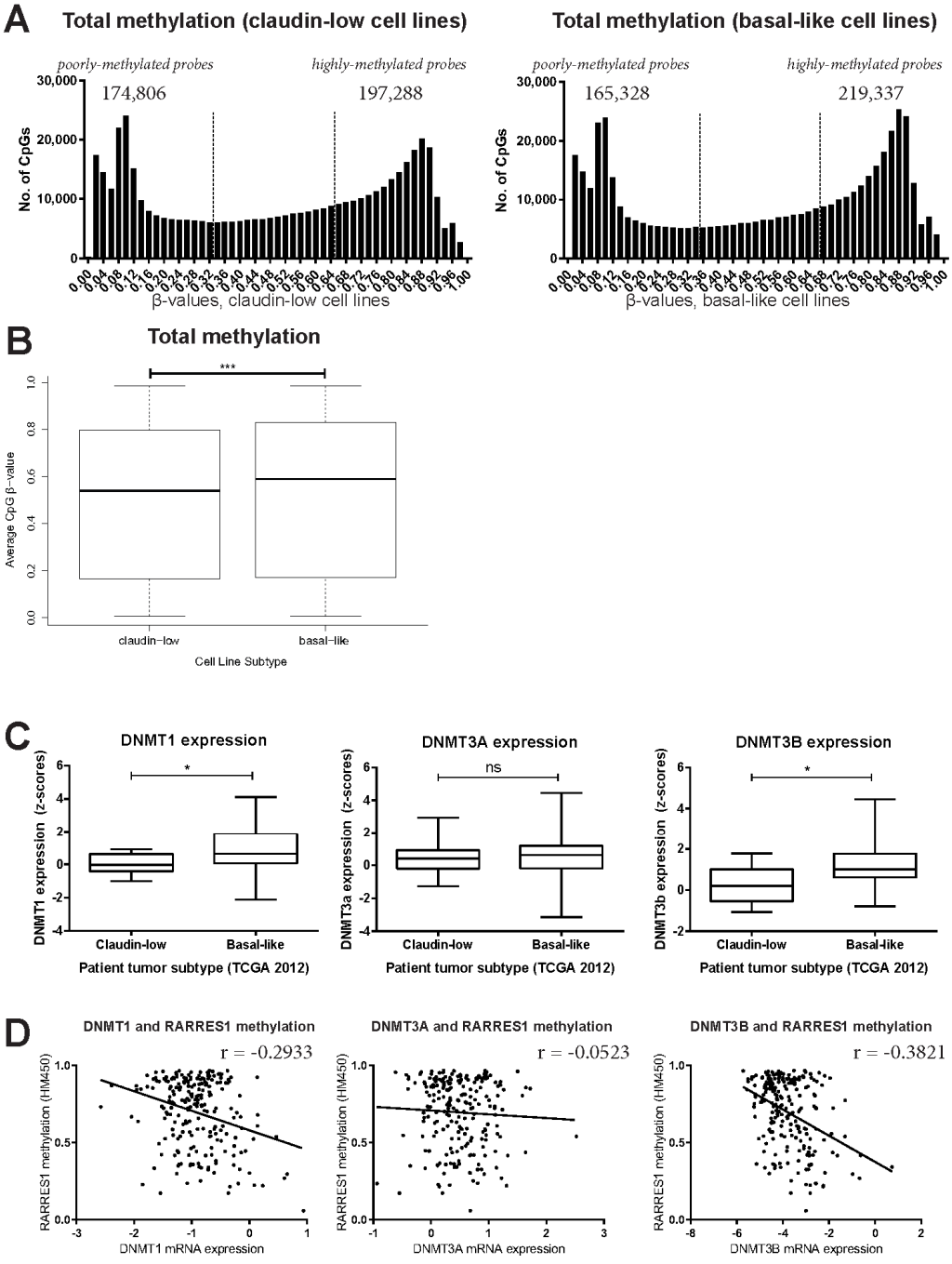

Figure 2-10 Basal-like breast cancer is more highly methylated than claudin-low breast cancer.

2.3.5 *Methylation Contributes to Differential Subtype-Specific RARRES1 Expression*

Having hypothesized subtype-specific hypomethylation of RARRES1, we determined if we could restore expression of RARRES1 in cell lines with low expression by treating the 26 cell lines described earlier with the demethylating agent decitabine (Stresemann and Lyko, 2008). qPCR illustrated that decitabine treatment restored RARRES1 in the luminal, HER-2-like and the majority of claudin-low cell lines, consistent with the hypermethylation of RARRES1 in these subtypes (Figure 2-11A). In contrast, expression of RARRES1 was decreased in basal-like cell lines, which is consistent with hypomethylation of RARRES1 in the basal-like subtype. The notable exceptions to this pattern were two basal-like cell lines HCC1599 and HCC1806, suggesting that they are hypermethylated (consistent with their low expression in Figure 2-2A); and the claudin-low cell line HCC38 (consistent with its high expression of RARRES1 as in Figure 2-2A). This pattern is consistent with the specific hypomethylation of RARRES1 in basal-like breast cancer.

Figure 2-11 RARRES1 is hypomethylated in basal-like breast cancer.

A. The panel of 24 cancerous and 2 normal breast cell lines were treated with 1 μM decitabine, and RARRES1 expression was measured by qPCR; data was compared by a paired student's t-test. (Subtypes: yellow, claudin-low; red, basal-like; black, other; pink, HER2-like; blue, luminal; green, normal.) **B.** The locations of the HumanMethylation450 (HM450) Illumina probes and the regions used for 5-methylcytosine ChIP are plotted in relation to the RARRES1 TSS and exons. **C.** Correlations between the β-value at each HM450 site and mRNA expression of RARRES1 within the TCGA data (The Cancer Genome Atlas Network, 2012) and HM450 cell line data are summarized by site. **D.** RARRES1 expression for each of 220 breast cancer samples and the 26 breast cell lines is plotted relative to the Illumina HM450 β-value at site 1. For all statistical comparisons, * $p < 0.05$, ** $p < 0.01$, *** $p < 0.001$.

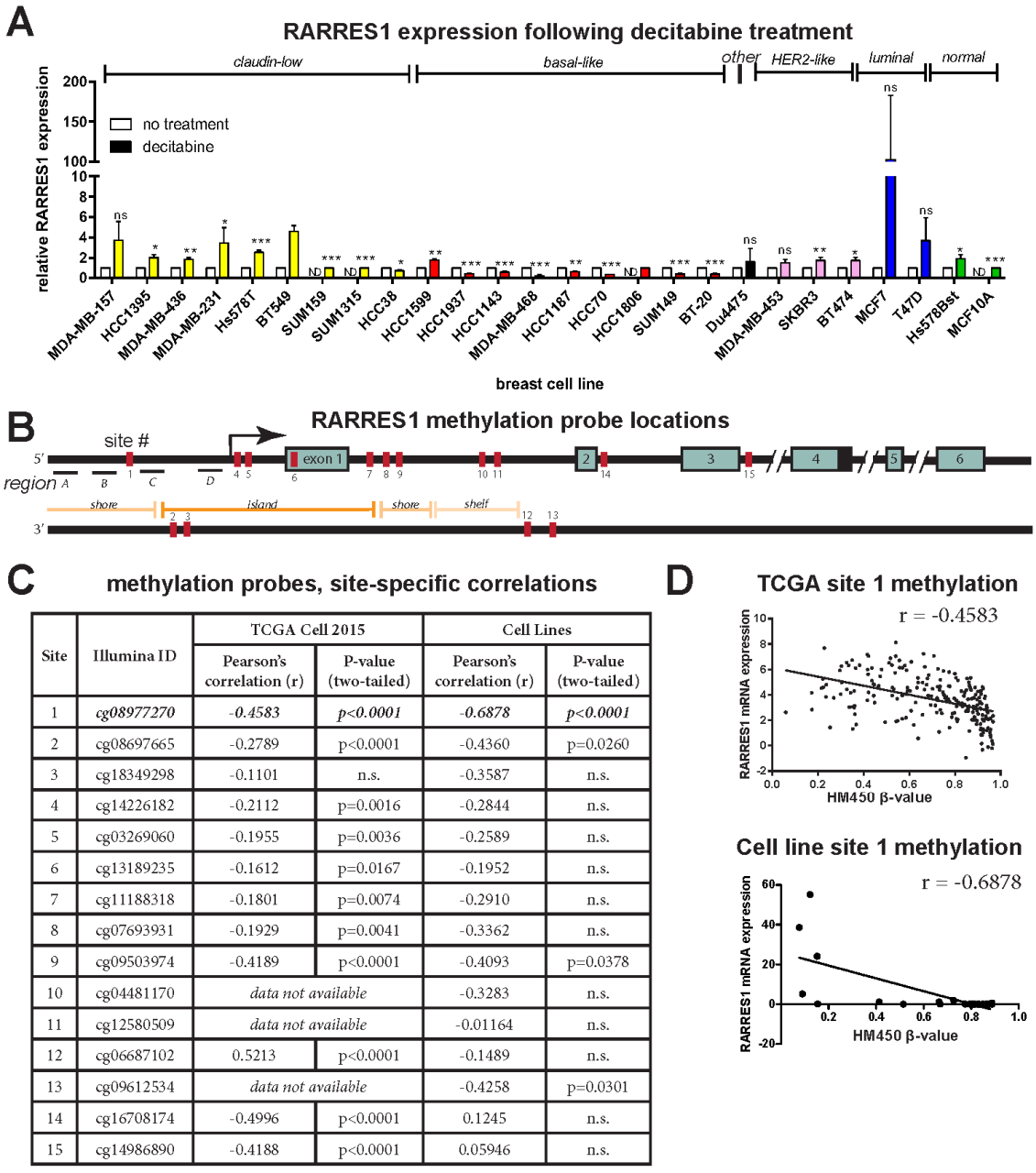

Site	Illumina ID	TCGA Cell 2015		Cell Lines	
		Pearson's correlation (r)	P-value (two-tailed)	Pearson's correlation (r)	P-value (two-tailed)
1	*cg08977270*	*-0.4583*	*p<0.0001*	*-0.6878*	*p<0.0001*
2	cg08697665	-0.2789	p<0.0001	-0.4360	p=0.0260
3	cg18349298	-0.1101	n.s.	-0.3587	n.s.
4	cg14226182	-0.2112	p=0.0016	-0.2844	n.s.
5	cg03269060	-0.1955	p=0.0036	-0.2589	n.s.
6	cg13189235	-0.1612	p=0.0167	-0.1952	n.s.
7	cg11188318	-0.1801	p=0.0074	-0.2910	n.s.
8	cg07693931	-0.1929	p=0.0041	-0.3362	n.s.
9	cg09503974	-0.4189	p<0.0001	-0.4093	p=0.0378
10	cg04481170	*data not available*		-0.3283	n.s.
11	cg12580509	*data not available*		-0.01164	n.s.
12	cg06687102	0.5213	p<0.0001	-0.1489	n.s.
13	cg09612534	*data not available*		-0.4258	p=0.0301
14	cg16708174	-0.4996	p<0.0001	0.1245	n.s.
15	cg14986890	-0.4188	p<0.0001	0.05946	n.s.

Figure 2-11 RARRES1 is hypomethylated in basal-like breast cancer.

Next, to determine the mechanism for the subtype-specific hypomethylation or silencing of the RARRES1 tumor suppressor, we analyzed HM450 data available from the TCGA data portal for 220 patient breast tumors. The HM450 array has 15 probes located in or near the RARRES1 gene (Figure 2-11B). These probes were overwhelmingly negatively correlated with RARRES1 expression (Figure 2-11C, Figure 2-12), suggesting that DNA hypermethylation may be silencing expression of RARRES1 in the luminal, HER2-like, and claudin-low subtypes. Utilizing our HM450 array data for the 26 cell lines, we identified a strong correlation at site 1 (Figure 2-11C, Figure 2-13), which is consistent with our findings in the TCGA 2015 data set (Figure 2-11D).

We then clustered the 26 cell lines based on methylation at sites 1 through 6, which revealed that site 1 is the primary region initiating progressive DNA methylation into the gene body and illustrates the clustering of basal-like breast cancers by specific hypomethylation of the region (Figure 2-14A). In validation of the importance of methylation of the promoter region of RARRES1, we performed 5-methylcytosine (5-mC) ChIP on RARRES1-silenced Hs578T cells using 4 locations ranging from ~1000bp upstream of the transcription start site (TSS) to within 100bp of the TSS (as described (Peng et al., 2012), indicated in Figure 2-11 as A-D). We observed a decrease in 5-mC following decitabine treatment which was most pronounced in Region C and D (Figure 2-14B), which is located nearest to site 1. This is consistent with our identification of a region containing site 1 as the region most important for initiating epigenetic silencing via DNA methylation.

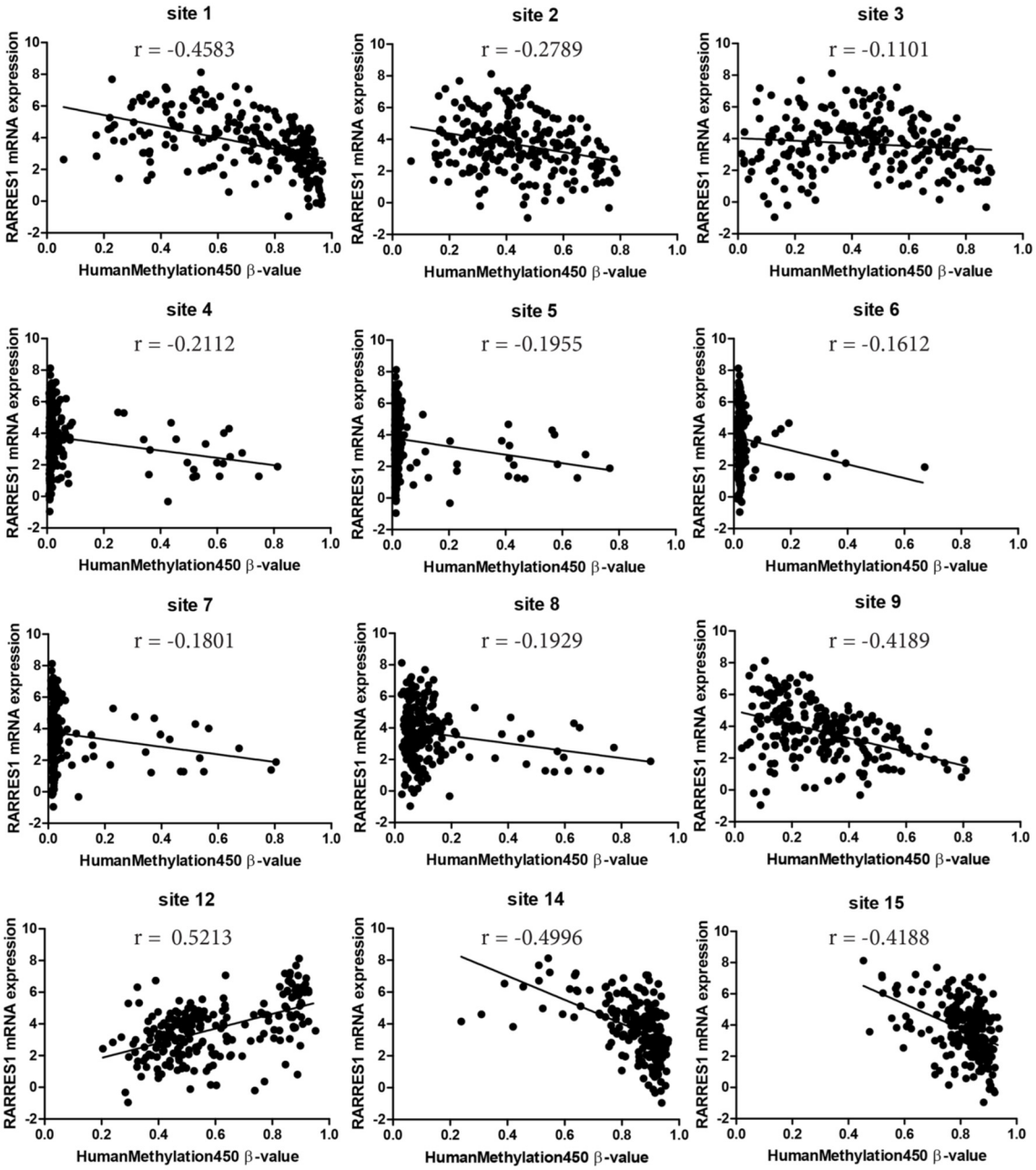

Figure 2-12 RARRES1 methylation in patient samples negatively correlates with mRNA expression.

Data from the TCGA Data Portal (Ciriello et al., 2015) using HM450 arrays was used to correlate mRNA expression of RARRES1 in patient tumors with the β-value at each probe location. Values on each graph represent linear correlations.

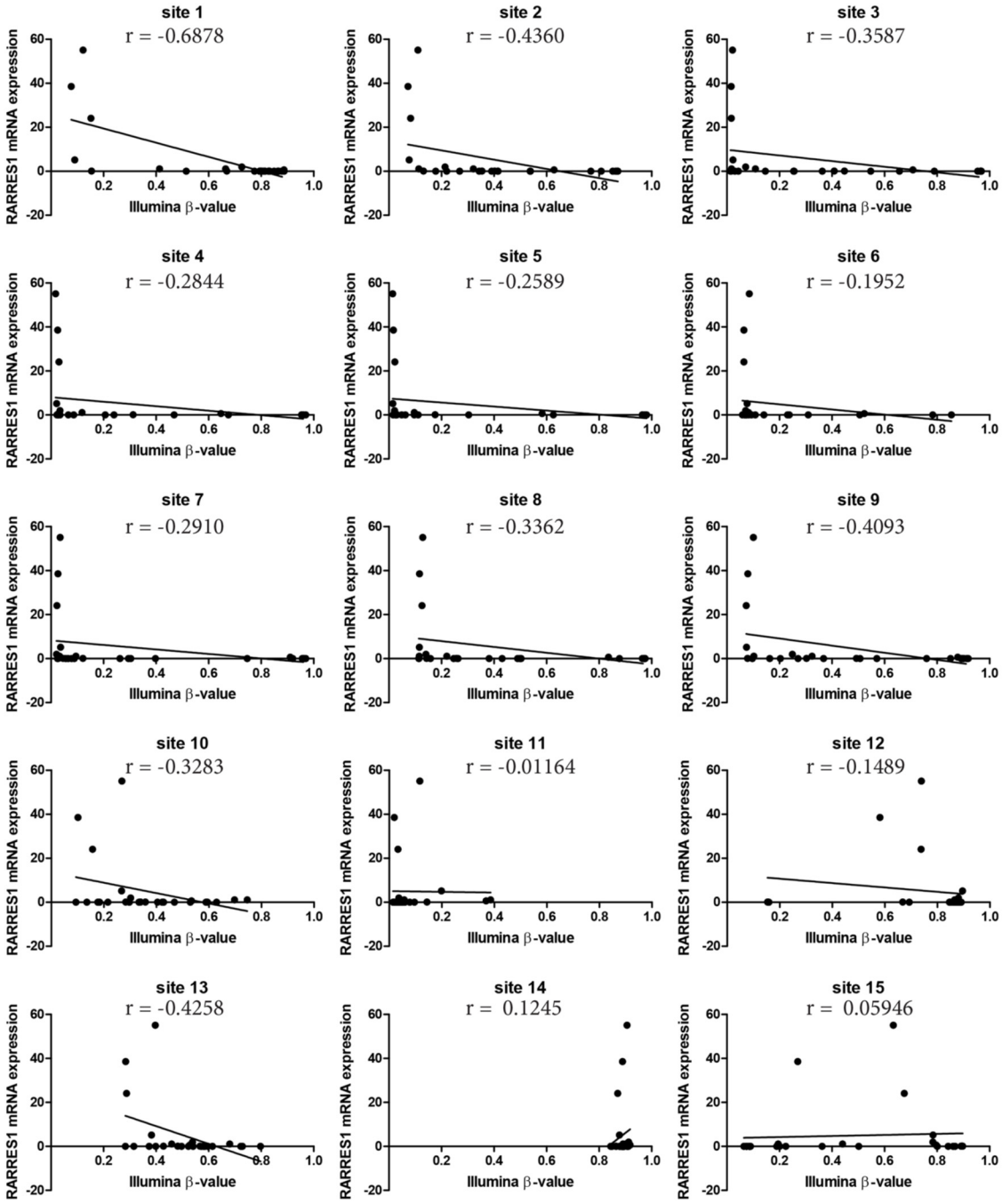

Figure 2-13 RARRES1 methylation in breast cancer cell lines negatively correlates with mRNA expression.

Using our own data from Illumina HM450 arrays and qPCR, mRNA expression of RARRES1 in 26 cell lines was correlated with the β-value at each probe location. Values on each graph represent linear correlations.

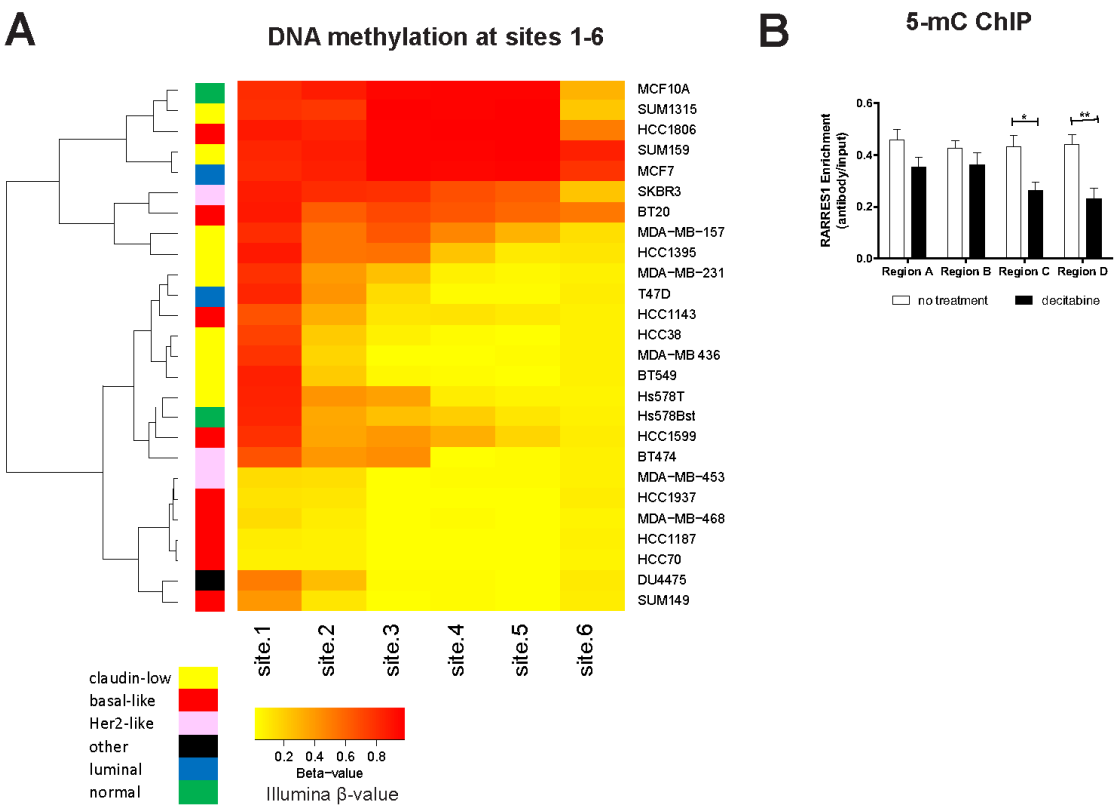

Figure 2-14 DNA methylation progressing from site 1 controls expression of RARRES1.

A. The panel of 24 cancerous and 2 normal breast cell lines were clustered (R function, heatmap.2) based on the relative methylation at RARRES1 sites 1-6 (as quantified by HM450 β values). **B.** RARRES1 enrichment as measured by qPCR following 5-methylcytosine ChIP in Hs578T cells treated with decitabine. Each region was compared using a student's t-test (* $p < 0.05$, ** $p < 0.01$).

2.3.6 *ALDH1A3 IS A SECONDARY FACTOR THAT DETERMINES RARRES1 EXPRESSION IN TNBC*

Although our data thus far suggest the importance of DNA methylation as a major factor dictating the expression of RARRES1 in breast cancer subtypes, our previous work and the presence of retinoic acid response elements (RAREs) in the gene suggest that the transcription mediator atRA also plays a role in subtype-specific expression of RARRES1. atRA is generated physiologically by the retinaldehyde dehydrogenases ALDH1A1, ALDH1A2, and ALDH1A3. Once synthesized, atRA binds to the retinoic acid and retinoid X receptors (RARs and RXRs) located at genomic RAREs (Chambon, 1996). This catalyzes the release of co-repressors and recruits co-activators to induce transcription of RARE-containing genes, such as RARRES1 (Torchia et al., 1998).

We first identified whether expression of the RARs and RXRs (α, β, and γ) correlated with expression of RARRES1 in the 2015 TCGA data set (Ciriello et al., 2015). We did not observe any relevant correlation between RARRES1 expression and RAR/RXR expression (Figure 2-15), suggesting that expression of these nuclear receptors was not dictating expression of RARRES1 in breast cancer. We continued upstream in retinoid signaling and investigated the possible connection between RARRES1 and the atRA-producing ALDH1A1, ALDH1A2, and ALDH1A3. In all 26 cell lines except SUM159 and BT474, ALDH1A3 was the most highly expressed isoform (Figure 2-16). Similar to our findings with RARRES1, we observed significantly higher expression of ALDH1A3 in the basal-like cell lines when compared to the claudin-low cell lines ($p<0.01$, Figure 2-17A). This suggests that if RA-producing enzymes are playing a role in RARRES1 subtype-specific regulation, ALDH1A3 is the most likely main contributor.

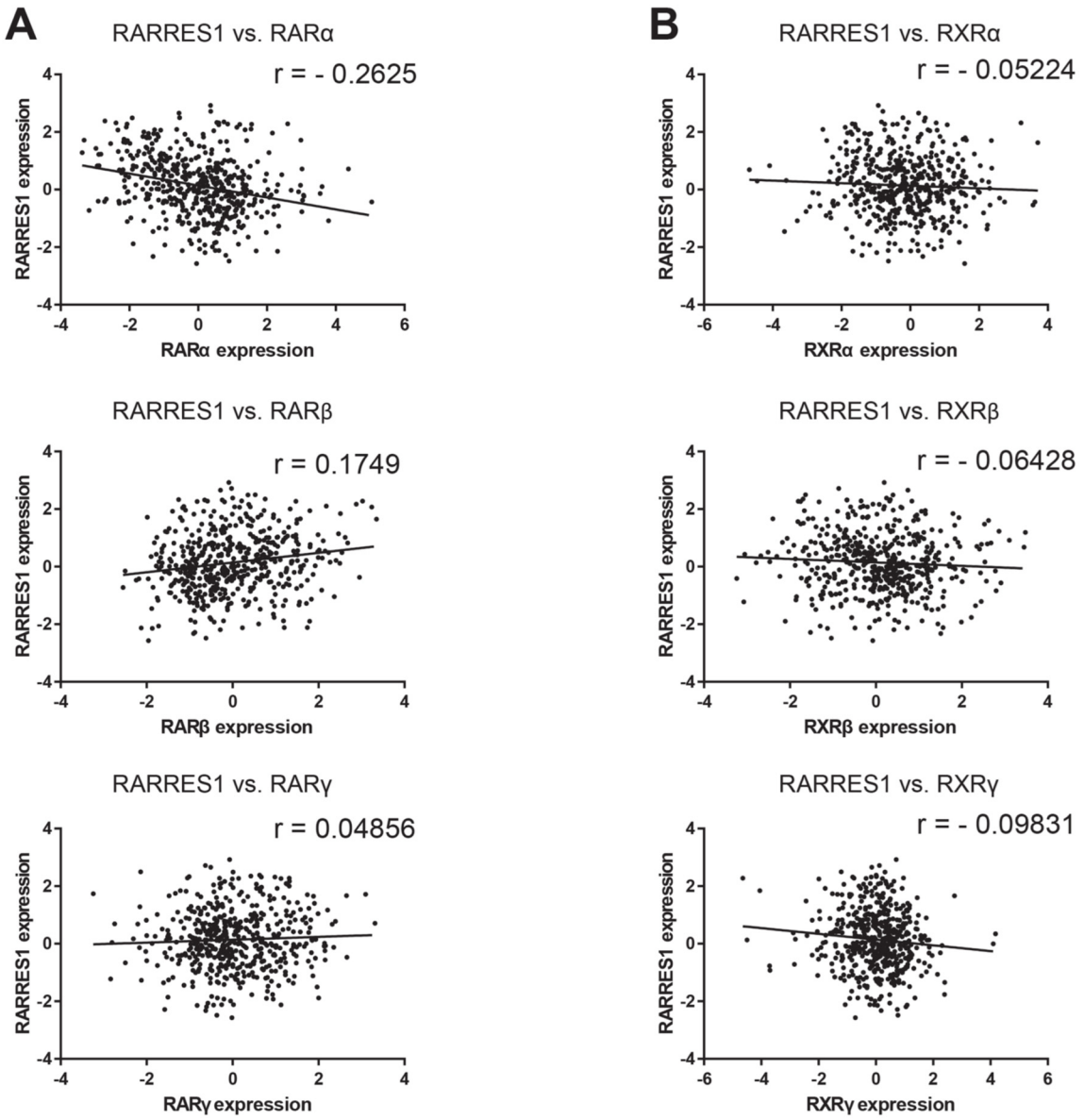

Figure 2-15 RARRES1 expression does not strongly correlate with expression of RAR and RXR isoforms.

Expression of RARRES1 mRNA in the TCGA (Ciriello et al., 2015) data set was correlated with expression of **A.** RARα, RARβ, and RARγ; and **B.** RXRα, RXRβ, and RXRγ.

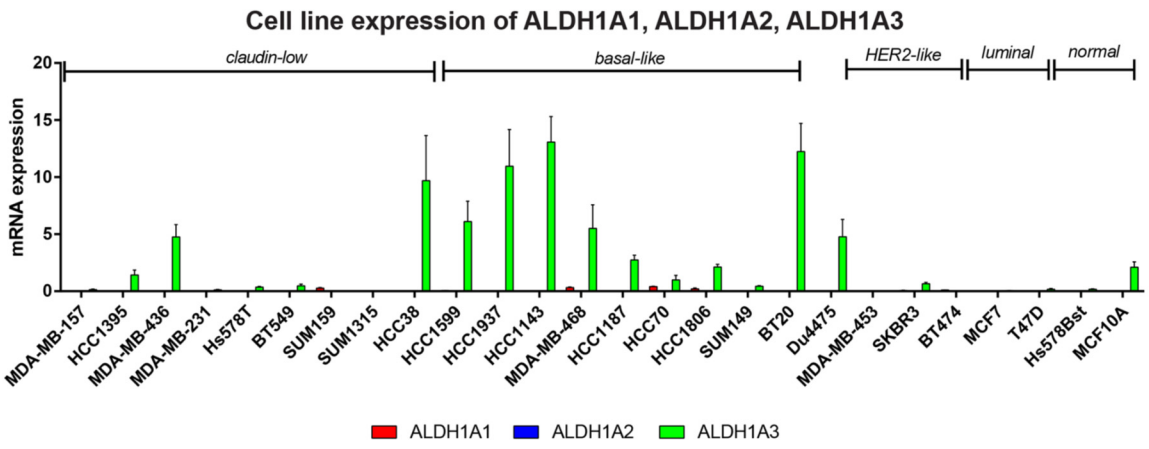

Figure 2-16 ALDH1A3 is the most highly expressed ALDH1a isoform in TNBC cell lines.

Expression of ALDH1A1, ALDH1A2, and ALDH1A3 mRNA in 26 cell lines was determined by qPCR.

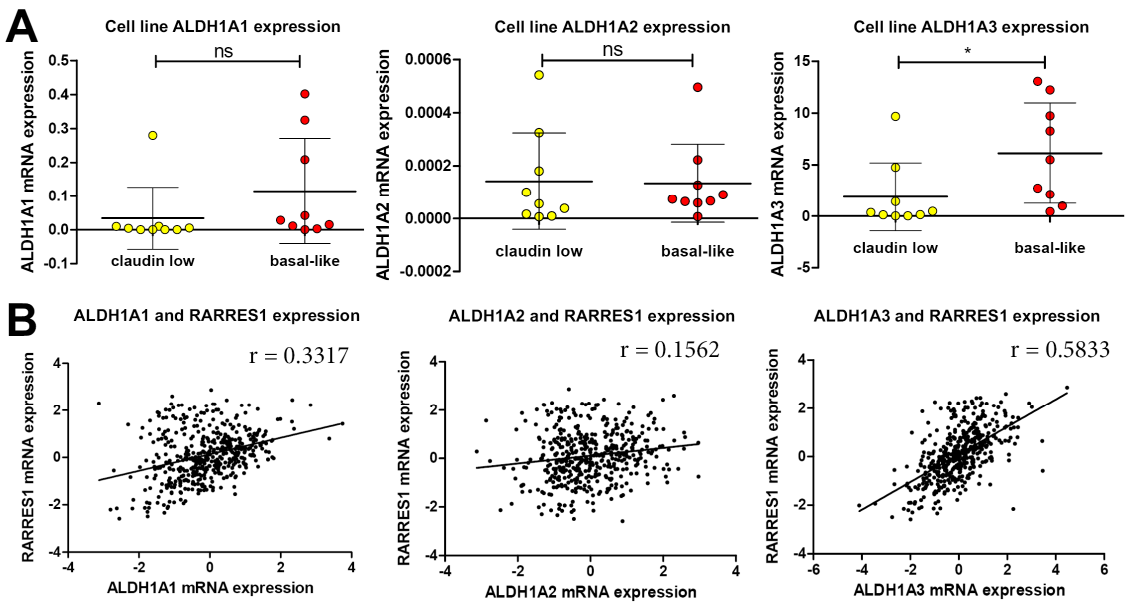

Figure 2-17 ALDH1A3 expression correlates with RARRES1 expression in patient tumors.

A. Expression of ALDH1A1, ALDH1A2 and ALDH1A3 was compared among all claudin-low and basal-like cell lines. **B.** Using the TCGA data via cBioportal (Ciriello et al., 2015), mRNA expression of ALDH1A1, ALDH1A3, and ALDH1A3 was correlated with RARRES1 via a linear correlation.

Next, we obtained data from TCGA (The Cancer Genome Atlas Network, 2012) that demonstrates weak correlations between RARRES1 and ALDH1A1, and ALDH1A2, but a moderately strong and significant correlation between RARRES1 and ALDH1A3 ($n=460$, $p < 0.001$) (Figure 2-17B). To investigate if this correlation exists beyond the mRNA level, we assessed RARRES1 and ALDH1A3 protein expression in 62 primary breast cancer tumors by immunofluorescence and found a significant correlation between the percentage of cells expressing ALDH1A3 and RARRES1 (Figure 2-18A and B). The expected random probabilities and the actual observed percentage of cells positive for both RARRES1 and ALDH1A3 were plotted as a histogram and fit with a Gaussian distribution (Figure 2-18C). The Gaussian distributions were compared (Figure 2-18C) and the mean actual percentage of double-positive cells (20.78%) is significantly higher than that expected due to random probability (12.83%, $p < 0.05$). These correlations between ALDH1A3 and RARRES1 suggests that expression of RARRES1 in breast cancer is not only controlled by methylation in the promoter region, but also by ALDH1A3 via its production of RA. Importantly, this assumption was corroborated by knockdown of ALDH1A3 in MDA-MB-468 cells (Marcato et al., 2015), which also reduced protein expression of RARRES1 (Figure 2-18D).

Figure 2-18 ALDH1A3 correlates with and contributes to RARRES1 expression.

A. Representative image of 62 formalin fixed primary breast cancer patient tumor samples stained for ALDH1A3 and RARRES1 protein expression by immunofluorescence. **B.** Quantification of the percentage of RARRES1-positive cells was correlated as a function of the percentage of ALDH1A3-positive cells in 62 individual patient tumor samples as detected by immunofluorescence (linear correlation). **C.** Based on the percent RARRES1^{+} cells and the percent ALDH1A3^{+} cells, a random expected distribution of double-positive cells was determined, plotted as a histogram, and fit with a Gaussian distribution. The actual observed distribution of double-positive cells was plotted as a histogram and fit with a Gaussian distribution. The distributions of random (expected) double-positive cells and actual (observed) double-positive were combined and compared using an extra sum-of-squares F test. **D.** RARRES1 expression was observed via Western blotting following shRNA knockdown of ALDH1A3 and/or RARRES1 in MDA-MB-468 cells.

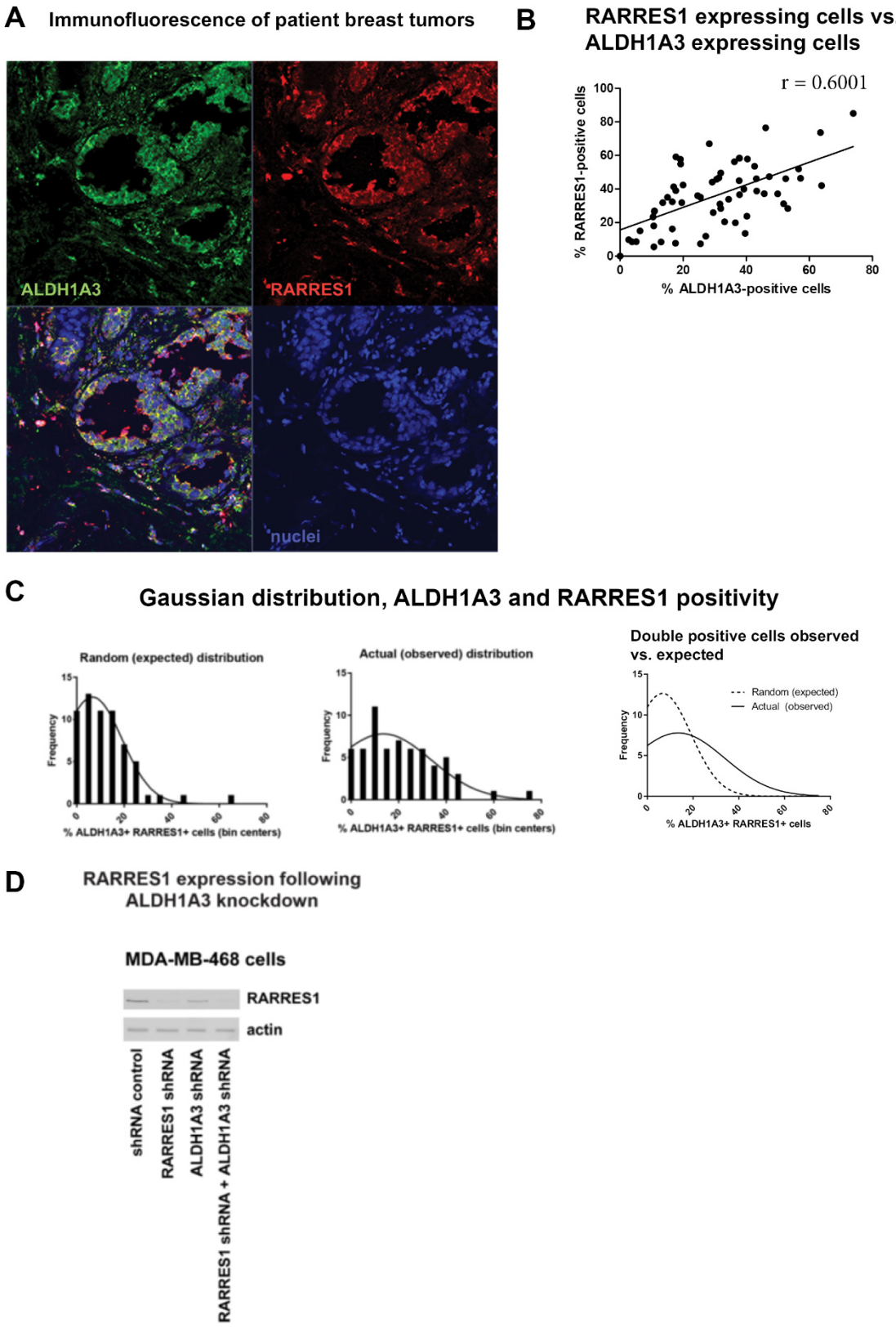

Figure 2-18 ALDH1A3 correlates with and contributes to RARRES1 expression.

2.3.7 *DNA Methylation and ALDH1A3/RA Co-Regulate Expression of RARRES1*

Having established that both DNA hypomethylation and high expression of RA-producing ALDH1A3 are factors in the subtype-specific expression of RARRES1, we next assessed how these factors control RARRES1 expression together. We examined the mRNA expression of RARRES1 following treatment with atRA, modulation of ALDH1A3 expression, decitabine, or a combination of both. Demethylation of RARRES1 with decitabine allows or enhances atRA-dependent transcription of the gene (Figure 2-19A). We observed consistent results when ALDH1A3 was overexpressed in MDA-MB-231 or knocked down in MDA-MB-468 (Figure 2-19B). This suggests that while DNA methylation is key in controlling the expression of RARRES1, physiological atRA produced by ALDH1A3 is also a determinant for RARRES1 expression.

We then used ChIP to validate atRA as an important secondary determinant in RARRES1 expression. Treatment of RARRES1-methylated MDA-MB-231 cells and RARRES1-unmethylated MDA-MB-468 cells with both atRA and decitabine is required for maximal demethylation of the RARRES1 gene, illustrated by decreased binding to the 5-mC antibody (Figure 2-19C and D). Additionally, atRA and decitabine are both required for maximal binding of both CTCF (a multipurpose DNA binding protein, Figure 2-19C), and RARα (the nuclear receptor of RA, Figure 2-19D) to their respective response elements in RARRES1. While CTCF can have multiple functions including transcriptional activation and repression (Holwerda and Laat, 2013), it appears to activate transcription at an unmethylated RARRES1 promoter (Peng et al., 2012).

Figure 2-19 RARRES1 expression is influenced by DNA methylation and retinoic acid signaling.

A. The effect of decitabine (DAC) and all-*trans* retinoic acid (atRA), alone or combined on RARRES1 expression was determined by qPCR in methylated cell lines (MDA-MB-231, MDA-MB-436, HCC1599), and unmethylated MDA-MB-468 cells. Treatments were compared using a repeated-measures ANOVA. **B.** The effect of ALDH1A3 overexpression in MDA-MB-231 cells (have low levels of intrinsic ALDH1A3) and ALDH1A3 knockdown in MDA-MB-468 cells (have high levels of intrinsic ALDH1A3) on RARRES1 expression was determined by qPCR. Decitabine-treated values were compared to no-treatment values using a paired student's t-test. To interrogate the RARRES1 promoter, ChIP and double ChIP assays were performed on the **C.** CTCF response element, and **D.** RARα response element, in MDA-MB-231 cells (have methylated RARRES1 promoter and low levels of ALDH1A3, which produces atRA) and MDA-MB-468 cells (have unmethylated RARRES1 promoter and intrinsic high ALDH1A3) that were either treated with decitabine (DAC), retinoic acid (atRA) or both. The assays were performed using antibodies against 5-mC, RARα and CTCF, as well as the control normal rabbit IgG, alone or in combination for the double ChIP assays. In the double ChIP assays, only DNA sequences that bind both proteins concurrently are detected by this assay.

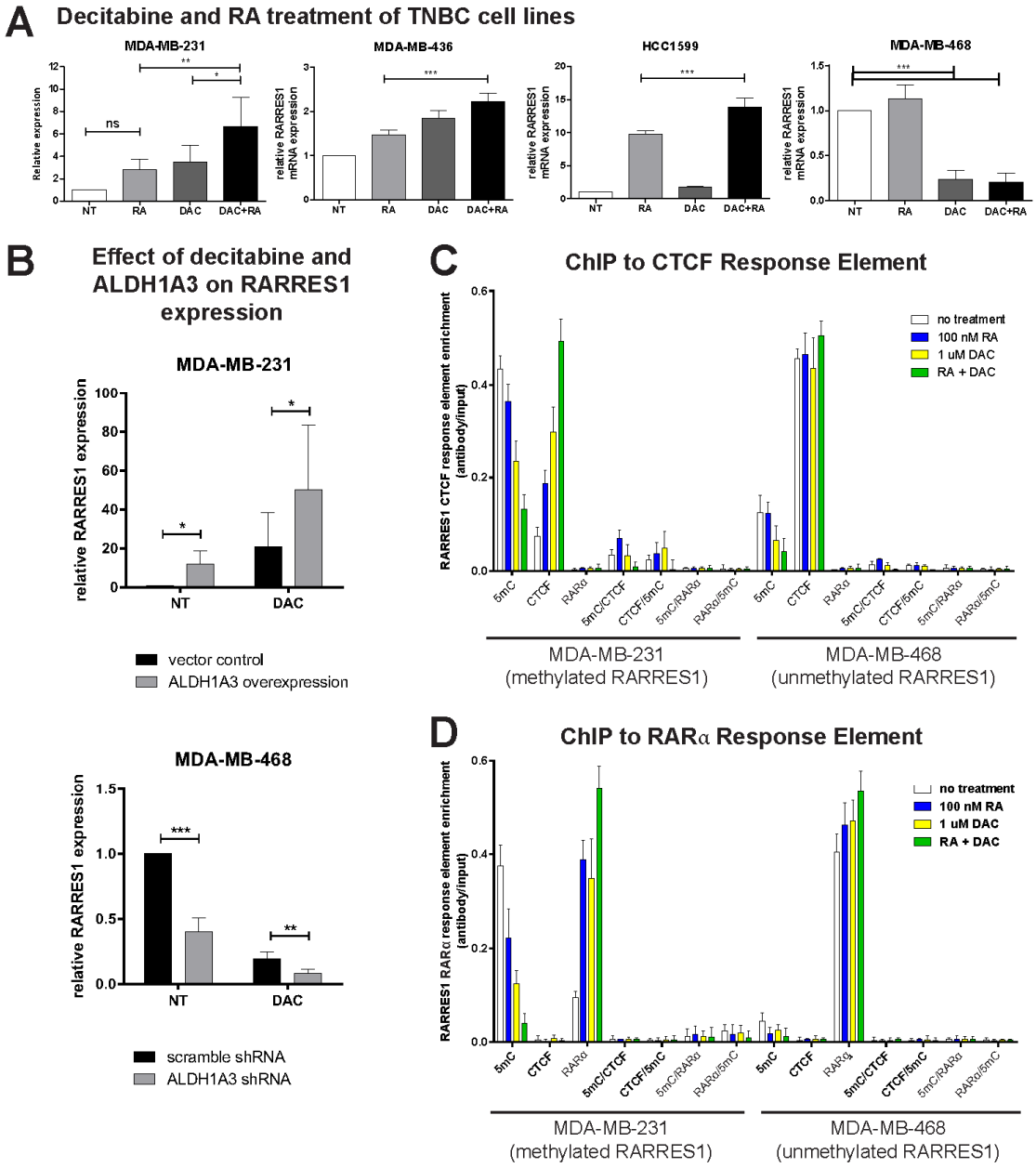

Figure 2-19 RARRES1 expression is influenced by DNA methylation and retinoic acid signaling.

The double-ChIP with 5-mC and CTCF (Figure 2-19C) or RARα (Figure 2-19D) demonstrates that CTCF and RARα bind minimally to methylated DNA. This supports our finding that demethylation is required for maximal induction of RARRES1 transcription and corroborates the wide range of RARRES1 expression values identified between the RARRES1-methylated claudin-low cell lines and the RARRES1-unmethylated basal-like cell lines.

2.4 Discussion

RARRES1 was first described as a novel retinoid response gene in skin raft cultures (Nagpal et al., 1996). RARRES1 is a commonly silenced hypermethylated locus in many cancer types including prostate cancer (Jing et al., 2002), hepatocellular carcinoma (X.-H. Chen et al., 2014), and breast cancer (Peng et al., 2012). Although generally described as a putative tumor suppressor gene, a recent report indicated a pro-tumorigenic role for RARRES1 in a rare form of breast cancer, inflammatory breast cancer (Wang et al., 2013). In contrast, in this study we identified RARRES1 as a tumor suppressor in TNBCs, and highly expressed specifically within the basal-like subtype. We determined that subtype-specific expression of this tumor suppressor is due to both its specific hypomethylation and ALDH1A3 expression within basal-like breast cancers, which provides its necessary transcription induction molecule, atRA, for nuclear hormone receptor RARα. Our characterization of the RARRES1 gene offers an example of a subtype-specific tumor suppressor that may be useful as a biomarker in subtype-specific therapies.

The heterogeneity of breast cancer complicates therapeutic decision making and affects patient outcomes. Recent research has focused on identifying gene expression

profiles, mutational maps, and methylation profiles to identify different subtypes of breast cancer (Ciriello et al., 2015; Perou et al., 2000; The Cancer Genome Atlas Network, 2012). These have revealed that the genes expressed in these different subtypes are important in determining the response of patients to anti-cancer therapies. Importantly, the specific expression and hypomethylation of RARRES1 in basal-like breast cancer adds RARRES1 to a list of genes which are differentially regulated and expressed in breast cancer subtypes (Parker et al., 2009; van ’t Veer et al., 2002). These genes may correlate with, or be causative factors in, the varying responses of different subtypes to various chemotherapy regimens.

In particular, RARRES1 is an atRA-inducible tumor suppressor gene. This is in direct contrast with the vast majority of tumor suppressors, which are currently considered as undruggable except by complex synthetic or conditional lethality models (Sellers, 2011). While atRA has achieved limited clinical success in breast cancer, an increasing body of work suggests that atRA affects key processes important for the progression and metastasis of breast cancer in a context-specific manner. For example, atRA signaling exhibits either cooperative or antagonistic interplay with estrogen signaling (Hua et al., 2009; Ross-Innes et al., 2010); atRA can promote either a pro-apoptotic or a pro-survival response (Jiménez-Lara et al., 2010); or atRA can promote or suppress TNBC tumor growth (Marcato et al., 2015). We recently hypothesized that differential methylation of tumor-suppressive and pro-growth genes in breast cancer may affect the response of breast cancers to atRA therapy (Marcato et al., 2015). RARRES1 is one example of a gene that fits this paradigm and may suggest that a specific subtype of breast cancer (i.e. basal-like breast cancers) could be treated with atRA.

2.5 Acknowledgements

The authors gratefully acknowledge the technical assistance of Dr. Alejandro Cohen.

Support was provided by grant funding to PM from the Canadian Institutes of Health Research (CIHR, MOP-130304), the Beatrice Hunter Cancer Research Institute (BHCRI), the Breast Cancer Society of Canada, and the QEII Health Sciences Center Foundation; by grant funding to ICGW from the Natural Sciences and Engineering Research Council of Canada (436204-2013); and by grant funding to PWKL and SG by CIHR. KMC, JPM, DV, MS, DC, MW, and MLT are supported by studentship or trainee awards from the BHCRI, Canadian Breast Cancer Foundation, and the Canadian Imperial Bank of Commerce. KMC and DC are supported by CGS-D awards, and MLT by a CGS-M award from CIHR. KMC, MLT, and DC are supported by the Nova Scotia Health Research Foundation. MLT is supported by NS Research and Innovation Graduate Scholarships. KMC is a Killam Scholar.

CHAPTER 3: PROFILING OF THE TRANSCRIPTIONAL RESPONSE TO ALL-*TRANS* RETINOIC ACID IN BREAST CANCER CELLS REVEALS RARE-INDEPENDENT MECHANISMS OF GENE EXPRESSION

Contribution statement

I designed the experiments, analysed the data, and wrote the manuscript with the guidance of Dr. Paola Marcato. I collected data with assistance as follows: Selena Maxwell, qPCR validation; Margaret Thomas, atRA/DAC/TSA sample collection. All authors reviewed and edited the manuscript.

3.1 INTRODUCTION

The evolutionarily-conserved retinoid signaling pathway governs expression of hundreds of genes and regulates a wide variety of fundamental biological processes, including differentiation, cell cycle arrest and cell proliferation (Coyle et al., 2013; Gudas and Wagner, 2011). Retinoid signaling has a controversial role in cancer, with evidence suggesting it can suppress or promote carcinogenesis (Coyle et al., 2013; R.-Z. Liu et al., 2011; X. Liu et al., 2011; Tang and Gudas, 2011), depending on the cancer and the cellular context (X. Liu et al., 2011; Marcato et al., 2015; Schug et al., 2007, 2008). For example, due to their ability to induce differentiation, retinoids are used very successfully to treat acute promyelocytic leukemia (Huang et al., 1988) and neuroblastoma (Peinemann et al., 2015). However, attempts to use retinoids and dietary precursors to treat other cancers (including breast cancer) have been unsuccessful and may even promote tumorigenesis (Alpha-Tocopherol, Beta Carotene Cancer Prevention Study Group, 1994; Chiesa et al., 2007; Singletary et al., 2002). A major hypothesis for these clinical disappointments is a failure to consider inter-tumoral heterogeneity (Garattini et al., 2014). As we better understand the complexities of retinoic acid signaling, we can characterize the divergent responses of breast cancer to retinoids and exploit this heterogeneity for improved cancer therapy.

In breast cancer, the effects of retinoids on cell growth are highly varied and likely depend upon which retinoic acid (RA)-inducible genes are expressed and additional non-genomic effects (R.-Z. Liu et al., 2011; Fontana, 1987; Cho et al., 1997; A. C. Chen et al., 1997; Hong and Lee-Kim, 2009; Wetherall and Taylor, 1986; Van heusden et al., 1998; Mira-Y-Lopez et al., 2000; Bolis et al., 2017; Carrier et al., 2016;

Persaud et al., 2016). The retinoid signaling pathway is often simplified to production of all-trans retinoic acid (atRA) by aldehyde dehydrogenase 1A (ALDH1A) enzymes, where it translocates to the nucleus and activates nuclear receptors, retinoic acid receptors (RARs) and retinoid X receptors (RXRs). These receptors induce the expression of genes with retinoic acid response elements (RAREs) in their promoters. The human genome contains over 14,000 RAREs; most of which are located in intragenic regions (3,249 RAREs are within 10kb of genes) (Lalevée et al., 2011). Many initial studies of RA-induced gene expression focused on straightforward induction of genes containing RARE sequences; however, RA-mediated gene expression is significantly more complex and governed by other cellular processes, including the interaction of co-repressors and co-activators.

There is strong evidence for hierarchical networks of nuclear receptors facilitating tissue-specific gene expression (Bookout et al., 2006). Significant choreography is required for the vast transcriptional responses to atRA (Liu et al., 2000; Zheng et al., 2005). The high complexity involved in retinoid signaling is unparalleled among nuclear hormone receptor pathways (Leid et al., 1992).

Although the majority of evidence supports atRA as a potent anti-cancer therapy which is able to suppress proliferation and induce differentiation or apoptosis (Altucci et al., 2001; Lin et al., 2017; Liu et al., 1996; Seewaldt et al., 1995), we and others have demonstrated that RA can also potentiate tumor growth (Manor et al., 2003; Marcato et al., 2015; Verma et al., 1982). Paradoxically, cancer stem cells have high levels of ALDH1A enzymes (Chen et al., 2009; Ginestier et al., 2007; E. H. Huang et al., 2009; Jiang et al., 2009; Marcato et al., 2011b; Sullivan et al., 2017), supporting higher than

normal levels of atRA biosynthesis and higher expression of RA-inducible genes (Moretti et al., 2016); however, atRA is also used as a differentiating agent which would theoretically eliminate those same cancer stem cells (Croker and Allan, 2012; Friedman et al., 2013; Ginestier et al., 2009; Lim et al., 2012). This demonstrates the importance of characterizing cellular responses to atRA in a variety of models and motivated the current study.

We sought to determine the relationship between the transcriptional profiles associated with ALDH1A3 expression and those corresponding to atRA treatment. We performed mRNA expression arrays (Affymetrix HuGene 2.0ST) with two triple-negative breast cancer (TNBC) cell lines, mesenchymal MDA-MB-231 and basal-like MDA-MB-468 cells. We have previously shown that atRA and ALDH1A3 expression potentiate growth of MDA-MB-231 xenografts, while atRA and ALDH1A3 expression inhibit the growth of MDA-MB-468 xenografts (Marcato et al., 2015). We identified distinct transcriptional responses with minor overlap to ALDH1A3 and atRA treatment in both cell lines. Among the atRA-inducible genes we identified were a number of known atRA-regulated genes, including keratin 7 (KRT7) (Nguyen et al., 2016), and prostaglandin E synthase (PTGES) (Mamidi et al., 2012). We also identified known regulators of the retinoid signaling pathway, including dehydrogenase reductase 3 (DHRS3) (Feng et al., 2010), nuclear receptor interaction protein 1 (NRIP1) (Heim et al., 2007), and cytochrome p450 family 26A1 (CYP26A1) (White et al., 1996).

Since it has been established that epigenetic modulation can enhance responses to retinoid-based treatments (Emionite et al., 2004; Kashyap and Gudas, 2010; Romero et al., 2017), we provide further evidence that DNA methylation can impact the atRA-

inducibility of select genes. On the other hand, the use of the histone deacetylase inhibitor, trichostatin A (TSA), revealed limited contributions of histone acetylation to the regulation of atRA-inducible genes. Very few of the genes we identified as atRA-inducible contained classical RAREs, and the vast majority of genes containing RAREs were not induced by atRA in either cell line. This again highlights the complexities of differential RA-regulated gene expression, which is cell-type specific and responsible for the diverse cellular effects induced by RA.

Although a major hypothesis for the opposing responses to atRA treatment is differential shuttling of atRA to RARα/β or to peroxisome proliferator-activated receptors (PPAR) β/δ (Schug et al., 2007; Shaw et al., 2003), our previous work had indicated that this was not a major contributing factor in the opposing responses to ALDH1A3 (Marcato et al., 2015). This study again indicates that PPARβ/δ-directed transcription is not a major regulator of the pro- or anti-tumor effects of atRA. Instead, we provide evidence for atRA-induced gene expression being predominantly RARE-independent (i.e. cathepsin S, CTSS) and dictated by expression of additional atRA-inducible transcription factors (i.e. interferon regulatory factor 1; IRF1). We demonstrate that IRF1 expression, which is atRA-inducible and epigenetically regulated, is required for full atRA inducibility of CTSS in MDA-MB-231 but not MDA-MB-468. This provides support to a complex network of interactions regulating the context-specific response of breast cancer cells to atRA.

3.2 MATERIALS AND METHODS

3.2.1 *CELL LINES, VECTORS, AND REAGENTS*

MDA-MB-231 and MDA-MB-468 cells were obtained from the American Type Culture Collection (ATCC) and cultured in Dulbecco's Modified Eagle's Medium (DMEM) with 10% fetal bovine serum and 1x antibiotic-antimycotic (Invitrogen). DDC Medical authenticated the cell lines by short tandem repeat (STR) profiling at 17 loci and verified them to be mycoplasma-negative (last performed 2015).

All-trans retinoic acid (atRA, Sigma) was used at 100 nM for 18 h. 5-aza-2′-deoxycitidine (decitabine, DAC, Sigma), was used at 1 μM for 72 h and replaced every 24 h. Trichostatin A (TSA, Sigma) was used at 100 nM for 18 h. When used in combination, atRA and TSA were added for the last 18 h of treatment.

IRF1 shRNA knockdown clones were generated using the pGipZ lentiviral vector packaged in HEK293T cells following standard protocols (IRF1kd-60: V3LHS_412360; IRF1kd-94: V2LHS_133394; Dharmacon). ALDH1A3-overexpressing and ALDH1A3 knockdown clones were generated and validated as previously described (Marcato et al., 2011b, 2015).

3.2.2 *QUANTITATIVE PCR*

Total RNA was extracted using Trizol reagent and the PureLink RNA kit (Invitrogen) with DNase treatment. Equal amounts of RNA were reverse transcribed using iScript (BioRad) and quantitative real-time PCR (qPCR) was performed using gene-specific primers (Table 3-1). Standard curves for each primer set were generated, and primer efficiencies were incorporated into the CFX Manager software (Bio-Rad). mRNA expression of all samples was calculated relative to two reference genes

[glyceraldehyde 3-phosphate dehydrogenase (GAPDH) and β-2- microglobulin (B2M)], and an indicated control sample. Relative mRNA expression was log-2 transformed prior to plotting and statistical analysis.

3.2.3 *Gene Expression Profiling*

MDA-MB-231 MSCV and ALDH1A3-overexpression cells, and MDA-MB-468 SMP and ALDH1A3-shRNA cells were treated with atRA and/or DAC as described (section 3.2.1) in triplicate. Sample preparation, amplification, hybridization to the Affymetrix HuGene 2.0 ST array, and data collection were performed by The Centre for Applied Genomics at the Hospital for Sick Children (Toronto, Ontario, Canada), and can be accessed by GEO Accession #GSE103426. Data was analyzed in the R environment using the oligo package with RMA normalization. Genes which were up-or down-regulated more than 1.6-fold ($\log_2$=0.678) at a significance level of $p<0.01$ were considered differentially expressed.

Table 3-1 Primers used for qPCR.

Gene	Primer sequence (5' - 3')		Reference
GAPDH	F	GGAGTCAACGGATTTGGTCGTA	(Marcato et al., 2015)
	R	TTCTCCATGGTGGTGAAGAC	
B2M	F	AGGCTATCCAGCGTACTCCA	(Coyle et al., 2016)
	R	CGGATGGATGAAACCCAGACA	
GDF15	F	TCCAGATTCCGAGAGTTGCG	
	R	CGAGGTCGGTGTTCGAATCT	
CDH5	F	CTTCACCCAGACCAAGTACACA	
	R	TCAACAAACAGAGAGCCCACA	
SCEL	F	CCAAAGTCTCGACAGCCTCA	
	R	CTGCTTTTGTTTGCTGAAGGGA	
IRF1	F	TCGGATGCGCATGAGACC	
	R	CATGCTTCCATGGGATCTGGA	
STAT1	F	TGCCAGCCTGGTTTGGTAAT	
	R	GTACCAAAGGATGGAGGCCC	
CTSS	F	ACATGGGTTCTTGTGGTGCT	
	R	AGTTGAGCAATCCACCAGGTT	
GBP4	F	TCCTTGACATGGCTAGCAACA	
	R	GCCAAGATATTTTGTCCCTACTCC	
RARRES3	F	GGCTGTTGCTATCGGGTCAA	
	R	GACCAACCATCTCCTTCGCA	
TNFSF10	F	TGCGTGCTGATCGTGATCTT	
	R	CTGCTTCAGCTCGTTGGTAAAG	
DHRS3	F	TCTGTGATGTGGGCAACCG	
	R	ATGGTGATGTCACCCACCTTC	
NRP2	F	CACCAGAACTGCGAGTGGAT	
	R	TGCAGTCGTGCTTCTCGATT	
PTGES	F	CTTTTGTCGCCTGGATGCAC	
	R	GTAGGTCACGGAGCGGATG	
RARB	F	GGTTTCACTGGCTTGACCAT	
	R	GGCAAAGGTGAACACAAGGT	
AMPH	F	ATCGTATTGAGTGGCTGCCC	
	R	CACCTGGGCAGGGGAATAAG	
SSX1	F	GAAGCCAGCAGAGGACGAAA	
	R	CAGAAATATTTGCTTTTCCTGGGGG	
ESM1	F	CGGTTCTGGGGCATAGGAAA	
	R	ACACAAACCACCAGTGGGTAA	
ARL14EPL	F	ACCCATGCCCGAAGTGTAAC	
	R	CCTGACTCAGTGACGATGGC	
CST2	F	AGGAGGACAGGATAATCGAGGG	
	R	AGTGGCCTTGTTATACTCGCTG	

Gene	Primer sequence (5’ - 3’)		Reference
LTBP3	F	AGATCTCAGCAGAAGTGCAGG	
	R	TTCGAGCTCTCAATGCGGT	
TINAGL1	F	CCTTTTCCCCCGATCCAAGG	
	R	GGTTCTTGGTCACACTGCCA	
CRISP2	F	GGTTGCCCTGATGACTGTGA	
	R	TGTTCACAGCCAGCTGTATTCT	
CRISP3	F	AAATACTTCATCCTGCTCTGGAAAC	
	R	GCAGTAAAAGCGGGATCCTTATC	
S100A7	F	CCAAGCCTGCTGACGATGA	
	R	GACATCGGCGAGGTAATTTGTG	
COLCA2	F	TGTCGGAAAAACCGAAGGTGTA	
	R	CCTGGTGTGCCCGTCTTT	
CD22	F	TGGGAGAAAAATGGCAGGCT	
	R	GGACGCTGTCTGTCCTATGG	
FOXA1	F	CATGAAACCAGCGACTGGAAC	
	R	TCATGTTGCTGACCGGGAC	
NFKBIZ	F	GTCCGCCTGTTGATGAGGAA	
	R	GGAACCAAATGCACTGGCTG	
SRPX2	F	ACCGGGGCTTTCGATTGATT	
	R	TGAATGGTAGTGCGTGGCAT	
TMPRSS4	F	TGAAGCTGCAGTTCCCACTC	
	R	TTCTGCTTCGTAAAGCCCCAT	
LINC00857	F	GAGGCCCTAATCCTCAAGGC	
	R	TCTTTTCCTTCACACCGCGT	

3.2.4 *Methylation Profiling*

DNA was collected from untreated, atRA-, and DAC-treated MDA-MB-231 and MDA-MB-468 cells using the PureLink DNA kit (Invitrogen). Methylation analyses using the HM450 bead chip array (Illumina) was performed by The Centre for Applied Genomics including bisulfite conversion, hybridization, background subtraction, and normalization (Geo Series Accession #GSE103425). β-values for Illumina probes near each gene of interest were extracted from the data, and location determined relative to the transcription start site (TSS).

3.2.5 *Transcription Factor Logos*

Genes with retinoic acid response elements (RAREs) were identified from published data (Lalevée et al., 2011) or from the oPOSSUM database (Kwon et al., 2012) within 10 kb of the TSS of the gene of interest. RARE sequences were entered into WebLogo (Crooks et al., 2004) with default settings. Where a gene was identified with more than 1 RARE within 10 kb of the TSS, all identified RARE sequences were utilized for logo generation.

3.2.6 *cBioportal Data Analysis*

Data from The Cancer Genome Atlas (TCGA) (Ciriello et al., 2015) were analyzed and extracted from the cBioportal interface (Cerami et al., 2012; J. Gao et al., 2013).

3.2.7 *Statistical Analyses*

All statistical analyses were calculated in GraphPad Prism 6. Paired t-tests were used to compare single treatments, one-way ANOVA was used to compare multiple vectors, and two-way ANOVA was used to compare combinations of treatments and/or

vectors. Pearson's correlations were calculated for TCGA data appearing in Figure 3-15. For all comparisons, * $p < 0.05$, ** $p < 0.01$, *** $p < 0.001$.

3.2.8 *Data Availability*

The microarray and DNA methylation datasets generated during and/or analysed during the current study are available in the GEO repository, at https://www.ncbi.nlm.nih.gov/geo/query/acc.cgi?acc=GSE103427. Other data and samples are available from the corresponding author on reasonable request.

3.3 RESULTS

3.3.1 *ALDH1A3 AND ATRA ACTIVATE DIFFERENT TRANSCRIPTIONAL RESPONSES*

We have previously characterized that expression of the cancer stem cell marker ALDH1A3 can have opposing effects in two models of TNBC: it can promote the growth of MDA-MB-231 xenografts while limiting the growth of MDA-MB-468 xenografts. We also demonstrated that this was due to differing transcriptional profiles (Marcato et al., 2015). We determined that the effect of ALDH1A3 on the growth of MDA-MB-231 and MDA-MB-468 xenografts in mice may be attributed to the upstream role of ALDH1A3 in atRA-associated gene expression, as a retinaldehyde dehydrogenase.

To assess what proportion of the transcriptional response to ALDH1A3 could be attributed to atRA, we performed gene expression microarrays (Affymetrix HuGene 2.0 ST). We used MDA-MB-231 cells (with or without ALDH1A3 overexpression), MDA-MB-468 cells (with or without ALDH1A3 shRNA), and treated cells with atRA in triplicate. We first identified genes upregulated by ALDH1A3 (knockdown or overexpression) from our microarray data in both MDA-MB-231 and MDA-MB-468 (Figure 3-1A). The overlap between the two cell lines is small (DHRS3), suggesting that ALDH1A3 can activate divergent gene expression profiles in these two selected cell lines. We selected a number of these genes for validation (Figure 3-1B, C, D). Of note, qPCR validation identified additional genes which were regulated by ALDH1A3 in both cell lines (i.e. RARB, SCEL, PTGES, as in Figure 3-1C).

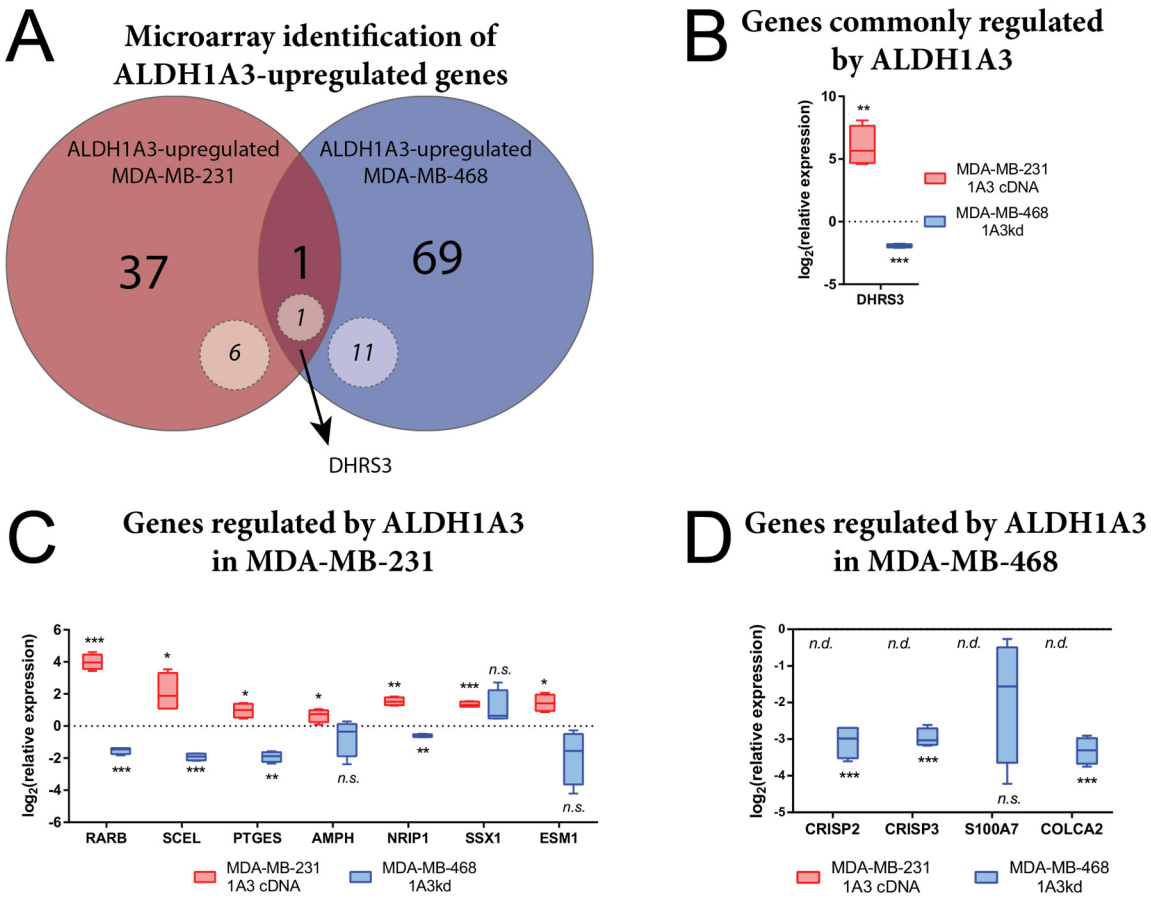

Figure 3-1 Microarray analysis identifies disparate transcriptional responses to ALDH1A3 manipulation in MDA-MB-231 and MDA-MB-468 cells.

A. Overlap of ALDH1A3-upregulated genes in MDA-MB-231 (ALDH1A3 cDNA / scramble vector) compared to MDA-MB-468 (scramble vector / ALDH1A3 shRNA knockdown). Gene-specific qPCR primers were used to validate genes regulated by ALDH1A3 in **B.** MDA-MB-231 and MDA-MB-468; **C.** MDA-MB-231 alone; and **D.** MDA-MB-468 alone. Statistical analysis was determined by paired student's t-tests (n=4). For all comparisons, * $p<0.05$, * $p<0.01$, *** $p<0.001$, *n.s.* not significant, and *n.d.* not detected.

We similarly identified genes upregulated by atRA treatment in MDA-MB-231 and MDA-MB-468 (Figure 3-2A) and validated the changes in expression of a number of these genes (Figure 3-2B, C, D). In almost all cases, qPCR validation supported the trends observed by microarray. Of note, according to the microarray data, SRPX2 was only upregulated by atRA in MDA-MB-468 (and not MDA-MB-231); however, in qPCR validation, even with atRA treatment, SRPX2 was below the limit of detection in MDA-MB-468 and was significantly induced by atRA in MDA-MB-231 (Figure 3-2D). The small number of genes consistently upregulated by atRA treatment in these two cell lines (Figure 3-2A) demonstrates that atRA can also activate divergent gene expression profiles depending on the cellular context (i.e. MDA-MB-231 versus MDA-MB-468).

To test our hypothesis that a substantial proportion of genes upregulated by ALDH1A3 could be attributed to transcriptional activation by atRA, we compared the ALDH1A3-upregulated genes with the atRA-upregulated genes (Figure 3-3). The overlap between the ALDH1A3-regulated genes and the RA-regulated genes is small but relevant in both MDA-MB-231 (Figure 3-3A) and MDA-MB-468 (Figure 3-3B). This demonstrates that exogenous application of atRA is not equivalent to manipulation of ALDH1A3 expression and suggests that ALDH1A3 may have atRA-independent effects on gene transcription.

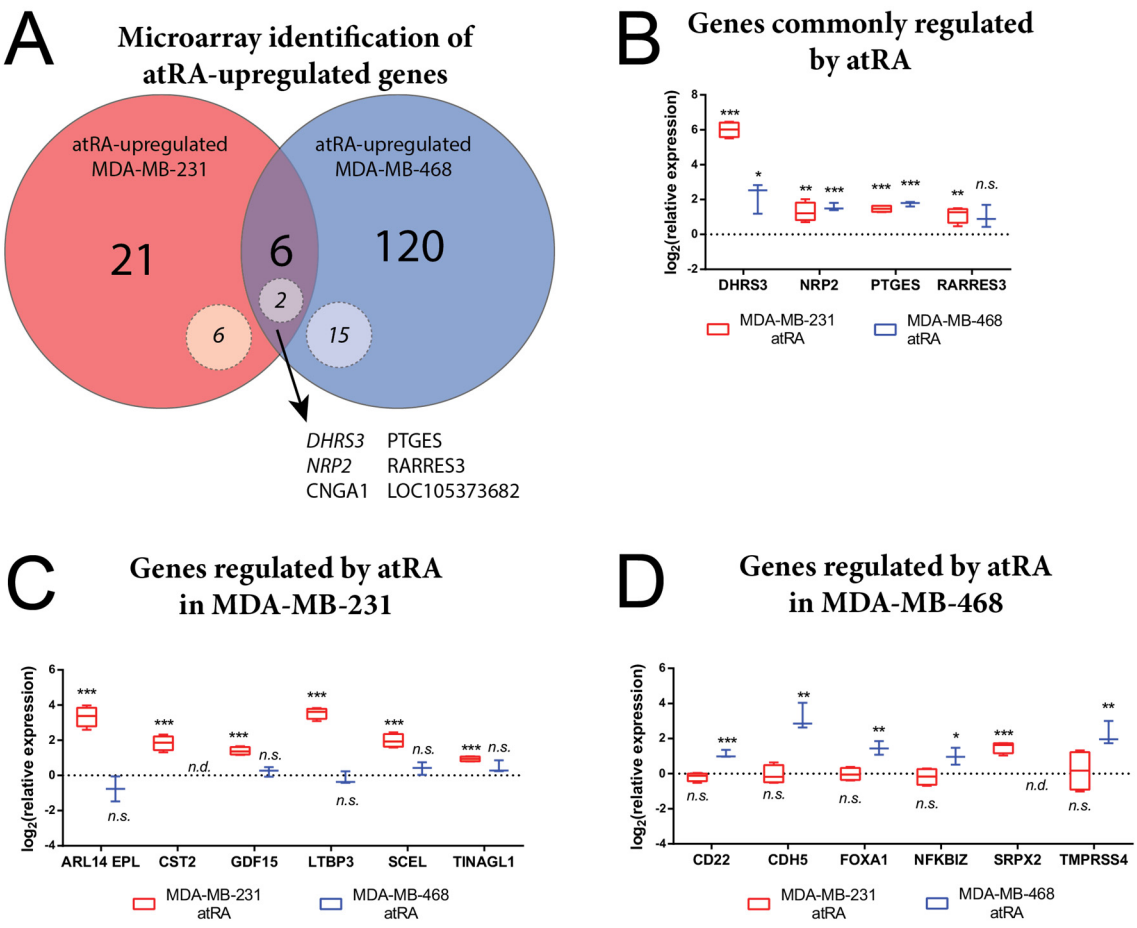

Figure 3-2 Microarray analysis identifies disparate transcriptional responses to atRA treatment in MDA-MB-231 and MDA-MB-468 cells.

A. Overlap of genes upregulated by 100 nM atRA in MDA-MB-231 and MDA-MB-468. Gene-specific primers were also used to validate the genes regulated by atRA in **B.** MDA-MB-231 and MDA-MB-468; **C.** MDA-MB-231 alone; and **D.** MDA-MB-468 alone. Statistical analysis was determined by paired student's t-tests (n=4 except for MDA-MB-468 where n=3). For all comparisons, * $p < 0.05$, * $p < 0.01$, *** $p < 0.001$, *n.s.* not significant, and *n.d.* not detected).

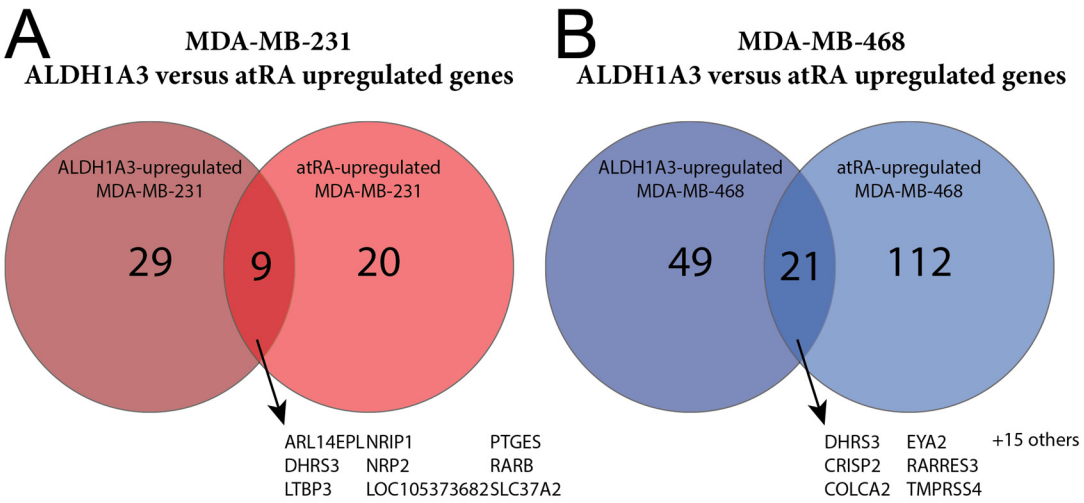

Figure 3-3 ALDH1A3 and atRA activate distinct transcriptional responses.

Comparison of ALDH1A3-upregulated and atRA-upregulated genes in **A.** MDA-MB-231 and **B.** MDA-MB-468.

It is possible that the differences between atRA-induced gene expression and ALDH1A3-induced gene expression is due to differences in the 'dosing' of atRA between exogenous application of atRA and expression of ALDH1A3 (i.e. genes may be upregulated by ALDH1A3 but not exceed the threshold set for differential expression). To eliminate this possibility, we compared all genes which were upregulated by either atRA or ALDH1A3 in either MDA-MB-231 or MDA-MB-468 (Figure 3-4). While there are several genes which are upregulated by both ALDH1A3 and atRA to different extents, this does not explain the majority of differences in gene expression. This indicates that a relevant subset of the ALDH1A3-regulated transcriptional response can be attributed to atRA, but that there is a significant proportion which cannot be attributed to atRA.

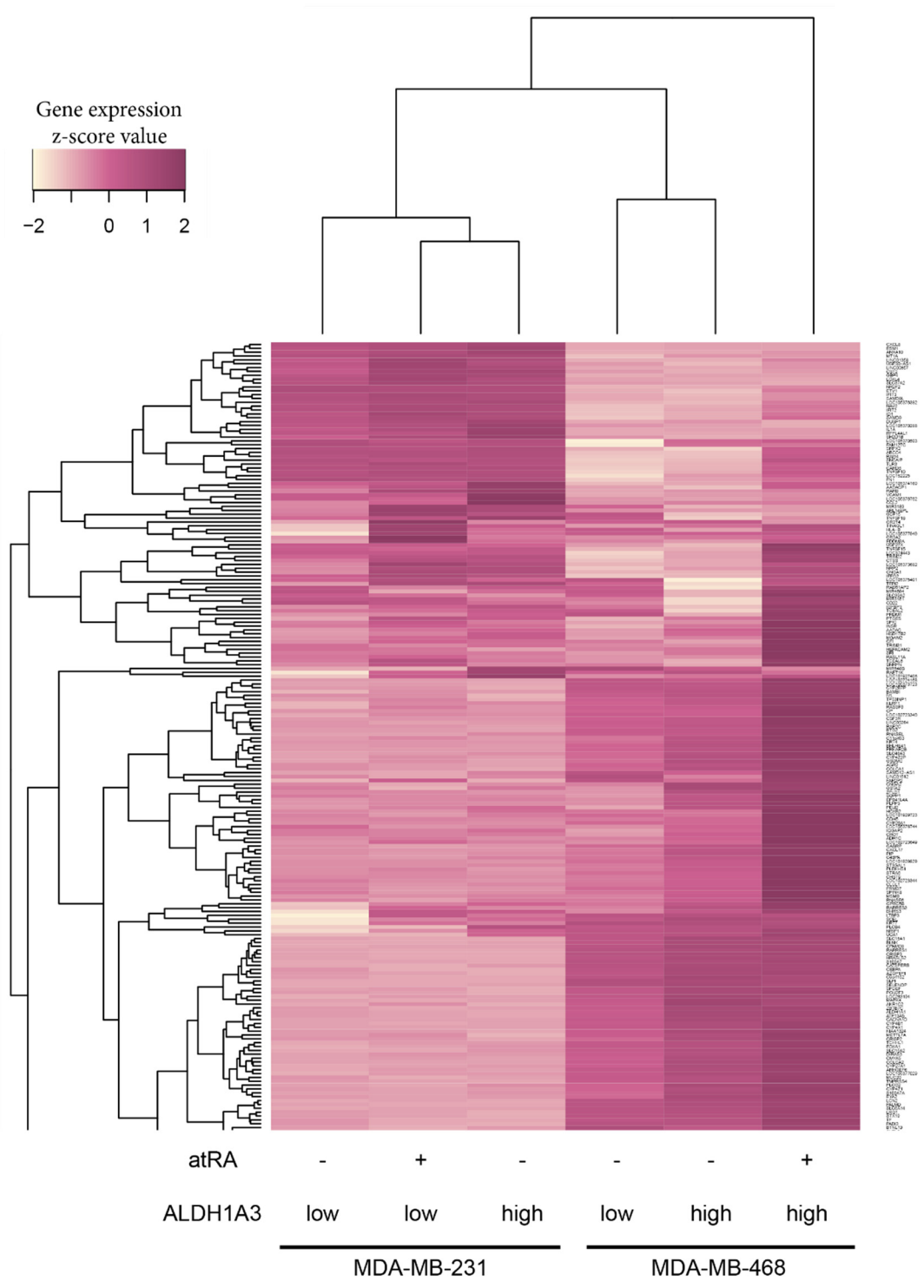

Figure 3-4 Hierarchical clustering of all genes regulated by atRA or ALDH1A3 in one or both cell lines.

Z-scores for each gene listed in the heatmap were taken and clustered by gene and sample using the heatmap.2 function in the R environment.

3.3.2 *Transcriptional Regulation by ALDH1A3 and atRA is Largely RARE-Independent*

We had previously described that the transcriptional response to ALDH1A3 was largely RARE-independent (Marcato et al., 2015). To confirm these findings in a new data set, we again identified genes with RAREs among those upregulated by ALDH1A3 in either MDA-MB-231 or MDA-MB-468 cells (dotted circles in Figure 3-1A). We compared the RARE sequences within 10 kb of a RARE DR5 predicted by *in silico* findings from Lalevée et al (Lalevée et al., 2011) and oPOSSUM (Kwon et al., 2012) using sequence logos (Figure 3-5, Table 3-2). The small number of genes identified within 10kb of a RARE DR5 (7 or 18.4% in MDA-MB-231, 12 or 17.1% in MDA-MB-468) and the nearly identical sequence logos allow us to conclude that the ALDH1A3-regulated transcriptional response is largely RARE-independent.

Given that ALDH1A3 appears to regulate the expression of a subset of genes independent of atRA, we hypothesized that a greater proportion of the transcriptional response to atRA would be primary and RARE-dependent. Among the atRA-upregulated genes, we again identified those genes which were located within 10kb of a RARE DR5 using data from Lalevée et al. (Lalevée et al., 2011) and oPOSSUM (Kwon et al., 2012) (Table 3-3). Only a small number of genes (8 or 29.6% in MDA-MB-231 and 17 or 13.5% in MDA-MB-468) were called as within 10kb of a RARE DR5. The small percentage of genes within regulatory distance of a RARE suggests that atRA-induced gene expression in these TNBC cell lines is primarily (>70%) RARE-independent. We generated TF logos from these genes (Figure 3-5). The logos all demonstrate a high degree of similarity with the core hexameric motif which comprises the RARE direct repeat, separated by 5 nucleotides (DR5): RGKTCA (Mader et al., 1993). This is

expected due to the methods to identify RARE-containing genes. Additionally, we noted no substantial variation between cell lines or between ALDH1A3-regulated or atRA-regulated genes. This suggests that there are no substantial preferences for minor variations in nucleotide sequence within the RARE DR5.

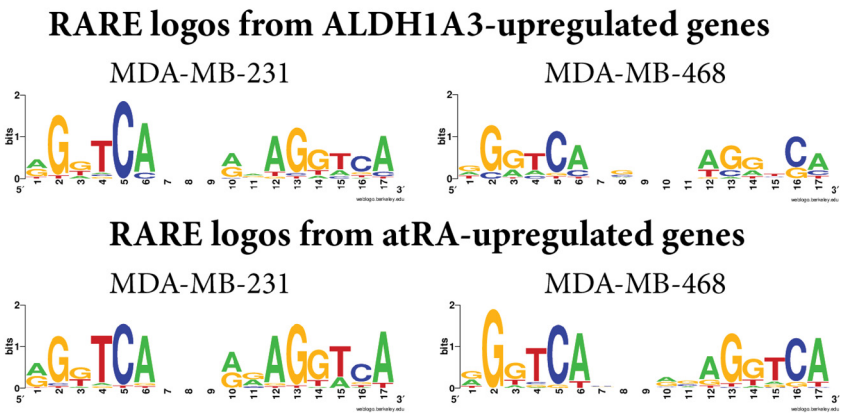

Figure 3-5 Similar sequence logos generated from ALDH1A3-and atRA-upregulated genes in two cell lines.

Sequence logos generated from all RAREs identified in ALDH1A3- or atRA-upregulated genes in MDA-MB-231 and MDA-MB-468.

Table 3-2 RARE sequences associated with ALDH1A3-upregulated genes.

Gene	RARE sequence
Associated with ALDH1A3-upregulated genes in MDA-MB-231	
CCL2	TGACCCCTCCTTCACCC
PTGFRN	TGAACCATTGATGACCC
DHRS3	GGTTCAGCCACAGGTCA
	GGGTCATGGAGAGGTCA
	AGGTCAGGGGAAGGACT
LTBP3	GTGTCATTGGGAGGTCA
NRIP1	AGGGCACCTGCAGTTCA
	AGTTCAACAGGAGGTAA
	AGGTCATTTAGAGGACA
	AGGTCACACAAAGGAGA
NRP2	AGGTCACTAAGGGGTCA
	AGTTCATTAAAATGTCA
	GGATCACAAAGAGGTGA
RARB	GGGTCATTTGAAGGTTA
	GGTTCACCGAAAGTTCA
	GGGTCACGGGCAGGTTA
Associated with ALDH1A3-upregulated genes in MDA-MB-468	
ALDH2	AGGTCAAGCTGAGTTGA
CEBPA	TGAACCAGAATTCACCC
CYP27A1	TGAACTTCTCTTCACCT
GSTA2	TCACCCTCGCCTGAACC
S100A7	GGGTGAAGTTGGGGTGA
S100A7A	TCACCCCAACTTCACCC
ARHGEF6	GGGTCAGGGGAAGGGGA
CACNA1D	GGGTTAGTGAGAGGTCA
	AGGACACGGAGAGGTCA
DHRS3	GGTTCAGCCACAGGTCA
	GGGTCATGGAGAGGTCA
	AGGTCAGGGGAAGGACT
EPB41L4A	AGGTCAGCATCAGGGCA
NFKBIZ	GGGTCATGGTGAAGTGA
PELI2	GGGTCACACACAGTTCA

Table 3-3 RARE sequences associated with atRA-upregulated genes.

Gene	RARE sequence
Associated with atRA-upregulated genes in MDA-MB-231	
ELF3	AGGTCAGAGGGAGGTCA
GBP4	TCAACTTGGAATGAACT
DHRS3	GGTTCAGCCACAGGTCA
	GGGTCATGGAGAGGTCA
	AGGTCAGGGGAAGGACT
LTBP3	GTGTCATTGGGAGGTCA
NRIP1	AGGGCACCTGCAGTTCA
	AGTTCAACAGGAGGTAA
	AGGTCATTTAGAGGACA
	AGGTCACACAAAGGAGA
NRP2	AGGTCACTAAGGGGTCA
	AGTTCATTAAAATGTCA
	GGATCACAAAGAGGTGA
RARB	GGGTCATTTGAAGGTTA
	GGTTCACCGAAAGTTCA
	GGGTCACGGGCAGGTTA
	AGTTCAACTAAAGTACA
TINAGL1	GGTTTGCAGGGAGGTCA
Associated with atRA-upregulated genes in MDA-MB-468	
ADH1C	GGGTCATTCAGAGTTCA
CYP26A1	GGGTCACAGGCGGGTCA
CYP27A1	TGAACTTCTCTTCACCT
FOXA1	TGACCTCCTCATGAACC
	AGGTCAGGGGGAGGGGA
SRPX2	TGACCTAAAGGTGAACT
STRA6	AGGTGAACCCAAGTTCA
TRIM31	AGGTCACAGCCAGTTCA
ARHGEF6	GGGTCAGGGGAAGGGGA
CLUL1	AGGTCACGCAAAGTTTA
CYP26A1	GGTTCACTAAGGGGTCA
	AGTTCACTCGGATGTCA
	GGGTCACAGGCGGGTCA
DHRS3	GGTTCAGCCACAGGTCA
	GGGTCATGGAGAGGTCA
	AGGTCAGGGGAAGGACT
EPB41L4A	AGGTCAGCATCAGGGCA
	GGTTCATGAGGAGGTCA
HOXB2	GGTTCAAGAAGAGTTCA
IFFO2	GGGTGTGGGGGAGGTCA
LRG1	TGGTCAGCTGGAGGTCA
	AGGGCAGGGGAGGGTCA

Gene	RARE sequence
Associated with atRA-upregulated genes in MDA-MB-468	
NAV2	TGGTCACTCACAGGTCA
	GGGGCAGGGACAGGTCA
NRP2	AGGTCACTAAGGGGTCA
	AGTTCATTAAAATGTCA
	GGATCACAAAGAGGTGA
PELI2	GGGTCACACACAGTTCA

3.3.3 *Epigenetic Silencing Restricts Transcriptional Response to atRA*

The utility of nuclear receptors depends on their ability to bind target DNA and activate transcription. We previously found that DNA methylation could restrict the expression of a number of ALDH1A3-inducible genes (Coyle et al., 2016; Marcato et al., 2015). Therefore, we hypothesized that DNA methylation may restrict the expression of potential atRA-inducible genes by preventing the induction of transcription and resulting in the disparate gene expression induced by atRA in MDA-MB-468 and MDA-MB-231 cells. To address this possibility, our microarray experiment also included three biological replicates treated with the cytidine analog and DNA methyl-transferase inhibitor, 5-aza-2'-deoxycytidine (also known as decitabine, DAC), alone or in combination with atRA treatment.

Next, we clustered the atRA-inducible genes in either cell lines based on their expression following atRA, DAC, or combination treatment (Figure 3-6). Of note, the 6 commonly upregulated genes did not cluster together (indicated with a red star). Although DAC did not globally enable atRA induction, we identified several clusters of genes where treatment with DAC appeared to enable atRA induction (indicated as "i", "ii", "iii", and "iv", Figure 3-6). The genes in these clusters, and the presence or absence of a RARE, are listed in Table 3-4. We selected several genes from these clusters for further investigation following treatment with atRA, DAC, and TSA, which inhibits class I and II histone deacetylases (HDACs). Among the genes we selected, GDF15 becomes atRA-inducible in the presence of DAC in MDA-MB-468 cells; CDH5 becomes atRA-inducible in the presence of DAC in MDA-MB-231 cells; and SCEL becomes atRA-inducible in the presence of DAC in MDA-MB-468 cells (Figure 3-7A).

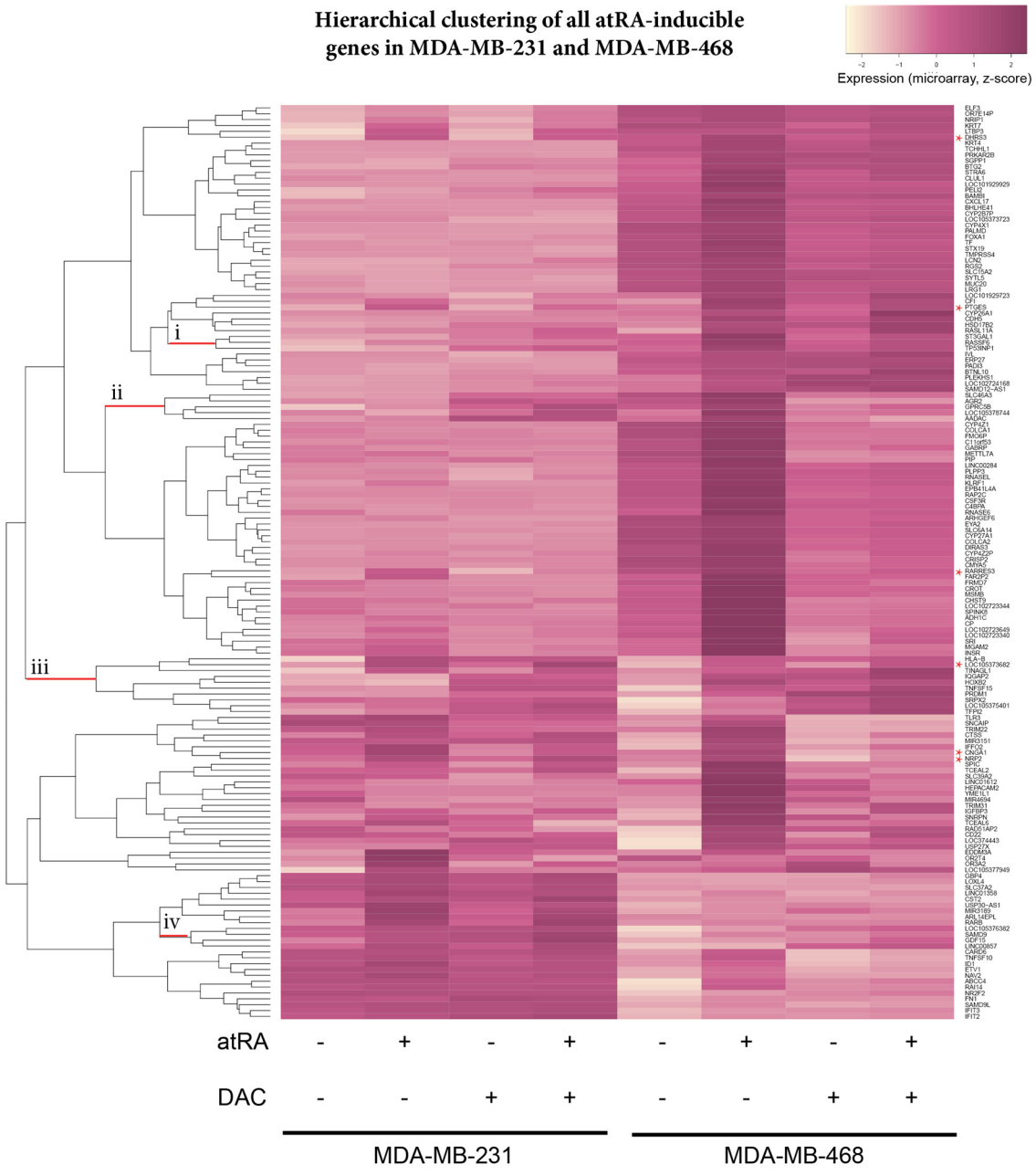

Figure 3-6 DAC treatment does not align atRA-induced transcriptional profiles.

Hierarchical clustering (heatmap.2, gplots) of microarray expression values from MDA-MB-231 and MDA-MB-468 cells treated with atRA, DAC, or both demonstrate that the use of DAC did not align the RA-inducible transcriptional profiles in these cell lines. Genes which were commonly upregulated in both cell lines are indicated by * on the right-hand side, while limited clusters of genes which displayed DAC-permissive atRA inducibility are indicated by lowercase Roman numerals. These genes are described in more detail in Table 3-4.

Table 3-4 Putative methylated atRA-inducible genes.

Cluster	Gene Symbol	RA-upregulated in?	RARE?
i	ST3GAL1	MDA-MB-468	
	RASSF6	MDA-MB-468	DR2 (Hosoda et al., 2015)
	TP53INP1	MDA-MB-468	
ii	SLC46A3	MDA-MB-468	
	AGR2	MDA-MB-468	
	GPRC5B	MDA-MB-468	
	LOC105378744	MDA-MB-468	
iii	HLA-B	MDA-MB-231	
	LOC105373682	MDA-MB-468 / MDA-MB-231	
	TINAGL1	MDA-MB-231	DR5 (oPOSSUM)
	IQGAP2	MDA-MB-468	
	HOXB2	MDA-MB-468	DR5 (oPOSSUM)
	TNFSF15	MDA-MB-468	
	PRDM1	MDA-MB-468	
	SRPX2	MDA-MB-468	DR5 (Lalevée et al., 2011)
	LOC105375401	MDA-MB-468	
	TFPI2	MDA-MB-468	
iv	LOC105376382	MDA-MB-468	
	SAMD9	MDA-MB-468	
	LINC00857	MDA-MB-231	

To further query the methylation of these genes, we utilized the HM450 array for MDA-MB-231 and MDA-MB-468 cells, with or without DAC treatment (GSE103425). We investigated the DNA methylation of GDF15, CDH5, and SCEL, using probes located +/−1500 bp from the transcription start site (TSS) (Figure 3-7B). Notably, while DAC has a substantial effect on expression of GDF15 in MDA-MB-468, only minor changes in methylation of GDF15 are seen with DAC treatment. The opposite is seen in CD22 and HOXB2, where DAC has substantial effects on DNA methylation, with no corresponding changes in gene expression (Figure 3-7C and D). Among those methylation-sensitive genes (i.e. GDF15, CDH5, and SCEL), we report no effect of atRA treatment on DNA methylation as measured by the HM450 array (Figure 3-7B). TSA did not appear to play a significant role in gene expression (except for TINAGL1 and PRDM1, Figure 3-8) which suggests that histone acetylation by HDACs 1, 3, 4, 6, or 10 is not a major contributory factor to the divergent gene expression profiles. The remainder of the genes investigated show no significant contributions of DAC treatment to the effects of atRA (e.g. GPRC5B, IQGAP2, Figure 3-8); however, there is a clear role for epigenetic regulation of expression in all genes examined.

Figure 3-7 Decitabine does not restore atRA inducibility of specific genes between cell lines.

A. MDA-MB-231 and MDA-MB-468 cells were treated with atRA, DAC, and/or TSA and relative expression of GDF15, CDH5, and SCEL were determined by qPCR. **B.** β-values representing the relative methylation (Illumina HM450 arrays) of distinct CpG sites in MDA-MB-231 and MDA-MB-468 cells treated with DAC are compared within 1500 bp of the transcription start site (TSS) for GDF15, CDH5, and SCEL; Similarly, **C.** relative expression and D. relative methylation for HOXB2 and CD22 are displayed. A. and C. A two-way analysis of variance was used to compare the effect of atRA treatment to the effects of DAC and/or TSA treatment (n=4, * $p < 0.05$, ** $p < 0.01$, *** $p < 0.001$). B. and D. n=3, GSE103425.

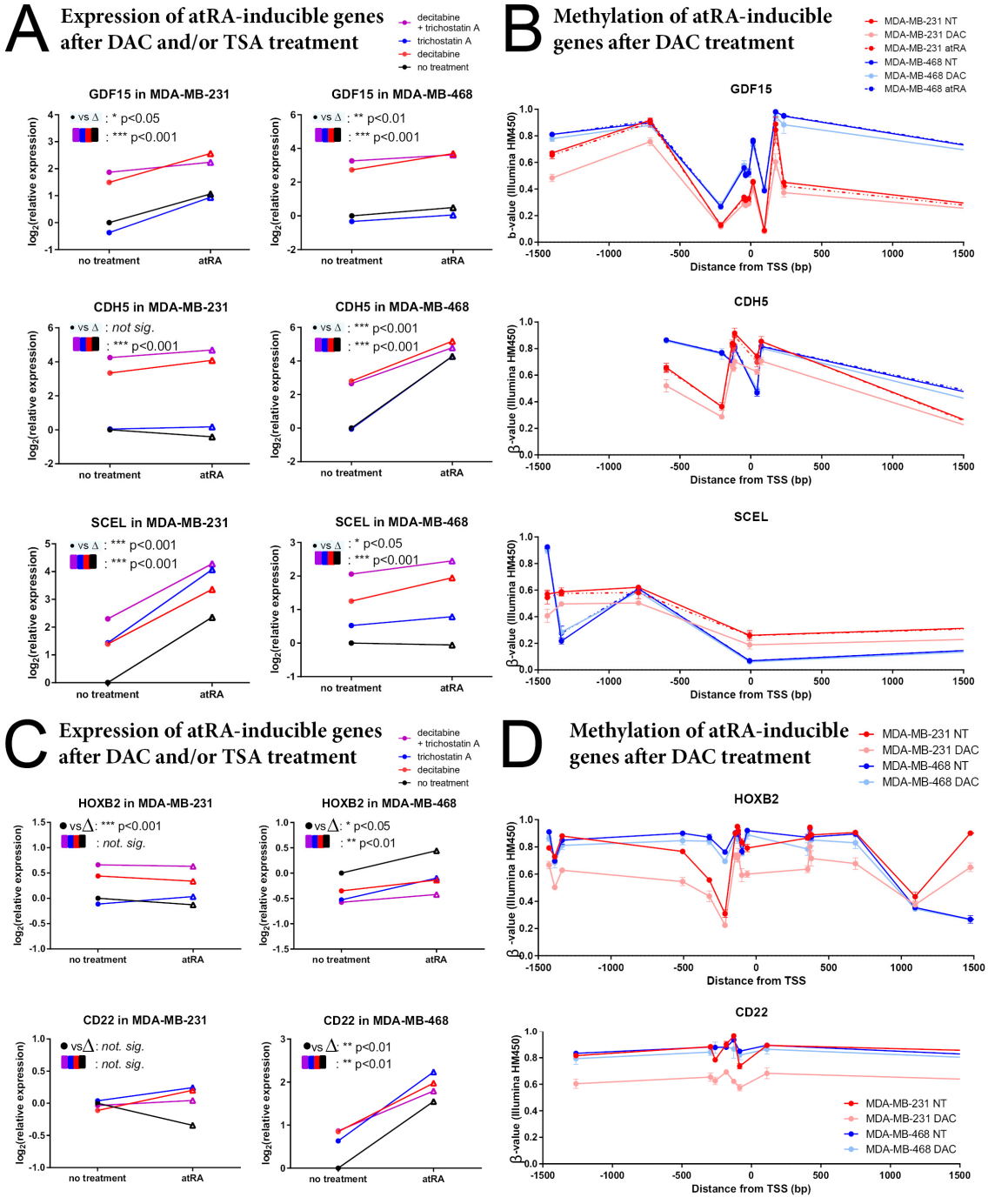

Figure 3-7 Decitabine does not restore atRA inducibility of specific genes between cell lines.

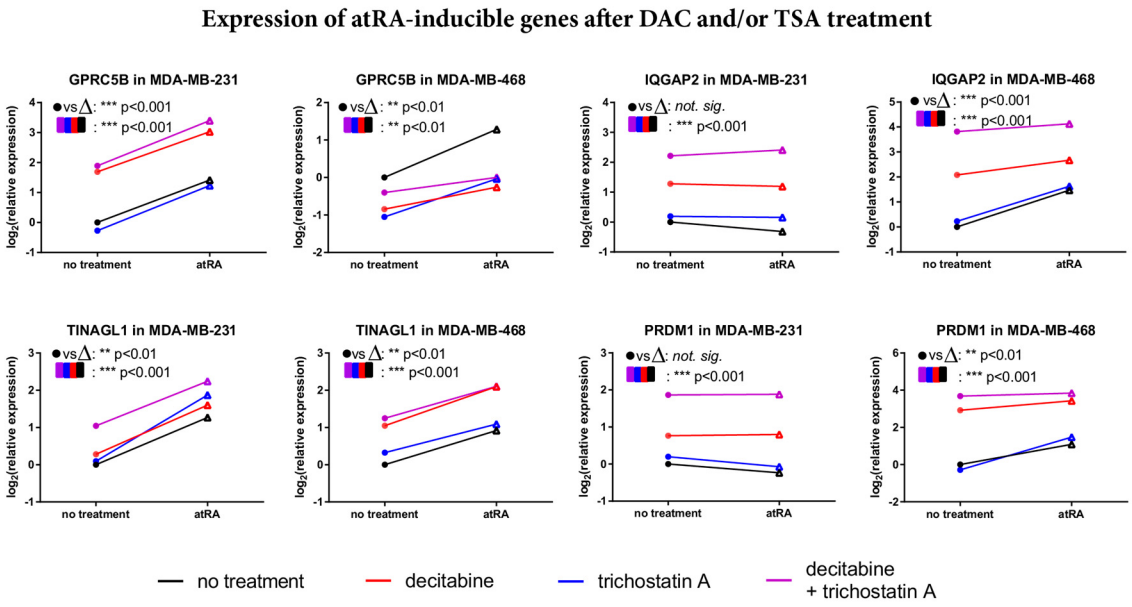

Figure 3-8 Changes in expression following DAC or atRA treatment are not accompanied by corresponding changes in DNA methylation.

qPCR was performed for GPRC5B, IQGAP2, TINAGL1, AND PRDM1 in MDA-MB-231 and MDA-MB-468 cells following treatment with combinations of atRA, decitabine and trichostatin A. Statistical significance was determined via a 2-way ANOVA (n=4; * $p < 0.05$; ** $p < 0.01$; *** $p < 0.001$).

Since these data suggested that DAC was unable to fully align the divergent transcriptional profiles, and that neither DNA methylation nor histone acetylation of the genes were concordant with the differences in mRNA expression, we then hypothesized that the expression of additional regulatory factors could be responsible for the differential transcriptional responses to atRA seen in these two TNBC models.

3.3.4 *IRF1 is Associated With atRA-Upregulated Genes in MDA-MB-231 and MDA-MB-468 Cells*

We used a discovery-motivated approach to identify potential regulatory transcriptional factors associated with the genes upregulated by atRA treatment in either MDA-MB-231 or MDA-MB-468. We used PASTAA (Predicting ASsociated Transcription factors from Annotated Affinities) (Roider et al., 2009) to identify transcription factors with high binding affinities within our upregulated gene lists. The top matrices in each cell line were identified and the corresponding transcriptional signatures. Using a cut-off of association > 2.0 and $p < 0.05$, 27 matrices were identified in MDA-MB-231 and 30 matrices were prioritized in MDA-MB-468 cells. This set of matrices corresponded to two lists of 19 and 21 transcription factors in MDA-MB-231 and MDA-MB-468 cells, respectively (Figure 3-9). Given that the genes upregulated by atRA were quite distinct (Figure 3-2A), it was not surprising that the transcription factors identified with high affinities for the gene lists from each cell line were also distinct. We also examined the transcription factors associated with down-regulated genes (summarized in Figure 3-10). Those with high association scores are consistent with previously published data which suggest that atRA can downregulate genes by interfering with promiscuous transcription factors such as AP1 (composed of a FOS/JUN heterodimer) (Benkoussa et al., 2002; Schüle et al., 1991).

Of note, the retinoic acid receptors α and β (RARα and RARβ) were only identified with high affinity in the MDA-MB-231 gene list. We did not investigate this canonical pathway as there is a substantial body of evidence indicating that methylation of RARβ contributes to differences in atRA-inducible transcription (Fazi et al., 2005; Xu et al., 1999; Zhang et al., 2004). It is also of interest that PPARα was only identified above our threshold in the MDA-MB-468 gene list. This suggests that redirection of atRA through FABP5 to PPARβ/δ is not a predominant mechanism for the promotion of tumor growth and proliferation by atRA in our model.

We identified interferon regulatory factor 1 (IRF1) and the myocyte enhancer factor 2 (MEF2) family of transcription factors as significantly associated with the gene lists from both MDA-MB-231 and MDA-MB-468 cells. atRA is known to activate MEF2C (Ren et al., 2007) and to induce expression of IRF1 (Luo and Ross, 2006). To prioritize further experiments, we then examined the expression of all indicated transcription factors in the microarray data (Figure 3-11). We selected IRF1 for further characterization due to its differential expression between MDA-MB-231 and MDA-MB-468 cells, an increase in expression following DAC treatment in MDA-MB-468 cells, and its RA-inducibility in both cell lines (Figure 3-11). In contrast, the MEF2 family of transcription factors showed no substantive response to RA (Figure 3-11).

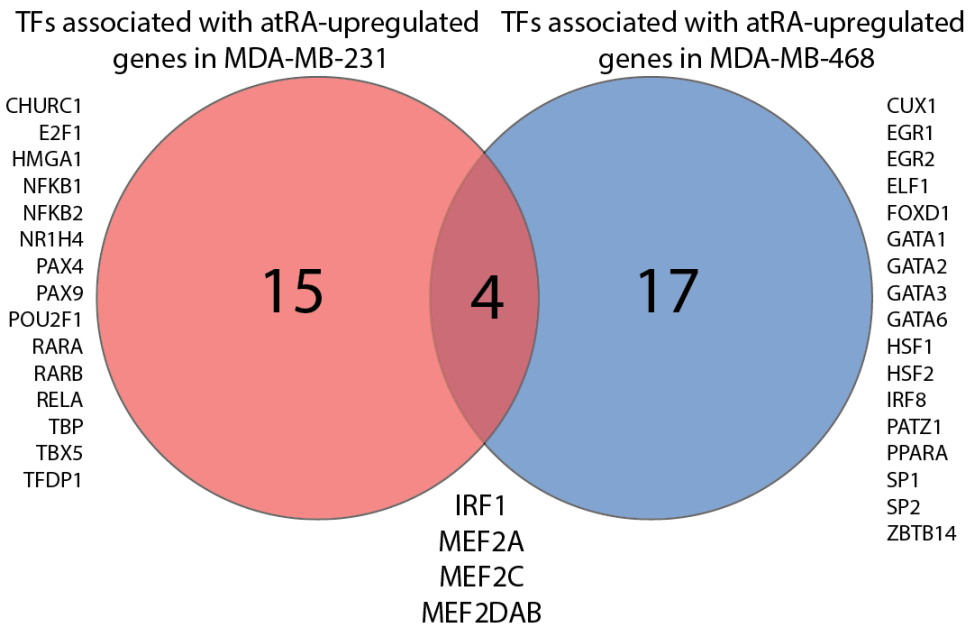

Figure 3-9 IRF1 is associated with atRA-upregulated genes in MDA-MB-231 and MDA-MB-468.

PASTAA analysis of transcription factor affinities identified disparate transcription factors associated with atRA-inducible genes in MDA-MB-231 as compared to MDA-MB-468.

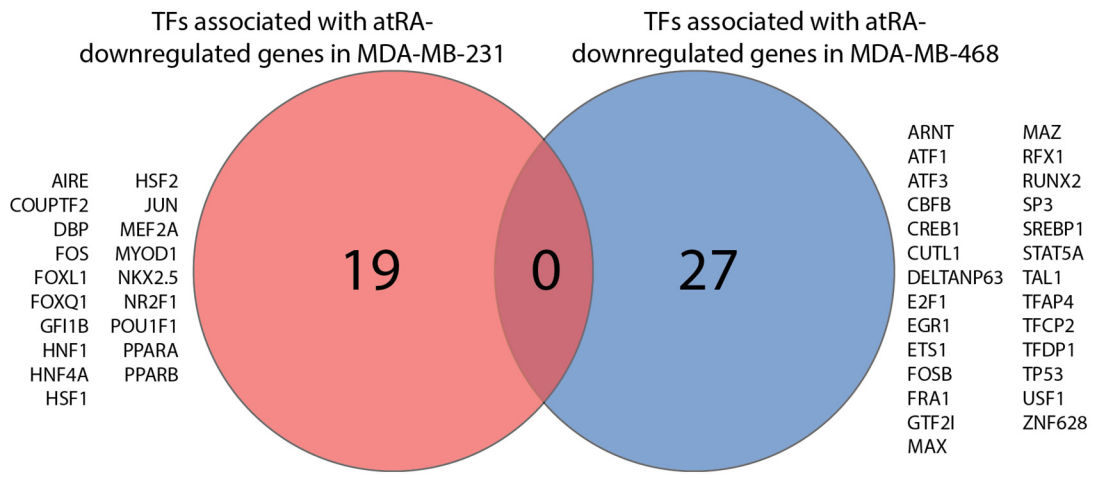

Figure 3-10 Transcription factors associated with atRA-downregulated genes are largely unrelated between MDA-MB-231 and MDA-MB-468 cells.

Transcription factors (TFs) identified by PASTAA analysis were compared between cell lines and the lack of overlap is demonstrated in a Venn diagram.

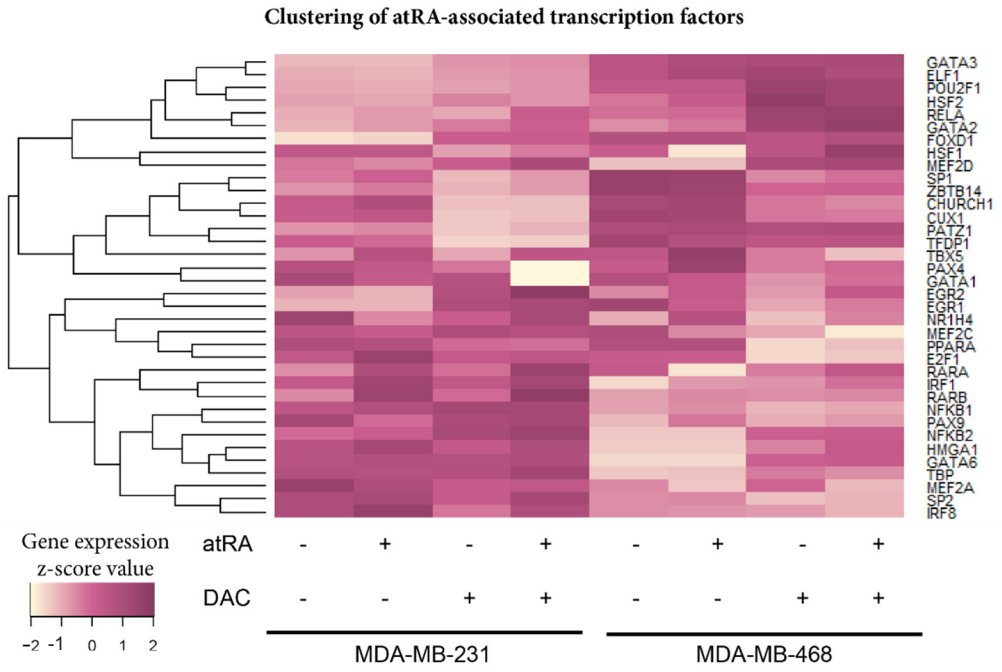

Figure 3-11 Hierarchical clustering of transcription factors associated with atRA-upregulated genes in MDA-MB-231 or MDA-MB-468 cells.

Z-scores for each transcription factor identified by PASTAA analysis (as in Figure 3-9) were taken and clustered by gene using the heatmap.2 function in the R environment.

IRF1 has been previously characterized with a RARE DR5; however, induction of IRF1 by atRA appears to be mediated by an interferon regulatory element (Pelicano et al., 1997). When we validated the expression by qPCR, we confirmed that IRF1 was more highly expressed in MDA-MB-231 cells (Figure 3-12A), and could be significantly induced by atRA in both cell lines (Figure 3-12B). Increased expression with DAC was only seen in MDA-MB-468 cells (Figure 3-12B). This suggests that differential expression of IRF1 may be a contributing factor to the divergent gene expression profiles in two TNBC cell line models. To confirm previous reports that the induction of IRF1 by atRA was independent of STAT1 (signal transducing activator of transcription 1) (Percario et al., 1999), we measured STAT1 mRNA expression in MDA-MB-231 cells following atRA treatment (Figure 3-12C). We observed no effect of atRA on STAT1 mRNA, suggesting that if atRA affects IRF1 expression via STAT1, it does so non-genomically.

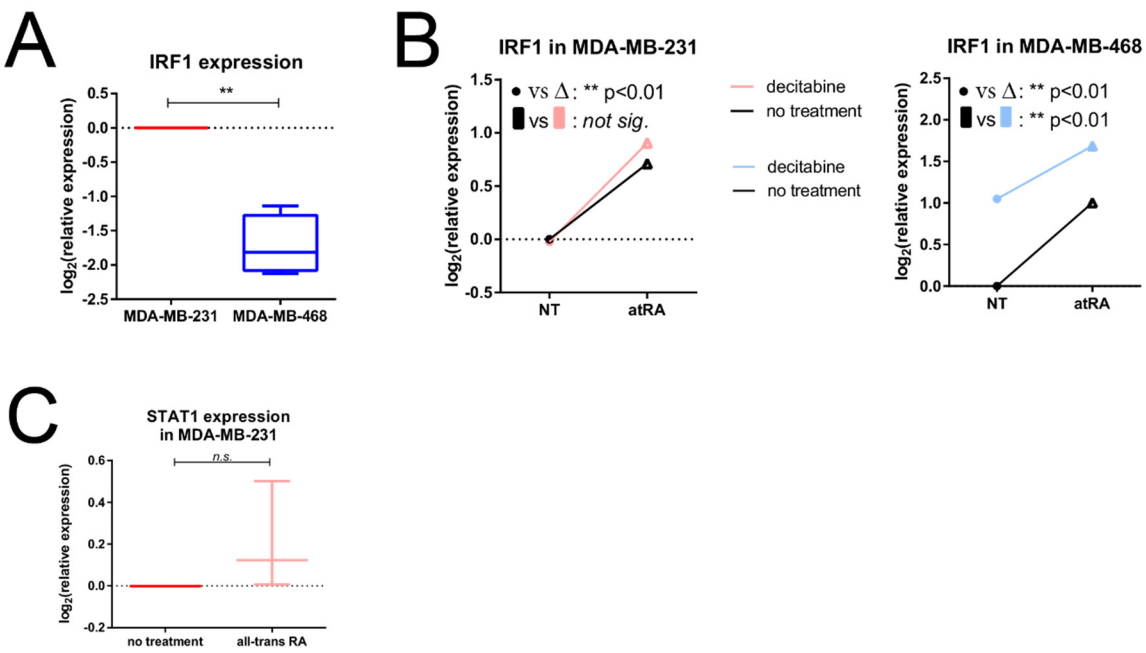

Figure 3-12 IRF1 is differentially expressed in MDA-MB-231 and MDA-MB-468 cells.

A. qPCR was used to detect expression of IRF1 in MDA-MB-231 and MDA-MB-468 cells. **B.** Relative expression of IRF1 following atRA and DAC treatment in MDA-MB-231 and MDA-MB-468 cells was determined by qPCR. A two-way analysis of variance was used to compare the effect of atRA treatment to the effect of DAC treatment. **C.** The expression of STAT1 was measured in MDA-MB-231 following atRA treatment and compared using a paired student's t-test. For all comparisons, * $p < 0.05$, ** $p < 0.01$, *n.s.* not significant.

3.3.5 *IRF1 Expression is Necessary for atRA Induction of CTSS Expression*

To further validate the role of IRF1 in differential RA transcriptional responses, we generated two shRNA knockdowns of IRF1 in MDA-MB-231 and MDA-MB-468 cells with varying efficiencies (Figure 3-13A). We then treated these vector-bearing cell lines with atRA and/or DAC, and measured the expression of several known IRF1 target genes (retinoic acid receptor response protein 3, RARRES3; guanylate binding protein 4, GBP4; and cathepsin S, CTSS) (Gravesande et al., 2002; Rettino and Clarke, 2013). Of these genes, RARRES3 and GBP4 possess RARE DR5s (Jiang et al., 2005; Lalevée et al., 2011). We demonstrate that although RARRES3 is more highly expressed in MDA-MB-468 cells, IRF1 knockdown has similar effects on its expression in both MDA-MB-231 and MDA-MB-468 cells (Figure 3-13B). Next, although GBP4 is more highly expressed in MDA-MB-231, IRF1 knockdown has similar effects on its expression in both cell lines (Figure 3-13C). We also examined the expression of TNFSF10 (tumor necrosis factor super family member 10; TNF-related apoptosis-inducing ligand, TRAIL), an important target of IRF1 transcription factor activity (Park et al., 2004), and determined that its expression in both MDA-MB-231 and MDA-MB-468 cells is largely IRF1-independent (Figure 3-13D).

Figure 3-13 IRF1 expression is required for CTSS expression in MDA-MB-231 cells.

A. shRNA knockdowns of IRF1 were generated in MDA-MB-231 and MDA-MB-468. Values were compared using a one-way analysis of variance with repeated measures (n=4). Expression of **B.** RARRES3, **C.** GBP4, **D.** TNFSF10, and **E.** CTSS was compared between MDA-MB-231 and MDA-MB-468 cells. Statistical significance was determined by paired student's t-test. Gene expression was measured in shRNA knockdowns following treatment with atRA and/or DAC. A two-way analysis of variance was used to determine the effect of IRF1 knockdown compared to atRA/DAC treatment (n=4). For all comparisons, n=4; * $p < 0.05$; ** $p < 0.01$; *** $p < 0.001$.

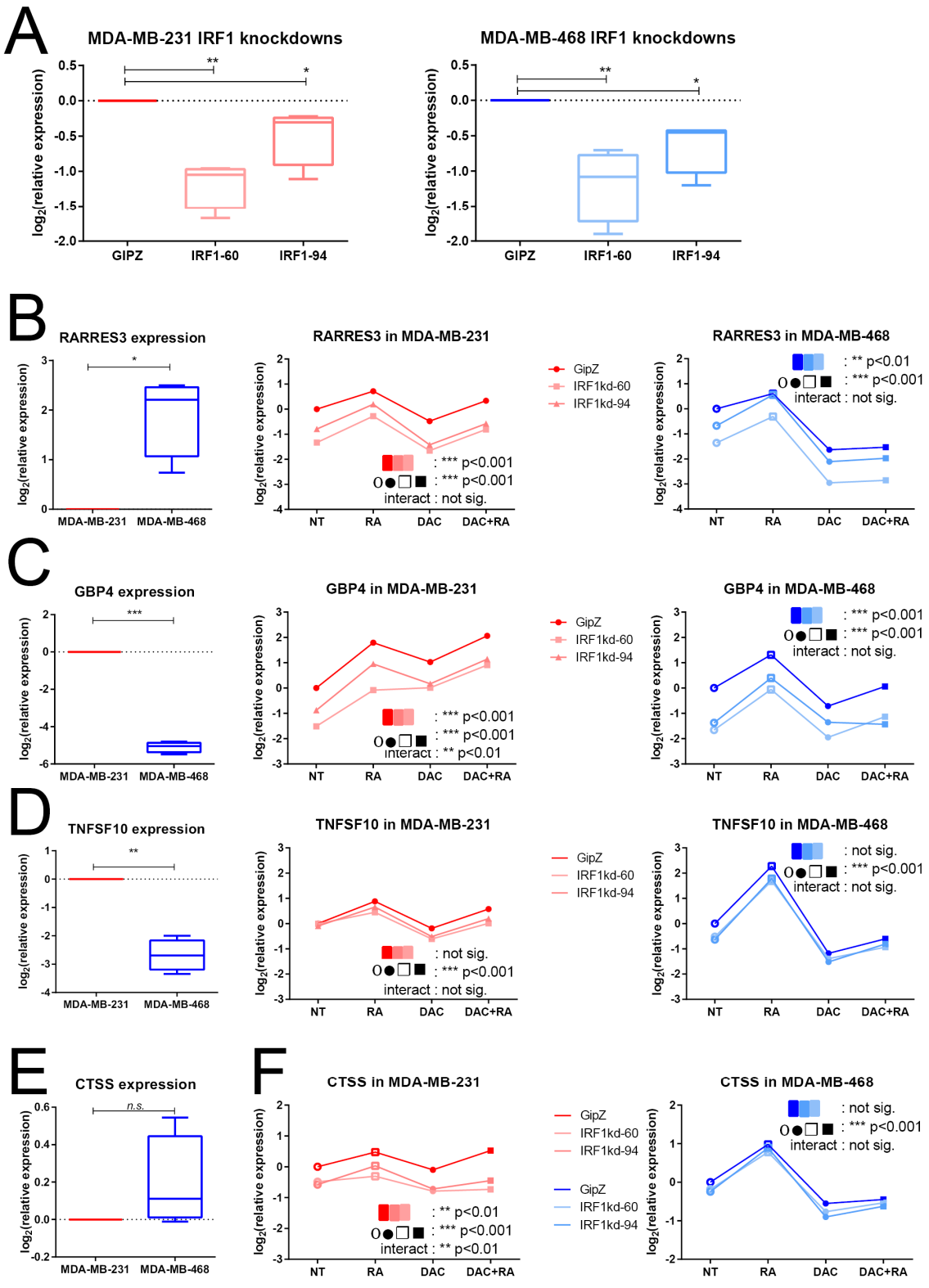

Figure 3-13 IRF1 expression is required for CTSS expression in MDA-MB-231 cells.

Of note, IRF1 expression was required for CTSS expression in MDA-MB-231 but not in MDA-MB-468 cells (Figure 3-13F). IRF1 expression was also required for full atRA-induced CTSS expression in MDA-MB-231 cells. While neither DAC nor TSA induced changes in CTSS expression (Figure 3-14A), CTSS displays differential methylation between MDA-MB-231 and MDA-MB-468 (Figure 3-14B). Our findings that IRF1 expression contributes to the regulation of RARRES3, GBP4, and CTSS, but not to the regulation of TNFSF10, are further validated by mRNA expression data from breast cancer patients. We observe strong correlations of IRF1 expression with GBP4 and CTSS, but only a weak correlation with RARRES3 and TNFSF10 expression (Figure 3-15).

In addition to the contributions of DNA methylation to the expression of atRA-inducible transcripts such as GDF15, CDH5, and SCEL, these findings demonstrate that baseline expression of additional regulatory transcriptional factors such as IRF1 can be sufficient to activate divergent transcriptional profiles in cells.

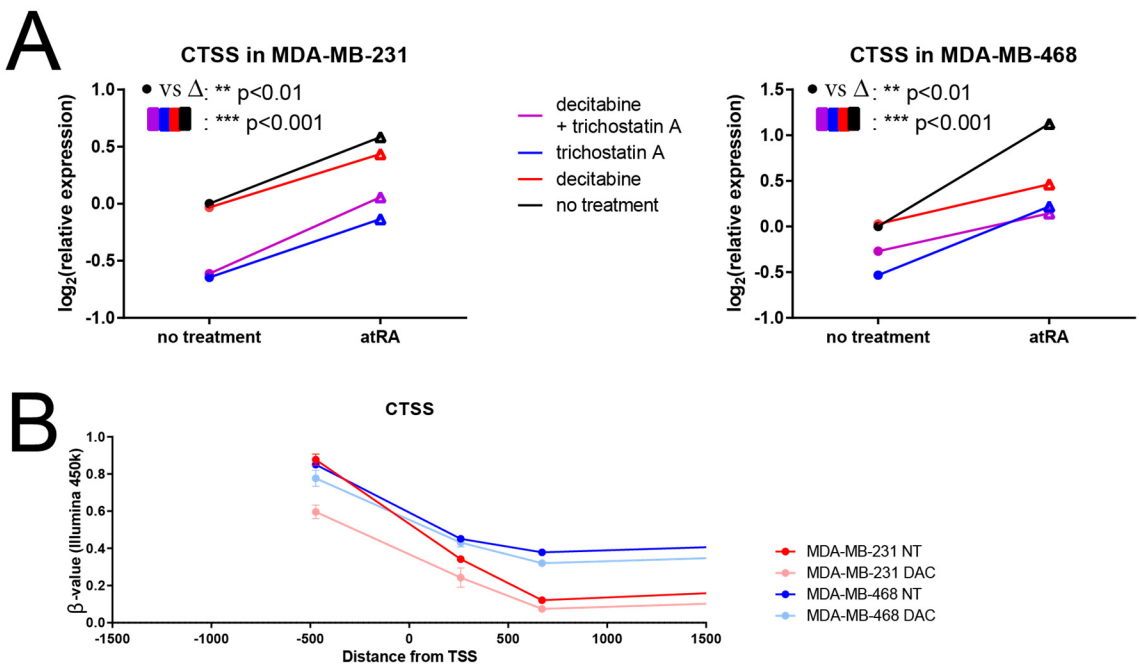

Figure 3-14 CTSS does not display significant epigenetic silencing.

A. MDA-MB-231 and MDA-MB-468 cells were treated with DAC and/or TSA and CTSS expression was measured by qPCR. Values were compared with a two-way analysis of variance (n=4). **B.** β-values representing the relative methylation (Illumina HM450 arrays) of distinct CpG sites in MDA-MB-231 and MDA-MB-468 cells treated with DAC are compared within 1500 bp of the transcription start site (TSS) (n=3, GSE103425). For all statistical comparisons, * $p < 0.05$, ** $p < 0.01$, *** $p < 0.001$.

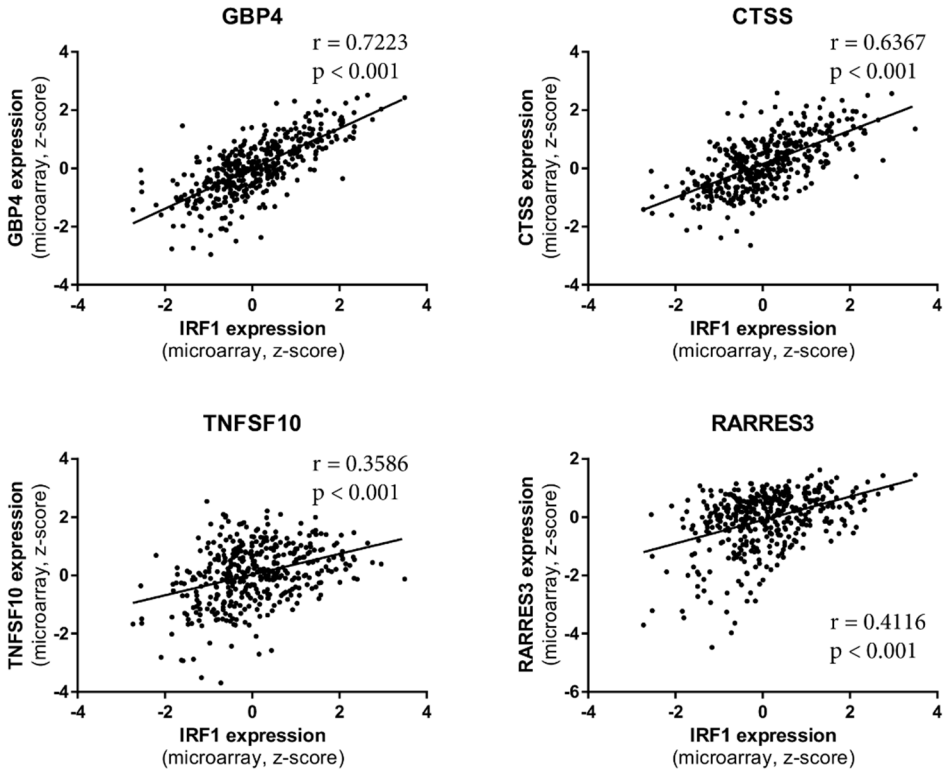

Figure 3-15 IRF1 expression strongly correlates with CTSS and GBP4 expression in breast cancer patient tumors.

The expression of IRF1 target genes CTSS, GBP4, TNFSF10, and RARRES3 in 421 breast cancer patient tumors are plotted against IRF1 expression (Ciriello et al., 2015). Correlation and significance are indicated for each plot.

3.4 DISCUSSION

Mechanisms of RARE-independent RA-mediated gene regulation have been proposed. For example, atRA can regulate gene expression via *trans*-mechanisms, such as interaction of the RARs with the transcription factors of other signaling pathways (e.g. estrogen receptor, ER, in ER^+ breast cancer cells) (Hua et al., 2009; Ross-Innes et al., 2010). RA-activated RARs can also act as epigenetic modifiers, altering chromatin structure and thus gene expression (Basu et al., 2017; Bhattacharyya et al., 1997; Kashyap et al., 2013). Through interactions with transcription complex proteins, RA bound RARs influence the addition or removal of epigenetic marks, such as histone methylation and acetylation, and DNA methylation. Interestingly, we did not see evidence of changes in gene methylation upon induction of gene expression by atRA, while we did note instances where DNA methylation contributes to differential RA-mediated gene expression. However, while promoter methylation contributes to the restricted atRA-inducible transcriptional responses in TNBC MDA-MB-231 and MDA-MB-468 cells, our data suggests that it is the expression of other regulatory factors such as IRF1 which mediate the expression of genes without RAREs. In fact, both atRA and DAC appear to modulate IRF1 expression in these cell lines. While most of this work focused on coding transcripts, several long non-coding RNAs were identified including linc00857 (upregulated in MDA-MB-231). Further work on understanding the regulation of non-coding transcripts by RA, and their subsequent regulation of the coding genome, will be important to contextualize the full cellular genomic context and cellular response to RA. This provides further evidence that the response of breast cancer cells to atRA is primarily non-classical, and indicates an area needing additional investigation if the full potential of atRA as a cancer therapeutic is to be achieved.

We further characterized the transcriptional response to ALDH1A3 manipulation by comparing it to atRA and DAC treatment in two TNBC cell lines. Although ALDH1A3 is characterized primarily as a retinaldehyde dehydrogenase, we identified limited overlap between the ALDH1A3-upregulated and the atRA-upregulated transcriptional profiles in both cell lines. While we and others have demonstrated a clear role for ALDH1A3 in initiating retinoid signaling and affecting the expression of RARE-containing genes including RARβ, the tumor suppressor gene RARRES1, and tissue transglutaminase (Coyle et al., 2016; Marcato et al., 2015; Sullivan et al., 2017), the sole contribution of ALDH1A3 as a retinaldehyde dehydrogenase in breast cancer and the stem cell phenotype (cancerous or non-cancerous) may be overstated (Chute et al., 2006; Duan et al., 2016; Ginestier et al., 2009; Marcato et al., 2011b, 2015; Thomas et al., 2016). Alternate functions of ALDH1A3 may contribute to breast cancer progression and stem-cell activity. We note that atRA has been used as an ALDH inhibitor in cancer stem cell studies (Croker and Allan, 2012; Young et al., 2015); however, considering that we demonstrate some overlap between ALDH1A3 and atRA regulated genes in breast cancer cells, the regulation of ALDH enzymes with atRA is likely to confound studies of the biological effects of ALDH1A3. The regulation of ALDH1A3 by atRA is likely to be context-dependent (Kedishvili, 2013).

One possible explanation is that other potential substrates of ALDH1A3 may further account for the observed discrepancies between transcriptional profiles in this study, including those involved in glycolysis (Mao et al., 2013) and the oxidation of lipid peroxidation-derived aldehydes (Singh et al., 2015, 2013). Additionally, the mouse ALDH1A3 (also known as RALDH3) has a high affinity for octanal, decanal, and

hexanal (Graham et al., 2006), which can affect gene expression (Lee et al., 2012) . There is a high degree of structural similarity between the ALDH1A isoforms, so ALDH1A3 may have yet uncharacterized enzymatic substrates, including 9-cis retinal (Moretti et al., 2016). These additional substrates may explain the lack of concordance between the ALDH1A3-induced and atRA-induced transcriptional profiles.

We demonstrate that the pleotropic effects of atRA on breast cancer cells may be related to non-genomic and multi-layered pathways; and restricting analysis of atRA-responsiveness in breast cancer to canonical RARE-containing genes limits the biological relevance. The cellular context of breast cancer cells (i.e. the expression of atRA-inducible transcription factors) is a major contributing factor to the divergent responses observed to atRA.

3.5 Acknowledgements

Support was provided by grant funding to PM from the Canadian Institutes of Health Research (CIHR, MOP-130304), the Beatrice Hunter Cancer Research Institute (BHCRI), the Breast Cancer Society of Canada, and the QEII Health Sciences Center Foundation. KMC and MLT are supported by studentship or trainee awards from the BHCRI, Canadian Breast Cancer Foundation, and the Canadian Imperial Bank of Commerce. KMC and MLT are supported by CGS-D awards from CIHR, by the Nova Scotia Health Research Foundation, and by the Killam Trusts at Dalhousie University. MLT is supported by NS Research and Innovation Graduate Scholarships.

CHAPTER 4: DNA METHYLATION AND GENE EXPRESSION AS BIOMARKERS FOR ALL-*TRANS* RETINOIC ACID THERAPY IN TRIPLE-NEGATIVE BREAST CANCER

This chapter will be submitted as: Coyle KM, Dean C, Giacomantonio CA, Helyer L, Marcato P. DNA methylation and gene expression as biomarkers for all-trans retinoic acid therapy in triple-negative breast cancer.

Contribution statement

I designed the experiments, analyzed the data, and wrote the manuscript with the guidance of Dr. Paola Marcato. I collected data with assistance as follows: Cheryl Dean, maintenance of clinical samples; Dr. Carman Giacomantonio and Dr. Lucy Helyer, collection of clinical samples.

4.1 INTRODUCTION

While breast cancer is commonly represented as one disease, it is highly heterogeneous. Many studies have observed molecular heterogeneity, which is associated with distinct drug responses and clinical outcomes (Ciriello et al., 2015; Curtis et al., 2012; Parker et al., 2009; Prat et al., 2010; Shah et al., 2012; The Cancer Genome Atlas Network, 2012). These classification approaches demonstrate consensus that basal-like and/or triple-negative breast cancers (TNBCs) have worse prognoses. TNBC is a diagnosis of exclusion, encompassing all breast cancers which lack expression of the estrogen receptor (ER) and progesterone receptor (PR), and lack amplification of the human epidermal growth factor receptor 2 (HER2). Thus, TNBC is itself a heterogeneous designation, and the molecular subtyping of TNBC can further identify distinct subtypes including luminal, basal-like, claudin-low or mesenchymal, and HER2-like (Lehmann et al., 2016, 2011; Parker et al., 2009; Prat et al., 2010; Prat and Perou, 2011).

All-*trans* retinoic acid (atRA) is clinically used in the treatment of acute promyelocytic leukemia (Huang et al., 1988; Lo-Coco et al., 2013), and has potential as a therapeutic option for breast cancer (Garattini et al., 2014; Marcato et al., 2015; Seewaldt et al., 1995; Toma et al., 2000a). However, clinical studies with atRA have demonstrated limited success, and recent preclinical work has demonstrated a high degree of variability in the response of breast cancers to atRA treatment. A review of past studies broadly characterizes TNBC as retinoid-resistant based on *in vitro* evaluation (Table 4-1). A thorough study characterizing the effects of atRA on TNBC *in vivo* has not yet been performed any may reveal effects not predictable based on predominantly *in vitro* approaches.

Table 4-1 Literature summary details varied responses of TNBC cell lines to retinoids.

TNBC cell line	Evaluation	Model	References
HCC1937	**Resistant**	In vitro	(Centritto et al., 2015; Wei et al., 2015)
SUM159	**Resistant**	In vitro	(Merino et al., 2016)
	Sensitive	Tumorsphere	(Ginestier et al., 2009)
		In vivo (intermediate)	(Merino et al., 2016)
SUM149	**Resistant**	Tumorsphere	(Wu et al., 2017, p. 2)
		In vitro	(Merino et al., 2016)
	Sensitive	Tumorsphere	(Ginestier et al., 2009)
HCC70	Sensitive	In vitro (intermediate)	(Centritto et al., 2015)
MDA-MB-453	**Resistant**	In vitro	(Centritto et al., 2015; Takatsuka et al., 1996; Tari et al., 2002)
MDA-MB-468	**Resistant**	In vitro	(Centritto et al., 2015; Liu et al., 1996)
		In vivo	(Marcato et al., 2015)
	Sensitive	In vivo	(Wei et al., 2015)
BT20	**Resistant**	In vitro	(Centritto et al., 2015; Liu et al., 1996)
		Tumorsphere	(Wu et al., 2017, p. 2)
HCC1806	Sensitive	In vitro (intermediate)	(Centritto et al., 2015; Lin et al., 2017)
HCC38	**Resistant**	In vitro	(Centritto et al., 2015)

TNBC cell line	Evaluation	Model	References
MDA-MB-231	**Resistant**	In vitro	(Centritto et al., 2015; Lin et al., 2017; Liu et al., 1996; Merino et al., 2016; Takatsuka et al., 1996; Wu et al., 1997)
		Tumorsphere	(Wu et al., 2017, p. 2)
		In vivo	(Merino et al., 2016)
	Promoted	In vivo	(Marcato et al., 2015)
	Resistant *(13-cis RA)*	*In vivo*	*(Halter et al., 1988)*
	Sensitive	In vivo In vitro (intermediate)	(Wei et al., 2015)
	Sensitive *(retinol, retinyl palmitate)*	*In vivo*	*(Fraker et al., 1984; Halter et al., 1988)*
Du4475	**Resistant**	In vitro	(Centritto et al., 2015)
HCC1187	*No evidence*		
MDA-MB-436	**Resistant**	In vitro	(Centritto et al., 2015)

N.B. 'Intermediate' refers to a classification of intermediate sensitivity

Retinoid-based therapies have low systemic toxicity, and the side-effects of atRA in treatment of APL are predominantly attributed to the differentiation of promyelocytes. This positions atRA as an under-utilized clinical agent which may be of benefit to patients with breast cancer if profiled accurately for response. We have previously demonstrated that atRA has varied effects on tumor growth: promoting the growth of MDA-MB-231 and MDA-MB-435 xenografts, while inhibiting the growth of MDA-MB-468 xenografts in the context of low ALDH1A3, induced by shRNA knockdown (Marcato et al., 2015). The present work further characterizes the response of TNBC cell line xenografts to systemic atRA treatment and identifies sensitive, resistant, and tumor-promoted phenotypes. We have previously demonstrated that some of the heterogeneity in the transcriptional responses of MDA-MB-231 and MDA-MB-468 cells to atRA can be attributed to variations in DNA methylation (Coyle et al., 2017b), and further investigate the contributions of DNA methylation to atRA sensitivity. We utilize the phenotypes determined in this thesis to supervise the determination of differential gene expression and DNA methylation in atRA-sensitive cell lines and demonstrate a profile of limited predictability for atRA sensitivity.

We validate our predictive DNA methylation profile, but not gene expression in predicting the response of four TNBC patient-derived xenografts (PDXs) to systemic atRA treatment. Our work demonstrates that atRA may be a clinically relevant choice for patients with TNBC and supports further consideration of atRA as a therapeutic option for TNBC. This also provides a paradigm for the utilization of differential DNA methylation as a predictive indicator of drug response.

4.2 Materials and Methods

4.2.1 *Ethics Statement*

All experiments were conducted in accordance with the Canadian Council on Animal Care standards and protocols approved by Dalhousie University Committee on Laboratory Animals (#15-013 and #17-011). PDX A and B patient samples were collected and analyzed in accordance with protocol #1007106, approved by the IWK Health Centre Research Ethics Board.

4.2.2 *Cell Culture and Reagents*

All cell lines were obtained from the American Tissue Type Collection (ATCC) and maintained as previously described (Coyle et al., 2016). Where indicated, all-trans retinoic acid (atRA, Sigma) was used at 100 nM for 18 h.

4.2.3 *Cell-Line Xenografts*

One day prior to tumor-cell implantation, experimental mice were implanted with a slow-release atRA pellet (5 mg / 60 days, Innovative Research of America). Cells were admixed 1:1 with high concentration Matrigel (BD Bioscience), and injected orthotopically into the mammary fat pad of female NOD-*scid* mice (HCC38, HCC70, MDA-MB-436, MDA-MB-453, HCC1187, BT20, HCC1937, Du4475: 5 x 10^6 cells/mouse; MDA-MB-231, MDA-MB-468, SUM159, SUM149: 2 x 10^6 cells/mouse; and HCC1806: 1 x 10^5 cells/mouse). Primary tumor volume was quantified (mm^3, length x width x depth / 2) for the duration of the experiment. Tumor-bearing mice were euthanized and tumor weight quantified.

4.2.4 *Patient-Derived Xenografts*

PDX A and B were derived from patients at the QEII Health Sciences Center (QEII HSC, Halifax). Surgical biopsies from primary tumors were harvested and stored in DMEM with 10% FBS for < 1 h until implantation. 2-3 mm^3 pieces were sutured to the thoracic mammary fat pad of female NOD-*scid* mice. Palpable tumors developed, after which mice were euthanized, tumors harvested, and 2-3 mm^3 pieces were successively implanted.

PDX C (BCM-3887) and PDX D (BCM-2665) were obtained from the laboratory of Dr. Michael Lewis (Baylor College of Medicine) as frozen samples (Zhang et al., 2013). Upon receipt, they were surgically implanted into the mammary fat pad of female NOD-*scid* mice for expansion, and subsequently preserved in liquid nitrogen.

4.2.5 *Quantitative PCR*

Total RNA was extracted using Trizol reagent and the PureLink RNA kit (Invitrogen) with DNase treatment. Equal amounts of RNA were reverse-transcribed using iScript (BioRad), and quantitative real-time PCR (qPCR) was performed using gene-specific primers (Table 4-2). Standard curves for each primer set were generated, and primer efficiencies were incorporated into the CFX Manager software (Bio-Rad). mRNA expression of all samples was calculated relative to two reference genes, glyceraldehyde 3-phosphate dehydrogenase (GAPDH) and β-2-microglobulin (B2M).

Table 4-2 Primers utilized for qPCR.

Gene Symbol	Primer Sequence (5' -- 3')		Reference
ALDH1A1	F	TGTTAGCTGATGCCGACTTG	(Marcato et al., 2011b)
	R	TTCTTAGCCCGCTCAACACT	
ALDH1A2	F	CTGGCAATAGTTCGGCTCTC	(Marcato et al., 2011b)
	R	TGATCCTGCAAACACTGCTC	
ALDH1A3	F	TCTCGACAAAGCCCTGAAGT	(Marcato et al., 2011b)
	R	TATTCGGCCAAAGCGTATTC	
ALDH8A1	F	TGGTGAGCATAGGTGCTCTG	(Marcato et al., 2011b)
	R	GTTATCACCGTGGGAAGCAT	
CRABP2	F	ACTGACCAACGATGGGGAAC	
	R	ACTCTCGGACGTAGACCCTG	
CRBP1	F	GTCGACTTCACTGGGTACTGG	
	R	GCTTCAGCAAGTTGGCGATT	
CYP26A1	F	TGTTGATCGAGCACTCGTGG	
	R	TCAGAGATGTGGCTGCACTG	
CYP26B1	F	CATGGGCTTCCCGCTCAT	
	R	TGGATCTTGGGCAGGTAACTC	
CYP26C1	F	GTTCCCTTCAGTGGCCTACG	
	R	CTTCTCAGAAATGGCCCCCTC	
EP300	F	ATCCAGGGCCTAACATGGGA	
	R	AGGCATCATCTGGTTTGGCA	
FABP5	F	CACAGCTGATGGCAGAAAAACT	
	R	CTTCCCATCCCACTCCTGATG	
NCOR2	F	CTGAAGCCACTGTCAACAACAG	
	R	ATTCTGCCCTGTGTCCTTGG	
RARα	F	CGGGTGATCACGCTGAAGAT	
	R	GGCCCTCTGAGTTCTCCAAC	
RARβ	F	GGTTTCACTGGCTTGACCAT	(Marcato et al., 2015)
	R	GGCAAAGGTGAACACAAGGT	
RARγ	F	CTGGAGATGGATGACACCGAG	
	R	GCTTGTCCACTTTTTCGGGC	
RXRα	F	CCAAGACCGAGACCTACGTG	
	R	CCACTCCACCAGGGTGAAAA	
RXRβ	F	TCCTCCTTGCCACAGGTCTT	
	R	GAGGGACCGATCAAAGATGGC	
RXRγ	F	GTTGTGAAGGCTGCAAAGGG	
	R	CGCTGACGCTTGTCAATGAG	
GAPDH	F	GGAGTCAACGGATTTGGTCGTA	(Marcato et al., 2015)
	R	TTCTCCATGGTGGTGAAGAC	
B2M	F	AGGCTATCCAGCGTACTCCA	(Coyle et al., 2016)
	R	CGGATGGATGAAACCCAGACA	

4.2.6 *Preparation of Cells from PDXs*

PDX-bearing mice were euthanized, and tumors harvested. Tumors were minced and incubated in collagenase (BioShop Canada Inc., 225 U/mL in HBSS, Invitrogen) at 37°C on an end-over-end shaker. After 2 h, cell suspension was passed through a 70 µm strainer (Fisher Scientific) and centrifuged for 5 min at 500 xg. Cells were resuspended in red blood cell lysis buffer (150 mM NH_4Cl, 10 mM $KHCO_3$, 0.1 mM Na_2EDTA). After 5 min, cells were centrifuged, resuspended in PBS, and passed through a 70 µm strainer. Cells were centrifuged, resuspended in Aldefluor buffer (Stem Cell Technologies, Inc.), and passed through a 70 µm strainer. Approximately 1 x 10^7 cells were incubated with anti-H-2Kd (1:1000 SF1-1.1, BioLegend) at 37°C with shaking. After 1 h, cells were centrifuged and resuspended in Aldefluor buffer with 7-AAD (1:10, eBioscience). Stained cells were gated on SSC and FSC to eliminate doublets. 7-AAD$^-$ H-2Kd$^-$ cells were sorted into ice-cold PBS with 5% BSA (Sigma-Aldrich). H-2Kd purity was assessed (FACS Aria).

4.2.7 *Preparation of Cell Line Samples for Oligonucleotide Arrays and Analysis*

TNBC cells were treated with atRA; total RNA was extracted as described. Sample preparation, amplification, hybridization to the Affymetrix HuGene 2.0 ST array, and data collection were performed by The Centre for Applied Genomics at the Hospital for Sick Children (Toronto, Ontario, Canada) and data will be accessible through the GEO repository. HuGene 2.0 ST data for MDA-MB-231 and MDA-MB-468 cells with and without atRA treatment was obtained from GSE103426 (Coyle et al., 2017b). Expression data was analyzed in the R environment using the oligo package with RMA normalization (Carvalho and Irizarry, 2010).

HM450 data for all cell lines was obtained from GSE78875 (Coyle et al., 2016), and analyzed in the R environment using the minfi package with functional normalization (Aryee et al., 2014; Fortin et al., 2014).

4.2.8 *Preparation of Patient-Derived Xenografts for Oligonucleotide Arrays and Analysis*

DNA was extracted from human cells using the PureLink DNA kit (Invitrogen), according to manufacturer's instructions. Sample preparation, bisulfite conversion, hybridization to the Illumina EPIC array (PDX C and D), and data collection were performed by The Centre for Applied Genomics (TCAG) at the Hospital for Sick Children (Toronto, Ontario, Canada) and will be accessible in the GEO repository. HM450 data (PDX A and B) was obtained from GSE78875 (Coyle et al., 2016). HM450 and EPIC data was analyzed in R with the minfi package and functional normalization (Fortin et al., 2017).

RNA was extracted from human cells of PDX A and B using Trizol reagent and the PureLink RNA kit (Invitrogen) with DNase treatment. Sample preparation, labelling, and hybridization to the Affymetrix HuGene 2.0ST array was performed by TCAG and will be accessible through the GEO repository. Normalized data from PDX C and D (Agilent UNC PerouLab 244K Custom Human Array version 5) was obtained from www.bcxenograft.org.

4.2.9 *Subtyping of Patient-Derived Xenografts*

Normalized gene expression data was obtained as described (section 4.2.7). PDXs were subtyped using SSP2003 *via* the genefu package in the R environment (Gendoo et

al., 2016; Sørlie et al., 2003). The claudin-low classification algorithm was also applied in genefu (Prat et al., 2010).

4.2.10 *cBioPortal Analyses*

Data from TCGA (Ciriello et al., 2015) was extracted using cBioPortal. Only those 533 patients with complete RNAseq and HM450 data were utilized (Cerami et al., 2012; J. Gao et al., 2013). Spearman's correlations were calculated between RNAseq and HM450 methylation.

4.2.11 *Statistical Analyses*

All statistical analyses beyond those described in section 4.2.7 were conducted with GraphPad Prism 6.0. Tumor weights were compared by student's t-test. The molecular subtype and the presence of alterations in driver genes were compared between sensitive cell lines and all remaining cell lines by a Fisher's exact test.

4.3 RESULTS

4.3.1 *BREAST CANCER CELL LINES DISPLAY A WIDE RANGE OF* IN VIVO *RESPONSES TO ATRA*

We have previously found that ALDH1A3 has opposing effects during the *in vivo* development of MDA-MB-231 and MDA-MB-468 cell line xenografts, via its generation of atRA (Marcato et al., 2015), and hypothesized that the response of TNBC xenografts to atRA may depend on the subtype: claudin-low TNBCs would be promoted by atRA, while basal-like TNBCs would be effectively treated with atRA. To test this hypothesis, we characterized the *in vivo* response of 13 TNBC cell lines (including MDA-MB-231 and MDA-MB-468) to atRA treatment by measuring resulting tumor volumes and final tumor weights. Based on the fold-change of final tumor weight, we characterized 4 as atRA-promoted (MDA-MB-231, Du4475, HCC1187, and MDA-MB-436; Figure 4-1A), 4 as atRA-resistant (MDA-MB-468, BT20, HCC1806, and HCC38; Figure 4-1B), and 5 as atRA-responsive (HCC1937, SUM159, SUM149, HCC70, and MDA-MB-453; Figure 4-1C). These experiments are summarized as single data points based on tumor weight (Figure 4-2A).

Since a Fisher's exact test revealed no significant relationship between molecular subtype and sensitivity to atRA (see Figure 4-2A), we compared the mutational profiles of these cell lines using data from the Cancer Cell Line Encyclopedia (CCLE) and other sources (Barnabas and Cohen, 2013; Barretina et al., 2012; Elstrodt et al., 2006) to determine if there were any obvious mutations which were correlated with atRA sensitivity. We found no correlation between mutations in breast cancer driver genes TP53, PIK3CA, MYC, PTEN, GATA3, RB1, BRCA1, or BRCA2, and sensitivity to atRA (Figure 4-2B).

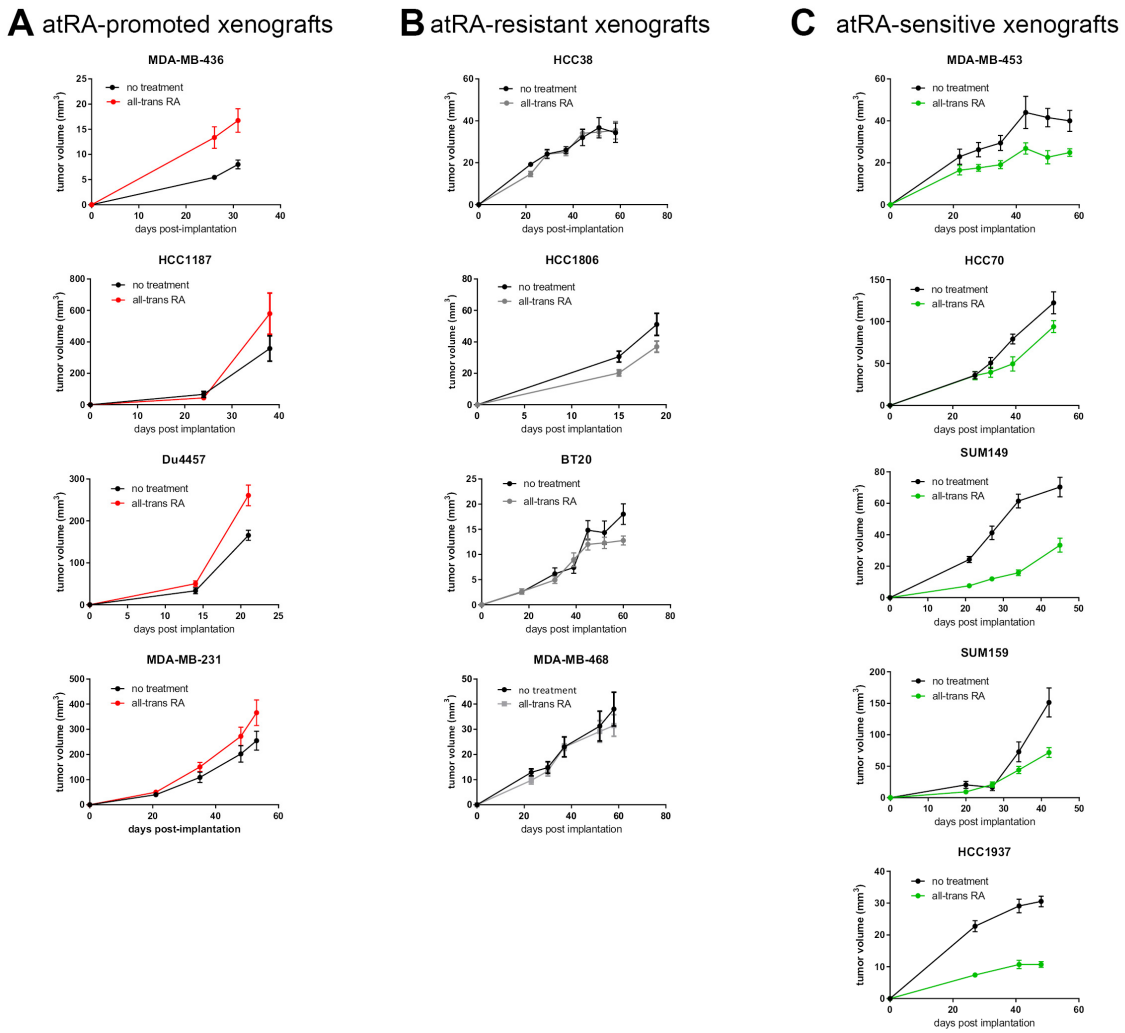

Figure 4-1 TNBC cell line xenografts display varied responses to atRA treatment.

Treatment of TNBC cell line xenografts with 5 mg / 60 day slow-release atRA pellets identified distinct phenotypes of **A.** atRA-promoted, **B.** atRA-resistant, and **C.** atRA-sensitive.

Figure 4-2 Classical retinoid signaling components do not correlate with atRA sensitivity in TNBC.

A. Cell line xenografts are summarized from Figure 4-1 based on their response to atRA treatment. Values represent fold-change in tumor weight, compared by student's t-test (* $p < 0.05$, ** $p < 0.01$, *** $p < 0.001$). **B.** Characterization of known mutations in cell lines from existing databases; dashed line represents distinction for Fisher's exact test. **C.** mRNA expression of FABP5 and CRABP2 was determined by qPCR and the ratio plotted. mRNA expression of **D.** RARα, β, γ and RXRα, β, γ, **E.** ALDH1A1, ALDH1A2, ALDH1A3, and ALDH8A1 was determined by qPCR. **F.** Changes in expression of ALDH isoforms after atRA treatment are represented by color gradient.

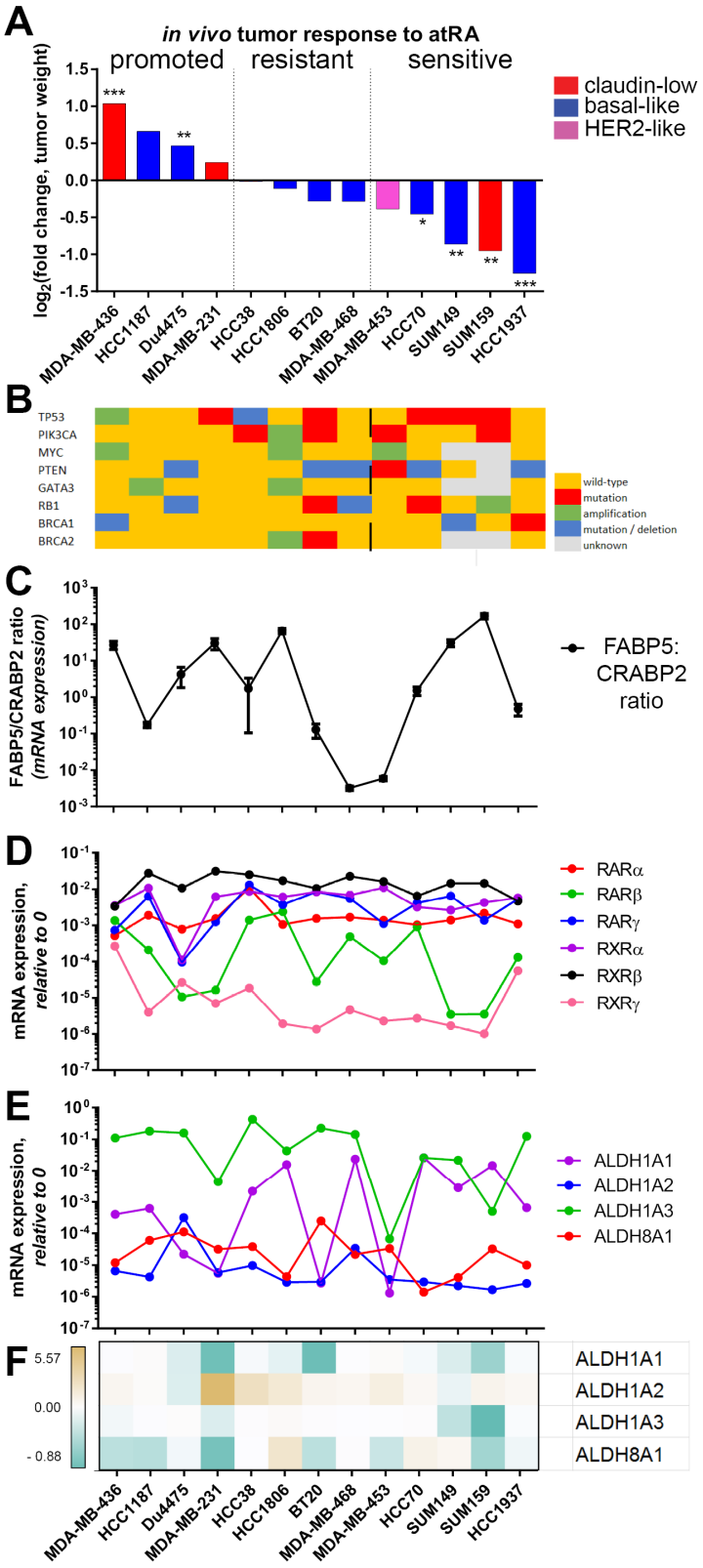

Figure 4-2 **Classical retinoid signaling components do not correlate with atRA sensitivity in TNBC.**

4.3.2 *Expression of Retinoid Pathway Genes does not Correlate With atRA Sensitivity*

Having found no correlation between atRA sensitivity and existing molecular subtypes or driver mutations, we next considered the hypothesis that the expression of retinoid processing and signaling genes dictates the response of breast cancers to atRA treatment. A primary hypothesis for differential effects of atRA is shuttling of atRA by FABP5 in the absence of CRABP2 to peroxisome proliferative response elements (PPREs) in the genome, as opposed to retinoic acid response elements (RAREs) (Schug et al., 2007, 2008). In contrast, we find no correlation between the FABP5:CRABP2 ratio and atRA sensitivity (Figure 4-2C, absolute expression shown in Figure 4-3A).

Another hypothesized determinant of atRA sensitivity is expression and methylation of RARβ2 (Liu et al., 1996); therefore, we queried both mRNA expression and DNA methylation. We found no relationship between the expression of any RAR or RXR isoforms and atRA sensitivity in the TNBC cell lines profiled (Figure 4-2D). Additionally, there was no significant correlation between RARβ methylation and atRA sensitivity (Figure 4-4). This suggests that while RAR or RXR expression may approximate sensitivity in luminal or HER2-like breast cancer (Centritto et al., 2015; Hayashi et al., 2003; Liu et al., 1996; Schneider et al., 2000), it does not carry the same weight in TNBCs.

We confirmed that ALDH1A3 is the most predominant retinaldehyde dehydrogenase mRNA expressed in TNBC (Figure 4-2E), except for HCC70 and SUM159. While the expression of retinaldehyde dehydrogenases may contribute to stemness properties in breast cancer, there is no correlation between atRA sensitivity and

the expression of ALDH1A1, ALDH1A2, ALDH1A3, or ALDH8A1 (Figure 4-2E); or with differential expression of these isoforms following atRA treatment (Figure 4-2F).

For a more comprehensive evaluation, we similarly profiled the expression of other retinoid processing and signaling genes (CYP26A1, CYP26B1, CYP26C1, CRBP1, NCOR2, and EP300) and identified no significant correlations with atRA sensitivity (Figure 4-3). These findings demonstrate that atRA sensitivity in TNBC is dependent on other factors which are likely independent of the classical retinoid signaling pathway.

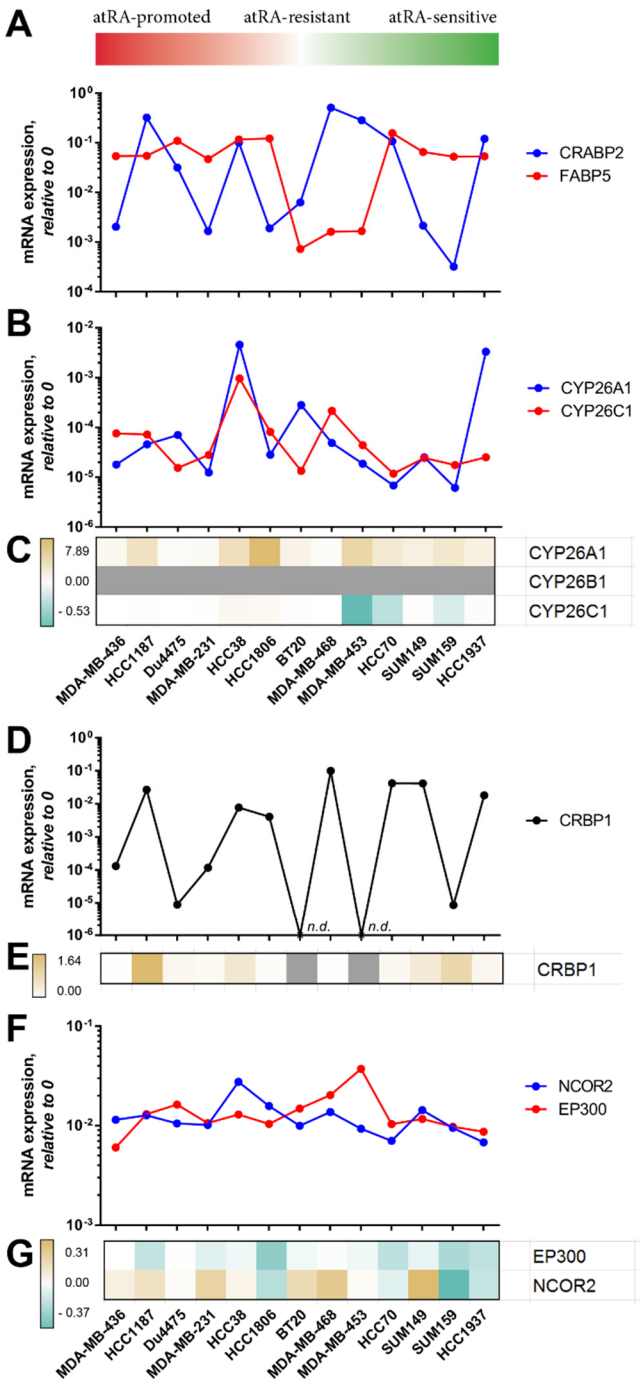

Figure 4-3 Expression of retinoid pathway genes does not correlate with atRA sensitivity.

mRNA expression of **A.** CRABP2 and FABP5 and **B.** CYP26 isoforms A1, B1, and C1. **C.** The response of CYP26 isoforms to *in vitro* atRA treatment **D.** mRNA expression of CRBP1. **E.** Response of CRBP1 to atRA treatment. **F.** mRNA expression of corepressor NCOR2 and coactivator EP300 was determined. **G.** Response of NCOR2 and EP300 to atRA. atRA response demonstrated by color gradients. (grey, *n.d.* not detected.)

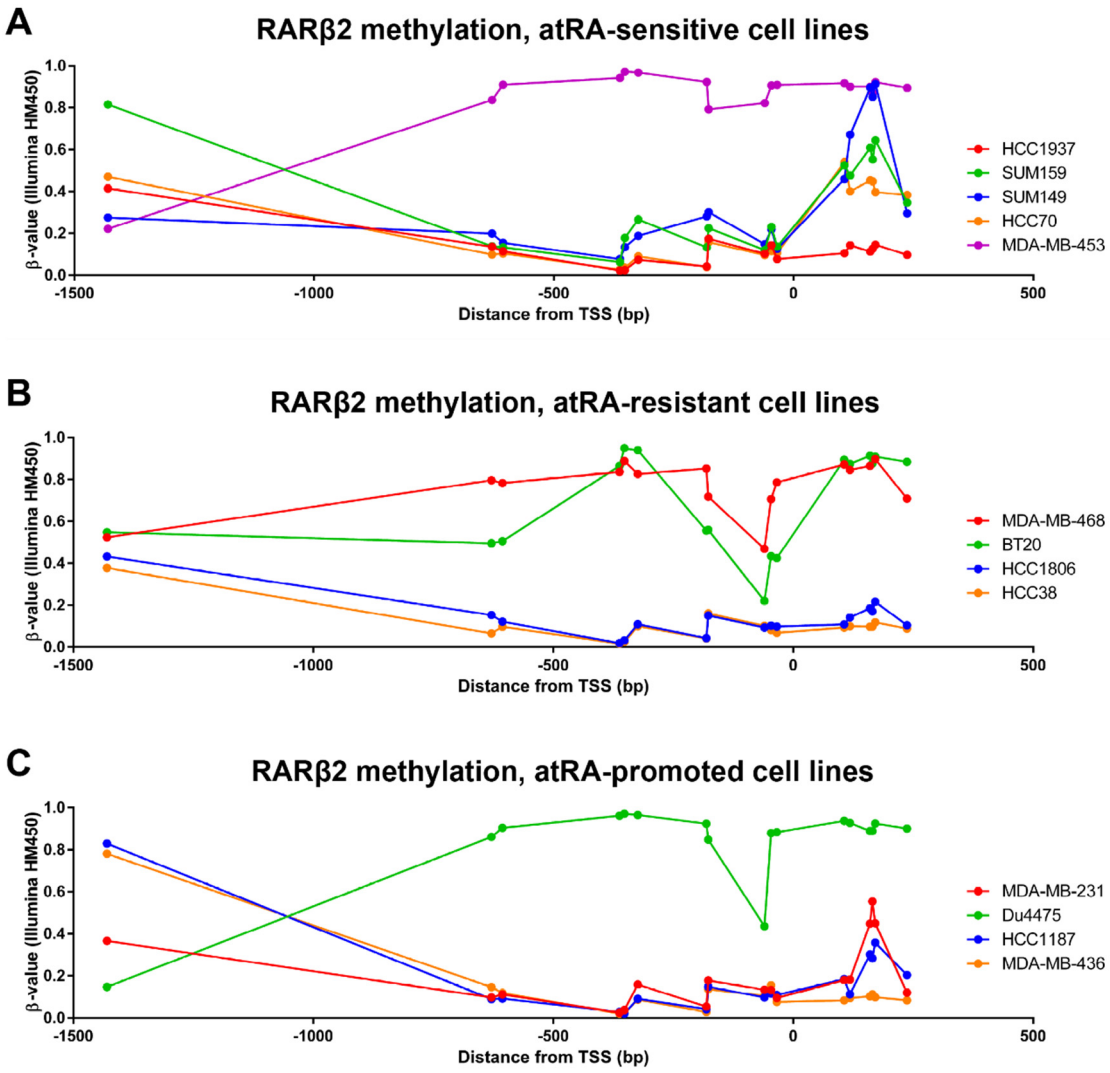

Figure 4-4 Methylation of RARβ2 does not correlate with atRA sensitivity.

β-values for the region extending ± 1500 bp from the transcription start site (TSS) of RARβ2 were extracted for all indicated cell lines from GEO #GSE78875 (Coyle et al., 2016). Values are plotted for **A.** atRA-sensitive cell lines; **B.** atRA-resistant cell lines; and **C.** atRA-promoted cell lines.

4.3.3 *Differential Gene Expression is Identified in atRA-Sensitive Cell Lines*

To determine the unknown factors affecting atRA sensitivity in TNBC, we performed gene expression analyses using Affymetrix Human Gene 2.0ST arrays in triplicate (GSE103426 and *data to be submitted*). When atRA-sensitive cell lines were compared to all other TNBC cell lines profiled, we identified 174 transcripts which were differentially expressed following atRA treatment (Figure 4-5, Table 4-3). We similarly identified 177 transcripts which were differentially expressed at basal levels between atRA-sensitive cell lines and all other TNBC lines utilized in this study (Figure 4-6, Table 4-4). Only ankyrin-repeat domain 6 (ANKRD6) is identified by both data sets. This suggests that while the induced genes could be informative in deciphering the mechanisms of atRA-induced tumor growth versus regression, they have little predictive value alone in the context of untreated patients with breast cancer. On the other hand, differential baseline gene expression may have predictive value.

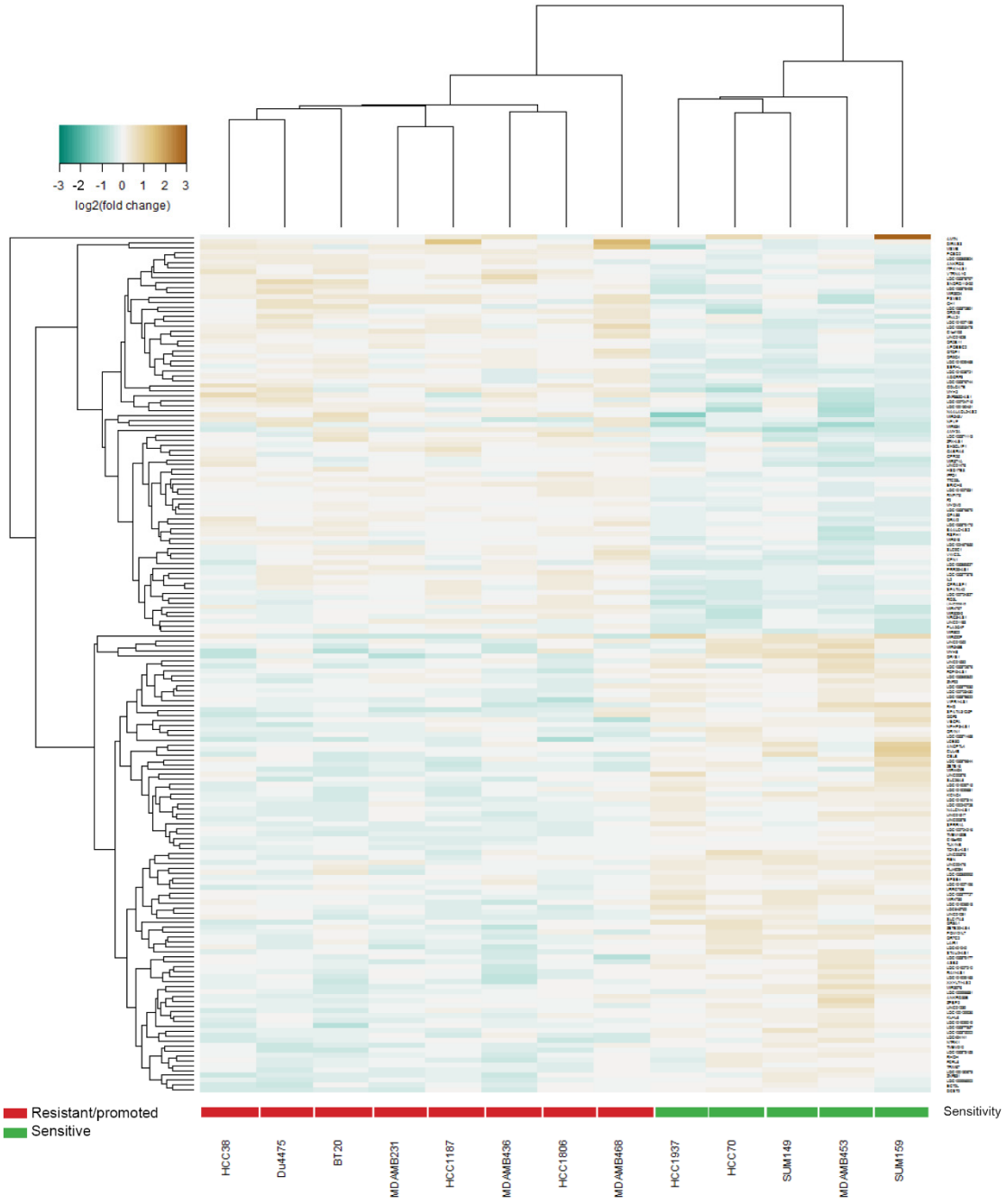

Figure 4-5 174 transcripts are differentially expressed following atRA treatment of TNBC cell lines.

Linear modelling of atRA-induced changes in gene expression between atRA-sensitive cell lines (HCC1937, HCC70, SUM149, SUM159, MDA-MB-453) identified 174 transcripts which were significantly different. These were clustered (heatmap.2, gplots) based on fold-change after 100 nM atRA treatment. Gene identifiers are displayed in Table 4-3.

Table 4-3 174 transcripts differentially expressed following atRA treatment of TNBC cell lines.

Transcript Name	Mean log_2(fold change) (sensitive)	Mean log_2(fold change) (resistant / promoted)
ADGRF3	-0.22293	0.050999
AMTN	0.849075	0.081004
AMY2A	-0.5557	-0.00242
ANGPTL4	0.336698	-0.03084
ANKRD33B	0.232499	-0.08449
ANKRD6	-0.16761	0.12155
APOBEC2	-0.1771	0.05643
ASB5	0.114512	-0.21703
BAALC-AS2	-0.18127	0.142717
C16orf90	0.011524	-0.17963
C1orf105	-0.08176	0.246905
CBLB	0.356613	-0.2041
CPN1	-0.2546	0.027361
CUL4B	0.29963	-0.01799
DCST2	-0.00066	-0.25032
DIRAS3	-0.14651	0.45867
ECT2L	0.031925	-0.19723
ERICH6	-0.09937	0.149798
F2	-0.19087	0.008421
FCRL6	0.071984	-0.18376
FGF10-AS1	0.259459	-0.09056
FLJ46284	0.244888	-0.01522
GABRA6	-0.21989	0.085995
GH1	-0.31253	0.216451
GOLGA7B	-0.21663	0.196206
GPA33	-0.17594	0.029162
GPR25	-0.21558	0.025469
GPRASP1	-0.30404	0.089897
HSD17B3	-0.15053	0.105437
IFFO1	-0.17041	0.093052
IFNA21	-0.12427	0.175245
IL2	-0.21221	0.095011
ITPK1-AS1	-0.1557	0.110175
KCNG4	0.160483	-0.12416
KLHL6	0.134141	-0.09005
LAIR1	0.137421	-0.11972
LCE3D	0.126981	-0.36068
LINC00376	0.262137	-0.09751
LINC00378	0.107959	-0.1735

Transcript Name	Mean log_2(fold change) (sensitive)	Mean log_2(fold change) (resistant / promoted)
LINC00476	0.328315	-0.03113
LINC00575	0.278175	-0.06377
LINC00615	-0.32085	-0.04404
LINC01052	0.30826	-0.03534
LINC01081	0.152266	-0.13089
LINC01183	-0.29488	0.05388
LINC01239	0.191053	-0.11169
LINC01476	-0.29046	0.01113
LINC01517	0.146296	-0.18763
LINC01532	0.274683	-0.06215
LINC01628	-0.15682	0.171878
LOC100129936	0.124027	-0.13118
LOC100130451	-0.28443	0.139756
LOC100130673	0.089374	-0.19169
LOC100240728	0.163068	-0.16012
LOC100505478	-0.3058	0.159014
LOC100996681	0.153058	-0.11254
LOC100996902	0.049873	-0.2333
LOC101926913	0.231679	-0.07907
LOC101927138	-0.15333	0.164336
LOC101927196	0.170479	-0.04103
LOC101927210	0.197148	-0.11524
LOC101927314	0.176912	-0.15118
LOC101927531	-0.19388	0.117541
LOC101928721	-0.32192	0.082837
LOC101929019	0.099721	-0.16514
LOC101929163	0.1627	-0.18636
LOC101929468	-0.22847	0.096953
LOC101929681	0.210859	-0.1588
LOC101929715	0.175445	-0.13092
LOC102467655	-0.27634	-0.01741
LOC102723430	0.139881	-0.13525
LOC102724216	0.080324	-0.1856
LOC102724327	-0.3054	0.019158
LOC102724715	-0.22188	0.112727
LOC105369352	0.2315	-0.0771
LOC105369527	-0.38433	0.005185
LOC105369804	-0.0871	0.184807
LOC105369995	0.185405	-0.08115
LOC105371113	-0.21083	0.150207
LOC105371468	0.083848	-0.1936

Transcript Name	Mean log_2(fold change) (sensitive)	Mean log_2(fold change) (resistant / promoted)
LOC105372676	0.198376	-0.15144
LOC105372891	-0.2481	0.150391
LOC105373153	0.069702	-0.2645
LOC105375002	0.17444	-0.12208
LOC105376493	-0.23454	0.168559
LOC105376644	0.203015	-0.12198
LOC105376679	-0.20559	0.059568
LOC105376744	-0.19256	0.017406
LOC105377357	0.133422	-0.217
LOC105377378	-0.14589	0.161146
LOC105377727	0.28542	-0.04803
LOC105377935	0.187282	-0.05669
LOC105378622	0.169685	-0.11997
LOC105378797	-0.13518	0.197476
LOC105379175	-0.18996	0.102744
LOC105379177	0.219494	-0.19668
LOC401040	0.130069	-0.18792
LOC494141	0.111617	-0.19969
LOC645752	0.299644	-0.10317
LRRC75B	0.115848	-0.1412
MIR329-2	-0.35818	0.037336
MIR371A	-0.25507	-0.00267
MIR3924	-0.23883	0.129794
MIR3976	0.278178	-0.15921
MIR4494	0.052794	-0.28517
MIR4739	0.305106	-0.07747
MIR4797	-0.38982	0.126211
MIR520F	0.538603	-0.17764
MIR548B	0.345038	-0.17283
MIR548V	-0.5416	0.200374
MIR618	-0.2892	0.021654
MIR634	-0.6252	0.044952
MIR802	-0.39018	0.015927
MSMB	-0.2855	0.348205
MYH2	-0.43709	0.17138
MYH8	0.251393	-0.22202
MYOM2	-0.14153	0.080707
NAALADL2-AS2	-0.44165	0.050374
NALCN-AS1	0.097451	-0.14833
NPHP3-AS1	0.152217	-0.19881
NPVF	-0.31869	0.081147

Transcript Name	Mean log_2(fold change) (sensitive)	Mean log_2(fold change) (resistant / promoted)
NRG3-AS1	-0.32438	0.011442
NTRK1	0.098759	-0.23342
ODF3	0.097771	-0.20238
OR1N1	0.148273	-0.1343
OR1S1	0.354983	-0.30822
OR2B11	-0.18225	0.087615
OR2M5	-0.25158	0.124395
OR7C2	0.302547	-0.13305
OR8A1	0.235366	-0.17546
OR9G4	-0.21377	0.107221
ORAI2	-0.13112	0.168804
OTOP1	-0.16268	0.102773
PGBD2	-0.0621	0.175066
PLA2G4F	-0.3006	0.006627
POM121L7	0.263694	-0.1367
PRR29-AS1	-0.2331	0.048073
PSMB9	-0.05613	0.33592
RAI1-AS1	0.141837	-0.15143
RD3L	-0.27801	-0.02945
REN	0.26495	-0.09481
RHD	0.256534	-0.20649
RHOH	0.149543	-0.14549
RNF175	-0.1672	0.077241
RSPH1	-0.20775	0.096202
SERHL	-0.2685	0.0451
SH3GL1P1	-0.17971	0.0978
SLC17A8	0.137024	-0.17619
SLC26A8	0.162287	-0.12263
SLC9C1	-0.12709	0.098698
SNORD115-25	-0.11152	0.23316
SPATA31D5P	0.238426	-0.28218
SPATA42	-0.31775	0.057774
SPRR1A	0.095743	-0.18004
SPSB4	0.187569	-0.04917
STAU2-AS1	0.147795	-0.18669
TLX1NB	0.118345	-0.14538
TMEM150B	0.065245	-0.20208
TMEM210	0.117865	-0.20609
TONSL-AS1	0.052737	-0.13964
TRIM67	0.053485	-0.12271
TTC23L	-0.10785	0.146671

Transcript Name	Mean log_2(fold change) (sensitive)	Mean log_2(fold change) (resistant / promoted)
VEGFA	0.249923	-0.12565
VIPR1-AS1	0.157445	-0.15873
VTRNA1-2	-0.24017	0.220471
VWC2L	-0.17741	0.129972
XXYLT1-AS2	0.098985	-0.23162
ZBTB16	0.241355	-0.2428
ZBTB20-AS4	0.355355	-0.14737
ZFX-AS1	-0.21379	0.101149
ZNF22	0.16469	-0.12775
ZNF385D-AS1	-0.24789	0.205281
ZNF831	0.06772	-0.23875
ZPBP2	0.186971	-0.11586

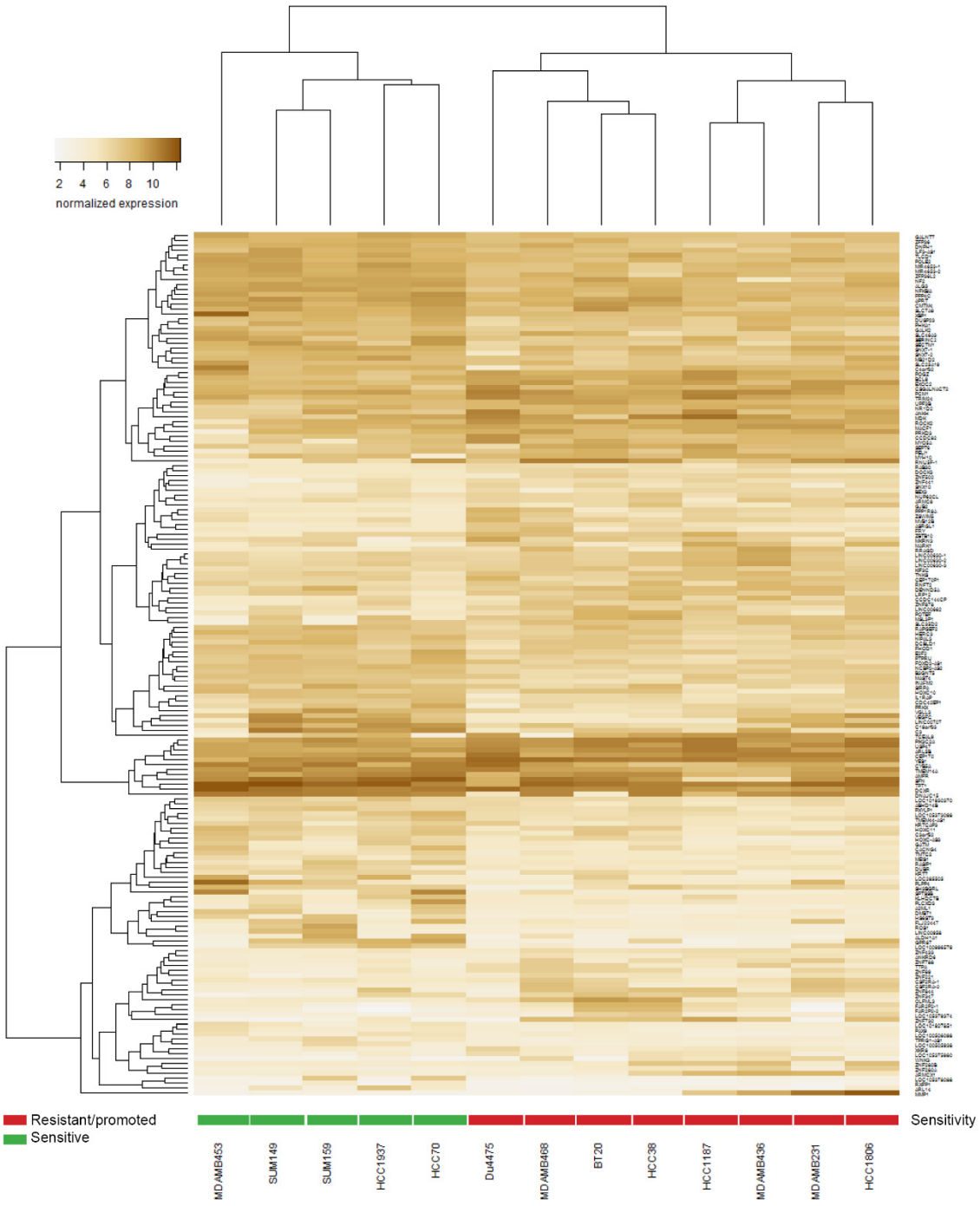

Figure 4-6 177 transcripts are differentially expressed at basal levels in atRA-sensitive cell lines.

Linear modelling of baseline gene expression between atRA-sensitive cell lines (HCC1937, HCC70, SUM149, SUM159, MDA-MB-453) identified 177 transcripts which were significantly different. These were clustered (heatmap.2, gplots) based on normalized expression. Gene identifiers are displayed in Table 4-4.

Table 4-4 177 transcripts differentially expressed at basal levels in TNBC cell lines.

Transcript name	Mean normalized expression (sensitive)	Mean normalized expression (resistant / promoted)
A2ML1	4.206784	5.684247
ABHD14B	5.737049	6.606271
ALDH1A1	3.905344	5.884162
ALG3	8.313749	9.224908
AMFR	9.160693	9.979377
ANKH	8.859306	7.509539
ANKRD6	5.214229	4.425731
APRT	8.556229	9.409447
ARL14	2.911448	4.813043
ARL5B	9.963327	9.12568
ARMC9	6.492315	5.692641
ARMCX1	6.23648	4.271927
ASRGL1	6.095106	4.959211
B3GNT5	6.494889	7.69586
BCL9	8.903552	8.012426
BEX3	5.904478	4.925141
C19orf33	7.162619	8.698847
C3	6.617267	9.061179
C3orf52	6.030167	7.01433
C4orf32	7.429519	8.808049
CACNG4	5.159459	6.492224
CCDC144CP	7.149503	5.437869
CCDC82	8.260503	7.173025
CDC42EP1	6.139129	7.091301
CEP170	10.04798	9.197336
CEP170P1	7.408404	6.496769
CMTM4	8.169512	9.122531
CSF2RA-1	6.296906	5.275305
CSF2RA-2	6.057728	4.500621
CSGALNACT2	8.954933	8.013197
CYB5A	8.706508	10.09153
DCBLD1	6.880424	7.765565
DCXR	10.11014	10.88402
DENND5A	7.737116	6.837548
DMBT1	4.230952	6.094967
DNAJC15	8.627791	10.52002
DNPH1	7.791241	8.618162
DOCK3	5.854214	5.064748
DUBR	5.225104	6.048731

Transcript name	Mean normalized expression (sensitive)	Mean normalized expression (resistant / promoted)
DUSP23	7.454629	8.24543
E2F2	6.783399	7.721153
EXOC2	9.03452	8.206538
FAR2P2-1	5.98672	4.018338
FAR2P2-2	5.393865	3.163749
FHOD1	6.565878	7.386179
FLJ22447	4.903679	6.751257
FOXD2-AS1	6.708284	7.66111
FRY	6.060238	4.875476
GALK2	7.086941	7.972501
GALNT7	7.845334	8.806687
GATM	4.95635	6.111376
GJB2	6.32254	5.035133
GPR87	4.573842	7.376397
HERC3	6.93858	7.773394
HOXC10	6.501491	7.798927
HOXC11	5.920004	7.237474
HOXC-AS3	5.222215	6.667249
HS6ST3	4.317737	5.810127
IL1RAP	6.096848	7.619178
ILF3-AS1	7.663121	8.546208
INAFM2	6.489289	7.320535
KIF3C	7.147387	6.24433
KLHDC7B	5.067173	6.249267
KRT7	5.393312	6.540305
KRTCAP3	5.440748	6.323529
LINC00630-1	7.351982	6.437359
LINC00630-2	7.289938	6.485037
LINC00630-3	7.519098	6.615467
LINC00662	7.032683	5.452146
LINC00707	6.101195	8.462645
LINC00958	4.036998	5.799037
LOC100505938	3.962022	4.9291
LOC100506098	4.088364	5.003576
LOC100996579	4.415305	6.427001
LOC101927851	4.243873	5.215799
LOC101930370	6.020076	6.960209
LOC105373098	5.820998	6.950912
LOC105375980	5.021449	3.82749
LOC105378088	3.006697	4.71501
LOC105379374	4.996058	3.533013

Transcript name	Mean normalized expression (sensitive)	Mean normalized expression (resistant / promoted)
LOC285505	4.647404	6.646643
LRP12	7.302664	6.290747
MACF1	8.991487	8.112621
MARK1	6.970559	5.250318
MAST4	6.64675	7.434542
MB21D2	7.434303	8.497035
MDK	9.349742	7.89373
MEIS1	4.971463	5.885761
MIR4653-1	7.814769	9.227144
MIR4653-2	7.625011	9.051721
MKRN3	7.07873	5.706927
MMP1	6.339124	2.909918
MSL3P1	7.832276	5.603704
MVB12B	6.761548	5.585246
MYH10	8.51193	6.846619
MYO5A	8.330751	6.758196
NCBP2-AS2	6.828369	7.857936
NF2	7.901532	9.034426
NFKBIA	8.194051	9.141888
NIPAL3	6.950847	7.832235
NR1D2	8.509067	7.701877
NUP62CL	6.586171	5.642134
OLFML3	6.59205	4.844084
PAX9	4.079746	5.011511
PCM1	9.612728	8.850594
PELI1	7.946492	6.614183
PHKA1	7.37997	8.237542
PIK3C2A	10.11646	9.241743
PLCXD3	4.962384	6.30076
PLPP4	5.569636	7.570282
POGZ	8.878742	8.118599
POLE2	8.117478	8.878988
POTEF	6.934055	5.511923
PPP1R9A	6.511508	5.260102
PPP4C	8.284986	9.094695
PRKD3	8.77884	7.353108
PRKX	6.040043	7.287887
PTPRU	6.313132	7.730296
PXYLP1	5.885737	6.921083
RAB30	6.034553	5.248046
RAPGEF2	7.051207	7.874077

Transcript name	Mean normalized expression (sensitive)	Mean normalized expression (resistant / promoted)
RASIP1	5.252517	6.544369
RNFT2	7.17413	6.231583
RNU5F-1	9.058961	6.518301
ROCK2	9.244527	7.930928
ROS1	4.304791	5.815597
RRAGD	6.958275	5.247045
RXFP1	2.577305	3.577295
SECTM1	6.959067	8.742051
SEPT6	8.282683	7.05538
SERINC2	7.668736	8.619058
SFN	9.06754	11.01726
SH3BGRL	5.681697	7.238838
SIRPA	6.672377	7.961317
SLC25A19	7.489121	8.261513
SLC35D2	7.388435	5.804808
SLC46A3	7.241826	8.564952
SLC7A6	8.142253	8.978741
SNX10	5.905858	4.882755
SNX7-1	7.973069	8.79698
SNX7-2	7.159761	8.230418
SPTSSB	4.467176	7.350113
TCEAL9	8.455187	6.036489
TLCD1	8.178663	8.97529
TMEM14A	9.144801	10.05265
TMEM44-AS1	5.804818	6.660688
TMTC2	5.252779	6.197962
TNKS	7.421255	6.593644
TPRG1-AS1	4.17523	5.163718
TPT1	10.60802	11.53616
TRIM24	9.367294	8.492887
TTPA	5.852811	4.417272
UPF3B	8.595803	7.627091
USP47	10.08761	9.208814
VEGFC	6.597429	8.271971
VGLL3	6.275894	7.78823
WNK3	4.789962	2.866692
XBP1	8.238538	9.240491
XKR6	5.145727	4.104599
YES1	10.66339	9.807989
ZBTB10	7.317641	5.980737
ZFP36	7.683321	8.595104

Transcript name	Mean normalized expression (sensitive)	Mean normalized expression (resistant / promoted)
ZFP36L2	8.031475	8.978388
ZNF221	5.227867	4.195711
ZNF280A	5.128249	3.81224
ZNF280B	6.138767	4.774016
ZNF347	6.29869	4.508711
ZNF433	5.652147	4.76961
ZNF441	6.00531	4.767891
ZNF502	6.346373	4.745236
ZNF69	5.903281	4.4035
ZNF730	6.596	3.280254
ZNF788	5.839002	4.452122
ZNF844	6.591047	4.612561
ZNF878	6.863112	5.553286
ZSWIM5	6.246344	5.1539

4.3.4 *DNA METHYLATION CONTRIBUTES TO DIFFERENTIAL GENE EXPRESSION BETWEEN ATRA-RESPONSIVE AND -RESISTANT TNBC CELL LINES*

We have previously demonstrated that DNA methylation contributes to both baseline expression and the inducibility of atRA-responsive genes (Coyle et al., 2016, 2017b). Therefore, we hypothesized that differences in DNA methylation may contribute to the atRA sensitivity of TNBC and could possibly be used to identify predictive atRA-inducible genes prior to treatment. Using the Illumina HM450 array, we first determined which CpG probes were differentially methylated ($p<0.01$) between atRA-sensitive and all other TNBC cell lines. We identified 1379 probes with differential methylation (Figure 4-7, Appendix 2). We note with interest that although the response to atRA was greatest in HCC1937, it appears to be more similar to the non-responsive cell lines by this clustering approach. The 1379 probes were associated with 644 unique gene identifiers. We hypothesized that genes which have differentially methylated CpG dinucleotides in combination with differential expression are likely regulated by DNA methylation. The overlap between these genes and those identified as differentially expressed upon atRA treatment and those which had differential basal expression was determined (Figure 4-8A), identifying 13 genes which we predicted would be regulated by DNA methylation. Using data available from The Cancer Genome Atlas (TCGA), we correlated expression of four genes (MKRN3, TPPA, ZNF280B and XKR6) with DNA methylation in 553 breast tumors (Figure 4-8B). We demonstrate strong correlations between methylation and expression for MKRN3, ZNF280B, and XKR6. Furthermore, we demonstrate that several of the CpG sites identified by this approach display varied patterns of DNA methylation within 1500 bp of the transcription start site (TSS) within the TNBC cell lines utilized in this work (Figure 4-9).

The HM450 array was designed with clear bias towards promoter-related CpG sites and genes of interest (Bibikova et al., 2011). Given the inherent bias of using a gene-centric view of data from HM450 arrays, we therefore maintained all 1379 probes (as in Figure 4-7) for further analysis. These probes and their locations are detailed in Appendix 2.

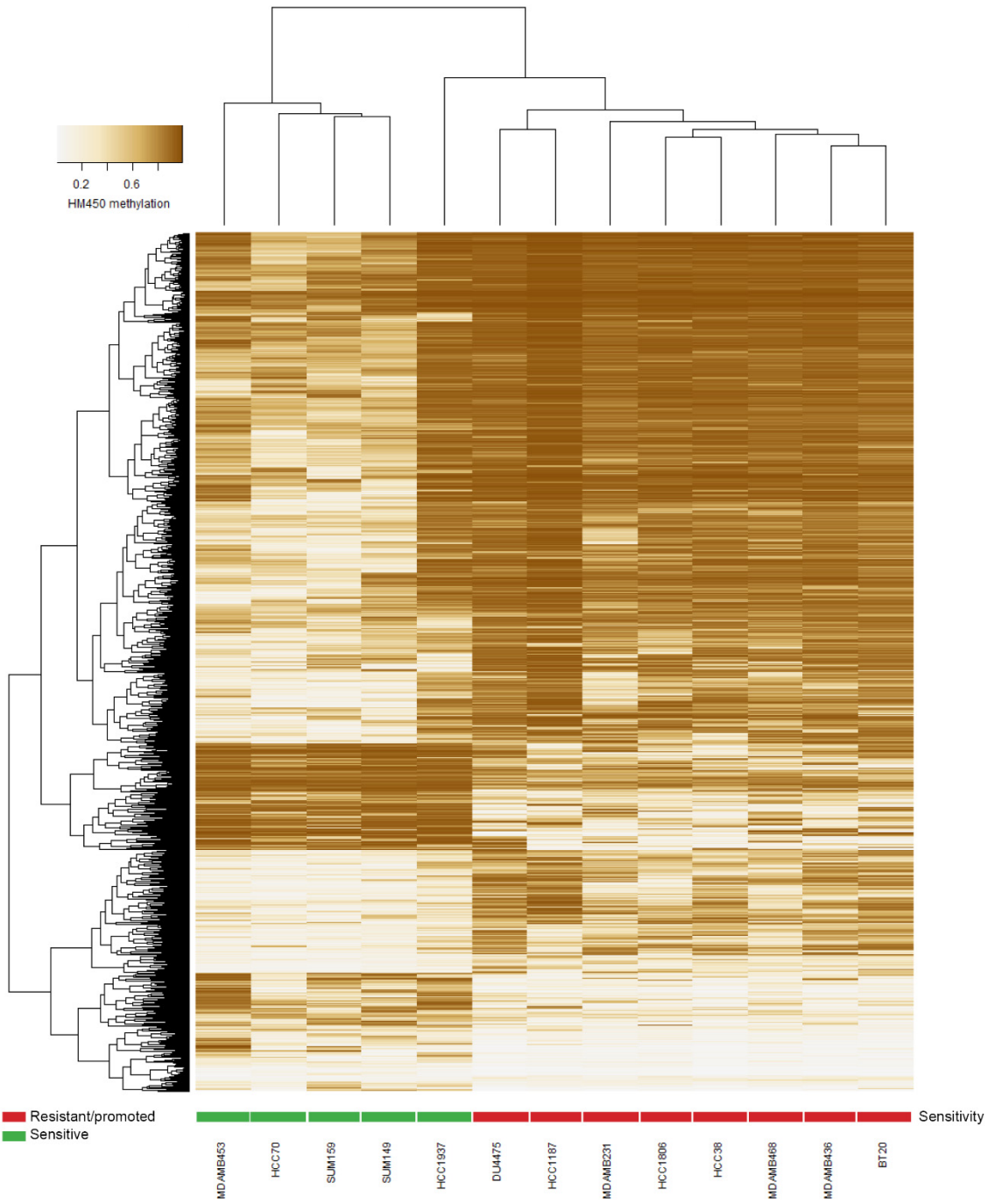

Figure 4-7 1379 CpG sites identified as differentially methylated between treatment response groups.

Linear modelling of differences in CpG probe methylation between atRA-sensitive cell lines (HCC1937, HCC70, SUM149, SUM159, MDA-MB-453) identified 1379 sites which were significantly different. These were clustered (heatmap.2, gplots) based on Illumina β-value. CpG identifiers were suppressed from the plot. Further data is presented in Appendix 2.

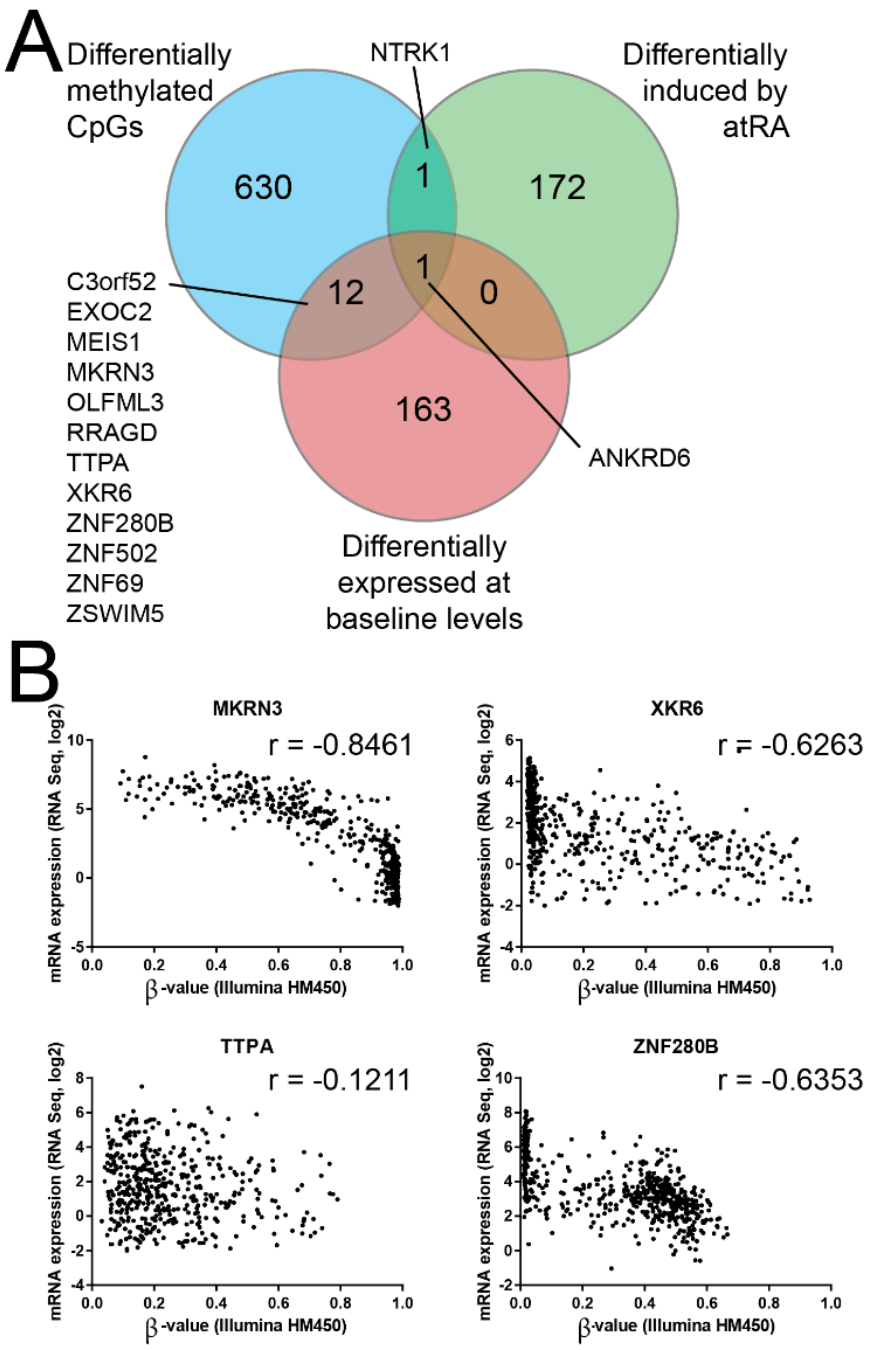

Figure 4-8 DNA methylation is a likely contributor to differences in baseline expression of identified genes.

A. Gene lists were compared between differentially methylated probes, differentially expressed transcripts, and differences in atRA-inducibility between atRA-sensitive and all other cell lines. **B.** DNA methylation and mRNA expression of four genes identified in the overlap of differential methylation and baseline gene expression were extracted from cBioportal. Spearman's correlations were calculated and displayed.

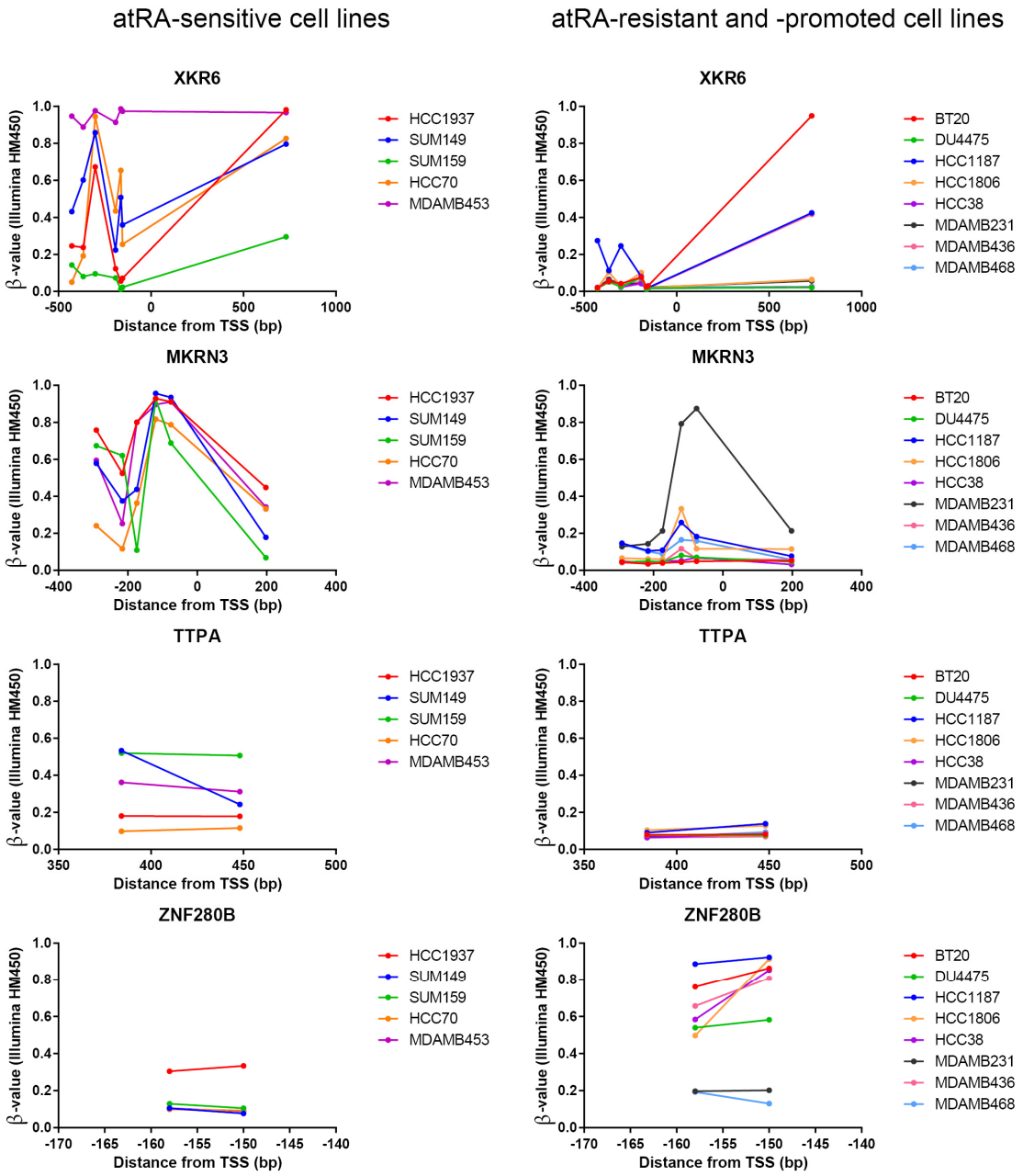

Figure 4-9 Patterns of methylation differ between atRA-sensitive cell lines and remaining TNBC cell lines.

Based on the 1379 differentially methylated probes identified, β-values for the selected probes within 1500 bp of the TSS of indicated genes were extracted from HM450 data for all cell lines as shown. atRA-sensitive cell lines are plotted independently of all other cell lines.

4.3.5 *DNA Methylation Predicts Sensitivity of 4 TNBC PDXs*

We derived two PDXs (A and B) from two independent surgical patients; and obtained BCM-3887 (PDX C) and BCM-2665 (PDX D) from the laboratory of Dr. Michael Lewis (Zhang et al., 2013). After successive passaging (PDX A, passage 2; PDX B, passage 42), we isolated live human cells by florescence-activated cell sorting (FACS) (Figure 4-10). Profiling of DNA methylation (PDX A and B, Illumina HM450; PDX C and D, Illumina EPIC) and gene expression (Affymetrix HuGene 2.0ST, PDX A and B) was performed on human cells. Normalized gene expression data for PDX C and D (Agilent UNC PerouLab 244K Custom Human Array version 5) was obtained from the Baylor College of Medicine (www.bcxenograft.org). Using the gene expression data for PDX A and B, we first characterized the intrinsic subtypes using the single-sample predictor and the claudin-low algorithm. PDX A and B were classified as basal-like, and PDX C and D have been previously identified as basal-like (Zhang et al., 2013).

We next identified gene-level gene expression for all four PDXs based on the subset of genes identified in Figure 4-6 which also could be queried with the Agilent custom data. This was compared to the expression of TNBC cell lines (Figure 4-11). Expression was column-centred by z-score for both PDXs and cell lines to minimize differences between platforms (HuGene 2.0ST vs custom array). Hierarchical clustering reveals that PDX A and B are most closely related to atRA-resistant or -promoted cell lines, while PDX C and D are highly dissimilar from all other data sets. This is likely a consequence of differences in probe-level measurements. Regardless, if baseline gene expression is predictive of response, we expect PDX A and B will be resistant to atRA treatment *in vivo*.

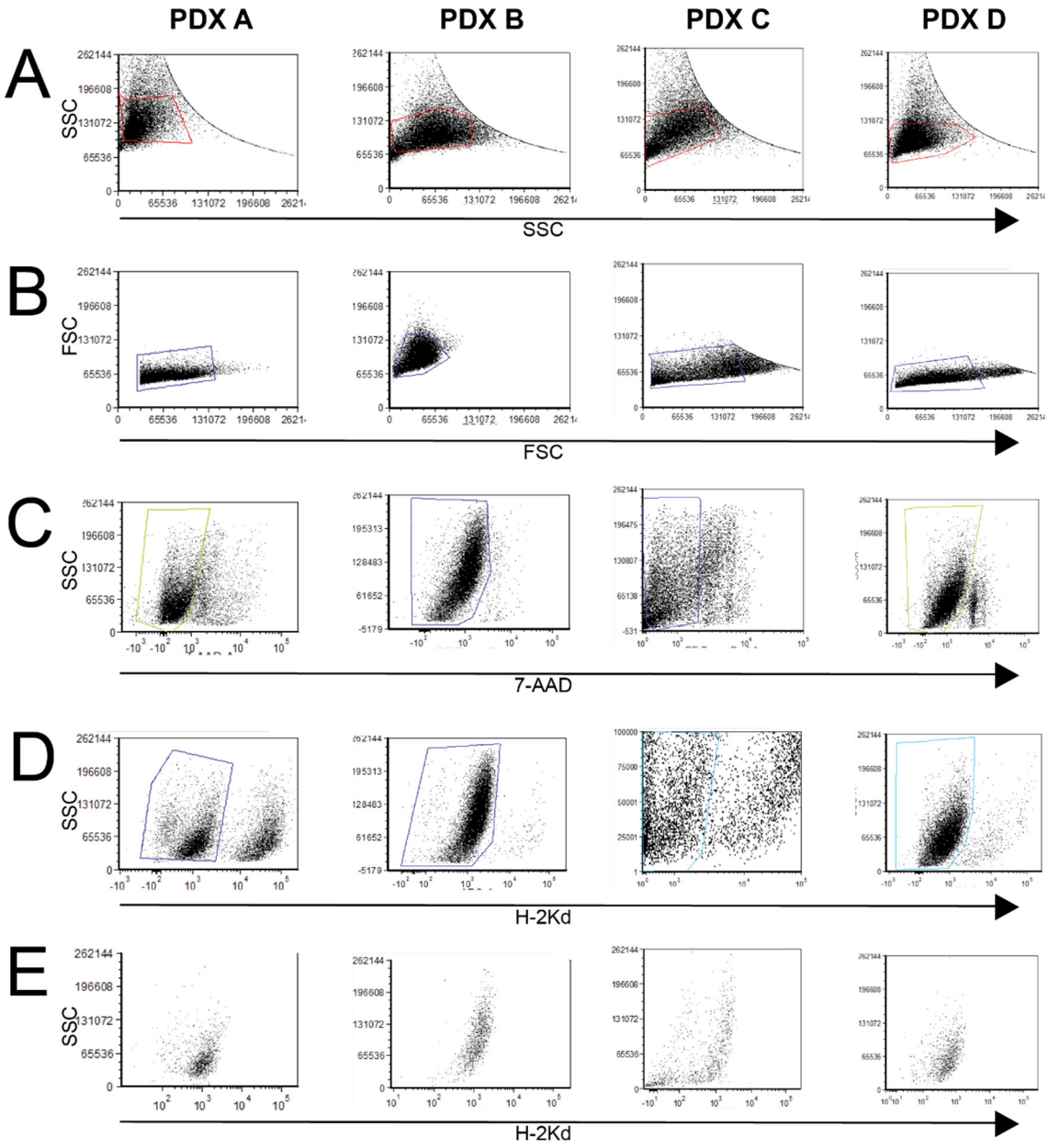

Figure 4-10 Live human cells are isolated from PDXs.

Prepared and stained cells from PDXs A-D were gated and sorted to **A.** exclude doublets based on side scatter (SSC); **B.** exclude doublets based on forward scatter (FSC); **C.** identify 7-AAD$^-$ live cells; and **D.** identify H-2Kd$^-$ human cells. **E.** H-2Kd purity of sorted cells was verified.

Figure 4-11 Hierarchical clustering of PDXs and cell lines based on gene expression is not a confident predictor for sensitivity.

Gene-level expression of transcripts identified via differential expression analysis of atRA-sensitive cell lines and PDXs are compared and clustered (gplots, heatmap.2 function). PDX A and B cluster most closely with atRA-resistant or -promoted cell lines; PDX C and D cluster independently of all other samples.

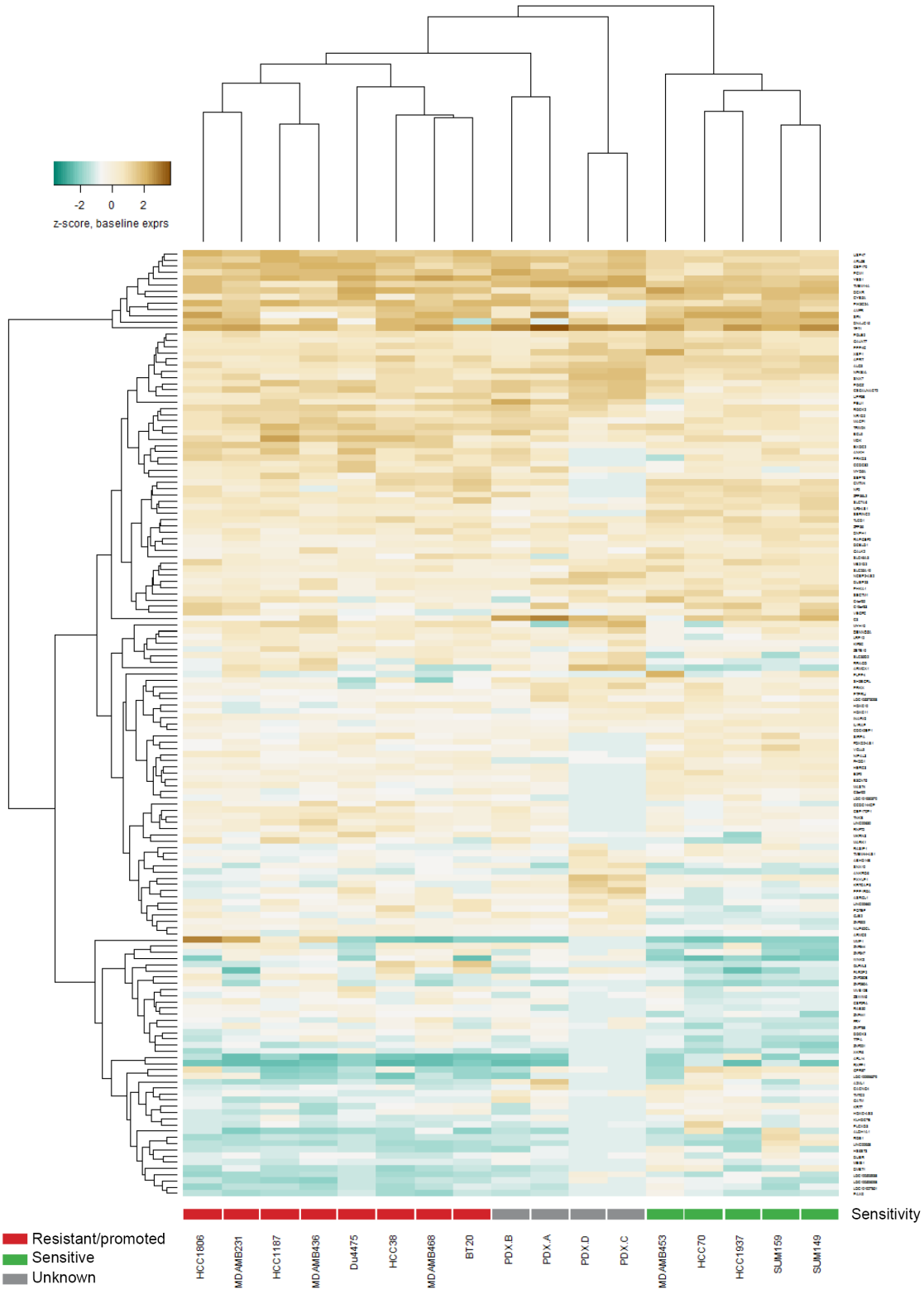

Figure 4-11 Hierarchical clustering of PDXs and cell lines based on gene expression is not a confident predictor for sensitivity.

We next investigated whether DNA methylation could provide a more robust model for predicting the sensitivity of PDXs. Using the 1379 CpG sites identified in Figure 4-7, we clustered the 13 TNBC cell lines and the 4 PDXs (Figure 4-12). This approach demonstrates that all four PDXs (A-D) are most similar to themselves, illustrating a key technical challenge in comparing PDXs to *in vitro* cell lines. Regardless, they are more closely related to the atRA-sensitive cell lines, and cluster with the highly sensitive HCC1937 cell line. Therefore, if DNA methylation is predictive of *in vivo* response to atRA, then all four PDXs would be sensitive to atRA treatment *in vivo*. Treatment of NOD-*scid* mice with 5 mg / 60 day slow release atRA pellets significantly decreased tumor volume and tumor weight of PDX A (Figure 4-13A), B (Figure 4-13B), C (Figure 4-13C), and D (Figure 4-13D), which validated our predictive DNA methylation profiling (Figure 4-12). This indicates successful preliminary identification of methylation biomarkers for atRA sensitivity.

Figure 4-12 PDXs cluster with atRA-sensitive HCC1937 based on CpG methylation.

β-values of CpG probes from analysis of atRA-sensitive cell lines and PDXs are compared and clustered (gplots, heatmap.2 function). PDXs A-D cluster most closely with each other and are most similar to atRA-sensitive HCC1937.

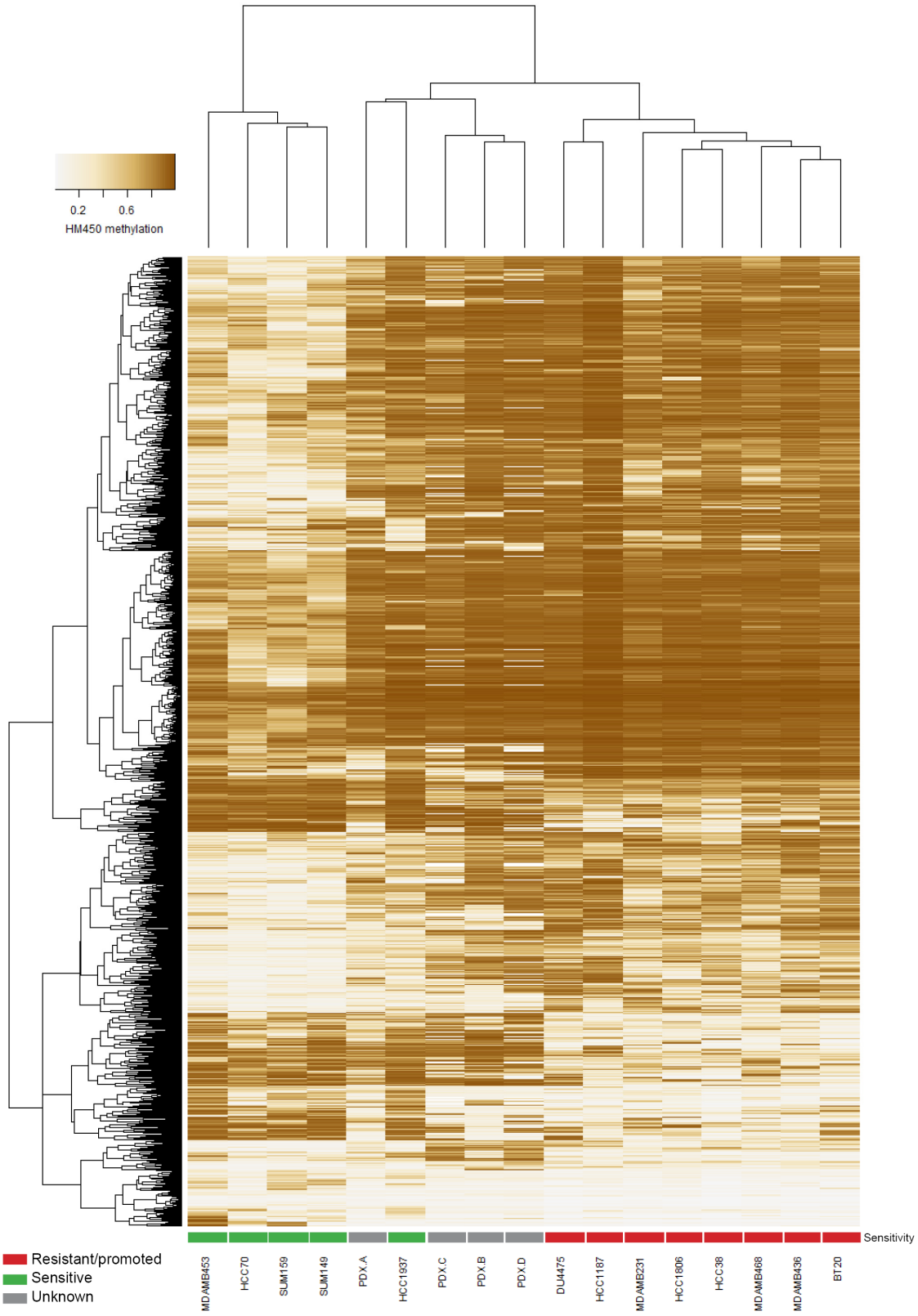

Figure 4-12 PDXs cluster with atRA-sensitive HCC1937 based on CpG methylation.

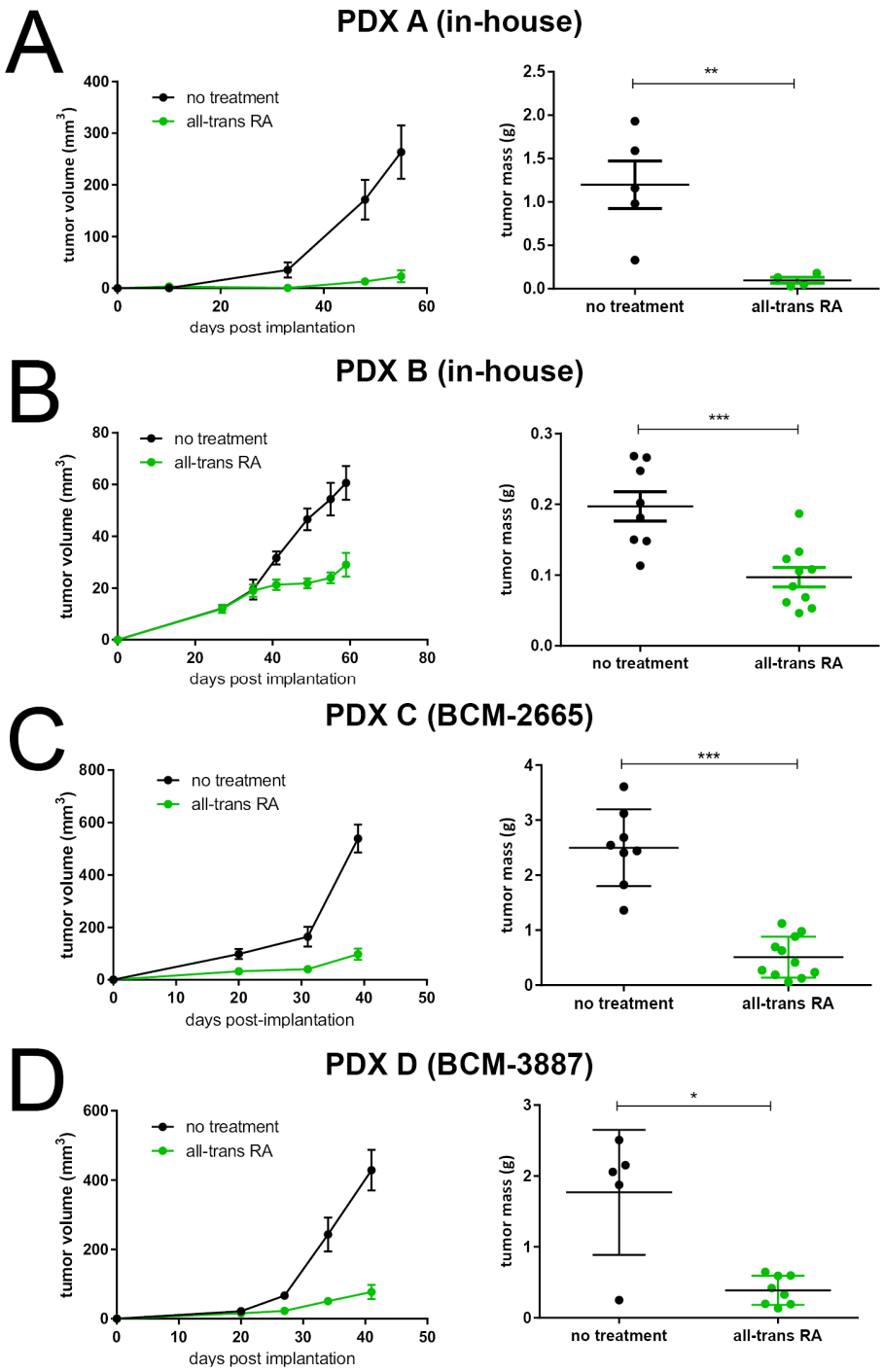

Figure 4-13 Treatment with atRA significantly inhibits the growth of four independent patient-derived xenografts.

Growth of **A.** PDX A, **B.** PDX B, **C.** PDX C (BCM-2665), and **D.** PDX D (BCM-3887) was quantified, and tumor weight determined at the conclusion of the experiment. Tumor weights were compared by student's t-test. For all comparisons, * $p < 0.05$, ** $p < 0.01$, *** $p < 0.001$.

4.4 DISCUSSION

Despite their promise as differentiating agents, retinoids have seen limited clinical success in solid tumors. The establishment of a signature describing sensitivity to atRA would thus be a useful tool in accelerating future clinical studies of atRA. While some efforts have been made to describe atRA sensitivity in breast cancer models, these predominantly *in vitro* studies have typically designated most TNBC cells as resistant. In contrast, using TNBC cell-line xenografts, we describe a high degree of variability in atRA sensitivity. The use of TNBC models exclusively allowed for the elimination of much variability originating from inter-subtype heterogeneity. To our knowledge, this is the first time a panel of TNBC xenografts have been characterized *in vivo* for atRA sensitivity.

We did not find any association or correlation between components of classical retinoid signaling (RAR or RXR isoforms, CYP26 isoforms), nor were we able to validate the FABP5:CRABP2 ratio as a determinant of atRA sensitivity. This is consistent with our previous findings that retinoid signaling is largely independent of classical RAREs or PPREs (Coyle et al., 2017b; Marcato et al., 2015)

It is possible that these discrepancies with existing literature are due to differences in atRA sensitivity between this study and previous, largely *in vitro*, studies (as described in Table 4-1); as well, this study uniquely considers the role of retinoid signaling in TNBC, thus eliminating much of the subtype-dependent variation in gene expression and DNA methylation. This does not exclude the possibility that RAR/RXR expression or the FABP5:CRABP2 ratio drive divergent gene expression; rather, it suggests that there are limited functional consequences to this hypothesis within TNBC.

Using data derived from 13 cell lines, we determined that a set of genes were differentially expressed between atRA-sensitive models and atRA-promoted or resistant models. Given our previous work that has described the contribution of DNA methylation to specific expression of atRA-inducible genes, we also investigated the methylation profiles between atRA-sensitive models and the remaining cell lines. Several of the genes we identified as differentially expressed also demonstrated differential methylation between response groups (e.g. TPPA, MKRN3, XKR6, ZNF280B). In addition, we were able to characterize a set of 1379 CpG probes which represented sites of dissimilar methylation between atRA-sensitive cell lines and the remaining cell lines.

We utilized these distinct gene expression and DNA methylation categories to predict atRA sensitivity of four basal-like PDXs. While gene expression was not a confident predictor for PDXs, likely due to differences in probe-level expression, DNA methylation predicted these PDXs as sensitive. This was validated upon *in vivo* atRA treatment of these PDXs. This is an important description of an atRA-sensitive DNA methylation profile which can be used for further investigation of atRA in clinical studies.

DNA methylation is not widely used as a biomarker. There are technical challenges from sample collection to bisulfite conversation which limit broad applicability of DNA methylation as a biomarker (Mikeska and Craig, 2014; Shiwa et al., 2016). While we did identify a consistent methylation profile between atRA-sensitive cell lines and PDXs, it is also likely that DNA methylation will vary depending on the growth environment: *in vitro*, *in vivo*, *ex vivo*, or in the natural host (Cope et al., 2014; Ehrich et al., 2008).We maintained all CpGs identified as differentially methylated because gene-

level methylation may not be the most predictive of gene expression (Aran et al., 2013; Aran and Hellman, 2013); however, the identification of functional effects of these CpGs thus requires substantial further exploration as they may be distal regulatory elements.

Considering the questionable clinical relevance of cell-line xenografts, we utilized four PDXs in this study and demonstrate potential benefit of atRA treatment. However, there is limited heterogeneity in the PDXs used (all four were basal-like TNBC). Although basal-like tumors represent the majority of TNBCs (Prat and Perou, 2011), the inclusion of other subtypes would give a broader applicability to potential clinical use of atRA. Further pre-clinical investigations which expand the modeling of atRA sensitivity and resistance in PDXs will improve the robustness of this predictive profile. The biomarkers identified in this study are purely correlative, and their functional relevance in the effects of atRA on cell proliferation or differentiation have not yet been investigated. Additionally, it is not clear whether these biomarkers represent cell-intrinsic or cell-extrinsic factors that may be confounded by the presence of non-tumor cells in clinical settings. This could explain why gene expression was a poor predictor in this study, as two PDXs were clustered with the resistant cell lines.

Future studies which address the contribution of paracrine signaling to the expression of biomarkers and evaluate the atRA sensitivity of an expanded set of PDXs will improve the predictive profile identified in this work and allow the clinical introduction of prospective identification for atRA sensitivity. Importantly, if proven successful for atRA, it may be possible to use a similar differential DNA methylation profiling strategy to predict sensitivity to other drugs.

4.5 ACKNOWLEDGEMENTS

Support was provided by grant funding to PM from the Canadian Institutes of Health Research (CIHR, MOP-130304), the Beatrice Hunter Cancer Research Institute (BHCRI), the Breast Cancer Society of Canada, and the QEII Health Sciences Center Foundation. KMC is supported by a CGS-D award from CIHR, by the Dalhousie Medical Research Foundation, by the Nova Scotia Health Research Foundation, by the Killam Trusts at Dalhousie University, and by the BHCRI with funds provided by the Canadian Imperial Bank of Commerce.

CHAPTER 5: *IN VIVO* GENOMIC RNAI SCREENING IDENTIFIES SCN1A AND GABRA3 AS PRO-TUMOR EFFECTORS OF ALL-*TRANS* RETINOIC ACID TREATMENT IN BREAST CANCER

Contribution statement

This work will be submitted as: Coyle KM, Dean C, Liu RZ, Pan LZ, Ahn DG, Sultan M, Mackey JR Godbout R, Lee PWK, Marcato P. *In vivo* genomic screening identifies SCN1A and GABRA3 as pro-tumor effectors of all-trans retinoic acid treatment in breast cancer.

I designed the experiments, analysed the data, and wrote the manuscript with the guidance of Dr. Paola Marcato. Generation of the lentiviral library in MDA-MB-231 was performed by Dr. LZ Pan, Dr. DG Ahn and Dr. P Marcato with guidance from Dr. PWK Lee. I collected data with assistance from Cheryl Dean and Mohammad Sultan. Clinical data and analysis was provided by Dr. RZ Liu, Dr. JR Mackey, and Dr. R Godbout.

5.1 INTRODUCTION

Retinoid signaling plays a controversial role in breast cancer. Despite triple-negative breast cancers (TNBCs) being largely characterized as resistant to retinoic acid (RA) treatment, our previous work (Chapter 4) described a wide range of possible responses to treatment with all-trans RA (atRA). Most strikingly, this study observed that atRA could promote tumor growth in four TNBC cell-line xenografts, including MDA-MB-231.

A pro-tumorigenic role of atRA is not unexpected. The expression and enzymatic activity of the retinaldehyde dehydrogenases ALDH1A1 and ALDH1A3 are often used to identify cancer stem cells (CSCs), particularly in breast cancer (Ginestier et al., 2007; Marcato et al., 2011b). The enrichment for tumor-initiating capabilities within these ALDH1A-high populations suggests that CSCs have a higher capacity for retinoid signaling than their non-CSC counterparts (Ginestier et al., 2009). In addition, several studies have shown that RAR antagonists are capable of inhibiting cancer cell proliferation (Hammond et al., 2001; Yang et al., 2001, 1999). In glioma, the combination of atRA and decitabine has been shown to increase the aggressiveness of xenografts (Schmoch et al., 2016)

While we have previously identified a predictive profile to identify TNBC tumors which could benefit from atRA treatment, this is primarily correlative and there is little to suggest that these biomarkers are functional. In addition, there is limited evidence surrounding pro-tumorigenic mediators of retinoid signaling. Beyond developing a more comprehensive biological network, the identification of these mediators may provide novel insight into mechanisms of intrinsic or acquired resistance to atRA.

We utilized a genomic loss-of-function screen to identify potential effectors of tumor promoting signals in MDA-MB-231 xenografts upon treatment with atRA. The lentiviral-based shRNA screen is annotated with molecular barcodes, which allow pool-based screening and detection via an oligonucleotide array. This has been used successfully to characterize the functional components of many pathways (Boettcher and Hoheisel, 2010; Liu-Sullivan et al., 2011; Schlabach et al., 2008; Silva et al., 2008). As well, a number of RNA interference (RNAi) screens have been performed using *in vivo* cancer models and have identified novel regulators and effectors of various tumor types (Bric et al., 2009; Schneider and Saur, 2016; Zender et al., 2008). Previous work has demonstrated that some essential mediators of cancer cell phenotypes are dispensable in cell culture (Meacham et al., 2009); therefore, we utilized an *in vivo* approach to identify functional effectors of retinoid signaling in MDA-MB-231. This approach allows experimental cells to interact with the tumor microenvironment and has substantial power to identify unknown mediators.

Given the propensity for false positives within a pooled shRNA screen, and the off-target effects possible with an RNA interference approach, we utilized a multi-step validation approach to confirm putative effectors as likely mediators of pro-tumorigenic retinoid screening. We identify SCN1A and GABRA3 as likely mediators of the tumor- and metastasis-promoting effects of atRA in MDA-MB-231 cells and provide preliminary evidence to support retinoid regulation of GABAergic signaling in this model.

This work identifies the importance of considering cross-talk between retinoid and other signaling pathways, and future work to characterize the role of GABAergic

signaling in breast cancer development and progression may identify therapeutic opportunities.

5.2 Materials and Methods

5.2.1 *Ethics Statement*

Animal investigations detailed in this manuscript have been conducted in accordance with the ethical standards and according to the Declaration of Helsinki and according to national and international guidelines. All experiments were conducted in accordance with the Canadian Council on Animal Care standards and a protocol approved by Dalhousie University Committee on Laboratory Animals (#13-010).

5.2.2 *Cell Lines and Reagents*

MDA-MB-231, MDA-MB-436, Du4475, HCC1187, and HEK293T cells were obtained from the American Type Culture Collection (ATCC) and RMF/EG cells were obtained from the laboratory of Dr. Robert Weinberg. MDA-MB-231, MDA-MB-436, Du4475, HCC1187 were cultured as previously described (Coyle et al., 2016). HEK293T and RMF/EG cells were cultured in DMEM (Invitrogen) with 10% FBS (Invitrogen) and 1x antibiotic-antimycotic (Invitrogen). DDC Medical authenticated MDA-MB-231 by short tandem repeat (STR) profiling at 17 loci and verified them to be mycoplasma-negative (last performed 2015). All-trans retinoic acid (atRA, Sigma) was used at 100 nM or at 1 μM (as indicated) for 18 h.

5.2.3 *Generation of shRNA Library in MDA-MB-231 Cells*

Three Decode lentiviral shRNA pools containing 10 000 shRNAs per pool (30 000 total), targeting approximately 12 000 human genes with well categorized biological functions or processes were purchased from Thermo Scientific (catalogue # RHS5339).

The titre of the shRNA pools was determined using HEK293T cells at $\geq 5 \times 10^8$ transfection units (TU)/mL. Using the pGipZ scramble shRNA control (catalogue # RHS4348), we determined the relative TU/mL for MDA-MB-231 compared to HEK293T cells (HEK293T: 4.53×10^8 TU/mL; MDA-MB-231: 1.09×10^8 TU/mL). The relative transduction efficiency of MDA-MB-231 was thus calculated as 0.24.

Following the manufacturer's instructions, we generated MDA-MB-231 shRNA pools with 100-fold representation of the shRNA library. Each pool was transduced into MDA-MB-231 using DMEM with 1% FBS and 8 μg/mL sequabrene (Sigma). To achieve 100-fold representation of each shRNA pool, the cells were infected at a multiplicity of infection (MOI) of 0.3. 4×10^6 MDA-MB-231 cells (cultured in 150 mm dishes) were transduced with 1.2×10^6 TU of each pool (11.0 μL). Lentivirus was left for 6 h before replacement with complete media (DMEM with 10% FBS and 1x AA).

Two days post-transduction, the expanded cells harbouring the shRNA sequences were selected with 1.5 μg/mL puromycin, maintained in 0.25 μg/mL, and immediately frozen to minimize changes in shRNA representation ($> 2 \times 10^6$ cells per vial).

5.2.4 IN VIVO *SHRNA SCREEN*

Six of 12 female NOD-*scid* mice were implanted with slow release atRA pellets (7.5 mg / 90 days, Innovative Research of America) one week prior to all mice being injected with 2×10^6 cells in their mammary fat pads (admixed 1:1 high concentration Matrigel) of pool 1, 2 or 3 MDA-MB-231 cells (n=2). Three weeks post tumor-cell implantation, mice were euthanized, and tumors harvested. Genomic DNA was extracted using the PureLink DNA kit (Invitrogen).

Genomic DNA was subjected to PCR with Phusion High Fidelity DNA polymerase (ThermoFisher) and the negative selection primers included with the Decode screen (RHS5339). 250-350 bp PCR products were purified using the QIAquick Gel Extraction kit (Qiagen). 1 μg DNA from each pool was combined for a total of 3 μg per sample.

Samples were labelled with Cy3 and Cy5, hybridized to microarrays (ThermoFisher, BCA5101), scanned, and data extracted and normalized by Ambry Genetics (California, USA) following the instructions in the Decode Array kit. Fold changes for each sample were calculated and shRNAs identified which were overrepresented and underrepresented in the experimental sample (MDA-MB-231 with atRA treatment).

5.2.5 *Lentiviral Vectors, Assembly, and Infection*

Individual shRNA knockdown clones were generated from pGipZ lentiviral vectors (Dharmacon, Table 5-1). Briefly, lentivirus was assembled in HEK293T cells using a second-generation packaging system (pMD2.G, pSPAX2). Lentiviral supernatants were collected and filtered (0.45 μm) prior to being applied to MDA-MB-231 cells. MDA-MB-231 cells were cultured in the presence of lentiviral supernatant for 4 hours before replacing with complete medium. Cells were selected with 1.5 μg/mL puromycin and maintained in the presence of 0.25 μg/mL puromycin.

Table 5-1 Lentiviral vectors utilized

Gene	Clone ID
COL11A2	V2LHS_192781
RNF138	V2LHS_115205
FAT2	V2LHS_131732
BTG3	V2LHS_257705
GCH1	V2LHS_83031
NCSTN	V2LHS_300632
	V2LHS_300630
TNNT3	V2LHS_84670
MUT	V2LHS_76342
FCRL3	V2LHS_118186
INDO	V2LHS_133258
CTSH	V2LHS_24107
ATP5A1	V2LHS_192755
LEPR	V2LHS_133949
IL22RA2	V2LHS_118324
BCL2L14	V2LHS_202519
DDX47	V2LHS_239028
RNF111	V2LHS_254793
MARK3	V2LHS_151569
SCN1A	V2LHS_94851
TET2	V2LHS_119120
GPR149	V2LHS_144667
PRSS12	V2LHS_27903
GABRA3	V2LHS_130704
TNFSF13B	V2LHS_196484
CS	V2LHS_172878
	V2LHS_172874
NRSN1	V2LHS_65344
SLC9A6	V2LHS_197128
HUS1	V2LHS_48957
NBEA	V2LHS_114586
SAT1	V2LHS_241156
ABCG4	V2LHS_205772
CORO2B	V2LHS_69591
CIR	V2LHS_67521
SPATA22	V2LHS_159467
PKHD1L1	V2LHS_210972
BCAM	V2LHS_62437
SCEL	V2LHS_16715
	V2LHS_16718

Gene	Clone ID
LOC645884	V2LHS_103737
MTA2	V2LHS_36305
	V2LHS_36306
HTR4	V2LHS_131042
	V2LHS_131038
TPP1	V2LHS_92761
PSG4	V2LHS_182868
SGPL1	V2LHS_47926
STK4	V2LHS_56692
LOC100130100	V2LHS_139377
COPS8	V2LHS_118860
UCN3	V2LHS_88456
CCL24	V2LHS_31054
JAK1	V2LHS_133563
BMP6	V2LHS_150044

5.2.6 IN VIVO *TUMOR GROWTH ASSAYS*

One day prior to tumor-cell implantation, experimental mice were implanted with a slow-release atRA pellet (5 mg / 60 days, Innovative Research of America). 2 x 10^6 MDA-MB-231 cells, admixed 1:1 with high concentration Matrigel (BD Bioscience), were injected orthotopically into the mammary fat pad of female NOD-*scid* mice and primary tumor growth was quantified (mm^3, length x width x depth / 2). Tumor-bearing mice were euthanized and tumor weight quantified.

5.2.7 *METASTASIS ASSAYS*

Lungs were collected from tumor-bearing mice. Tissue was finely minced and passed through a 40 μm filter. Cells were incubated in red blood cell lysis buffer (150 mM NH_4Cl, 10 mM $KHCO_3$, 100 nM Na_2EDTA, pH 7.3) for 5 min. Cells were analyzed by flow cytometry (FACS Calibur) for GFP expression. Lungs from a tumor-naïve mouse were used as a negative control; GFP-expressing MDA-MB-231 cells were used as a positive control.

5.2.8 *QUANTITATIVE PCR*

Total RNA was extracted using Trizol reagent and the PureLink RNA kit (Invitrogen) with DNase treatment. Equal amounts of RNA were reverse-transcribed using iScript (BioRad) and quantitative real-time PCR (qPCR) was performed using gene-specific primers (Table 5-2). Standard curves for each primer set were generated, and primer efficiencies were incorporated into the CFX Manager software (Bio-Rad). mRNA expression of all samples was calculated relative to two reference genes [glyceraldehyde 3-phosphate dehydrogenase (GAPDH) and β-2-microglobulin (B2M)], and an indicated control sample.

Table 5-2 Primers utilized for qPCR.

Gene Symbol	Primer (5' – 3')		Reference
GAPDH	F	GGAGTCAACGGATTTGGTCGTA	(Marcato et al., 2015)
	R	TTCTCCATGGTGGTGAAGAC	
B2M	F	AGGCTATCCAGCGTACTCCA	(Coyle et al., 2016)
	R	CGGATGGATGAAACCCAGACA	
COL11A2	F	CTGATGTGGCCTACCGAGTG	
	R	CGGACAACAGTCAGCAGAGA	
RNF138	F	AGACAGCGTTTACTGGATCACT	
	R	TCTGGCTAGGATCTCCCCAA	
BTG3	F	ATCGAGGGAATGGCCATCAG	
	R	ATGTCACTGGAATTGGGCGA	
GCH1	F	AAGTCCTTGGCCTCAGCAAA	
	R	TTGTAAGGCGCTCCTGAACTT	
NCSTN	F	CCTGCTCAACGCCACTCAT	
	R	GGGGCCATCAGTCAATACCC	
MUT	F	TCCGCCAGTATGCTGGTTTT	
	R	TCGCCAGATCAAAGGCAACT	
FCRL3	F	TGGCCCCAAAAGCTGTACTT	
	R	CTGCTGCATATGAGAGCCACT	
IDO1	F	GGGAAGCTTATGACGCCTGT	
	R	CTGGCTTGCAGGAATCAGGA	
CTSH	F	CATCGCAACCGGAAAGATGC	
	R	ATACTCGAAAGCCTGGCTGG	
ATP5A1	F	AAAGACTGGGACTGCTGAGATG	
	R	ATGTACGCGGGCAATACCAT	
LEPR	F	TGTCAGTCTCCCAGTTCCAGA	
	R	TGTGTAGGCTGGATTGCTCC	
BCL2L14	F	GCTCAGGGTCAAAGGACGTT	
	R	GACTTTGGGGTCCACAGCTT	
DDX47	F	TGCCCTAGTTCTTACCCCGA	
	R	ATCACAGCACTCTGCACTCC	
RNF111	F	GGACCTGAGCAACAGTGGTAT	
	R	GGCCTGATGGCCAAAGATTG	
SCN1A	F	TTGTGTCTGCAAGATCGCCA	
	R	CTATCCACTCCCCACACAGC	
TET2	F	ACACAGCAACCCCAAACTGA	
	R	CATACAGGCATGTGGCTTGC	
PRSS12	F	GACCCGACCGCAGTGATTAT	
	R	AGAGTGGTAAACAGGCTGGC	
GABRA3	F	CATGACCAGCCTTGGGATTCT	
	R	AAAGTCCCCGGGTTCTTGTC	

Gene Symbol	Primer (5' – 3')		Reference
TNFSF13B	F	CCACAGAAAGGGAGCAGTCA	
	R	GGACAGAGGGGCTTTCCTTC	
CS	F	CCCCATGTCTCAGCTCAGTG	
	R	TTGGTTCGGCTGATACCCTG	
NRSN1	F	ACACCCAGCCGGTTACAAAA	
	R	TCAGGTTGCCAGTAGAGGCT	
SLC9A6	F	CAGCGCCCCAAGGAGATTTA	
	R	ATTGGAAGAACCAGGCGTGT	
HUS1	F	TATGTCAAGCAGTAGCCGCA	
	R	GGGACCACCGGTTCTTGTAA	
NBEA	F	TATGGTCTGCCACAAGCCAG	
	R	TGCCAGCGCTGAGTCATATT	
SAT1	F	GGTTGCAGAAGTGCCGAAAG	
	R	TGCCAATCCACGGGTCATAG	
ABCG4	F	GGGGCTGGCAAGTCTACATT	
	R	TCCCGTGGCCTTCCATTAAC	
CORO2B	F	GACTCTCAAGGGCCTGATCG	
	R	GTGCCTGGTGTCATTGGGTA	
CIR	F	GTTCCCACTGATGGCTCAGG	
	R	TTGCGGTCAAGTTTCTCCCC	
BCAM	F	TCGTTGCTGTCTTCTACTGCG	
	R	GGCGGAGCCCCCTTCT	
SCEL	F	CCAAAGTCTCGACAGCCTCA	
	R	CTGCTTTTGTTTGCTGAAGGGA	
MTA2	F	AGGCACCCCTGAAACCAAAA	
	R	GCCCGTTTCACCATAATGCC	
HTR4	F	CCCTGTGCATCATCATGGGT	
	R	AGGAAAGCAGTCCACACCTG	
TPP1	F	TTGACCTCACAAGACGTGGG	
	R	GCAAAGTTGCCACCGAAGAG	
SGPL1	F	AAGATTGTGCGGGTCCCATT	
	R	GTGGGGTAGAACAGACGAGC	
STK4	F	AGAGACCGGCCAGATTGTTG	
	R	ATGAGGGCTGTCACATTGCT	
LOC100130100	F	CGGGCAAGTCAGGGCATTA	
	R	CCACTGAACCGAGATGGGAC	
COPS8	F	ATCGCCGATGATTTTGCAGC	
	R	TGGTGGAATCAGCTTGCCAT	
CCL24	F	GCAGGCCTGATGACCATAGTA	
	R	CAGAGCCCGTAGGGATGATG	
JAK1	F	TCAGTGTGGCGTCATTCTCC	
	R	CAGTGAGCTGGCATCAAGGA	

Gene Symbol	Primer (5’ – 3’)		Reference
BMP6	F	CCTTACGACAAGCAGCCCTT	
	R	TGGGACTGGGTAGAGCGATT	
GAD1	F	AATACCACTAACCTGCGCCC	
	R	CTTCCAGGCTGTTGGTCCTT	
GAD2	F	AATACCACTAACCTGCGCCC	
	R	CTTCCAGGCTGTTGGTCCTT	

5.2.9 *Metabolomics Screen*

Samples were prepared and analyzed as described previously (Yuan et al., 2012). MDA-MB-231 and RMF-EG cells were grown in 6-well plates and treated with or without 100 nM atRA. Cells were collected in 250 µL of 80% ice cold methanol. 25 µl of cells or media were combined with 225 µl of hydrophilic interaction liquid chromatography (HILIC) loading buffer: 5% (v/v) acetonitrile, 2 mM ammonium hydroxide, 2 mM ammonium acetate, pH 9.0. 50 µL injections of the samples were loaded in triplicate on a Acquity UPLC BEH Amide, 1.7 µm particle size, 2.1 x 100 mm column (Waters #186004801). Metabolite levels were analyzed using multiple reaction monitoring (MRM) with an in-house triple quadrupole mass spectrometer Sciex 5500 QTRAP. Based on known Q1 (precursor ion) and Q3 (fragment ion) transitions, the metabolite name, the dwell time and the appropriate collision energies (CEs) for both positive and negative ion modes were identified. Using this protocol, a selected reaction monitoring transition list of 289 (approximately 10–14 scans per metabolite peak) metabolites can be accurately identified. Skyline software was used to integrate the peak areas from the Q3 TIC values across the chromatographic elution. Each peak area from every sample was manually confirmed.

5.2.10 *Patient Cohort and Survival Analysis*

The cohort of patients utilized in this study has been previously described (Marcato et al., 2015). RNA isolation from frozen human breast tumor samples, gene microarray analysis (GEO accession #GSE22820) and data processing were as previously described (R.-Z. Liu et al., 2011). The mRNA levels were estimated based on normalized

gene microarray signal intensity. The cut-off values to define “high” and “low” levels for each gene were determined with receiver operating characteristic (ROC) curve analysis.

5.2.11 *Statistical Analyses*

All statistical analyses were calculated in GraphPad Prism 6. Paired t-tests were used to compare single treatments, one-way ANOVA was used to compare multiple vectors, and two-way ANOVA was used to compare combinations of treatments and/or vectors. Multiple fitted curves were compared for goodness of fit using the AIC method (without H_0 testing). For all comparisons, * $p < 0.05$, ** $p < 0.01$, *** $p < 0.001$.

5.3 RESULTS

5.3.1 *RNAi SCREEN IDENTIFIES 135 POTENTIAL EFFECTORS*

RA is generally regarded as a differentiation agent with broad anti-tumor activities. Although resistance to atRA has been described in the literature (Centritto et al., 2015; Lin et al., 2017; Liu et al., 1996; Merino et al., 2016; Takatsuka et al., 1996; Tari et al., 2002; Wei et al., 2015), there are few reports of tumor promoting effects of atRA (Marcato et al., 2015; Schug et al., 2007). We have previously reported that atRA is capable of promoting tumor growth in several TNBC cell lines: MDA-MB-231, MDA-MB-435, MDA-MB-436, HCC11887, and Du4475 (Marcato et al., 2015). The ALDH-high enrichment of CSCs and the successful use of RAR antagonists also point to cell-intrinsic retinoid signaling as tumor promoting in these models.

We selected the well-studied MDA-MB-231 cell line to identify and characterize putative effectors of tumorigenic retinoid signaling. Consistent with our previous observations (Marcato et al., 2015), we observed that atRA treatment increased the growth of MDA-MB-231 xenografts (Figure 5-1A). Most functional studies of atRA have focused on its tumor inhibiting effects (Wei et al., 2015; Zanetti et al., 2015); and, existing hypotheses for the tumor-promoting role of atRA, such as alternative shuttling of atRA to peroxisome proliferator response elements (PPREs) via binding to fatty acid binding protein 5 (FABP5), do not seem to be of great importance in the models we have tested (Chapter 4; Coyle et al., 2017b; Marcato et al., 2015). As such, we utilized an unbiased genome-wide RNAi screen to identify putative novel effectors responsible for the tumor-promoting effects of atRA in MDA-MB-231 (Figure 5-1B).

We performed the RNAi screen *in vivo* to allow for cell-extrinsic factors to affect the identification of mediators in this model. We performed two biological replicates in NOD-*scid* mice (Figure 5-1C). Representation of each barcode was calculated in each replicate relative to the untreated control, and mean fold-change was determined (Figure 5-1D). We identified 135 genes which were depleted more than 2-fold in atRA-treated MDA-MB-231 xenografts (Figure 5-1E). DAVID analysis of the top 135 genes did not reveal any enriched pathways or Gene Ontology designations.

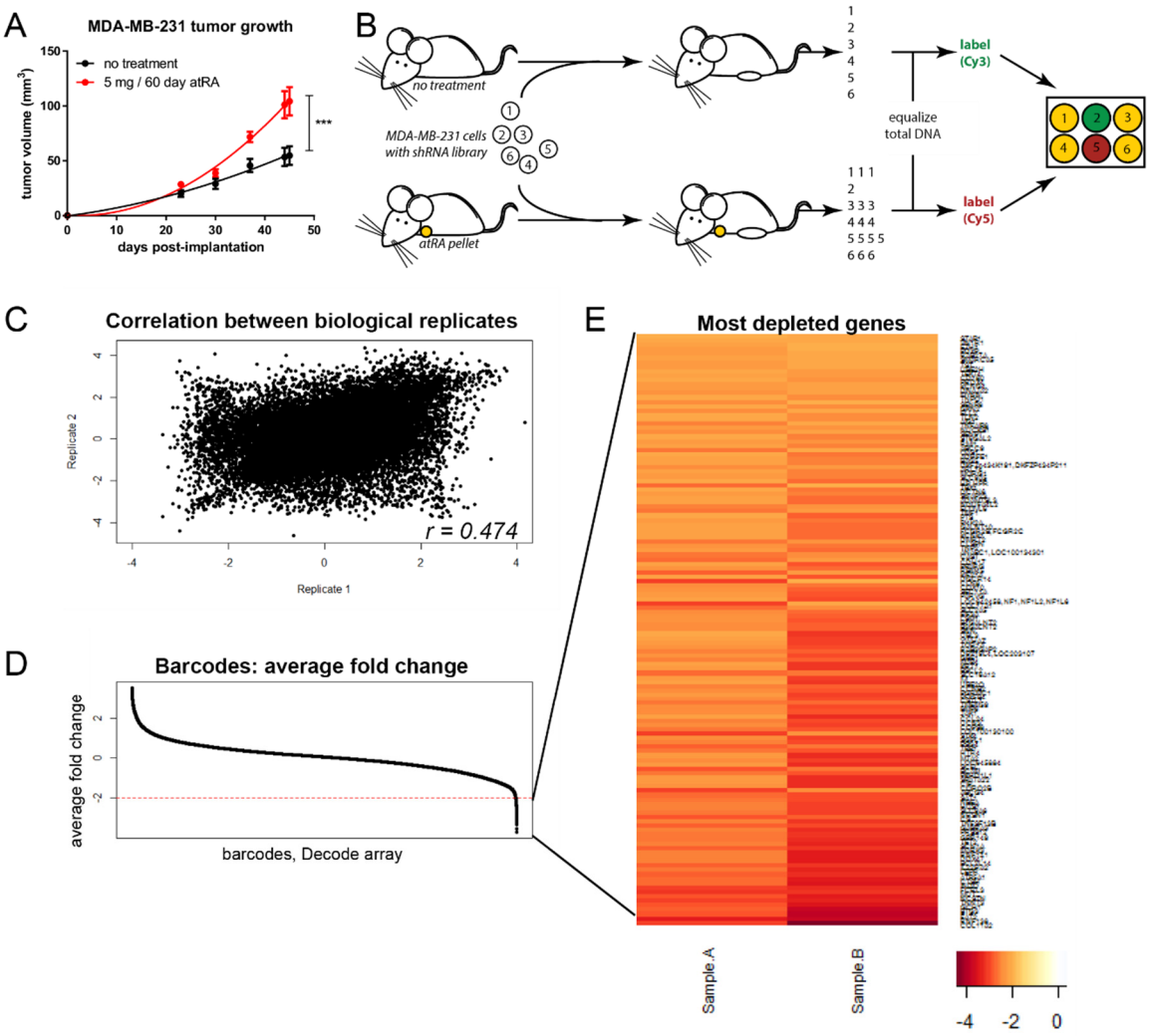

Figure 5-1 Genomic loss-of-function screening identifies 135 putative mediators of pro-tumorigenic retinoid signaling.

A. Growth of MDA-MB-231 xenografts is enhanced in NOD-*scid* mice in the presence of 5 mg/ 60 day slow-release atRA pellet. **B.** Lentiviral-containing MDA-MB-231 cells were implanted in mice with or without atRA pellets; DNA was extracted, labelled, and hybridized to microarray. **C.** Fold-change of each barcode in two biological replicates are plotted and compared by linear correlation. **D.** Average fold change between two biological replicates is plotted and **E.** individual fold-change vales for the 135 genes depleted more than 2-fold are shown.

5.3.2 IN VITRO *GENE-LIST PRIORITIZATION*

We prioritized the genes associated with the 50 most depleted barcodes for further validation (Table 5-3). To validate on-target effects of the identified shRNAs, we generated individual clones utilizing the sequences identified in the screen. These clones were validated by gene-specific qPCR (Figure 5-2A). Genes which were not effectively targeted by the indicated shRNA were eliminated from further validation. This approach eliminated six genes from the top 50, which represents 12% and is a reasonable proportion of off-target effects. This percentage may be higher based on verification of the 13 incomplete knockdowns (shown as *n.d.* in Figure 5-2A). This illustrates the importance of validating the gene hits from the shRNA screen.

Following the validation of the identified shRNA sequences, we examined whether screen hits were regulated by atRA. Using MDA-MB-231 cells treated with 1 μM atRA, genes were queried by qPCR (Figure 5-2B). Fewer than half of the genes examined were differentially regulated in the presence of atRA. This reductive approach does not eliminate the possibility that the putative effectors participate in the retinoid signaling pathway in other ways. Genes may still affect retinoid catabolism, RAR phosphorylation and localization, or the activity of coactivators or corepressors.

We utilized the validation of gene knockdowns and potential regulation by atRA to prioritize six genes for *in vivo* investigation.

Table 5-3 Average fold depletion for 50 prioritized genes.

Gene symbol	Average fold depletion	Gene description
COL11A2	-3.71	collagen, type XI, alpha 2
RNF138	-3.54	ring finger protein 138
FAT2	-3.34	FAT tumor suppressor homolog 2 (Drosophila)
BTG3	-3.25	BTG family, member 3
GCH1	-3.15	GTP cyclohydrolase 1
TNNT3	-3.15	troponin T type 3 (skeletal, fast)
NCSTN	-3.14	nicastrin
MUT	-3.13	methylmalonyl Coenzyme A mutase
FCRL3	-3.13	Fc receptor-like 3
INDO	-3.12	indoleamine-pyrrole 2,3 dioxygenase
CTSH	-3.03	cathepsin H
ATP5A1	-3.00	ATP synthase, H+ transporting, mitochondrial F1 complex, alpha subunit 1, cardiac muscle
LEPR	-2.96	leptin receptor
IL22RA2	-2.96	interleukin 22 receptor, alpha 2
BCL2L14	-2.94	BCL2-like 14 (apoptosis facilitator)
DDX47	-2.93	DEAD (Asp-Glu-Ala-Asp) box polypeptide 47
RNF111	-2.92	ring finger protein 111
MARK3	-2.91	MAP/microtubule affinity-regulating kinase 3
SCN1A	-2.90	sodium channel, voltage-gated, type I, alpha subunit
TET2	-2.89	tet oncogene family member 2
GPR149	-2.88	G protein-coupled receptor 149
PRSS12	-2.85	protease, serine, 12 (neurotrypsin, motopsin)
GABRA3	-2.84	gamma-aminobutyric acid (GABA) A receptor, alpha 3
TNFSF13B	-2.84	tumor necrosis factor (ligand) superfamily, member 13b
CS	-2.83	citrate synthase
NRSN1	-2.82	neurensin 1
SLC9A6	-2.79	solute carrier family 9 (sodium/hydrogen exchanger), member 6
HUS1	-2.79	HUS1 checkpoint homolog (S. pombe)
NBEA	-2.79	neurobeachin
SAT1	-2.78	spermidine/spermine N1-acetyltransferase 1
ABCG4	-2.76	ATP-binding cassette, sub-family G (WHITE), member 4
CORO2B	-2.76	coronin, actin binding protein, 2B
CIR	-2.75	CBF1 interacting corepressor
SPATA22	-2.74	spermatogenesis associated 22
PKHD1L1	-2.74	polycystic kidney and hepatic disease 1 (autosomal recessive)-like 1

Gene symbol	Average fold depletion	Gene description
BCAM	-2.73	basal cell adhesion molecule (Lutheran blood group)
SCEL	-2.73	sciellin
LOC645884	-2.73	similar to 40S ribosomal protein S7 (S8)
MTA2	-2.72	metastasis associated 1 family, member 2
HTR4	-2.71	5-hydroxytryptamine (serotonin) receptor 4
TPP1	-2.70	tripeptidyl peptidase I
PSG4	-2.70	pregnancy specific beta-1-glycoprotein 4
SGPL1	-2.70	sphingosine-1-phosphate lyase 1
STK4	-2.70	serine/threonine kinase 4
LOC100130100	-2.70	similar to hCG26659
COPS8	-2.69	COP9 constitutive photomorphogenic homolog subunit 8 (Arabidopsis)
UCN3	-2.69	urocortin 3 (stresscopin)
CCL24	-2.69	chemokine (C-C motif) ligand 24
JAK1	-2.67	Janus kinase 1 (a protein tyrosine kinase)
BMP6	-2.67	bone morphogenetic protein 6

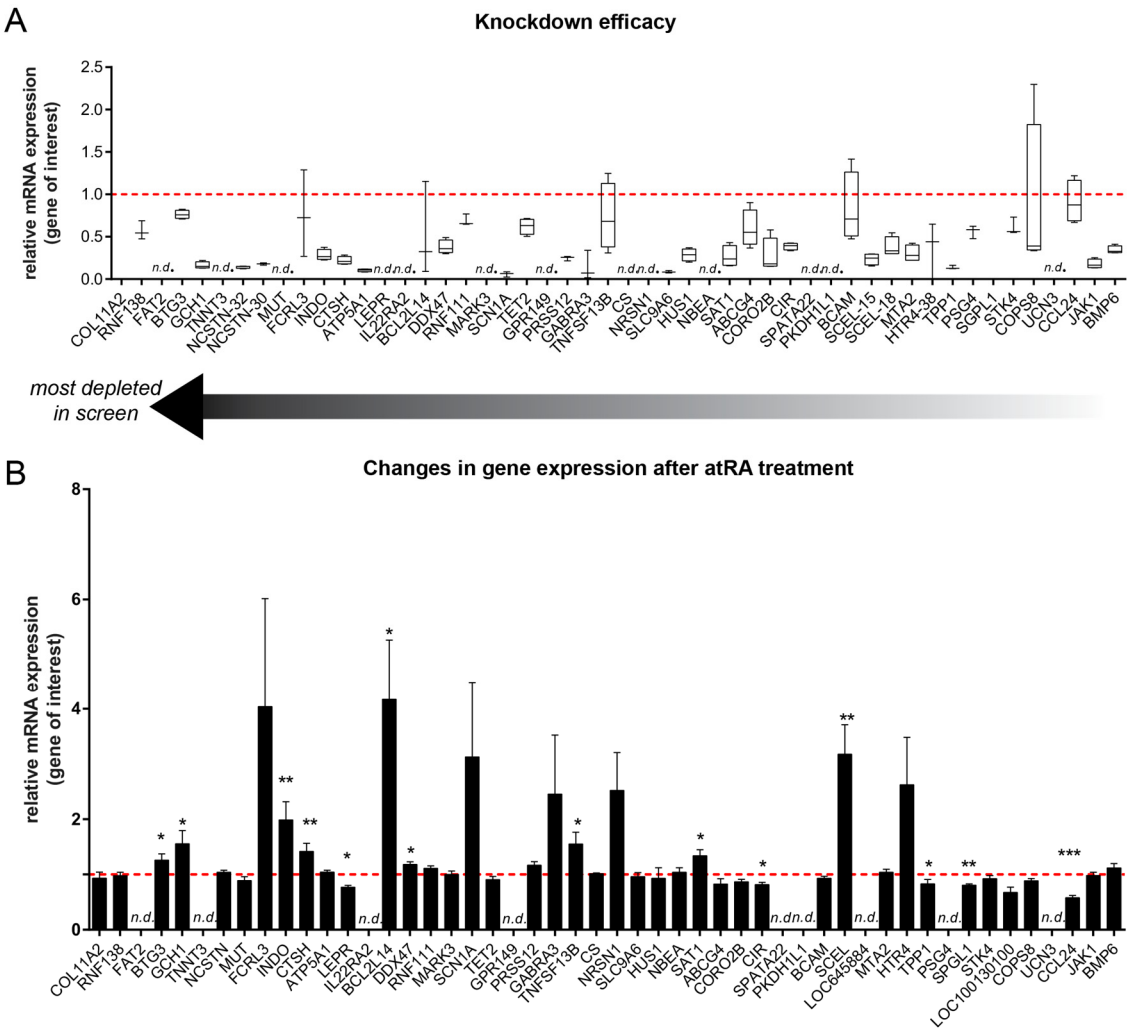

Figure 5-2 Putative effectors of retinoid signaling are targets of retinoid signaling.

A. Individual shRNA knockdowns were generated using the vectors identified in the screen. qPCR was used to determine expression of the target gene relative to pGipZ-bearing scramble control cells (n=3-4). **B.** MDA-MB-231 cells were treated with 1 μM atRA for 18h and qPCR was used to determine expression of the target gene relative to untreated cells. A paired student's t-test was used to determine statistical significance. For all comparisons, * $p < 0.05$, ** $p < 0.01$, *** $p < 0.001$, *n.d.* not determined.

5.3.3 *Knockdown of SCN1A or GABRA3 Diminishes Pro-Tumor Effect of atRA in MDA-MB-231*

Using the same single-gene knockdowns identified in the screen and generated in Figure 5-2A, we performed tumor xenograft experiments with knockdown clones of HTR4, SCN1A, GABRA3, NCSTN, SCEL, and IDO1 in two independent experiments. First, we demonstrate that atRA treatment significantly increases the growth of MDA-MB-231 (Figure 5-3A). Comparison of fitted curves (Figure 5-3B) demonstrated that shRNA knockdown of HTR4, SCN1A, and GABRA3 abrogated this pro-tumorigenic effect of atRA. Similarly, atRA treatment increased the growth of MDA-MB-231 (Figure 5-3C), and shRNA knockdown of SCEL and IDO1 abrogated this effect (Figure 5-3D). Knockdown of NCSTN did not alter the growth of atRA-treated MDA-MB-231 xenografts. This points to a functional role for HTR4, SCN1A, GABRA3, SCEL, and IDO1 in retinoid signaling.

We have previously demonstrated that atRA treatment increases pulmonary metastasis of MDA-MB-231 cells in NOD-*scid* mice (Marcato et al., 2015). Although we did not utilize the shRNA screen to identify metastatic mediators, we considered whether any of the genes which affected *in vivo* tumor growth similarly impacted pulmonary metastasis. We used the GFP-positive nature of the vector-bearing cells to determine the percentage of tumor cells in the lungs of tumor-bearing mice (as in Figure 5-3E). We noted that only GABRA3 and SCN1A shRNA knockdowns effectively reduced the percentage of metastatic cells (Figure 5-3F); while SCEL knockdown appeared to increase metastasis despite the associated decrease in tumor size (Figure 5-3G). SCN1A and GABRA3 were thus prioritized for further investigation.

Importantly, essential further validation of these gene hits with second shRNAs will eliminate the possibility of off-target effects; comparisons between atRA-treated and untreated shRNA xenografts will allow us to determine if the role of each gene in retinoid signaling is dependent on atRA treatment. Additionally, we will seek to confirm the role of these genes in MDA-MB-436 and Du4475, two additional TNBC cell lines which are promoted by atRA treatment (Chapter 4).

Figure 5-3 SCN1A, GABRA3, HTR4, SCEL and IDO1 knockdowns abrogate effects of atRA *in vivo*.

A. and **C.** The growth of MDA-MB-231 xenografts is enhanced by the presence of atRA. **B.** shRNA knockdowns of HTR4 (n=5), SCN1A (n=5), and GABRA3 (n=4) were injected into mice previously implanted with a slow-release atRA pellet. Tumor growth was measured and compared to scramble shRNA control with atRA pellet (n=5). **D.** shRNA knockdowns of NCSTN (n=4), SCEL (n=6), and IDO1 (n=5) were injected into mice previously implanted with a slow-release atRA pellet. Tumor growth was measured and compared to scramble shRNA control with atRA pellet (n=7). **E.** Representative images demonstrate the use of GFP and flow cytometry to determine the percentage of metastatic cells. **F, G.** Percentage metastatic cells measured by flow cytometry in lung tissue. Values were compared by one-way ANOVA, * $p < 0.05$. B. and D. non-linear (exponential) curves were individually compared to the curve representing growth of scramble shRNA xenograft with atRA treatment. Models were tested by AIC.

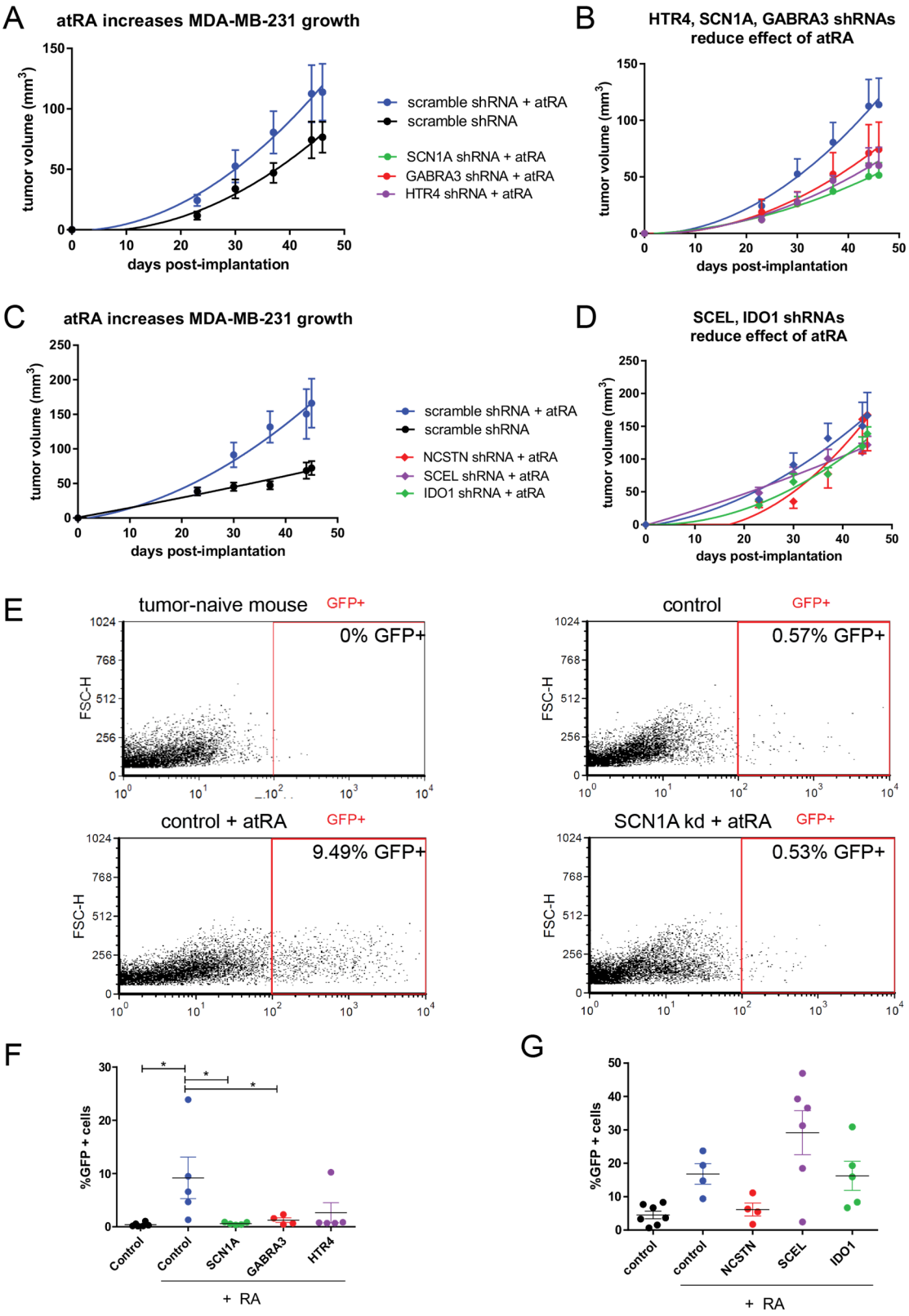

Figure 5-3 **SCN1A, GABRA3, HTR4, SCEL and IDO1 knockdowns abrogate effects of atRA *in vivo*.**

5.3.4 *GABAergic Signaling in MDA-MB-231*

SCN1A (voltage-gated sodium channel α subunit type 1) and GABRA3 (gamma-aminobutyric acid receptor subunit α3) are both indicated as critical mediators in the central nervous system (CNS), and have also been detected in cancerous tissues (Gao et al., 2010; Gumireddy et al., 2016). The identification of both SCN1A and GABRA3 (a ligand-gated chloride channel subunit) as contributors to the pro-tumorigenic effects suggested that ion channels may mediate atRA signaling; alternatively, crosstalk between SCN1A and GABAergic signaling has been indicated in neuronal models (Han et al., 2012). Studies of GABAergic differentiation in mouse embryos revealed an essential role for RA (Chatzi et al., 2011). This evidence suggested that the GABAergic pathway may be connected to atRA signaling. To determine if atRA affects GABA signaling, we detected γ-amino butyrate via a mass spectrometry metabolomics approach (Figure 5-4A). We hypothesized that changes in GABAergic signaling in tumor cells may be supported or influenced by alterations to cancer-associated fibroblasts, thus we utilized MDA-MB-231 cells and the non-cancerous immortalized RMF/EG fibroblast cells, previously generated from a reduction mammoplasty (Kuperwasser et al., 2004). We observed a small but relevant decrease in GABA levels upon atRA treatment in MDA-MB-231 cells, but no measurable change in GABA in RMF/EG cells (Figure 5-4).

We investigated the expression of GABRA3 and glutamic acid decarboxylases 1 and 2 (GAD1, GAD2) in MDA-MB-231 and RMF/EG cells (Figure 5-4B). The high expression of GAD1 and GAD2 in MDA-MB-231 cells as compared to RMF/EG is consistent with the levels of GABA detected in our mass spectrometry approach.

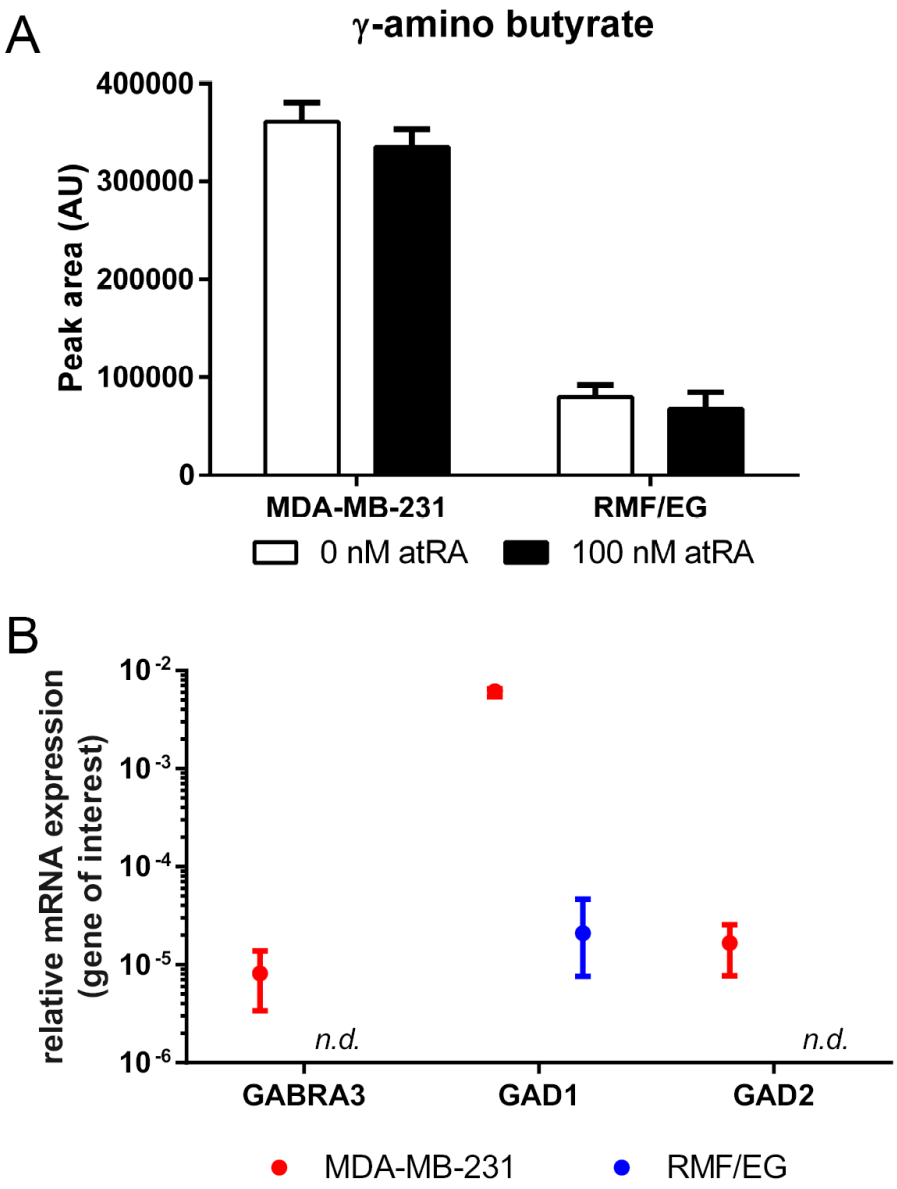

Figure 5-4 GABAergic signaling is likely initiated by tumor cells, not mammary fibroblasts.

A. Levels of GABA were determined by mass spectrometry in MDA-MB-231 and RMF/EG cells with or without atRA treatment. Errors represent standard deviation from three technical replicates. **B.** mRNA expression of GABRA3, GAD1, and GAD2 were determined in MDA-MB-231 and RMF/EG cells. *n.d.* not detected

5.3.5 *Expression of SCN1A and GABRA3 are Associated With Expression of ALDH1A3*

Since we demonstrated that both SCN1A and GABRA3 can be upregulated upon atRA treatment (Figure 5-2A), we also sought to characterize whether these genes could be regulated by the atRA-producing enzyme, ALDH1A3. Using ALDH1A3-overexpressing MDA-MB-231 cells which we have previously validated (Marcato et al., 2015), we observed small increases in expression of SCN1A and GABRA3 when ALDH1A3 is overexpressed (Figure 5-5). This is also consistent with the observed tumor-promoting effects of ALDH1A3 overexpression and atRA treatment in MDA-MB-231 cells (Marcato et al., 2015).

Similarly, in a cohort of breast cancer patients, expression of both SCN1A and GABRA3 are strongly correlated with ALDH1A3 but not ALDH1A1 (Figure 5-6). High expression of GABRA3 or SCN1A is associated with decreased survival probability in the same patient cohort (hazard ratios 2.01, 1.54 respectively). This confirms previous findings with GABRA3 (Gumireddy et al., 2016).

This connection between ALDH1A3, SCN1A, and GABRA3 as tumorigenic mediators warrants future exploration of the role of these signaling components in CSCs. It is possible that the hypothesized role for GABA signaling in mediating metastasis of breast cancer cells is related to the tumorigenic capabilities of CSCs. Identification of additional models for these effects will permit future work in this area.

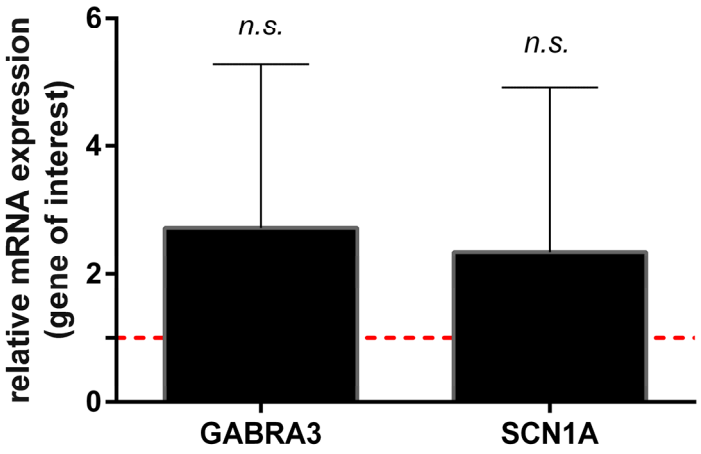

Figure 5-5 GABRA3 and SCN1A exhibit modest increases in expression when ALDH1A3 is overexpressed.

qPCR was used to determine expression of the GABRA3 or SCN1A in ALDH1A3-overexpressing MDA-MB-231 cells compared to MSCV scramble control cells (n=3). Values were compared by a paired student's t-test.

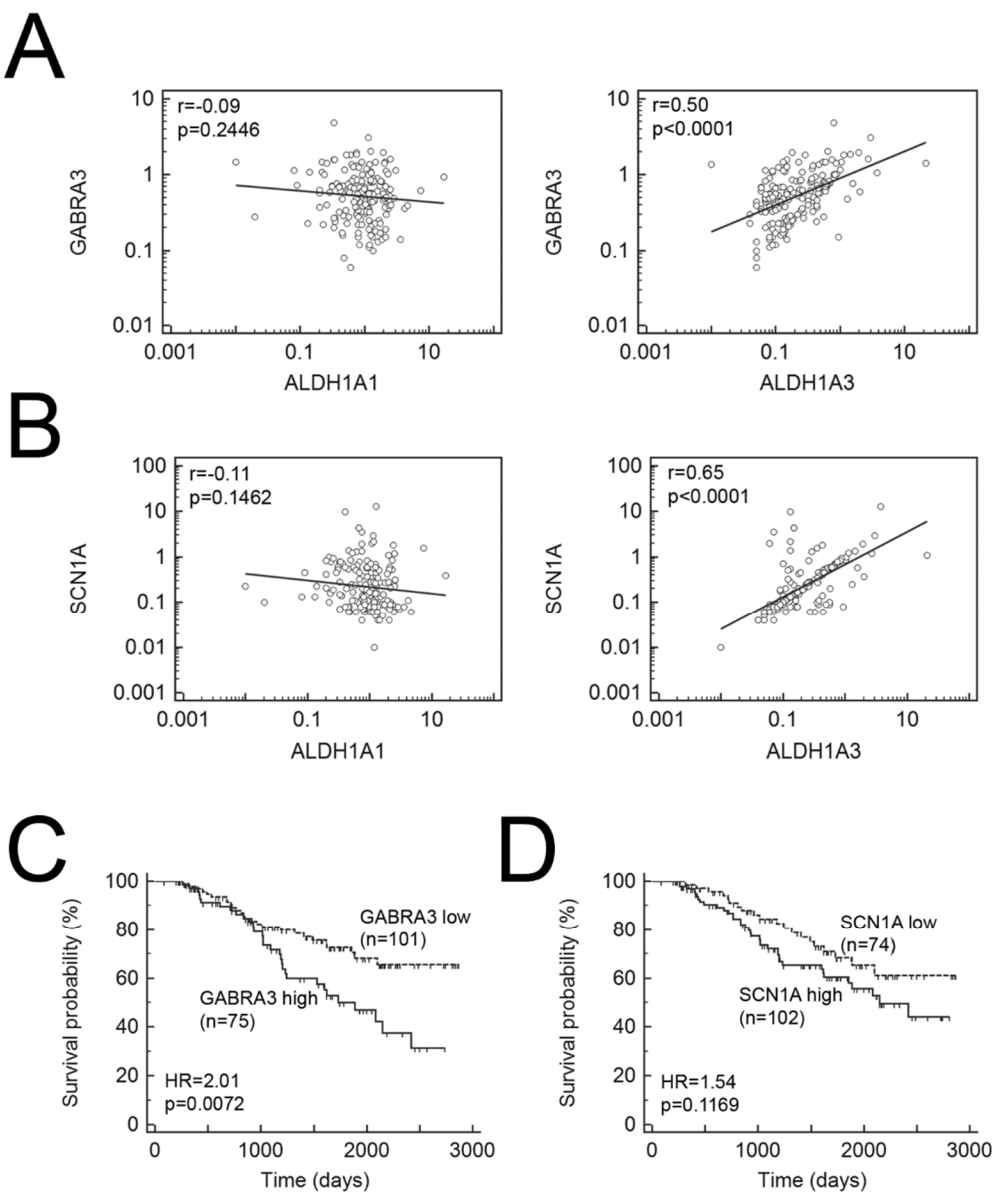

Figure 5-6 Expression of SCN1A and GABRA3 associate specifically with ALDH1A3 expression and worse patient outcomes.

A. Expression of SCN1A correlated significantly with ALDH1A3 but not ALDH1A1. **B.** Similarly, expression of GABRA3 correlated significantly with ALDH1A3 and not ALDH1A1. Kaplan-Meier survival analysis of this patient cohort revealed that high expression of **C.** GABRA3 is significantly correlated with reduced survival probability, and high expression of **D.** SCN1A is associated with reduced patient survival (not significant).

5.3.6 *Characterization of Cell Lines for Future Work*

We have previously identified that atRA promotes the growth of four TNBC cell-line xenografts: MDA-MB-231, HCC1187, Du4475, and MDA-MB-436. Having characterized contributions of GABRA3 and SCN1A to the growth and pulmonary metastasis of MDA-MB-231 cells *in vivo*, we next investigated the expression of GABRA3 and SCN1A in these additional TNBC cell lines by qPCR (Figure 5-7). We note that GABRA3 is most highly expressed in Du4475 cells (Figure 5-7A), while its expression is similar across the other cell lines. On the other hand, SCN1A is expressed at similar levels in MDA-MB-231 and Du4475 cells, while its expression is slightly higher in MDA-MB-436 cells (Figure 5-7B). SCN1A was not detected in HCC1187 cells. We thus suggest MDA-MB-436 and Du4475 for future exploration of the pro-tumorigenic role of GABRA3 and SCN1A.

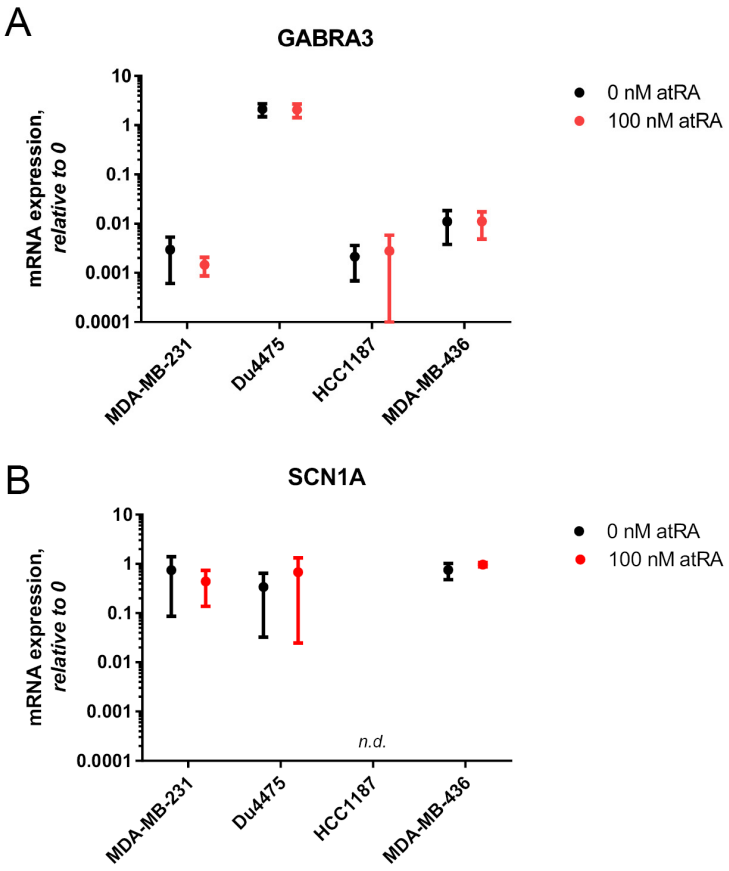

Figure 5-7 GABRA3 and SCN1A are expressed at varying levels in atRA-promoted TNBC cell lines.

Expression of **A.** GABRA3 and **B.** SCN1A was determined by qPCR in four TNBC cell lines which are promoted by atRA. Cells were treated with 100 nM atRA for 18 h. *n.d.* not detected.

5.4 DISCUSSION

In this study, we performed an *in vivo* genomic RNAi screen to identify putative effectors of the tumor-promoting effects of atRA in TNBC. We identified 135 putative mediators in MDA-MB-231, and selectively pursued validation of 50 genes. While we have previously described non-classical effects of atRA, including the possibility of non-genomic effects (Coyle et al., 2017b), part of our validation included increased mRNA expression in response to *in vivo* atRA treatment. Genes which were screened out by this approach may still play a role in potentiating or inhibiting retinoid signaling.

The lack of concordance between the genes identified in this screen and existing biomarkers for retinoid resistance (such as those described in Chapter 4) may reflect the *in vivo* nature of the screen. Conducting an RNAi screen in a solid tumor model allowed cell-extrinsic factors to impact proliferation. Both SCN1A and GABRA3 are membrane-bound proteins, which can respond to extracellular GABA, Na^+, or Cl^-. Similarly, tumor microenvironments may be best suited to studies of altered membrane potentials, given the abundance of nutrients in traditional cell culture media.

In this study, we describe the contribution of sodium channel subunit SCN1A and GABA receptor subunit GABRA3 to tumorigenesis and provide evidence of cross-talk between GABAergic and retinoid signaling. While this work illustrates a clear role for GABRA3 and SCN1A in atRA-mediated tumor progression, the precise mechanism is not clear. Retinoid mediation of ion channels may have non-genomic effects, such as on electrical potentials which in turn affect cytoskeleton and cellular migration. Alternatively, cross-talk between GABAergic and retinoid signaling may have genomic effects which potentiate pro-growth retinoid signaling.

There is existing evidence connecting GABA signaling with retinoids. In mouse neurons, atRA treatment affects the membrane localization of GABA receptors (Sarti et al., 2013). Treatment of embryonic stem cells with atRA can also induce differentiation into GABAergic interneurons (Addae et al., 2012; Chatzi et al., 2011). The nature of the cross-talk is not clear, and may include physical interactions (Song et al., 2005) or it may be related to more classical transcriptional activities of atRA.

While we followed up on GABAergic signaling as a potential mediator of the effects of atRA, we note that both GABRA3 and SCN1A function as components of ion channels. GABRA3 is a ligand-gated calcium channel and SCN1A is a voltage-gated sodium channel. Alterations in the action potential of cell membranes (i.e. the voltage across the plasma membrane, V_m) can impact proliferation as well as cell migration (Yang and Brackenbury, 2013). Further investigation of V_m following atRA treatment with or without SCN1A and GABRA3 knockdown would provide additional insight into these phenomena.

The detection of GABA in MDA-MB-231 cell culture, prior to any adaptation to a neural niche as may be required for metastasis to the brain, suggests that this may be an inherent capability of some breast cancers. Future determination of GABA levels within other breast cancer cell lines and comparison to their metastatic capabilities may support preliminary findings that GABAergic signaling is essential for metastasis to the brain (Neman et al., 2014; Sizemore et al., 2014; Zhang et al., 2014).

Despite our successful validation of two related signaling components to the response of MDA-MB-231 cells to atRA, the use of an *in vivo* genomic RNAi screen posed several technical challenges. We demonstrate a low correlation between replicate

samples. This likely represents a substantial amount of stochastic drift. As such, the 100-fold representation of shRNAs in this experiment may have been insufficient to detect all types of functional mediators (Gargiulo et al., 2014). It is also worth considering that the fold-representation of shRNAs was calculated relative to the untreated control, and input samples were not characterized. It is highly likely that barcodes corresponding to genes essential for engraftment in a murine host were lost in this approach (Fernandez et al., 2014; Nolan-Stevaux et al., 2013). The identification of factors contributing to successful xenografting will contribute to generation of more diverse *in vivo* models of breast cancer.

The identification of pro-tumorigenic mediators in atRA-treated MDA-MB-231 xenografts may suggest opportunities for combination therapies. If further characterization of SCN1A and GABRA3 confirms them as mediators of resistance in additional atRA-resistant models, targeting ion channels in combination with atRA therapy may improve the application of atRA in clinical management of TNBC.

5.5 ACKNOWLEDGEMENTS

The authors acknowledge the financial and technical support of the Dalhousie Medical Research Foundation (DMRF) Olwen Dorothy Farrel Enhanced Gene Analysis and Discovery Core Facility. The technical assistance of Dr. Barry Kennedy and Dr. J Patrick Murphy is also gratefully acknowledged.

Support was provided by grant funding to PM from the Canadian Institutes of Health Research (CIHR, MOP-130304), the Beatrice Hunter Cancer Research Institute (BHCRI), the Breast Cancer Society of Canada, and the QEII Health Sciences Center Foundation. MS and KMC are supported by the BHCRI with funds provided by the Canadian Imperial Bank of Commerce and by the Nova Scotia Health Research Foundation. MS received support from the Dalhousie Cancer Awareness and Research Society. KMC is supported by a CGS-D award from CIHR, by the Dalhousie Medical Research Foundation, and by the Killam Trusts at Dalhousie University.

CHAPTER 6: DISCUSSION

6.1 SUMMARY OF WORK

This work had five broad objectives which set the stage for consideration of atRA as a clinical agent in TNBC:

1. establish a single-gene paradigm for DNA methylation as a determinant of retinoid signaling (Chapter 2);

2. characterize and compare the broad transcriptional responses of two TNBC cell lines to atRA and ALDH1A3 (Chapter 3);

3. determine the range of *in vivo* responses to atRA in TNBC cell line xenografts and PDXs (Chapter 4);

4. identify and validate a transcriptional and epigenetic signature which predicts the response of TNBCs to atRA *in vivo* (Chapter 4); and,

5. identify and confirm functional effectors of the pro-tumor responses of TNBC models to atRA (Chapter 5).

6.1.1 *EPIGENETIC FACTORS ARE SECONDARY DETERMINANTS OF RETINOID SIGNALING*

Our characterization of the broad range of expression of RARRES1 suggests that the context-specific expression of genes, related to the impact of epigenetic factors and expression of regulatory factors, may be important in determining the response of patients to anti-cancer therapies. This provided the impetus for broader characterization of the transcriptional response to atRA, as well as for the use of multiple models in studying the therapeutic relevance of atRA for TNBC.

6.1.2 *atRA-Induced Transcriptional Response is Largely RARE-Independent*

Through characterization of the transcriptional response to atRA in two TNBC cell lines from different subtypes, this study revealed a larger network of interactions (e.g. atRA-IRF1-CTSS) as well as epigenetic regulatory factors (i.e. DNA methylation) that govern the expression of genes upon atRA treatment. This response was largely independent of the presence of canonical RAREs in the induced genes. I concluded that restricting analysis of atRA-responsiveness in breast cancer to canonical RARE-containing genes would limit the biological relevance of future studies.

This study identified a lack of concordance between the ALDH1A3-induced and atRA-induced transcriptional profiles and suggested alternate substrates which may account for this discrepancy. Studies of the impact of ALDH1A3 in breast cancer, particularly as a CSC marker, should thus consider non-atRA mediated effects (i.e. alternative substrates as discussed in Chapter 3).

6.1.3 *TNBC Exhibits a Range of Cellular Responses to atRA*

To our knowledge, this is the first *in vivo* characterization of the response of TNBC cell-line and PDXs to atRA treatment. In contrast to predominantly *in vitro* literature findings, I identify a subset of TNBCs which are sensitive to atRA treatment and confirm this using four PDXs. After examining the presence of driver mutations and expression of key retinoid pathway genes, I conclude that key hypotheses for retinoid sensitivity (FABP5:CRABP2, RARβ methylation) are not applicable to the TNBC models utilized in this work.

6.1.4 *Predicting the Response of TNBCs to atRA*

Driven by the hypothesis that the cellular context of breast cancer cells (i.e. the expression of atRA-inducible transcription factors) is a major contributing factor to the divergent responses observed to atRA, we used a data-driven approach to identify predictive biomarkers in our training set of 13 TNBC cell lines. We identified gene-expression and DNA methylation profiles which were associated with atRA sensitivity of five TNBC cell lines and applied this to four PDXs. While gene expression profiling predicted two PDXs as resistant or promoted (two could not be clustered), DNA methylation predicted all four PDXs as sensitive to atRA treatment. All PDXs tested were sensitive to *in vivo* atRA treatment, suggesting that DNA methylation is the most predictive of sensitivity.

6.1.5 *Identification of Functional Effectors*

We utilized a loss-of-function RNAi screen to discover genes which were functionally relevant to the pro-tumorigenic effects of atRA in MDA-MB-231. This study provided preliminary validation of the contribution of SCN1A and GABRA3 to the effects of atRA in MDA-MB-231 and evaluated a potential role for the tumor microenvironment in providing supportive signaling. We provide preliminary evidence supporting GABAergic signaling as a potential novel mechanism by which atRA may promote tumor growth.

6.2 Complexity in Retinoid Signaling Enables Diverse Responses

6.2.1 *Retinoid Signaling is a Complex Hierarchical Network*

Retinoid signaling plays important roles in development, cell and tissue differentiation, and proliferation and apoptosis (Gudas, 1994; Gudas and Wagner, 2011).

The pleiotropic effects of retinoid signaling which are both possible and necessary require diversity in signaling molecules as well as a complex network of interactions. Among nuclear hormone receptors, the diversity of signaling options in retinoid signaling is unparalleled (Leid et al., 1992).

The classical retinoid signaling pathway relies on RARs and RXRs as signaling effectors. Previous studies of cancer-associated RA signaling has indicated potential roles for the RAR and RXR NHRs in mediating sensitivity and resistance to RA. There are a number of studies which attribute resistance to epigenetic silencing of the RARβ2 promoter (Hayashi et al., 2003; Liu et al., 1996; Widschwendter et al., 2000). In contrast, this study found no correlation between methylation of RARβ2 and sensitivity of TNBC models to atRA treatment (Figure 4-4). Extending beyond RARβ2, other studies suggest that the activation of distinct genes requires different RAR or RXR isoforms (Cheung et al., 1996; Klaassen et al., 2001). I identified no correlation between the expression of RAR or RXR isoforms and expression of the RARE-containing gene RARRES1, nor was there any correlation with atRA sensitivity (Figure 2-15, Figure 4-2). It is possible that these discrepancies with existing literature are due to differences in atRA sensitivity between this study and previous, largely *in vitro*, studies (as described in Table 4-1). As well, this study uniquely considers the role of retinoid signaling in TNBC, thus eliminating much of the subtype-dependent variation in gene expression and DNA methylation. This does not exclude the possibility that RAR/RXR expression drives divergent gene expression; rather, it suggests that there are limited functional consequences to this hypothesis within TNBC.

Along with the lack of evidence supporting differences in RAR/RXR expression as a determinant of atRA sensitivity, I also demonstrate the relative paucity of classical DR5 RAREs in genes induced by atRA in either MDA-MB-231 or MDA-MB-468, and which has also been demonstrated in MCF-7 (Chen et al., 2006). This is a clear illustration of the need to consider non-classical gene expression responses to atRA and demonstrates the limitations of a selective and biased gene-by-gene approach. This study did not discuss the presence of non-classical RAREs (i.e. non-DR5 RAREs) in the respective gene lists identified; future bioinformatic analysis and motif discovery could provide a more detailed description of the nature of atRA-induced gene expression. This will be particularly relevant given a recent description of the prevalence of DR2 RAREs in the luminal MCF-7 and $HER2^+$ BT474 cells (Carrier et al., 2016).

I considered the growing body of evidence describing interactions between RARs or RXRs and other transcription factors, including thyroid hormone receptor, ER, AP-1, or PPAR (Glass et al., 1989; Hua et al., 2009; Lu and Benbrook, 2006; Ross-Innes et al., 2010; Schug et al., 2007) and did not identify a significant role for any of these known interactions (detailed in Chapters 3 and 4). Instead, I provide evidence for a dense network of interactions that governs the cellular transcriptional response to atRA. Using the example of IRF1, I also demonstrate that these interactions are dependent on the cellular context: IRF1 has no effect on CTSS expression in MDA-MB-468 cells, while significantly affecting CTSS expression in MDA-MB-231 cells. The cell-specific response to retinoid signaling in this study was not limited to the use of atRA; despite limited overlap between ALDH1A3-induced and atRA-induced transcriptional profiles, the transcriptional response to ALDH1A3 was similarly dependent on the cellular

context. This contextual diversity has previously been described for other signaling pathways such as estrogen, NF-κB and MYB (Kawashima et al., 2002; Lee et al., 2011; Ness et al., 1993; Tzukerman et al., 1994). This study provides strong evidence for a non-classical hierarchical network which contributes to the atRA-induced transcriptional heterogeneity observed in TNBC.

6.2.2 *Hierarchical Signaling Enables Heterogeneity in Transcription*

This study adds an important description of the heterogeneity of transcriptional responses to retinoid signaling. To date, this has not been well characterized in cancer models as most studies have focused on the expression of specific genes or of canonical RARE-containing genes (Centritto et al., 2015; Joshi et al., 2007). In fact, our initial study in MDA-MB-231 and MDA-MB-468 cells, which manipulated ALDH1A3 expression, is an early example of global transcriptional heterogeneity in retinoid responses (Marcato et al., 2015). Considering that this study and our previous work identified gene expression patterns which were independent of classical RAREs, the selective profiling of known retinoid response genes is unnecessarily reductionist, and may contribute to the over-identification of RARs, RXRs, or cellular retinoid binding proteins as predictors of atRA sensitivity.

It is also notable that most previous work on retinoid signaling in breast cancer focused on luminal cancers or broadly generalized TNBCs as retinoid-resistant (as in Table 4-1). The focus on TNBC models in this study adds an important dimension to the study of retinoids in breast cancer. In this study, I describe variable expression of an atRA-inducible tumor suppressor, RARRES1, across breast cancer patients, and particularly within the TNBC subtype (Figure 2-1). Furthermore, direct comparison of

the transcriptional response to atRA between MDA-MB-231 and MDA-MB-468 cells revealed significant diversity (Figure 3-1). This was further supported by gene expression analyses of 11 additional cell lines (Figure 4-5, Figure 4-6), which provides further evidence for a combinatorial network allowing context-specific retinoid signaling. Initial hypotheses for this context-specific regulation focused on the localized availability of RA, and observed that the spatial and temporal distribution of retinaldehyde dehydrogenases and RA-catabolizing genes were associated with the embryonic patterning attributed to retinoid signaling (Dolle et al., 1990; McCaffery et al., 1992; McCaffery and Dräger, 1994; Ruberte et al., 1993). Further work determined that the response to RA was not completely defined by these observations, and posit that the identity of the gene is also important in determining retinoid-mediated gene expression (Colbert et al., 1995).

Additional research has characterized diverse responses to RA in stem cells (Kashyap and Gudas, 2010; Mahony et al., 2011; Wu et al., 2017, p. 2) and suggested that the differentiation status of cells will affect the transcriptional response to RA. The models of TNBC utilized in this study may represent different differentiation states of the cell-of-origin, which positions claudin-low breast cancers as most similar to the mammary stem cell, while basal-like and luminal breast cancers are respectively more differentiated (Prat et al., 2010). However, this study demonstrates wide heterogeneity in transcriptional responses to atRA even within cell lines from a single subtype, suggesting that the specific cell context may be a larger determinant than differentiation status. Further work using models of breast cell differentiation may characterize this more accurately.

This study demonstrated that expression of retinoid pathway enzymes was not a primary contributor to the atRA-induced transcriptional heterogeneity identified in TNBC (Figure 4-2,Figure 4-3). Importantly, this study focused on the classical retinoid pathway, although it is known that additional enzymes may contribute to this pathway (Marill et al., 2000). Neither the global expression profiling nor the functional RNAi screening suggested any additional CYP enzymes or other retinoid-related genes which could play a role. This study does not exclude the possibility that genes identified as predictive biomarkers (Chapter 4) or putative functional effectors (Chapter 5, Appendix 1) may play a role in potentiating or inhibiting classical retinoid signaling, as the functional contribution of genes was only explored for RARRES1 (Chapter 2), SCN1A, and GABRA3 (Chapter 5).

The lack of correlations identified between atRA sensitivity and the expression of classical signaling components led to the investigation of DNA methylation as a context-dependent mediator of gene expression; and, by extension, of retinoid sensitivity.

6.2.3 *DNA Methylation Contributes to Cellular Responses to atRA*

Our own early profiling of transcriptional responses to ALDH1A3, and other work describing the differences between cell types, suggested that epigenetic control of retinoid-responsive genes could be a major contributor to the transcriptional diversity observed in this study (Kashyap and Gudas, 2010; Marcato et al., 2015). The subtype-specific epigenetic alterations described in RARRES1 (Figure 2-11) contributes to an emerging body of work which is now characterizing epigenomic differences between molecular subtypes of breast cancer (Chen et al., 2016; Holm et al., 2016; Karsli-Ceppioglu et al., 2017; Stefansson et al., 2015). After establishing RARRES1 as a

paradigm for epigenetic control over an atRA-inducible tumor suppressor, global transcriptional profiling of the response to atRA and decitabine in MDA-MB-231 and MDA-MB-468 demonstrated that DNA methylation contributes to global differential gene expression; however, modulating DNA methylation did not fully align the diverse gene expression responses (Figure 3-6). This pointed to a more complex network of yet-unknown factors which controls gene expression in a hierarchical manner (e.g. IRF1).

Interestingly, there some evidence which indicates that atRA contributes to changes in the epigenome: altering DNA methylation via micro RNAs (miRNAs) or modulating histone modifications (Das et al., 2010; Lu et al., 2011; Urvalek and Gudas, 2014). This study did not find any significant effect of atRA on DNA methylation of selected genes (i.e. Figure 3-7); however, a global analysis for atRA-induced changes in DNA methylation was not performed. The role of histone modifications in the response to atRA was not considered in this study beyond a limited use of the HDAC inhibitor, TSA, in Chapter 3. The subset of genes examined following TSA treatment did not show any significant effect of HDAC inhibition on gene expression (Figure 3-7, Figure 3-8). It is likely that the effect of atRA on both DNA methylation and histone modifications are specific to the cellular context. An integrative analysis which combines the changes in gene expression described in this study with consideration of DNA methylation and histone modifications may provide a more comprehensive overview of the cellular responses to atRA.

It is possible that DNA methylation could be used as a surrogate for gene expression (Jones and Laird, 1999); however, more substantial correlative work is required to decipher the meaning of individual 5-mC marks. Considering the major

contribution of DNA methylation to the transcriptional diversity observed in the TNBC models utilized in this study, I sought to characterize the association between differential gene expression, DNA methylation, and retinoid sensitivity (Chapter 4). The prediction of drug sensitivity based on epigenetic features is an emerging field of research. I have defined key differences in genomic methylation between atRA-sensitive and atRA-resistant models of TNBC (Figure 4-7). These differences were recapitulated in the atRA-sensitive PDXs, supporting their use as predictive biomarkers (Figure 4-12).

Much early work with atRA suggested it could be an effective chemopreventative agent; however, given the wide range of responses observed to atRA in this work, and the context-specific nature of those responses, I would strongly caution against widespread use of vitamin A as a preventative therapy.

6.2.4 *Signaling Cross-Talk: FABP5/CRABP2*

Ligand crossover between PPARs and RARs allows for additional diversity in non-classical retinoid signaling, and a major hypothesis for the differential effects of atRA on cell proliferation centers on alternative shuttling of atRA by FABP5 to PPREs in the absence of adequate CRABP2 (as in Figure 1-6). atRA binds CRABP2 with much higher affinity, thus the pro-proliferative effects as a result of binding to FABP5 will only be apparent when CRABP2 is not highly abundant (Schug et al., 2007). This study did not confirm this mechanism as a key contributor to the opposing effects of atRA in the selected TNBC models. My characterization of the FAPB5:CRABP2 ratio across 13 TNBC cell lines indicates no correlation with atRA sensitivity (Figure 4-2).

The initial characterization of FABP5 as a tumor-promoting signal transducer focused on a select number of PPAR-inducible genes in two cell lines which were from

highly different subtypes (luminal MCF-7, HER2-like tumors derived from MMTV/neu transgenic mice) (Schug et al., 2007). Considering that HER2-induced signaling may itself affect retinoid signaling (Siwak et al., 2003; Tari et al., 2002), this comparison may not be as relevant in the TNBC models used in my work.

In TNBC specifically, one study has characterized high FABP5 expression across the subtype (R.-Z. Liu et al., 2011, p. 5); however, this cannot explain the diversity of responses to atRA treatment observed in Chapter 4 (Figure 4-2). By exclusively focusing on TNBC, it was possible to eliminate much of the inter-subtype variation. Given the body of work which describes context-specific retinoid signaling, the inclusion of multiple TNBC cell lines in this study also eliminates many of the isolated phenomena which may occur when comparing individual cell lines. The use of multiple models to eliminate cell-line-specific phenotypes also necessitated a curtailed approach to biomarker discovery.

6.3 A Reductive Approach to Biomarker Discovery

Given the challenges in accurately describing the complex nature of interactions governing the transcriptional response to atRA (discussed in section 6.2), as well as the context-specific nature of this work, it was necessary to take a reductive approach to biomarker discovery. Additionally, the use of atRA as a clinical agent in non-APL malignancies predominantly predated the genomics revolution (Budd et al., 1998; Sutton et al., 1997; Toma et al., 2000b); therefore, clinical samples could not be used as a robust predictive or validation tool in this study.

There are limited examples of prognostic or predictive gene expression signatures which have been appropriately validated in clinical settings. Most cancer biomarkers lack

the required specificity and sensitivity for reasonable application in the clinic. One prominent exception is the detection of HER2 amplification in breast cancer, and successful treatment with the monoclonal antibody trastuzumab (Bartsch et al., 2007). Although transcriptional profiling is commonly used for research classification and disease subtyping, it has demonstrated little value for clinical decision making in breast cancer treatment (Azim et al., 2013).

One explanation for the lack of translatability is the failure of preclinical models to appropriately reflect heterogeneity in the tumor and microenvironment. Considering the exclusion of stroma and infiltrating immune cells from the *in vitro* and *in vivo* models utilized for this study, it would be ideal to perform pathway and network analysis as these are least likely to be confounded by additional non-tumor cells (Bruning et al., 2016; Liang and Cookson, 2014); however, I identified significant challenges in attempting pathway and network analysis in this study. There is limited consideration of the cellular context and conditions as they affect pathways, while that is a major implication of my work. Additionally, the pleotropic effects of RA on cells are not well characterized by existing annotations (Khatri et al., 2012). More preclinical modeling with additional PDX models and comparisons to clinical samples will improve the robustness of this work and ensure that it is not confounded by inter- and intra-tumoral heterogeneity.

The reductive approach to biomarker discovery detailed in this study also necessitated a focus on classical retinoid signaling; given many of the non-classical findings of this work, it is likely that non-classical retinoid signaling is an important factor to consider in studying the response of TNBCs to atRA.

6.3.1 *Tumor Heterogeneity*

Tumor cells in solid tumors do not exist as clonal populations in isolation. Tumors are typically comprised of tumor cells, supportive stromal cells, vasculature, invading immune cells, and components of an extracellular matrix (i.e. as in Figure 1-4). While these components of a tumor undoubtedly contribute to observable phenotypes and drug responses (Figure 6-1), their addition to experimental models can complicate and obscure our attempts to further characterize already complex biological pathways. The retinoid signaling pathway is considered to be one of the most complex, and this study demonstrates that much remains to be characterized. As such, the models chosen for the biomarker aspect of this study did not investigate the contributions of these cells to the drug responses during *in vitro*, *in vivo*, or *in silico* characterization.

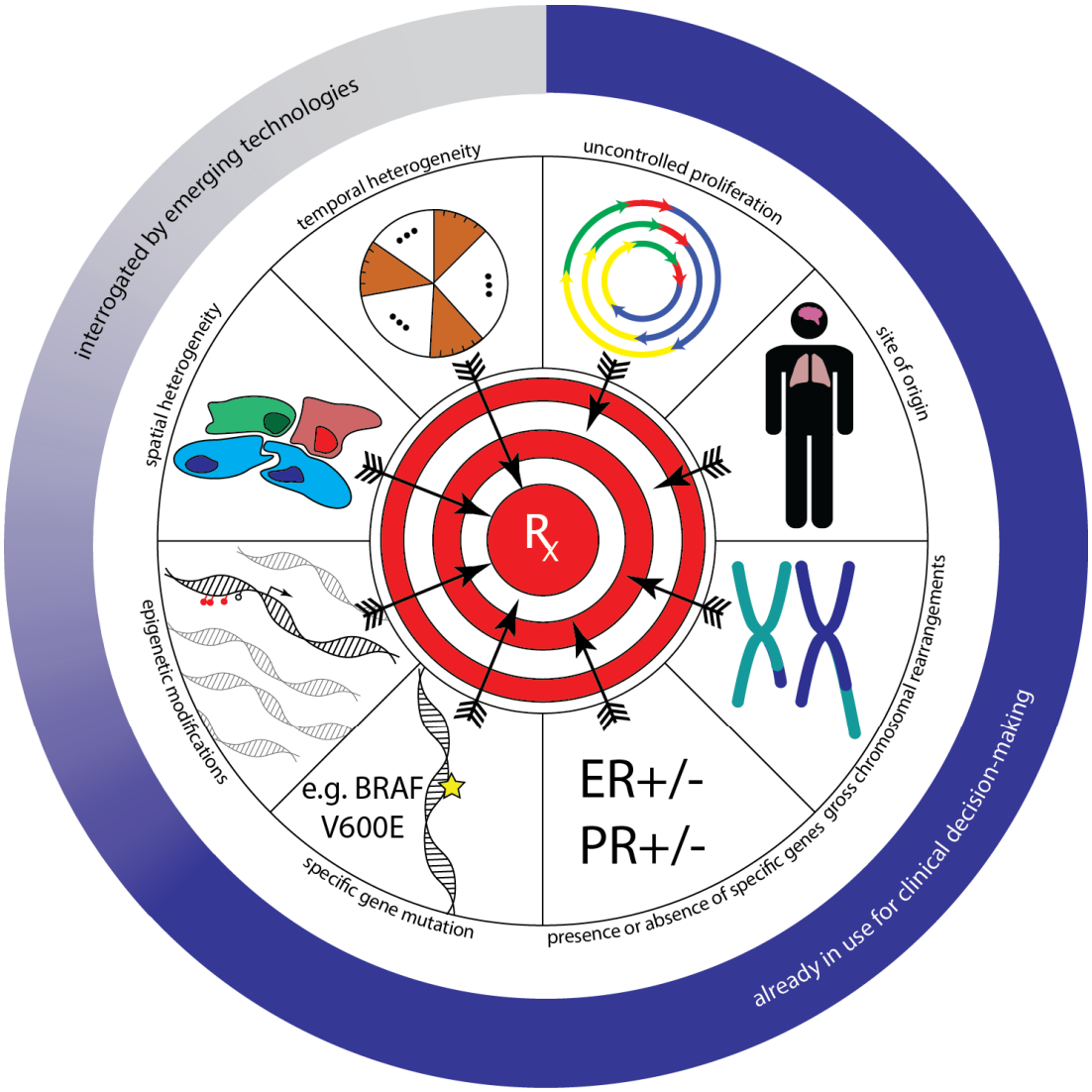

Figure 6-1 Comprehensive evaluation of tumors can enhance clinical responses.

Treatment approaches have evolved from a "one-size-fits-all" strategy based on the uncontrolled proliferation of cells and the site of a tumor's origin. Current approaches incorporate gross chromosomal rearrangements and the presence or absence of specific genes which can provide insight into the potential for therapeutic efficacy. Limited precision strategies which target specific mutations are also in use. Emerging technologies will provide a comprehensive view of cancer and allow clinical decision-making and drug development strategies to incorporate epigenetic modifications, spatial heterogeneity, and temporal heterogeneity that can enable acquired resistance to targeted therapy.

Reproduced from (Coyle et al., 2017a) with permission granted under the terms of the Creative Commons Attribution License.

Given existing descriptions of the transcriptional response to atRA, and the findings from this study, as highly dependent on the cellular context, it was necessary to take a reductionist approach to further characterization of the role of atRA and retinoid signaling in TNBC. This study considered the transcriptional response of TNBC cells to atRA and excluded possible responses of additional cells within the tumor microenvironment. The lack of concordance between the predictive biomarkers described in Chapter 4 and the putative functional mediators described in Chapter 5 and Appendix 1 highlight the limitations of this reductive approach. To consider this profile more confidently in the precision application of atRA for patients with breast cancer, it will be important to determine the effect of atRA on various other components of the tumor microenvironment, and any subsequent effects on tumor cells.

Immune function.

Characterizing the possible range of responses to atRA in TNBC required the use of multiple cell line and patient-derived xenografts. The use of these xenografts allowed this study to consider the large heterogeneity observed in patients with TNBC (as described in section 1.1.4). However, this necessitated the use of immunocompromised models. The exclusive use of NOD-*scid* mice as a host for the *in vivo* work described in this study effectively prohibits the study of interactions between atRA and immune function. This limitation is of particular importance considering the known roles of atRA in modulating immune responses (as described in section 1.4.2).

While there is limited data on the impact of atRA or vitamin A status in immune regulation during cancer therapy, it is highly likely that systemic administration of atRA will influence anti-tumor immunity. These effects may be anti-tumorigenic, by reducing

the population of myeloid-derived suppressor cells and improving antigen specific T-cell responses (Mirza et al., 2006); however, atRA may contribute to immune tolerance by supporting the development of regulatory T cells (Benson et al., 2007; Dunham et al., 2013; Nolting et al., 2009). The varied roles for atRA in immune function and modulation suggest that the specific context of each tumor will be important in predicting the impact of atRA.

The effects of atRA on the immune system will also likely depend on the nature of cell death elicited during treatment. The models used in this study did not distinguish between cytostatic or cytotoxic effects, and the type of cell death was not determined. Future work to distinguish the cytotoxicity of atRA from cytostatic effects could also characterize the immunogenicity of any observed cell death (Galluzzi et al., 2017).

Cancer associated fibroblasts.

Given that the effects we obtain with atRA treatment are distinct from literature findings based on *in vitro* evaluations of drug sensitivity, we hypothesize that the effects of atRA on CAFs play an important role in supporting the response to therapy. It should be noted, however, that while the contribution of CAFs in our model is likely to be highly similar between experiments (utilizing mice from the same genetic background, performing orthotopic implantations), that the response to therapy was still dependent on the cell-line xenograft studied. This provides further support for our evaluation of atRA sensitivity as highly tumor cell-context specific.

The supportive stromal cells in the tumor microenvironment are an important source of paracrine signaling and evidence suggests that they are an important mediator

of the effects of atRA (Guan and Chen, 2014; Papi et al., 2012). The importance of retinoid signaling in the stromal cells has been characterized in an MMTV/neu model where $RARB^{-/-}$ mice were resistant to tumorigenesis (X. Liu et al., 2011). However, this points again to the complex interplay between Her2 and retinoid signaling, and further work in luminal and basal-like breast tumors would provide additional insight to the role of the stromal cells in propagating retinoid signaling.

While our *in vitro* models lack tumor stroma, PDX models *in vivo* include murine stroma. Although this does not allow the coevolution of stromal cells with the tumor, it does permit some degree of paracrine signaling. For example, supplementation with estradiol can enhance the take-rate of ER^- xenografts (Zhang et al., 2013). Limited consideration of this is demonstrated in Chapter 5, where I evaluated the GABA release of stromal RMF/EG cells (Figure 5-4). However, I concluded that GABA signaling in MDA-MB-231 tumorigenicity is likely mediated by the cancer cells, and not the supportive stromal cells. Future consideration of paracrine signaling as it contributes to classical and non-classical retinoid signaling may improve our understanding of discrepancies between this *in vivo* work and published *in vitro* findings with models of TNBC.

Clonal heterogeneity.

The use of PDX models allowed my research to reflect aspects of clonal heterogeneity beyond those permitted by exclusive use of cancer cell lines. Evidence suggests that PDXs can retain significant heterogeneity through successive passaging (Eirew et al., 2015; Whittle et al., 2015; Zhang et al., 2013). The contributions of clonal heterogeneity to the effects of atRA may impact the clinical translation of this research

(Figure 6-1); and single-cell evaluation of clonal dynamics in response to atRA may provide important context for this.

This work describes an understudied complexity of clonal heterogeneity: breast CSCs, among the most tumorigenic cells of a tumor, can be identified by high enzymatic activity of ALDH enzymes. We have identified ALDH1A3 as a primary contributor to this activity in breast cancer, and I demonstrate that ALDH1A3 is the most highly expressed ALDH1A isoform in TNBC, with few exceptions (Figure 2-16Figure 4-2). My findings on the context-specific nature of retinoid signaling, and the role of ALDH1A3 in initiating RA signaling, leave the contribution of ALDH1A3 and subsequent generation of RA to stemness as an outstanding question.

6.3.2 *Non-Classical Explanations for Retinoid Sensitivity*

While this study identified non-classical gene expression as a determinant for sensitivity, there is limited evidence to support a causal relationship between the predictive profile and the sensitivity of TNBC models to atRA. Specifically, there is virtually no overlap between the predictive profile identified in Chapter 4 and the putative functional mediators identified in Chapter 5 or Appendix 1. Thus, the literature and evidence from this study supports future characterization of non-classical mediators to identify precise interactions contributing to sensitivity or resistance.

The most successful use of atRA in cancer therapy is as a differentiation agent in APL. Recent work suggests that the primary anti-leukemic effect of atRA is due to degradation of the PML-RAR fusion peptide, and can be uncoupled from the transcriptional activating properties (Ablain et al., 2013). There is additional evidence for non-genomic effects of atRA affecting cell growth. For example, CRABP1, bound to

atRA, can delay cell cycle progression independently of RAR, by activating ERK1/2 or PP2A (Persaud et al., 2016, 2013). The identification of SCN1A and GABRA3 as potential atRA-resistance mediators (Chapter 5) further points to non-classical mechanisms governing the response of TNBC to atRA.

Non-coding RNAs.

While non-coding RNAs (ncRNAs) were not a focus of this work, I did confirm atRA regulation of one long intergenic non-coding RNA (lincRNA), linc00857. Work examining NHR signaling pathways have identified ncRNAs functioning as cofactors, such as steroid receptor RNA activator (SRA) which can serve as a cofactor for RAR and other NHRs (Colley and Leedman, 2011; Cooper et al., 2011; Lanz et al., 1999).

Additionally, there is substantial support for regulation of miRNAs by retinoic acid (Das et al., 2010; Fisher et al., 2015; Zhang et al., 2015). I did not evaluate miRNA expression as a primary effect or a regulatory feature and this poses an alternative explanation for the RARE-independent transcriptional effects described in this work.

6.4 Towards Clinical Application: Key Considerations

While my study demonstrates a clear potential for positive responses to atRA (Figure 4-1,Figure 4-13), I have not compared atRA therapy to standard-of-care chemotherapies in this research. This will be an essential future pre-clinical investigation, prior to pursuing clinical use of atRA. There are additional limitations of the work I have undertaken which must be considered if this research is to be translated to clinical trialling and practice.

6.4.1 IN VIVO *MODELING*

There are several limitations to the *in vivo* modeling approach used in my characterization of retinoid signaling in TNBC. The use of cell lines and PDXs in this work will bias my findings towards highly aggressive and late-stage disease (Burdall et al., 2003). However, it is unlikely that atRA will be used as a first-line agent, thus the work described herein is highly relevant to the potential application of atRA in clinical management of TNBC. Similarly, this work is biased towards models which are capable of engraftment in foreign hosts. The relative paucity of claudin-low PDX models illustrates that some of these factors may be subtype-associated; it may therefore be impossible to properly recapitulate the heterogeneity of human tumors in murine models. This also demonstrates a challenge in the use of paired PDX models for clinical trials: claudin-low tumors are associated with poor prognoses but cannot be appropriately engrafted. It is not clear yet whether the treatment of PDX models will accurately reflect the treatment of tumors in human clinical settings; however, initial studies suggest that this comparison is valid in the use of cytotoxic chemotherapies (Gao et al., 2015; Zhang et al., 2013).

Our model of treating mice at, or immediately prior to, cell-line or patient-derived tumor implantation primarily reflects that atRA delays or slows tumor engraftment. This could be applied to models testing preventative interventions; however, it is not truly representative of the clinical experience of a patient with an established tumor. In future *in vivo* cell-line xenograft experiments, the tumors should be allowed to reach a minimum palpable size prior to surgical resection; atRA treatment could be examined as an adjuvant chemotherapy. Although this study utilized previously established PDXs,

further pre-clinical validation or the use of PDXs as a first step in clinical validation will present a different challenge: it is possible that atRA will affect the engraftment ability rather than characteristics of the cancer cells.

While this work details potential mechanisms for primary resistance, alternative *in vivo* models may allow for the examination of acquired resistance to atRA treatment.

6.4.2 *Pharmacokinetics of atRA*

This study utilized commercially-synthesized atRA. *In vitro*, atRA is rarely isomerized to 9cRA or 13cRA, and atRA is relatively stable for up to 24 h in serum-supplemented media (Sharow et al., 2012). On the other hand, isomerization of atRA to 13cRA occurs *in vivo* (Takitani et al., 1995); however, all effects observed in this work have been exclusively attributed to atRA. This does not exclude the possibility that *in vivo* isomerization to 9cRA or 13cRA could have biological importance, nor does it exclude the possibility that oxidative metabolites of RA have biological activity *in vitro* or *in vivo* (Pijnappel et al., 1993; Sonneveld et al., 1999). Further work with more selective, synthetic ligands could characterize the contribution of these isomers or oxidative metabolites to cancer-associated signaling.

Previous investigation of the slow-release atRA pellet produced by Innovative Research of America (utilized in Chapter 4 and 5) demonstrated sustained release over the indicated duration (Westervelt et al., 2002); however, the study indicated that with 10 mg / 21 days, average plasma atRA was approximately 30-67 ng/mL which is about 5-10 times lower than that achieved in the serum of APL patients. Further characterization of the serum levels of atRA in treated mice (5 mg / 60 days) would provide an indication of the appropriate dosing scheme for human tumors. The half-life of atRA in *Mus musculus*

is estimated at approximately 30 minutes, while it slightly longer in humans with estimates at 45 minutes (Arnold et al., 2015; Smith et al., 1992).

These limitations are essential considerations when translating the pre-clinical work described here to clinical applications, and further limitations are described below.

6.4.3 *Application of Predictive Profile*

Although I have discussed several advantages to the reductionist approach in characterizing retinoid signaling in TNBC, there are key limitations to consider in looking towards the clinical use of the predictive profile developed in this study.

The biomarkers which were identified and used in Chapter 4 to develop a predictive profile for atRA sensitivity were identified from *in vitro* models. Application and validation of this profile will be complicated by the presence of non-tumor cells in a clinical sample (described in section 1.4.1). Recent literature characterizing molecular subtyping in colorectal cancer biopsies and PDX models illustrates that it is difficult to separate tumor-derived features from stromal-derived features in a heterogenous sample (Becht et al., 2016; Dunne et al., 2016; Isella et al., 2015). Given that the profile developed in this study was built from tumor cells exclusively, future research will be necessary which considers how non-tumor cells in the microenvironment contribute to the gene expression and epigenetic modifications contained within the profile (Aran et al., 2015; Bradford et al., 2016; Gandellini et al., 2015; Isella et al., 2017; Natrajan et al., 2016). One approach may be to use laser-capture microdissection to distinguish between the tumor-cell-intrinsic and -extrinsic factors which affect measures of both mRNA expression and DNA methylation; alternatively, bioinformatic approaches may be able to distinguish between cellular compartments (Bradford et al., 2016).

Temporal heterogeneity is a major consideration for therapeutic decisions. The timing of tissue sampling often limits the application and validation of predictive biomarkers. The selective pressure of neoadjuvant or adjuvant chemotherapy can significantly alter the clonal dynamics of a tumor (Almendro et al., 2014; Findlay et al., 2016; Shah et al., 2012). The process of metastasis will also alter the makeup of a tumor from the initial local presentation (Turajlic and Swanton, 2016). The application of predictive profiling will only be as powerful as the sample from which it is determined.

6.4.4 *Signaling Complexity Implicates Potential Combination Therapies*

This thesis provides additional evidence that complexity in retinoid signaling is associated with other cellular pathways, including interferon signaling (Chapter 3) and GABAergic signaling (Chapter 5). Alongside future research investigating mechanisms of acquired retinoid resistance in TNBC, these pathway interactions demonstrate opportunities for combination therapy which could be investigated in the models described throughout my study.

Interferon signaling.

Given that I identified interferon signaling as associated with atRA signaling in MDA-MB-231 and MDA-MB-468, the modulation of this pathway is a potential therapeutic target. However, this may be similarly complicated as interferon signaling can have opposing functions in cancer: enhancing immunogenic cell death (ICD) or increasing therapeutic resistance. The evaluation of markers of ICD in response to atRA treatment of the TNBC models utilized throughout this thesis can provide additional insight into the appropriateness of manipulating interferon signaling in combination with atRA treatment. Characterization of atRA sensitivity within an immunocompetent model

will also allow the investigation of the impact of atRA-mediated interferon signaling on PD-L1 expression and additional immunosuppressive mechanisms. Following these investigations, use of interferon supplementation or interferon inhibitors (e.g. ruxolitinib, tofacitinib) in combination with atRA *in vivo* would provide further support to this combination.

GABAergic signaling.

While GABAergic signaling was classically restricted to the nervous system, evidence suggests that it may play a role in peripheral tissues, including in cancer (Song et al., 2005; Zhang et al., 2014). Our detection of GABA in MDA-MB-231 cells (Figure 5-4) supports this potential role for GABAergic signaling within breast cancer. Evidence from neural studies suggests that molecules such as dopamine or the benzodiazepine flumazenil may modulate this signaling (Johnston, 2013; Wang et al., 2002). These are primarily neurological drugs; however, as our understanding of GABA moves outside of the CNS, it is possible that new interactions may be discovered. The existing agents and novel classes may help temper pro-tumorigenic effects of atRA which are mediated by GABA.

6.4.5 *Applying This Approach to Other Cancers*

Describing substantial heterogeneity within the TNBC subtype and identifying a signature for atRA-sensitive tumors presents a novel opportunity to investigate molecular heterogeneity within other cancer types with the goal of describing retinoid sensitivity.

The use of 13cRA in neuroblastoma has improved event-free survival for a number of high-risk patients; however, there are still patients who receive no benefit from

this therapy (Reynolds et al., 2003). Recent work in neuroblastoma has attempted to develop improved strategies for risk determination (Stricker et al., 2014). Beyond improving the use of these technologies in prognostic profiling, they may also be predictive of therapeutic benefit. Identifying a molecular signature which defines success of 13cRA in neuroblastoma may allow patients with intrinsically-resistant tumors to seek alternative therapies earlier.

Retinoid use in glioblastoma is also disappointing to date. Treatment with 13cRA has been described as only 'modestly beneficial' (See et al., 2004). RA naphthalene triazole (RANT), a newer retinoid derivative which overcomes some of the toxicities associated with high-dose cRA, was associated with improved outcomes (Jia et al., 2015). There is thus some indication that retinoids may be appropriate in the clinical management of glioblastomas; however, defining the factors dictating the response of these tumors would undoubtedly improve this application.

In vitro and early clinical studies of the effects of retinoids on thyroid (Schmutzler and Köhrle, 2000), ovarian (Wu et al., 1998), and pancreatic cancers (Gupta et al., 2012; Michael et al., 2007) present additional opportunities to classify the mechanisms of atRA resistance and sensitivity in order to stratify patients successfully.

6.5 Summary of Limitations and Potential Investigations

The limitations of my work as discussed above can be broadly summarized in three categories: classical retinoid signaling, *in vivo* modeling, and clinical factors. These are reiterated with possible future directions to consider in this line of investigation.

6.5.1 *Classical Retinoid Signaling*

Throughout my investigation of the effects of atRA on TNBC, I primarily considered a classical retinoid pathway (as in Figure 1-6). Given the presence of non-classical RAREs (i.e. DR0-DR10 elements) which have been previously described, mediators of retinoid signaling may have been missed. Future analysis of atRA-regulated genes identified in this work should consider these non-classical elements.

In a similar vein, it is possible that the genes identified as putative functional effectors (Chapter 5, Appendix 1) may potentiate or inhibit retinoid signaling, and not be direct genomic targets of atRA. My prioritization of these genes based on regulation by atRA and the presence of DR5 RAREs may have limited the possible functions identified. As such, further consideration of non-classical signaling may identify additional important mediators from this data.

This work has attributed all effects of *in vivo* or *in vitro* atRA treatment to atRA, without considering the likely isomerization to 9cRA or 13cRA, especially *in vivo*. Measuring the serum levels of retinoids and the oxidative derivatives can provide essential pharmacokinetic information. Additionally, *in vitro* characterization of transcriptional overlap between retinoid isomers and derivatives may allow the consideration of non-classical explanations to transcriptional regulation.

Finally, this work did not highlight the role of retinoids in affecting DNA methylation or histone modifications. An integrative analysis, which includes gene expression, DNA methylation, and histone modifications, may help explain some of the RARE-independent mechanisms of gene regulation which I identified.

6.5.2 IN VIVO *MODELING*

While the use of human TNBC cell lines and PDXs necessitated the use of immunocompromised NOD-*scid* models, this limits the direct translation of our preclinical data to clinical settings. atRA will play a key regulatory role in tumor immunity which must be elucidated before clinical testing.

The administration of atRA prior to engraftment of cells and PDXs also prevented this work from appropriately modeling clinical settings. A model which includes resection of tumors with neo-adjuvant or adjuvant atRA treatment will provide stronger clinical evidence. While Chapter 4 attempts to describe primary resistance to atRA, alternative *in vivo* models may also allow the study of acquired resistance. In addition, comparing the effect size of atRA treatment to that of conventional chemotherapies in these *in vivo* models will provide support for the use of atRA in clinical management of TNBC.

The engraftment of human cells in murine hosts also imposes certain limitations: it is well understood that CAFs coevolve with a tumor and are an important source of paracrine signaling. The introduction of malignant cells into a non-transformed stroma eliminates the effects of this simultaneous evolution and may have a significant impact on cell-cell signaling. Additionally, the species mismatch between human tumor cells and murine stromal cells has certainly affected cell-cell signaling.

Another important limitation of the *in vivo* work I performed is the absence of claudin-low PDX models. Without appropriate modeling of the range of heterogeneity within TNBC, it is difficult to develop a robust predictive tool. More intensive efforts

should be directed to derivation of claudin-low PDXs. This will also provide an interesting opportunity to study the factors required for engraftment in NOD-*scid* mice.

6.5.3 *Clinical Factors*

Given the known interactions between retinoid and estrogen signaling, and between retinoid and HER2 signaling, the exclusive use of TNBC models limits the application of these findings to broad clinical settings. Future pre-clinical work which compares biomarkers in luminal or $HER2^+$ models to our novel findings in TNBC may clarify the application of this predictive approach. Finally, identifying an appropriate bioinformatics approach to distinguish between cell-intrinsic and -extrinsic factors in our PDX models as well as clinical samples, will support maximum application of the predictive profile generated by my research.

6.6 Conclusions

This study describes the contributions of DNA methylation and non-classical retinoid signaling to cellular responses to atRA, using breast cancer as a representative system. Using heterogeneous models of TNBC, I demonstrate a novel opportunity for precision use of retinoid-based therapies in breast cancer. This is an important finding which will enhance future work on both cancerous and non-cancerous retinoid signaling, and which will support the construction of a detailed network which describes the range of cellular responses to retinoids. The effects of atRA described in this work identify opportunities for the use of atRA in combination with existing cytotoxic chemotherapies, which may improve patient survival and decrease off-target toxicity. This research demonstrates a clear potential for the application of molecular profiling to existing therapeutic agents for improved clinical benefit.

BIBLIOGRAPHY

Ablain, J., Leiva, M., Peres, L., Fonsart, J., Anthony, E., Thé, H. de, 2013. Uncoupling RARA transcriptional activation and degradation clarifies the bases for APL response to therapies. J. Exp. Med. 210, 647–653. https://doi.org/10.1084/jem.20122337

Abramson, V.G., Mayer, I.A., 2014. Molecular heterogeneity of triple negative breast cancer. Curr. Breast Cancer Rep. 6, 154–158. https://doi.org/10.1007/s12609-014-0152-1

Adams, J.M., Strasser, A., 2008. Is tumor growth sustained by rare cancer stem cells or dominant clones? Cancer Res. 68, 4018–4021. https://doi.org/10.1158/0008-5472.CAN-07-6334

Addae, C., Yi, X., Gernapudi, R., Cheng, H., Musto, A., Martinez-Ceballos, E., 2012. All-trans-retinoid acid induces the differentiation of encapsulated mouse embryonic stem cells into GABAergic neurons. Differentiation 83, 233–241. https://doi.org/10.1016/j.diff.2012.03.001

Al-Hajj, M., Wicha, M.S., Benito-Hernandez, A., Morrison, S.J., Clarke, M.F., 2003. Prospective identification of tumorigenic breast cancer cells. Proc. Natl. Acad. Sci. 100, 3983–3988. https://doi.org/10.1073/pnas.0530291100

Ali, H.R., Chlon, L., Pharoah, P.D.P., Markowetz, F., Caldas, C., 2016. Patterns of immune infiltration in breast cancer and their clinical implications: A gene-expression-based retrospective Study. PLOS Med. 13, e1002194. https://doi.org/10.1371/journal.pmed.1002194

Almendro, V., Cheng, Y.-K., Randles, A., Itzkovitz, S., Marusyk, A., Ametller, E., Gonzalez-Farre, X., Muñoz, M., Russnes, H.G., Helland, Å., Rye, I.H., Borresen-Dale, A.-L., Maruyama, R., van Oudenaarden, A., Dowsett, M., Jones, R.L., Reis-Filho, J., Gascon, P., Gönen, M., Michor, F., Polyak, K., 2014. Inference of tumor evolution during chemotherapy by computational modeling and in situ analysis of cellular diversity for genetic and phenotypic features. Cell Rep. 6, 514–527. https://doi.org/10.1016/j.celrep.2013.12.041

Alpha-Tocopherol, Beta Carotene Cancer Prevention Study Group, 1994. The effect of vitamin E and beta carotene on the incidence of lung cancer and other cancers in male smokers. N. Engl. J. Med. 330, 1029–1035. https://doi.org/10.1056/NEJM199404143301501

Altucci, L., Leibowitz, M.D., Ogilvie, K.M., de Lera, A.R., Gronemeyer, H., 2007. RAR and RXR modulation in cancer and metabolic disease. Nat. Rev. Drug Discov. 6, 793–810. https://doi.org/10.1038/nrd2397

Altucci, L., Rossin, A., Raffelsberger, W., Reitmair, A., Chomienne, C., Gronemeyer, H., 2001. Retinoic acid-induced apoptosis in leukemia cells is mediated by paracrine action of tumor-selective death ligand TRAIL. Nat. Med. 7, 680–686. https://doi.org/10.1038/89050

Ameri, A., Alidoosti, A., Hosseini, S.Y., Parvin, M., Emranpour, M.H., Taslimi, F., Salehi, E., Fadavip, P., 2011. Prognostic value of promoter hypermethylation of retinoic acid receptor beta (RARB) and CDKN2 (p16/MTS1) in prostate cancer. Chin. J. Cancer Res. 23, 306–311. https://doi.org/10.1007/s11670-011-0306-x

Aran, D., Hellman, A., 2013. DNA methylation of transcriptional enhancers and cancer predisposition. Cell 154, 11–13. https://doi.org/10.1016/j.cell.2013.06.018
Aran, D., Sabato, S., Hellman, A., 2013. DNA methylation of distal regulatory sites characterizes dysregulation of cancer genes. Genome Biol. 14, R21. https://doi.org/10.1186/gb-2013-14-3-r21
Aran, D., Sirota, M., Butte, A.J., 2015. Systematic pan-cancer analysis of tumour purity. Nat. Commun. 6. https://doi.org/10.1038/ncomms9971
Aribi, A., Kantarjian, H.M., Estey, E.H., Koller, C.A., Thomas, D.A., Kornblau, S.M., Faderl, S.H., Laddie, N.M., Garcia-Manero, G., Cortes, J.E., 2007. Combination therapy with arsenic trioxide, all-trans retinoic acid, and gemtuzumab ozogamicin in recurrent acute promyelocytic leukemia. Cancer 109, 1355–1359. https://doi.org/10.1002/cncr.22524
Arnold, S.L.M., Kent, T., Hogarth, C.A., Griswold, M.D., Amory, J.K., Isoherranen, N., 2015. Pharmacological inhibition of ALDH1A in mice decreases all-trans retinoic acid concentrations in a tissue specific manner. Biochem. Pharmacol. 95, 177. https://doi.org/10.1016/j.bcp.2015.03.001
Aryee, M.J., Jaffe, A.E., Corrada-Bravo, H., Ladd-Acosta, C., Feinberg, A.P., Hansen, K.D., Irizarry, R.A., 2014. Minfi: a flexible and comprehensive Bioconductor package for the analysis of Infinium DNA methylation microarrays. Bioinformatics 30, 1363–1369. https://doi.org/10.1093/bioinformatics/btu049
Azim, H.A., Michiels, S., Zagouri, F., Delaloge, S., Filipits, M., Namer, M., Neven, P., Symmans, W.F., Thompson, A., André, F., Loi, S., Swanton, C., 2013. Utility of prognostic genomic tests in breast cancer practice: The IMPAKT 2012 Working Group Consensus Statement. Ann. Oncol. 24, 647–654. https://doi.org/10.1093/annonc/mds645
Bacus, S.S., Kiguchi, K., Chin, D., King, C.R., Huberman, E., 1990. Differentiation of cultured human breast cancer cells (AU-565 and MCF-7) associated with loss of cell surface HER-2/neu antigen. Mol. Carcinog. 3, 350–362.
Balmain, A., 2002. Cancer: New-age tumour suppressors. Nature 417, 235–237. https://doi.org/10.1038/417235a
Balmaña, J., Tung, N.M., Isakoff, S.J., Graña, B., Ryan, P.D., Saura, C., Lowe, E.S., Frewer, P., Winer, E., Baselga, J., Garber, J.E., 2014. Phase I trial of olaparib in combination with cisplatin for the treatment of patients with advanced breast, ovarian and other solid tumors. Ann. Oncol. Off. J. Eur. Soc. Med. Oncol. 25, 1656–1663. https://doi.org/10.1093/annonc/mdu187
Bardot, O., Aldridge, T.C., Latruffe, N., Green, S., 1993. PPAR-RXR heterodimer activates a peroxisome proliferator response element upstream of the bifunctional enzyme gene. Biochem. Biophys. Res. Commun. 192, 37–45. https://doi.org/10.1006/bbrc.1993.1378
Barnabas, N., Cohen, D., 2013. Phenotypic and molecular characterization of MCF10DCIS and SUM breast cancer cell lines. Int. J. Breast Cancer 2013, 872743. https://doi.org/10.1155/2013/872743
Barretina, J., Caponigro, G., Stransky, N., Venkatesan, K., Margolin, A.A., Kim, S., Wilson, C.J., Lehár, J., Kryukov, G.V., Sonkin, D., Reddy, A., Liu, M., Murray, L., Berger, M.F., Monahan, J.E., Morais, P., Meltzer, J., Korejwa, A., Jané-Valbuena, J., Mapa, F.A., Thibault, J., Bric-Furlong, E., Raman, P., Shipway, A.,

Engels, I.H., Cheng, J., Yu, G.K., Yu, J., Aspesi, P., de Silva, M., Jagtap, K., Jones, M.D., Wang, L., Hatton, C., Palescandolo, E., Gupta, S., Mahan, S., Sougnez, C., Onofrio, R.C., Liefeld, T., MacConaill, L., Winckler, W., Reich, M., Li, N., Mesirov, J.P., Gabriel, S.B., Getz, G., Ardlie, K., Chan, V., Myer, V.E., Weber, B.L., Porter, J., Warmuth, M., Finan, P., Harris, J.L., Meyerson, M., Golub, T.R., Morrissey, M.P., Sellers, W.R., Schlegel, R., Garraway, L.A., 2012. The Cancer Cell Line Encyclopedia enables predictive modelling of anticancer drug sensitivity. Nature 483, 603–607. https://doi.org/10.1038/nature11003

Bartsch, R., Wenzel, C., Steger, G.G., 2007. Trastuzumab in the management of early and advanced stage breast cancer. Biol. Targets Ther. 1, 19–31.

Basu, M., Khan, M.W., Chakrabarti, P., Das, C., 2017. Chromatin reader ZMYND8 is a key target of all trans retinoic acid-mediated inhibition of cancer cell proliferation. Biochim. Biophys. Acta BBA - Gene Regul. Mech. 1860, 450–459. https://doi.org/10.1016/j.bbagrm.2017.02.004

Baylin, S.B., 2005. DNA methylation and gene silencing in cancer. Nat. Clin. Pract. Oncol. 2, S4–S11. https://doi.org/10.1038/ncponc0354

Becht, E., Reyniès, A. de, Giraldo, N.A., Pilati, C., Buttard, B., Lacroix, L., Selves, J., Sautès-Fridman, C., Laurent-Puig, P., Fridman, W.H., 2016. Immune and stromal classification of colorectal cancer is associated with molecular subtypes and relevant for precision immunotherapy. Clin. Cancer Res. 22, 4057–4066. https://doi.org/10.1158/1078-0432.CCR-15-2879

Bediaga, N.G., Acha-Sagredo, A., Guerra, I., Viguri, A., Albaina, C., Diaz, I.R., Rezola, R., Alberdi, M.J., Dopazo, J., Montaner, D., Renobales, M. de, Fernández, A.F., Field, J.K., Fraga, M.F., Liloglou, T., Pancorbo, M.M. de, 2010. DNA methylation epigenotypes in breast cancer molecular subtypes. Breast Cancer Res. 12, R77. https://doi.org/10.1186/bcr2721

Ben-David, U., Ha, G., Khadka, P., Jin, X., Wong, B., Franke, L., Golub, T.R., 2016. The landscape of chromosomal aberrations in breast cancer mouse models reveals driver-specific routes to tumorigenesis. Nat. Commun. 7, ncomms12160. https://doi.org/10.1038/ncomms12160

Benkoussa, M., Brand, C., Delmotte, M.-H., Formstecher, P., Lefebvre, P., 2002. Retinoic acid receptors inhibit AP1 activation by regulating extracellular signal-regulated kinase and CBP recruitment to an AP1-responsive promoter. Mol. Cell. Biol. 22, 4522–4534.

Benson, M.J., Pino-Lagos, K., Rosemblatt, M., Noelle, R.J., 2007. All-trans retinoic acid mediates enhanced T reg cell growth, differentiation, and gut homing in the face of high levels of co-stimulation. J. Exp. Med. 204, 1765–1774. https://doi.org/10.1084/jem.20070719

Berman, J.N., Chiu, P.P.L., Dellaire, G., 2014. Chapter 8 - Preclinical Animal Models for Cancer Genomics, in: Cancer Genomics. Academic Press, Boston, pp. 109–131. https://doi.org/10.1016/B978-0-12-396967-5.00008-6

Bernardino, J., Roux, C., Almeida, A., Vogt, N., Gibaud, A., Gerbault-Seureau, M., Magdelenat, H., Bourgeois, C.A., Malfoy, B., Dutrillaux, B., 1997. DNA hypomethylation in breast cancer: an independent parameter of tumor progression? Cancer Genet. Cytogenet. 97, 83–89.

Berns, E.M., Klijn, J.G., van Staveren, I.L., Portengen, H., Noordegraaf, E., Foekens, J.A., 1992. Prevalence of amplification of the oncogenes c-myc, HER2/neu, and int-2 in one thousand human breast tumours: correlation with steroid receptors. Eur. J. Cancer Oxf. Engl. 1990 28, 697–700.

Bestor, T.H., 2003. Unanswered questions about the role of promoter methylation in carcinogenesis. Ann. N. Y. Acad. Sci. 983, 22–27. https://doi.org/10.1111/j.1749-6632.2003.tb05959.x

Bhattacharyya, N., Dey, A., Minucci, S., Zimmer, A., John, S., Hager, G., Ozato, K., 1997. Retinoid-induced chromatin structure alterations in the retinoic acid receptor beta2 promoter. Mol. Cell. Biol. 17, 6481–6490. https://doi.org/10.1128/MCB.17.11.6481

Bianchini, G., Balko, J.M., Mayer, I.A., Sanders, M.E., Gianni, L., 2016. Triple-negative breast cancer: challenges and opportunities of a heterogeneous disease. Nat. Rev. Clin. Oncol. 13, 674. https://doi.org/10.1038/nrclinonc.2016.66

Bibikova, M., Barnes, B., Tsan, C., Ho, V., Klotzle, B., Le, J.M., Delano, D., Zhang, L., Schroth, G.P., Gunderson, K.L., Fan, J.-B., Shen, R., 2011. High density DNA methylation array with single CpG site resolution. Genomics 98, 288–295. https://doi.org/10.1016/j.ygeno.2011.07.007

Bird, A., 2002. DNA methylation patterns and epigenetic memory. Genes Dev. 16, 6–21. https://doi.org/10.1101/gad.947102

Bird, A., Taggart, M., Frommer, M., Miller, O.J., Macleod, D., 1985. A fraction of the mouse genome that is derived from islands of nonmethylated, CpG-rich DNA. Cell 40, 91–99. https://doi.org/10.1016/0092-8674(85)90312-5

Birgisdottir, V., Stefansson, O.A., Bodvarsdottir, S.K., Hilmarsdottir, H., Jonasson, J.G., Eyfjord, J.E., 2006. Epigenetic silencing and deletion of the BRCA1 gene in sporadic breast cancer. Breast Cancer Res. 8, R38. https://doi.org/10.1186/bcr1522

Bissell, M.J., Radisky, D.C., Rizki, A., Weaver, V.M., Petersen, O.W., 2002. The organizing principle: microenvironmental influences in the normal and malignant breast. Differ. Res. Biol. Divers. 70, 537–546. https://doi.org/10.1046/j.1432-0436.2002.700907.x

Blaner, W.S., Olsen, J.A., 1994. Retinol and retinoic acid metabolism., in: The Retinoids: Biology, Chemistry, and Medicine. Raven Press, New York, pp. 229–255.

Boerman, M.H., Napoli, J.L., 1995. Characterization of a microsomal retinol dehydrogenase: a short-chain alcohol dehydrogenase with integral and peripheral membrane forms that interacts with holo-CRBP (type I). Biochemistry (Mosc.) 34, 7027–7037.

Boettcher, M., Hoheisel, J.D., 2010. Pooled RNAi screens - technical and biological aspects. Curr. Genomics 11, 162–167. https://doi.org/10.2174/138920210791110988

Bolis, M., Garattini, E., Paroni, G., Zanetti, A., Kurosaki, M., Castrignanò, T., Garattini, S.K., Biancardi, F., Barzago, M.M., Gianni', M., Terao, M., Pattini, L., Fratelli, M., 2017. Network-guided modeling allows tumor-type independent prediction of sensitivity to all-trans-retinoic acid. Ann. Oncol. 28, 611–621. https://doi.org/10.1093/annonc/mdw660

Bolmer, S.D., Wolf, G., 1982. Retinoids and phorbol esters alter release of fibronectin from enucleated cells. Proc. Natl. Acad. Sci. U. S. A. 79, 6541–6545.
Bookout, A.L., Jeong, Y., Downes, M., Yu, R.T., Evans, R.M., Mangelsdorf, D.J., 2006. Anatomical profiling of nuclear receptor expression reveals a hierarchical transcriptional network. Cell 126, 789–799. https://doi.org/10.1016/j.cell.2006.06.049
Bosch, A., Bertran, S.P., Lu, Y., Garcia, A., Jones, A.M., Dawson, M.I., Farias, E.F., 2012. Reversal by RARα agonist Am580 of c-Myc-induced imbalance in RARα/RARγ expression during MMTV-Myc tumorigenesis. Breast Cancer Res. BCR 14, R121. https://doi.org/10.1186/bcr3247
Bosma, G.C., Custer, R.P., Bosma, M.J., 1983. A severe combined immunodeficiency mutation in the mouse. Nature 301, 527–530.
Botton, S.D., Dombret, H., Sanz, M., Miguel, J.S., Caillot, D., Zittoun, R., Gardembas, M., Stamatoulas, A., Condé, E., Guerci, A., Gardin, C., Geiser, K., Makhoul, D.C., Reman, O., Serna, J. de la, Lefrere, F., Chomienne, C., Chastang, C., Degos, L., Fenaux, P., Group, the E.A., 1998. Incidence, clinical features, and outcome of all trans-retinoic acid syndrome in 413 cases of newly diagnosed acute promyelocytic leukemia. Blood 92, 2712–2718.
Bouillet, P., Sapin, V., Chazaud, C., Messaddeq, N., Décimo, D., Dollé, P., Chambon, P., 1997. Developmental expression pattern of Stra6, a retinoic acid-responsive gene encoding a new type of membrane protein. Mech. Dev. 63, 173–186.
Bour, G., Lalevée, S., Rochette-Egly, C., 2007. Protein kinases and the proteasome join in the combinatorial control of transcription by nuclear retinoic acid receptors. Trends Cell Biol. 17, 302–309. https://doi.org/10.1016/j.tcb.2007.04.003
Bouterfa, H., Picht, T., Kess, D., Herbold, C., Noll, E., Black, P.M., Roosen, K., Tonn, J.C., 2000. Retinoids inhibit human glioma cell proliferation and migration in primary cell cultures but not in established cell lines. Neurosurgery 46, 419–430.
Bradford, J.R., Wappett, M., Beran, G., Logie, A., Delpuech, O., Brown, H., Boros, J., Camp, N.J., McEwen, R., Mazzola, A.M., D'Cruz, C., Barry, S.T., 2016. Whole transcriptome profiling of patient-derived xenograft models as a tool to identify both tumor and stromal specific biomarkers. Oncotarget 7, 20773–20787. https://doi.org/10.18632/oncotarget.8014
Brentnall, T.A., Lai, L.A., Coleman, J., Bronner, M.P., Pan, S., Chen, R., 2012. Arousal of cancer-associated stroma: overexpression of palladin activates fibroblasts to promote tumor invasion. PloS One 7, e30219. https://doi.org/10.1371/journal.pone.0030219
Bric, A., Miething, C., Bialucha, C.U., Scuoppo, C., Zender, L., Krasnitz, A., Xuan, Z., Zuber, J., Wigler, M., Hicks, J., McCombie, R.W., Hemann, M.T., Hannon, G.J., Powers, S., Lowe, S.W., 2009. Functional identification of tumor-suppressor genes through an in vivo RNA interference screen in a mouse lymphoma model. Cancer Cell 16, 324–335. https://doi.org/10.1016/j.ccr.2009.08.015
Brill, B., Boecher, N., Groner, B., Shemanko, C.S., 2008. A sparing procedure to clear the mouse mammary fat pad of epithelial components for transplantation analysis. Lab. Anim. 42, 104–110. https://doi.org/10.1258/la.2007.06003e

Bronzert, D.A., Greene, G.L., Lippman, M.E., 1985. Selection and characterization of a breast cancer cell line resistant to the antiestrogen LY 117018. Endocrinology 117, 1409–1417. https://doi.org/10.1210/endo-117-4-1409

Brown, K.E., Baxter, J., Graf, D., Merkenschlager, M., Fisher, A.G., 1999. Dynamic repositioning of genes in the nucleus of lymphocytes preparing for cell division. Mol. Cell 3, 207–217.

Bruck, N., Vitoux, D., Ferry, C., Duong, V., Bauer, A., de Thé, H., Rochette-Egly, C., 2009. A coordinated phosphorylation cascade initiated by p38MAPK/MSK1 directs RARα to target promoters. EMBO J. 28, 34–47. https://doi.org/10.1038/emboj.2008.256

Bruna, A., Rueda, O.M., Greenwood, W., Batra, A.S., Callari, M., Batra, R.N., Pogrebniak, K., Sandoval, J., Cassidy, J.W., Tufegdzic-Vidakovic, A., Sammut, S.-J., Jones, L., Provenzano, E., Baird, R., Eirew, P., Hadfield, J., Eldridge, M., McLaren-Douglas, A., Barthorpe, A., Lightfoot, H., O'Connor, M.J., Gray, J., Cortes, J., Baselga, J., Marangoni, E., Welm, A.L., Aparicio, S., Serra, V., Garnett, M.J., Caldas, C., 2016. A biobank of breast cancer explants with preserved intra-tumor heterogeneity to screen anticancer compounds. Cell 167, 260-274.e22. https://doi.org/10.1016/j.cell.2016.08.041

Bruning, O., Rodenburg, W., Wackers, P.F.K., van Oostrom, C., Jonker, M.J., Dekker, R.J., Rauwerda, H., Ensink, W.A., de Vries, A., Breit, T.M., 2016. Confounding factors in the transcriptome analysis of an in-vivo exposure experiment. PLoS ONE 11, e0145252. https://doi.org/10.1371/journal.pone.0145252

Bryan, M., Pulte, E.D., Toomey, K.C., Pliner, L., Pavlick, A.C., Saunders, T., Wieder, R., 2011. A pilot phase II trial of all-<Emphasis Type="Italic">trans</Emphasis> retinoic acid (Vesanoid) and paclitaxel (Taxol) in patients with recurrent or metastatic breast cancer. Invest. New Drugs 29, 1482–1487. https://doi.org/10.1007/s10637-010-9478-3

Buchholz, T.A., Weil, M.M., Story, M.D., Strom, E.A., Brock, W.A., McNeese, M.D., 1999. Tumor suppressor genes and breast cancer. Radiat. Oncol. Investig. 7, 55–65. https://doi.org/10.1002/(SICI)1520-6823(1999)7:2<55::AID-ROI1>3.0.CO;2-#

Budd, G.T., Adamson, P.C., Gupta, M., Homayoun, P., Sandstrom, S.K., Murphy, R.F., McLain, D., Tuason, L., Peereboom, D., Bukowski, R.M., Ganapathi, R., 1998. Phase I/II trial of all-trans retinoic acid and tamoxifen in patients with advanced breast cancer. Clin. Cancer Res. 4, 635–642.

Burdall, S.E., Hanby, A.M., Lansdown, M.R., Speirs, V., 2003. Breast cancer cell lines: friend or foe? Breast Cancer Res. 5, 89–95.

Cadieux, B., Ching, T.-T., VandenBerg, S.R., Costello, J.F., 2006. Genome-wide hypomethylation in human glioblastomas associated with specific copy number alteration, methylenetetrahydrofolate reductase allele status, and increased proliferation. Cancer Res. 66, 8469–8476. https://doi.org/10.1158/0008-5472.CAN-06-1547

Cahill, D.P., Kinzler, K.W., Vogelstein, B., Lengauer, C., 1999. Genetic instability and darwinian selection in tumours. Trends Cell Biol. 9, M57–M60. https://doi.org/10.1016/S0962-8924(99)01661-X

Cailleau, R., Olivé, M., Cruciger, Q.V.J., 1978. Long-term human breast carcinoma cell lines of metastatic origin: Preliminary characterization. In Vitro 14, 911–915. https://doi.org/10.1007/BF02616120

Canadian Cancer Society's Advisory Committee on Cancer Statistics, 2017. Canadian Cancer Statistics 2017 [WWW Document]. URL http://www.cancer.ca/Canadian-Cancer-Statistics-2017-EN.pdf (accessed 9.9.17).

Cardiff, R.D., Anver, M.R., Gusterson, B.A., Hennighausen, L., Jensen, R.A., Merino, M.J., Rehm, S., Russo, J., Tavassoli, F.A., Wakefield, L.M., Ward, J.M., Green, J.E., 2000. The mammary pathology of genetically engineered mice: the consensus report and recommendations from the Annapolis meeting. Oncogene 19, 968–988.

Carrier, M., Joint, M., Lutzing, R., Page, A., Rochette-Egly, C., 2016. Phosphoproteome and transcriptome of RA-responsive and RA-resistant breast cancer cell lines. PLOS ONE 11, e0157290. https://doi.org/10.1371/journal.pone.0157290

Carvalho, B.S., Irizarry, R.A., 2010. A framework for oligonucleotide microarray preprocessing. Bioinformatics 26, 2363–2367. https://doi.org/10.1093/bioinformatics/btq431

Cassidy, J.W., Caldas, C., Bruna, A., 2015. Maintaining tumour heterogeneity in patient-derived tumour xenografts. Cancer Res. 75, 2963–2968. https://doi.org/10.1158/0008-5472.CAN-15-0727

Centritto, F., Paroni, G., Bolis, M., Garattini, S.K., Kurosaki, M., Barzago, M.M., Zanetti, A., Fisher, J.N., Scott, M.F., Pattini, L., Lupi, M., Ubezio, P., Piccotti, F., Zambelli, A., Rizzo, P., Gianni', M., Fratelli, M., Terao, M., Garattini, E., 2015. Cellular and molecular determinants of all-trans retinoic acid sensitivity in breast cancer: Luminal phenotype and RARα expression. EMBO Mol. Med. 7, 950–972. https://doi.org/10.15252/emmm.201404670

Cerami, E., Gao, J., Dogrusoz, U., Gross, B.E., Sumer, S.O., Aksoy, B.A., Jacobsen, A., Byrne, C.J., Heuer, M.L., Larsson, E., Antipin, Y., Reva, B., Goldberg, A.P., Sander, C., Schultz, N., 2012. The cBio cancer genomics portal: an open platform for exploring multidimensional cancer genomics data. Cancer Discov. 2, 401–404. https://doi.org/10.1158/2159-8290.CD-12-0095

Chambers, A.F., 2009. MDA-MB-435 and M14 Cell Lines: Identical but not M14 Melanoma? Cancer Res. 69, 5292–5293. https://doi.org/10.1158/0008-5472.CAN-09-1528

Chambon, P., 1996. A decade of molecular biology of retinoic acid receptors. FASEB J. 10, 940–954.

Chan, J.S.K., Sng, M.K., Teo, Z.Q., Chong, H.C., Twang, J.S., Tan, N.S., 2017. Targeting nuclear receptors in cancer-associated fibroblasts as concurrent therapy to inhibit development of chemoresistant tumors. Oncogene. https://doi.org/10.1038/onc.2017.319

Chang, H.Y., Sneddon, J.B., Alizadeh, A.A., Sood, R., West, R.B., Montgomery, K., Chi, J.-T., van de Rijn, M., Botstein, D., Brown, P.O., 2004. Gene expression signature of fibroblast serum response predicts human cancer progression: similarities between tumors and wounds. PLoS Biol. 2, e7. https://doi.org/10.1371/journal.pbio.0020007

Chang, S.-J., Ou-Yang, F., Tu, H.-P., Lin, C.-H., Huang, S.-H., Kostoro, J., Hou, M.-F., Chai, C.-Y., Kwan, A.-L., 2016. Decreased expression of autophagy protein LC3 and stemness (CD44+/CD24−/low) indicate poor prognosis in triple-negative breast cancer. Hum. Pathol. 48, 48–55. https://doi.org/10.1016/j.humpath.2015.09.034

Charafe-Jauffret, E., Ginestier, C., Iovino, F., Wicinski, J., Cervera, N., Finetti, P., Hur, M.-H., Diebel, M.E., Monville, F., Dutcher, J., Brown, M., Viens, P., Xerri, L., Bertucci, F., Stassi, G., Dontu, G., Birnbaum, D., Wicha, M.S., 2009. Breast Cancer Cell Lines Contain Functional Cancer Stem Cells with Metastatic Capacity and a Distinct Molecular Signature. Cancer Res. 69, 1302–1313. https://doi.org/10.1158/0008-5472.CAN-08-2741

Chatzi, C., Brade, T., Duester, G., 2011. Retinoic acid functions as a key GABAergic differentiation signal in the basal ganglia. PLoS Biol. 9, e1000609. https://doi.org/10.1371/journal.pbio.1000609

Chen, A.C., Guo, X., Derguini, F., Gudas, L.J., 1997. Human breast cancer cells and normal mammary epithelial cells: retinol metabolism and growth inhibition by the retinol metabolite 4-oxoretinol. Cancer Res. 57, 4642–4651.

Chen, H., Lin, R.J., Schiltz, R.L., Chakravarti, D., Nash, A., Nagy, L., Privalsky, M.L., Nakatani, Y., Evans, R.M., 1997. Nuclear Receptor Coactivator ACTR Is a Novel Histone Acetyltransferase and Forms a Multimeric Activation Complex with P/CAF and CBP/p300. Cell 90, 569–580. https://doi.org/10.1016/S0092-8674(00)80516-4

Chen, H.L., Gabrilovich, D., Tampé, R., Girgis, K.R., Nadaf, S., Carbone, D.P., 1996. A functionally defective allele of TAP1 results in loss of MHC class I antigen presentation in a human lung cancer. Nat. Genet. 13, 210–213. https://doi.org/10.1038/ng0696-210

Chen, J.D., Evans, R.M., 1995. A transcriptional co-repressor that interacts with nuclear hormone receptors. Nature 377, 454–457. https://doi.org/10.1038/377454a0

Chen, X., Hu, H., He, L., Yu, X., Liu, X., Zhong, R., Shu, M., 2016. A novel subtype classification and risk of breast cancer by histone modification profiling. Breast Cancer Res. Treat. 157, 267–279. https://doi.org/10.1007/s10549-016-3826-8

Chen, X.-H., Wu, W.-G., Ding, J., 2014. Aberrant TIG1 methylation associated with its decreased expression and clinicopathological significance in hepatocellular carcinoma. Tumour Biol. J. Int. Soc. Oncodevelopmental Biol. Med. 35, 967–971. https://doi.org/10.1007/s13277-013-1129-9

Chen, Y., Dokmanovic, M., Stein, W.D., Ardecky, R.J., Roninson, I.B., 2006. Agonist and antagonist of retinoic acid receptors cause similar changes in gene expression and induce senescence-like growth arrest in MCF-7 breast carcinoma cells. Cancer Res. 66, 8749–8761. https://doi.org/10.1158/0008-5472.CAN-06-0581

Chen, Y., McGee, J., Chen, X., Doman, T.N., Gong, X., Zhang, Y., Hamm, N., Ma, X., Higgs, R.E., Bhagwat, S.V., Buchanan, S., Peng, S.-B., Staschke, K.A., Yadav, V., Yue, Y., Kouros-Mehr, H., 2014. Identification of druggable cancer driver genes amplified across TCGA datasets. PLOS ONE 9, e98293. https://doi.org/10.1371/journal.pone.0098293

Chen, Y.-C., Chen, Y.-W., Hsu, H.-S., Tseng, L.-M., Huang, P.-I., Lu, K.-H., Chen, D.-T., Tai, L.-K., Yung, M.-C., Chang, S.-C., Ku, H.-H., Chiou, S.-H., Lo, W.-L.,

2009. Aldehyde dehydrogenase 1 is a putative marker for cancer stem cells in head and neck squamous cancer. Biochem. Biophys. Res. Commun. 385, 307–313. https://doi.org/10.1016/j.bbrc.2009.05.048

Cheung, B., Hocker, J.E., Smith, S.A., Reichert, U., Norris, M.D., Haber, M., Stewart, B.W., Marshall, G.M., 1996. Retinoic acid receptors β and γ distinguish retinoid signals for growth inhibition and neuritogenesis in human neuroblastoma cells. Biochem. Biophys. Res. Commun. 229, 349–354. https://doi.org/10.1006/bbrc.1996.1804

Chiesa, M.D., Passalacqua, R., Michiara, M., Franciosi, V., Di Costanzo, F., Bisagni, G., Camisa, R., Buti, S., Tomasello, G., Cocconi, G., Italian Oncology Group for Clinical Research, 2007. Tamoxifen vs Tamoxifen plus 13-cis-retinoic acid vs Tamoxifen plus Interferon alpha-2a as first-line endocrine treatments in advanced breast cancer: updated results of a phase II, prospective, randomised multicentre trial. Acta Bio-Medica Atenei Parm. 78, 204–209.

Cho, Y., Tighe, A.P., Talmage, D.A., 1997. Retinoic acid induced growth arrest of human breast carcinoma cells requires protein kinase C alpha expression and activity. J. Cell. Physiol. 172, 306–313. https://doi.org/10.1002/(SICI)1097-4652(199709)172:3<306::AID-JCP4>3.0.CO;2-S

Chute, J.P., Muramoto, G.G., Whitesides, J., Colvin, M., Safi, R., Chao, N.J., McDonnell, D.P., 2006. Inhibition of aldehyde dehydrogenase and retinoid signaling induces the expansion of human hematopoietic stem cells. Proc. Natl. Acad. Sci. 103, 11707–11712. https://doi.org/10.1073/pnas.0603806103

Ciriello, G., Gatza, M.L., Beck, A.H., Wilkerson, M.D., Rhie, S.K., Pastore, A., Zhang, H., McLellan, M., Yau, C., Kandoth, C., Bowlby, R., Shen, H., Hayat, S., Fieldhouse, R., Lester, S.C., Tse, G.M.K., Factor, R.E., Collins, L.C., Allison, K.H., Chen, Y.-Y., Jensen, K., Johnson, N.B., Oesterreich, S., Mills, G.B., Cherniack, A.D., Robertson, G., Benz, C., Sander, C., Laird, P.W., Hoadley, K.A., King, T.A., TCGA Research Network, Perou, C.M., 2015. Comprehensive molecular portraits of invasive lobular breast cancer. Cell 163, 506–519. https://doi.org/10.1016/j.cell.2015.09.033

Clagett-Dame, M., DeLuca, H.F., 2002. The role of vitamin A in mammalian reproduction and embryonic development. Annu. Rev. Nutr. 22, 347–381. https://doi.org/10.1146/annurev.nutr.22.010402.102745E

Clarke, R., 1996. Human breast cancer cell line xenografts as models of breast cancer. The immunobiologies of recipient mice and the characteristics of several tumorigenic cell lines. Breast Cancer Res. Treat. 39, 69–86.

Cobb, B.S., Morales-Alcelay, S., Kleiger, G., Brown, K.E., Fisher, A.G., Smale, S.T., 2000. Targeting of Ikaros to pericentromeric heterochromatin by direct DNA binding. Genes Dev. 14, 2146–2160.

Cobleigh, M.A., Vogel, C.L., Tripathy, D., Robert, N.J., Scholl, S., Fehrenbacher, L., Wolter, J.M., Paton, V., Shak, S., Lieberman, G., Slamon, D.J., 1999. Multinational study of the efficacy and safety of humanized anti-HER2 monoclonal antibody in women who have HER2-overexpressing metastatic breast cancer that has progressed after chemotherapy for metastatic disease. J. Clin. Oncol. Off. J. Am. Soc. Clin. Oncol. 17, 2639–2648. https://doi.org/10.1200/JCO.1999.17.9.2639

Colbert, M.C., Rubin, W.W., Linney, E., LaMantia, A.-S., 1995. Retinoid signaling and the generation of regional and cellular diversity in the embryonic mouse spinal cord. Dev. Dyn. 204, 1–12. https://doi.org/10.1002/aja.1002040102
Cole, M.P., Jones, C.T., Todd, I.D., 1971. A new anti-oestrogenic agent in late breast cancer. An early clinical appraisal of ICI46474. Br. J. Cancer 25, 270–275.
Colley, S.M., Leedman, P.J., 2011. Steroid receptor RNA activator - A nuclear receptor coregulator with multiple partners: Insights and challenges. Biochimie 93, 1966–1972. https://doi.org/10.1016/j.biochi.2011.07.004
Cooper, C., Vincett, D., Yan, Y., Hamedani, M.K., Myal, Y., Leygue, E., 2011. Steroid receptor RNA activator bi-faceted genetic system: Heads or tails? Biochimie 93, 1973–1980. https://doi.org/10.1016/j.biochi.2011.07.002
Cooper, D.N., Taggart, M.H., Bird, A.P., 1983. Unmethlated domains in vertebrate DNA. Nucleic Acids Res. 11, 647–658. https://doi.org/10.1093/nar/11.3.647
Cope, L.M., Fackler, M.J., Lopez-Bujanda, Z., Wolff, A.C., Visvanathan, K., Gray, J.W., Sukumar, S., Umbricht, C.B., 2014. Do breast cancer cell lines provide a relevant model of the patient tumor methylome? PLOS ONE 9, e105545. https://doi.org/10.1371/journal.pone.0105545
Cowell, C.F., Weigelt, B., Sakr, R.A., Ng, C.K.Y., Hicks, J., King, T.A., Reis-Filho, J.S., 2013. Progression from ductal carcinoma in situ to invasive breast cancer: Revisited. Mol. Oncol. 7, 859–869. https://doi.org/10.1016/j.molonc.2013.07.005
Coyle, K.M., Boudreau, J.E., Marcato, P., 2017a. Genetic mutations and epigenetic modifications: Driving cancer and informing precision medicine. BioMed Res. Int. 2017, 9620870. https://doi.org/10.1155/2017/9620870
Coyle, K.M., Marcato, P., 2013. Cancer stem cells: Clinical relevance. Can. J. Pathol. 5, 141–149.
Coyle, K.M., Maxwell, S., Thomas, M.L., Marcato, P., 2017b. Profiling of the transcriptional response to all-trans retinoic acid in breast cancer cells reveals RARE-independent mechanisms of gene expression. Sci. Rep. 7, 16684. https://doi.org/10.1038/s41598-017-16687-6
Coyle, K.M., Murphy, J.P., Vidovic, D., Vaghar-Kashani, A., Dean, C.A., Sultan, M., Clements, D., Wallace, M., Thomas, M.L., Hundert, A., Giacomantonio, C.A., Helyer, L., Gujar, S.A., Lee, P.W.K., Weaver, I.C.G., Marcato, P., 2016. Breast cancer subtype dictates DNA methylation and ALDH1A3-mediated expression of tumor suppressor RARRES1. Oncotarget 7, 44096–44112. https://doi.org/10.18632/oncotarget.9858
Coyle, K.M., Sultan, M., Thomas, M.L., Kashani, A. V, Marcato, P., 2013. Retinoid Signaling in Cancer and Its Promise for Therapy. J. Carcinog. Mutagen. 0–14. https://doi.org/10.4172/2157-2518.S7-006
Croker, A.K., Allan, A.L., 2012. Inhibition of aldehyde dehydrogenase (ALDH) activity reduces chemotherapy and radiation resistance of stem-like ALDHhi CD44+ human breast cancer cells. Breast Cancer Res. Treat. 133, 75–87. https://doi.org/10.1007/s10549-011-1692-y
Crooks, G.E., Hon, G., Chandonia, J.-M., Brenner, S.E., 2004. WebLogo: a sequence logo generator. Genome Res. 14, 1188–1190. https://doi.org/10.1101/gr.849004
Curtis, C., Shah, S.P., Chin, S.-F., Turashvili, G., Rueda, O.M., Dunning, M.J., Speed, D., Lynch, A.G., Samarajiwa, S., Yuan, Y., Gräf, S., Ha, G., Haffari, G.,

Bashashati, A., Russell, R., McKinney, S., Group, M., Langerød, A., Green, A., Provenzano, E., Wishart, G., Pinder, S., Watson, P., Markowetz, F., Murphy, L., Ellis, I., Purushotham, A., Børresen-Dale, A.-L., Brenton, J.D., Tavaré, S., Caldas, C., Aparicio, S., 2012. The genomic and transcriptomic architecture of 2,000 breast tumours reveals novel subgroups. Nature 486, 346. https://doi.org/10.1038/nature10983

D'Andrea, F.P., Safwat, A., Kassem, M., Gautier, L., Overgaard, J., Horsman, M.R., 2011. Cancer stem cell overexpression of nicotinamide N-methyltransferase enhances cellular radiation resistance. Radiother. Oncol. 99, 373–378. https://doi.org/10.1016/j.radonc.2011.05.086

Das, S., Foley, N., Bryan, K., Watters, K.M., Bray, I., Murphy, D.M., Buckley, P.G., Stallings, R.L., 2010. MicroRNA mediates DNA demethylation events triggered by retinoic acid during neuroblastoma cell differentiation. Cancer Res. 70, 7874–7881. https://doi.org/10.1158/0008-5472.CAN-10-1534

de Bono, J., Ramanathan, R.K., Mina, L., Chugh, R., Glaspy, J., Rafii, S., Kaye, S., Sachdev, J., Heymach, J., Smith, D.C., Henshaw, J.W., Herriott, A., Patterson, M., Curtin, N.J., Byers, L.A., Wainberg, Z.A., 2017. Phase I, dose-escalation, two-part trial of the PARP inhibitor talazoparib in patients with advanced germline BRCA1/2 mutations and selected sporadic cancers. Cancer Discov. 7, 620–629. https://doi.org/10.1158/2159-8290.CD-16-1250

de Capoa, A., Musolino, A., Della Rosa, S., Caiafa, P., Mariani, L., Del Nonno, F., Vocaturo, A., Donnorso, R.P., Niveleau, A., Grappelli, C., 2003. DNA demethylation is directly related to tumour progression: evidence in normal, pre-malignant and malignant cells from uterine cervix samples. Oncol. Rep. 10, 545–549.

De Palo, G., Mariani, L., Camerini, T., Marubini, E., Formelli, F., Pasini, B., Decensi, A., Veronesi, U., 2002. Effect of fenretinide on ovarian carcinoma occurrence. Gynecol. Oncol. 86, 24–27.

De Palo, G., Veronesi, U., Camerini, T., Formelli, F., Mascotti, G., Boni, C., Fosser, V., Del Vecchio, M., Campa, T., Costa, A., 1995. Can fenretinide protect women against ovarian cancer? J. Natl. Cancer Inst. 87, 146–147.

De, S., Michor, F., 2011. DNA secondary structures and epigenetic determinants of cancer genome evolution. Nat. Struct. Mol. Biol. 18, 950–955. https://doi.org/10.1038/nsmb.2089

de Thé, H., Lavau, C., Marchio, A., Chomienne, C., Degos, L., Dejean, A., 1991. The PML-RAR alpha fusion mRNA generated by the t(15;17) translocation in acute promyelocytic leukemia encodes a functionally altered RAR. Cell 66, 675–684.

Debnath, J., Brugge, J.S., 2005. Modelling glandular epithelial cancers in three-dimensional cultures. Nat. Rev. Cancer 5, 675–688. https://doi.org/10.1038/nrc1695

Decensi, A., Robertson, C., Guerrieri-Gonzaga, A., Serrano, D., Cazzaniga, M., Mora, S., Gulisano, M., Johansson, H., Galimberti, V., Cassano, E., Moroni, S.M., Formelli, F., Lien, E.A., Pelosi, G., Johnson, K.A., Bonanni, B., 2009. Randomized double-blind 2 x 2 trial of low-dose tamoxifen and fenretinide for breast cancer prevention in high-risk premenopausal women. J. Clin. Oncol. Off. J. Am. Soc. Clin. Oncol. 27, 3749–3756. https://doi.org/10.1200/JCO.2008.19.3797

Dedieu, S., Lefebvre, P., 2006. Retinoids interfere with the AP1 signalling pathway in human breast cancer cells. Cell. Signal. 18, 889–898. https://doi.org/10.1016/j.cellsig.2005.08.001

DeSantis, C.E., Fedewa, S.A., Goding Sauer, A., Kramer, J.L., Smith, R.A., Jemal, A., 2016. Breast cancer statistics, 2015: Convergence of incidence rates between black and white women. CA. Cancer J. Clin. 66, 31–42. https://doi.org/10.3322/caac.21320

Dey, A., Minucci, S., Ozato, K., 1994. Ligand-dependent occupancy of the retinoic acid receptor beta 2 promoter in vivo. Mol. Cell. Biol. 14, 8191–8201. https://doi.org/10.1128/MCB.14.12.8191

Dias, K., Dvorkin-Gheva, A., Hallett, R.M., Wu, Y., Hassell, J., Pond, G.R., Levine, M., Whelan, T., Bane, A.L., 2017. Claudin-low breast cancer; Clinical & pathological characteristics. PLOS ONE 12, e0168669. https://doi.org/10.1371/journal.pone.0168669

Dietze, E.C., Caldwell, L.E., Marcom, K., Collins, S.J., Yee, L., Swisshelm, K., Hobbs, K.B., Bean, G.R., Seewaldt, V.L., 2002. Retinoids and retinoic acid receptors regulate growth arrest and apoptosis in human mammary epithelial cells and modulate expression of CBP/p300. Microsc. Res. Tech. 59, 23–40. https://doi.org/10.1002/jemt.10174

Dietze, E.C., Troch, M.M., Bowie, M.L., Yee, L., Bean, G.R., Seewaldt, V.L., 2003. CBP/p300 induction is required for retinoic acid sensitivity in human mammary cells. Biochem. Biophys. Res. Commun. 302, 841–848. https://doi.org/10.1016/S0006-291X(03)00266-3

Dion, L.D., Blalock, J.E., Gifford, G.E., 1977. Vitamin A-induced density-dependent inhibition of L-cell proliferation. J. Natl. Cancer Inst. 58, 795–801.

Di-Poï, N., Tan, N.S., Michalik, L., Wahli, W., Desvergne, B., 2002. Antiapoptotic role of PPARβ in keratinocytes via transcriptional control of the Akt1 signaling pathway. Mol. Cell 10, 721–733. https://doi.org/10.1016/S1097-2765(02)00646-9

Dirix, L.Y., Takacs, I., Nikolinakos, P., Jerusalem, G., Arkenau, H.-T., Hamilton, E.P., Heydebreck, A. von, Grote, H.-J., Chin, K., Lippman, M.E., 2016. Abstract S1-04: Avelumab (MSB0010718C), an anti-PD-L1 antibody, in patients with locally advanced or metastatic breast cancer: A phase Ib JAVELIN solid tumor trial. Cancer Res. 76, S1-04-S1-04. https://doi.org/10.1158/1538-7445.SABCS15-S1-04

Dissemond, J., Götte, P., Mörs, J., Lindeke, A., Goos, M., Ferrone, S., Wagner, S.N., 2003. Association of TAP1 downregulation in human primary melanoma lesions with lack of spontaneous regression. Melanoma Res. 13, 253–258. https://doi.org/10.1097/01.cmr.0000056237.78713.65

Dobbin, Z.C., Katre, A.A., Steg, A.D., Erickson, B.K., Shah, M.M., Alvarez, R.D., Conner, M.G., Schneider, D., Chen, D., Landen, C.N., 2014. Using heterogeneity of the patient-derived xenograft model to identify the chemoresistant population in ovarian cancer. Oncotarget 5, 8750–8764.

Dobrovic, A., Simpfendorfer, D., 1997. Methylation of the BRCA1 gene in sporadic breast cancer. Cancer Res. 57, 3347–3350.

Dolle, P., Ruberte, E., Leroy, P., Morriss-Kay, G., Chambon, P., 1990. Retinoic acid receptors and cellular retinoid binding proteins. I. A systematic study of their

differential pattern of transcription during mouse organogenesis. Development 110, 1133–1151.
Dong, D., Ruuska, S.E., Levinthal, D.J., Noy, N., 1999. Distinct roles for cellular retinoic acid-binding proteins I and II in regulating signaling by retinoic acid. J. Biol. Chem. 274, 23695–23698. https://doi.org/10.1074/jbc.274.34.23695
Dong, J., Grunstein, J., Tejada, M., Peale, F., Frantz, G., Liang, W.-C., Bai, W., Yu, L., Kowalski, J., Liang, X., Fuh, G., Gerber, H.-P., Ferrara, N., 2004. VEGF-null cells require PDGFR alpha signaling-mediated stromal fibroblast recruitment for tumorigenesis. EMBO J. 23, 2800–2810. https://doi.org/10.1038/sj.emboj.7600289
Duan, J.-J., Cai, J., Guo, Y.-F., Bian, X.-W., Yu, S.-C., 2016. ALDH1A3, a metabolic target for cancer diagnosis and therapy. Int. J. Cancer 139, 965–975. https://doi.org/10.1002/ijc.30091
Dubois, C., Schlageter, M.H., Gentile, A. de, Guidez, F., Balitrand, N., Toubert, M.E., Krawice, I., Fenaux, P., Castaigne, S., Najean, Y., 1994. Hematopoietic growth factor expression and ATRA sensitivity in acute promyelocytic blast cells. Blood 83, 3264–3270.
Dumontet, C., Jordan, M.A., 2010. Microtubule-binding agents: a dynamic field of cancer therapeutics. Nat. Rev. Drug Discov. 9, 790–803. https://doi.org/10.1038/nrd3253
Dunham, R.M., Thapa, M., Velazquez, V.M., Elrod, E.J., Denning, T.L., Pulendran, B., Grakoui, A., 2013. Hepatic stellate cells preferentially induce Foxp3+ regulatory T cells by production of retinoic acid. J. Immunol. 190, 2009–2016. https://doi.org/10.4049/jimmunol.1201937
Dunne, P.D., McArt, D.G., Bradley, C.A., O'Reilly, P.G., Barrett, H.L., Cummins, R., O'Grady, T., Arthur, K., Loughrey, M.B., Allen, W.L., McDade, S.S., Waugh, D.J., Hamilton, P.W., Longley, D.B., Kay, E.W., Johnston, P.G., Lawler, M., Salto-Tellez, M., Schaeybroeck, S.V., 2016. Challenging the cancer molecular stratification dogma: Intratumoral heterogeneity undermines consensus molecular subtypes and potential diagnostic value in colorectal cancer. Clin. Cancer Res. 22, 4095–4104. https://doi.org/10.1158/1078-0432.CCR-16-0032
Dupé, V., Matt, N., Garnier, J.-M., Chambon, P., Mark, M., Ghyselinck, N.B., 2003. A newborn lethal defect due to inactivation of retinaldehyde dehydrogenase type 3 is prevented by maternal retinoic acid treatment. Proc. Natl. Acad. Sci. 100, 14036–14041. https://doi.org/10.1073/pnas.2336223100
Ehrich, M., Turner, J., Gibbs, P., Lipton, L., Giovanneti, M., Cantor, C., Boom, D. van den, 2008. Cytosine methylation profiling of cancer cell lines. Proc. Natl. Acad. Sci. 105, 4844–4849. https://doi.org/10.1073/pnas.0712251105
Ehrlich, M., 2009. DNA hypomethylation in cancer cells. Epigenomics 1, 239–259. https://doi.org/10.2217/epi.09.33
Ehrlich, M., 2002. DNA methylation in cancer: too much, but also too little. Oncogene 21, 5400–5413. https://doi.org/10.1038/sj.onc.1205651
Ehrlich, M., Buchanan, K.L., Tsien, F., Jiang, G., Sun, B., Uicker, W., Weemaes, C.M.R., Smeets, D., Sperling, K., Belohradsky, B.H., Tommerup, N., Misek, D.E., Rouillard, J.-M., Kuick, R., Hanash, S.M., 2001. DNA methyltransferase 3B

mutations linked to the ICF syndrome cause dysregulation of lymphogenesis genes. Hum. Mol. Genet. 10, 2917–2931. https://doi.org/10.1093/hmg/10.25.2917

Eirew, P., Steif, A., Khattra, J., Ha, G., Yap, D., Farahani, H., Gelmon, K., Chia, S., Mar, C., Wan, A., Laks, E., Biele, J., Shumansky, K., Rosner, J., McPherson, A., Nielsen, C., Roth, A.J.L., Lefebvre, C., Bashashati, A., de Souza, C., Siu, C., Aniba, R., Brimhall, J., Oloumi, A., Osako, T., Bruna, A., Sandoval, J.L., Algara, T., Greenwood, W., Leung, K., Cheng, H., Xue, H., Wang, Y., Lin, D., Mungall, A.J., Moore, R., Zhao, Y., Lorette, J., Nguyen, L., Huntsman, D., Eaves, C.J., Hansen, C., Marra, M.A., Caldas, C., Shah, S.P., Aparicio, S., 2015. Dynamics of genomic clones in breast cancer patient xenografts at single-cell resolution. Nature 518, 422–426. https://doi.org/10.1038/nature13952

Elias, P.M., Grayson, S., Caldwell, T.M., McNutt, N.S., 1980. Gap junction proliferation in retinoic acid-treated human basal cell carcinoma. Lab. Investig. J. Tech. Methods Pathol. 42, 469–474.

Ellison, G., Klinowska, T., Westwood, R.F.R., Docter, E., French, T., Fox, J.C., 2002. Further evidence to support the melanocytic origin of MDA-MB-435. Mol. Pathol. MP 55, 294–299.

Elstrodt, F., Hollestelle, A., Nagel, J.H.A., Gorin, M., Wasielewski, M., van den Ouweland, A., Merajver, S.D., Ethier, S.P., Schutte, M., 2006. BRCA1 mutation analysis of 41 human breast cancer cell lines reveals three new deleterious mutants. Cancer Res. 66, 41–45. https://doi.org/10.1158/0008-5472.CAN-05-2853

Emionite, L., Galmozzi, F., Grattarola, M., Boccardo, F., Vergani, L., Toma, S., 2004. Histone deacetylase inhibitors enhance retinoid response in human breast cancer cell Lines. Anticancer Res. 24, 4019–4024.

Engel, L.W., Young, N.A., Tralka, T.S., Lippman, M.E., O'Brien, S.J., Joyce, M.J., 1978. Establishment and characterization of three new continuous cell lines derived from human breast carcinomas. Cancer Res. 38, 3352–3364.

Esteller, M., 2011. Non-coding RNAs in human disease. Nat. Rev. Genet. 12, 861–874. https://doi.org/10.1038/nrg3074

Ethier, S.P., Kokeny, K.E., Ridings, J.W., Dilts, C.A., 1996. erbB family receptor expression and growth regulation in a newly isolated human breast cancer cell line. Cancer Res. 56, 899–907.

Ethier, S.P., Mahacek, M.L., Gullick, W.J., Frank, T.S., Weber, B.L., 1993. Differential isolation of normal luminal mammary epithelial cells and breast cancer cells from primary and metastatic sites using selective media. Cancer Res. 53, 627–635.

Fan, P., Jordan, V.C., 2014. Acquired Resistance to Selective Estrogen Receptor Modulators (SERMs) in Clinical Practice (Tamoxifen & Raloxifene) by Selection Pressure in Breast Cancer Cell Populations. Steroids 90, 44–52. https://doi.org/10.1016/j.steroids.2014.06.002

Fan, X., Molotkov, A., Manabe, S.-I., Donmoyer, C.M., Deltour, L., Foglio, M.H., Cuenca, A.E., Blaner, W.S., Lipton, S.A., Duester, G., 2003. Targeted disruption of Aldh1a1 (Raldh1) provides evidence for a complex mechanism of retinoic acid synthesis in the developing retina. Mol. Cell. Biol. 23, 4637–4648. https://doi.org/10.1128/MCB.23.13.4637-4648.2003

Fazi, F., Travaglini, L., Carotti, D., Palitti, F., Diverio, D., Alcalay, M., McNamara, S., Miller, W.H., Coco, F.L., Pelicci, P.G., Nervi, C., 2005. Retinoic acid targets DNA-methyltransferases and histone deacetylases during APL blast differentiation in vitro and in vivo. Oncogene 24, 1820–1830. https://doi.org/10.1038/sj.onc.1208286

Feinberg, A.P., Vogelstein, B., 1983. Hypomethylation of ras oncogenes in primary human cancers. Biochem. Biophys. Res. Commun. 111, 47–54.

Feng, L., Hernandez, R.E., Waxman, J.S., Yelon, D., Moens, C.B., 2010. Dhrs3a regulates retinoic acid biosynthesis through a feedback inhibition mechanism. Dev. Biol. 338, 1–14. https://doi.org/10.1016/j.ydbio.2009.10.029

Ferguson-Smith, A.C., 2011. Genomic imprinting: the emergence of an epigenetic paradigm. Nat. Rev. Genet. 12, 565–575. https://doi.org/10.1038/nrg3032

Fernandez, M.G., Holmfeldt, P., Marathe, H., Hall, T., Pardieck, J., McKinney-Freeman, S., 2014. Functional screen identifies novel regulators of murine hematopoietic stem cell engraftment. Blood 124, 4321–4321.

Fernández-Medarde, A., Santos, E., 2011. Ras in cancer and developmental diseases. Genes Cancer 2, 344–358. https://doi.org/10.1177/1947601911411084

Fex, G., Hansson, B., 1979. Retinol-binding protein from human urine and its interaction with retinol and prealbumin. Eur. J. Biochem. 94, 307–313.

Findlay, J.M., Castro-Giner, F., Makino, S., Rayner, E., Kartsonaki, C., Cross, W., Kovac, M., Ulahannan, D., Palles, C., Gillies, R.S., MacGregor, T.P., Church, D., Maynard, N.D., Buffa, F., Cazier, J.-B., Graham, T.A., Wang, L.-M., Sharma, R.A., Middleton, M., Tomlinson, I., 2016. Differential clonal evolution in oesophageal cancers in response to neo-adjuvant chemotherapy. Nat. Commun. 7, 11111. https://doi.org/10.1038/ncomms11111

Fisher, J.N., Terao, M., Fratelli, M., Kurosaki, M., Paroni, G., Zanetti, A., Gianni, M., Bolis, M., Lupi, M., Tsykin, A., Goodall, G.J., Garattini, E., 2015. MicroRNA networks regulated by all-trans retinoic acid and Lapatinib control the growth, survival and motility of breast cancer cells. Oncotarget 6, 13176–13200. https://doi.org/10.18632/oncotarget.3759

Fogh, J., Wright, W.C., Loveless, J.D., 1977. Absence of HeLa cell contamination in 169 cell lines derived from human tumors. J. Natl. Cancer Inst. 58, 209–214.

Fontana, J.A., 1987. Interaction of retinoids and tamoxifen on the inhibition of human mammary carcinoma cell proliferation. Exp. Cell Biol. 55, 136–144.

Forbes, S.A., Beare, D., Gunasekaran, P., Leung, K., Bindal, N., Boutselakis, H., Ding, M., Bamford, S., Cole, C., Ward, S., Kok, C.Y., Jia, M., De, T., Teague, J.W., Stratton, M.R., McDermott, U., Campbell, P.J., 2015. COSMIC: exploring the world's knowledge of somatic mutations in human cancer. Nucleic Acids Res. 43, D805-811. https://doi.org/10.1093/nar/gku1075

Forozan, F., Veldman, R., Ammerman, C.A., Parsa, N.Z., Kallioniemi, A., Kallioniemi, O.-P., Ethier, S.P., 1999. Molecular cytogenetic analysis of 11 new breast cancer cell lines. Br. J. Cancer 81, 1328–1334. https://doi.org/10.1038/sj.bjc.6695007

Fortin, J.-P., Labbe, A., Lemire, M., Zanke, B.W., Hudson, T.J., Fertig, E.J., Greenwood, C.M., Hansen, K.D., 2014. Functional normalization of 450k methylation array data improves replication in large cancer studies. Genome Biol. 15, 503. https://doi.org/10.1186/s13059-014-0503-2

Fortin, J.-P., Triche, T.J., Hansen, K.D., 2017. Preprocessing, normalization and integration of the Illumina HumanMethylationEPIC array with minfi. Bioinformatics 33, 558–560. https://doi.org/10.1093/bioinformatics/btw691

Fraker, L.D., Halter, S.A., Forbes, J.T., 1984. Growth inhibition by retinol of a human breast carcinoma cell line in vitro and in athymic mice. Cancer Res. 44, 5757–5763.

Frankel, S.R., Eardley, A., Lauwers, G., Weiss, M., Warrell, R.P., 1992. The "retinoic acid syndrome" in acute promyelocytic leukemia. Ann. Intern. Med. 117, 292–296.

Friedman, M.D., Jeevan, D.S., Tobias, M., Murali, R., Jhanwar-Uniyal, M., 2013. Targeting cancer stem cells in glioblastoma multiforme using mTOR inhibitors and the differentiating agent all-trans retinoic acid. Oncol. Rep. 30, 1645–1650.

Fritz, H., Kennedy, D., Fergusson, D., Fernandes, R., Doucette, S., Cooley, K., Seely, A., Sagar, S., Wong, R., Seely, D., 2011. Vitamin A and retinoid derivatives for lung cancer: A systematic review and meta analysis. PLoS ONE 6. https://doi.org/10.1371/journal.pone.0021107

Fukumura, D., Xavier, R., Sugiura, T., Chen, Y., Park, E.C., Lu, N., Selig, M., Nielsen, G., Taksir, T., Jain, R.K., Seed, B., 1998. Tumor induction of VEGF promoter activity in stromal cells. Cell 94, 715–725.

Furth, P.A., St Onge, L., Böger, H., Gruss, P., Gossen, M., Kistner, A., Bujard, H., Hennighausen, L., 1994. Temporal control of gene expression in transgenic mice by a tetracycline-responsive promoter. Proc. Natl. Acad. Sci. U. S. A. 91, 9302–9306.

Gaffney, E.V., 1982. A cell line (HBL-100) established from human breast milk. Cell Tissue Res. 227, 563–568.

Galli, S., Colombo, L., Vanzuli, S., Daroqui, M.C., del Carmen Vidal, M., Jasnis, M.A., Sacerdote de Lustig, E., Eijan, A.M., 2000. Characterization of a fibroblastoid mammary carcinoma cell line (LM2) originated from a mouse adenocarcinoma. Int. J. Oncol. 17, 1259–1324.

Galluzzi, L., Buqué, A., Kepp, O., Zitvogel, L., Kroemer, G., 2017. Immunogenic cell death in cancer and infectious disease. Nat. Rev. Immunol. 17, 97. https://doi.org/10.1038/nri.2016.107

Galvin, K.C., Dyck, L., Marshall, N.A., Stefanska, A.M., Walsh, K.P., Moran, B., Higgins, S.C., Dungan, L.S., Mills, K.H.G., 2013. Blocking retinoic acid receptor-α enhances the efficacy of a dendritic cell vaccine against tumours by suppressing the induction of regulatory T cells. Cancer Immunol. Immunother. CII 62, 1273–1282. https://doi.org/10.1007/s00262-013-1432-8

Gandellini, P., Andriani, F., Merlino, G., D'Aiuto, F., Roz, L., Callari, M., 2015. Complexity in the tumour microenvironment: Cancer associated fibroblast gene expression patterns identify both common and unique features of tumour-stroma crosstalk across cancer types. Semin. Cancer Biol., Complexity in Cancer Biology 35, 96–106. https://doi.org/10.1016/j.semcancer.2015.08.008

Gao, H., Korn, J.M., Ferretti, S., Monahan, J.E., Wang, Y., Singh, M., Zhang, C., Schnell, C., Yang, G., Zhang, Y., Balbin, O.A., Barbe, S., Cai, H., Casey, F., Chatterjee, S., Chiang, D.Y., Chuai, S., Cogan, S.M., Collins, S.D., Dammassa, E., Ebel, N., Embry, M., Green, J., Kauffmann, A., Kowal, C., Leary, R.J., Lehar,

J., Liang, Y., Loo, A., Lorenzana, E., Iii, E.R.M., McLaughlin, M.E., Merkin, J., Meyer, R., Naylor, T.L., Patawaran, M., Reddy, A., Röelli, C., Ruddy, D.A., Salangsang, F., Santacroce, F., Singh, A.P., Tang, Y., Tinetto, W., Tobler, S., Velazquez, R., Venkatesan, K., Arx, F.V., Wang, H.Q., Wang, Z., Wiesmann, M., Wyss, D., Xu, F., Bitter, H., Atadja, P., Lees, E., Hofmann, F., Li, E., Keen, N., Cozens, R., Jensen, M.R., Pryer, N.K., Williams, J.A., Sellers, W.R., 2015. High-throughput screening using patient-derived tumor xenografts to predict clinical trial drug response. Nat. Med. 21, 1318. https://doi.org/10.1038/nm.3954

Gao, J., Aksoy, B.A., Dogrusoz, U., Dresdner, G., Gross, B., Sumer, S.O., Sun, Y., Jacobsen, A., Sinha, R., Larsson, E., Cerami, E., Sander, C., Schultz, N., 2013. Integrative analysis of complex cancer genomics and clinical profiles using the cBioPortal. Sci. Signal. 6, pl1. https://doi.org/10.1126/scisignal.2004088

Gao, R., Shen, Y., Cai, J., Lei, M., Wang, Z., 2010. Expression of voltage-gated sodium channel α subunit in human ovarian cancer. Oncol. Rep. 23, 1293–1299.

Gao, T., He, B., Pan, Y., Li, R., Xu, Y., Chen, L., Nie, Z., Gu, L., Wang, S., 2013. The association of retinoic acid receptor beta 2 (RARβ2) methylation status and prostate cancer risk: A systematic review and meta-analysis. PLOS ONE 8, e62950. https://doi.org/10.1371/journal.pone.0062950

Garattini, E., Bolis, M., Garattini, S.K., Fratelli, M., Centritto, F., Paroni, G., Gianni', M., Zanetti, A., Pagani, A., Fisher, J.N., Zambelli, A., Terao, M., 2014. Retinoids and breast cancer: From basic studies to the clinic and back again. Cancer Treat. Rev. 40, 739–749. https://doi.org/10.1016/j.ctrv.2014.01.001

Gargiulo, G., Serresi, M., Cesaroni, M., Hulsman, D., Lohuizen, M. van, 2014. *In vivo* shRNA screens in solid tumors. Nat. Protoc. 9, 2880. https://doi.org/10.1038/nprot.2014.185

Gasser, S.M., 2001. Positions of potential: nuclear organization and gene expression. Cell 104, 639–642.

Gazdar, A.F., Kurvari, V., Virmani, A., Gollahon, L., Sakaguchi, M., Westerfield, M., Kodagoda, D., Stasny, V., Cunningham, H.T., Wistuba, I.I., Tomlinson, G., Tonk, V., Ashfaq, R., Leitch, A.M., Minna, J.D., Shay, J.W., 1998. Characterization of paired tumor and non-tumor cell lines established from patients with breast cancer. Int. J. Cancer 78, 766–774.

Gendoo, D.M.A., Ratanasirigulchai, N., Schröder, M.S., Paré, L., Parker, J.S., Prat, A., Haibe-Kains, B., 2016. Genefu: an R/Bioconductor package for computation of gene expression-based signatures in breast cancer. Bioinformatics 32, 1097–1099. https://doi.org/10.1093/bioinformatics/btv693

Giannì, M., Parrella, E., Raska, I., Gaillard, E., Nigro, E.A., Gaudon, C., Garattini, E., Rochette-Egly, C., 2006. P38MAPK-dependent phosphorylation and degradation of SRC-3/AIB1 and RARalpha-mediated transcription. EMBO J. 25, 739–751. https://doi.org/10.1038/sj.emboj.7600981

Ginestier, C., Hur, M.H., Charafe-Jauffret, E., Monville, F., Dutcher, J., Brown, M., Jacquemier, J., Viens, P., Kleer, C.G., Liu, S., Schott, A., Hayes, D., Birnbaum, D., Wicha, M.S., Dontu, G., 2007. ALDH1 is a marker of normal and malignant human mammary stem cells and a predictor of poor clinical outcome. Cell Stem Cell 1, 555–567. https://doi.org/10.1016/j.stem.2007.08.014

Ginestier, C., Wicinski, J., Cervera, N., Monville, F., Finetti, P., Bertucci, F., Wicha, M.S., Birnbaum, D., Charafe-Jauffret, E., 2009. Retinoid signaling regulates breast cancer stem cell differentiation. Cell Cycle 8, 3297–3302. https://doi.org/10.4161/cc.8.20.9761

Glass, C.K., Lipkin, S.M., Devary, O.V., Rosenfeld, M.G., 1989. Positive and negative regulation of gene transcription by a retinoic acid-thyroid hormone receptor heterodimer. Cell 59, 697–708. https://doi.org/10.1016/0092-8674(89)90016-0

Glass, C.K., Rosenfeld, M.G., 2000. The coregulator exchange in transcriptional functions of nuclear receptors. Genes Dev. 14, 121–141. https://doi.org/10.1101/gad.14.2.121

Graham, C.E., Brocklehurst, K., Pickersgill, R.W., Warren, M.J., 2006. Characterization of retinaldehyde dehydrogenase 3. Biochem. J. 394, 67–75. https://doi.org/10.1042/BJ20050918

Gravesande, K.S. van's, Layne, M.D., Ye, Q., Le, L., Baron, R.M., Perrella, M.A., Santambrogio, L., Silverman, E.S., Riese, R.J., 2002. IFN regulatory factor-1 regulates IFN-γ-dependent cathepsin S expression. J. Immunol. 168, 4488–4494. https://doi.org/10.4049/jimmunol.168.9.4488

Grigoriadis, A., Mackay, A., Noel, E., Wu, P.J., Natrajan, R., Frankum, J., Reis-Filho, J.S., Tutt, A., 2012. Molecular characterisation of cell line models for triple-negative breast cancers. BMC Genomics 13, 619. https://doi.org/10.1186/1471-2164-13-619

Guan, J., Chen, J., 2014. Tumor microenvironment: The promising target for tumor therapy. Cancer Cell Microenviron. 1. https://doi.org/10.14800/ccm.81

Gudas, L.J., 1994. Retinoids and vertebrate development. J. Biol. Chem. 269, 15399–15402.

Gudas, L.J., Wagner, J.A., 2011. Retinoids regulate stem cell differentiation. J. Cell. Physiol. 226, 322–330. https://doi.org/10.1002/jcp.22417

Guenther, M.G., Barak, O., Lazar, M.A., 2001. The SMRT and N-CoR crepressors are activating cofactors for histone deacetylase 3. Mol. Cell. Biol. 21, 6091–6101. https://doi.org/10.1128/MCB.21.18.6091-6101.2001

Gumireddy, K., Li, A., Kossenkov, A.V., Sakurai, M., Yan, J., Li, Y., Xu, H., Wang, J., Zhang, P.J., Zhang, L., Showe, L.C., Nishikura, K., Huang, Q., 2016. The mRNA-edited form of GABRA3 suppresses GABRA3-mediated Akt activation and breast cancer metastasis. Nat. Commun. 7, 10715. https://doi.org/10.1038/ncomms10715

Guo, Y., Pino-Lagos, K., Ahonen, C.A., Bennett, K.A., Wang, J., Napoli, J.L., Blomhoff, R., Sockanathan, S., Chandraratna, R.A., Dmitrovsky, E., Turk, M.J., Noelle, R.J., 2012. A retinoic acid--rich tumor microenvironment provides clonal survival cues for tumor-specific CD8(+) T cells. Cancer Res. 72, 5230–5239. https://doi.org/10.1158/0008-5472.CAN-12-1727

Gupta, P., Ho, P.-C., Huq, M.M., Ha, S.G., Park, S.W., Khan, A.A., Tsai, N.-P., Wei, L.-N., 2008. Retinoic acid-stimulated sequential phosphorylation, PML recruitment, and SUMOylation of nuclear receptor TR2 to suppress Oct4 expression. Proc. Natl. Acad. Sci. U. S. A. 105, 11424–11429. https://doi.org/10.1073/pnas.0710561105

Gupta, S., Pramanik, D., Mukherjee, R., Campbell, N.R., Elumalai, S., de Wilde, R.F., Hong, S.-M., Goggins, M.G., De Jesus-Acosta, A., Laheru, D., Maitra, A., 2012. Molecular determinants of retinoic acid sensitivity in pancreatic cancer. Clin. Cancer Res. Off. J. Am. Assoc. Cancer Res. 18, 280–289. https://doi.org/10.1158/1078-0432.CCR-11-2165

Hackett, A.J., Smith, H.S., Springer, E.L., Owens, R.B., Nelson-Rees, W.A., Riggs, J.L., Gardner, M.B., 1977. Two syngeneic cell lines from human breast tissue: the aneuploid mammary epithelial (Hs578T) and the diploid myoepithelial (Hs578Bst) cell lines. J. Natl. Cancer Inst. 58, 1795–1806.

Hagan, C.R., Lange, C.A., 2014. Molecular determinants of context-dependent progesterone receptor action in breast cancer. BMC Med. 12, 32. https://doi.org/10.1186/1741-7015-12-32

Hajdu, S.I., 2004. Greco-Roman thought about cancer. Cancer 100, 2048–2051. https://doi.org/10.1002/cncr.20198

Hall, A.G., Tilby, M.J., 1992. Mechanisms of action of, and modes of resistance to, alkylating agents used in the treatment of haematological malignancies. Blood Rev. 6, 163–173.

Halter, S.A., Fraker, L.D., Adcock, D., Vick, S., 1988. Effect of retinoids on xenotransplanted human mammary carcinoma cells in athymic mice. Cancer Res. 48, 3733–3736.

Hammes, S.R., Davis, P.J., 2015. Overlapping nongenomic and genomic actions of thyroid hormone and steroids. Best Pract. Res. Clin. Endocrinol. Metab. 29, 581–593. https://doi.org/10.1016/j.beem.2015.04.001

Hammond, L.A., Krinks, C.H.V., Durham, J., Tomkins, S.E., Burnett, R.D., Jones, E.L., Chandraratna, R.A.S., Brown, G., 2001. Antagonists of retinoic acid receptors (RARs) are potent growth inhibitors of prostate carcinoma cells. Br. J. Cancer 85, 453–462. https://doi.org/10.1054/bjoc.2001.1939

Han, S., Tai, C., Westenbroek, R.E., Yu, F.H., Cheah, C.S., Potter, G.B., Rubenstein, J.L., Scheuer, T., Iglesia, H.O. de la, Catterall, W.A., 2012. Autistic-like behaviour in *Scn1a*$^{+/-}$ mice and rescue by enhanced GABA-mediated neurotransmission. Nature 489, 385. https://doi.org/10.1038/nature11356

Hanahan, D., Weinberg, R.A., 2011. Hallmarks of cancer: The next generation. Cell 144, 646–674. https://doi.org/10.1016/j.cell.2011.02.013

Hanahan, D., Weinberg, R.A., 2000. The hallmarks of cancer. Cell 100, 57–70. https://doi.org/10.1016/S0092-8674(00)81683-9

Harbeck, N., Rody, A., 2012. Lost in translation? Estrogen receptor status and endocrine responsiveness in breast cancer. J. Clin. Oncol. 30, 686–689. https://doi.org/10.1200/JCO.2011.38.9619

Harper, M.J., Walpole, A.L., 1967. A new derivative of triphenylethylene: effect on implantation and mode of action in rats. J. Reprod. Fertil. 13, 101–119.

Hartman, H.B., Yu, J., Alenghat, T., Ishizuka, T., Lazar, M.A., 2005. The histone-binding code of nuclear receptor co-repressors matches the substrate specificity of histone deacetylase 3. EMBO Rep. 6, 445–451. https://doi.org/10.1038/sj.embor.7400391

Hayashi, K., Goodison, S., Urquidi, V., Tarin, D., Lotan, R., Tahara, E., 2003. Differential effects of retinoic acid on the growth of isogenic metastatic and non-

metastatic breast cancer cell lines and their association with distinct expression of retinoic acid receptor β isoforms 2 and 4. Int. J. Oncol. 22, 623–629.
Hayden, L.J., Satre, M.A., 2002. Alterations in cellular retinol metabolism contribute to differential retinoid responsiveness in normal human mammary epithelial cells versus breast cancer cells. Breast Cancer Res. Treat. 72, 95–105.
Heim, K.C., White, K.A., Deng, D., Tomlinson, C.R., Moore, J.H., Freemantle, S.J., Spinella, M.J., 2007. Selective repression of retinoic acid target genes by RIP140 during induced tumor cell differentiation of pluripotent human embryonal carcinoma cells. Mol. Cancer 6, 57. https://doi.org/10.1186/1476-4598-6-57
Heinzel, T., Lavinsky, R.M., Mullen, T.-M., Söderström, M., Laherty, C.D., Torchia, J., Yang, W.-M., Brard, G., Ngo, S.D., Davie, J.R., Seto, E., Eisenman, R.N., Rose, D.W., Glass, C.K., Rosenfeld, M.G., 1997. A complex containing N-CoR, mSln3 and histone deacetylase mediates transcriptional repression. Nature 387, 43–48. https://doi.org/10.1038/387043a0
Heiser, L.M., Wang, N.J., Talcott, C.L., Laderoute, K.R., Knapp, M., Guan, Y., Hu, Z., Ziyad, S., Weber, B.L., Laquerre, S., Jackson, J.R., Wooster, R.F., Kuo, W.L., Gray, J.W., Spellman, P.T., 2009. Integrated analysis of breast cancer cell lines reveals unique signaling pathways. Genome Biol. 10, R31. https://doi.org/10.1186/gb-2009-10-3-r31
Helle, S.I., Jonat, W., Giurescu, M., Ekse, D., Holly, J.M.P., Lønning, P.E., 1998. Influence of treatment with onapristone on the IGF-system in breast cancer patients. J. Steroid Biochem. Mol. Biol. 66, 159–163. https://doi.org/10.1016/S0960-0760(98)00046-6
Hennekens, C.H., Buring, J.E., Manson, J.E., Stampfer, M., Rosner, B., Cook, N.R., Belanger, C., LaMotte, F., Gaziano, J.M., Ridker, P.M., Willett, W., Peto, R., 1996. Lack of effect of long-term supplementation with beta carotene on the incidence of malignant neoplasms and cardiovascular disease. N. Engl. J. Med. 334, 1145–1149. https://doi.org/10.1056/NEJM199605023341801
Hernandez, L., Wilkerson, P.M., Lambros, M.B., Campion-Flora, A., Rodrigues, D.N., Gauthier, A., Cabral, C., Pawar, V., Mackay, A., A'Hern, R., Marchiò, C., Palacios, J., Natrajan, R., Weigelt, B., Reis-Filho, J.S., 2012. Genomic and mutational profiling of ductal carcinomas in situ and matched adjacent invasive breast cancers reveals intra-tumour genetic heterogeneity and clonal selection. J. Pathol. 227, 42–52. https://doi.org/10.1002/path.3990
Heselmeyer-Haddad, K., Berroa Garcia, L.Y., Bradley, A., Ortiz-Melendez, C., Lee, W.-J., Christensen, R., Prindiville, S.A., Calzone, K.A., Soballe, P.W., Hu, Y., Chowdhury, S.A., Schwartz, R., Schäffer, A.A., Ried, T., 2012. Single-cell genetic analysis of ductal carcinoma in situ and invasive breast cancer reveals enormous tumor heterogeneity yet conserved genomic imbalances and gain of MYC during progression. Am. J. Pathol. 181, 1807–1822. https://doi.org/10.1016/j.ajpath.2012.07.012
Heyman, R.A., Mangelsdorf, D.J., Dyck, J.A., Stein, R.B., Eichele, G., Evans, R.M., Thaller, C., 1992. 9-cis retinoic acid is a high affinity ligand for the retinoid X receptor. Cell 68, 397–406. https://doi.org/10.1016/0092-8674(92)90479-V
Hickey, T.E., Robinson, J.L.L., Carroll, J.S., Tilley, W.D., 2012. Minireview: The androgen receptor in breast tissues: growth inhibitor, tumor suppressor,

oncogene? Mol. Endocrinol. 26, 1252–1267. https://doi.org/10.1210/me.2012-1107
Hollander, D., Muralidhara, K.S., 1977. Vitamin A1 intestinal absorption in vivo: influence of luminal factors on transport. Am. J. Physiol.-Endocrinol. Metab. 232, E471. https://doi.org/10.1152/ajpendo.1977.232.5.E471
Hollern, D.P., Andrechek, E.R., 2014. A genomic analysis of mouse models of breast cancer reveals molecular features of mouse models and relationships to human breast cancer. Breast Cancer Res. 16, R59. https://doi.org/10.1186/bcr3672
Holliday, D.L., Speirs, V., 2011. Choosing the right cell line for breast cancer research. Breast Cancer Res. 13, 215. https://doi.org/10.1186/bcr2889
Holm, K., Staaf, J., Lauss, M., Aine, M., Lindgren, D., Bendahl, P.-O., Vallon-Christersson, J., Barkardottir, R.B., Höglund, M., Borg, Å., Jönsson, G., Ringnér, M., 2016. An integrated genomics analysis of epigenetic subtypes in human breast tumors links DNA methylation patterns to chromatin states in normal mammary cells. Breast Cancer Res. 18, 27. https://doi.org/10.1186/s13058-016-0685-5
Holwerda, S.J.B., Laat, W. de, 2013. CTCF: the protein, the binding partners, the binding sites and their chromatin loops. Phil Trans R Soc B 368, 20120369. https://doi.org/10.1098/rstb.2012.0369
Hong, T.-K., Lee-Kim, Y.C., 2009. Effects of retinoic acid isomers on apoptosis and enzymatic antioxidant system in human breast cancer cells. Nutr. Res. Pract. 3, 77–83. https://doi.org/10.4162/nrp.2009.3.2.77
Hörlein, A.J., Näär, A.M., Heinzel, T., Torchia, J., Gloss, B., Kurokawa, R., Ryan, A., Kamei, Y., Söderström, M., Glass, C.K., Rosenfeld, M.G., 1995. Ligand-independent repression by the thyroid hormone receptor mediated by a nuclear receptor co-repressor. Nature 377, 397–404. https://doi.org/10.1038/377397a0
Hosoda, K., Sato, M., Yanai, K., 2015. Identification and characterization of human genomic binding sites for retinoic acid receptor/retinoid X receptor heterodimers. Adv. Biol. Chem. 05, 58. https://doi.org/10.4236/abc.2015.52006
Hosoya, K., Yamashita, S., Ando, T., Nakajima, T., Itoh, F., Ushijima, T., 2009. Adenomatous polyposis coli 1A is likely to be methylated as a passenger in human gastric carcinogenesis. Cancer Lett. 285, 182–189. https://doi.org/10.1016/j.canlet.2009.05.016
Hsu, L.C., Chang, W.C., Hiraoka, L., Hsieh, C.L., 1994. Molecular cloning, genomic organization, and chromosomal localization of an additional human aldehyde dehydrogenase gene, ALDH6. Genomics 24, 333–341. https://doi.org/10.1006/geno.1994.1624
Hu, Y., Sun, H., Drake, J., Kittrell, F., Abba, M.C., Deng, L., Gaddis, S., Sahin, A., Baggerly, K., Medina, D., Aldaz, C.M., 2004. From mice to humans: Identification of commonly deregulated genes in mammary cancer via comparative SAGE studies. Cancer Res. 64, 7748–7755. https://doi.org/10.1158/0008-5472.CAN-04-1827
Hua, S., Kittler, R., White, K.P., 2009. Genomic antagonism between retinoic acid and estrogen signaling in breast cancer. Cell 137, 1259–1271. https://doi.org/10.1016/j.cell.2009.04.043

Huang, D.W., Sherman, B.T., Lempicki, R.A., 2009a. Systematic and integrative analysis of large gene lists using DAVID bioinformatics resources. Nat. Protoc. 4, 44–57. https://doi.org/10.1038/nprot.2008.211

Huang, D.W., Sherman, B.T., Lempicki, R.A., 2009b. Bioinformatics enrichment tools: paths toward the comprehensive functional analysis of large gene lists. Nucleic Acids Res. 37, 1–13. https://doi.org/10.1093/nar/gkn923

Huang, E.H., Hynes, M.J., Zhang, T., Ginestier, C., Dontu, G., Appelman, H., Fields, J.Z., Wicha, M.S., Boman, B.M., 2009. Aldehyde dehydrogenase 1 Is a marker for normal and malignant human colonic stem cells (SC) and tracks SC overpopulation during colon tumorigenesis. Cancer Res. 69, 3382–3389. https://doi.org/10.1158/0008-5472.CAN-08-4418

Huang, M.E., Ye, Y.C., Chen, S.R., Chai, J.R., Lu, J.X., Zhoa, L., Gu, L.J., Wang, Z.Y., 1988. Use of all-trans retinoic acid in the treatment of acute promyelocytic leukemia. Blood 72, 567–572.

Hwang, R.F., Moore, T., Arumugam, T., Ramachandran, V., Amos, K.D., Rivera, A., Ji, B., Evans, D.B., Logsdon, C.D., 2008. Cancer-associated stromal fibroblasts promote pancreatic tumor progression. Cancer Res. 68, 918–926. https://doi.org/10.1158/0008-5472.CAN-07-5714

Idowu, M.O., Kmieciak, M., Dumur, C., Burton, R.S., Grimes, M.M., Powers, C.N., Manjili, M.H., 2012. CD44+/CD24−/low cancer stem/progenitor cells are more abundant in triple-negative invasive breast carcinoma phenotype and are associated with poor outcome. Hum. Pathol. 43, 364–373. https://doi.org/10.1016/j.humpath.2011.05.005

Irvine, R.A., Lin, I.G., Hsieh, C.-L., 2002. DNA methylation has a local effect on transcription and histone acetylation. Mol. Cell. Biol. 22, 6689–6696. https://doi.org/10.1128/MCB.22.19.6689-6696.2002

Isella, C., Brundu, F., Bellomo, S.E., Galimi, F., Zanella, E., Porporato, R., Petti, C., Fiori, A., Orzan, F., Senetta, R., Boccaccio, C., Ficarra, E., Marchionni, L., Trusolino, L., Medico, E., Bertotti, A., 2017. Selective analysis of cancer-cell intrinsic transcriptional traits defines novel clinically relevant subtypes of colorectal cancer. Nat. Commun. 8, 15107. https://doi.org/10.1038/ncomms15107

Isella, C., Terrasi, A., Bellomo, S.E., Petti, C., Galatola, G., Muratore, A., Mellano, A., Senetta, R., Cassenti, A., Sonetto, C., Inghirami, G., Trusolino, L., Fekete, Z., Ridder, M.D., Cassoni, P., Storme, G., Bertotti, A., Medico, E., 2015. Stromal contribution to the colorectal cancer transcriptome. Nat. Genet. 47, 312. https://doi.org/10.1038/ng.3224

Ishizuka, T., Lazar, M.A., 2003. The N-CoR/histone deacetylase 3 complex is required for repression by thyroid hormone receptor. Mol. Cell. Biol. 23, 5122–5131. https://doi.org/10.1128/MCB.23.15.5122-5131.2003

Ito, M., Hiramatsu, H., Kobayashi, K., Suzue, K., Kawahata, M., Hioki, K., Ueyama, Y., Koyanagi, Y., Sugamura, K., Tsuji, K., Heike, T., Nakahata, T., 2002. NOD/SCID/γ mouse: an excellent recipient mouse model for engraftment of human cells. Blood 100, 3175–3182. https://doi.org/10.1182/blood-2001-12-0207

Jack, J., Rotroff, D., Motsinger-Reif, A., 2014. Cell lines: Models of drug response: successes and lessons from this pharmacogenomic model. Curr. Mol. Med. 14, 833–840.

Jaeckle, K.A., Hess, K.R., Yung, W.K.A., Greenberg, H., Fine, H., Schiff, D., Pollack, I.F., Kuhn, J., Fink, K., Mehta, M., Cloughesy, T., Nicholas, M.K., Chang, S., Prados, M., North American Brain Tumor Consortium, 2003. Phase II evaluation of temozolomide and 13-cis-retinoic acid for the treatment of recurrent and progressive malignant glioma: a North American Brain Tumor Consortium study. J. Clin. Oncol. 21, 2305–2311. https://doi.org/10.1200/JCO.2003.12.097

Jaiyesimi, I.A., Buzdar, A.U., Hortobagyi, G., 1992. Inflammatory breast cancer: a review. J. Clin. Oncol. 10, 1014–1024. https://doi.org/10.1200/JCO.1992.10.6.1014

Jenuwein, T., Allis, C.D., 2001. Translating the histone code. Science 293, 1074–1080. https://doi.org/10.1126/science.1063127

Jia, P.-F., Gu, W.-T., Zhang, W.-F., Li, F., 2015. Treatment of recurrent malignant gliomas with 13-cis-retinoic acid naphthalene triazole. Neurol. Sci. 36, 717–721. https://doi.org/10.1007/s10072-014-2025-9

Jiang, F., Qiu, Q., Khanna, A., Todd, N.W., Deepak, J., Xing, L., Wang, H., Liu, Z., Su, Y., Stass, S.A., Katz, R.L., 2009. Aldehyde dehydrogenase 1 Is a tumor stem cell-associated marker in lung cancer. Mol. Cancer Res. 7, 330–338. https://doi.org/10.1158/1541-7786.MCR-08-0393

Jiang, G., Zhang, S., Yazdanparast, A., Li, M., Pawar, A.V., Liu, Y., Inavolu, S.M., Cheng, L., 2016. Comprehensive comparison of molecular portraits between cell lines and tumors in breast cancer. BMC Genomics 17. https://doi.org/10.1186/s12864-016-2911-z

Jiang, S.-Y., Wu, M.-S., Chen, L.-M., Hung, M.-W., Lin, H.-E., Chang, G.-G., Chang, T.-C., 2005. Identification and characterization of the retinoic acid response elements in the human RIG1 gene promoter. Biochem. Biophys. Res. Commun. 331, 630–639. https://doi.org/10.1016/j.bbrc.2005.03.214

Jiménez-Lara, A.M., Aranda, A., Gronemeyer, H., 2010. Retinoic acid protects human breast cancer cells against etoposide-induced apoptosis by NF-kappaB-dependent but cIAP2-independent mechanisms. Mol. Cancer 9, 15. https://doi.org/10.1186/1476-4598-9-15

Jing, C., El-Ghany, M.A., Beesley, C., Foster, C.S., Rudland, P.S., Smith, P., Ke, Y., 2002. Tazarotene-induced gene 1 (TIG1) expression in prostate carcinomas and its relationship to tumorigenicity. J. Natl. Cancer Inst. 94, 482–490.

Johansson, H.J., Sanchez, B.C., Mundt, F., Forshed, J., Kovacs, A., Panizza, E., Hultin-Rosenberg, L., Lundgren, B., Martens, U., Máthé, G., Yakhini, Z., Helou, K., Krawiec, K., Kanter, L., Hjerpe, A., Stål, O., Linderholm, B.K., Lehtiö, J., 2013. Retinoic acid receptor alpha is associated with tamoxifen resistance in breast cancer. Nat. Commun. 4, 2175. https://doi.org/10.1038/ncomms3175

Johnston, G.A.R., 2013. Advantages of an antagonist: bicuculline and other GABA antagonists. Br. J. Pharmacol. 169, 328–336. https://doi.org/10.1111/bph.12127

Jonat, W., Bachelot, T., Ruhstaller, T., Kuss, I., Reimann, U., Robertson, J.F.R., 2013. Randomized phase II study of lonaprisan as second-line therapy for progesterone receptor-positive breast cancer. Ann. Oncol. 24, 2543–2548. https://doi.org/10.1093/annonc/mdt216

Jones, P.A., 2012. Functions of DNA methylation: islands, start sites, gene bodies and beyond. Nat. Rev. Genet. 13, 484–492. https://doi.org/10.1038/nrg3230

Jones, P.A., Laird, P.W., 1999. Cancer-epigenetics comes of age. Nat. Genet. 21, 163–167. https://doi.org/10.1038/5947

Jordan, V.C., 2008. Tamoxifen: catalyst for the change to targeted therapy. Eur. J. Cancer 44, 30–38. https://doi.org/10.1016/j.ejca.2007.11.002

Joshi, S., Guleria, R.S., Pan, J., DiPette, D., Singh, U.S., 2007. Heterogeneity in retinoic acid signaling in neuroblastomas: Role of matrix metalloproteinases in retinoic acid-induced differentiation. Biochim. Biophys. Acta Mol. Basis Dis. 1772, 1093–1102. https://doi.org/10.1016/j.bbadis.2007.05.009

Kakizuka, A., Miller, W.H., Umesono, K., Warrell, R.P., Frankel, S.R., Murty, V.V., Dmitrovsky, E., Evans, R.M., 1991. Chromosomal translocation t(15;17) in human acute promyelocytic leukemia fuses RAR alpha with a novel putative transcription factor, PML. Cell 66, 663–674.

Kaleagasioglu, F., Doepner, G., Biesalski, H.K., Berger, M.R., 1993. Antiproliferative activity of retinoic acid and some novel retinoid derivatives in breast and colorectal cancer cell lines of human origin. Arzneimittelforschung. 43, 487–490.

Kandoth, C., McLellan, M.D., Vandin, F., Ye, K., Niu, B., Lu, C., Xie, M., Zhang, Q., McMichael, J.F., Wyczalkowski, M.A., Leiserson, M.D.M., Miller, C.A., Welch, J.S., Walter, M.J., Wendl, M.C., Ley, T.J., Wilson, R.K., Raphael, B.J., Ding, L., 2013. Mutational landscape and significance across 12 major cancer types. Nature 502, 333–339. https://doi.org/10.1038/nature12634

Kang, Y., Siegel, P.M., Shu, W., Drobnjak, M., Kakonen, S.M., Cordón-Cardo, C., Guise, T.A., Massagué, J., 2003. A multigenic program mediating breast cancer metastasis to bone. Cancer Cell 3, 537–549.

Kao, J., Salari, K., Bocanegra, M., Choi, Y.-L., Girard, L., Gandhi, J., Kwei, K.A., Hernandez-Boussard, T., Wang, P., Gazdar, A.F., Minna, J.D., Pollack, J.R., 2009. Molecular profiling of breast cancer cell lines defines relevant tumor models and provides a resource for cancer gene discovery. PloS One 4, e6146. https://doi.org/10.1371/journal.pone.0006146

Karsli-Ceppioglu, S., Dagdemir, A., Judes, G., Lebert, A., Penault-Llorca, F., Bignon, Y.-J., Bernard-Gallon, D., 2017. The epigenetic landscape of promoter genome-wide analysis in breast cancer. Sci. Rep. 7, 6597. https://doi.org/10.1038/s41598-017-06790-z

Kashyap, V., Gudas, L.J., 2010. Epigenetic regulatory mechanisms distinguish retinoic acid-mediated transcriptional responses in stem cells and fibroblasts. J. Biol. Chem. 285, 14534–14548. https://doi.org/10.1074/jbc.M110.115345

Kashyap, V., Laursen, K.B., Brenet, F., Viale, A.J., Scandura, J.M., Gudas, L.J., 2013. RARγ is essential for retinoic acid induced chromatin remodeling and transcriptional activation in embryonic stem cells. J Cell Sci 126, 999–1008. https://doi.org/10.1242/jcs.119701

Kawaguchi, R., Yu, J., Honda, J., Hu, J., Whitelegge, J., Ping, P., Wiita, P., Bok, D., Sun, H., 2007. A Membrane Receptor for Retinol Binding Protein Mediates Cellular Uptake of Vitamin A. Science 315, 820–825. https://doi.org/10.1126/science.1136244

Kawashima, K., Yamakawa, K., Takahashi, W., Takizawa, S., Yin, P., Sugiyama, N., Kanba, S., Arita, J., 2002. The estrogen-occupied estrogen receptor functions as a negative regulator to inhibit cell proliferation induced by insulin/IGF-1: A cell

context-specific antimitogenic action of estradiol on rat lactotrophs in culture. Endocrinology 143, 2750–2758. https://doi.org/10.1210/endo.143.7.8915
Kedishvili, N.Y., 2013. Enzymology of retinoic acid biosynthesis and degradation. J. Lipid Res. 54, 1744–1760. https://doi.org/10.1194/jlr.R037028
Keniry, M., Parsons, R., 2008. The role of PTEN signaling perturbations in cancer and in targeted therapy. Oncogene 27, 5477. https://doi.org/10.1038/onc.2008.248
Keriel, A., Stary, A., Sarasin, A., Rochette-Egly, C., Egly, J.-M., 2002. XPD mutations prevent TFIIH-dependent transactivation by nuclear receptors and phosphorylation of RARα. Cell 109, 125–135. https://doi.org/10.1016/S0092-8674(02)00692-X
Keydar, I., Chen, L., Karby, S., Weiss, F.R., Delarea, J., Radu, M., Chaitcik, S., Brenner, H.J., 1979. Establishment and characterization of a cell line of human breast carcinoma origin. Eur. J. Cancer 15, 659–670.
Khatri, P., Sirota, M., Butte, A.J., 2012. Ten years of pathway analysis: Current approaches and outstanding challenges. PLOS Comput. Biol. 8, e1002375. https://doi.org/10.1371/journal.pcbi.1002375
Khuri, F.R., Lotan, R., Kemp, B.L., Lippman, S.M., Wu, H., Feng, L., Lee, J.J., Cooksley, C.S., Parr, B., Chang, E., Walsh, G.L., Lee, J.S., Hong, W.K., Xu, X.C., 2000. Retinoic acid receptor-beta as a prognostic indicator in stage I non-small-cell lung cancer. J. Clin. Oncol. 18, 2798–2804. https://doi.org/10.1200/JCO.2000.18.15.2798
Kitamura, T., Qian, B.-Z., Pollard, J.W., 2015. Immune cell promotion of metastasis. Nat. Rev. Immunol. 15, 73–86. https://doi.org/10.1038/nri3789
Klaassen, I., Brakenhoff, R.H., Smeets, S.J., Snow, G.B., Braakhuis, B.J.M., 2001. Expression of retinoic acid receptor gamma correlates with retinoic acid sensitivity and metabolism in head and neck squamous cell carcinoma cell lines. Int. J. Cancer 92, 661–665. https://doi.org/10.1002/1097-0215(20010601)92:5<661::AID-IJC1251>3.0.CO;2-O
Kliewer, S.A., Umesono, K., Noonan, D.J., Heyman, R.A., Evans, R.M., 1992. Convergence of 9-cis retinoic acid and peroxisome proliferator signalling pathways through heterodimer formation of their receptors. Nature 358, 771–774. https://doi.org/10.1038/358771a0
Klijn, J.G.M., Jong, F.H. de, Bakker, G.H., Lamberts, S.W.J., Rodenburg, C.J., Alexieva-Figusch, J., 1989. Antiprogestins, a new form of endocrine therapy for human breast cancer. Cancer Res. 49, 2851–2856.
Knudson, A.G., 2001. Two genetic hits (more or less) to cancer. Nat. Rev. Cancer 1, 157–162. https://doi.org/10.1038/35101031
Knudson, A.G., 1971. Mutation and cancer: statistical study of retinoblastoma. Proc. Natl. Acad. Sci. U. S. A. 68, 820–823.
Konantz, M., Balci, T.B., Hartwig, U.F., Dellaire, G., André, M.C., Berman, J.N., Lengerke, C., 2012. Zebrafish xenografts as a tool for in vivo studies on human cancer. Ann. N. Y. Acad. Sci. 1266, 124–137. https://doi.org/10.1111/j.1749-6632.2012.06575.x
Kopelman, M., Cogan, U., Mokady, S., Shinitzky, M., 1976. The interaction between retinol-binding proteins and prealbumins studied by fluorescence polarization. Biochim. Biophys. Acta 439, 449–460.

Korch, C., Hall, E.M., Dirks, W.G., Ewing, M., Faries, M., Varella-Garcia, M., Robinson, S., Storts, D., Turner, J.A., Wang, Y., Burnett, E.C., Healy, L., Kniss, D., Neve, R.M., Nims, R.W., Reid, Y.A., Robinson, W.A., Capes-Davis, A., 2018. Authentication of M14 melanoma cell line proves misidentification of MDA-MB-435 breast cancer cell line. Int. J. Cancer 142, 561–572. https://doi.org/10.1002/ijc.31067

Kuperwasser, C., Chavarria, T., Wu, M., Magrane, G., Gray, J.W., Carey, L., Richardson, A., Weinberg, R.A., 2004. Reconstruction of functionally normal and malignant human breast tissues in mice. Proc. Natl. Acad. Sci. U. S. A. 101, 4966–4971. https://doi.org/10.1073/pnas.0401064101

Kuperwasser, C., Dessain, S., Bierbaum, B.E., Garnet, D., Sperandio, K., Gauvin, G.P., Naber, S.P., Weinberg, R.A., Rosenblatt, M., 2005. A mouse model of human breast cancer metastasis to human bone. Cancer Res. 65, 6130–6138. https://doi.org/10.1158/0008-5472.CAN-04-1408

Kurokawa, R., Söderström, M., Hörlein, A., Halachmi, S., Brown, M., Rosenfeld, M.G., Glass, C.K., 1995. Polarity-specific activities of retinoic acid receptors determined by a co-repressor. Nature 377, 451–454. https://doi.org/10.1038/377451a0

Kwok, W.K., Pang, J.C.S., Lo, K.W., Ng, H.-K., 2009. Role of the RARRES1 gene in nasopharyngeal carcinoma. Cancer Genet. Cytogenet. 194, 58–64. https://doi.org/10.1016/j.cancergencyto.2009.06.005

Kwon, A.T., Arenillas, D.J., Worsley Hunt, R., Wasserman, W.W., 2012. oPOSSUM-3: advanced analysis of regulatory motif over-representation across genes or ChIP-Seq datasets. G3 Bethesda Md 2, 987–1002. https://doi.org/10.1534/g3.112.003202

Lacroix, M., Leclercq, G., 2004. Relevance of breast cancer cell lines as models for breast tumours: an update. Breast Cancer Res. Treat. 83, 249–289. https://doi.org/10.1023/B:BREA.0000014042.54925.cc

Laganière, J., Deblois, G., Giguère, V., 2005. Functional genomics identifies a mechanism for estrogen activation of the retinoic acid receptor α1 gene in breast cancer cells. Mol. Endocrinol. 19, 1584–1592. https://doi.org/10.1210/me.2005-0040

Lalevée, S., Anno, Y.N., Chatagnon, A., Samarut, E., Poch, O., Laudet, V., Benoit, G., Lecompte, O., Rochette-Egly, C., 2011. Genome-wide in silico identification of new conserved and functional retinoic acid receptor response elements (direct repeats separated by 5 bp). J. Biol. Chem. 286, 33322–33334. https://doi.org/10.1074/jbc.M111.263681

Langlois, A.J., Holder, W.D., Iglehart, J.D., Nelson-Rees, W.A., Wells, S.A., Bolognesi, D.P., 1979. Morphological and biochemical properties of a new human breast cancer cell line. Cancer Res. 39, 2604–2613.

Lanz, R.B., McKenna, N.J., Onate, S.A., Albrecht, U., Wong, J., Tsai, S.Y., Tsai, M.J., O'Malley, B.W., 1999. A steroid receptor coactivator, SRA, functions as an RNA and is present in an SRC-1 complex. Cell 97, 17–27.

Lapidot, T., Sirard, C., Vormoor, J., Murdoch, B., Hoang, T., Caceres-Cortes, J., Minden, M., Paterson, B., Caligiuri, M.A., Dick, J.E., 1994. A cell initiating human acute

myeloid leukaemia after transplantation into SCID mice. Nature 367, 645–648. https://doi.org/10.1038/367645a0
Larson, R.S., Brown, D.C., Sklar, L.A., 1997. Retinoic acid induces aggregation of the acute promyelocytic leukemia cell line NB-4 by utilization of LFA-1 and ICAM-2. Blood 90, 2747–2756.
Lasfargues, E.Y., Coutinho, W.G., Redfield, E.S., 1978. Isolation of two human tumor epithelial cell lines from solid breast carcinomas. J. Natl. Cancer Inst. 61, 967–978.
Lasfargues, E.Y., Ozzello, L., 1958. Cultivation of human breast carcinomas. J. Natl. Cancer Inst. 21, 1131–1147.
Lau, J.C.Y., Hanel, M.L., Wevrick, R., 2004. Tissue-specific and imprinted epigenetic modifications of the human NDN gene. Nucleic Acids Res. 32, 3376–3382. https://doi.org/10.1093/nar/gkh671
Lee, E.Y.H.P., Muller, W.J., 2010. Oncogenes and tumor suppressor genes. Cold Spring Harb. Perspect. Biol. 2. https://doi.org/10.1101/cshperspect.a003236
Lee, H.S., Yoon, J.-S., Song, M., Shin, C.-Y., Chung, H.S., Ryu, J.-C., 2012. Gene expression profiling of low dose exposure of saturated aliphatic aldehydes in A549 human alveolar epithelial cells. Toxicol. Environ. Health Sci. 4, 211–217. https://doi.org/10.1007/s13530-012-0140-7
Lee, S.T., Li, Z., Wu, Z., Aau, M., Guan, P., Karuturi, R.K.M., Liou, Y.C., Yu, Q., 2011. Context-specific regulation of NF-κB target gene expression by EZH2 in breast cancers. Mol. Cell 43, 798–810. https://doi.org/10.1016/j.molcel.2011.08.011
Lefebvre, P., Mouchon, A., Lefebvre, B., Formstecher, P., 1998. Binding of retinoic acid receptor heterodimers to DNA. A role for histones NH2 termini. J. Biol. Chem. 273, 12288–12295.
Lehmann, B.D., Bauer, J.A., Chen, X., Sanders, M.E., Chakravarthy, A.B., Shyr, Y., Pietenpol, J.A., 2011. Identification of human triple-negative breast cancer subtypes and preclinical models for selection of targeted therapies. J. Clin. Invest. 121, 2750–2767. https://doi.org/10.1172/JCI45014
Lehmann, B.D., Jovanović, B., Chen, X., Estrada, M.V., Johnson, K.N., Shyr, Y., Moses, H.L., Sanders, M.E., Pietenpol, J.A., 2016. Refinement of triple-negative breast cancer molecular subtypes: Implications for neoadjuvant chemotherapy selection. PloS One 11, e0157368. https://doi.org/10.1371/journal.pone.0157368
Leid, M., Kastner, P., Chambon, P., 1992. Multiplicity generates diversity in the retinoic acid signalling pathways. Trends Biochem. Sci. 17, 427–433.
Lengauer, C., Kinzler, K.W., Vogelstein, B., 1998. Genetic instabilities in human cancers. Nature 396, 643–649. https://doi.org/10.1038/25292
Leo, C., Chen, J.D., 2000. The SRC family of nuclear receptor coactivators. Gene 245, 1–11. https://doi.org/10.1016/S0378-1119(00)00024-X
Levanon, D., Bernstein, Y., Negreanu, V., Bone, K.R., Pozner, A., Eilam, R., Lotem, J., Brenner, O., Groner, Y., 2011. Absence of Runx3 expression in normal gastrointestinal epithelium calls into question its tumour suppressor function: Absence of Runx3 in normal GIT epithelium. EMBO Mol. Med. 3, 593–604. https://doi.org/10.1002/emmm.201100168
Li, J., Wang, Jin, Wang, Jianxiang, Nawaz, Z., Liu, J.M., Qin, J., Wong, J., 2000. Both corepressor proteins SMRT and N-CoR exist in large protein complexes

containing HDAC3. EMBO J. 19, 4342–4350. https://doi.org/10.1093/emboj/19.16.4342
Li, N., Li, S., 2015. Epigenetic inactivation of SOX1 promotes cell migration in lung cancer. Tumor Biol. 36, 4603–4610. https://doi.org/10.1007/s13277-015-3107-x
Liacini, A., Sylvester, J., Li, W.Q., Zafarullah, M., 2002. Inhibition of interleukin-1-stimulated MAP kinases, activating protein-1 (AP-1) and nuclear factor kappa B (NF-κB) transcription factors down-regulates matrix metalloproteinase gene expression in articular chondrocytes. Matrix Biol. 21, 251–262. https://doi.org/10.1016/S0945-053X(02)00007-0
Liang, L., Cookson, W.O.C., 2014. Grasping nettles: cellular heterogeneity and other confounders in epigenome-wide association studies. Hum. Mol. Genet. 23, R83–R88. https://doi.org/10.1093/hmg/ddu284
Lim, Y.C., Kang, H.J., Kim, Y.S., Choi, E.C., 2012. All-trans-retinoic acid inhibits growth of head and neck cancer stem cells by suppression of Wnt/β-catenin pathway. Eur. J. Cancer 48, 3310–3318. https://doi.org/10.1016/j.ejca.2012.04.013
Lin, C.M., Jaswal, J., Vandenberg, T., Tuck, A., Brackstone, M., 2013. Weakly hormone receptor–positive breast cancer and use of adjuvant hormonal therapy. Curr. Oncol. 20, e612–e613. https://doi.org/10.3747/co.20.1598
Lin, G., Zhu, S., Wu, Y., Song, C., Wang, W., Zhang, Y., Chen, Y.-L., He, Z., 2017. ω-3 free fatty acids and all-trans retinoic acid synergistically induce growth inhibition of three subtypes of breast cancer cell lines. Sci. Rep. 7, 2929. https://doi.org/10.1038/s41598-017-03231-9
Lin, J.H., 2007. Pharmacokinetic and pharmacodynamic variability: a daunting challenge in drug therapy. Curr. Drug Metab. 8, 109–136.
Lin, M., Napoli, J.L., 2000. cDNA cloning and expression of a human aldehyde dehydrogenase (ALDH) active with 9-cis-retinal and identification of a rat ortholog, ALDH12. J. Biol. Chem. 275, 40106–40112. https://doi.org/10.1074/jbc.M008027200
Lintig, J. von, Vogt, K., 2000. Filling the gap in vitamin A research: Molecular identification of an enzyme cleaving β-carotene to retinal. J. Biol. Chem. 275, 11915–11920. https://doi.org/10.1074/jbc.275.16.11915
Liu, R.-Z., Graham, K., Glubrecht, D.D., Germain, D.R., Mackey, J.R., Godbout, R., 2011. Association of FABP5 expression with poor survival in triple-negative breast cancer: implication for retinoic acid therapy. Am. J. Pathol. 178, 997–1008. https://doi.org/10.1016/j.ajpath.2010.11.075
Liu, T.-X., Zhang, J.-W., Tao, J., Zhang, R.-B., Zhang, Q.-H., Zhao, C.-J., Tong, J.-H., Lanotte, M., Waxman, S., Chen, S.-J., Mao, M., Hu, G.-X., Zhu, L., Chen, Z., 2000. Gene expression networks underlying retinoic acid–induced differentiation of acute promyelocytic leukemia cells. Blood 96, 1496–1504.
Liu, X., Giguère, V., 2014. Inactivation of RARβ inhibits Wnt1-induced mammary tumorigenesis by suppressing epithelial-mesenchymal transition. Nucl. Recept. Signal. 12. https://doi.org/10.1621/nrs.12004
Liu, X., Nugoli, M., Laferrière, J., Saleh, S.M., Rodrigue-Gervais, I.G., Saleh, M., Park, M., Hallett, M.T., Muller, W.J., Giguère, V., 2011. Stromal retinoic acid receptor

beta promotes mammary gland tumorigenesis. Proc. Natl. Acad. Sci. U. S. A. 108, 774–779. https://doi.org/10.1073/pnas.1011845108

Liu, Y., Lee, M.O., Wang, H.G., Li, Y., Hashimoto, Y., Klaus, M., Reed, J.C., Zhang, X., 1996. Retinoic acid receptor beta mediates the growth-inhibitory effect of retinoic acid by promoting apoptosis in human breast cancer cells. Mol. Cell. Biol. 16, 1138–1149. https://doi.org/10.1128/MCB.16.3.1138

Liu-Sullivan, N., Zhang, J., Bakleh, A., Marchica, J., Li, J., Siolas, D., Laquerre, S., Degenhardt, Y.Y., Wooster, R., Chang, K., Hannon, G.F., Powers, S., 2011. Pooled shRNA screen for sensitizers to inhibition of the mitotic regulator polo-like kinase (PLK1). Oncotarget 2, 1254–1264. https://doi.org/10.18632/oncotarget.406

Lo-Coco, F., Avvisati, G., Vignetti, M., Thiede, C., Orlando, S.M., Iacobelli, S., Ferrara, F., Fazi, P., Cicconi, L., Di Bona, E., Specchia, G., Sica, S., Divona, M., Levis, A., Fiedler, W., Cerqui, E., Breccia, M., Fioritoni, G., Salih, H.R., Cazzola, M., Melillo, L., Carella, A.M., Brandts, C.H., Morra, E., von Lilienfeld-Toal, M., Hertenstein, B., Wattad, M., Lübbert, M., Hänel, M., Schmitz, N., Link, H., Kropp, M.G., Rambaldi, A., La Nasa, G., Luppi, M., Ciceri, F., Finizio, O., Venditti, A., Fabbiano, F., Döhner, K., Sauer, M., Ganser, A., Amadori, S., Mandelli, F., Döhner, H., Ehninger, G., Schlenk, R.F., Platzbecker, U., Gruppo Italiano Malattie Ematologiche dell'Adulto, German-Austrian Acute Myeloid Leukemia Study Group, Study Alliance Leukemia, 2013. Retinoic acid and arsenic trioxide for acute promyelocytic leukemia. N. Engl. J. Med. 369, 111–121. https://doi.org/10.1056/NEJMoa1300874

Longley, D.B., Harkin, D.P., Johnston, P.G., 2003. 5-Fluorouracil: mechanisms of action and clinical strategies. Nat. Rev. Cancer 3, 330.

Lotan, R., 1979. Different susceptibilities of human melanoma and breast carcinoma cell lines to retinoic acid-induced growth inhibition. Cancer Res. 39, 1014–1019.

Lu, L., Ma, J., Li, Z., Lan, Q., Chen, M., Liu, Y., Xia, Z., Wang, J., Han, Y., Shi, W., Quesniaux, V., Ryffel, B., Brand, D., Li, B., Liu, Z., Zheng, S.G., 2011. All-trans retinoic acid promotes TGF-β-induced Tregs via histone modification but not DNA demethylation on Foxp3 gene locus. PLOS ONE 6, e24590. https://doi.org/10.1371/journal.pone.0024590

Lu, S., Benbrook, D.M., 2006. Role of AP-1 antagonism in growth inhibition of cervical cancer cell lines by retinoids. Am. J. Pharmacol. Toxicol. 1, 40–47. https://doi.org/10.3844/ajptsp.2006.40.47

Lumachi, F., Brunello, A., Maruzzo, M., Basso, U., Basso, S.M.M., 2013. Treatment of estrogen receptor-positive breast cancer. Curr. Med. Chem. 20, 596–604.

Luo, X.M., Ross, A.C., 2006. Retinoic acid exerts dual regulatory actions on the expression and nuclear localization of interferon regulatory factor-1. Exp. Biol. Med. Maywood NJ 231, 619–631.

Luo, Y., Dallaglio, K., Chen, Y., Robinson, W.A., Robinson, S.E., McCarter, M.D., Wang, J., Gonzalez, R., Thompson, D.C., Norris, D.A., Roop, D.R., Vasiliou, V., Fujita, M., 2012. ALDH1A isozymes are markers of human melanoma stem cells and potential therapeutic targets. STEM CELLS 30, 2100–2113. https://doi.org/10.1002/stem.1193

Ma, S., Chan, K.W., Lee, T.K.-W., Tang, K.H., Wo, J.Y.-H., Zheng, B.-J., Guan, X.-Y., 2008. Aldehyde dehydrogenase discriminates the CD133 liver cancer stem cell populations. Mol. Cancer Res. 6, 1146–1153. https://doi.org/10.1158/1541-7786.MCR-08-0035

Madeira, M., Mattar, A., Logullo, Â.F., Soares, F.A., Gebrim, L.H., 2013. Estrogen receptor alpha/beta ratio and estrogen receptor beta as predictors of endocrine therapy responsiveness–a randomized neoadjuvant trial comparison between anastrozole and tamoxifen for the treatment of postmenopausal breast cancer. BMC Cancer 13, 425. https://doi.org/10.1186/1471-2407-13-425

Mader, S., Leroy, P., Chen, J.Y., Chambon, P., 1993. Multiple parameters control the selectivity of nuclear receptors for their response elements. Selectivity and promiscuity in response element recognition by retinoic acid receptors and retinoid X receptors. J. Biol. Chem. 268, 591–600.

Madsen, B., Georg, B., Vissing, H., Fahrenkrug, J., 1998. Retinoic acid down-regulates the expression of the vasoactive intestinal polypeptide receptor type-1 in human breast carcinoma cell lines. Cancer Res. 58, 4845–4850.

Mahmoud, S.M.A., Paish, E.C., Powe, D.G., Macmillan, R.D., Grainge, M.J., Lee, A.H.S., Ellis, I.O., Green, A.R., 2011. Tumor-infiltrating CD8+ lymphocytes predict clinical outcome in breast cancer. J. Clin. Oncol. 29, 1949–1955. https://doi.org/10.1200/JCO.2010.30.5037

Mahony, S., Mazzoni, E.O., McCuine, S., Young, R.A., Wichterle, H., Gifford, D.K., 2011. Ligand-dependent dynamics of retinoic acid receptor binding during early neurogenesis. Genome Biol. 12, R2. https://doi.org/10.1186/gb-2011-12-1-r2

Makova, K.D., Hardison, R.C., 2015. The effects of chromatin organization on variation in mutation rates in the genome. Nat. Rev. Genet. 16, 213–223. https://doi.org/10.1038/nrg3890

Mamidi, S., Hofer, T.P.J., Hoffmann, R., Ziegler-Heitbrock, L., Frankenberger, M., 2012. All-trans retinoic acid up-regulates prostaglandin-E synthase expression in human macrophages. Immunobiology 217, 593–600. https://doi.org/10.1016/j.imbio.2011.10.022

Manders, K., van de Poll-Franse, L.V., Creemers, G.-J., Vreugdenhil, G., van der Sangen, M.J.C., Nieuwenhuijzen, G.A.P., Roumen, R.M.H., Voogd, A.C., 2006. Clinical management of women with metastatic breast cancer: a descriptive study according to age group. BMC Cancer 6, 179. https://doi.org/10.1186/1471-2407-6-179

Manjili, M.H., 2011. Revisiting cancer immunoediting by understanding cancer immune complexity. J. Pathol. 224, 5–9. https://doi.org/10.1002/path.2865

Manor, D., Shmidt, E.N., Budhu, A., Flesken-Nikitin, A., Zgola, M., Page, R., Nikitin, A.Y., Noy, N., 2003. Mammary Carcinoma Suppression by Cellular Retinoic Acid Binding Protein-II. Cancer Res. 63, 4426–4433.

Mao, P., Joshi, K., Li, J., Kim, S.-H., Li, P., Santana-Santos, L., Luthra, S., Chandran, U.R., Benos, P.V., Smith, L., Wang, M., Hu, B., Cheng, S.-Y., Sobol, R.W., Nakano, I., 2013. Mesenchymal glioma stem cells are maintained by activated glycolytic metabolism involving aldehyde dehydrogenase 1A3. Proc. Natl. Acad. Sci. U. S. A. 110, 8644–8649. https://doi.org/10.1073/pnas.1221478110

Marcato, P., Dean, C.A., Giacomantonio, C.A., Lee, P.W.K., 2011a. Aldehyde dehydrogenase: its role as a cancer stem cell marker comes down to the specific isoform. Cell Cycle 10, 1378–1384. https://doi.org/10.4161/cc.10.9.15486

Marcato, P., Dean, C.A., Liu, R.-Z., Coyle, K.M., Bydoun, M., Wallace, M., Clements, D., Turner, C., Mathenge, E.G., Gujar, S.A., Giacomantonio, C.A., Mackey, J.R., Godbout, R., Lee, P.W.K., 2015. Aldehyde dehydrogenase 1A3 influences breast cancer progression via differential retinoic acid signaling. Mol. Oncol. 9, 17–31. https://doi.org/10.1016/j.molonc.2014.07.010

Marcato, P., Dean, C.A., Pan, D., Araslanova, R., Gillis, M., Joshi, M., Helyer, L., Pan, L., Leidal, A., Gujar, S., Giacomantonio, C.A., Lee, P.W.K., 2011b. Aldehyde dehydrogenase activity of breast cancer stem cells is primarily due to isoform ALDH1A3 and its expression is predictive of metastasis. Stem Cells 29, 32–45. https://doi.org/10.1002/stem.563

Marchetti, M., Falanga, A., Giovanelli, S., Oldani, E., Barbui, T., 1996. All-trans-retinoic acid increases adhesion to endothelium of the human promyelocytic leukaemia cell line NB4. Br. J. Haematol. 93, 360–366. https://doi.org/10.1046/j.1365-2141.1996.4911029.x

Marill, J., Cresteil, T., Lanotte, M., Chabot, G.G., 2000. Identification of human cytochrome P450s involved in the formation of all-trans-retinoic acid principal metabolites. Mol. Pharmacol. 58, 1341–1348.

Maring, J.G., Groen, H.J.M., Wachters, F.M., Uges, D.R.A., de Vries, E.G.E., 2005. Genetic factors influencing Pyrimidine-antagonist chemotherapy. Pharmacogenomics J. 5, 226–243. https://doi.org/10.1038/sj.tpj.6500320

Marth, C., Mayer, I., Daxenbichler, G., 1984. Effect of retinoic acid and 4-hydroxytamoxifen on human breast cancer cell lines. Biochem. Pharmacol. 33, 2217–2221.

Masters, J.R., Thomson, J.A., Daly-Burns, B., Reid, Y.A., Dirks, W.G., Packer, P., Toji, L.H., Ohno, T., Tanabe, H., Arlett, C.F., Kelland, L.R., Harrison, M., Virmani, A., Ward, T.H., Ayres, K.L., Debenham, P.G., 2001. Short tandem repeat profiling provides an international reference standard for human cell lines. Proc. Natl. Acad. Sci. U. S. A. 98, 8012–8017. https://doi.org/10.1073/pnas.121616198

Matthay, K.K., Villablanca, J.G., Seeger, R.C., Stram, D.O., Harris, R.E., Ramsay, N.K., Swift, P., Shimada, H., Black, C.T., Brodeur, G.M., Gerbing, R.B., Reynolds, C.P., 1999. Treatment of high-risk neuroblastoma with intensive chemotherapy, radiotherapy, autologous bone marrow transplantation, and 13-cis-retinoic acid. Children's Cancer Group. N. Engl. J. Med. 341, 1165–1173. https://doi.org/10.1056/NEJM199910143411601

Mazzocca, A., Fransvea, E., Dituri, F., Lupo, L., Antonaci, S., Giannelli, G., 2010. Down-regulation of connective tissue growth factor by inhibition of transforming growth factor beta blocks the tumor-stroma cross-talk and tumor progression in hepatocellular carcinoma. Hepatology 51, 523–534. https://doi.org/10.1002/hep.23285

McCaffery, P., Dräger, U.C., 1994. Hot spots of retinoic acid synthesis in the developing spinal cord. Proc. Natl. Acad. Sci. U. S. A. 91, 7194–7197.

McCaffery, P., Lee, M.O., Wagner, M.A., Sladek, N.E., Dräger, U.C., 1992. Asymmetrical retinoic acid synthesis in the dorsoventral axis of the retina. Development 115, 371–382.
McDonald, P.J., Carpenter, R., Royle, G.T., Taylor, I., 1990. Poor response of breast cancer to tamoxifen. Postgrad. Med. J. 66, 1029–1031. https://doi.org/10.1136/pgmj.66.782.1029
Meacham, C.E., Ho, E.E., Dubrovsky, E., Gertler, F.B., Hemann, M.T., 2009. In vivo RNAi screening identifies regulators of actin dynamics as key determinants of lymphoma progression. Nat. Genet. 41, 1133–1137. https://doi.org/10.1038/ng.451
Meltzer, P., Leibovitz, A., Dalton, W., Villar, H., Kute, T., Davis, J., Nagle, R., Trent, J., 1991. Establishment of two new cell lines derived from human breast carcinomas with HER-2/neu amplification. Br. J. Cancer 63, 727–735.
Merino, V.F., Nguyen, N., Jin, K., Sadik, H., Cho, S., Korangath, P., Han, L., Foster, Y.M.N., Zhou, X.C., Zhang, Z., Connolly, R.M., Stearns, V., Ali, S.Z., Adams, C., Chen, Q., Pan, D., Huso, D.L., Ordentlich, P., Brodie, A., Sukumar, S., 2016. Combined treatment with epigenetic, differentiating, and chemotherapeutic agents cooperatively targets tumor-initiating cells in triple-negative breast cancer. Cancer Res. 76, 2013–2024. https://doi.org/10.1158/0008-5472.CAN-15-1619
Metzger-Filho, O., Tutt, A., de Azambuja, E., Saini, K.S., Viale, G., Loi, S., Bradbury, I., Bliss, J.M., Azim, H.A., Ellis, P., Di Leo, A., Baselga, J., Sotiriou, C., Piccart-Gebhart, M., 2012. Dissecting the heterogeneity of triple-negative breast cancer. J. Clin. Oncol. 30, 1879–1887. https://doi.org/10.1200/JCO.2011.38.2010
Michael, A., Hill, M., Maraveyas, A., Dalgleish, A., Lofts, F., 2007. 13-cis-Retinoic acid in combination with gemcitabine in the treatment of locally advanced and metastatic pancreatic cancer--report of a pilot phase II study. Clin. Oncol. 19, 150–153.
Mikeska, T., Craig, J.M., 2014. DNA methylation biomarkers: Cancer and beyond. Genes 5, 821–864. https://doi.org/10.3390/genes5030821
Miller, W.H., 1998. The emerging role of retinoids and retinoic acid metabolism blocking agents in the treatment of cancer. Cancer 83, 1471–1482.
Miller, W.H., Moy, D., Li, A., Grippo, J.F., Dmitrovsky, E., 1990. Retinoic acid induces down-regulation of several growth factors and proto-oncogenes in a human embryonal cancer cell line. Oncogene 5, 511–517.
Miller, W.R., 2003. Aromatase inhibitors: mechanism of action and role in the treatment of breast cancer. Semin. Oncol. 30, 3–11.
Minucci, S., Maccarana, M., Cioce, M., De Luca, P., Gelmetti, V., Segalla, S., Di Croce, L., Giavara, S., Matteucci, C., Gobbi, A., Bianchini, A., Colombo, E., Schiavoni, I., Badaracco, G., Hu, X., Lazar, M.A., Landsberger, N., Nervi, C., Pelicci, P.G., 2000. Oligomerization of RAR and AML1 transcription factors as a novel mechanism of oncogenic activation. Mol. Cell 5, 811–820.
Mira-Y-Lopez, R., Zheng, W.L., Kuppumbatti, Y.S., Rexer, B., Jing, Y., Ong, D.E., 2000. Retinol conversion to retinoic acid is impaired in breast cancer cell lines relative to normal cells. J. Cell. Physiol. 185, 302–309. https://doi.org/10.1002/1097-4652(200011)185:2<302::AID-JCP15>3.0.CO;2-#

Mirza, N., Fishman, M., Fricke, I., Dunn, M., Neuger, A.M., Frost, T.J., Lush, R.M., Antonia, S., Gabrilovich, D.I., 2006. All-trans-retinoic acid improves differentiation of myeloid cells and immune response in cancer patients. Cancer Res. 66, 9299–9307. https://doi.org/10.1158/0008-5472.CAN-06-1690

Modrich, P., 1994. Mismatch repair, genetic stability, and cancer. Science 266, 1959–1960.

Mohandas, T., Sparkes, R.S., Shapiro, L.J., 1981. Reactivation of an inactive human X chromosome: evidence for X inactivation by DNA methylation. Science 211, 393–396. https://doi.org/10.1126/science.6164095

Montesinos, P., Sanz, M.A., 2011. The differentiation syndrome in patients with acute promyelocytic leukemia: Experience of the Pethema Group and review of the literature. Mediterr. J. Hematol. Infect. Dis. 3. https://doi.org/10.4084/MJHID.2011.059

Moretti, A., Li, J., Donini, S., Sobol, R.W., Rizzi, M., Garavaglia, S., 2016. Crystal structure of human aldehyde dehydrogenase 1A3 complexed with NAD(+) and retinoic acid. Sci. Rep. 6, 35710. https://doi.org/10.1038/srep35710

Nagpal, S., Patel, S., Asano, A.T., Johnson, A.T., Duvic, M., Chandraratna, R.A., 1996. Tazarotene-induced gene 1 (TIG1), a novel retinoic acid receptor-responsive gene in skin. J. Invest. Dermatol. 106, 269–274.

Nagy, L., Kao, H.-Y., Chakravarti, D., Lin, R.J., Hassig, C.A., Ayer, D.E., Schreiber, S.L., Evans, R.M., 1997. Nuclear receptor repression mediated by a complex containing SMRT, mSin3A, and histone deacetylase. Cell 89, 373–380. https://doi.org/10.1016/S0092-8674(00)80218-4

Nakamura, M., Yonekawa, Y., Kleihues, P., Ohgaki, H., 2001. Promoter hypermethylation of the RB1 gene in glioblastomas. Lab. Investig. J. Tech. Methods Pathol. 81, 77–82.

Nakshatri, H., Srour, E.F., Badve, S., 2009. Breast Cancer Stem Cells and Intrinsic Subtypes: Controversies Rage On. Curr. Stem Cell Res. Ther. 4, 50–60. https://doi.org/10.2174/157488809787169110

Nanda, R., Chow, L.Q., Dees, E.C., Berger, R., Gupta, S., Geva, R., Pusztai, L., Dolled-Filhart, M., Emancipator, K., Gonzalez, E.J., Houp, J., Pathiraja, K., Karantza, V., Iannone, R., Gause, C.K., Cheng, J.D., Buisseret, L., 2015. Abstract S1-09: A phase Ib study of pembrolizumab (MK-3475) in patients with advanced triple-negative breast cancer. Cancer Res. 75, S1-09-S1-09. https://doi.org/10.1158/1538-7445.SABCS14-S1-09

Natrajan, R., Sailem, H., Mardakheh, F.K., Garcia, M.A., Tape, C.J., Dowsett, M., Bakal, C., Yuan, Y., 2016. Microenvironmental heterogeneity parallels breast cancer progression: A histology–genomic integration analysis. PLOS Med. 13, e1001961. https://doi.org/10.1371/journal.pmed.1001961

Nehls, M., Pfeifer, D., Schorpp, M., Hedrich, H., Boehm, T., 1994. New member of the winged-helix protein family disrupted in mouse and rat nude mutations. Nature 372, 103–107. https://doi.org/10.1038/372103a0

Neman, J., Termini, J., Wilczynski, S., Vaidehi, N., Choy, C., Kowolik, C.M., Li, H., Hambrecht, A.C., Roberts, E., Jandial, R., 2014. Human breast cancer metastases to the brain display GABAergic properties in the neural niche. Proc. Natl. Acad. Sci. 111, 984–989. https://doi.org/10.1073/pnas.1322098111

Nerlich, A.G., Bachmeier, B.E., 2013. Density-dependent lineage instability of MDA-MB-435 breast cancer cells. Oncol. Lett. 5, 1370–1374.
Ness, S.A., Kowenz-Leutz, E., Casini, T., Graf, T., Leutz, A., 1993. Myb and NF-M: combinatorial activators of myeloid genes in heterologous cell types. Genes Dev. 7, 749–759. https://doi.org/10.1101/gad.7.5.749
Neve, R.M., Chin, K., Fridlyand, J., Yeh, J., Baehner, F.L., Fevr, T., Clark, L., Bayani, N., Coppe, J.-P., Tong, F., Speed, T., Spellman, P.T., DeVries, S., Lapuk, A., Wang, N.J., Kuo, W.-L., Stilwell, J.L., Pinkel, D., Albertson, D.G., Waldman, F.M., McCormick, F., Dickson, R.B., Johnson, M.D., Lippman, M., Ethier, S., Gazdar, A., Gray, J.W., 2006. A collection of breast cancer cell lines for the study of functionally distinct cancer subtypes. Cancer Cell 10, 515–527. https://doi.org/10.1016/j.ccr.2006.10.008
Newell-Price, J., Clark, A.J.L., King, P., 2000. DNA methylation and silencing of gene expression. Trends Endocrinol. Metab. 11, 142–148. https://doi.org/10.1016/S1043-2760(00)00248-4
Nguyen, P.H., Giraud, J., Staedel, C., Chambonnier, L., Dubus, P., Chevret, E., Bœuf, H., Gauthereau, X., Rousseau, B., Fevre, M., Soubeyran, I., Belleannée, G., Evrard, S., Collet, D., Mégraud, F., Varon, C., 2016. All-trans retinoic acid targets gastric cancer stem cells and inhibits patient-derived gastric carcinoma tumor growth. Oncogene 35, 5619–5628. https://doi.org/10.1038/onc.2016.87
Niederreither, K., Subbarayan, V., Dollé, P., Chambon, P., 1999. Embryonic retinoic acid synthesis is essential for early mouse post-implantation development. Nat. Genet. 21, 444–448. https://doi.org/10.1038/7788
Nolan-Stevaux, O., Tedesco, D., Ragan, S., Makhanov, M., Chenchik, A., Ruefli-Brasse, A., Quon, K., Kassner, P.D., 2013. Measurement of cancer cell growth heterogeneity through lentiviral barcoding identifies clonal dominance as a characteristic of in vivo tumor engraftment. PLOS ONE 8, e67316. https://doi.org/10.1371/journal.pone.0067316
Nolting, J., Daniel, C., Reuter, S., Stuelten, C., Li, P., Sucov, H., Kim, B.-G., Letterio, J.J., Kretschmer, K., Kim, H.-J., von Boehmer, H., 2009. Retinoic acid can enhance conversion of naive into regulatory T cells independently of secreted cytokines. J. Exp. Med. 206, 2131–2139. https://doi.org/10.1084/jem.20090639
Ohkura-Hada, S., Kondoh, N., Hada, A., Arai, M., Yamazaki, Y., Shindoh, M., Kitagawa, Y., Takahashi, M., Ando, T., Sato, Y., Yamamoto, M., 2008. Carbonyl reductase 3 (CBR3) mediates 9-cis-retinoic acid-induced cytostatis and is a potential prognostic marker for oral malignancy. Open Dent. J. 2, 78–88. https://doi.org/10.2174/1874210600802010078
Oldridge, E.E., Walker, H.F., Stower, M.J., Simms, M.S., Mann, V.M., Collins, A.T., Pellacani, D., Maitland, N.J., 2013. Retinoic acid represses invasion and stem cell phenotype by induction of the metastasis suppressors RARRES1 and LXN. Oncogenesis 2, e45. https://doi.org/10.1038/oncsis.2013.6
Omenn, G.S., Goodman, G.E., Thornquist, M.D., Balmes, J., Cullen, M.R., Glass, A., Keogh, J.P., Meyskens, F.L.J., Valanis, B., Williams, J.H.J., Barnhart, S., Hammar, S., 1996. Effects of a combination of beta carotene and vitamin A on lung cancer and cardiovascular disease. N. Engl. J. Med. 334, 1150–1155. https://doi.org/10.1056/NEJM199605023341802

Ong, D.E., 1987. Cellular retinoid-binding proteins. Arch. Dermatol. 123, 1693-1695a.
Osborne, C.K., 1998. Tamoxifen in the treatment of breast cancer. N. Engl. J. Med. 339, 1609–1618. https://doi.org/10.1056/NEJM199811263392207
Paez-Ribes, M., Man, S., Xu, P., Kerbel, R.S., 2016. Development of patient derived xenograft models of overt spontaneous breast cancer metastasis: A cautionary note. PLOS ONE 11, e0158034. https://doi.org/10.1371/journal.pone.0158034
Paine, T.M., Soule, H.D., Pauley, R.J., Dawson, P.J., 1992. Characterization of epithelial phenotypes in mortal and immortal human breast cells. Int. J. Cancer 50, 463–473.
Papi, A., Guarnieri, T., Storci, G., Santini, D., Ceccarelli, C., Taffurelli, M., Carolis, S.D., Avenia, N., Sanguinetti, A., Sidoni, A., Orlandi, M., Bonafé, M., 2012. Nuclear receptors agonists exert opposing effects on the inflammation dependent survival of breast cancer stem cells. Cell Death Differ. 19, 1208. https://doi.org/10.1038/cdd.2011.207
Pappas, J.J., Toulouse, A., Basik, M., Lévesque, L., Bradley, W.E.C., 2011. Knockdown of RARB2 identifies a dual role in cancer. Genes. Chromosomes Cancer 50, 700–714. https://doi.org/10.1002/gcc.20892
Park, C., Qian, W., Zhang, J., 2012. Genomic evidence for elevated mutation rates in highly expressed genes. EMBO Rep. 13, 1123–1129. https://doi.org/10.1038/embor.2012.165
Park, S.Y., Kwon, H.J., Choi, Y., Lee, H.E., Kim, S.-W., Kim, J.H., Kim, I.A., Jung, N., Cho, N.-Y., Kang, G.H., 2012. Distinct patterns of promoter CpG island methylation of breast cancer subtypes are associated with stem cell phenotypes. Mod. Pathol. 25, 185–196. https://doi.org/10.1038/modpathol.2011.160
Park, S.-Y., Seol, J.-W., Lee, Y.-J., Cho, J.-H., Kang, H.-S., Kim, I.-S., Park, S.-H., Kim, T.-H., Yim, J.H., Kim, M., Billiar, T.R., Seol, D.-W., 2004. IFN-gamma enhances TRAIL-induced apoptosis through IRF-1. Eur. J. Biochem. 271, 4222–4228. https://doi.org/10.1111/j.1432-1033.2004.04362.x
Parker, J.S., Mullins, M., Cheang, M.C.U., Leung, S., Voduc, D., Vickery, T., Davies, S., Fauron, C., He, X., Hu, Z., Quackenbush, J.F., Stijleman, I.J., Palazzo, J., Marron, J.S., Nobel, A.B., Mardis, E., Nielsen, T.O., Ellis, M.J., Perou, C.M., Bernard, P.S., 2009. Supervised risk predictor of breast cancer based on intrinsic subtypes. J. Clin. Oncol. 27, 1160–1167. https://doi.org/10.1200/JCO.2008.18.1370
Peinemann, F., van Dalen, E.C., Tushabe, D.A., Berthold, F., 2015. Retinoic acid post consolidation therapy for high-risk neuroblastoma patients treated with autologous hematopoietic stem cell transplantation. Cochrane Database Syst. Rev. 1, CD010685. https://doi.org/10.1002/14651858.CD010685.pub2
Pelicano, L., Li, F., Schindler, C., Chelbi-Alix, M.K., 1997. Retinoic acid enhances the expression of interferon-induced proteins: evidence for multiple mechanisms of action. Oncogene 15, 2349–2359. https://doi.org/10.1038/sj.onc.1201410
Pelleitier, M., Montplaisir, S., 1975. The nude mouse: a model of deficient T-cell function. Methods Achiev. Exp. Pathol. 7, 149–166.
Peng, Z., Shen, R., Li, Y.-W., Teng, K.-Y., Shapiro, C.L., Lin, H.-J.L., 2012. Epigenetic repression of RARRES1 is mediated by methylation of a proximal promoter and a loss of CTCF binding. PloS One 7, e36891. https://doi.org/10.1371/journal.pone.0036891

Percario, Z.A., Giandomenico, V., Fiorucci, G., Chiantore, M.V., Vannucchi, S., Hiscott, J., Affabris, E., Romeo, G., 1999. Retinoic acid is able to induce interferon regulatory factor 1 in squamous carcinoma cells via a STAT-1 independent signalling pathway. Cell Growth Differ. Mol. Biol. J. Am. Assoc. Cancer Res. 10, 263–270.

Pereira, B., Chin, S.-F., Rueda, O.M., Vollan, H.-K.M., Provenzano, E., Bardwell, H.A., Pugh, M., Jones, L., Russell, R., Sammut, S.-J., Tsui, D.W.Y., Liu, B., Dawson, S.-J., Abraham, J., Northen, H., Peden, J.F., Mukherjee, A., Turashvili, G., Green, A.R., McKinney, S., Oloumi, A., Shah, S., Rosenfeld, N., Murphy, L., Bentley, D.R., Ellis, I.O., Purushotham, A., Pinder, S.E., Børresen-Dale, A.-L., Earl, H.M., Pharoah, P.D., Ross, M.T., Aparicio, S., Caldas, C., 2016. The somatic mutation profiles of 2,433 breast cancers refine their genomic and transcriptomic landscapes. Nat. Commun. 7, 11479. https://doi.org/10.1038/ncomms11479

Perez, E.A., Thompson, E.A., Ballman, K.V., Anderson, S.K., Asmann, Y.W., Kalari, K.R., Eckel-Passow, J.E., Dueck, A.C., Tenner, K.S., Jen, J., Fan, J.-B., Geiger, X.J., McCullough, A.E., Chen, B., Jenkins, R.B., Sledge, G.W., Winer, E.P., Gralow, J.R., Reinholz, M.M., 2015. Genomic analysis reveals that immune function genes are strongly linked to clinical outcome in the North Central Cancer Treatment Group N9831 adjuvant trastuzumab trial. J. Clin. Oncol. 33, 701–708. https://doi.org/10.1200/JCO.2014.57.6298

Perissi, V., Aggarwal, A., Glass, C.K., Rose, D.W., Rosenfeld, M.G., 2004. A corepressor/coactivator exchange complex required for transcriptional activation by nuclear receptors and other regulated transcription factors. Cell 116, 511–526. https://doi.org/10.1016/S0092-8674(04)00133-3

Perou, C.M., Sørlie, T., Eisen, M.B., van de Rijn, M., Jeffrey, S.S., Rees, C.A., Pollack, J.R., Ross, D.T., Johnsen, H., Akslen, L.A., Fluge, O., Pergamenschikov, A., Williams, C., Zhu, S.X., Lønning, P.E., Børresen-Dale, A.L., Brown, P.O., Botstein, D., 2000. Molecular portraits of human breast tumours. Nature 406, 747–752. https://doi.org/10.1038/35021093

Perrault, D., Eisenhauer, E.A., Pritchard, K.I., Panasci, L., Norris, B., Vandenberg, T., Fisher, B., 1996. Phase II study of the progesterone antagonist mifepristone in patients with untreated metastatic breast carcinoma: a National Cancer Institute of Canada Clinical Trials Group study. J. Clin. Oncol. 14, 2709–2712. https://doi.org/10.1200/JCO.1996.14.10.2709

Persaud, S.D., Lin, Y.-W., Wu, C.-Y., Kagechika, H., Wei, L.-N., 2013. Cellular retinoic acid binding protein I mediates rapid non-canonical activation of ERK1/2 by all-trans retinoic acid. Cell. Signal. 25, 19–25. https://doi.org/10.1016/j.cellsig.2012.09.002

Persaud, S.D., Park, S.W., Ishigami-Yuasa, M., Koyano-Nakagawa, N., Kagechika, H., Wei, L.-N., 2016. All trans-retinoic acid analogs promote cancer cell apoptosis through non-genomic Crabp1 mediating ERK1/2 phosphorylation. Sci. Rep. 6, 22396. https://doi.org/10.1038/srep22396

Peterson, C.L., Laniel, M.-A., 2004. Histones and histone modifications. Curr. Biol. 14, R546–R551. https://doi.org/10.1016/j.cub.2004.07.007

Peterson, T.J., Karmakar, S., Pace, M.C., Gao, T., Smith, C.L., 2007. The silencing mediator of retinoic acid and thyroid hormone receptor (SMRT) corepressor is

required for full estrogen receptor α transcriptional activity. Mol. Cell. Biol. 27, 5933–5948. https://doi.org/10.1128/MCB.00237-07
Petitjean, A., Achatz, M.I.W., Borresen-Dale, A.L., Hainaut, P., Olivier, M., 2007. *TP53* mutations in human cancers: functional selection and impact on cancer prognosis and outcomes. Oncogene 26, 2157. https://doi.org/10.1038/sj.onc.1210302
Pfitzner, E., Kirfel, J., Becker, P., Rolke, A., Schüle, R., 1998. Physical interaction between retinoic acid receptor and the oncoprotein Myb inhibits retinoic acid-dependent transactivation. Proc. Natl. Acad. Sci. 95, 5539–5544.
Pijnappel, W.W., Hendriks, H.F., Folkers, G.E., van den Brink, C.E., Dekker, E.J., Edelenbosch, C., van der Saag, P.T., Durston, A.J., 1993. The retinoid ligand 4-oxo-retinoic acid is a highly active modulator of positional specification. Nature 366, 340–344. https://doi.org/10.1038/366340a0
Prat, A., Karginova, O., Parker, J.S., Fan, C., He, X., Bixby, L., Harrell, J.C., Roman, E., Adamo, B., Troester, M., Perou, C.M., 2013. Characterization of cell lines derived from breast cancers and normal mammary tissues for the study of the intrinsic molecular subtypes. Breast Cancer Res. Treat. 142, 237–255. https://doi.org/10.1007/s10549-013-2743-3
Prat, A., Parker, J.S., Karginova, O., Fan, C., Livasy, C., Herschkowitz, J.I., He, X., Perou, C.M., 2010. Phenotypic and molecular characterization of the claudin-low intrinsic subtype of breast cancer. Breast Cancer Res. 12, R68. https://doi.org/10.1186/bcr2635
Prat, A., Perou, C.M., 2011. Deconstructing the molecular portraits of breast cancer. Mol. Oncol. 5, 5–23. https://doi.org/10.1016/j.molonc.2010.11.003
Price, J.E., 1996. Metastasis from human breast cancer cell lines. Breast Cancer Res. Treat. 39, 93–102. https://doi.org/10.1007/BF01806081
Price, J.E., Polyzos, A., Zhang, R.D., Daniels, L.M., 1990. Tumorigenicity and metastasis of human breast carcinoma cell lines in nude mice. Cancer Res. 50, 717–721.
Rae, J.M., Creighton, C.J., Meck, J.M., Haddad, B.R., Johnson, M.D., 2007. MDA-MB-435 cells are derived from M14 melanoma cells--a loss for breast cancer, but a boon for melanoma research. Breast Cancer Res. Treat. 104, 13–19. https://doi.org/10.1007/s10549-006-9392-8
Rangarajan, A., Hong, S.J., Gifford, A., Weinberg, R.A., 2004. Species- and cell type-specific requirements for cellular transformation. Cancer Cell 6, 171–183. https://doi.org/10.1016/j.ccr.2004.07.009
Rangarajan, A., Weinberg, R.A., 2003. Opinion: Comparative biology of mouse versus human cells: modelling human cancer in mice. Nat. Rev. Cancer 3, 952–959. https://doi.org/10.1038/nrc1235
Redmond, T.M., Gentleman, S., Duncan, T., Yu, S., Wiggert, B., Gantt, E., Cunningham, F.X., 2001. Identification, expression, and substrate specificity of a mammalian β-carotene 15,15′-dioxygenase. J. Biol. Chem. 276, 6560–6565. https://doi.org/10.1074/jbc.M009030200
Ren, J., Liu, S., Cui, C., Ten Dijke, P., 2017. Invasive behavior of human breast cancer cells in embryonic zebrafish. J. Vis. Exp. JoVE. https://doi.org/10.3791/55459
Ren, X., Li, Y., Ma, X., Zheng, L., Xu, Y., Wang, J., 2007. Activation of p38/MEF2C pathway by all-trans retinoic acid in cardiac myoblasts. Life Sci. 81, 89–96. https://doi.org/10.1016/j.lfs.2007.04.037

Resetkova, E., Reis-Filho, J.S., Jain, R.K., Mehta, R., Thorat, M.A., Nakshatri, H., Badve, S., 2010. Prognostic impact of ALDH1 in breast cancer: a story of stem cells and tumor microenvironment. Breast Cancer Res. Treat. 123, 97–108. https://doi.org/10.1007/s10549-009-0619-3

Restifo, N.P., Esquivel, F., Kawakami, Y., Yewdell, J.W., Mulé, J.J., Rosenberg, S.A., Bennink, J.R., 1993. Identification of human cancers deficient in antigen processing. J. Exp. Med. 177, 265–272.

Rettino, A., Clarke, N.M., 2013. Genome-wide identification of IRF1 binding sites reveals extensive occupancy at cell death associated genes. J. Carcinog. Mutagen. https://doi.org/10.4172/2157-2518.S6-009

Rexer, B.N., Zheng, W.L., Ong, D.E., 2001. Retinoic acid biosynthesis by normal human breast epithelium is via aldehyde dehydrogenase 6, absent in MCF-7 cells. Cancer Res. 61, 7065–7070.

Reynolds, C.P., Matthay, K.K., Villablanca, J.G., Maurer, B.J., 2003. Retinoid therapy of high-risk neuroblastoma. Cancer Lett. 197, 185–192. https://doi.org/10.1016/S0304-3835(03)00108-3

Reynolds, C.P., Schindler, P.F., Jones, D.M., Gentile, J.L., Proffitt, R.T., Einhorn, P.A., 1994. Comparison of 13-cis-retinoic acid to trans-retinoic acid using human neuroblastoma cell lines. Prog. Clin. Biol. Res. 385, 237–244.

Riaz, M., van Jaarsveld, M.T.M., Hollestelle, A., Prager-van der Smissen, W.J.C., Heine, A.A.J., Boersma, A.W.M., Liu, J., Helmijr, J., Ozturk, B., Smid, M., Wiemer, E.A., Foekens, J.A., Martens, J.W.M., 2013. miRNA expression profiling of 51 human breast cancer cell lines reveals subtype and driver mutation-specific miRNAs. Breast Cancer Res. 15, R33. https://doi.org/10.1186/bcr3415

Roberts, C., Ivins, S.M., James, C.T., Scambler, P.J., 2005. Retinoic acid down-regulates Tbx1 expression in vivo and in vitro. Dev. Dyn. 232, 928–938. https://doi.org/10.1002/dvdy.20268

Robertson, J.F.R., Willsher, P.C., Winterbottom, L., Blamey, R.W., Thorpe, S., 1999. Onapristone, a progesterone receptor antagonist, as first-line therapy in primary breast cancer. Eur. J. Cancer 35, 214–218. https://doi.org/10.1016/S0959-8049(98)00388-8

Rochette-Egly, C., 2003. Nuclear receptors: integration of multiple signalling pathways through phosphorylation. Cell. Signal. 15, 355–366. https://doi.org/10.1016/S0898-6568(02)00115-8

Rogaia, D., Grignani, F., Grignani, F., Nicoletti, I., Pelicci, P.G., 1995. The acute promyelocytic leukemia-specific PML/RAR alpha fusion protein reduces the frequency of commitment to apoptosis upon growth factor deprivation of GM-CSF-dependent myeloid cells. Leukemia 9, 1467–1472.

Roider, H.G., Manke, T., O'Keeffe, S., Vingron, M., Haas, S.A., 2009. PASTAA: identifying transcription factors associated with sets of co-regulated genes. Bioinformatics 25, 435–442. https://doi.org/10.1093/bioinformatics/btn627

Roll, J.D., Rivenbark, A.G., Sandhu, R., Parker, J.S., Jones, W.D., Carey, L.A., Livasy, C.A., Coleman, W.B., 2013. Dysregulation of the epigenome in triple-negative breast cancers: Basal-like and claudin-low breast cancers express aberrant DNA hypermethylation. Exp. Mol. Pathol. 95, 276–287. https://doi.org/10.1016/j.yexmp.2013.09.001

Roman, S.D., Ormandy, C.J., Manning, D.L., Blamey, R.W., Nicholson, R.I., Sutherland, R.L., Clarke, C.L., 1993. Estradiol induction of retinoic acid receptors in human breast cancer cells. Cancer Res. 53, 5940–5945.
Romero, O.A., Verdura, S., Torres-Diz, M., Gomez, A., Moran, S., Condom, E., Esteller, M., Villanueva, A., Sanchez-Cespedes, M., 2017. Sensitization of retinoids and corticoids to epigenetic drugs in MYC-activated lung cancers by antitumor reprogramming. Oncogene 36, 1287–1296. https://doi.org/10.1038/onc.2016.296
Romieu, G., Maudelonde, T., Ulmann, A., Pujol, H., Grenier, J., Cavalie, G., Khalaf, S., Rochefort, H., 1987. The antiprogestin RU486 in advanced breast cancer: preliminary clinical trial. Bull. Cancer (Paris) 74, 455–461.
Ross, D.T., Scherf, U., Eisen, M.B., Perou, C.M., Rees, C., Spellman, P., Iyer, V., Jeffrey, S.S., Van de Rijn, M., Waltham, M., Pergamenschikov, A., Lee, J.C., Lashkari, D., Shalon, D., Myers, T.G., Weinstein, J.N., Botstein, D., Brown, P.O., 2000. Systematic variation in gene expression patterns in human cancer cell lines. Nat. Genet. 24, 227–235. https://doi.org/10.1038/73432
Ross-Innes, C.S., Stark, R., Holmes, K.A., Schmidt, D., Spyrou, C., Russell, R., Massie, C.E., Vowler, S.L., Eldridge, M., Carroll, J.S., 2010. Cooperative interaction between retinoic acid receptor-alpha and estrogen receptor in breast cancer. Genes Dev. 24, 171–182. https://doi.org/10.1101/gad.552910
Roy, A., Ramalinga, M., Kim, O.J., Chijioke, J., Lynch, S., Byers, S., Kumar, D., 2017. Multiple roles of RARRES1 in prostate cancer: Autophagy induction and angiogenesis inhibition. PLOS ONE 12, e0180344. https://doi.org/10.1371/journal.pone.0180344
Ruberte, E., Friederich, V., Chambon, P., Morriss-Kay, G., 1993. Retinoic acid receptors and cellular retinoid binding proteins. III. Their differential transcript distribution during mouse nervous system development. Development 118, 267–282.
Sabatier, R., Finetti, P., Guille, A., Adelaide, J., Chaffanet, M., Viens, P., Birnbaum, D., Bertucci, F., 2014. Claudin-low breast cancers: clinical, pathological, molecular and prognostic characterization. Mol. Cancer 13, 228. https://doi.org/10.1186/1476-4598-13-228
Sabbattini, P., 2001. Binding of Ikaros to the lambda5 promoter silences transcription through a mechanism that does not require heterochromatin formation. EMBO J. 20, 2812–2822. https://doi.org/10.1093/emboj/20.11.2812
Sahab, Z.J., Hall, M.D., Me Sung, Y., Dakshanamurthy, S., Ji, Y., Kumar, D., Byers, S.W., 2011. Tumor suppressor RARRES1 interacts with cytoplasmic carboxypeptidase AGBL2 to regulate the α-tubulin tyrosination cycle. Cancer Res. 71, 1219–1228. https://doi.org/10.1158/0008-5472.CAN-10-2294
Salbert, G., Fanjul, A., Piedrafita, F.J., Lu, X.P., Kim, S.J., Tran, P., Pfahl, M., 1993. Retinoic acid receptors and retinoid X receptor-alpha down-regulate the transforming growth factor-beta 1 promoter by antagonizing AP-1 activity. Mol. Endocrinol. 7, 1347–1356. https://doi.org/10.1210/mend.7.10.8264664
Salvatori, L., Ravenna, L., Caporuscio, F., Principessa, L., Coroniti, G., Frati, L., Russo, M.A., Petrangeli, E., 2011. Action of retinoic acid receptor on EGFR gene transactivation and breast cancer cell proliferation: Interplay with the estrogen receptor. Biomed. Pharmacother. 65, 307–312. https://doi.org/10.1016/j.biopha.2011.03.007

Sandell, L.L., Lynn, M.L., Inman, K.E., McDowell, W., Trainor, P.A., 2012. RDH10 oxidation of vitamin A Is a critical control step in synthesis of retinoic acid during mouse embryogenesis. PLOS ONE 7, e30698. https://doi.org/10.1371/journal.pone.0030698

Santin, A.D., Hermonat, P.L., Ravaggi, A., Chiriva-Internati, M., Pecorelli, S., Parham, G.P., 1998. Retinoic acid up-regulates the expression of major histocompatibility complex molecules and adhesion/costimulation molecules (specifically, intercellular adhesion molecule ICAM-1) in human cervical cancer. Am. J. Obstet. Gynecol. 179, 1020–1025.

Sarti, F., Zhang, Z., Schroeder, J., Chen, L., 2013. Rapid suppression of inhibitory synaptic transmission by retinoic acid. J. Neurosci. 33, 11440–11450. https://doi.org/10.1523/JNEUROSCI.1710-13.2013

Sauer, B., 1998. Inducible gene targeting in mice using the Cre/lox system. Methods 14, 381–392. https://doi.org/10.1006/meth.1998.0593

Saumet, A., Vetter, G., Bouttier, M., Antoine, E., Roubert, C., Orsetti, B., Theillet, C., Lecellier, C.-H., 2012. Estrogen and retinoic acid antagonistically regulate several microRNA genes to control aerobic glycolysis in breast cancer cells. Mol. Biosyst. 8, 3242–3253. https://doi.org/10.1039/C2MB25298H

Schlabach, M.R., Luo, J., Solimini, N.L., Hu, G., Xu, Q., Li, M.Z., Zhao, Z., Smogorzewska, A., Sowa, M.E., Ang, X.L., Westbrook, T.F., Liang, A.C., Chang, K., Hackett, J.A., Harper, J.W., Hannon, G.J., Elledge, S.J., 2008. Cancer proliferation gene discovery through functional genomics. Science 319, 620–624. https://doi.org/10.1126/science.1149200

Schmoch, T., Gal, Z., Mock, A., Mossemann, J., Lahrmann, B., Grabe, N., Schmezer, P., Lasitschka, F., Beckhove, P., Unterberg, A., Herold-Mende, C., 2016. Combined treatment of ATRA with epigenetic drugs increases aggressiveness of glioma xenografts. Anticancer Res. 36, 1489–1496.

Schmutzler, C., Köhrle, J., 2000. Retinoic acid redifferentiation therapy for thyroid cancer. Thyroid 10, 393–406. https://doi.org/10.1089/thy.2000.10.393

Schneider, G., Saur, D., 2016. In vivo RNAi screening for pancreatic cancer drivers: PILOTing the WDR5-MYC axis. Trends Cancer 2, 391–392. https://doi.org/10.1016/j.trecan.2016.07.002

Schneider, S.M., Offterdinger, M., Huber, H., Grunt, T.W., 2000. Activation of retinoic acid receptor alpha is sufficient for full induction of retinoid responses in SK-BR-3 and T47D human breast cancer cells. Cancer Res. 60, 5479–5487.

Schug, T.T., Berry, D.C., Shaw, N.S., Travis, S.N., Noy, N., 2007. Opposing effects of retinoic acid on cell growth result from alternate activation of two different nuclear receptors. Cell 129, 723–733. https://doi.org/10.1016/j.cell.2007.02.050

Schug, T.T., Berry, D.C., Toshkov, I.A., Cheng, L., Nikitin, A.Y., Noy, N., 2008. Overcoming retinoic acid-resistance of mammary carcinomas by diverting retinoic acid from PPARbeta/delta to RAR. Proc. Natl. Acad. Sci. U. S. A. 105, 7546–7551. https://doi.org/10.1073/pnas.0709981105

Schüle, R., Rangarajan, P., Yang, N., Kliewer, S., Ransone, L.J., Bolado, J., Verma, I.M., Evans, R.M., 1991. Retinoic acid is a negative regulator of AP-1-responsive genes. Proc. Natl. Acad. Sci. U. S. A. 88, 6092–6096.

Schuster-Böckler, B., Lehner, B., 2012. Chromatin organization is a major influence on regional mutation rates in human cancer cells. Nature 488, 504–507. https://doi.org/10.1038/nature11273

Seale, J., Delva, L., Renesto, P., Balitrand, N., Dombret, H., Scrobohaci, M.L., Degos, L., Paul, P., Chomienne, C., 1996. All-trans retinoic acid rapidly decreases cathepsin G synthesis and mRNA expression in acute promyelocytic leukemia. Leukemia 10, 95–101.

See, S.-J., Levin, V.A., Yung, W.-K.A., Hess, K.R., Groves, M.D., 2004. 13-cis-retinoic acid in the treatment of recurrent glioblastoma multiforme. Neuro-Oncol. 6, 253–258. https://doi.org/10.1215/S1152851703000607

Seewaldt, V.L., Johnson, B.S., Parker, M.B., Collins, S.J., Swisshelm, K., 1995. Expression of retinoic acid receptor beta mediates retinoic acid-induced growth arrest and apoptosis in breast cancer cells. Cell Growth Differ. Mol. Biol. J. Am. Assoc. Cancer Res. 6, 1077–1088.

Segars, J.H., Nagata, T., Bours, V., Medin, J.A., Franzoso, G., Blanco, J.C., Drew, P.D., Becker, K.G., An, J., Tang, T., 1993. Retinoic acid induction of major histocompatibility complex class I genes in NTera-2 embryonal carcinoma cells involves induction of NF-kappa B (p50-p65) and retinoic acid receptor beta-retinoid X receptor beta heterodimers. Mol. Cell. Biol. 13, 6157–6169.

Seifert, H.-H., Schmiemann, V., Mueller, M., Kazimirek, M., Onofre, F., Neuhausen, A., Florl, A.R., Ackermann, R., Boecking, A., Schulz, W.A., Grote, H.J., 2007. In situ detection of global DNA hypomethylation in exfoliative urine cytology of patients with suspected bladder cancer. Exp. Mol. Pathol. 82, 292–297. https://doi.org/10.1016/j.yexmp.2006.08.002

Sellappan, S., Grijalva, R., Zhou, X., Yang, W., Eli, M.B., Mills, G.B., Yu, D., 2004. Lineage infidelity of MDA-MB-435 cells: expression of melanocyte proteins in a breast cancer cell line. Cancer Res. 64, 3479–3485. https://doi.org/10.1158/0008-5472.CAN-3299-2

Sellers, W.R., 2011. A blueprint for advancing genetics-based cancer therapy. Cell 147, 26–31. https://doi.org/10.1016/j.cell.2011.09.016

Semba, R.D., 1998. The role of vitamin A and related retinoids in immune function. Nutr. Rev. 56, S38–S48. https://doi.org/10.1111/j.1753-4887.1998.tb01643.x

Shah, S.P., Roth, A., Goya, R., Oloumi, A., Ha, G., Zhao, Y., Turashvili, G., Ding, J., Tse, K., Haffari, G., Bashashati, A., Prentice, L.M., Khattra, J., Burleigh, A., Yap, D., Bernard, V., McPherson, A., Shumansky, K., Crisan, A., Giuliany, R., Heravi-Moussavi, A., Rosner, J., Lai, D., Birol, I., Varhol, R., Tam, A., Dhalla, N., Zeng, T., Ma, K., Chan, S.K., Griffith, M., Moradian, A., Cheng, S.-W.G., Morin, G.B., Watson, P., Gelmon, K., Chia, S., Chin, S.-F., Curtis, C., Rueda, O.M., Pharoah, P.D., Damaraju, S., Mackey, J., Hoon, K., Harkins, T., Tadigotla, V., Sigaroudinia, M., Gascard, P., Tlsty, T., Costello, J.F., Meyer, I.M., Eaves, C.J., Wasserman, W.W., Jones, S., Huntsman, D., Hirst, M., Caldas, C., Marra, M.A., Aparicio, S., 2012. The clonal and mutational evolution spectrum of primary triple-negative breast cancers. Nature 486, 395–399. https://doi.org/10.1038/nature10933

Sharow, K.A., Temkin, B., Asson-Batres, M.A., 2012. Retinoic acid stability in stem cell cultures. Int. J. Dev. Biol. 56, 273–278. https://doi.org/10.1387/ijdb.113378ks

Shaw, N., Elholm, M., Noy, N., 2003. Retinoic acid is a high affinity selective ligand for the peroxisome proliferator-activated receptor β/δ. J. Biol. Chem. 278, 41589–41592. https://doi.org/10.1074/jbc.C300368200

Sheikh, M.S., Shao, Z.M., Li, X.S., Dawson, M., Jetten, A.M., Wu, S., Conley, B.A., Garcia, M., Rochefort, H., Fontana, J.A., 1994. Retinoid-resistant estrogen receptor-negative human breast carcinoma cells transfected with retinoic acid receptor-alpha acquire sensitivity to growth inhibition by retinoids. J. Biol. Chem. 269, 21440–21447.

Shen, Z.-X., Shi, Z.-Z., Fang, J., Gu, B.-W., Li, J.-M., Zhu, Y.-M., Shi, J.-Y., Zheng, P.-Z., Yan, H., Liu, Y.-F., Chen, Y., Shen, Y., Wu, W., Tang, W., Waxman, S., De Thé, H., Wang, Z.-Y., Chen, S.-J., Chen, Z., 2004. All-trans retinoic acid/As2O3 combination yields a high quality remission and survival in newly diagnosed acute promyelocytic leukemia. Proc. Natl. Acad. Sci. U. S. A. 101, 5328–5335. https://doi.org/10.1073/pnas.0400053101

Shih, S.C., Claffey, K.P., 2001. Role of AP-1 and HIF-1 transcription factors in TGF-beta activation of VEGF expression. Growth Factors 19, 19–34.

Shipitsin, M., Campbell, L.L., Argani, P., Weremowicz, S., Bloushtain-Qimron, N., Yao, J., Nikolskaya, T., Serebryiskaya, T., Beroukhim, R., Hu, M., Halushka, M.K., Sukumar, S., Parker, L.M., Anderson, K.S., Harris, L.N., Garber, J.E., Richardson, A.L., Schnitt, S.J., Nikolsky, Y., Gelman, R.S., Polyak, K., 2007. Molecular definition of breast tumor heterogeneity. Cancer Cell 11, 259–273. https://doi.org/10.1016/j.ccr.2007.01.013

Shiwa, Y., Hachiya, T., Furukawa, R., Ohmomo, H., Ono, K., Kudo, H., Hata, J., Hozawa, A., Iwasaki, M., Matsuda, K., Minegishi, N., Satoh, M., Tanno, K., Yamaji, T., Wakai, K., Hitomi, J., Kiyohara, Y., Kubo, M., Tanaka, H., Tsugane, S., Yamamoto, M., Sobue, K., Shimizu, A., 2016. Adjustment of cell-type composition minimizes systematic bias in blood DNA methylation profiles derived by DNA collection protocols. PLOS ONE 11, e0147519. https://doi.org/10.1371/journal.pone.0147519

Shultz, L.D., Ishikawa, F., Greiner, D.L., 2007. Humanized mice in translational biomedical research. Nat. Rev. Immunol. 7, 118–130. https://doi.org/10.1038/nri2017

Shultz, L.D., Schweitzer, P.A., Christianson, S.W., Gott, B., Schweitzer, I.B., Tennent, B., McKenna, S., Mobraaten, L., Rajan, T.V., Greiner, D.L., 1995. Multiple defects in innate and adaptive immunologic function in NOD/LtSz-scid mice. J. Immunol. Baltim. Md 1950 154, 180–191.

Silva, J.M., Marran, K., Parker, J.S., Silva, J., Golding, M., Schlabach, M.R., Elledge, S.J., Hannon, G.J., Chang, K., 2008. Profiling essential genes in human mammary cells by multiplex RNAi screening. Science 319, 617–620. https://doi.org/10.1126/science.1149185

Singh, M., Kapoor, A., Bhatnagar, A., 2015. Oxidative and reductive metabolism of lipid-peroxidation derived carbonyls. Chem. Biol. Interact. 234, 261–273. https://doi.org/10.1016/j.cbi.2014.12.028

Singh, S., Brocker, C., Koppaka, V., Ying, C., Jackson, B., Matsumoto, A., Thompson, D.C., Vasiliou, V., 2013. Aldehyde dehydrogenases in cellular responses to

oxidative/electrophilic stress. Free Radic. Biol. Med. 56, 89–101. https://doi.org/10.1016/j.freeradbiomed.2012.11.010
Singh, S.K., Clarke, I.D., Terasaki, M., Bonn, V.E., Hawkins, C., Squire, J., Dirks, P.B., 2003. Identification of a cancer stem cell in human brain tumors. Cancer Res. 63, 5821–5828.
Singletary, S.E., Atkinson, E.N., Hoque, A., Sneige, N., Sahin, A.A., Fritsche, H.A., Lotan, R., Lu, T., Hittelman, W.N., Bevers, T.B., Stelling, C.B., Lippman, S.M., 2002. Phase II clinical trial of N-(4-Hydroxyphenyl)retinamide and tamoxifen administration before definitive surgery for breast neoplasia. Clin. Cancer Res. 8, 2835–2842.
Sirchia, S.M., Ren, M., Pili, R., Sironi, E., Somenzi, G., Ghidoni, R., Toma, S., Nicolò, G., Sacchi, N., 2002. Endogenous reactivation of the RARβ2 tumor suppressor gene epigenetically silenced in breast cancer. Cancer Res. 62, 2455–2461.
Sivaprasadarao, A., Boudjelal, M., Findlay, J.B.C., 1994. Solubilization and purification of the retinol-binding protein receptor from human placental membranes. Biochem. J. 302, 245–251. https://doi.org/10.1042/bj3020245
Siwak, D.R., Mendoza-Gamboa, E., Tari, A.M., 2003. HER2/neu uses Akt to suppress retinoic acid response element binding activity in MDA-MB-453 breast cancer cells. Int. J. Oncol. 23, 1739–1745.
Sizemore, G.M., Sizemore, S.T., Seachrist, D.D., Keri, R.A., 2014. GABA(A) Receptor Pi (GABRP) Stimulates Basal-like Breast Cancer Cell Migration through Activation of Extracellular-regulated Kinase 1/2 (ERK1/2). J. Biol. Chem. 289, 24102–24113. https://doi.org/10.1074/jbc.M114.593582
Skobe, M., Fusenig, N.E., 1998. Tumorigenic conversion of immortal human keratinocytes through stromal cell activation. Proc. Natl. Acad. Sci. U. S. A. 95, 1050–1055.
Slamon, D.J., Leyland-Jones, B., Shak, S., Fuchs, H., Paton, V., Bajamonde, A., Fleming, T., Eiermann, W., Wolter, J., Pegram, M., Baselga, J., Norton, L., 2001. Use of chemotherapy plus a monoclonal antibody against HER2 for metastatic breast cancer that overexpresses HER2. N. Engl. J. Med. 344, 783–792. https://doi.org/10.1056/NEJM200103153441101
Smarda, J., Sugarman, J., Glass, C., Lipsick, J., 1995. Retinoic acid receptor alpha suppresses transformation by v-myb. Mol. Cell. Biol. 15, 2474–2481. https://doi.org/10.1128/MCB.15.5.2474
Smiraglia, D.J., Rush, L.J., Frühwald, M.C., Dai, Z., Held, W.A., Costello, J.F., Lang, J.C., Eng, C., Li, B., Wright, F.A., Caligiuri, M.A., Plass, C., 2001. Excessive CpG island hypermethylation in cancer cell lines versus primary human malignancies. Hum. Mol. Genet. 10, 1413–1419. https://doi.org/10.1093/hmg/10.13.1413
Smith, H.S., Wolman, S.R., Dairkee, S.H., Hancock, M.C., Lippman, M., Leff, A., Hackett, A.J., 1987. Immortalization in culture: occurrence at a late stage in the progression of breast cancer. J. Natl. Cancer Inst. 78, 611–615.
Smith, M.A., Adamson, P.C., Balis, F.M., Feusner, J., Aronson, L., Murphy, R.F., Horowitz, M.E., Reaman, G., Hammond, G.D., Fenton, R.M., 1992. Phase I and pharmacokinetic evaluation of all-trans-retinoic acid in pediatric patients with

cancer. J. Clin. Oncol. 10, 1666–1673. https://doi.org/10.1200/JCO.1992.10.11.1666
Soares, J., Pinto, A.E., Cunha, C.V., André, S., Barão, I., Sousa, J.M., Cravo, M., 1999. Global DNA hypomethylation in breast carcinoma: correlation with prognostic factors and tumor progression. Cancer 85, 112–118.
Somenzi, G., Sala, G., Rossetti, S., Ren, M., Ghidoni, R., Sacchi, N., 2007. Disruption of retinoic acid receptor alpha reveals the growth promoter face of retinoic acid. PloS One 2, e836. https://doi.org/10.1371/journal.pone.0000836
Song, X.-Q., Meng, F., Ramsey, D.J., Ripps, H., Qian, H., 2005. The GABA ρ1 subunit interacts with a cellular retinoic acid binding protein in mammalian retina. Neuroscience 136, 467–475. https://doi.org/10.1016/j.neuroscience.2005.08.018
Sonneveld, E., van den Brink, C.E., Tertoolen, L.G., van der Burg, B., van der Saag, P.T., 1999. Retinoic acid hydroxylase (CYP26) is a key enzyme in neuronal differentiation of embryonal carcinoma cells. Dev. Biol. 213, 390–404. https://doi.org/10.1006/dbio.1999.9381
Sørlie, T., Tibshirani, R., Parker, J., Hastie, T., Marron, J.S., Nobel, A., Deng, S., Johnsen, H., Pesich, R., Geisler, S., Demeter, J., Perou, C.M., Lønning, P.E., Brown, P.O., Børresen-Dale, A.-L., Botstein, D., 2003. Repeated observation of breast tumor subtypes in independent gene expression data sets. Proc. Natl. Acad. Sci. U. S. A. 100, 8418–8423. https://doi.org/10.1073/pnas.0932692100
Soule, H.D., Maloney, T.M., Wolman, S.R., Peterson, W.D., Brenz, R., McGrath, C.M., Russo, J., Pauley, R.J., Jones, R.F., Brooks, S.C., 1990. Isolation and characterization of a spontaneously immortalized human breast epithelial cell line, MCF-10. Cancer Res. 50, 6075–6086.
Spencer, T.E., Jenster, G., Burcin, M.M., Allis, C.D., Zhou, J., Mizzen, C.A., McKenna, N.J., Onate, S.A., Tsai, S.Y., Tsai, M.-J., O'Malley, B.W., 1997. Steroid receptor coactivator-1 is a histone acetyltransferase. Nature 389, 194–198. https://doi.org/10.1038/38304
Sproul, D., Nestor, C., Culley, J., Dickson, J.H., Dixon, J.M., Harrison, D.J., Meehan, R.R., Sims, A.H., Ramsahoye, B.H., 2011. Transcriptionally repressed genes become aberrantly methylated and distinguish tumors of different lineages in breast cancer. Proc. Natl. Acad. Sci. U. S. A. 108, 4364–4369. https://doi.org/10.1073/pnas.1013224108
Stefansson, O.A., Moran, S., Gomez, A., Sayols, S., Arribas-Jorba, C., Sandoval, J., Hilmarsdottir, H., Olafsdottir, E., Tryggvadottir, L., Jonasson, J.G., Eyfjord, J., Esteller, M., 2015. A DNA methylation-based definition of biologically distinct breast cancer subtypes. Mol. Oncol. 9, 555–568. https://doi.org/10.1016/j.molonc.2014.10.012
Steg, A.D., Bevis, K.S., Katre, A.A., Ziebarth, A., Alvarez, R.D., Zhang, K., Conner, M., Landen, C.N., 2012. Stem cell pathways contribute to clinical chemoresistance in ovarian cancer. Clin. Cancer Res. 18, 869–881. https://doi.org/10.1158/1078-0432.CCR-11-2188
Stephens, P.J., McBride, D.J., Lin, M.-L., Varela, I., Pleasance, E.D., Simpson, J.T., Stebbings, L.A., Leroy, C., Edkins, S., Mudie, L.J., Greenman, C.D., Jia, M., Latimer, C., Teague, J.W., Lau, K.W., Burton, J., Quail, M.A., Swerdlow, H., Churcher, C., Natrajan, R., Sieuwerts, A.M., Martens, J.W.M., Silver, D.P.,

Langerød, A., Russnes, H.E.G., Foekens, J.A., Reis-Filho, J.S., van 't Veer, L., Richardson, A.L., Børresen-Dale, A.-L., Campbell, P.J., Futreal, P.A., Stratton, M.R., 2009. Complex landscapes of somatic rearrangement in human breast cancer genomes. Nature 462, 1005–1010. https://doi.org/10.1038/nature08645

Strahl, B.D., Allis, C.D., 2000. The language of covalent histone modifications. Nature 403, 41–45. https://doi.org/10.1038/47412

Stratton, M.R., Campbell, P.J., Futreal, P.A., 2009. The cancer genome. Nature 458, 719–724. https://doi.org/10.1038/nature07943

Stresemann, C., Lyko, F., 2008. Modes of action of the DNA methyltransferase inhibitors azacytidine and decitabine. Int. J. Cancer J. Int. Cancer 123, 8–13. https://doi.org/10.1002/ijc.23607

Stricker, T.P., Morales La Madrid, A., Chlenski, A., Guerrero, L., Salwen, H.R., Gosiengfiao, Y., Perlman, E.J., Furman, W., Bahrami, A., Shohet, J.M., Zage, P.E., Hicks, M.J., Shimada, H., Suganuma, R., Park, J.R., So, S., London, W.B., Pytel, P., Maclean, K.H., Cohn, S.L., 2014. Validation of a prognostic multi-gene signature in high-risk neuroblastoma using the high throughput digital NanoString nCounter™ system. Mol. Oncol. 8, 669–678. https://doi.org/10.1016/j.molonc.2014.01.010

Sullivan, K.E., Rojas, K., Cerione, R.A., Nakano, I., Wilson, K.F., 2017. The stem cell/cancer stem cell marker ALDH1A3 regulates the expression of the survival factor tissue transglutaminase, in mesenchymal glioma stem cells. Oncotarget 8, 22325–22343. https://doi.org/10.18632/oncotarget.16479

Sundaram, M., Sivaprasadarao, A., DeSousa, M.M., Findlay, J.B.C., 1998. The transfer of retinol from serum retinol-binding protein to cellular retinol-binding protein is mediated by a membrane receptor. J. Biol. Chem. 273, 3336–3342. https://doi.org/10.1074/jbc.273.6.3336

Sussman, F., de Lera, A.R., 2005. Ligand recognition by RAR and RXR receptors: Binding and selectivity. J. Med. Chem. 48, 6212–6219. https://doi.org/10.1021/jm050285w

Sutton, L.M., Warmuth, M.A., Petros, W.P., Winer, E.P., 1997. Pharmacokinetics and clinical impact of all-trans retinoic acid in metastatic breast cancer: a phase II trial. Cancer Chemother. Pharmacol. 40, 335–341. https://doi.org/10.1007/s002800050666

Swaby, R.F., Sharma, C.G.N., Jordan, V.C., 2007. SERMs for the treatment and prevention of breast cancer. Rev. Endocr. Metab. Disord. 8, 229–239. https://doi.org/10.1007/s11154-007-9034-4

Szklarczyk, D., Franceschini, A., Wyder, S., Forslund, K., Heller, D., Huerta-Cepas, J., Simonovic, M., Roth, A., Santos, A., Tsafou, K.P., Kuhn, M., Bork, P., Jensen, L.J., von Mering, C., 2015. STRING v10: protein-protein interaction networks, integrated over the tree of life. Nucleic Acids Res. 43, D447-452. https://doi.org/10.1093/nar/gku1003

Takatsuka, J., Takahashi, N., de Luca, L.M., 1996. Retinoic acid metabolism and inhibition of cell proliferation: an unexpected liaison. Cancer Res. 56, 675–678.

Takitani, K., Tamai, H., Morinobu, T., Kawamura, N., Miyake, M., Fujimoto, T., Mino, M., 1995. Pharmacokinetics of all-trans retinoic acid in pediatric patients with

leukemia. Jpn. J. Cancer Res. 86, 400–405. https://doi.org/10.1111/j.1349-7006.1995.tb03070.x

Tallman, M.S., Andersen, J.W., Schiffer, C.A., Appelbaum, F.R., Feusner, J.H., Ogden, A., Shepherd, L., Rowe, J.M., François, C., Larson, R.S., Wiernik, P.H., 2000. Clinical description of 44 patients with acute promyelocytic leukemia who developed the retinoic acid syndrome. Blood 95, 90–95.

Tamborero, D., Gonzalez-Perez, A., Perez-Llamas, C., Deu-Pons, J., Kandoth, C., Reimand, J., Lawrence, M.S., Getz, G., Bader, G.D., Ding, L., Lopez-Bigas, N., 2013. Comprehensive identification of mutational cancer driver genes across 12 tumor types. Sci. Rep. 3, 2650. https://doi.org/10.1038/srep02650

Tan, N.-S., Shaw, N.S., Vinckenbosch, N., Liu, P., Yasmin, R., Desvergne, B., Wahli, W., Noy, N., 2002. Selective cooperation between fatty acid binding proteins and peroxisome proliferator-activated receptors in regulating transcription. Mol. Cell. Biol. 22, 5114–5127. https://doi.org/10.1128/MCB.22.14.5114-5127.2002

Tan, X., Sande, J.L., Pufnock, J.S., Blattman, J.N., Greenberg, P.D., 2011. Retinoic acid as a vaccine adjuvant enhances CD8+ T cell response and mucosal protection from viral challenge. J. Virol. 85, 8316–8327. https://doi.org/10.1128/JVI.00781-11

Taneja, R., Rochette-Egly, C., Plassat, J.-L., Penna, L., Gaub, M.-P., Chambon, P., 1997. Phosphorylation of activation functions AF-1 and AF-2 of RARα and RARγ is indispensable for differentiation of F9 cells upon retinoic acid and cAMP treatment. EMBO J. 16, 6452–6465. https://doi.org/10.1093/emboj/16.21.6452

Tang, D., Kryvenko, O.N., Mitrache, N., Do, K.C., Jankowski, M., Chitale, D.A., Trudeau, S., Rundle, A., Belinsky, S.A., Rybicki, B.A., 2013. Methylation of the RARB gene increases prostate cancer risk in black americans. J. Urol. 190, 317–324. https://doi.org/10.1016/j.juro.2013.01.083

Tang, X.-H., Gudas, L.J., 2011. Retinoids, retinoic acid receptors, and cancer. Annu. Rev. Pathol. 6, 345–364. https://doi.org/10.1146/annurev-pathol-011110-130303

Tanumihardjo, S.A., 2011. Vitamin A: Biomarkers of nutrition for development. Am. J. Clin. Nutr. 94, 658S-665S. https://doi.org/10.3945/ajcn.110.005777

Tari, A.M., Lim, S.-J., Hung, M.-C., Esteva, F.J., Lopez-Berestein, G., 2002. Her2/neu induces all-trans retinoic acid (ATRA) resistance in breast cancer cells. Oncogene 21, 5224–5232. https://doi.org/10.1038/sj.onc.1205660

Tentler, J.J., Tan, A.C., Weekes, C.D., Jimeno, A., Leong, S., Pitts, T.M., Arcaroli, J.J., Messersmith, W.A., Eckhardt, S.G., 2012. Patient-derived tumour xenografts as models for oncology drug development. Nat. Rev. Clin. Oncol. 9, 338–350. https://doi.org/10.1038/nrclinonc.2012.61

Terao, M., Fratelli, M., Kurosaki, M., Zanetti, A., Guarnaccia, V., Paroni, G., Tsykin, A., Lupi, M., Gianni, M., Goodall, G.J., Garattini, E., 2011. Induction of miR-21 by retinoic acid in estrogen receptor-positive breast carcinoma cells: Biological correlates and molecular targets. J. Biol. Chem. 286, 4027–4042. https://doi.org/10.1074/jbc.M110.184994

Thatcher, J.E., Isoherranen, N., 2009. The role of CYP26 enzymes in retinoic acid clearance. Expert Opin. Drug Metab. Toxicol. 5, 875–886. https://doi.org/10.1517/17425250903032681

The Cancer Genome Atlas Network, 2012. Comprehensive molecular portraits of human breast tumours. Nature 490, 61–70. https://doi.org/10.1038/nature11412

Thomas, M.L., de Antueno, R., Coyle, K.M., Sultan, M., Cruickshank, B.M., Giacomantonio, M.A., Giacomantonio, C.A., Duncan, R., Marcato, P., 2016. Citral reduces breast tumor growth by inhibiting the cancer stem cell marker ALDH1A3. Mol. Oncol. 10, 1485–1496. https://doi.org/10.1016/j.molonc.2016.08.004

Thompson, A., Brennan, K., Cox, A., Gee, J., Harcourt, D., Harris, A., Harvie, M., Holen, I., Howell, A., Nicholson, R., Steel, M., Streuli, C., 2008. Evaluation of the current knowledge limitations in breast cancer research: A gap analysis. Breast Cancer Res. 10, R26. https://doi.org/10.1186/bcr1983

Timp, W., Feinberg, A.P., 2013. Cancer as a dysregulated epigenome allowing cellular growth advantage at the expense of the host. Nat. Rev. Cancer 13, 497–510. https://doi.org/10.1038/nrc3486

Toma, S., Raffo, P., Isnardi, L., 2000a. Effects of all-trans retinoic acid and 13-cis retinoic acid on breast cancer cell lines, in: Vitamin A and Retinoids: An Update of Biological Aspects and Clinical Applications. Springer International Publishing, Birkhäuser, Basel, pp. 209–219. https://doi.org/10.1007/978-3-0348-8454-9_16

Toma, S., Raffo, P., Nicolo, G., Canavese, G., Margallo, E., Vecchio, C., Dastoli, G., Iacona, I., Regazzi-Bonora, M., 2000b. Biological activity of all-trans-retinoic acid with and without tamoxifen and alpha-interferon 2a in breast cancer patients. Int. J. Oncol. 17, 991–1991.

Torchia, J., Glass, C., Rosenfeld, M.G., 1998. Co-activators and co-repressors in the integration of transcriptional responses. Curr. Opin. Cell Biol. 10, 373–383. https://doi.org/10.1016/S0955-0674(98)80014-8

Toyota, M., Issa, J.-P.J., 2005. Epigenetic changes in solid and hematopoietic tumors. Semin. Oncol. 32, 521–530. https://doi.org/10.1053/j.seminoncol.2005.07.003

Trempe, G.L., 1976. Human breast cancer in culture. Recent Results Cancer Res. 33–41.

Tugwood, J.D., Issemann, I., Anderson, R.G., Bundell, K.R., McPheat, W.L., Green, S., 1992. The mouse peroxisome proliferator activated receptor recognizes a response element in the 5' flanking sequence of the rat acyl CoA oxidase gene. EMBO J. 11, 433–439.

Turajlic, S., Swanton, C., 2016. Metastasis as an evolutionary process. Science 352, 169–175. https://doi.org/10.1126/science.aaf2784

Tuxhorn, J.A., Ayala, G.E., Smith, M.J., Smith, V.C., Dang, T.D., Rowley, D.R., 2002. Reactive stroma in human prostate cancer: induction of myofibroblast phenotype and extracellular matrix remodeling. Clin. Cancer Res. 8, 2912–2923.

Tzukerman, M.T., Esty, A., Santiso-Mere, D., Danielian, P., Parker, M.G., Stein, R.B., Pike, J.W., McDonnell, D.P., 1994. Human estrogen receptor transactivational capacity is determined by both cellular and promoter context and mediated by two functionally distinct intramolecular regions. Mol. Endocrinol. 8, 21–30. https://doi.org/10.1210/mend.8.1.8152428

Urvalek, A.M., Gudas, L.J., 2014. Retinoic acid and histone deacetylases regulate epigenetic changes in embryonic stem cells. J. Biol. Chem. 289, 19519–19530. https://doi.org/10.1074/jbc.M114.556555

Van heusden, J., Wouters, W., Ramaekers, F.C., Krekels, M.D., Dillen, L., Borgers, M., Smets, G., 1998. All-trans-retinoic acid metabolites significantly inhibit the proliferation of MCF-7 human breast cancer cells in vitro. Br. J. Cancer 77, 26–32.

Van Poznak, C., Somerfield, M.R., Bast, R.C., Cristofanilli, M., Goetz, M.P., Gonzalez-Angulo, A.M., Hicks, D.G., Hill, E.G., Liu, M.C., Lucas, W., Mayer, I.A., Mennel, R.G., Symmans, W.F., Hayes, D.F., Harris, L.N., 2015. Use of biomarkers to guide decisions on systemic therapy for women with metastatic breast cancer: American Society of Clinical Oncology Clinical Practice Guideline. J. Clin. Oncol. 33, 2695–2704. https://doi.org/10.1200/JCO.2015.61.1459

Van Roy, N., De Preter, K., Hoebeeck, J., Van Maerken, T., Pattyn, F., Mestdagh, P., Vermeulen, J., Vandesompele, J., Speleman, F., 2009. The emerging molecular pathogenesis of neuroblastoma: implications for improved risk assessment and targeted therapy. Genome Med. 1, 74. https://doi.org/10.1186/gm74

van Staveren, W.C.G., Solís, D.Y.W., Hébrant, A., Detours, V., Dumont, J.E., Maenhaut, C., 2009. Human cancer cell lines: Experimental models for cancer cells in situ? For cancer stem cells? Biochim. Biophys. Acta 1795, 92–103. https://doi.org/10.1016/j.bbcan.2008.12.004

van ’t Veer, L.J., Dai, H., van de Vijver, M.J., He, Y.D., Hart, A.A.M., Mao, M., Peterse, H.L., van der Kooy, K., Marton, M.J., Witteveen, A.T., Schreiber, G.J., Kerkhoven, R.M., Roberts, C., Linsley, P.S., Bernards, R., Friend, S.H., 2002. Gene expression profiling predicts clinical outcome of breast cancer. Nature 415, 530–536. https://doi.org/10.1038/415530a

Vasiliou, V., Nebert, D.W., 2005. Analysis and update of the human aldehyde dehydrogenase (ALDH) gene family. Hum. Genomics 2, 138–143.

Verma, A.K., Conrad, E.A., Boutwell, R.K., 1982. Differential effects of retinoic acid and 7,8-benzoflavone on the induction of mouse skin tumors by the complete carcinogenesis process and by the initiation-promotion regimen. Cancer Res. 42, 3519–3525.

Veronesi, U., De Palo, G., Marubini, E., Costa, A., Formelli, F., Mariani, L., Decensi, A., Camerini, T., Del Turco, M.R., Di Mauro, M.G., Muraca, M.G., Del Vecchio, M., Pinto, C., D’Aiuto, G., Boni, C., Campa, T., Magni, A., Miceli, R., Perloff, M., Malone, W.F., Sporn, M.B., 1999. Randomized trial of fenretinide to prevent second breast malignancy in women with early breast cancer. J. Natl. Cancer Inst. 91, 1847–1856.

Veronesi, U., Mariani, L., Decensi, A., Formelli, F., Camerini, T., Miceli, R., Di Mauro, M.G., Costa, A., Marubini, E., Sporn, M.B., De Palo, G., 2006. Fifteen-year results of a randomized phase III trial of fenretinide to prevent second breast cancer. Ann. Oncol. Off. J. Eur. Soc. Med. Oncol. 17, 1065–1071. https://doi.org/10.1093/annonc/mdl047

Vertuani, S., De Geer, A., Levitsky, V., Kogner, P., Kiessling, R., Levitskaya, J., 2003. Retinoids act as multistep modulators of the major histocompatibility class I presentation pathway and sensitize neuroblastomas to cytotoxic lymphocytes. Cancer Res. 63, 8006–8013.

Vertuani, S., Dubrovska, E., Levitsky, V., Jager, M.J., Kiessling, R., Levitskaya, J., 2007. Retinoic acid elicits cytostatic, cytotoxic and immunomodulatory effects on uveal

melanoma cells. Cancer Immunol. Immunother. 56, 193–204. https://doi.org/10.1007/s00262-006-0185-z
Villablanca, J.G., Khan, A.A., Avramis, V.I., Seeger, R.C., Matthay, K.K., Ramsay, N.K., Reynolds, C.P., 1995. Phase I trial of 13-cis-retinoic acid in children with neuroblastoma following bone marrow transplantation. J. Clin. Oncol. 13, 894–901. https://doi.org/10.1200/JCO.1995.13.4.894
Villablanca, J.G., London, W.B., Naranjo, A., McGrady, P., Ames, M.M., Reid, J.M., McGovern, R.M., Buhrow, S.A., Jackson, H., Stranzinger, E., Kitchen, B.J., Sondel, P.M., Parisi, M.T., Shulkin, B., Yanik, G.A., Cohn, S.L., Reynolds, C.P., 2011. Phase II study of oral capsular 4-hydroxyphenylretinamide (4-HPR/fenretinide) in pediatric patients with refractory or recurrent neuroblastoma: a report from the Children's Oncology Group. Clin. Cancer Res. 17, 6858–6866. https://doi.org/10.1158/1078-0432.CCR-11-0995
Vincent, K.M., Findlay, S.D., Postovit, L.M., 2015. Assessing breast cancer cell lines as tumour models by comparison of mRNA expression profiles. Breast Cancer Res. 17. https://doi.org/10.1186/s13058-015-0613-0
Vogelstein, B., Kinzler, K.W., 2004. Cancer genes and the pathways they control. Nat. Med. 10, 789–799. https://doi.org/10.1038/nm1087
Vonderheide, R.H., LoRusso, P.M., Khalil, M., Gartner, E.M., Khaira, D., Soulieres, D., Dorazio, P., Trosko, J.A., Rüter, J., Mariani, G.L., Usari, T., Domchek, S.M., 2010. Tremelimumab in combination with exemestane in patients with advanced breast cancer and treatment-associated modulation of inducible costimulator expression on patient T cells. Clin. Cancer Res. 16, 3485–3494. https://doi.org/10.1158/1078-0432.CCR-10-0505
Wajjwalku, W., Takahashi, M., Miyaishi, O., Lu, J., Sakata, K., Yokoi, T., Saga, S., Imai, M., Matsuyama, M., Hoshino, M., 1991. Tissue distribution of mouse mammary tumor virus (MMTV) antigens and new endogenous MMTV loci in Japanese laboratory mouse strains. Jpn. J. Cancer Res. 82, 1413–1420.
Wald, G., 1968. Molecular basis of visual excitation. Science 162, 230–239.
Wang, X., Penzes, P., Napoli, J.L., 1996. Cloning of a cDNA encoding an aldehyde dehydrogenase and its expression in Escherichia coli. Recognition of retinal as substrate. J. Biol. Chem. 271, 16288–16293.
Wang, X., Saso, H., Iwamoto, T., Xia, W., Gong, Y., Pusztai, L., Woodward, W.A., Reuben, J.M., Warner, S.L., Bearss, D.J., Hortobagyi, G.N., Hung, M.-C., Ueno, N.T., 2013. TIG1 promotes the development and progression of inflammatory breast cancer through activation of Axl kinase. Cancer Res. 73, 6516–6525. https://doi.org/10.1158/0008-5472.CAN-13-0967
Wang, X., Zhong, P., Yan, Z., 2002. Dopamine D4 Receptors Modulate GABAergic Signaling in Pyramidal Neurons of Prefrontal Cortex. J. Neurosci. 22, 9185–9193.
Warwick, G.P., 1963. The mechanism of action of alkylating agents. Cancer Res. 23, 1315–1333.
Weber, M., Hellmann, I., Stadler, M.B., Ramos, L., Pääbo, S., Rebhan, M., Schübeler, D., 2007. Distribution, silencing potential and evolutionary impact of promoter DNA methylation in the human genome. Nat. Genet. 39, 457. https://doi.org/10.1038/ng1990

Wei, S., Kozono, S., Kats, L., Nechama, M., Li, W., Guarnerio, J., Luo, M., You, M.-H., Yao, Y., Kondo, A., Hu, H., Bozkurt, G., Moerke, N.J., Cao, S., Reschke, M., Chen, C.-H., Rego, E.M., Lo-Coco, F., Cantley, L.C., Lee, T.H., Wu, H., Zhang, Y., Pandolfi, P.P., Zhou, X.Z., Lu, K.P., 2015. Active Pin1 is a key target of all-trans retinoic acid in acute promyelocytic leukemia and breast cancer. Nat. Med. 21, 457–466. https://doi.org/10.1038/nm.3839

Wen, J., Kawamata, Y., Tojo, H., Tanaka, S., Tachi, C., 1995. Expression of whey acidic protein (WAP) genes in tissues other than the mammary gland in normal and transgenic mice expressing mWAP/hGH fusion gene. Mol. Reprod. Dev. 41, 399–406. https://doi.org/10.1002/mrd.1080410402

Westervelt, P., Pollock, J.L., Oldfather, K.M., Walter, M.J., Ma, M.K., Williams, A., DiPersio, J.F., Ley, T.J., 2002. Adaptive immunity cooperates with liposomal all-trans-retinoic acid (ATRA) to facilitate long-term molecular remissions in mice with acute promyelocytic leukemia. Proc. Natl. Acad. Sci. U. S. A. 99, 9468–9473. https://doi.org/10.1073/pnas.132657799

Wetherall, N.T., Taylor, C.M., 1986. The effects of retinoid treatment and antiestrogens on the growth of T47D human breast cancer cells. Eur. J. Cancer Clin. Oncol. 22, 53–59.

White, J.A., Guo, Y.D., Baetz, K., Beckett-Jones, B., Bonasoro, J., Hsu, K.E., Dilworth, F.J., Jones, G., Petkovich, M., 1996. Identification of the retinoic acid-inducible all-trans-retinoic acid 4-hydroxylase. J. Biol. Chem. 271, 29922–29927.

Whittle, J.R., Lewis, M.T., Lindeman, G.J., Visvader, J.E., 2015. Patient-derived xenograft models of breast cancer and their predictive power. Breast Cancer Res. 17, 17. https://doi.org/10.1186/s13058-015-0523-1

Widschwendter, M., Berger, J., Hermann, M., Müller, H.M., Amberger, A., Zeschnigk, M., Widschwendter, A., Abendstein, B., Zeimet, A.G., Daxenbichler, G., Marth, C., 2000. Methylation and silencing of the retinoic acid receptor-β2 gene in breast cancer. J. Natl. Cancer Inst. 92, 826–832. https://doi.org/10.1093/jnci/92.10.826

Widschwendter, M., Berger, J., Müller, H.M., Zeimet, A.G., Marth, C., 2001. Epigenetic downregulation of the retinoic acid receptor-beta2 gene in breast cancer. J. Mammary Gland Biol. Neoplasia 6, 193–201.

Wistuba, I.I., Behrens, C., Milchgrub, S., Syed, S., Ahmadian, M., Virmani, A.K., Kurvari, V., Cunningham, T.H., Ashfaq, R., Minna, J.D., Gazdar, A.F., 1998. Comparison of features of human breast cancer cell lines and their corresponding tumors. Clin. Cancer Res. 4, 2931–2938.

Wu, C.-C., Tsai, F.-M., Shyu, R.-Y., Tsai, Y.-M., Wang, C.-H., Jiang, S.-Y., 2011. G protein-coupled receptor kinase 5 mediates Tazarotene-induced gene 1-induced growth suppression of human colon cancer cells. BMC Cancer 11, 175. https://doi.org/10.1186/1471-2407-11-175

Wu, K., Kim, H.T., Rodriquez, J.L., Munoz-Medellin, D., Mohsin, S.K., Hilsenbeck, S.G., Lamph, W.W., Gottardis, M.M., Shirley, M.A., Kuhn, J.G., Green, J.E., Brown, P.H., 2000. 9-cis-Retinoic acid suppresses mammary tumorigenesis in C3(1)-simian virus 40 T antigen-transgenic mice. Clin. Cancer Res. 6, 3696–3704.

Wu, M.-J., Kim, M.R., Chen, Y.-S., Yang, J.-Y., Chang, C.-J., 2017. Retinoic acid directs breast cancer cell state changes through regulation of TET2-PKCζ pathway. Oncogene 36, 3193. https://doi.org/10.1038/onc.2016.467

Wu, Q., Chen, Z., Su, W., 2002. Anticancer effect of retinoic acid via AP-1 activity repression is mediated by retinoic acid receptor α and β in gastric cancer cells. Int. J. Biochem. Cell Biol. 34, 1102–1114. https://doi.org/10.1016/S1357-2725(02)00030-4

Wu, Q., Dawson, M.I., Zheng, Y., Hobbs, P.D., Agadir, A., Jong, L., Li, Y., Liu, R., Lin, B., Zhang, X.K., 1997. Inhibition of trans-retinoic acid-resistant human breast cancer cell growth by retinoid X receptor-selective retinoids. Mol. Cell. Biol. 17, 6598–6608.

Wu, S., Zhang, D., Zhang, Z.P., Soprano, D.R., Soprano, K.J., 1998. Critical role of both retinoid nuclear receptors and retinoid-X-receptors in mediating growth inhibition of ovarian cancer cells by all-trans retinoic acid. Oncogene 17, 2839–2849. https://doi.org/10.1038/sj.onc.1202208

Wyss, A., Wirtz, G., Woggon, W., Brugger, R., Wyss, M., Friedlein, A., Bachmann, H., Hunziker, W., 2000. Cloning and expression of beta,beta-carotene 15,15'-dioxygenase. Biochem. Biophys. Res. Commun. 271, 334–336. https://doi.org/10.1006/bbrc.2000.2619

Xia, J., Han, L., Zhao, Z., 2012. Investigating the relationship of DNA methylation with mutation rate and allele frequency in the human genome. BMC Genomics 13, 1–9. https://doi.org/10.1186/1471-2164-13-S8-S7

Xu, X.-C., Liu, X., Tahara, E., Lippman, S.M., Lotan, R., 1999. Expression and up-regulation of retinoic acid receptor-β is associated with retinoid sensitivity and colony formation in esophageal cancer cell lines. Cancer Res. 59, 2477–2483.

Yaar, M., Stanley, J.R., Katz, S.I., 1981. Retinoic acid delays the terminal differentiation of keratinocytes in suspension culture. J. Invest. Dermatol. 76, 363–366.

Yamashina, T., Baghdadi, M., Yoneda, A., Kinoshita, I., Suzu, S., Dosaka-Akita, H., Jinushi, M., 2014. Cancer stem-like cells derived from chemoresistant tumors have a unique capacity to prime tumorigenic myeloid cells. Cancer Res. 74, 2698–2709. https://doi.org/10.1158/0008-5472.CAN-13-2169

Yamauchi, H., Woodward, W.A., Valero, V., Alvarez, R.H., Lucci, A., Buchholz, T.A., Iwamoto, T., Krishnamurthy, S., Yang, W., Reuben, J.M., Hortobágyi, G.N., Ueno, N.T., 2012. Inflammatory breast cancer: What we know and what we need to learn. The Oncologist 17, 891–899. https://doi.org/10.1634/theoncologist.2012-0039

Yang, J., Mani, S.A., Donaher, J.L., Ramaswamy, S., Itzykson, R.A., Come, C., Savagner, P., Gitelman, I., Richardson, A., Weinberg, R.A., 2004. Twist, a master regulator of morphogenesis, plays an essential role in tumor metastasis. Cell 117, 927–939. https://doi.org/10.1016/j.cell.2004.06.006

Yang, L., Munoz-Medellin, D., Kim, H.T., Ostrowski, J., Reczek, P., Brown, P.H., 1999. Retinoic acid receptor antagonist BMS453 inhibits the growth of normal and malignant breast cells without activating RAR-dependent gene expression. Breast Cancer Res. Treat. 56, 277–291.

Yang, L., Ostrowski, J., Reczek, P., Brown, P., 2001. The retinoic acid receptor antagonist, BMS453, inhibits normal breast cell growth by inducing active TGFβ

and causing cell cycle arrest. Oncogene 20, 8025. https://doi.org/10.1038/sj.onc.1204911
Yang, M., Brackenbury, W.J., 2013. Membrane potential and cancer progression. Front. Physiol. 4. https://doi.org/10.3389/fphys.2013.00185
Yang, R.M., 2016. Understanding the role of the MYB oncogene in human breast cancer: targets and functions. https://doi.org/10.14264/uql.2016.1135
Yang, W., Soares, J., Greninger, P., Edelman, E.J., Lightfoot, H., Forbes, S., Bindal, N., Beare, D., Smith, J.A., Thompson, I.R., Ramaswamy, S., Futreal, P.A., Haber, D.A., Stratton, M.R., Benes, C., McDermott, U., Garnett, M.J., 2013. Genomics of Drug Sensitivity in Cancer (GDSC): a resource for therapeutic biomarker discovery in cancer cells. Nucleic Acids Res. 41, D955–D961. https://doi.org/10.1093/nar/gks1111
Yao, T.P., Ku, G., Zhou, N., Scully, R., Livingston, D.M., 1996. The nuclear hormone receptor coactivator SRC-1 is a specific target of p300. Proc. Natl. Acad. Sci. 93, 10626–10631.
Yi, M., Huo, L., Koenig, K.B., Mittendorf, E.A., Meric-Bernstam, F., Kuerer, H.M., Bedrosian, I., Buzdar, A.U., Symmans, W.F., Crow, J.R., Bender, M., Shah, R.R., Hortobagyi, G.N., Hunt, K.K., 2014. Which threshold for ER positivity? a retrospective study based on 9639 patients. Ann. Oncol. 25, 1004–1011. https://doi.org/10.1093/annonc/mdu053
Yoshida, A., Hsu, L.C., Davé, V., 1992. Retinal oxidation activity and biological role of human cytosolic aldehyde dehydrogenase. Enzyme 46, 239–244.
Young, M.-J., Wu, Y.-H., Chiu, W.-T., Weng, T.-Y., Huang, Y.-F., Chou, C.-Y., 2015. All-trans retinoic acid downregulates ALDH1-mediated stemness and inhibits tumour formation in ovarian cancer cells. Carcinogenesis 36, 498–507. https://doi.org/10.1093/carcin/bgv018
Yuan, M., Breitkopf, S.B., Yang, X., Asara, J.M., 2012. A positive/negative ion-switching, targeted mass spectrometry-based metabolomics platform for bodily fluids, cells, and fresh and fixed tissue. Nat. Protoc. 7, 872–881. https://doi.org/10.1038/nprot.2012.024
Yung, W.K., Kyritsis, A.P., Gleason, M.J., Levin, V.A., 1996. Treatment of recurrent malignant gliomas with high-dose 13-cis-retinoic acid. Clin. Cancer Res. 2, 1931–1935.
Yuspa, S.H., Ben, T., Steinert, P., 1982. Retinoic acid induces transglutaminase activity but inhibits cornification of cultured epidermal cells. J. Biol. Chem. 257, 9906–9908.
Zámborszky, J., Szikriszt, B., Gervai, J.Z., Pipek, O., Póti, Á., Krzystanek, M., Ribli, D., Szalai-Gindl, J.M., Csabai, I., Szallasi, Z., Swanton, C., Richardson, A.L., Szüts, D., 2017. Loss of BRCA1 or BRCA2 markedly increases the rate of base substitution mutagenesis and has distinct effects on genomic deletions. Oncogene 36, 746. https://doi.org/10.1038/onc.2016.243
Zanetti, A., Affatato, R., Centritto, F., Fratelli, M., Kurosaki, M., Barzago, M.M., Bolis, M., Terao, M., Garattini, E., Paroni, G., 2015. All-trans retinoic acid modulates the plasticity and inhibits the motility of breast cancer cells: role of NOTCH1 and TGFβ. J. Biol. Chem. jbc.M115.638510. https://doi.org/10.1074/jbc.M115.638510

Zender, L., Xue, W., Zuber, J., Semighini, C.P., Krasnitz, A., Ma, B., Zender, P., Kubicka, S., Luk, J.M., Schirmacher, P., Richard McCombie, W., Wigler, M., Hicks, J., Hannon, G.J., Powers, S., Lowe, S.W., 2008. An oncogenomics-based in vivo RNAi screen identifies tumor suppressors in liver cancer. Cell 135, 852–864. https://doi.org/10.1016/j.cell.2008.09.061

Zhang, D., Li, X., Yao, Z., Wei, C., Ning, N., Li, J., 2014. GABAergic signaling facilitates breast cancer metastasis by promoting ERK1/2-dependent phosphorylation. Cancer Lett. 348, 100–108. https://doi.org/10.1016/j.canlet.2014.03.006

Zhang, J., Gao, Y., Yu, M., Wu, H., Ai, Z., Wu, Y., Liu, H., Du, J., Guo, Z., Zhang, Y., 2015. Retinoic acid induces embryonic stem cell differentiation by altering both encoding RNA and microRNA expression. PLOS ONE 10, e0132566. https://doi.org/10.1371/journal.pone.0132566

Zhang, J., Liu, L., Pfeifer, G.P., 2004. Methylation of the retinoid response gene TIG1 in prostate cancer correlates with methylation of the retinoic acid receptor beta gene. Oncogene 23, 2241–2249. https://doi.org/10.1038/sj.onc.1207328

Zhang, X., Claerhout, S., Prat, A., Dobrolecki, L.E., Petrovic, I., Lai, Q., Landis, M.D., Wiechmann, L., Schiff, R., Giuliano, M., Wong, H., Fuqua, S.W., Contreras, A., Gutierrez, C., Huang, J., Mao, S., Pavlick, A.C., Froehlich, A.M., Wu, M.-F., Tsimelzon, A., Hilsenbeck, S.G., Chen, E.S., Zuloaga, P., Shaw, C.A., Rimawi, M.F., Perou, C.M., Mills, G.B., Chang, J.C., Lewis, M.T., 2013. A renewable tissue resource of phenotypically stable, biologically and ethnically diverse, patient-derived human breast cancer xenograft models. Cancer Res. 73, 4885–4897. https://doi.org/10.1158/0008-5472.CAN-12-4081

Zhang, X., Jeyakumar, M., Petukhov, S., Bagchi, M.K., 1998. A nuclear receptor corepressor modulates transcriptional activity of antagonist-occupied steroid hormone receptor. Mol. Endocrinol. 12, 513–524. https://doi.org/10.1210/mend.12.4.0089

Zhao, D., McCaffery, P., Ivins, K.J., Neve, R.L., Hogan, P., Chin, W.W., Dräger, U.C., 1996. Molecular identification of a major retinoic-acid-synthesizing enzyme, a retinaldehyde-specific dehydrogenase. Eur. J. Biochem. 240, 15–22.

Zhao, H., Langerød, A., Ji, Y., Nowels, K.W., Nesland, J.M., Tibshirani, R., Bukholm, I.K., Kåresen, R., Botstein, D., Børresen-Dale, A.-L., Jeffrey, S.S., 2004. Different gene expression patterns in invasive lobular and ductal carcinomas of the breast. Mol. Biol. Cell 15, 2523–2536. https://doi.org/10.1091/mbc.E03-11-0786

Zhao, H.H., Herrera, R.E., Coronado-Heinsohn, E., Yang, M.C., Ludes-Meyers, J.H., Seybold-Tilson, K.J., Nawaz, Z., Yee, D., Barr, F.G., Diab, S.G., Brown, P.H., Fuqua, S.A.W., Osborne, C.K., 2001. Forkhead homologue in rhabdomyosarcoma functions as a bifunctional nuclear receptor-interacting protein with both coactivator and corepressor functions. J. Biol. Chem. 276, 27907–27912. https://doi.org/10.1074/jbc.M104278200

Zheng, P.-Z., Wang, K.-K., Zhang, Q.-Y., Huang, Q.-H., Du, Y.-Z., Zhang, Q.-H., Xiao, D.-K., Shen, S.-H., Imbeaud, S., Eveno, E., Zhao, C.-J., Chen, Y.-L., Fan, H.-Y., Waxman, S., Auffray, C., Jin, G., Chen, S.-J., Chen, Z., Zhang, J., 2005. Systems analysis of transcriptome and proteome in retinoic acid/arsenic trioxide-induced

cell differentiation/apoptosis of promyelocytic leukemia. Proc. Natl. Acad. Sci. U. S. A. 102, 7653–7658. https://doi.org/10.1073/pnas.0502825102
Zhou, G.-B., Zhang, J., Wang, Z.-Y., Chen, S.-J., Chen, Z., 2007. Treatment of acute promyelocytic leukaemia with all-trans retinoic acid and arsenic trioxide: a paradigm of synergistic molecular targeting therapy. Philos. Trans. R. Soc. Lond. B. Biol. Sci. 362, 959–971. https://doi.org/10.1098/rstb.2007.2026
Zunino, F., Capranico, G., 1990. DNA topoisomerase II as the primary target of anti-tumor anthracyclines. Anticancer. Drug Des. 5, 307–317.

APPENDIX 1: *IN VIVO* GENOMIC RNAI SCREENING IDENTIFIES NOVEL EFFECTORS OF ALDH1A3-MEDIATED TUMOR SUPPRESSION

Contribution statement

I designed the experiments, analyzed the data, and wrote this chapter with the guidance of Dr. Paola Marcato. qPCR and *in vitro* cell proliferation data was collected with the assistance of Shelby Clattenburg. The lentiviral library was prepared and provided as indicated in Chapter 5.

A1.1 INTRODUCTION

Retinoid signaling in breast cancer poses an intriguing paradox. Elevated retinoid signaling is associated with cancer stem cells (CSCs) via their enrichment through Aldefluor activity. On the other hand, retinoid treatment is associated with differentiation and anti-tumor effects in several breast cancer models, including several aggressive models of triple-negative breast cancer (TNBC).

Retinoic acid (RA) is generated from the oxidation of retinaldehyde (retinal) by aldehyde dehydrogenases (ALDHs). In mammals, the implicated enzymes are ALDH1A1, ALDH1A2, ALDH1A3, and ALDH8A1 (Hsu et al., 1994; Lin and Napoli, 2000; Rexer et al., 2001; Wang et al., 1996; Yoshida et al., 1992; Zhao et al., 1996). We have previously demonstrated that ALDH1A3 is the primary contributor to Aldefluor activity of MDA-MB-468 (Marcato et al., 2015); ALDH1A3 is also the most highly expressed retinaldehyde dehydrogenase in most TNBC models we have evaluated (see Coyle et al. 2016; Chapter 4). While we have demonstrated the importance of both ALDH1A3 and all-*trans* (at)RA in tumor growth, we have also previously described limited overlap in transcriptional profiles between ALDH1A3 and atRA treatment in MDA-MB-468 cells (Coyle et al., 2017b). This suggests that yet-unknown, non-genomic mediators may be essential for the effects of ALDH1A3 on tumor growth.

Considering the importance of non-classical transcriptional effects of retinoid signaling, as well as the hypothesized and known extra-genomic effects of both ALDH1A3 and all-trans retinoic acid (atRA), we sought to use a functional RNA interference (RNAi) approach to discover novel mediators of the effects of ALDH1A3 in MDA-MB-468. Knockdown of ALDH1A3 in this cell line results in increased tumor

growth, suggesting a tumor suppressive role for ALDH1A3 which is highly dependent on the cellular context.

While we have previously identified a predictive profile to identify TNBC tumors which could benefit from atRA treatment (Chapter 4), this is primarily correlative and there is little to suggest that these biomarkers are functional. In addition, there is limited evidence regarding non-classical mediators of retinoid resistance. Beyond developing a more comprehensive biological network, the identification of these mediators may provide novel insight into mechanisms of resistance to atRA.

We utilized a genomic loss-of-function screen to identify potential effectors of tumor inhibiting signals in MDA-MB-468 xenografts following knockdown of ALDH1A3. The lentiviral-based shRNA screen and the *in vivo* approach are described n Chapter 5. We similarly utilized a multi-step validation approach to confirm potential mediators of the tumor suppressive effects of ALDH1A3. We identify PIGX, CYP26A1, and MYB as putative effectors of this response; and suggest MYB as a signaling hub for this pathway. We perform initial investigations of PIGX, CYP26A1 and MYB in retinoid-sensitive luminal cell lines MCF-7 and T-47d. This work demonstrates the added value of functional screening, even within a pathway which is primarily transcriptional in nature.

A1.2 Materials and Methods

A1.2.1 Cell Lines and Cell Culture

MDA-MB-468, HEK293T, MCF-7 and T-47d cells were obtained from the American Type Culture Collection (ATCC). All cells were cultured in Dulbecco's Modified Eagle's Medium (DMEM, Invitrogen) with 10% fetal bovine serum (FBS, Invitrogen) and 1x antibiotic-antimycotic (Invitrogen). DDC Medical authenticated MDA-MB-468 by short tandem repeat (STR) profiling at 17 loci and verified them to be mycoplasma-negative (last performed 2015). Where indicated, all-trans retinoic acid (atRA, Sigma) was used at 1 μM for 18 h.

A1.2.2 Generation of shRNA Library in MDA-MB-468 cells

Three Decode lentiviral shRNA pools containing 10 000 shRNAs per pool (30 000 total), targeting approximately 12 000 human genes with well categorized biological functions or processes were purchased from Thermo Scientific (catalogue # RHS5339). The titre of the shRNA pools was determined using HEK293T cells at $\geq 5 \times 10^8$ transfection units (TU)/mL. Using the pGipZ scramble shRNA control (catalogue # RHS4348), we determined the relative TU/mL for MDA-MB-468 compared to HEK293T cells (HEK293T: 4.53×10^8 TU/mL; MDA-MB-468: 7.81 $X10^7$ TU/mL). The relative transduction efficiency of MDA-MB-468 was thus calculated as 0.17.

Following the manufacturer's instructions, we generated MDA-MB-468 shRNA pools with 100-fold representation of the shRNA library. Each pool was transduced into MDA-MB-468 using DMEM with 1% FBS and 8 μg/mL sequabrene (Sigma). To achieve 100-fold representation of each shRNA pool, the cells were infected at a multiplicity of infection (MOI) of 0.3. 4×10^6 MDA-MB-468 cells (cultured in 150 mm

dishes) were transduced with 1.2 x 10^6 TU of each pool (15.4 µL). Lentivirus was left for 6 h before replacement with complete media (DMEM with 10% FBS and 1x AA).

Two days post transduction, the expanded cells harbouring the shRNA sequences were selected with 1.5 µg/mL puromycin, maintained in 0.25 µg/mL, and immediately frozen to minimize changes in shRNA representation (> 2 x 10^6 cells per vial).

To generate the library with or without ALDH1A3 knockdown, pool 1, 2, 3 harbouring cells were thawed and cultured in 15 cm dishes. Approximately 1 x 10^7 cells per pool (in two 15 cm dishes per pool) were transduced with 5 mL of 0.45 µM filtered retrovirus pSMB scramble control shRNA or pSMB harbouring ALDH1A3 shRNA supernatants admixed 1:1 with media (10 mL total with 8 µg/mL sequabrene). 6 h post-transduction, the media was replaced. After 2 days, the expanded cells were selected with 5 µg/mL blasticidin, resulting in greater than 80% death. This confirmed that the cells were infected at < 0.3 MOI, and that 100-fold library representation had been maintained.

A1.2.3 In Vivo shRNA Screen

NOD-*scid* mice were injected with 2 x 10^6 cells in their mammary fat pads (admixed 1:1 high concentration Matrigel) of pool 1, 2 or 3 MDA-MB-468 cells (n=3). Three weeks post tumor-cell-implantation, mice were euthanized, and tumors harvested. Genomic DNA was extracted using the PureLink DNA kit (Invitrogen).

Genomic DNA was subjected to PCR with Phusion High Fidelity DNA polymerase (ThermoFisher) and the negative selection primers included with the Decode screen (RHS5339). 250-350 bp PCR products were purified using the QIAquick Gel

Extraction kit (Qiagen). 1 μg DNA from each pool was combined for a total of 3 μg per sample.

Samples were labelled with Cy3 and Cy5, hybridized to microarrays (ThermoFisher, BCA5101), scanned, and data extracted and normalized by Ambry Genetics (California, USA) following the instructions in the Decode Array kit. Fold changes for each sample were calculated and shRNAs identified which were overrepresented and underrepresented (MDA-MB-468 with atRA treatment).

A1.2.4 Lentiviral Vectors, Assembly, and Infection

Individual shRNA knockdown clones were generated from pGipZ lentiviral vectors (Dharmacon, Table A1-1). Briefly, lentivirus was assembled in HEK293T cells using a second-generation packaging system (pMD2.G, pSPAX2). Lentiviral supernatants were collected and filtered (0.44 μm) prior to being applied to MDA-MB-468 cells. MDA-MB-468 cells were cultured in the presence of lentiviral supernatant for 4 hours before replacing with complete medium. Cells were selected with 1.5 μg/mL puromycin and maintained in the presence of 0.25 μg/mL puromycin.

Table A1-1 Lentiviral vectors.

Gene Name	Vector ID
PIGX	V2LHS_174188
MEI1	V2LHS_102131
MGC33894	V2LHS_247834
UBE2L6	V2LHS_28431
SEPW1	V2LHS_278642
EPHX2	V2LHS_151434
PPP2R3A	V2LHS_39816
TRERF1	V2LHS_175495
NUAK1	V2LHS_231711
TMEM105	V2LHS_270962
RREB1	V2LHS_31951
COX7A2	V2LHS_150823
RBBP4	V2LHS_57089
SNAPC4	V2LHS_153232
CACNA1D	V2LHS_112215
SYNGR2	V2LHS_36936
DEFB123	V2LHS_39799
PCDH15	V2LHS_236681
NUPR1	V2LHS_48846
CYP26A1	V2LHS_112498
PRPF4B	V2LHS_47787
GNG3	V2LHS_21058
CACNA1C	V2LHS_112213
ENPP3	V2LHS_19973
MYB shRNA 1	V2LHS_36797
MYB shRNA 2	V2LHS_36796
MYB shRNA 3	V2LHS_36794
DICER1	V2LHS_239140
RARG	V2LHS_239272

A1.2.5 IN VITRO *PROLIFERATION ASSAYS*

2.5 x10^4 cells were seeded in six-well plates. 24 h post-seeding, live cells were counted by Trypan Blue (Invitrogen) dye exclusion. 96 h later, live cells were counted again. Growth rates were calculated relative to the 24 h cell count and the control sample.

A1.2.6 QUANTITATIVE PCR

Total RNA was extracted using Trizol reagent and the PureLink RNA kit (Invitrogen) with DNase treatment. Equal amounts of RNA were reverse-transcribed using iScript (BioRad) and quantitative real-time PCR (qPCR) was performed using gene-specific primers (Table A1-2). Standard curves for each primer set were generated, and primer efficiencies were incorporated into the CFX Manager software (Bio-Rad). mRNA expression of all samples was calculated relative to two reference genes, glyceraldehyde 3-phosphate dehydrogenase (GAPDH) and β-2-microglobulin (B2M), and an indicated control sample.

A1.2.7 STATISTICAL ANALYSES

Student's t-test was used to compare qPCR data and *in vitro* cell proliferation data. All analyses were conducted in GraphPad Prism 6.0. For all analyses, * $p < 0.05$, ** $p < 0.01$, *** $p < 0.001$.

Table A1-2 qPCR primers utilized.

Gene	Primer sequence (5'- 3')		Reference
GAPDH	F	GGAGTCAACGGATTTGGTCGTA	(Marcato et al., 2015)
	R	TTCTCCATGGTGGTGAAGAC	
B2M	F	AGGCTATCCAGCGTACTCCA	(Coyle et al., 2016)
	R	CGGATGGATGAAACCCAGACA	
PIGX	F	TGTGCACTGCCGCTATCATC	
	R	AGCCAGCTTGGTCACAAAACA	
UBE2L6	F	GCAGTGAGAACTGGAAGCCT	
	R	GCAGGGGCTCCCTGATATTC	
SEPW1	F	CCGAGTCGTTTATTGTGGCG	
	R	GCCGGGGAACTCATCTTCTAA	
EPHX2	F	ACTTCGTGCTCGTTCCTCAG	
	R	TGTCCATCTGTGTCCAGTGC	
PPP2R3A	F	GATCCCTTTGCGGTCCAGAA	
	R	TTCCTCTGCAACAAGCGTCT	
TRERF1	F	CTCTCAGGGGTTCACCAACAG	
	R	TTCCTGGGGATTTCGAGCAC	
NUAK1	F	AACTTGAAGCACCGCTACGA	
	R	CACTCGGCCAGAAAACCTCT	
RREB1	F	TGCTGGCTTCCACGACTTAG	
	R	CAGGTTTGTTTCGCACCAGG	
COX7A2	F	GGCCATTTTCGTTGGTGGTG	
	R	ACGAAGAGCCAGCAGATTCC	
RBBP4	F	GCCCGTTATATGCCCCAGAA	
	R	GGGTTGCACTCTCCAGAAGG	
SNAPC4	F	CAGCCCCCAGCCAATATGAA	
	R	GCTTCTGCAGGACTTTGGGA	
CACNA1D	F	TGGGGTCAAGCCATCTCAAAA	
	R	ACCAGCCAGTAAAACGTGACA	
SYNGR2	F	TCCATCTTCTCCTGGGGTGT	
	R	CGGAGTGGGGTCAACGTAAT	
NUPR1	F	AGAGAGAAGCTGCTGCCAAC	
	R	CCCCTCGCTTCTTCCTCTCT	
CYP26A1	F	TTCGAGGAAATGACCCGCAA	Coyle et al. (Chapter 4)
	R	CGAATGTTCTGCTCGATGCG	
GNG3	F	AGCCAGCTTGTGTCGGATAAA	
	R	GAAGGGGTTCTCCGAAGTGG	
MYB	F	ACAGATGGGCAGAAATCGCA	
	R	TTCCTGTTCGACCTTCCGAC	

Gene	Primer sequence (5'- 3')		Reference
DICER1	F	TGTGGTGTTGACACGGGAAA	
	R	GCTTCCACACAGTCCGCTAT	
RARG	F	CTGTGCGAAATGACCGGAAC	
	R	GTCTCCTGATGGGCTTTGCT	

A1.3 RESULTS

A1.3.1 GENOMIC shRNA SCREEN REVEALS NOVEL PUTATIVE EFFECTORS OF ALDH1A3 SIGNALING

We have previously demonstrated that ALDH1A3 expression in MDA-MB-468 cells suppresses tumor growth, and that the role of ALDH1A3 in TNBC is context-specific (Marcato et al., 2015). Given that the effects of ALDH1A3 cannot be completely attributed to its enzymatic production of atRA from retinal (Coyle et al., 2017b), we sought to determine the functional effectors of the anti-tumor effects of ALDH1A3 in MDA-MB-468. A genomic RNAi screen (Figure A1-1A) identified 170 barcodes enriched and 23 barcodes depleted more than 2-fold in three biological replicates (Figure A1-1B). We prioritized study of the genes targeted by the enriched barcodes as these correspond to genes which may mediate the tumor-suppressing role of ALDH1A3 in this model. The 170 enriched barcodes corresponded to 167 unique genomic identifiers (Figure A1-1C).

Notably, the list of enriched barcodes suggested that RARγ and MYB could be important transcription factors affecting the response to ALDH1A3. We identified those targets within the 167 unique identifiers which had a canonical retinoic acid response element (RARE) within 10 kb of the transcription start site (TSS), based on in silico data from Laleveé et al. (2011), and those which had a MYB-binding site. This approach led us to prioritize 23 genes for further investigation and validation (Table A1-3).

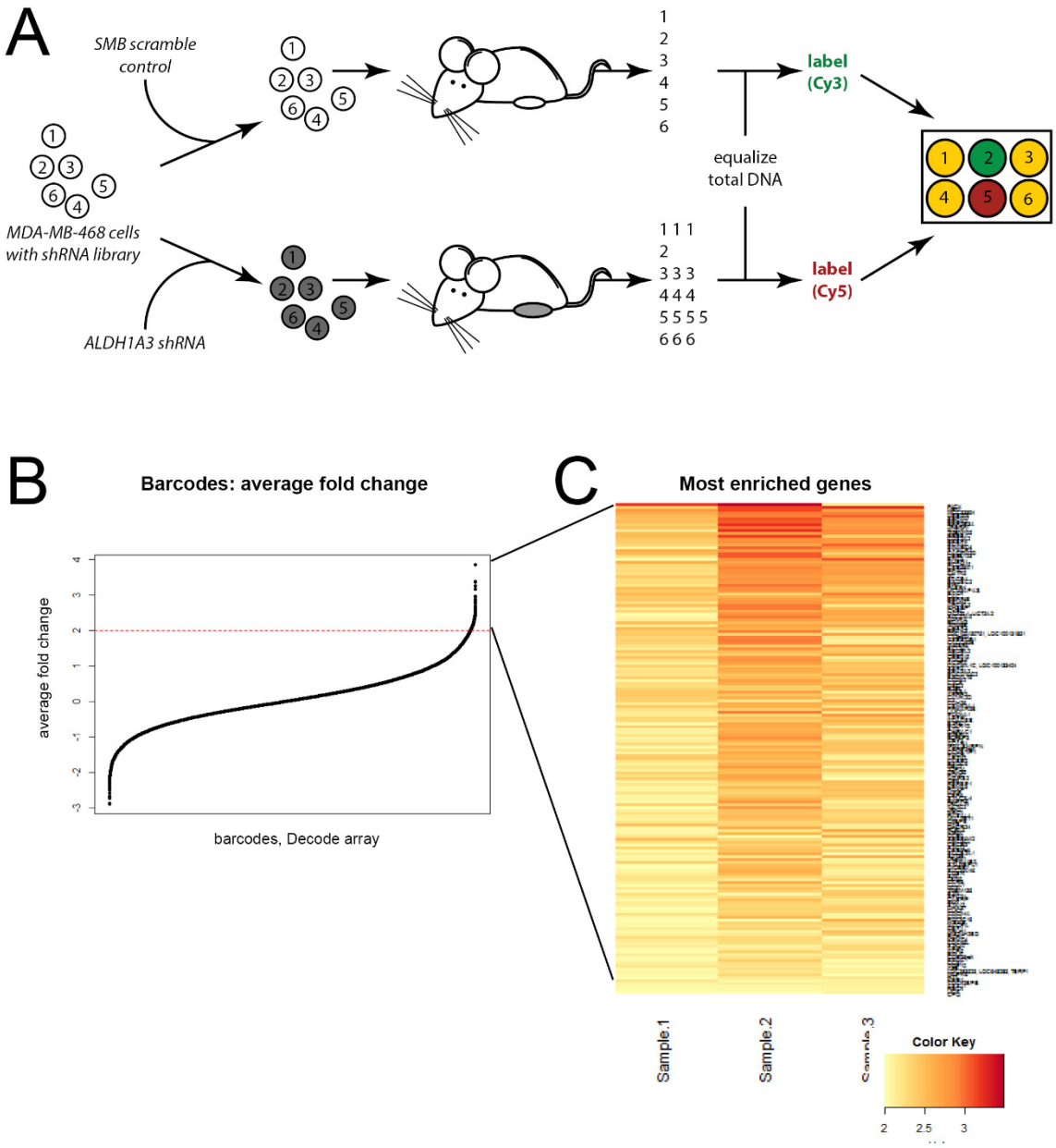

Figure A1-1 ***In vivo*** **genomic screening identifies 167 putative mediators of tumor-inhibiting effects of ALDH1A3.**

A. ALDH1A3 shRNA or control shRNA was added to lentiviral-containing MDA-MB-468 cells prior to implantation in mice; DNA was extracted, labelled, and hybridized to microarray. **B.** Average fold change between three biological replicates is plotted and **C.** individual fold-change vales for the 167 genes enriched more than 2-fold are shown.

Table A1-3: Genes prioritized for further validation.

Gene Symbol	Gene Name	Average Fold Enrichm't	Fold Enrichm't Rank	RARE Sequence	MYB binding site
PIGX	phosphatidylinositol glycan anchor biosynthesis, class X	2.95	1		
MEI1	meiosis inhibitor 1	2.93	2		X
UBE2L6	ubiquitin-conjugating enzyme E2L 6	2.84	4		
SEPW1	selenoprotein W, 1	2.83	5		
EPHX2	epoxide hydrolase 2, cytoplasmic	2.82	6		
PPP2R3A	protein phosphatase 2, regulatory subunit B, alpha	2.8	7		
TRERF1	transcriptional regulating factor 1	2.77	8	X	X
NUAK1	NUAK family, SNF1-like kinase, 1	2.75	9		X
TMEM105	transmembrane protein 105	2.75	10	X	
RREB1	ras responsive element binding protein 1	2.69	11		X
COX7A2	cytochrome c oxidase subunit	2.68	12		
RBBP4	retinoblastoma binding protein 4	2.68	13		X
SNAPC4	small nuclear RNA activating complex, polypeptide 4	2.67	14		
CACNA1D	calcium channel, voltage-dependent, L type, alpha 1D subunit	2.66	16		X
SYNGR2	synaptogyrin 2	2.65	17		
PCDH15	protocadherin-related 15	2.65	19		X
NUPR1	nuclear protein, transcriptional regulator, 1	2.65	20		
CYP26A1	cytochrome P450, family 26, subfamily A, polypeptide 1	2.63	22	X	

Gene Symbol	Gene Name	Average Fold Enrichm't	Fold Enrichm't Rank	RARE Sequence	MYB binding site
GNG3	guanine nucleotide binding protein (G protein), gamma 3	2.45	48		X
CACNA1C	calcium channel, voltage-dependent, L type, alpha 1C subunit	2.44	51		X
MYB	v-myb avian myeloblastosis viral oncogene homolog	2.30	108		
DICER1	dicer 1, ribonuclease type III	2.26	122		X
RARG	retinoic acid receptor, gamma	2.21	145		X

The discovery-oriented approach to prioritization and the nature of RNAi screening necessitated initial validation by confirming that the screen-identified shRNAs affected the expression of the target gene. We generated individual shRNA knockdown of the 23 genes listed in Table A1-3 and attempted to validate the knockdowns by gene-specific qPCR (Figure A1-2). Targets which were not significantly knocked down by the specified shRNA, or which could not be detected in control cells, were excluded from further analysis.

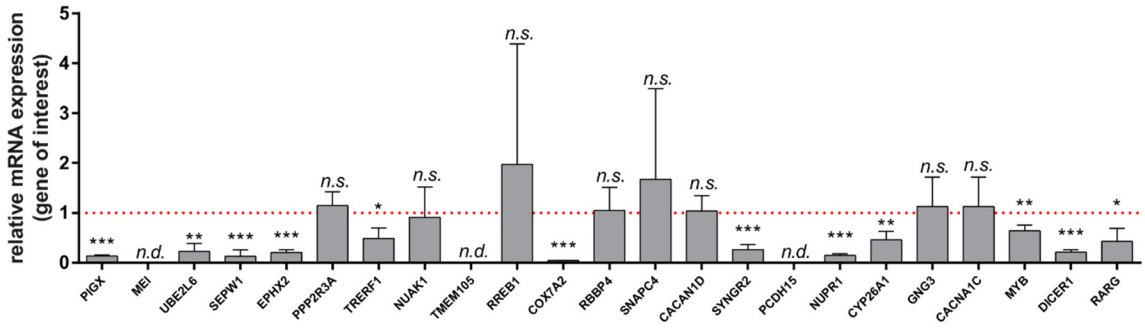

Figure A1-2 shRNA knockdowns validate barcodes identified by genomic RNAi screen.

Individual shRNA knockdowns were generated using the vectors identified in the screen. qPCR was used to determine expression of the target gene relative to pGipZ-bearing scramble control cells (n=4). Values compared to scramble control by paired student's t-test (* $p < 0.05$, ** $p < 0.01$, *** $p < 0.001$, *n.s.* not significant, *n.d.* not determined, gene expression below limit of detection).

A1.3.2 *CYP26A1, MYB, AND PIGX MEDIATE ANTI-PROLIFERATIVE EFFECTS OF ATRA* IN VITRO

After confirming the selective effects of indicated knockdowns on mRNA expression, we sought to characterize the role of these genes on the *in vitro* proliferation of MDA-MB-468 cells. Our initial work focused on wild-type (i.e. ALDH1A3-expressing) MDA-MB-468 cells. *In vitro* characterization of the shRNA knockdowns revealed important effects of CYP26A1, MYB, and PIGX on cell proliferation (Figure A1-3A). At this point, it is not clear whether these effects are ALDH1A3-dependent. Additionally, it is possible that the knockdowns which did not affect cell proliferation in this experiment have ALDH1A3-dependent effects; the role of these genes may be affected by cell-extrinsic factors not provided *in vitro*. Thus, all putative hits were carried through to further screening steps.

A1.3.3 SCREEN-IDENTIFIED EFFECTORS ARE ALTERED BY THE PRESENCE OF ATRA AND/OR ALDH1A3

We next investigated the expression of the screen-identified genes in response to atRA treatment or manipulations of ALDH1A3 expression. All candidate effectors validated in Figure A1-2 were investigated. We used qPCR to determine mRNA expression in MDA-MB-468 cells with or without atRA treatment, and with or without ALDH1A3 expression (Figure A1-3B).

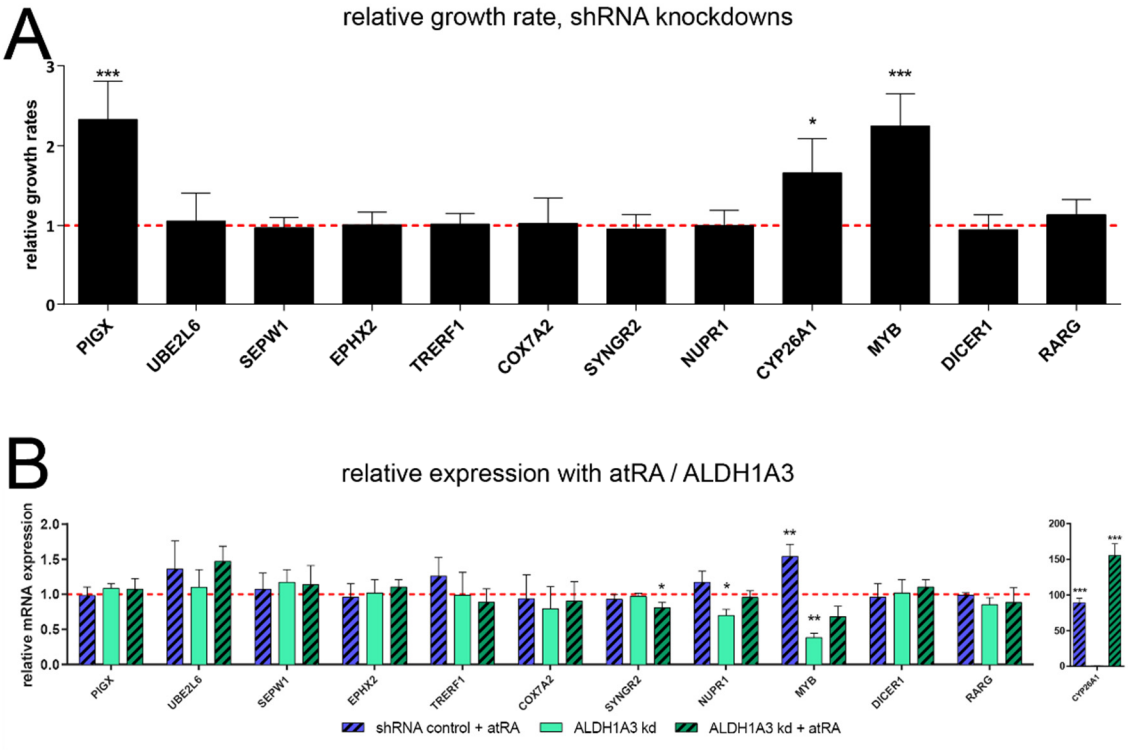

Figure A1-3 Effect of shRNA knockdown on cell proliferation.

A. The relative *in vitro* growth rate of MDA-MB-468 cells bearing single-gene shRNAs as validated in Figure A1-2 was determined. A paired student's t-test was used to compare shRNA knockdowns to scramble control (growth rate = 1, n=3. **B.** MDA-MB-468 cells with or without ALDH1A3 shRNA knockdown (kd) were treated with 100 nM atRA for 18h. qPCR was used to determine expression of the target gene relative to untreated scramble control cells. An ANOVA was used to determine statistical significance. For all comparisons, * $p < 0.05$, ** $p < 0.01$, *** $p < 0.001$.

A1.3.4 SCREEN HIT MYB IS A PUTATIVE SIGNALING HUB

Our initial prioritization (Table A1-1) focused on the presence of RAR or MYB binding sites. Our screening of the effects of atRA treatment on gene expression revealed that the presence of RARE sequences did not effectively identify atRA-inducible genes. We thus undertook a different approach to discern the role of MYB as a signaling hub in the anti-tumor effects of ALDH1A3 in the MDA-MB-468 model. Having already determined that MYB is important for cell proliferation, we generated shRNA knockdowns of MYB in MDA-MB-468 cells (Figure A1-4A) and evaluated the mRNA expression of MYB target genes TRERF1, NUAK1, RREB1, CACNA1D, GNG3, DICER1, and RARγ (Figure A1-4B). Only the expression of TRERF1 was affected by MYB knockdown.

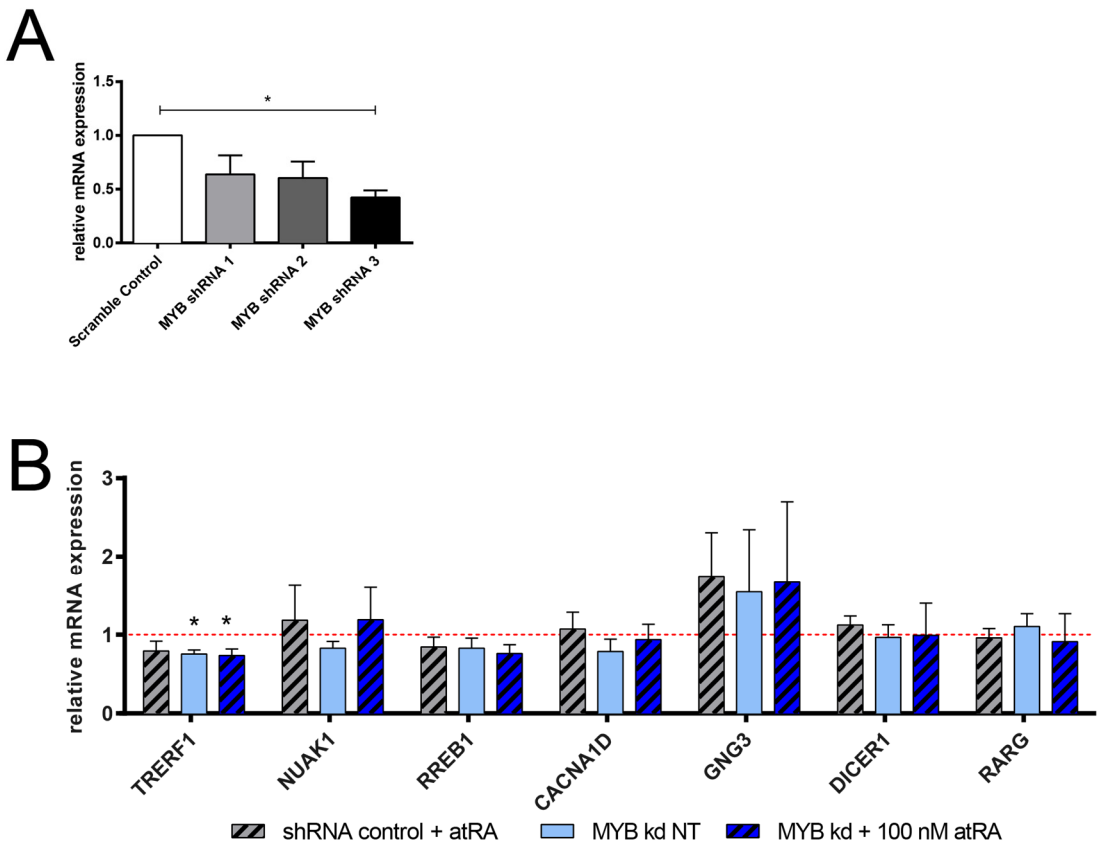

Figure A1-4 MYB knockdown affects expression of TRERF1.

A. shRNA knockdowns of MYB were generated in MDA-MB-468 cells and validated by qPCR. One-way ANOVA was used for comparisons. **B.** Scramble control and MYB shRNA-bearing cells were treated with 100 nM atRA for 18 h and gene expression of MYB target genes was determined by qPCR. For all comparisons, * $p < 0.05$.

A1.3.5 Screen-identified genes are also regulated by atRA in atRA-sensitive luminal cell lines

We have previously attributed a portion of the tumor-suppressive effects of ALDH1A3 expression in MDA-MB-468 cells to its role as a retinaldehyde dehydrogenase. While TNBC cells have been typically characterized as atRA-resistant, luminal breast cancer cells are widely thought to be sensitive to atRA treatment. We hypothesized that some of the genes identified in this genomic RNAi screen might also have important implications for the sensitivity of luminal cells to atRA. We characterized the mRNA expression of screen-identified genes in ER+ cell lines MCF-7 and T-47d by qPCR (Figure A1-5). CYP26A1 was upregulated by atRA in both cell lines. PPP2R3A and TRERF1 were both downregulated following atRA treatment, which suggests a yet-unknown mechanism for the regulation of these genes in response to atRA. The evidence from MCF-7 and T-47d suggests that the genes identified by the RNAi screening in MDA-MB-468 may be relevant to the anti-tumor effects of atRA in other cell lines; however, this requires further investigation.

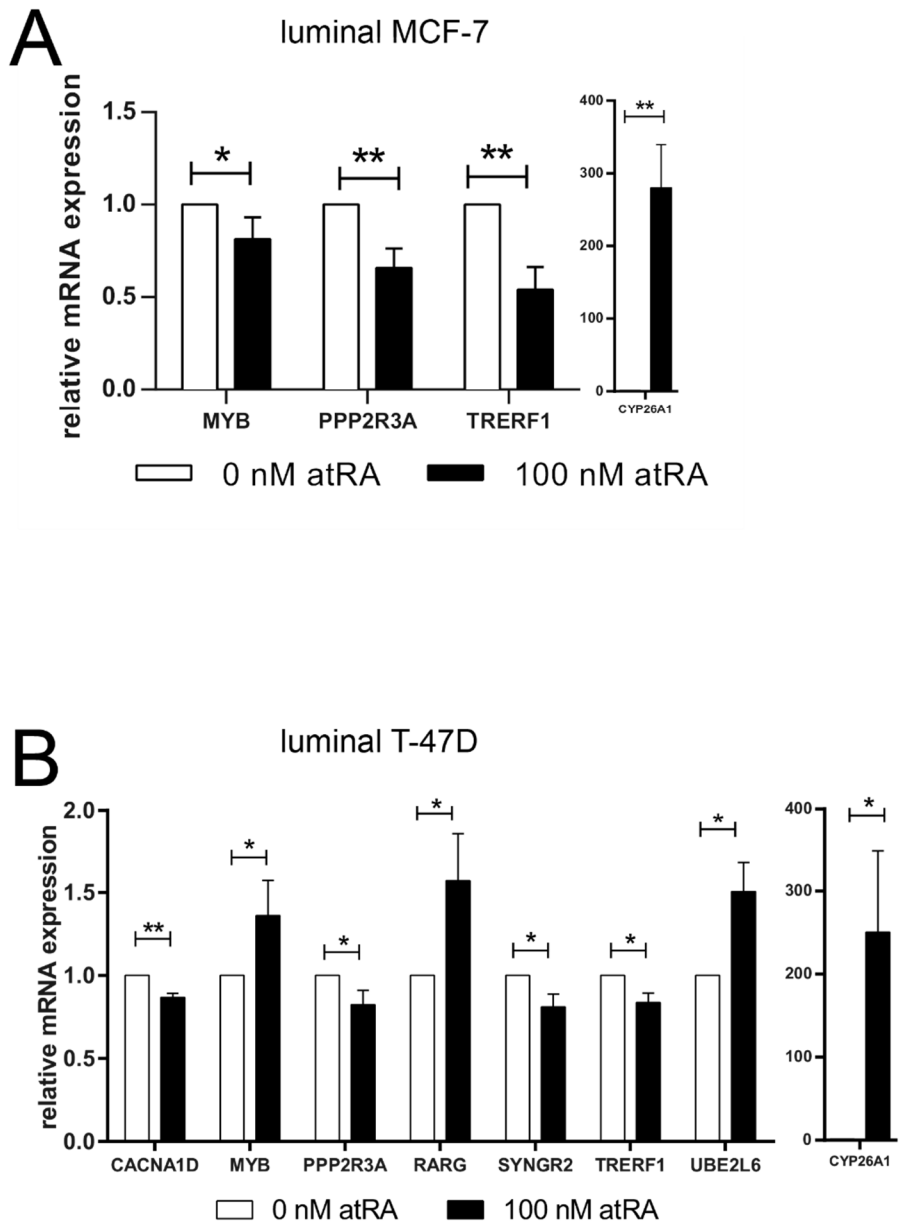

Figure A1-5 Effectors identified in MDA-MB-468 may be relevant to luminal breast cancer.

Luminal **A.** MCF-7 and **B.** T-47d cells were treated with 100 nM atRA for 18h, and expression of target genes was determined by qPCR. Values were compared by paired student's t-test, * $p < 0.05$, ** $p < 0.01$, *** $p < 0.001$.

A1.4 DISCUSSION

We utilize an *in vivo* genomic loss-of-function screen to identify novel mediators of the anti-tumor effectors of ALDH1A3. We validate a role for MYB, CYP26A1, and PIGX in the tumorigenicity of MDA-MB-468 cells, although future work will examine if these effects are ALDH1A3- or atRA-specific. In MDA-MB-468, we suggest MYB as a potential signaling hub, demonstrating that expression of MYB contributes to the expression of MYB target gene and screen hit TRERF1. Previous work has suggested that ALDH1A3 may be a direct target of MYB which supports our identified connection in this work (Yang, 2016). There are potentially other direct interactions between retinoid signaling and MYB such as between MYB and RARs (Pfitzner et al., 1998; Smarda et al., 1995). This supports a complex network of interactions which may regulate the response of TNBC cells to ALDH1A1 or atRA (as discussed in Chapter 6).

Additionally, we confirmed a role for CYP26A1 in this phenotype. CYP26A1 expression contributes to the growth of MDA-MB-468 cells, even without the exogenous application of pharmacological levels of atRA. This suggests that endogenous retinoid signaling (mediated by high endogenous expression of ALDH1A3) can contribute to the tumorigenicity of MDA-MB-468. Utilizing other cell lines with high expression of ALDH1A3 may also identify a functional role for CYP26A1 in cell growth.

This work was conducted prior to our description of largely RARE-independent responses to ALDH1A3 and atRA, thus our prioritization of genes based on the presence of classical RAREs (Table A1-3) further limited our investigations. We note that despite the identification of RAREs in several putative effectors, the mRNA expression of most genes did not change in response to atRA treatment. Genes for future investigation

include those where at least 2 shRNAs were enriched more than 2-fold: ADP ribosylation factor interacting protein 2 (ARFIP2), carbonyl reductase 4 (CBR4), and cadherin 26 (CDH26). There is evidence which supports a role for carbonyl reductases in mediating retinoid signaling (Ohkura-Hada et al., 2008), which makes this a promising screen hit for future experiments.

There are several important flaws in this work which prevent broad interpretation and limit future investigations. The composition of the lentiviral library in MDA-MB-468 cells was not assessed prior to or after the introduction of ALDH1A3 shRNA-bearing retrovirus and was not assessed prior to implantation in NOD-*scid* mice. Thus, it is impossible to determine whether representation was maintained throughout these manipulations. Given that 100-fold representation may already be insufficient to assess mechanisms of resistance or identify tumor suppressor genes and oncogenes (Gargiulo et al., 2014), this further restricted the identification of putative effectors.

Despite these limitations, we describe novel roles for MYB, PIGX, and CYP26A1 in the growth of MDA-MB-468 cells. Future *in vivo* investigation as well as manipulation of ALDH1A3 levels in concert with these shRNA knockdowns will demonstrate whether the effects of these genes are dependent on ALDH1A3 expression. Furthermore, the validation of genes associated with the depleted barcodes in this screen may identify potential mediators of intrinsic or acquired resistance to atRA. This could support the development of combination regimens for breast cancers.

A1.5 ACKNOWLEDGEMENTS

The authors acknowledge the financial and technical support of the Dalhousie Medical Research Foundation (DMRF) Olwen Dorothy Farrel Enhanced Gene Analysis and Discovery Core Facility.

Support was provided by grant funding to PM from the Canadian Institutes of Health Research (CIHR, MOP-130304), the Beatrice Hunter Cancer Research Institute (BHCRI), the Breast Cancer Society of Canada, and the QEII Health Sciences Center Foundation. KMC is supported by the BHCRI with funds provided by the Canadian Imperial Bank of Commerce, by a CGS-D award from CIHR, by the Dalhousie Medical Research Foundation, by the Nova Scotia Health Research Foundation, and by the Killam Trusts at Dalhousie University.

Appendix 2: 1379 CpG Probes Differentially Methylated in TNBC Cell Lines

CpG	Chromosome	Location	Mean β-value (sensitive)	Mean β-value (resistant / promoted)
cg18810664	10	31074367	0.9668	0.3659
cg26675876	8	11059176	0.7094	0.0587
cg06277900	16	67198029	0.9450	0.3496
cg20866694	6	27181670	0.9577	0.3319
cg20464719	19	17889512	0.9349	0.4043
cg25405984	10	31074039	0.9203	0.2970
cg16145703	8	10917024	0.5288	0.0212
cg20792895	15	23810334	0.9052	0.2306
cg04657224	8	11059038	0.4433	0.0149
cg20709110	22	19946873	0.9534	0.3948
cg11051055	8	11058145	0.7732	0.2477
cg25612391	19	19216451	0.9789	0.4911
cg05952543	15	23810378	0.8463	0.1984
cg21385746	2	105118572	0.8923	0.2796
cg27024127	8	27522576	0.8057	0.2398
cg14216285	6	28778124	0.7896	0.2772
cg25098208	11	8190659	0.8740	0.2924
cg00951395	1	232941775	0.8853	0.3284
cg22990158	14	24802150	0.8931	0.3599
cg17056069	2	9409242	0.9465	0.4186
cg04277055	4	185749877	0.9095	0.3178
cg02152120	1	118727840	0.9258	0.4704
cg02630677	8	3102222	0.8213	0.2693
cg03146452	2	234777078	0.4641	0.0171
cg17690832	4	185939537	0.4852	0.0588
cg09559047	8	10916868	0.6453	0.1160
cg16569273	6	27247725	0.8371	0.3172
cg00929798	10	135150139	0.9000	0.3588
cg06621126	16	67198243	0.9065	0.3393
cg11845785	2	105118547	0.8975	0.3230
cg16332936	22	19748910	0.8607	0.3681
cg06307939	19	12984645	0.9445	0.4277
cg26063563	5	113697330	0.3769	0.0538
cg22869818	4	182714319	0.7680	0.2533
cg00040007	15	41222276	0.4177	0.0231
cg04515667	3	89282776	0.8415	0.3121
cg22812684	1	70035392	0.7779	0.2670
cg24631970	8	11059029	0.3365	0.0211

CpG	Chromosome	Location	Mean β-value (sensitive)	Mean β-value (resistant / promoted)
cg06822340	7	147355839	0.7532	0.2224
cg17222645	3	197808017	0.4380	0.0515
cg15535638	7	31467	0.6090	0.1934
cg27025752	8	11059303	0.3635	0.0509
cg24797574	17	42988849	0.9506	0.4873
cg00799826	6	30071200	0.5636	0.0957
cg14945790	13	112980399	0.8003	0.3400
cg07099606	12	133051136	0.9344	0.4586
cg06935979	1	232941706	0.9298	0.4527
cg14866032	15	98195808	0.7563	0.2851
cg23378546	17	76352717	0.8432	0.3708
cg18584387	12	4384879	0.6851	0.2173
cg09437135	15	23810163	0.5691	0.0835
cg12621171	5	88185768	0.7817	0.2868
cg05291429	17	1494566	0.8516	0.4323
cg19242923	10	52750995	0.7680	0.2833
cg11449070	X	53449647	0.3451	0.0126
cg10856724	12	34555212	0.6574	0.2286
cg20698924	15	28344730	0.7792	0.2634
cg05209917	3	1134730	0.9272	0.4603
cg04580872	16	67198367	0.8784	0.3434
cg10144400	16	53407678	0.4035	0.0370
cg14438019	17	46702558	0.4725	0.0580
cg03811260	16	67198215	0.8541	0.3567
cg05952494	12	4378316	0.8125	0.3315
cg05314124	14	56471704	0.9143	0.4360
cg24549277	6	28778121	0.8373	0.3720
cg06624036	2	117257137	0.6134	0.1581
cg17817564	8	1312765	0.7045	0.1986
cg01078197	2	234777085	0.5313	0.0619
cg02869929	13	28527832	0.6589	0.1753
cg04153563	16	61323411	0.7955	0.2732
cg23217097	14	42074635	0.8294	0.4437
cg12294121	4	47033575	0.8173	0.3333
cg02734505	12	54763081	0.9478	0.5381
cg11859607	18	909154	0.9245	0.4998
cg18117228	1	65775772	0.3937	0.0423
cg13480357	2	219906406	0.8226	0.3662
cg14973421	1	102462821	0.7883	0.3205
cg22611504	10	52750754	0.8121	0.3207

CpG	Chromosome	Location	Mean β-value (sensitive)	Mean β-value (resistant / promoted)
cg22052659	8	114444989	0.9722	0.6684
cg21013756	2	234777080	0.4905	0.0500
cg00336164	2	219906404	0.8112	0.3569
cg14730815	5	24645147	0.6064	0.1701
cg16131766	15	23810280	0.5023	0.0817
cg17571266	12	54763211	0.9315	0.5244
cg05650846	16	3078142	0.9654	0.6153
cg05214218	17	79988749	0.3914	0.0284
cg19768950	2	182521921	0.6502	0.2159
cg00517270	15	54638342	0.6714	0.2437
cg19846991	15	72411513	0.8526	0.4740
cg13268603	7	26415606	0.6116	0.1395
cg14527639	14	79359526	0.8222	0.3855
cg09160477	9	95820913	0.3842	0.0516
cg24340926	X	129305036	0.9567	0.5958
cg23445878	12	127545350	0.7088	0.2674
cg15121364	19	40324993	0.6176	0.1825
cg05107246	7	31441	0.6137	0.2048
cg01274524	7	145280278	0.9100	0.4695
cg02380802	16	53407808	0.5815	0.1209
cg02469186	5	161277234	0.6853	0.2146
cg23543766	X	129091396	0.5304	0.1707
cg09697696	5	139488623	0.7171	0.2757
cg17831934	7	147264850	0.9373	0.5461
cg14242696	14	73361964	0.7767	0.3089
cg02026801	19	58817442	0.6220	0.1899
cg19532307	3	164912664	0.7237	0.2761
cg18690729	10	128250156	0.9336	0.5912
cg12303981	6	2244766	0.8874	0.4862
cg11125758	14	83591622	0.5830	0.1807
cg08125821	8	114445779	0.8813	0.4888
cg00611227	2	116122048	0.7205	0.2751
cg16196968	8	86976101	0.7898	0.3451
cg26664752	11	123940635	0.8926	0.4984
cg20134295	X	37031028	0.6483	0.2338
cg09840968	15	37394840	0.6933	0.2816
cg04788987	14	48096041	0.6489	0.2390
cg16617910	7	93204959	0.7060	0.2917
cg00919411	6	28584078	0.9348	0.5828
cg25303761	1	31256028	0.5478	0.1582

CpG	Chromosome	Location	Mean β-value (sensitive)	Mean β-value (resistant / promoted)
cg22020227	1	114521775	0.8193	0.3984
cg15013177	3	1134366	0.9075	0.4826
cg23855505	12	104852439	0.3301	0.0380
cg16144799	2	66892642	0.6605	0.2384
cg14291622	9	19127549	0.2370	0.0150
cg14181355	19	12984996	0.9506	0.6106
cg01365152	1	159683813	0.8053	0.3969
cg12012426	4	1366463	0.6941	0.2888
cg19923114	2	80247297	0.8465	0.4022
cg20620751	13	112979998	0.6622	0.2303
cg25745201	2	118380992	0.4962	0.0901
cg09012594	10	21464258	0.6146	0.1698
cg02487491	8	4183726	0.5256	0.1563
cg19854521	7	93520452	0.7504	0.3117
cg14331377	X	10588732	0.5607	0.1590
cg14983172	5	73244708	0.8259	0.3946
cg10209886	18	34833563	0.8631	0.4419
cg11250576	5	132386346	0.9041	0.4982
cg23257935	1	118727834	0.8442	0.4410
cg03892457	1	159157066	0.7078	0.2776
cg02353937	X	53449152	0.3055	0.0245
cg21351647	6	31081905	0.8655	0.4386
cg17594131	17	43046361	0.9090	0.5493
cg23694371	15	26967579	0.6403	0.2124
cg02756845	22	51038542	0.5921	0.2130
cg24119717	5	139488731	0.9143	0.5488
cg01443488	1	159557514	0.8593	0.4744
cg14530233	8	11059241	0.4002	0.0693
cg04080595	1	2985649	0.5557	0.1627
cg22260952	12	104852446	0.2522	0.0263
cg26279745	14	24801970	0.8477	0.4327
cg07055845	X	10588667	0.4401	0.1036
cg02217159	6	62996697	0.6186	0.2081
cg10946435	1	154843044	0.6688	0.2909
cg20769842	15	23810238	0.3782	0.0718
cg11237207	1	158911377	0.6462	0.2226
cg09558850	7	93520445	0.6567	0.2478
cg20302975	2	105468274	0.6375	0.2262
cg07749454	19	56028883	0.7790	0.3556
cg16759813	2	104988400	0.4961	0.1182

CpG	Chromosome	Location	Mean β-value (sensitive)	Mean β-value (resistant / promoted)
cg16854630	12	127348285	0.8323	0.3898
cg08268798	20	42955472	0.3417	0.0928
cg09815642	16	59602460	0.4508	0.1048
cg19457237	12	34500585	0.6722	0.2971
cg00961640	1	110933767	0.8234	0.4779
cg20187719	3	13691967	0.5714	0.2146
cg23631062	1	102462806	0.5604	0.1670
cg14293999	14	101840368	0.7076	0.3122
cg12984905	13	20692744	0.3271	0.0766
cg22745781	7	16461244	0.4325	0.1053
cg13434396	19	1508555	0.7672	0.3988
cg10318063	14	42075122	0.6161	0.2019
cg16027403	1	247978791	0.5978	0.2369
cg27349460	18	76000984	0.7852	0.4126
cg08145292	6	73867933	0.8193	0.4905
cg08230215	19	18208303	0.9344	0.6509
cg20940153	8	11059066	0.3536	0.0655
cg05278500	14	48096021	0.8174	0.4995
cg24855781	10	68688167	0.8335	0.4759
cg06707970	20	59962861	0.5078	0.1700
cg07838098	1	228872185	0.4563	0.1438
cg05836145	7	20827117	0.7795	0.3893
cg13178766	12	71113470	0.6128	0.2372
cg02515354	7	147256123	0.8684	0.5030
cg03654560	5	178266175	0.8954	0.5523
cg08681685	16	53407594	0.5528	0.1800
cg14005019	2	79220881	0.6557	0.2746
cg18121171	2	234776883	0.4544	0.0918
cg06366833	4	183710473	0.9554	0.7137
cg19556343	21	22370046	0.8459	0.4747
cg04614053	19	12250778	0.2995	0.0604
cg18492126	21	22369802	0.8822	0.5422
cg21185255	4	149763983	0.7492	0.3603
cg06792368	6	27599652	0.8888	0.5716
cg08081379	13	41496707	0.9643	0.7465
cg04493558	13	100635730	0.5113	0.1787
cg17001717	8	4439501	0.3779	0.0751
cg18112785	X	144903000	0.4497	0.1223
cg21172458	8	86350927	0.8681	0.5479
cg09039475	8	27629592	0.3994	0.0955

CpG	Chromosome	Location	Mean β-value (sensitive)	Mean β-value (resistant / promoted)
cg09052244	8	1496751	0.9257	0.6724
cg00765922	1	156626839	0.8654	0.5137
cg04431119	7	73039108	0.7599	0.4040
cg26753208	2	18569314	0.7412	0.3709
cg00578220	6	62996702	0.5464	0.2158
cg14248106	17	43046371	0.9120	0.6194
cg26810336	X	28605742	0.7490	0.3718
cg11644057	19	409408	0.3328	0.0749
cg07640648	19	39993697	0.1864	0.0403
cg23926793	6	62996664	0.5126	0.1804
cg27274426	2	86791087	0.8174	0.4637
cg23018689	1	159173540	0.7917	0.4556
cg07077665	15	37395084	0.8971	0.5938
cg00589791	5	30429329	0.4063	0.1139
cg08125031	4	21699373	0.3964	0.1159
cg04609045	11	66035544	0.4143	0.1386
cg12843448	3	193789466	0.7491	0.3994
cg13221363	2	12859103	0.3334	0.0780
cg10695325	4	81106463	0.6621	0.3076
cg12289251	10	18689471	0.5215	0.1816
cg26081071	13	20701668	0.4941	0.1881
cg04555941	4	175444268	0.3204	0.0646
cg23076370	14	107095027	0.3152	0.0621
cg06447474	16	6067747	0.7074	0.3567
cg22507354	17	62493832	0.6677	0.2872
cg22932677	19	12983876	0.5669	0.2322
cg17527484	17	62039082	0.7483	0.4180
cg07700524	16	62988282	0.3670	0.0762
cg24562465	2	105191709	0.8852	0.6000
cg22845496	15	54303927	0.7208	0.3642
cg09725439	X	23801440	0.3767	0.1080
cg13806106	8	63998228	0.3390	0.0771
cg11471354	10	52420019	0.8244	0.4804
cg14927724	8	41559608	0.6978	0.3635
cg13717684	3	111830803	0.5977	0.2767
cg13328713	7	93520527	0.5017	0.1935
cg01185766	16	6033648	0.3541	0.0975
cg03887094	16	67198826	0.8768	0.5656
cg17467752	17	38218738	0.3880	0.1281
cg00881894	2	166930521	0.8322	0.5191

CpG	Chromosome	Location	Mean β-value (sensitive)	Mean β-value (resistant / promoted)
cg03588460	10	89623442	0.2125	0.0375
cg13321688	3	125120406	0.7502	0.4112
cg07588442	11	60673866	0.2030	0.0451
cg11648471	X	14891001	0.3273	0.0885
cg11279021	7	14028690	0.4644	0.1661
cg25724246	3	190595776	0.8160	0.5083
cg11654553	13	22248917	0.2931	0.0645
cg02069150	12	9556998	0.8997	0.6374
cg09877299	X	34149485	0.8389	0.5183
cg02836020	3	183145946	0.1618	0.0358
cg19722082	5	83681563	0.8681	0.5682
cg04818845	1	6580167	0.4973	0.1805
cg04586722	21	26734336	0.9041	0.7099
cg10810847	19	47950499	0.5376	0.2320
cg02172018	4	46390832	0.3164	0.0907
cg22807241	7	147709862	0.5393	0.2344
cg09667379	3	21447501	0.9315	0.7233
cg17083099	2	42007901	0.5906	0.2784
cg21125207	15	22547896	0.8226	0.5287
cg21650765	19	9434433	0.4511	0.1749
cg00295948	9	124261807	0.3476	0.1018
cg20464732	8	111073225	0.6804	0.3750
cg22927247	8	86351195	0.9032	0.6801
cg22122603	2	60797006	0.5739	0.2713
cg27046052	15	23810652	0.2739	0.0816
cg01726287	14	93812936	0.6108	0.2967
cg22238923	2	74781587	0.3730	0.1203
cg26297688	12	107349093	0.2843	0.0930
cg15777553	12	34493996	0.3039	0.0980
cg03082821	6	138785451	0.8880	0.6453
cg10314139	10	71560231	0.7984	0.5410
cg10130811	11	66277720	0.7301	0.4334
cg18193230	2	118381179	0.4682	0.1866
cg26690414	1	154528408	0.8704	0.6124
cg01768395	16	13873833	0.5573	0.2630
cg09696486	16	7270014	0.4529	0.1854
cg05149617	16	30033242	0.2433	0.0637
cg12726014	13	57484467	0.9161	0.7187
cg07278153	16	87524192	0.8044	0.5243
cg17423207	19	17958892	0.7590	0.4848

CpG	Chromosome	Location	Mean β-value (sensitive)	Mean β-value (resistant / promoted)
cg21462596	19	843995	0.3728	0.1317
cg15879316	22	46934089	0.1822	0.0481
cg04296578	1	45671659	0.1104	0.0236
cg12031217	17	63133186	0.5196	0.2405
cg04288999	2	66667852	0.8833	0.6649
cg13704629	14	73396469	0.5554	0.2838
cg13325417	1	9161644	0.9272	0.7590
cg05446414	11	71710982	0.7585	0.4783
cg17181476	1	16871838	0.9013	0.7174
cg20344434	11	20385170	0.1236	0.0261
cg20997159	9	139559897	0.3159	0.1075
cg19006211	2	116183919	0.3031	0.1151
cg15029285	X	45060311	0.9087	0.7340
cg16523643	15	37395171	0.7917	0.5394
cg23602533	8	63998164	0.2711	0.0938
cg27340648	8	3254739	0.2348	0.0813
cg06830800	18	21167517	0.5638	0.3025
cg16799188	13	20692766	0.3534	0.1435
cg17173639	6	162384350	0.8895	0.6951
cg03284440	1	245318734	0.2104	0.0684
cg25423416	22	46934860	0.2644	0.0959
cg04084348	10	75677011	0.8080	0.5896
cg27562595	7	146603166	0.8644	0.7153
cg18112117	8	101965903	0.2316	0.0976
cg19865561	6	31465898	0.1051	0.0258
cg05865202	20	36156789	0.1110	0.0395
cg13666267	2	232317487	0.8750	0.6974
cg21106136	3	194405973	0.8468	0.6494
cg18051798	12	51453432	0.9016	0.7581
cg24839145	8	5028854	0.8510	0.6368
cg23689426	10	44167053	0.8588	0.6560
cg17489897	10	89623432	0.1939	0.0637
cg13897627	16	49378497	0.1901	0.0646
cg03157610	6	33377317	0.9208	0.7828
cg16260700	11	62414786	0.9038	0.7451
cg26968387	19	37569268	0.0868	0.0280
cg10447095	16	60678710	0.2848	0.1228
cg02471760	11	569587	0.6964	0.4746
cg10999157	7	74020711	0.4219	0.2143
cg04420141	17	63133231	0.2259	0.0984

CpG	Chromosome	Location	Mean β-value (sensitive)	Mean β-value (resistant / promoted)
cg02653364	16	58283706	0.1158	0.0414
cg22792461	10	97850322	0.5266	0.2953
cg24762359	13	25254447	0.2833	0.1254
cg17787710	17	79989039	0.3010	0.1281
cg05263649	11	63916644	0.9270	0.8141
cg18473234	19	5097819	0.9299	0.8122
cg04236329	5	443585	0.0486	0.0179
cg02243665	8	146013792	0.7888	0.5993
cg03041532	11	71711021	0.9143	0.7939
cg15912040	3	113871809	0.1836	0.0770
cg18542377	19	4172961	0.2594	0.1129
cg14851700	1	182362230	0.8687	0.7086
cg01192572	2	234372854	0.8990	0.7821
cg10533624	12	3143428	0.6201	0.4150
cg15564240	11	20385176	0.0487	0.0180
cg23497016	2	66666684	0.9548	0.8909
cg08029909	5	176245078	0.1377	0.0631
cg10052368	12	48163063	0.8415	0.6968
cg07565150	14	69244243	0.8220	0.6644
cg19773547	2	216252792	0.8780	0.7603
cg17024944	6	74443302	0.6081	0.4134
cg14033737	3	162129530	0.7331	0.5672
cg27640302	11	57296133	0.8010	0.6452
cg04948014	12	120241494	0.8916	0.7911
cg06329807	16	68554737	0.0732	0.0343
cg07228441	8	681215	0.0607	0.0306
cg04852280	1	26496234	0.0521	0.0225
cg14724364	11	17410554	0.0598	0.0288
cg18045461	22	29601862	0.0617	0.0311
cg00397059	6	132031294	0.7699	0.6250
cg20382626	1	85156797	0.1593	0.0821
cg26087862	1	150602029	0.3264	0.2003
cg23604683	7	75779470	0.5897	0.7415
cg21613754	2	219133847	0.8396	0.9148
cg04025307	7	1156635	0.7298	0.8430
cg08311803	2	231854570	0.9286	0.9655
cg03435488	2	131591344	0.7245	0.8454
cg23676151	6	108491372	0.8605	0.9309
cg12204262	20	1249928	0.8747	0.9401
cg09033219	17	73714598	0.8321	0.9169

CpG	Chromosome	Location	Mean β-value (sensitive)	Mean β-value (resistant / promoted)
cg16576052	14	68038799	0.8129	0.9073
cg11100450	6	513211	0.8803	0.9433
cg21229954	17	5076857	0.8045	0.9030
cg01797043	16	2004686	0.4242	0.6126
cg00266389	11	2867748	0.8678	0.9401
cg04704247	4	1672920	0.9262	0.9677
cg01757548	6	170730413	0.8538	0.9344
cg09575542	17	48704296	0.4399	0.6325
cg20996561	22	40082316	0.9224	0.9685
cg02398342	17	80708632	0.8682	0.9453
cg07058234	17	159236	0.5506	0.7302
cg14204241	9	128167459	0.7539	0.8863
cg05131771	10	3446995	0.8303	0.9256
cg08649501	3	41997107	0.8059	0.9125
cg02095530	6	88105544	0.8166	0.9232
cg10623213	3	69070440	0.6431	0.8183
cg21441674	8	56805218	0.7524	0.8823
cg13444392	4	1608283	0.7711	0.8988
cg00455747	18	8659509	0.6862	0.8431
cg04609959	16	88980609	0.8708	0.9472
cg26113593	5	1001881	0.5235	0.7201
cg03471150	1	201797198	0.6961	0.8498
cg07793724	1	53609371	0.7821	0.8957
cg19735533	2	241196887	0.8469	0.9377
cg09744243	10	70653884	0.5861	0.7740
cg09624942	20	25584456	0.6713	0.8427
cg12053891	11	62168512	0.2374	0.4427
cg27607838	17	29728	0.3941	0.6110
cg26916607	16	56994770	0.7489	0.8859
cg07605410	1	16828163	0.7858	0.9061
cg16871667	6	32025975	0.9021	0.9656
cg02141929	16	56681544	0.5635	0.7700
cg04691634	11	69625284	0.8981	0.9633
cg00360866	15	65627661	0.6905	0.8517
cg06203137	6	169965255	0.9077	0.9687
cg13978447	11	1764985	0.7188	0.8782
cg13492520	7	73012206	0.8149	0.9266
cg27347104	12	6233657	0.7074	0.8584
cg03396896	3	194117107	0.5590	0.7682
cg26815396	6	34495393	0.6131	0.7940

CpG	Chromosome	Location	Mean β-value (sensitive)	Mean β-value (resistant / promoted)
cg11404380	4	41215359	0.0512	0.1376
cg07631407	6	43243961	0.7384	0.8870
cg07955741	1	16821502	0.7959	0.9173
cg04841337	3	194782915	0.6529	0.8329
cg06339396	16	57736130	0.9028	0.9654
cg15307777	11	130271767	0.7543	0.8898
cg24623694	19	40919760	0.3457	0.5646
cg26368842	10	23004020	0.6807	0.8379
cg06051213	10	121085229	0.8309	0.9337
cg03870234	12	133118683	0.6761	0.8538
cg15798873	8	67417740	0.9223	0.9746
cg10264354	6	129505619	0.7727	0.9098
cg03096732	17	6946527	0.2696	0.4898
cg14898433	11	1629936	0.6386	0.8180
cg19322788	12	125831167	0.0747	0.1907
cg14426785	9	101876671	0.7804	0.9163
cg26697650	18	57637908	0.7822	0.9150
cg18276808	11	1086863	0.8069	0.9237
cg20099906	19	13344820	0.6523	0.8348
cg01084635	7	1975411	0.6778	0.8562
cg09822291	1	28560027	0.7333	0.8887
cg09115960	16	1481278	0.7329	0.8908
cg00855396	16	87705655	0.8242	0.9419
cg13566141	9	132050607	0.7455	0.8961
cg14832183	7	72413540	0.7877	0.9171
cg04475193	5	132303723	0.7809	0.9198
cg25104437	2	45170725	0.6589	0.8491
cg22622183	5	1640178	0.6907	0.8731
cg26330321	19	39236571	0.7744	0.9064
cg26973177	16	56898967	0.6935	0.8511
cg15837280	5	135415258	0.6034	0.8062
cg07474672	6	90142171	0.8217	0.9379
cg02572606	16	20753499	0.7732	0.9082
cg06106633	6	73969316	0.7976	0.9300
cg16294620	20	13280181	0.7993	0.9260
cg22656544	11	1893975	0.7570	0.9063
cg12529917	7	6889129	0.3077	0.5447
cg13935206	15	99752192	0.7028	0.8798
cg03384959	2	238305427	0.6794	0.8638
cg27301280	3	194783348	0.6158	0.8218

CpG	Chromosome	Location	Mean β-value (sensitive)	Mean β-value (resistant / promoted)
cg13027184	17	1657448	0.6778	0.8514
cg06964595	11	1665238	0.5579	0.7843
cg13710542	9	140261971	0.7416	0.8970
cg03536654	22	31688645	0.0836	0.2285
cg05921260	6	28484915	0.0616	0.1803
cg26241863	8	145849419	0.7717	0.9149
cg12958891	4	7706547	0.7237	0.8900
cg14124376	20	24987139	0.7673	0.9099
cg15259920	17	73997287	0.4680	0.7102
cg21021110	4	1625732	0.7335	0.8969
cg08584665	7	23471813	0.7617	0.9177
cg26570776	15	101690228	0.7578	0.9033
cg03282543	16	84065224	0.6880	0.8651
cg07942497	10	15037403	0.6301	0.8386
cg15915028	1	27528084	0.6603	0.8617
cg26158150	8	10448863	0.2432	0.4503
cg14635466	8	101661245	0.7063	0.8672
cg04489573	1	26394009	0.7576	0.9079
cg02335306	11	2559880	0.8406	0.9523
cg15233961	10	96990543	0.7567	0.9134
cg20624953	19	38344455	0.7584	0.9118
cg26003993	7	1866358	0.7103	0.8890
cg15314212	14	90094328	0.8043	0.9388
cg18539988	16	14926152	0.6188	0.8367
cg20493283	17	48912164	0.8017	0.9388
cg06050631	6	140098850	0.7333	0.9008
cg04528054	8	145955016	0.7906	0.9254
cg14210632	14	93155030	0.7322	0.8956
cg23835453	12	53646929	0.7383	0.8856
cg27038480	21	38374377	0.6852	0.8776
cg02517711	2	26700914	0.1533	0.3381
cg11596779	5	77188947	0.7637	0.9104
cg00241002	10	26931912	0.0498	0.1533
cg02641844	17	72913966	0.7070	0.8890
cg21277505	19	50978348	0.8125	0.9334
cg27588093	1	3276413	0.1227	0.3084
cg01671212	14	23981341	0.2795	0.5307
cg18824596	6	32972970	0.7145	0.8897
cg10244525	2	237146748	0.6867	0.8709
cg13607082	12	122652224	0.7338	0.8953

CpG	Chromosome	Location	Mean β-value (sensitive)	Mean β-value (resistant / promoted)
cg26211724	18	57636670	0.7742	0.9218
cg13427828	3	42301921	0.7226	0.9022
cg21446981	7	37534909	0.0837	0.2225
cg03327494	3	195938048	0.8116	0.9416
cg00985040	6	37553208	0.3962	0.6604
cg16515815	1	3522768	0.7233	0.9036
cg05664061	2	233256979	0.7723	0.9306
cg13608979	9	101871229	0.7358	0.9020
cg03069267	9	134699490	0.1649	0.3842
cg22850258	7	16438702	0.6851	0.8853
cg25968469	10	49687287	0.7482	0.9193
cg17529235	17	21451571	0.4414	0.7010
cg10215414	16	67361708	0.5094	0.7548
cg25013838	22	26137524	0.7325	0.9046
cg15931168	5	72528678	0.7979	0.9320
cg04663194	11	66315239	0.7193	0.9031
cg00912164	12	133020327	0.7806	0.9291
cg21911490	3	194909350	0.7964	0.9204
cg05879527	1	35333886	0.7778	0.9329
cg07585610	6	46656612	0.7781	0.9198
cg25114855	2	113465072	0.8005	0.9416
cg02475539	2	10665802	0.4549	0.7174
cg22203829	12	65155719	0.7432	0.9093
cg09576978	8	41554080	0.7169	0.9011
cg12146447	17	47926239	0.7257	0.9113
cg15584792	3	44763977	0.5136	0.7663
cg23284338	10	73569605	0.7615	0.9218
cg16296417	8	126285443	0.0712	0.2128
cg20224991	7	65511110	0.7260	0.9113
cg05286724	X	49159887	0.1733	0.4008
cg25599012	19	39827384	0.6806	0.8887
cg23586959	20	30073209	0.2754	0.5330
cg17404787	1	3340625	0.6899	0.8901
cg10316527	15	82242305	0.1348	0.3371
cg15142913	8	142440250	0.6881	0.8742
cg12387865	1	16942481	0.6723	0.8744
cg04944527	18	12068065	0.4871	0.7494
cg18865257	1	204329775	0.4878	0.7418
cg14667799	17	17253104	0.7670	0.9250
cg12107580	8	142431437	0.6658	0.8805

CpG	Chromosome	Location	Mean β-value (sensitive)	Mean β-value (resistant / promoted)
cg20098420	22	51155589	0.7990	0.9453
cg09512406	16	609103	0.6397	0.8644
cg00917181	17	76925901	0.5400	0.7997
cg14349956	15	74637483	0.7713	0.9278
cg06798483	3	98504973	0.5830	0.8337
cg11888270	10	113941466	0.5782	0.8293
cg22614518	7	77492522	0.7255	0.9161
cg03302135	20	61040825	0.5383	0.7992
cg18552983	2	237128101	0.7440	0.9120
cg25316120	2	106986197	0.6346	0.8515
cg12235877	12	323392	0.1673	0.3792
cg05347613	9	101748082	0.7003	0.8929
cg18982066	11	67407195	0.4077	0.6786
cg06836872	16	1447994	0.5652	0.8096
cg17756131	12	133059921	0.6447	0.8551
cg03489965	15	65368982	0.7622	0.9249
cg16189817	22	22093983	0.7286	0.9118
cg18803251	4	7374622	0.7739	0.9394
cg08469540	1	948627	0.0505	0.1310
cg07467199	5	14874832	0.7405	0.9104
cg24832721	11	70023142	0.6041	0.8453
cg21239997	2	24398519	0.3376	0.6215
cg03062454	21	30362034	0.7760	0.9404
cg22158051	5	143172092	0.6619	0.8550
cg00279529	X	153523467	0.7352	0.9169
cg16469307	11	69612825	0.6654	0.8829
cg16293569	11	2870208	0.2129	0.4427
cg26550330	1	228396009	0.6547	0.8749
cg07766916	16	88853845	0.7418	0.9280
cg04480665	8	142439791	0.6217	0.8362
cg06116594	X	70180220	0.0502	0.1859
cg24006770	1	92056542	0.6760	0.8922
cg10109943	17	52563	0.6363	0.8679
cg01619107	12	52515354	0.5488	0.8179
cg27178922	1	213476578	0.6095	0.8396
cg03560973	2	25390400	0.7143	0.9117
cg22355506	19	3773230	0.6557	0.8821
cg03536289	14	94443120	0.4761	0.7543
cg02347105	16	21557425	0.8613	0.9608
cg04970064	17	266066	0.5029	0.7826

CpG	Chromosome	Location	Mean β-value (sensitive)	Mean β-value (resistant / promoted)
cg21604450	1	66998563	0.4709	0.7381
cg05128056	15	100911974	0.5750	0.8205
cg13647536	7	27260466	0.7437	0.9267
cg02570888	1	225864873	0.7460	0.9189
cg02141208	10	81320623	0.1641	0.3874
cg09787580	7	140227335	0.3562	0.6411
cg25799059	3	45134300	0.7665	0.9264
cg04678570	10	3280494	0.7521	0.9311
cg15577126	2	218932178	0.0992	0.2768
cg08155994	19	2388502	0.7636	0.9299
cg08009313	3	130682432	0.2524	0.5248
cg04095810	15	57668087	0.7811	0.9349
cg14989988	7	105319819	0.7618	0.9298
cg08846959	2	10666713	0.4362	0.7308
cg27369328	4	1638220	0.7766	0.9407
cg26974318	16	88760471	0.8653	0.9668
cg10306247	6	28108608	0.7369	0.9216
cg03369432	5	179442399	0.6011	0.8475
cg04251828	16	75252744	0.6891	0.8888
cg00063748	1	3352986	0.2462	0.5142
cg15805490	19	3503113	0.4131	0.7056
cg16875554	12	6897731	0.7476	0.9284
cg21041579	14	95907997	0.2648	0.5300
cg12852407	13	22613841	0.1963	0.4681
cg18498565	10	3173604	0.6933	0.8947
cg23035597	1	1063527	0.6168	0.8469
cg05933789	2	97190408	0.7254	0.9185
cg22496996	6	27471291	0.0908	0.2928
cg25459301	8	10941183	0.6779	0.8920
cg24709511	1	2251570	0.8409	0.9579
cg06551661	2	10691849	0.7238	0.9136
cg00187981	8	142984613	0.7448	0.9310
cg23913904	11	70590130	0.6750	0.8902
cg03632245	5	72590921	0.5600	0.8236
cg14321837	2	106812100	0.7419	0.9351
cg01840740	21	45705175	0.7010	0.9057
cg12115928	15	45248806	0.6078	0.8443
cg19526076	13	74713082	0.4415	0.7186
cg07882302	16	87948277	0.2463	0.5071
cg02082342	11	124622373	0.6420	0.8784

CpG	Chromosome	Location	Mean β-value (sensitive)	Mean β-value (resistant / promoted)
cg02276263	15	40781779	0.5014	0.7664
cg23460851	4	1604456	0.7714	0.9403
cg11288260	13	100117058	0.4343	0.7271
cg21691753	13	114321595	0.5230	0.8032
cg10224783	7	138413359	0.7575	0.9284
cg15772157	10	22766320	0.5557	0.8105
cg13569868	14	89734827	0.7171	0.9155
cg09002677	17	5999	0.9017	0.9779
cg21570811	4	3362574	0.7004	0.8958
cg24944959	8	142445786	0.8750	0.9758
cg12439130	22	21714051	0.5362	0.7964
cg20790618	X	128978347	0.1856	0.4465
cg23564309	21	45582448	0.7266	0.9230
cg10832938	2	45170365	0.6190	0.8749
cg11938738	6	134999799	0.6820	0.8908
cg02582912	20	62421950	0.7560	0.9264
cg25413347	7	44279938	0.7741	0.9487
cg23682879	8	124836410	0.6583	0.8760
cg14028829	20	62422127	0.7115	0.8941
cg04036070	16	53957219	0.7238	0.9200
cg14001748	15	31093040	0.4222	0.7126
cg12268531	1	92102055	0.6695	0.9029
cg08627621	X	74965938	0.4469	0.7373
cg07158881	17	49227858	0.7109	0.9195
cg17860198	3	5138170	0.5555	0.8089
cg15678513	8	142431934	0.5734	0.8316
cg03882270	4	3384736	0.7262	0.9210
cg00537709	16	89320298	0.7118	0.9202
cg03334307	16	58234168	0.6805	0.8973
cg19879906	19	16392219	0.5373	0.8121
cg23032184	2	121523682	0.8415	0.9653
cg14290040	9	133866498	0.3411	0.6504
cg24629455	1	3163970	0.6653	0.8984
cg23246911	17	154671	0.6749	0.9042
cg01373319	7	72711913	0.6606	0.8799
cg14143574	9	127247660	0.8563	0.9696
cg03436722	7	1643298	0.4587	0.7703
cg14443472	9	129266352	0.5634	0.8533
cg19835040	3	46538742	0.7298	0.9310
cg11259254	10	52366029	0.4982	0.7826

CpG	Chromosome	Location	Mean β-value (sensitive)	Mean β-value (resistant / promoted)
cg09936845	1	156849818	0.9014	0.9795
cg03004270	14	65747480	0.6637	0.9027
cg00953069	1	155991941	0.7535	0.9380
cg22468055	3	122334227	0.1283	0.3767
cg26745520	10	121108997	0.7019	0.9134
cg12267069	1	156407809	0.2989	0.5965
cg00808132	14	23511306	0.6585	0.8956
cg26529044	13	43354767	0.0818	0.2512
cg24312879	1	6422118	0.5475	0.8249
cg01931792	2	20211771	0.4805	0.7620
cg16127759	1	110613596	0.2956	0.5971
cg08100284	17	35242990	0.5412	0.8266
cg21330313	7	44259047	0.8541	0.9713
cg13523731	17	76607622	0.6163	0.8635
cg14429381	9	103342099	0.5928	0.8293
cg15949553	5	141879669	0.5259	0.7906
cg25683570	1	203051472	0.6174	0.8680
cg09725286	8	134419335	0.4141	0.7118
cg07390459	2	121582002	0.4730	0.7751
cg10648197	10	22634578	0.6274	0.8857
cg03988297	1	219060547	0.5253	0.7880
cg12073083	14	89749549	0.6686	0.8949
cg18169835	10	134612155	0.5502	0.8429
cg27534424	8	10966224	0.7154	0.9272
cg21865844	11	69661197	0.5806	0.8572
cg04279801	17	19314319	0.6073	0.8794
cg24767237	5	172662724	0.4826	0.7764
cg21245300	7	155675943	0.2145	0.4944
cg23034437	10	92912529	0.2930	0.6069
cg15725989	17	35098710	0.5884	0.8640
cg16308540	8	101017845	0.7103	0.9087
cg13104880	7	155790512	0.5522	0.8345
cg08332866	17	35017916	0.6856	0.9038
cg24345184	22	19751899	0.6062	0.8760
cg18284022	20	2676474	0.6616	0.8989
cg16974832	2	238188707	0.6170	0.8732
cg05292376	17	79095236	0.6309	0.8886
cg13474090	9	92027541	0.6995	0.9202
cg26219458	14	95916220	0.6759	0.9098
cg19971102	14	100135277	0.3213	0.6277

CpG	Chromosome	Location	Mean β-value (sensitive)	Mean β-value (resistant / promoted)
cg01381130	8	142431473	0.5709	0.8437
cg27305939	1	2285115	0.6605	0.9020
cg12267497	8	11053804	0.6527	0.8955
cg04598224	19	11784514	0.4448	0.7534
cg01082602	1	7726441	0.2893	0.6031
cg09585974	10	31076192	0.7151	0.9279
cg02049180	1	156828202	0.7270	0.9221
cg01694331	12	109273766	0.5532	0.8433
cg17775003	20	33562606	0.2447	0.5232
cg20325547	1	9431594	0.6843	0.9230
cg26992949	5	13919339	0.5493	0.8185
cg25051134	2	181938260	0.5864	0.8656
cg26925688	19	4303957	0.3698	0.6772
cg03779097	20	62727043	0.2007	0.4853
cg24844971	15	70127556	0.3819	0.6930
cg07378067	14	103388859	0.6070	0.8695
cg21203984	5	92549171	0.6645	0.9099
cg06071058	9	96716091	0.7499	0.9469
cg10861390	14	94442922	0.3270	0.6365
cg21843586	11	2397201	0.6283	0.8876
cg19869037	6	116732515	0.4557	0.7572
cg26261563	4	8372758	0.5961	0.8714
cg14074284	17	48912075	0.5929	0.8640
cg12641135	10	15055196	0.6547	0.8948
cg19388050	11	2562647	0.6624	0.9138
cg27649037	8	53322510	0.6169	0.8454
cg10729312	5	140289	0.6026	0.8691
cg04145539	3	46618527	0.7372	0.9344
cg18190433	17	10573397	0.5358	0.8202
cg05040232	3	194117403	0.5271	0.8141
cg16678522	20	32149963	0.0805	0.2764
cg16527444	7	138364464	0.6220	0.8781
cg23141914	3	125900824	0.6825	0.9138
cg05759166	8	10452896	0.7661	0.9470
cg10658438	3	194117018	0.7410	0.9301
cg17463527	20	42187837	0.5778	0.8564
cg00528351	7	44348318	0.7301	0.9292
cg05743883	8	142277447	0.6428	0.8917
cg25313698	12	133182638	0.4860	0.7813
cg11964358	11	69499059	0.6811	0.9154

CpG	Chromosome	Location	Mean β-value (sensitive)	Mean β-value (resistant / promoted)
cg07978996	1	2288299	0.6566	0.8927
cg26468878	5	112501418	0.6308	0.9038
cg18247090	13	30062835	0.4338	0.7421
cg25019707	11	69994152	0.7146	0.9235
cg15150248	7	111380914	0.6166	0.8779
cg23306526	2	45171583	0.3806	0.7015
cg05911990	7	112063449	0.6500	0.8761
cg02002258	2	26700976	0.1790	0.4491
cg18200389	6	30170340	0.6671	0.9010
cg03901836	2	232456624	0.5990	0.8806
cg23592735	6	56357077	0.7257	0.9433
cg16365421	2	121523609	0.5650	0.8413
cg25362648	12	109273780	0.5146	0.8361
cg15551981	8	28552181	0.3842	0.6904
cg06772671	16	85123778	0.6712	0.9146
cg07465602	20	44830440	0.6445	0.8857
cg11213983	17	63652954	0.3328	0.6532
cg16072661	14	21058422	0.4454	0.7543
cg24365121	11	1860114	0.5369	0.8277
cg11852218	2	105859083	0.5216	0.8221
cg04106633	4	1044584	0.6001	0.8586
cg17894008	17	59668604	0.4843	0.7805
cg25388451	7	111784478	0.6122	0.8703
cg13694662	9	140214551	0.6445	0.9062
cg14818812	8	142362180	0.5494	0.8311
cg14518098	9	135085065	0.4958	0.7973
cg15734436	6	33047185	0.3677	0.6882
cg08556107	5	429891	0.3983	0.7117
cg08931849	3	138174025	0.5969	0.8674
cg26792948	16	25115092	0.4428	0.7669
cg26321066	3	183769987	0.4851	0.7750
cg17593342	6	14037614	0.6501	0.8987
cg04986567	9	128776861	0.5162	0.8128
cg18062860	2	224866636	0.5440	0.8474
cg09649266	2	88583529	0.3576	0.6810
cg09438605	15	80757169	0.5869	0.8484
cg02947498	14	90139566	0.3769	0.6913
cg25389863	8	130492175	0.6307	0.8666
cg10982280	1	40238140	0.5806	0.8714
cg15163151	8	100906373	0.4328	0.7473

CpG	Chromosome	Location	Mean β-value (sensitive)	Mean β-value (resistant / promoted)
cg03622314	15	50838905	0.6943	0.9330
cg20090561	3	185704268	0.6011	0.8499
cg22643918	X	119078200	0.3307	0.6855
cg23873525	10	103070221	0.2535	0.5918
cg08971041	16	87911340	0.7339	0.9415
cg08096812	8	142440046	0.8593	0.9653
cg08426962	5	94076140	0.0787	0.3029
cg06979726	16	84851070	0.6245	0.8918
cg01593969	14	23851239	0.1165	0.3501
cg03838714	10	125996372	0.2843	0.5928
cg10255486	2	121726317	0.7651	0.9406
cg00356045	1	22461890	0.5505	0.8466
cg17342141	10	124459311	0.5415	0.8269
cg01646784	22	37976725	0.6780	0.9106
cg21467692	17	26176717	0.5135	0.8099
cg02772379	1	18149599	0.6915	0.9207
cg13963891	15	28343577	0.5848	0.8353
cg07069342	15	28353101	0.6206	0.8768
cg21481966	2	233280609	0.3187	0.6441
cg07630274	10	71583235	0.5362	0.8506
cg14361119	9	116971621	0.7282	0.9316
cg23728588	10	118304610	0.1669	0.4787
cg17828456	17	48056033	0.5664	0.8582
cg02140425	11	120972246	0.5810	0.8709
cg02710552	15	73611321	0.2498	0.5938
cg03972040	13	103345722	0.6241	0.8675
cg18738220	4	115077178	0.5005	0.7902
cg13960894	15	83415633	0.5405	0.8482
cg01693638	17	63283010	0.6537	0.8887
cg24775773	15	100512663	0.6336	0.9017
cg03084652	4	7638050	0.6493	0.9018
cg00979695	7	138363322	0.5275	0.8292
cg02179492	11	69981382	0.6206	0.8939
cg22657659	4	8608361	0.2412	0.5687
cg16708012	12	108992114	0.6662	0.9135
cg26019584	19	1302689	0.5825	0.8770
cg23152931	11	1027560	0.8081	0.9574
cg03907849	3	195544555	0.6029	0.8749
cg20589691	13	51672329	0.5434	0.8244
cg21721022	6	29407834	0.0772	0.3183

CpG	Chromosome	Location	Mean β-value (sensitive)	Mean β-value (resistant / promoted)
cg04018210	6	168473234	0.6670	0.9160
cg26978611	6	90271866	0.6360	0.8986
cg21858516	14	59103353	0.2542	0.5721
cg19690704	15	100739985	0.7388	0.9422
cg20550154	14	52487779	0.3935	0.7226
cg23400413	14	89959574	0.2668	0.5823
cg20482223	7	138347826	0.6819	0.9226
cg13484324	2	235359663	0.6275	0.9021
cg15227522	3	13112502	0.6439	0.9168
cg18527241	7	105319558	0.5768	0.8743
cg10257895	21	45584142	0.5403	0.8529
cg24478595	11	2817646	0.6639	0.9157
cg10172068	11	2431333	0.2694	0.5850
cg16785502	4	7666180	0.6288	0.8998
cg07136254	1	145412774	0.4702	0.7930
cg14219900	1	156119542	0.3999	0.7271
cg16465369	16	89678764	0.4232	0.7676
cg15484406	14	94461913	0.2702	0.6017
cg08888905	21	47008098	0.1236	0.4303
cg15768620	10	133938604	0.5333	0.8466
cg09126559	7	44261162	0.7534	0.9461
cg27640020	19	19002253	0.6784	0.9120
cg24913825	2	198134173	0.5173	0.8125
cg09366379	16	87905824	0.5490	0.8516
cg01824618	16	85315212	0.4032	0.7393
cg01534765	1	39979415	0.5760	0.8787
cg09499095	2	241564943	0.1989	0.5124
cg11160572	4	169706422	0.7356	0.9459
cg02470287	8	10823068	0.1832	0.4912
cg07791834	19	48800382	0.7203	0.9338
cg00770372	8	37237473	0.0847	0.3495
cg24864097	10	121127614	0.4759	0.8149
cg02390947	10	105273633	0.6413	0.9098
cg15161251	19	1305252	0.6635	0.9208
cg14565752	19	47955003	0.1268	0.3992
cg06322983	7	128492245	0.4509	0.7723
cg10982692	8	142367177	0.6211	0.8950
cg03267419	2	75423622	0.5457	0.8321
cg14532497	4	174439756	0.6522	0.8957
cg19642727	1	853876	0.4420	0.7771

CpG	Chromosome	Location	Mean β-value (sensitive)	Mean β-value (resistant / promoted)
cg10838469	11	2211741	0.4841	0.8452
cg02059823	2	240872433	0.6985	0.9406
cg07081739	6	27214794	0.0797	0.3300
cg03040530	1	228558193	0.5518	0.8554
cg13049398	18	74157682	0.2314	0.5625
cg06304190	14	91283606	0.5490	0.8695
cg18311498	7	151093196	0.8079	0.9725
cg10336925	14	77647482	0.3868	0.7133
cg01407419	7	75442962	0.5292	0.8662
cg12368694	11	70391098	0.4424	0.7815
cg05294813	19	53541287	0.0833	0.3285
cg00927495	9	96715687	0.5308	0.8578
cg00317879	11	68920611	0.7452	0.9443
cg03608583	2	232761931	0.5275	0.8381
cg26580332	8	143919495	0.5478	0.8577
cg10562649	2	95695011	0.5891	0.8847
cg08895562	6	32034322	0.5840	0.8798
cg01149415	20	44745522	0.6610	0.9181
cg02801277	18	44334713	0.6041	0.8826
cg08800414	22	39965495	0.6190	0.9026
cg01620410	16	46791076	0.7037	0.9402
cg06901893	7	73400692	0.5151	0.8371
cg16786458	5	149108820	0.3367	0.6724
cg08231696	1	16349079	0.5594	0.8769
cg04791601	1	204159016	0.4474	0.7878
cg06051662	X	153096786	0.2662	0.6267
cg01416043	2	11053694	0.7654	0.9533
cg27511525	15	100642482	0.5851	0.8805
cg09459581	2	173685275	0.4416	0.7745
cg14171516	1	2252860	0.4145	0.7760
cg27106950	16	11367916	0.4266	0.7517
cg19368582	10	88716646	0.5650	0.8640
cg16909685	4	88722338	0.6546	0.9100
cg04064452	2	242486462	0.1673	0.4842
cg23817627	2	69043460	0.4659	0.7818
cg04848913	7	105651736	0.3415	0.6942
cg10517919	1	226707583	0.2441	0.5763
cg11585605	1	52401955	0.3397	0.7041
cg27079322	17	59530436	0.5881	0.8788
cg00461578	4	146819333	0.5642	0.8591

CpG	Chromosome	Location	Mean β-value (sensitive)	Mean β-value (resistant / promoted)
cg05573434	4	7648540	0.4529	0.7917
cg17345277	6	2641053	0.6334	0.9034
cg17229197	11	2542688	0.6502	0.9255
cg23283187	4	8593019	0.3066	0.6670
cg14388170	9	129224091	0.6650	0.9262
cg20801892	20	2678368	0.2906	0.6578
cg04454237	7	155636106	0.3364	0.6977
cg07461414	19	12024676	0.1403	0.3892
cg19504089	1	146495202	0.0996	0.3812
cg17819168	15	23807180	0.5845	0.8692
cg07574896	6	401453	0.2431	0.6089
cg24762452	12	117487037	0.8506	0.9788
cg14222474	1	2286612	0.6088	0.9010
cg13907754	6	90117574	0.7002	0.9360
cg04305539	1	247171728	0.2840	0.6411
cg05768565	4	7553433	0.6655	0.9083
cg13148921	15	80853140	0.4405	0.7751
cg23273843	13	111449880	0.0965	0.3582
cg13976496	5	135156607	0.3798	0.7142
cg24634055	8	10996424	0.5534	0.8737
cg23849410	2	210822981	0.2969	0.6519
cg12630714	4	54975894	0.7048	0.9328
cg26705688	19	58238435	0.2725	0.6166
cg22897193	14	94406618	0.3712	0.7381
cg03907847	13	28495908	0.5041	0.8176
cg26639596	12	124371660	0.1512	0.4769
cg09155774	9	96723033	0.5084	0.8143
cg14373611	13	20798734	0.2665	0.6321
cg08024103	17	131848	0.6116	0.9140
cg05117693	22	40006573	0.2179	0.5490
cg11870309	3	12927951	0.4358	0.8039
cg06652392	5	1560727	0.3261	0.6947
cg14274019	9	134184504	0.6587	0.9226
cg25734785	20	62738310	0.3070	0.6650
cg19593680	4	7374669	0.7763	0.9612
cg11691189	2	47743741	0.4924	0.8065
cg27488680	4	7638222	0.5376	0.8483
cg09660670	5	677592	0.6207	0.8945
cg05146395	20	61314143	0.3408	0.7187
cg21079946	3	58622915	0.4635	0.8013

CpG	Chromosome	Location	Mean β-value (sensitive)	Mean β-value (resistant / promoted)
cg17836177	8	22735111	0.2879	0.6398
cg14975015	7	138459783	0.6016	0.9049
cg20455802	13	112062882	0.1912	0.5332
cg12332536	3	46450983	0.5320	0.8639
cg01978937	20	2671574	0.6190	0.9158
cg19586352	13	25120195	0.6736	0.9383
cg17945140	17	239634	0.6546	0.9197
cg20290360	1	204956391	0.6582	0.9084
cg06726099	3	195940674	0.6242	0.9124
cg23370548	1	6471486	0.6184	0.8941
cg06032919	1	22666910	0.5626	0.8365
cg24472574	10	103070503	0.1832	0.5216
cg06155697	11	8120396	0.5658	0.8846
cg14251805	9	129222402	0.6715	0.9338
cg26429140	5	94782293	0.4342	0.7794
cg14693391	2	183731563	0.2941	0.6633
cg14880079	3	194120150	0.2966	0.6459
cg12874479	22	21028739	0.4909	0.8137
cg11403374	17	48680410	0.6037	0.9074
cg00136173	5	176045746	0.6045	0.9002
cg07795916	2	108885152	0.3903	0.7532
cg10428230	X	54526673	0.3249	0.6679
cg11530289	8	67350852	0.4360	0.7897
cg14400528	12	121417986	0.4168	0.7567
cg24219966	2	224950887	0.5304	0.8616
cg21485521	6	44773698	0.5541	0.8848
cg22852840	6	47749714	0.1556	0.4887
cg03712837	10	94183680	0.5889	0.8731
cg19137726	6	4082055	0.5669	0.8749
cg14022995	11	2397350	0.6094	0.9099
cg04538289	11	72305989	0.2659	0.6247
cg17524924	19	56879207	0.5667	0.8709
cg08825075	16	3934709	0.1550	0.4059
cg24987667	4	8518709	0.3860	0.7600
cg12013258	12	776351	0.4466	0.8259
cg02309609	15	66918297	0.5857	0.8981
cg22805356	15	93286499	0.2699	0.6358
cg07654843	22	26138429	0.5862	0.8981
cg02937055	3	171489625	0.3871	0.7531
cg19815720	3	183770650	0.5077	0.8384

CpG	Chromosome	Location	Mean β-value (sensitive)	Mean β-value (resistant / promoted)
cg02169542	9	19932609	0.3352	0.6868
cg22495191	1	154834293	0.5129	0.8530
cg13376953	11	1750381	0.3957	0.7581
cg06961473	15	65369801	0.6634	0.9174
cg03621279	5	140009	0.6203	0.9077
cg20671150	6	32172151	0.4260	0.7537
cg03983364	7	101272096	0.4365	0.7841
cg19107291	15	100537865	0.7544	0.9595
cg01975786	8	142428968	0.3988	0.7635
cg02035348	11	69624697	0.5380	0.8789
cg17951488	10	51487759	0.5986	0.8836
cg09000302	3	43414570	0.5192	0.8580
cg14451926	8	23562918	0.6410	0.9204
cg03872804	4	1594280	0.7766	0.9737
cg11235583	1	16369437	0.6718	0.9301
cg18949794	7	130123340	0.4560	0.7934
cg23441248	15	50140549	0.0582	0.3036
cg24154779	2	177038538	0.1914	0.5718
cg03421624	22	18984376	0.4620	0.8086
cg10035737	17	42840005	0.5333	0.8807
cg20489946	13	52731078	0.4577	0.8060
cg06442844	X	117958793	0.1338	0.4829
cg26400835	12	107103889	0.3686	0.7265
cg25880954	1	47900630	0.6354	0.9354
cg21125628	12	10605936	0.3890	0.7473
cg15575009	1	48179471	0.3465	0.7022
cg18070442	22	39965918	0.4125	0.7674
cg26087651	13	22836354	0.1847	0.5411
cg13805052	1	2283063	0.4774	0.8511
cg18334977	3	128272847	0.5739	0.8986
cg26685375	11	120039029	0.6278	0.9267
cg23199907	13	33305966	0.4168	0.7734
cg24897141	5	139283199	0.5291	0.8657
cg20563269	2	129104576	0.7956	0.9705
cg17413302	11	2360997	0.4270	0.8058
cg07161061	12	133057193	0.3366	0.7240
cg13593548	9	101745309	0.5219	0.8693
cg12449813	15	69853608	0.4969	0.8485
cg06149981	11	1243947	0.1611	0.4659
cg05034363	7	75443193	0.3773	0.7871

CpG	Chromosome	Location	Mean β-value (sensitive)	Mean β-value (resistant / promoted)
cg27441486	1	201708522	0.2902	0.6557
cg02035102	7	23603991	0.1805	0.5239
cg21079113	1	110010089	0.2857	0.6654
cg12546355	7	155333337	0.2012	0.5479
cg21966656	8	10897405	0.6829	0.9415
cg10843707	14	52510701	0.3693	0.7570
cg13845692	9	94259238	0.2978	0.6789
cg02824443	7	108093448	0.5794	0.8902
cg16336436	14	76178685	0.2536	0.6305
cg00470505	9	139596117	0.2273	0.5432
cg08790158	8	126709639	0.5141	0.8535
cg19912559	1	40204330	0.1171	0.4516
cg21105924	17	79133388	0.5724	0.9008
cg05803296	7	105319615	0.4902	0.8674
cg13975344	2	45170979	0.2319	0.5900
cg26452811	15	65666640	0.4036	0.7835
cg01379009	20	57041622	0.7653	0.9665
cg07701579	1	2262232	0.1999	0.5224
cg14018797	7	1849782	0.7433	0.9581
cg25030888	1	67156909	0.3266	0.7130
cg25722727	10	125751983	0.4869	0.8329
cg07576525	22	51146088	0.3905	0.7920
cg17149030	15	99549047	0.3086	0.6907
cg10165864	2	173419899	0.1661	0.5453
cg24127593	4	1648399	0.6946	0.9490
cg12302875	7	2499975	0.7304	0.9613
cg01273802	8	10871371	0.0636	0.3452
cg06476663	17	113701	0.6270	0.9227
cg24492749	6	167063318	0.2059	0.6066
cg24690715	20	62455532	0.5908	0.9197
cg18931977	1	228567311	0.4926	0.8367
cg18098089	17	146487	0.4669	0.8356
cg16720578	14	54410717	0.4217	0.7834
cg13257129	3	127109560	0.5064	0.8735
cg00345025	8	743875	0.3163	0.6964
cg11723772	1	44979652	0.4604	0.8267
cg03102788	20	62738880	0.3424	0.7226
cg03880722	9	108416630	0.4145	0.7884
cg00490075	13	27359547	0.1827	0.5714
cg08209336	2	128409268	0.6421	0.9426

CpG	Chromosome	Location	Mean β-value (sensitive)	Mean β-value (resistant / promoted)
cg07699149	8	10987869	0.6171	0.9292
cg26789888	11	119872718	0.4035	0.7637
cg02522367	9	139640325	0.5926	0.9182
cg21134737	11	2871400	0.4270	0.8131
cg07016979	5	79288583	0.4932	0.8579
cg19901940	14	22689870	0.2666	0.6739
cg25303462	1	183357929	0.2230	0.5966
cg25456020	17	159130	0.3160	0.6909
cg20243424	6	32059605	0.1772	0.5217
cg14619064	17	56355331	0.4863	0.8368
cg13603914	8	41518004	0.5525	0.8848
cg19733042	1	148193658	0.4226	0.7757
cg20279493	17	42059996	0.3058	0.6973
cg12634208	8	41570802	0.2998	0.6813
cg01932308	1	3337800	0.2885	0.6807
cg11614093	6	155406298	0.5085	0.8835
cg09518670	16	88150515	0.3226	0.7190
cg12645891	5	139912	0.7737	0.9771
cg06636485	5	889694	0.6486	0.9511
cg25801300	2	131975758	0.2864	0.6824
cg02018326	19	51670251	0.0701	0.3611
cg23213876	1	53924164	0.2021	0.5301
cg08040755	14	76716894	0.5408	0.8931
cg17153775	1	3512117	0.5285	0.8977
cg12996100	8	11470690	0.4758	0.8397
cg22869369	4	1608593	0.6188	0.9298
cg18339098	8	10892823	0.1838	0.5744
cg17434008	1	38974111	0.1643	0.5080
cg25793191	20	61038971	0.5575	0.9042
cg03097114	7	155679586	0.4752	0.8406
cg23768117	17	79134486	0.4515	0.8456
cg01293207	7	23218577	0.4520	0.8262
cg21619637	7	979643	0.5479	0.9066
cg01184387	5	176306590	0.6023	0.9191
cg12901038	11	2815078	0.5227	0.8967
cg12989498	22	22236465	0.3261	0.7393
cg24121503	6	151650834	0.4296	0.8147
cg00735599	6	168629370	0.3502	0.7524
cg21663666	2	232220549	0.7659	0.9715
cg00988577	6	32978548	0.3654	0.7466

CpG	Chromosome	Location	Mean β-value (sensitive)	Mean β-value (resistant / promoted)
cg14467690	9	135120707	0.4457	0.8372
cg14198221	14	67983484	0.3100	0.7134
cg02731390	10	98367715	0.5084	0.8759
cg22526491	8	143912895	0.3576	0.7389
cg05598581	1	48179783	0.3155	0.7000
cg10692700	4	1599344	0.4628	0.8448
cg02847185	4	8589313	0.5633	0.9024
cg04687040	8	142427117	0.3205	0.7433
cg21752270	11	2813528	0.4188	0.8186
cg22610106	6	167136367	0.5484	0.8881
cg16714273	20	30455386	0.5564	0.8978
cg00176309	21	46303258	0.5879	0.9137
cg07339138	3	42820274	0.5657	0.9199
cg09389370	16	30685678	0.4402	0.8390
cg00323014	10	125928304	0.5410	0.8958
cg11855156	19	51446953	0.1841	0.5495
cg10735632	2	106681831	0.2404	0.6329
cg24244478	11	75374608	0.5068	0.8538
cg21163444	12	54765670	0.2464	0.6284
cg04813159	17	79127459	0.4741	0.8517
cg00417197	7	111817978	0.4195	0.8052
cg14481124	10	71500729	0.3099	0.7109
cg03533051	7	1865705	0.7968	0.9796
cg02008826	8	41505696	0.4612	0.8516
cg02597644	11	1898970	0.5270	0.9022
cg17336615	6	401429	0.2293	0.6330
cg18845375	2	237173852	0.2060	0.6162
cg02068596	6	14068147	0.4108	0.7919
cg08587313	8	130215373	0.3258	0.7286
cg10719664	22	22863663	0.1487	0.5394
cg04533751	6	168491686	0.2001	0.6043
cg13913990	5	172970	0.2459	0.6581
cg03390717	22	39966585	0.5383	0.8941
cg19350679	6	32710506	0.2416	0.6378
cg01322142	4	786718	0.4418	0.8229
cg23332027	3	13681764	0.4165	0.8202
cg26847490	7	95115289	0.4410	0.8189
cg23335916	8	42578842	0.5755	0.9200
cg02814590	7	130416119	0.4625	0.8387
cg03634073	22	45068420	0.4267	0.8138

CpG	Chromosome	Location	Mean β-value (sensitive)	Mean β-value (resistant / promoted)
cg10399850	1	1089668	0.5299	0.8965
cg07757702	3	126401175	0.3501	0.7657
cg00441301	8	33458593	0.2223	0.6232
cg16912848	10	3250774	0.5726	0.9161
cg09619488	7	155817478	0.6353	0.9269
cg08318587	2	216484453	0.1333	0.4997
cg07209624	10	13627505	0.4275	0.8353
cg26876001	16	88951664	0.6971	0.9659
cg12871937	3	14394404	0.5451	0.8942
cg07486732	2	237150793	0.3956	0.7937
cg19600494	2	106959525	0.4854	0.8436
cg21785010	6	901035	0.4089	0.8280
cg21725652	8	10918152	0.6123	0.9159
cg07936323	19	3802504	0.4265	0.8200
cg20718570	17	140716	0.6667	0.9473
cg14006405	4	1537799	0.5908	0.9206
cg19628874	4	7131247	0.4327	0.8370
cg13773631	9	96715843	0.4994	0.8817
cg14090208	5	1632226	0.4605	0.8748
cg24109790	12	113575128	0.4519	0.8220
cg14098223	1	2262333	0.4108	0.8266
cg07496078	9	92216935	0.2607	0.6353
cg07720540	1	3477442	0.4450	0.8509
cg04769798	16	87714169	0.4682	0.8654
cg24281777	3	166162926	0.1463	0.4780
cg17226042	1	37973652	0.4313	0.8138
cg08840010	1	8000314	0.4760	0.8642
cg00525931	16	29084744	0.4612	0.8407
cg15149275	3	129744648	0.4484	0.8419
cg11789804	1	219958132	0.4132	0.7967
cg16703333	19	42470790	0.4169	0.8266
cg27152299	11	71238225	0.2558	0.6485
cg18496318	3	13117754	0.1671	0.5034
cg14029959	11	1047720	0.5432	0.9133
cg05200628	1	160681760	0.5208	0.8607
cg05161119	4	785696	0.5119	0.8895
cg01719832	1	11752772	0.4589	0.8367
cg10125399	13	113328979	0.3931	0.8113
cg02966200	2	224866483	0.5042	0.8973
cg07494130	5	139132458	0.3178	0.7258

CpG	Chromosome	Location	Mean β-value (sensitive)	Mean β-value (resistant / promoted)
cg27609217	11	46258039	0.3280	0.7436
cg16333374	2	88579997	0.3036	0.7086
cg21752660	15	52824726	0.3956	0.7911
cg05868531	2	232348602	0.6589	0.9626
cg21091226	4	7395612	0.5242	0.9082
cg00285902	3	46605616	0.4680	0.8787
cg18088931	3	141381413	0.3625	0.7860
cg07961637	4	7637856	0.5664	0.9144
cg11410726	11	69625409	0.7496	0.9787
cg19635401	6	118873071	0.2201	0.6583
cg05607801	3	125903092	0.3920	0.7949
cg11832717	11	2434218	0.7155	0.9633
cg03059896	1	27560050	0.4463	0.8344
cg03841627	16	88935862	0.4697	0.8637
cg01447854	1	228556332	0.2565	0.6765
cg17566541	11	1912287	0.5226	0.9022
cg00716704	8	20048583	0.2550	0.6960
cg00730780	10	30316187	0.3293	0.7557
cg18855080	1	172748189	0.2058	0.6101
cg22830663	2	131975750	0.3086	0.7278
cg02202589	2	241101064	0.2714	0.7012
cg03152880	16	48019794	0.1147	0.5149
cg13026754	14	94392718	0.3392	0.7420
cg22092606	2	109887294	0.5811	0.9128
cg17548395	10	60461164	0.2428	0.6697
cg21875839	2	129308196	0.4842	0.8862
cg17459387	17	79134666	0.6677	0.9572
cg19344878	12	131369535	0.4330	0.8300
cg05129489	15	100664728	0.3963	0.8303
cg00280235	7	107797076	0.2810	0.6881
cg22387113	15	89535439	0.4052	0.8200
cg11247615	11	1029336	0.6417	0.9670
cg08957279	16	202311	0.2868	0.7007
cg26485844	5	77256916	0.2694	0.6559
cg13852784	9	101265948	0.2495	0.6496
cg03984758	4	57944634	0.5043	0.8701
cg17942219	2	132160418	0.1436	0.5765
cg23541923	12	70382434	0.1857	0.6322
cg11717883	10	76052393	0.4930	0.8621
cg14583103	19	373432	0.2642	0.6817

CpG	Chromosome	Location	Mean β-value (sensitive)	Mean β-value (resistant / promoted)
cg06810011	7	110562986	0.3367	0.7616
cg16218340	3	126422260	0.3856	0.7883
cg11868634	7	155797461	0.4481	0.8480
cg13778078	4	785160	0.6797	0.9566
cg18954658	11	47451623	0.2540	0.7128
cg20338182	7	92857276	0.5071	0.8597
cg09809224	3	41782779	0.3920	0.8037
cg17876294	15	90115219	0.2934	0.7020
cg22439459	7	138345249	0.4394	0.8550
cg03969260	1	153122203	0.2096	0.6135
cg26373716	8	53474030	0.3116	0.7133
cg20200711	11	2211776	0.4009	0.8486
cg24782378	15	100672379	0.4705	0.8729
cg19914124	1	3073626	0.5192	0.9048
cg16231066	6	168482485	0.2448	0.6433
cg02066784	6	28231033	0.3817	0.7570
cg07247405	1	2484626	0.2754	0.6793
cg05046306	17	46698273	0.3293	0.7752
cg12121166	11	2376275	0.2512	0.6437
cg16513326	8	10877312	0.1291	0.4915
cg03222632	11	111431381	0.4562	0.8524
cg16737517	20	62406677	0.4026	0.8457
cg25499537	3	151177940	0.1814	0.6016
cg02232988	14	53340748	0.1054	0.5048
cg00720629	22	19752228	0.5043	0.9087
cg02976009	6	32068226	0.1576	0.5577
cg07770360	16	5039472	0.2698	0.6968
cg13330050	5	114632793	0.2872	0.7379
cg01468562	6	97371373	0.4765	0.8909
cg06646262	19	12428544	0.3322	0.7758
cg06793967	11	464665	0.4408	0.8170
cg24574147	8	10918572	0.3680	0.7767
cg11007362	6	901022	0.3141	0.7666
cg03713640	15	101088289	0.2982	0.7035
cg08439276	2	68937224	0.1339	0.5870
cg10979436	7	27242005	0.5686	0.9220
cg01613189	8	10875246	0.2431	0.6584
cg03972560	X	17877110	0.1722	0.5918
cg08895013	11	2468332	0.3881	0.8514
cg07136920	1	53970693	0.4219	0.8026

CpG	Chromosome	Location	Mean β-value (sensitive)	Mean β-value (resistant / promoted)
cg07532405	14	22948498	0.2925	0.7405
cg06689180	21	35831010	0.5101	0.9180
cg19007167	2	242755350	0.3037	0.7116
cg25101863	11	69650231	0.5679	0.9273
cg16083838	11	2889809	0.2919	0.7375
cg05357152	20	61049813	0.4968	0.8991
cg07865216	10	98910008	0.0948	0.4766
cg07725967	4	7663352	0.7091	0.9702
cg20173428	12	108167502	0.1308	0.5587
cg15104839	19	46932612	0.2627	0.7162
cg09387749	2	177028680	0.3688	0.7799
cg26686068	4	7700686	0.5439	0.9140
cg11547104	4	7593493	0.6229	0.9461
cg22118369	6	32972157	0.4215	0.8421
cg06172235	6	168482099	0.6328	0.9671
cg14391016	6	167523797	0.2416	0.6810
cg16818372	17	46270817	0.4977	0.9009
cg04882216	1	3101820	0.1039	0.5268
cg20993253	15	100535343	0.4224	0.8484
cg22551546	5	76916591	0.2437	0.6888
cg07369569	6	55444821	0.3179	0.7647
cg05383332	14	74804420	0.3367	0.7893
cg12964647	17	46234525	0.3956	0.8340
cg06938699	11	1037775	0.5713	0.9437
cg11791288	1	31988382	0.4541	0.9026
cg03282889	3	125706919	0.3614	0.8398
cg09233395	8	116678582	0.0642	0.4661
cg00273198	9	139069298	0.2334	0.6652
cg07105499	16	55909393	0.1365	0.5976
cg24801230	17	43978533	0.3576	0.7602
cg02770688	6	168491649	0.5030	0.8944
cg02235871	3	44062006	0.3420	0.7928
cg10923036	4	57931299	0.2655	0.7004
cg18294158	7	103849187	0.3415	0.7811
cg01470599	9	38422794	0.4973	0.9300
cg21428990	7	155790277	0.4282	0.8646
cg02022247	X	25029872	0.3772	0.8208
cg01004762	9	34956991	0.2462	0.7236
cg13096809	6	32189126	0.1202	0.5354
cg10023855	6	32710516	0.0922	0.4944

CpG	Chromosome	Location	Mean β-value (sensitive)	Mean β-value (resistant / promoted)
cg13403003	20	3392757	0.3056	0.7720
cg19785810	17	52346	0.5917	0.9534
cg14443606	9	40536407	0.2329	0.7117
cg10876767	4	7637533	0.5166	0.8855
cg04481189	7	138364700	0.3072	0.7602
cg22718169	1	2264352	0.3926	0.8579
cg19094530	10	79470169	0.2689	0.7152
cg02239163	4	7720084	0.2917	0.7565
cg18752412	19	47161689	0.1351	0.5841
cg02588889	10	124829211	0.1188	0.5869
cg00225618	3	133392210	0.2790	0.7560
cg26252077	1	61607055	0.1263	0.5542
cg09374123	6	150379008	0.5855	0.9464
cg04845171	16	31384854	0.2757	0.7141
cg03438558	8	10982836	0.4996	0.9066
cg21438602	21	45713510	0.4930	0.9163
cg08355045	6	80787529	0.0924	0.5091
cg02717470	2	241559792	0.3427	0.7922
cg09537533	20	592957	0.3772	0.8377
cg23968213	11	2481965	0.4625	0.8823
cg18239253	20	238156	0.1760	0.6541
cg03848831	11	2397685	0.4289	0.8522
cg27369423	16	56228901	0.1687	0.6651
cg14018024	9	133908909	0.3467	0.8174
cg04278110	2	198063759	0.1872	0.6631
cg23824845	1	53921414	0.2492	0.7531
cg16966243	15	76408398	0.3406	0.8077
cg10454937	9	96715047	0.3021	0.7187
cg25389791	5	176307836	0.5486	0.9285
cg14549078	15	48752032	0.1417	0.5887
cg08430277	16	15858790	0.1233	0.5616
cg07475394	17	79466438	0.5394	0.9338
cg04258133	11	1953661	0.3185	0.7781
cg00441918	17	47113407	0.1081	0.5825
cg25952964	2	109607272	0.2780	0.7474
cg21496187	6	100624512	0.1846	0.6741
cg17737776	17	79122455	0.3437	0.8376
cg08015883	20	61049884	0.1825	0.6358
cg20895877	14	94254586	0.2380	0.7107
cg05465935	5	43515805	0.1747	0.6602

CpG	Chromosome	Location	Mean β-value (sensitive)	Mean β-value (resistant / promoted)
cg07472943	19	437061	0.1946	0.7030
cg06762750	1	3534422	0.5980	0.9690
cg20637438	8	10771386	0.1436	0.5467
cg24310722	19	47019524	0.4012	0.8698
cg00678050	4	184838207	0.4038	0.8400
cg03470671	11	45115584	0.4167	0.8782
cg05489661	16	88975108	0.5775	0.9673
cg13897134	3	147120248	0.3304	0.7985
cg06441116	1	2500814	0.4312	0.9180
cg19246110	19	58238928	0.3532	0.7820
cg08450752	15	73611451	0.4846	0.8892
cg27433479	1	1687481	0.3670	0.8390
cg16144345	10	103982587	0.3557	0.8293
cg16661628	20	32857227	0.3826	0.8618
cg27570984	16	55125644	0.5053	0.9259
cg24706674	10	134679704	0.2401	0.7260
cg06819296	8	10982668	0.4189	0.8769
cg04123498	8	142283564	0.4911	0.9074
cg01823853	7	27646144	0.0943	0.5846
cg19213703	3	177554561	0.2506	0.7712
cg18480717	11	2366949	0.3680	0.8574
cg02502358	17	26221089	0.1398	0.6539
cg04841358	8	10897293	0.1781	0.6578
cg08382534	16	84058601	0.1539	0.6619
cg21541083	19	7701212	0.4410	0.9081
cg02633398	16	88974944	0.2428	0.7559
cg26598540	8	10753147	0.2872	0.7406
cg27655954	8	10753160	0.1631	0.6258
cg01223204	22	22863655	0.1395	0.6598
cg08436104	5	38168076	0.1981	0.7107
cg01266390	10	125034002	0.2387	0.7232
cg27066989	13	51640362	0.2290	0.7209
cg05917273	7	116200522	0.1975	0.6523
cg11036640	22	22865950	0.0873	0.6036
cg09131332	22	50482045	0.1187	0.6426
cg26813483	13	111980537	0.0661	0.5258
cg17167536	8	10906938	0.1515	0.6794
cg04835091	17	35406	0.3200	0.8115
cg17315454	7	75443174	0.1721	0.5901
cg09263513	11	2295852	0.4765	0.9248

CpG	Chromosome	Location	Mean β-value (sensitive)	Mean β-value (resistant / promoted)
cg11977686	19	58238987	0.2704	0.7801
cg18623649	10	125034066	0.3223	0.8271
cg13675721	7	140227273	0.3906	0.8301
cg23287435	4	57937220	0.3525	0.8643
cg07356412	8	11044280	0.3739	0.9034
cg14435720	9	139565087	0.5261	0.9296
cg26350007	11	2013524	0.4630	0.9505
cg08048222	19	58239012	0.2149	0.6941
cg10738003	11	120233535	0.1814	0.6751
cg18541042	7	140227195	0.3137	0.7911
cg06950309	1	154843314	0.2233	0.8164
cg27272246	3	38664451	0.1238	0.7130
cg02310165	8	10892734	0.3504	0.9086
cg26512469	13	113688268	0.4261	0.9235
cg16528678	5	94830	0.2393	0.7804
cg13672736	9	135114066	0.2896	0.8500
cg21783198	5	95541	0.4218	0.9493
cg26069044	11	124613956	0.2550	0.7648
cg02792168	10	101281924	0.2720	0.8371
cg05906769	5	129794	0.2445	0.8480
cg13683939	9	136152547	0.3209	0.8927

APPENDIX 3: GENE ABBREVIATIONS

A1CF	APOBEC1 complementation factor
A2ML1	alpha-2-macroglobulin like 1
AADAC	arylacetamide deacetylase
AADACP1	arylacetamide deacetylase pseudogene 1
ABCC4	ATP binding cassette subfamily C member 4
ABCD1	ATP binding cassette subfamily D member 1
ABHD14B	abhydrolase domain containing 14B
ACADSB	acyl-CoA dehydrogenase, short/branched chain
ACAP1	ArfGAP with coiled-coil, ankyrin repeat and PH domains 1
ACP5	acid phosphatase 5, tartrate resistant
ACTG2	actin, gamma 2, smooth muscle, enteric
ADH1C	alcohol dehydrogenase 1C (class I), gamma polypeptide
AFP	alpha fetoprotein
AGR2	anterior gradient 2, protein disulphide isomerase family member
AGTR2	angiotensin II receptor type 2
AHCYL2	adenosylhomocysteinase like 2
AIP	aryl hydrocarbon receptor interacting protein
AKR1C2	aldo-keto reductase family 1 member C2
AKR1C3	aldo-keto reductase family 1 member C3
ALDH1A1	aldehyde dehydrogenase 1 family member A1
ALDH2	aldehyde dehydrogenase 2 family (mitochondrial)
ALG3	ALG3, alpha-1,3- mannosyltransferase
AMFR	autocrine motility factor receptor
ANAPC5	anaphase promoting complex subunit 5
ANKH	ANKH inorganic pyrophosphate transport regulator
ANKHD1	ankyrin repeat and KH domain containing 1
ANKRD6	ankyrin repeat domain 6
ANXA10	annexin A10
ANXA8	annexin A8
AP1M2	adaptor related protein complex 1 mu 2 subunit
APIP	APAF1 interacting protein
APOB	apolipoprotein B
APOOL	apolipoprotein O like
APRT	adenine phosphoribosyltransferase
ARFIP2	ADP ribosylation factor interacting protein 2
ARHGEF6	Rac/Cdc42 guanine nucleotide exchange factor 6
ARL14	ADP ribosylation factor like GTPase 14
ARL14EPL	ADP ribosylation factor like GTPase 14 effector protein like
ARL5B	ADP ribosylation factor like GTPase 5B
ARL8B	ADP ribosylation factor like GTPase 8B
ARMC10	armadillo repeat containing 10
ARMC9	armadillo repeat containing 9

ARMCX1	armadillo repeat containing, X-linked 1
ASPH	aspartate beta-hydroxylase
ASPSCR1	ASPSCR1, UBX domain containing tether for SLC2A4
ASRGL1	asparaginase like 1
ASXL1	additional sex combs like 1, transcriptional regulator
ATF7IP2	activating transcription factor 7 interacting protein 2
ATP13A5	ATPase 13A5
ATP6V1E2	ATPase H+ transporting V1 subunit E2
AZGP1P1	alpha-2-glycoprotein 1, zinc-binding pseudogene 1
B2M	beta-2-microglobulin
B3GALT5	beta-1,3-galactosyltransferase 5
B3GNT5	UDP-GlcNAc:betaGal beta-1,3-N-acetylglucosaminyltransferase 5
BACE1	beta-secretase 1
BAG4	BCL2 associated athanogene 4
BAMBI	BMP and activin membrane bound inhibitor
BCL2A1	BCL2 related protein A1
BCL9	B-cell CLL/lymphoma 9
BHLHE41	basic helix-loop-helix family member e41
BLNK	B-cell linker
BNC2	basonuclin 2
BPHL	biphenyl hydrolase like
BSG	basigin (Ok blood group)
BTF3L1	basic transcriptionfactor 3 pseudogene 11
BTG2	BTG anti-proliferation factor 2
BTNL10	butyrophilin like 10
C11orf53	chromosome 11 open reading frame 53
C12orf51	chromosome 12 open reading frame 51
C19orf33	chromosome 19 open reading frame 33
C1QBP	complement C1q binding protein
C2	complement C2
C20orf24	chromosome 20 open reading frame 24
C3	complement C3
C3orf52	chromosome 3 open reading frame 52
C4BPA	complement component 4 binding protein alpha
C4BPB	complement component 4 binding protein beta
C4orf32	chromosome 4 open reading frame 32
C6orf132	chromosome 6 open reading frame 132
C9orf152	chromosome 9 open reading frame 152
CACNA1C	calcium voltage-gated channel subunit alpha1 C
CACNA1D	calcium voltage-gated channel subunit alpha1 D
CACNG4	calcium voltage-gated channel auxiliary subunit gamma 4
CACYBP	calcyclin binding protein
CAMK2D	calcium/calmodulin dependent protein kinase II delta
CARD6	caspase recruitment domain family member 6

CATSPERB	cation channel sperm associated auxiliary subunit beta
CBR4	carbonyl reductase 4
CBY1	chibby family member 1, beta catenin antagonist
CCBP2	atypical chemokine receptor 2 (ACKR2)
CCDC12	coiled-coil domain containing 12
CCDC144CP	coiled-coil domain containing 144C, pseudogene
CCDC82	coiled-coil domain containing 82
CCL2	C-C motif chemokine ligand 2
CCNB1IP1	cyclin B1 interacting protein 1
CCNI	cyclin I
CCR8	C-C motif chemokine receptor 8
CD151	CD151 molecule (Raph blood group)
CD22	CD22 molecule
CDC14A	cell division cycle 14A
CDC42BPB	CDC42 binding protein kinase beta
CDC42EP1	CDC42 effector protein 1
CDC45L	cell division cycle 45 related
CDH26	cadherin 26
CDH5	cadherin 5
CDKN2AIP	CDKN2A interacting protein
CDSN	corneodesmosin
CDV3	CDV3 homolog
CEBPA	CCAAT/enhancer binding protein alpha
CECR3	cat eye syndrome chromosome region, candidate 3 (non-protein coding)
CEP170	centrosomal protein 170
CEP170P1	centrosomal protein 170 pseudogene 1
CFI	complement factor I
CHCHD6	coiled-coil-helix-coiled-coil-helix domain containing 6
CHD1	chromodomain helicase DNA binding protein 1
CHMP2A	charged multivesicular body protein 2A
CHMP4B	charged multivesicular body protein 4B
CHRAC1	chromatin accessibility complex 1
CHST9	carbohydrate sulfotransferase 9
CHSY3	chondroitin sulfate synthase 3
CHURC1	churchill domain containing 1
CIAPIN1	cytokine induced apoptosis inhibitor 1
CLDN2	claudin 2
CLK2	CDC like kinase 2
CLPTM1L	CLPTM1 like
CLUL1	clusterin like 1
CMSS1	cms1 ribosomal small subunit homolog (yeast)
CMTM4	CKLF like MARVEL transmembrane domain containing 4
CMYA5	cardiomyopathy associated 5
CNBP	CCHC-type zinc finger nucleic acid binding protein

CNGA1	cyclic nucleotide gated channel alpha 1
CNGA2	cyclic nucleotide gated channel alpha 2
CNPY2	canopy FGF signaling regulator 2
CNPY3	canopy FGF signaling regulator 3
CNTN5	contactin 5
COLCA1	colorectal cancer associated 1
COLCA2	colorectal cancer associated 2
COPG2	coatomer protein complex subunit gamma 2
CORO1B	coronin 1B
COX5B	cytochrome c oxidase subunit 5B
COX7A2	cytochrome c oxidase subunit 7A2
COX7A2L	cytochrome c oxidase subunit 7A2 like
COX8A	cytochrome c oxidase subunit 8A
CP	ceruloplasmin
CPAMD8	C3 and PZP like, alpha-2-macroglobulin domain containing 8
CPD	carboxypeptidase D
CPO	carboxypeptidase O
CRISP2	cysteine rich secretory protein 2
CRISP3	cysteine rich secretory protein 3
CROT	carnitine O-octanoyltransferase
CRY2	cryptochrome circadian clock 2
CSF2RA	colony stimulating factor 2 receptor alpha subunit
CSF3R	colony stimulating factor 3 receptor
CSGALNACT2	chondroitin sulfate N-acetylgalactosaminyltransferase 2
CSNK1A1	casein kinase 1 alpha 1
CST2	cystatin SA
CTCF	CCCTC-binding factor
CTGF	connective tissue growth factor
CTSS	cathepsin S
CUL2	cullin 2
CUX1	cut like homeobox 1
CXCL17	C-X-C motif chemokine ligand 17
CXCL8	C-X-C motif chemokine ligand 8
CYB5A	cytochrome b5 type A
CYP26A1	cytochrome P450 family 26 subfamily A member 1
CYP27A1	cytochrome P450 family 27 subfamily A member 1
CYP2B7P	cytochrome P450 family 2 subfamily B member 7, pseudogene
CYP4B1	cytochrome P450 family 4 subfamily B member 1
CYP4X1	cytochrome P450 family 4 subfamily X member 1
CYP4Z1	cytochrome P450 family 4 subfamily Z member 1
CYP4Z2P	cytochrome P450 family 4 subfamily Z member 2, pseudogene
DCBLD1	discoidin, CUB and LCCL domain containing 1
DCXR	dicarbonyl and L-xylulose reductase
DDX51	DEAD-box helicase 51
DEFB123	defensin beta 123

DENND5A	DENN domain containing 5A
DHCR24	24-dehydrocholesterol reductase
DHRS3	dehydrogenase/reductase 3
DHX35	DEAH-box helicase 35
DHX37	DEAH-box helicase 37
DICER1	dicer 1, ribonuclease III
DIRAS3	DIRAS family GTPase 3
DMBT1	deleted in malignant brain tumors 1
DNAJC15	DnaJ heat shock protein family (Hsp40) member C15
DNPH1	2'-deoxynucleoside 5'-phosphate N-hydrolase 1
DOCK3	dedicator of cytokinesis 3
DRG1	developmentally regulated GTP binding protein 1
DSG2	desmoglein 2
DSTN	destrin, actin depolymerizing factor
DUBR	DPPA2 upstream binding RNA
DUSP1	dual specificity phosphatase 1
DUSP23	dual specificity phosphatase 23
DUT	deoxyuridine triphosphatase
DYNC1LI2	dynein cytoplasmic 1 light intermediate chain 2
DYNLL2	dynein light chain LC8-type 2
E2F1	E2F transcription factor 1
E2F2	E2F transcription factor 2
E2F6	E2F transcription factor 6
ECI1	enoyl-CoA delta isomerase 1
EDDM3A	epididymal protein 3A
EGR1	early growth response 1
EGR2	early growth response 2
EHD4	EH domain containing 4
EIF2A	eukaryotic translation initiation factor 2A
ELAC2	elaC ribonuclease Z 2
ELF1	E74 like ETS transcription factor 1
ELF3	E74 like ETS transcription factor 3
ELMO3	engulfment and cell motility 3
EML5	echinoderm microtubule associated protein like 5
ENAH	enabled homolog (Drosophila)
ENPP3	ectonucleotide pyrophosphatase/phosphodiesterase 3
EPB41L4A	erythrocyte membrane protein band 4.1 like 4A
EPHX2	epoxide hydrolase 2
EPN1	epsin 1
ERGIC1	endoplasmic reticulum-golgi intermediate compartment 1
ERLEC1	endoplasmic reticulum lectin 1
ERMP1	endoplasmic reticulum metallopeptidase 1
ERP27	endoplasmic reticulum protein 27
ERVK3	endogenous retrovirus group K3
ESM1	endothelial cell specific molecule 1

ETF1	eukaryotic translation termination factor 1
ETV1	ETS variant 1
EXOC2	exocyst complex component 2
EXOC6	exocyst complex component 6
EXOC8	exocyst complex component 8
EXOSC2	exosome component 2
EYA2	EYA transcriptional coactivator and phosphatase 2
FABP4	fatty acid binding protein 4
FAM105B	OTU deubiquitinase with linear linkage specificity (OTULIN)
FAM120A	family with sequence similarity 120A
FAM127C	family with sequence similarity 127 member C
FAM26F	family with sequence similarity 26 member F
FAM98B	family with sequence similarity 98 member B
FAR2P2	fatty acyl-CoA reductase 2 pseudogene 2
FCRL5	Fc receptor like 5
FDX1	ferredoxin 1
FGFBP3	fibroblast growth factor binding protein 3
FHOD1	formin homology 2 domain containing 1
FIP1L1	factor interacting with PAPOLA and CPSF1
FKBP1A	FK506 binding protein 1A
FMO6P	flavin containing monooxygenase 6 pseudogene
FMR1	fragile X mental retardation 1
FN1	fibronectin 1
FOXA1	forkhead box A1
FOXD1	forkhead box D1
FOXD2-AS1	FOXD2 antisense RNA 1 (head to head)
FRMD7	FERM domain containing 7
FRY	FRY microtubule binding protein
FSTL1	follistatin like 1
FXN	frataxin
GABRP	gamma-aminobutyric acid type A receptor pi subunit
GADD45B	growth arrest and DNA damage inducible beta
GAL	galanin and GMAP prepropeptide
GALK2	galactokinase 2
GALNT7	polypeptide N-acetylgalactosaminyltransferase 7
GATA1	GATA binding protein 1
GATA2	GATA binding protein 2
GATA3	GATA binding protein 3
GATA6	GATA binding protein 6
GATM	glycine amidinotransferase
GBP4	guanylate binding protein 4
GCH1	GTP cyclohydrolase 1
GDF15	growth differentiation factor 15
GJB2	gap junction protein beta 2
GLB1	galactosidase beta 1

GNA13	G protein subunit alpha 13
GNE	glucosamine (UDP-N-acetyl)-2-epimerase/N-acetylmannosamine kinase
GNG3	G protein subunit gamma 3
GP6	glycoprotein VI platelet
GPR115	adhesion G protein-coupled receptor F4 (ADGFR4)
GPR87	G protein-coupled receptor 87
GPRC5A	G protein-coupled receptor class C group 5 member A
GPRC5B	G protein-coupled receptor class C group 5 member B
GSDMC	gasdermin C
GSTA2	glutathione S-transferase alpha 2
GSTA4	glutathione S-transferase alpha 4
GSTM3	glutathione S-transferase mu 3
GYPC	glycophorin C (Gerbich blood group)
H1FX	H1 histone family member X
HEPACAM2	HEPACAM family member 2
HERC3	HECT and RLD domain containing E3 ubiquitin protein ligase 3
HIST1H2AD	histone cluster 1 H2A family member D
HIST1H2BD	histone cluster 1 H2B family member d
HK1	hexokinase 1
HLA-B	major histocompatibility complex, class I, B
HMGA1	high mobility group AT-hook 1
HNRNPA1	heterogeneous nuclear ribonucleoprotein A1
HNRNPF	heterogeneous nuclear ribonucleoprotein F
HOXB2	homeobox B2
HOXC10	homeobox C10
HOXC11	homeobox C11
HOXC-AS3	HOXC cluster antisense RNA 3
HRASLS2	HRAS like suppressor 2
HS6ST3	heparan sulfate 6-O-sulfotransferase 3
HSD17B2	hydroxysteroid 17-beta dehydrogenase 2
HSF1	heat shock transcription factor 1
HSF2	heat shock transcription factor 2
HTT	huntingtin
ID1	inhibitor of DNA binding 1, HLH protein
IDH3g	isocitrate dehydrogenase 3 (NAD(+)) gamma
IFFO2	intermediate filament family orphan 2
IFIT2	interferon induced protein with tetratricopeptide repeats 2
IFIT3	interferon induced protein with tetratricopeptide repeats 3
IGBP1	immunoglobulin (CD79A) binding protein 1
IGFBP3	insulin like growth factor binding protein 3
IKBKE	inhibitor of kappa light polypeptide gene enhancer in B-cells, kinase epsilon
IL1A	interleukin 1 alpha

IL1RAP	interleukin 1 receptor accessory protein
ILF3-AS1	ILF3 antisense RNA 1 (head to head)
IMP4	IMP4 homolog, U3 small nucleolar ribonucleoprotein
INAFM2	InaF motif containing 2
INPP5K	inositol polyphosphate-5-phosphatase K
INSR	insulin receptor
IPO11	importin 11
IPW	imprinted In Prader-Willi syndrome (non-protein coding)
IQGAP2	IQ motif containing GTPase activating protein 2
IRF1	interferon regulatory factor 1
IRF2BP2	interferon regulatory factor 2 binding protein 2
IRF8	interferon regulatory factor 8
IVL	involucrin
JRKL	JRK-like
KDELR2	KDEL endoplasmic reticulum protein retention receptor 2
KERA	keratocan
KHSRP	KH-type splicing regulatory protein
KIAA1324	KIAA1324
KIDINS220	kinase D-interacting substrate 220kDa
KIF3C	kinesin family member 3C
KIF5A	kinesin family member 5A
KLHDC7B	kelch domain containing 7B
KLK5	kallikrein related peptidase 5
KLRF1	killer cell lectin like receptor F1
KNDC1	kinase non-catalytic C-lobe domain containing 1
KPNA3	karyopherin subunit alpha 3
KPNA4	karyopherin subunit alpha 4
KRT4	keratin 4
KRT7	keratin 7
KRTAP4-12	keratin associated protein 4-12
KRTCAP3	keratinocyte associated protein 3
LAGE3	L antigen family member 3
LAMA5	laminin subunit alpha 5
LAMTOR1	late endosomal/lysosomal adaptor, MAPK and MTOR activator 1
LCN2	lipocalin 2
LCTL	lactase like
LDLR	low density lipoprotein receptor
LIG4	DNA ligase 4
LINC00630	long intergenic non-protein coding RNA 630
LINC00662	long intergenic non-protein coding RNA 662
LINC00958	long intergenic non-protein coding RNA 958
LOC100130751	uncharacterized LOC100130751
LOC100505938	uncharacterized LOC100505938
LOC100506098	uncharacterized LOC100506098

LOC100996579	uncharacterized LOC100996579
LOC101927851	uncharacterized LOC101927851
LOC101930370	uncharacterized LOC101930370
LOC105373098	uncharacterized LOC105373098
LONP2	lon peptidase 2, peroxisomal
LOXL4	lysyl oxidase like 4
LPCAT4	lysophosphatidylcholine acyltransferase 4
LPHN1	latrophilin 1
LRG1	leucine rich alpha-2-glycoprotein 1
LRP12	LDL receptor related protein 12
LSM5	LSM5 homolog, U6 small nuclear RNA and mRNA degradation associated
LTBP3	latent transforming growth factor beta binding protein 3
LYPLA1	lysophospholipase I
MACF1	microtubule-actin crosslinking factor 1
MAD1L1	MAD1 mitotic arrest deficient like 1
MAN2A1	mannosidase alpha class 2A member 1
MAN2C1	mannosidase alpha class 2C member 1
MAPK4	mitogen-activated protein kinase 4
MAPK6	mitogen-activated protein kinase 6
MAPRE1	microtubule associated protein RP/EB family member 1
MARK1	microtubule affinity regulating kinase 1
MAST4	microtubule associated serine/threonine kinase family member 4
MAT2B	methionine adenosyltransferase 2B
MATR3	matrin 3
MB21D2	Mab-21 domain containing 2
MBD1	methyl-CpG binding domain protein 1
MBL2	mannose binding lectin 2
MCM3APAS	MCM3 minichromosome maintenance deficient 3 associated protein antisense
MDK	midkine (neurite growth-promoting factor 2)
MEF2A	myocyte enhancer factor 2A
MEF2C	myocyte enhancer factor 2C
MEF2D	myocyte enhancer factor 2D
MEI1	meiotic double-stranded break formation protein 1
MEIS1	Meis homeobox 1
METTL7A	methyltransferase like 7A
MFSD10	major facilitator superfamily domain containing 10
MGAM2	maltase-glucoamylase 2 (putative)
MGP	matrix Gla protein
MIR3151	microRNA 3151
MIR3189	microRNA 3189
MIR3910-2	microRNA 3910-2
MIR4694	microRNA 4694

MIR548B	microRNA 548b
MIR548H1	microRNA 548h-1
MKRN3	makorin ring finger protein 3
MLL	mixed lineage leukemia gene
MMP1	matrix metallopeptidase 1
MMP10	matrix metallopeptidase 10
MSMB	microseminoprotein beta
MT1A	metallothionein 1A
MT1G	metallothionein 1G
MTSS1	MTSS1, I-BAR domain containing
MUC20	mucin 20, cell surface associated
MVB12B	multivesicular body subunit 12B
MYB	MYB proto-oncogene, transcription factor
MYH10	myosin heavy chain 10
MYH11	myosin heavy chain 11
MYO5A	myosin VA
NAGPA	N-acetylglucosamine-1-phosphodiester alpha-N-acetylglucosaminidase
NARS2	asparaginyl-tRNA synthetase 2, mitochondrial (putative)
NAT10	N-acetyltransferase 10
NAV2	neuron navigator 2
NCBP2-AS2	NCBP2 antisense RNA 2 (head to head)
NCOA5	nuclear receptor coactivator 5
NCOR2	nuclear receptor corepressor 2
NDUFA6	NADH:ubiquinone oxidoreductase subunit A6
NDUFS7	NADH:ubiquinone oxidoreductase core subunit S7
NEURL2	neuralized E3 ubiquitin protein ligase 2
NF2	neurofibromin 2
NFKB1	nuclear factor kappa B subunit 1
NFKB2	nuclear factor kappa B subunit 2
NFKBIA	NFKB inhibitor alpha
NFKBIZ	NFKB inhibitor zeta
NFYB	nuclear transcription factor Y subunit beta
NHLH1	nescient helix-loop-helix 1
NIPAL3	NIPA like domain containing 3
NME4	NME/NM23 nucleoside diphosphate kinase 4
NOSIP	nitric oxide synthase interacting protein
NR1D2	nuclear receptor subfamily 1 group D member 2
NR1H4	nuclear receptor subfamily 1 group H member 4
NR2F2	nuclear receptor subfamily 2 group F member 2
NRG1	neuregulin 1
NRIP1	nuclear receptor interacting protein 1
NRK	Nik related kinase
NRP2	neuropilin 2
NT5E	5'-nucleotidase ecto

NTMT1	N-terminal Xaa-Pro-Lys N-methyltransferase 1
NUAK1	NUAK family kinase 1
NUP62CL	nucleoporin 62 C-terminal like
NUPR1	nuclear protein 1, transcriptional regulator
OCIAD1	OCIA domain containing 1
OLFML3	olfactomedin like 3
OR2T4	olfactory receptor family 2 subfamily T member 4
OR3A2	olfactory receptor family 3 subfamily A member 2
OR7E14P	olfactory receptor family 7 subfamily E member 14 pseudogene
OSBPL2	oxysterol binding protein like 2
OSM1	osmotin-like gene
OXR1	oxidation resistance 1
PADI3	peptidyl arginine deiminase 3
PAFAH1B1	platelet activating factor acetylhydrolase 1b regulatory subunit 1
PAICS	phosphoribosylaminoimidazole carboxylase; phosphoribosylaminoimidazolesuccinocarboxamide synthase
PALMD	palmdelphin
PATZ1	POZ/BTB and AT hook containing zinc finger 1
PAX4	paired box 4
PAX9	paired box 9
PBK	PDZ binding kinase
PCDH15	protocadherin related 15
PCM1	pericentriolar material 1
PDCD1LG2	programmed cell death 1 ligand 2
PDCD4	programmed cell death 4 (neoplastic transformation inhibitor)
PDXP	pyridoxal phosphatase
PEBP1	phosphatidylethanolamine binding protein 1
PELI1	pellino E3 ubiquitin protein ligase 1
PELI2	pellino E3 ubiquitin protein ligase family member 2
PHKA1	phosphorylase kinase regulatory subunit alpha 1
PI3	peptidase inhibitor 3
PIF1	PIF1 5'-to-3' DNA helicase
PIGT	phosphatidylinositol glycan anchor biosynthesis class T
PIGX	phosphatidylinositol glycan anchor biosynthesis class X
PIK3C2A	phosphatidylinositol-4-phosphate 3-kinase catalytic subunit type 2 alpha
PIN1	peptidylprolyl cis/trans isomerase, NIMA-interacting 1
PIP	prolactin induced protein
PLA2G16	phospholipase A2 group XVI
PLAA	phospholipase A2 activating protein
PLCB4	phospholipase C beta 4
PLCG2	phospholipase C gamma 2
PLCXD3	phosphatidylinositol specific phospholipase C X domain containing 3

PLEKHS1	pleckstrin homology domain containing S1
PLP2	proteolipid protein 2
PLPP3	phospholipid phosphatase 3
PLPP4	phospholipid phosphatase 4
PLXNA1	plexin A1
PMCH	pro-melanin concentrating hormone
PNO1	partner of NOB1 homolog
PNP	purine nucleoside phosphorylase
POGZ	pogo transposable element with ZNF domain
POLDIP2	DNA polymerase delta interacting protein 2
POLE2	DNA polymerase epsilon 2, accessory subunit
POLR1D	RNA polymerase I subunit D
POMC	proopiomelanocortin
POTEF	POTE ankyrin domain family member F
POU2F1	POU class 2 homeobox 1
POU2F3	POU class 2 homeobox 3
PPARA	peroxisome proliferator activated receptor alpha
PPFIBP1	PPFIA binding protein 1
PPIA	peptidylprolyl isomerase A
PPP1R9A	protein phosphatase 1 regulatory subunit 9A
PPP2R3A	protein phosphatase 2 regulatory subunit B"alpha
PPP4C	protein phosphatase 4 catalytic subunit
PPTC7	PTC7 protein phosphatase homolog
PRDM1	PR/SET domain 1
PRDX3	peroxiredoxin 3
PRKAR2B	protein kinase cAMP-dependent type II regulatory subunit beta
PRKD3	protein kinase D3
PRKX	protein kinase, X-linked
PRPF4B	pre-mRNA processing factor 4B
PSMB1	proteasome subunit beta 1
PSMB4	proteasome subunit beta 4
PSPH	phosphoserine phosphatase
PTGES	prostaglandin E synthase
PTGFRN	prostaglandin F2 receptor inhibitor
PTPN2	protein tyrosine phosphatase, non-receptor type 2
PTPRU	protein tyrosine phosphatase, receptor type U
PXYLP1	2-phosphoxylose phosphatase 1
PYCR1	pyrroline-5-carboxylate reductase 1
PYGO2	pygopus family PHD finger 2
RAB30	RAB30, member RAS oncogene family
RAD51AP2	RAD51 associated protein 2
RAET1K	retinoic acid early transcript 1K pseudogene
RAI14	retinoic acid induced 14
RAP2C	RAP2C, member of RAS oncogene family
RAPGEF2	Rap guanine nucleotide exchange factor 2

RARA	retinoic acid receptor alpha
RARB	retinoic acid receptor beta
RARG	retinoic acid receptor gamma
RARRES1	retinoic acid receptor responder 1
RARRES3	retinoic acid receptor responder 3
RASAL1	RAS protein activator like 1
RASIP1	Ras interacting protein 1
RASL11A	RAS like family 11 member A
RASSF6	Ras association domain family member 6
RBBP4	RB binding protein 4, chromatin remodeling factor
RBM45	RNA binding motif protein 45
RCAN3	RCAN family member 3
RCL1	RNA terminal phosphate cyclase like 1
REG4	regenerating family member 4
RELA	RELA proto-oncogene, NF-kB subunit
RFC3	replication factor C subunit 3
RFPL4AL1	ret finger protein like 4A like 1
RGS2	regulator of G-protein signaling 2
RMDN3	regulator of microtubule dynamics 3
RNASE6	ribonuclease A family member k6
RNASEL	ribonuclease L
RNFT2	ring finger protein, transmembrane 2
ROCK2	Rho associated coiled-coil containing protein kinase 2
ROS1	ROS proto-oncogene 1, receptor tyrosine kinase
RPL37A	ribosomal protein L37a
RPS27	ribosomal protein S27
RPS8	ribosomal protein S8
RRAGD	Ras related GTP binding D
RRAS	related RAS viral (r-ras) oncogene homolog
RREB1	ras responsive element binding protein 1
RRM1	ribonucleotide reductase catalytic subunit M1
RRM2	ribonucleotide reductase regulatory subunit M2
RTN3	reticulon 3
RTN4	reticulon 4
RXFP1	relaxin/insulin like family peptide receptor 1
RYBP	RING1 and YY1 binding protein
S100A7	S100 calcium binding protein A7
S100A7A	S100 calcium binding protein A7A
SAMD12-AS1	SAMD12 antisense RNA 1
SAMD9	sterile alpha motif domain containing 9
SAMD9L	sterile alpha motif domain containing 9 like
SAR1A	secretion associated Ras related GTPase 1A
SCEL	sciellin
SCGB2A1	secretoglobin family 2A member 1
SCN1A	sodium voltage-gated channel alpha subunit 1

SDF2	stromal cell derived factor 2
SDHAF2	succinate dehydrogenase complex assembly factor 2
SDHD	succinate dehydrogenase complex subunit D
SECTM1	secreted and transmembrane 1
SEL1L	SEL1L ERAD E3 ligase adaptor subunit
SELENOP	selenoprotein P
SEPT6	septin 6
SEPT8	septin 8
SEPW1	selenoprotein W
SERINC2	serine incorporator 2
SERPINI2	serpin family I member 2
SESN3	sestrin 3
SET	SET nuclear proto-oncogene
SF3B5	splicing factor 3b subunit 5
SFN	stratifin
SFXN1	sideroflexin 1
SGPL1	sphingosine-1-phosphate lyase 1
SGPP1	sphingosine-1-phosphate phosphatase 1
SH2D1B	SH2 domain containing 1B
SH3BGRL	SH3 domain binding glutamate rich protein like
SIRPA	signal regulatory protein alpha
SLC15A1	solute carrier family 15 member 1
SLC15A2	solute carrier family 15 member 2
SLC25A19	solute carrier family 25 member 19
SLC25A46	solute carrier family 25 member 46
SLC27A2	solute carrier family 27 member 2
SLC2A1	solute carrier family 2 member 1
SLC35D2	solute carrier family 35 member D2
SLC37A2	solute carrier family 37 member 2
SLC39A2	solute carrier family 39 member 2
SLC46A3	solute carrier family 46 member 3
SLC6A14	solute carrier family 6 member 14
SLC7A6	solute carrier family 7 member 6
SLPI	secretory leukocyte peptidase inhibitor
SMARCA2	SWI/SNF related, matrix associated, actin dependent regulator of chromatin, subfamily a, member 2
SNAPC4	small nuclear RNA activating complex polypeptide 4
SNCAIP	synuclein alpha interacting protein
SNRPN	small nuclear ribonucleoprotein polypeptide N
SNX10	sorting nexin 10
SNX7	sorting nexin 7
SOCS4	suppressor of cytokine signaling 4
SP1	Sp1 transcription factor
SP2	Sp2 transcription factor
SPATA2	spermatogenesis associated 2

SPDEF	SAM pointed domain containing ETS transcription factor
SPG21	spastic paraplegia 21 (autosomal recessive, Mast syndrome)
SPIC	Spi-C transcription factor
SPINK8	serine peptidase inhibitor, Kazal type 8 (putative)
SPRYD7	SPRY domain containing 7
SRI	sorcin
SRPX2	sushi repeat containing protein, X-linked 2
SSH2	slingshot protein phosphatase 2
SSR1	signal sequence receptor subunit 1
ST3GAL1	ST3 beta-galactoside alpha-2,3-sialyltransferase 1
ST5	suppression of tumorigenicity 5
ST7L	suppression of tumorigenicity 7 like
STAG3L4	stromal antigen 3-like 4 (pseudogene)
STAMBPL1	STAM binding protein like 1
STAT2	signal transducer and activator of transcription 2
STK10	serine/threonine kinase 10
STK39	serine/threonine kinase 39
STRA6	stimulated by retinoic acid 6
STT3B	STT3B, catalytic subunit of the oligosaccharyltransferase complex
STX12	syntaxin 12
STX19	syntaxin 19
SUMF2	sulfatase modifying factor 2
SUMO2	small ubiquitin-like modifier 2
SYNGR2	synaptogyrin 2
SYPL1	synaptophysin like 1
SYTL5	synaptotagmin like 5
tAKR	aldo-keto reductase family 1 member C6, pseudogene
TBP	TATA-box binding protein
TBX5	T-box 5
TCEAL2	transcription elongation factor A like 2
TCEAL6	transcription elongation factor A like 6
TCHHL1	trichohyalin like 1
TERF1	telomeric repeat-binding factor 1
TF	transferrin
TFAM	transcription factor A, mitochondrial
TFDP1	transcription factor Dp-1
TFPI2	tissue factor pathway inhibitor 2
TG	thyroglobulin
THOC7	THO complex 7
THYN1	thymocyte nuclear protein 1
TIMM10	translocase of inner mitochondrial membrane 10
TIMM8B	translocase of inner mitochondrial membrane 8 homolog B
TINAGL1	tubulointerstitial nephritis antigen like 1
TK1	thymidine kinase 1

TLCD1	TLC domain containing 1
TLR3	toll like receptor 3
TM9SF2	transmembrane 9 superfamily member 2
TM9SF3	transmembrane 9 superfamily member 3
TMED10	transmembrane p24 trafficking protein 10
TMEM105	transmembrane protein 105
TMEM136	transmembrane protein 136
TMEM14A	transmembrane protein 14A
TMEM14C	transmembrane protein 14C
TMEM230	transmembrane protein 230
TMEM259	transmembrane protein 259
TMEM44-AS1	TMEM44 antisense RNA 1
TMPO	thymopoietin
TMPRSS4	transmembrane protease, serine 4
TMTC2	transmembrane and tetratricopeptide repeat containing 2
TNFSF10	tumor necrosis factor superfamily member 10
TNFSF15	tumor necrosis factor superfamily member 15
TNFSF18	tumor necrosis factor superfamily member 18
TNKS	tankyrase
TOP2A	topoisomerase (DNA) II alpha
TP53INP1	tumor protein p53 inducible nuclear protein 1
TPT1	tumor protein, translationally-controlled 1
TRERF1	transcriptional regulating factor 1
TRIM22	tripartite motif containing 22
TRIM24	tripartite motif containing 24
TRIM25	tripartite motif containing 25
TRIM31	tripartite motif containing 31
TRMT61A	tRNA methyltransferase 61A
TSR1	TSR1, ribosome maturation factor
TTN	titin
TTPA	alpha tocopherol transfer protein
U2SURP	U2 snRNP associated SURP domain containing
UBA5	ubiquitin like modifier activating enzyme 5
UBE2D3	ubiquitin conjugating enzyme E2 D3
UBE2L6	ubiquitin conjugating enzyme E2 L6
UBL5	ubiquitin like 5
UCA1	urothelial cancer associated 1 (non-protein coding)
UGT2A1	UDP glucuronosyltransferase family 2 member A1 complex locus
ULK1	unc-51 like autophagy activating kinase 1
UNC5CL	unc-5 family C-terminal like
UPF3B	UPF3 regulator of nonsense transcripts homolog B (yeast)
USP27X	ubiquitin specific peptidase 27, X-linked
USP30-AS1	USP30 antisense RNA 1
USP47	ubiquitin specific peptidase 47

UTP6	UTP6, small subunit processome component
VCAM1	vascular cell adhesion molecule 1
VDAC3	voltage dependent anion channel 3
VEGFC	vascular endothelial growth factor C
VEZF1	vascular endothelial zinc finger 1
VGLL3	vestigial like family member 3
VPS35	VPS35, retromer complex component
WARS2	tryptophanyl tRNA synthetase 2, mitochondrial
WNK3	WNK lysine deficient protein kinase 3
XBP1	X-box binding protein 1
XKR6	XK related 6
XRCC1	X-ray repair cross complementing 1
YES1	YES proto-oncogene 1, Src family tyrosine kinase
YLYAR	Ly1 antibody reactive
YME1L1	YME1 like 1 ATPase
YTHDC1	YTH domain containing 1
ZBTB10	zinc finger and BTB domain containing 10
ZBTB14	zinc finger and BTB domain containing 14
ZBTB7C	zinc finger and BTB domain containing 7C
ZFP36	ZFP36 ring finger protein
ZFP36L2	ZFP36 ring finger protein like 2
ZMYM2	zinc finger MYM-type containing 2
ZNF221	zinc finger protein 221
ZNF280A	zinc finger protein 280A
ZNF280B	zinc finger protein 280B
ZNF347	zinc finger protein 347
ZNF441	zinc finger protein 441
ZNF502	zinc finger protein 502
ZNF706	zinc finger protein 706
ZNF788	zinc finger family member 788
ZNF844	zinc finger protein 844
ZPLD1	zona pellucida like domain containing 1
ZSWIM5	zinc finger SWIM-type containing 5

APPENDIX 4: COPYRIGHT PERMISSIONS

Chapter 1:

Coyle KM, Sultan M, Thomas ML, Vaghar-Kashani A, Marcato P. Retinoid signaling in cancer and its promise for therapy. Journal of Carcinogenesis and Mutagenesis 2013; S7:006.

Coyle KM, Boudreau JE, Marcato P. Genetic mutations and epigenetic modifications: Driving cancer and informing precision medicine. BioMed Research International. 2017; 2017: 9620870.

Chapter 2:

Coyle KM, Murphy JP, Vidovic D, Vaghar-Kashani A, Dean CA, Sultan M, Clements D, Wallace M, Thomas ML, Hundert A, Giacomantonio CA, Helyer L, Gujar SA, Lee PWK, Weaver ICG, Marcato P. Breast cancer subtype dictates DNA methylation and ALDH1A3-mediated expression of tumor suppressor RARRES1. Oncotarget 2016; 7(28):44096-44112.

Chapter 3:

Coyle KM, Maxwell S, Thomas ML, Marcato P. Profiling of the transcriptional response to all-trans retinoic acid in breast cancer cells reveals RARE-independent mechanisms of gene expression. Scientific Reports. 2017; 7(1):16684.